

**CORRELATION FUNCTION OF MACROMOLECULES  
IN SOLUTION :  
CLUSTER THEORETIC CALCULATION IN THE  
HYPERNETTED CHAIN APPROXIMATION**

**A Thesis Submitted  
in Partial Fulfilment of the Requirements  
for the Degree of  
DOCTOR OF PHILOSOPHY**

**by  
BEDAMATI DAS**

**to the  
DEPARTMENT OF CHEMISTRY  
INDIAN INSTITUTE OF TECHNOLOGY, KANPUR**

**October, 1993**

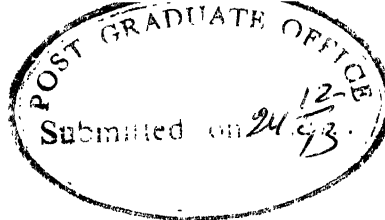
4 JUL 1996  
CENTRAL LIBRARY  
I.I.T KANPUR

Ms. No. A. 121821

✓ CHM-1883-D-DAS-COR



A121821



## CERTIFICATE

I hereby declare that the work embodied in this thesis entitled, "CORRELATION FUNCTION OF MACROMOLECULES IN SOLUTION: Cluster Theoretic Calculation in the Hypernetted Chain Approximation" is the result of investigations carried out by me in the Department of Chemistry, Indian Institute of Technology, Kanpur, India, under the supervision of Professor P. Gupta Bhaya.

In keeping with scientific tradition, wherever work done by others has been utilized, due acknowledgement has been made.

*Bedamati Das*  
Bedamati Das

Kanpur

Decemberr, 1993

## CERTIFICATE I

Certified that the work presented in this thesis entitled,  
"CORRELATION FUNCTION OF MACROMOLECULES IN SOLUTION Cluster  
Theoretic Calculation in the Hypernetted Chain Approximation" by  
Ms. Bedamati Das has been carried out under my supervision and  
has not been submitted elsewhere for a degree.

*P. nani Gupta Bhaya*

(Professor P. Gupta Bhaya)  
Thesis Supervisor  
Department of Chemistry  
I.I.T. Kanpur

Kanpur  
December, 1993



DEPARTMENT OF CHEMISTRY  
INDIAN INSTITUTE OF TECHNOLOGY KANPUR, INDIA

CERTIFICATE II

This is to certify that Ms. Bedamati Das has satisfactorily completed all the courses required for the Ph.D. degree program. The courses include:

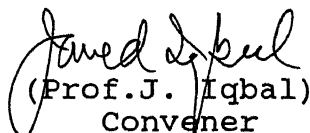
Chm 525N Principles of Physical Chemistry  
Chm 545N Principles of Inorganic Chemistry  
Chm 521N Chemical Binding  
Chm 505N Principles of Organic Chemistry  
Chm 524N Modern Physical Methods  
Chm 542N Advance Inorganic Chemistry II  
Chm 626N Solid State Chemistry  
Chm 800N General Seminar  
Chm 801N Special Seminar  
Chm 900N Ph.D. Thesis

Ms. Bedamati Das was admitted to the candidacy for the Ph.D. degree in March 3, 1987 after she successfully completed the written and oral qualifying examinations.



(Prof. P.K. Ghosh)  
Head

Department of Chemistry  
I.I.T. Kanpur



(Prof. J. Iqbal)  
Convener  
Departmental Postgraduate Committee  
I.I.T. Kanpur

## ACKNOWLEDGEMENTS

I like to thank my thesis supervisor Dr. Pinaki Gupta-Bhaya for affectionate guidance, sincere concern for my academic and personal welfare and stimulating discussions. Working with him has been a rich experience, both academic and personal.

I am also indebted to his mother, Dr. Renu Gupta; wife, Dr. Sumana Gupta; for their affection and care. They took personal care of me in many ways but for which the completion of this work would have been difficult. Finally I apologise to his daughter Shahana, who missed her precious holidays for the progress of this work.

I have taken help from many people for the accomplishment of this work. I am quoting their name below. My sincere thanks to each one of them.

Dr. Kalyan Banerjee,  
Dr. D.C. Khan,  
Dr.A.K. Majumdar,  
Dr. S.D. Joglekar,  
Dr. Swapan Saha,  
Dr. S.P. Mohanty,  
Dr. P.C. Das,  
Dr. Pravir Dutt,  
Dr. R.K.S.Rathore,  
Dr. Aparna Dar,  
Dr. Divakar Sharma,  
Dr. S.Manogaran,  
Dr. A.Sengupta  
Mr. Vishal Saxena,  
Dr. N. Subba Rao,  
Dr. Y. Kamlakara Rao  
Mr. Ashok Naik  
Mr. Avik Ghosh  
Mr. Sayan Kar

I thank Mr. Raghunath Behera, Mr. Tapan Kumar Khan and Mr. Sib Sankar Kundu from my heart for rendering me special help just when I needed them.

I thank my friends Dr. Nishi Gupta, Ms. Prachla Vig, Arati Nanda, Sushma Sinha, Snigdha Saxena, M. Sujata, V. Vidyavathi, Jaya Sharma, Bhabana Pati, Sujata Mohanty, Sarabjit Kaur, Sharmisht Parija, Vaishali Kulkarni, Rita Singh, R.R.N. Shailaja, Charu Gupta for providing me a friendly atmosphere.

I thank Mr. U.S. Mishra for the neat and efficient typing. Mr.L.S. Bajpai, Mr. Ghanshyam and Mr. A.K.Srivastava also typed a sizable part of the thesis. I thank them. I also thank Mr. N.K. Metia for ably taking the final print of the thesis.

I thank my mother Mrs. Madhuri Das, whose aspirations compelled me to undertake this journey. I thank my brothers, sister, sister-in-law and my nephew who have waited patiently for me to complete this work.

-Bedamati Das

## ABSTRACT

The static correlation functions in macroionic solution are calculated in the Hypernetted-chain approximation. The effect of the polarization of highly charged macroionic dielectric by other ions in solution is considered and it is found that the effect is significant only in non-spherical macroions. The method of calculation of energy terms arising from the polarization of the macroion is discussed in detail to make the underlying physics clear. The effect of polarization is taken into account by making the screening constant of Coulombic interaction dependent on distance. This is the content of Chapter II.

The cluster theoretic method that leads to the Allnatt equation for the treatment of ionic fluids in the hypernetted chain approximation is described in Chapter III. It is extended (Section 9) to the treatment of systems where polarization effect is important, i.e. screening constant is a function of  $r$ .

Systems with angle-dependent potential are considered in Chapter IV. The method of Jepsen and Friedman is described. It is extended to the treatment of ion-dipole mixtures at finite concentrations of both. It is pointed out that the Allnatt equation holds for angle-dependent potential also. The method for the calculation of correlation function in these systems is described. The question of convergence of cluster expansion is discussed.

In Chapter V, the numerical results on macroion-macroion pair correlation function of charged non-polar macroions as a function of size, charge density and concentration of macroion and background electrolyte present in solution are given and the trends are discussed. It is found that the use of Allnatt equation makes the HNC theory applicable to asymmetric electrolytes having a particle charge and a packing fraction much larger than that found possible in recent investigations. As compared to recent work, calculations reported in this thesis, can handle particle charges almost an order of magnitude larger at a packing fraction 1.5 times larger. The calculation on a charged polar macroionic system could not be done extensively. A single graph is given to show that the program works and dipole moment of the macroion affects the correlation function.

## CONTENTS

|  | PAGE |
|--|------|
| <b>Chapter I</b>   |      |
| Introduction .....   | 1    |
| 1.1 Forces between Macromolecular Assemblies :<br>Relevance .....  | 2    |
| 1.2 Experiments : Hydration Forces .....   | 4    |
| 1.3 Dispersive Forces .....  | 5    |
| 1.4 Measurement of Dispersive and Inductive Forces:<br>Role of Theory .....                                | 14   |
| 1.5 Particle Size, Polarization Effect, Dipolar<br>Interaction .....                                       | 16   |
| 1.6 Macromolecular Suspension as an Inhomogeneous<br>Dielectric .....                                      | 18   |
| 1.7 Integral Equation Theories .....   | 19   |
| 1.8 Highly Assymmetric Electrolytes : Polarizable Ions .   | 21   |
| 1.9 Effect of Long Range Correlation in Charged<br>Micelles .....  | 22   |
| 1.10 Correlation Function Calculations : Models .....  | 26   |
| 1.11 Essential Role of Integral Equation Theories .....  | 28   |
| 1.12 MSA : Measure of Macroion Charges .....   | 29   |
| 1.13 HNC Calculation on Polyelectrolytes .....   | 35   |
| 1.14 Ion-Dipole Mixture .....  | 44   |
| 1.15 Bridge Functions .....  | 49   |
| 1.16 Integral Equation in Treatment of External Field<br>and Planar Interface .....                        | 51   |
| 1.17 Molecular Recognition at a Distance .....   | 51   |
| 1.18 Structure of this Thesis .....  | 52   |
| References .....   | 54   |
| <b>Chapter II</b>  |      |
| Coulombic Interaction in Macroionic Solution :<br>Effect of Polarization of Macroionic<br>Dielectric ..... | 65   |
| 2.1 Introduction .....   | 66   |
| 2.2 Screening Constant of a System of Two Point<br>Ions .....  | 75   |
| 2.3 Energy of a System of Charges in the Presence<br>of a Dielectric .....                                 | 78   |
| 2.4 Screening Constant of a System of an Ion and<br>a Macroion .....                                       | 83   |
| 2.5 Point ion-Macroion Interaction, viewed from<br>the Macroion and the Point ion .....                    | 93   |

|     |  |     |
|-----|--|-----|
| 2.6 | Screening Constant of a System of Two Interacting Macroions .....  | 97  |
| 2.7 | Numerical Estimates of Effective Screening Constant : Significant Modification of the Screening Constant for a Nonspherical Particle ..... | 98  |
| 2.8 | Polarized Charge Distribution at the Macroion Surface .....  | 101 |
|     | References .....   | 102 |

### Chapter III

|      |   |     |
|------|---|-----|
|      | HNC Theory of Macromolecules Interacting Through Central Potential .....                          | 104 |
|      | Introduction .....  | 105 |
| 3.1  | Statistical Mechanical Preliminaries .....  | 105 |
| 3.2  | Distribution Function .....   | 107 |
| 3.3  | Potential of Average Force .....  | 111 |
| 3.4  | Clusters .....  | 112 |
| 3.5  | Topological Classification .....  | 115 |
| 3.6  | Theory of Ionic Solution .....  | 118 |
| 3.7  | Cluster Summation of Potential of Average Force and Radial Distribution Function .....            | 125 |
| 3.8  | Solution of Integral Equation .....   | 157 |
| 3.9  | Calculation of $q$ -function for an Ionic System with Distance Dependent Screening Constant ..... | 160 |
| 3.10 | The Question of Convergence .....   | 172 |
| 3.11 | Problems in Calculation of the Transform of the Coulomb Potential .....                           | 176 |
|      | References .....  | 179 |

### Chapter IV

|     |  |     |
|-----|--|-----|
|     | HNC Calculations on Macroionic Solution: Angle Dependent Potential .....             | 180 |
|     | Introduction .....   | 181 |
| 4.1 | Jepsen and Friedman Theory .....   | 181 |
| 4.2 | Extension of Friedman-Jepsen Method to Mixtures .....                                | 214 |
| 4.3 | Calculation of Initial value of $\tau$ .....   | 243 |
| 4.4 | Calculation of $g(r, \Gamma)$ .....  | 253 |
| 4.5 | Calculation of $q$ for a Mixture of Ions only from the Equations Derived Above ..... | 270 |
| 4.6 | Problem of Convergence of the Cluster Expansion of Angle Dependent $q$ .....         | 271 |

|     |   |     |
|-----|---|-----|
| 4.7 | Validity of Allnatt Equation for<br>Angle Dependent Potential ..... | 274 |
|     | Appendix .....  | 275 |
|     | References .....  | 282 |

## Chapter V

|            |   |     |
|------------|---|-----|
|            | Numerical Results .....   | 283 |
| 5.1        | Calculation of Convolution Integrals<br>a*b .....   | 284 |
| 5.2        | Number of Points in F.T. Operations .....   | 292 |
| 5.3        | The Problem of Nonconvergent Iteration<br>in Solution of HNC Equation .....                                       | 294 |
| 5.4        | Features of the $g(r)$ versus $r$ Plots .....   | 298 |
| 5.5        | Calculation of Transform of Coulomb<br>Potential for Systems with Distance-<br>Dependent Screening Constant ..... | 315 |
| 5.6        | Systems with Angle-dependent Inter-<br>action .....   | 317 |
|            | References .....  | 394 |
| Appendix-1 | .....   | 396 |
| Appendix-2 | .....   | 413 |
| Appendix-3 | .....   | 435 |



# CHAPTER I

## INTRODUCTION

### 1.1 Forces between Macromolecular Assemblies: Relevance

Force between macroions and their association is an important quantity in Molecular Biology and Biotechnology. The nature of forces determine strong and specific association under exquisite control and is a key to the understanding of the regulation of cellular activity. Fusion of cells is at the root of many biological processes viz. fertilization. It has also found technological application in the production of plant seeds of high yielding variety and in the production of monoclonal antibodies, an important product in medicine and pharmaceutical industry. Fusion can be induced by chemical agents viz.  $\text{Ca}^{2+}$  ion and polyethylene glycol. More recently, electric fields have been used. Use of electric field is definitely going to have a major impact in fusion technology. It is more amenable to control and does not modify the cell on a chemical level. It is important to be able to calculate the effect of electric field on the forces between cells to make it possible for the experimenter to design a fusion experiment that will have high yield for a given system. The field of membrane fusion has been reviewed extensively. A recent collection of articles has most of the relevant information and literature references (1). A good introduction to forces in membrane systems can be found in a text book by Silver (2).

Forces between highly charged macroions introduce very long range correlations between particles. The usual chemical

molecules do not have such long correlation lengths. A macromolecular solution, as will be discussed below can be treated as an equivalent gas of macroions, interacting through a mean effective potential. The gas can show highly interesting phenomena arising from very long range interparticle correlation including phase transitions. The study of macroionic solution is of interest in understanding of fluids, in general, apart from being of intrinsic interest in macromolecular physical chemistry. At the other end, the dispersive and inductive forces of shorter range between macromolecules, of interest in cell fusion research, assume importance also in the context of understanding them. Quantitative measure of the dependence of dispersive and inductive interaction on chemical nature, shape and size of macroions, will lead to improved understanding of these forces. Small molecules, by virtue of their smallness, do not show many features, that become amenable to investigation only in the study of macromolecular suspensions.

An understanding of the forces in biomolecular systems may be crucial in deciphering the details of biological specificity and bimolecular recognition. Recognition of a molecule by a cell surface or a macromolecular assembly may not be a process that requires intimate contact at distances where valence forces become operative as is known in great detail in enzyme-substrate interaction. It may operate even at larger distances. In the case of angle dependent forces, it is possible that a dipolar

molecule (almost all biological molecules carry dipole moment) may have favoured direction of approach, which allow them to land at specific sites on a cell surface.

## 1.2 Experiments: Hydration Forces

Theoretical studies on forces between membranes has received strong impetus from the ingenious experiments of Parsegian and Israelachvili, in which direct measurement of forces between membrane bilayers and between mica surfaces have been measured. The forces between mica surfaces show interesting oscillations at distances of a few nanometers (2). Neutral bilayers such as DPPC, DPLC and DMPC separated by small distances repel each other with an enormous force that obeys an exponential law given by

$$P = P_0 \exp \left( - \frac{d\omega}{\lambda} \right), \quad (1)$$

where  $P_0 = 7 \times 10^9$  dynes/cm<sup>2</sup> and  $\lambda = 2.56 \text{ \AA}$  (2). The relationship holds for separation  $d_\omega$  of  $\sim 3$  to  $25 \text{ \AA}$  and for a wide variety of phospholipids. This large repulsive forces at short distances are balanced by attractive Vander Waal's forces at short distances and result in an equilibrium distance between neutral bilayers in crystals. It is known that the distance increases to a maximum value with addition of water (2). The proportion of lipid and water determines the equilibrium distances because the repulsive forces owe their origin to water. Qualitatively this so called structural or hydration force originates from the detailed microscopic solvent structure and its modification due

to the presence of bilayers at close proximity. At a larger distance than a few nanometers this force disappears and a description of solvent as a continuum holds. Interesting recent papers have appeared on direct force measurement between counter-ion condensed DNA double helices (3,4), that between linear polysaccharides (5) and on the origin of hydration force (6,7). A recent review has appeared (8).

### 1.3 Dispersive Forces

Vander Waal's force between atoms as well as macroscopic bodies, has been thoroughly investigated (9,10). This force owes its origin to fluctuating multipoles of two atoms or molecules interacting through the electromagnetic field that they emit. For larger molecular assemblies the forces are not pairwise additive, because the fluctuations of different particles in these assemblies are correlated. It is a complicated many body problem. A complete quantum electrodynamical theory has been worked out by Lifshitz (11). Its application requires a knowledge of only the macroscopic properties of the bodies and the intervening medium. The microscopic details are not necessary. Whereas the pre-Lifshitz theories, that ignore correlation between fluctuations, predict attraction under all circumstances, Lifshitz theory predicts new effects viz. repulsion, deviation from  $r^{-6}$  law, forces of extraordinary strength at large distances. The theory is based on interaction between

$$\begin{aligned}
&= \lim_{\alpha \rightarrow 0} \int_0^{\infty} \frac{e^{-\alpha r}}{Dr} \frac{\sin tr}{tr} 4\pi r^2 dr \\
&= \frac{4\pi}{Dt} \lim_{\alpha \rightarrow 0} \int_0^{\infty} e^{-\alpha r} \sin tr dr \\
&= \lim_{\alpha \rightarrow 0} \frac{4\pi}{D(\alpha^2 + t^2)} = \frac{4\pi}{Dt^2} \quad * \quad (113)
\end{aligned}$$

$$\left\{ \text{we recall } \lambda = \frac{\epsilon^2}{kT} \text{ and define } \delta = \frac{4\pi\epsilon^2}{DkT} = \frac{4\pi\lambda}{D} \right\}$$

Then, for our system

$$\left[ I - Z'(-\lambda H') \right] = \begin{bmatrix} 1 + \rho_+ Z_+^2 \delta/t^2 & + \rho_+ Z_+^2 \delta/t^2 & + \rho_+ Z_+^2 \lambda \tilde{g}'_{+m} \\ + \rho_- Z_-^2 \delta/t^2 & 1 + \rho_- Z_-^2 \delta/t^2 & + \rho_- Z_-^2 \lambda \tilde{g}'_{-m} \\ + \rho_m Z_m^2 \lambda \tilde{g}'_{m+} & + \rho_m Z_m^2 \lambda \tilde{g}'_{m-} & 1 + \rho_m Z_m^2 \lambda \tilde{g}'_{mm} \end{bmatrix} \quad (114)$$

We now work out the matrix  $\left[ I - Z'(-\lambda H') \right]^{-1}$ .

From equation (108), we see that calculation of  $\tilde{q}_{XY}(t)$  needs finding XY element of the matrix  $\left[ (-\lambda H') \left[ I - Z'(-\lambda H') \right]^{-1} \right]$ . That needs finding inverse of the matrix  $\left[ I - Z'(-\lambda H') \right]$  and multiplying the inverse matrix by the matrix  $(-\lambda H')$ .

$$\begin{aligned}
&\det \left[ I - Z'(-\lambda H') \right] \\
&= \left( 1 + \rho_+ Z_+^2 \frac{\delta}{t^2} + \rho_- Z_-^2 \frac{\delta}{t^2} + \rho_m Z_m^2 \lambda \tilde{g}'_{mm} + \rho_- \rho_m Z_-^2 Z_m^2 \frac{\delta}{t^2} \lambda \tilde{g}'_{mm} \right. \\
&\quad \left. - \rho_- \rho_m Z_-^2 Z_m^2 \lambda \tilde{g}'_{m-} \lambda \tilde{g}'_{-m} + \rho_+ \rho_m Z_+^2 Z_m^2 \frac{\delta}{t^2} \lambda \tilde{g}'_{mm} - \rho_+ \rho_m Z_+^2 Z_m^2 \frac{\delta}{t^2} \lambda \tilde{g}'_{m-} \lambda \tilde{g}'_{-m} \right. \\
&\quad \left. + \rho_+ \rho_- \rho_m Z_+^2 Z_-^2 Z_m^2 \frac{\delta}{t^2} \lambda \tilde{g}'_{-m} \lambda \tilde{g}'_{m+} + \rho_+ \rho_- \rho_m Z_+^2 Z_-^2 Z_m^2 \frac{\delta}{t^2} \lambda \tilde{g}'_{+m} \lambda \tilde{g}'_{m-} \right)
\end{aligned}$$

fluctuating dipoles and the fluctuation-dissipation theorem.

Two isotropic nonpolar molecules interact in vacuum, through Vander Waals forces. Since permanent electric multipole moments are all zero, interaction owes its origin to fluctuating multipoles. The fluctuating multipoles on one molecule is correlated to that on another in such a way that their mutual orientations are not random. The mutual orientations that release energy are preferred, as in the case of permanent dipoles. The net effect is a favourable energy of interaction, called Vander Waals bond. The strength of the interaction depends on the magnitude of the fluctuating dipole that generates field, as well as on its frequency distribution. The response of the other molecule depends on its electric polarizability at the frequencies of the electromagnetic field emitted by the fluctuating dipoles. Thus we anticipate that polarizability will appear in the expression of Van der Waals forces. Just as a tuning fork transmits best at the frequency at which it resonates best, molecules fluctuate spontaneously with a frequency distribution exactly paralleling those at which it responds most effectively. Polarizability controls the fluctuations and through them the frequency spectrum of the transmitted radiation.

A quantitative calculation of Vander Waals force requires values of polarizability as a function of frequency. For free molecules in vacuum, one needs polarizability in vacuum and this is obtainable from spectroscopic data. All one does in

of all functions  $g(r, \alpha)$  which reduce to  $g(r)$  in the limit  $\alpha \rightarrow 0$  need not give  $1/t^2$  when it is applied on the transform of  $g(r, \alpha)$ . It has not been proven in general that for all  $g(r, \alpha)$ , we will have  $\lim_{\alpha \rightarrow 0} \tilde{g}(t, \alpha) = 1/t^2$ . Such proofs exist for other cases and are called Tauberian theorems in mathematics. Friedman (2) has derived  $g(t) = \frac{1}{t^2}$  starting from Gauss's Law of electrostatics, using divergence theorem and then Fourier transforming the resulting equation.  $g(r)$  is then obtained from  $g(t)$  to be  $\frac{1}{4\pi r}$ . The procedure is reverse of what was done earlier, i.e., to obtain  $g(t)$  from  $g(r)$ . Possible "physical" interpretations of the convergence factor  $e^{-\alpha r}$  has been discussed by Friedman (2) and are shown to be unsatisfactory. Thus, it is a purely mathematical device and its success is entirely dependent on agreement of results so derived with experiments.

In Chapter 4, we derive expressions of  $q(t)$  for ion-dipole mixtures, starting from Coulomb  $g$  bonds following a method of Friedman and Jepsen (15). The procedure adopted by Friedman and Jepsen (15) avoids the divergence problem by assuming that Coulomb potential is zero within a sphere of small radius  $a$  and is the usual Coulomb potential outside this sphere and then letting  $a \rightarrow 0$ . We will show there that in a system containing only positive and negative ions (and no dipoles),  $q(t)$  once again turns out to be  $1/t^2$  as  $a \rightarrow 0$ .



spectroscopy is to probe the system with oscillating electromagnetic field. The peaks in spectra appear when the characteristic frequency of the molecule is in resonance with the frequency of the incident field. Our interest is in large assemblies of importance in biology. Their spontaneous thermal fluctuations have a frequency spectrum. Fluctuation-Dissipation theorem tells us that the response of a system to an external disturbance, in the limit of linear response, can be predicted from the characteristics of its spontaneous thermal fluctuations at thermal equilibrium. This connection is parallel to the tuning fork analogy given earlier. The response of a system to an electromagnetic field allows us to determine the nature of the electrical (and magnetic) fluctuations within the system in the absence of the field. The response is manifested by the conventional spectral characteristics and at low frequencies by the dielectric permeability. The tools needed for calculating Vander Waals force are conventional optical spectroscopic and dielectric spectroscopy.

McLachlan (12,13) has derived the expression of free energy of interaction between two isotropic bodies in free space separated by a distance  $r$  large compared with their dimensions

$$G = - \frac{6kT}{r^6} \sum_{n=0}' \alpha_1 (i\omega_n) \alpha_2 (i\omega_n) \quad (2)$$

The prime on the summation sign indicates that the  $n=0$  term is multiplied by  $1/2$ .  $\omega_n = n (2\pi kT/\hbar)$  and  $\alpha_1 (i\omega_n)$  can be obtained

by taking the expression of frequency dependent polarizability and replacing  $\omega$  by  $i\omega$ , where  $i = (-1)^{1/2}$ . For atoms, a good approximation for electronic polarizability is

$$\alpha_e(\omega_n) = fe^2/m (\omega_e^2 - \omega_n^2),$$

where  $\omega$  is the frequency of electromagnetic radiation,  $e$  and  $m$  the charge and mass of the electron and  $f$  the effective number of oscillating electrons. The polarizability has a maximum at  $\omega = \omega_e$ . Thus  $\alpha_e(i\omega_n) = fe^2/m (\omega_e^2 + \omega_n^2)$ . Numerical estimates show that for atoms the values of  $\alpha_e(i\omega_n)$  that contribute most to  $G$  will be in the ultraviolet and the static polarizability plays a negligible role. The term in  $n=0$  does not contribute to the dispersion energy since it contains only the static polarization. The sum over the terms for  $n > 0$  can be shown under normal physical conditions to give

$$G_{n>0} = - \frac{3\hbar}{2r^6} \frac{\omega_{1e}\omega_{2e}}{(\omega_{1e}+\omega_{2e})} \alpha_{1e}(0)\alpha_{2e}(0) \quad (3)$$

This is London's formula for dispersion energy of two atoms in vacuum. If two isotropic particles are separated by a medium rather than a vacuum. McLachlan's formula is modified to

$$G = - \frac{6kT}{r^6} \sum_{n=0}^{\infty} ' \alpha_1^*(i\omega_n) \alpha_2^*(i\omega_n) / \epsilon_3^2(i\omega_n) \quad (4)$$

(the prime has the same significance as the prime in Eq.(2)).

$\epsilon_3(i\omega)$  is the dielectric permeability of the medium at imaginary frequencies. At  $\omega = 0$ ,  $\epsilon_3(0)$  is the static dielectric constant. Formulae for  $\epsilon(i\omega)$  at nonzero frequency are known in terms of

$$(16) M_n^1 = \int \varphi(r, i \rightarrow r) r^1 D_{on}^1(i \rightarrow r) d^3\vec{r} \quad (20)$$

$\varphi \rightarrow$  charge distribution of molecule  $i$  and the axes of integration coordinates are fixed to molecule.

$$(17) \bar{f}_{12} \begin{pmatrix} l_1 & l_2 & l \\ m_1 & m_2 & r_{12} \end{pmatrix} = \sum_{l_1 l_2 l} \bar{F}_{12} \begin{pmatrix} l_1 & l_2 & l \\ m_1 & m_2 & r_{12} \\ n_1 & n_2 & -n \end{pmatrix} (-)^{m_1} \begin{bmatrix} l_1 & l_2 & l \\ n_1 & n_2 & n \end{bmatrix}_{3j} \quad (21)$$

A function of the coordinates of two molecules  $i$  and  $j$  depends on only six coordinates rather than twelve implied by their dependence on  $\{i\}$  and  $\{j\}$  separately. The coordinates are

$r_{ij}$ , the distance between their centres

$\alpha(r_{ij} \rightarrow i) - \alpha(r_{ij} \rightarrow j)$

$\beta(r_{ij} \rightarrow i)$

$\beta(r_{ij} \rightarrow j)$

$\gamma(r_{ij} \rightarrow i)$

$\gamma(r_{ij} \rightarrow j)$

Such functions of the coordinates of two molecules which depend on six coordinates are called invariant pairwise functions, since they do not change if the pair of molecules are translated or rotated as a whole. Hence it is applied to assemblies of molecules in the absence of external field.

Fourier transform of such functions is done in two steps.

(i) In the first step dependence on rotational coordinates is eliminated.

(ii) In the second step, dependence on the distance  $r_{12}$  is eliminated.

experimentally measured dielectric constant values (9). The expression of the retarded dispersion energies given by Casimir and Polder (14) are similar in appearance to London's formulae for atoms (Eq. (3) above) given above, but have a  $r^{-7}$  dependence on distance

$$G = - \frac{23\hbar c}{4\pi r^7} \alpha_{1e}(0) \alpha_{2e}(0) \quad \text{for } \omega_e \gg c/r \quad (5)$$

$\alpha_{1e}(0)$  is the polarizability of particle 1 due to electronic displacements only. The distance at which the onset of retardation becomes significant depends on  $\omega_e$ . Since a particle may have appreciable spontaneous fluctuations at a variety of frequencies, it follows that for each frequency there is a nonretarded and a retarded range of distances for the dispersion force and that the larger the frequency the shorter is the distance at which one range passes into the other. Because of the  $1/r^6$  dependence of the non-retarded term and the  $1/r^7$  dependence of the retarded terms, the distance dependence of Vander Waals energy is complicated. When two small isotropic particles are immersed in a medium, rather than a vacuum, the retarded energy is given by (12,13)

$$G = - 23\hbar c \alpha_1^*(0) \alpha_2^*(0) / 4\pi \epsilon_s^{5/2} r^7 \quad (6)$$

In the expressions of free energy of interaction in the presence of a dielectric medium, we notice that the intensity of the electric field of the radiation is lowered by  $1/\epsilon_s$  and since both

(ii) Invariant Pairwise Function

$f_{12} \rightarrow$  An invariant pairwise function. This is independent of  $\vec{r}_1$  at fixed  $\vec{r}_{12}$  (i.e. this is a function of  $\vec{r}_{12}$ )

$$\begin{aligned}
 \tilde{f}_{12} &= \int \Psi_{\langle 1 \rangle} (\{1\}) f_{12} \Psi_{\langle 2 \rangle}^* (\{2\}) d\{1\} d\{2\} \\
 &= \int_{\text{cube}} \left( \frac{2l_1+1}{8\pi^2} \right)^{1/2} \exp(i\vec{e}_1 \cdot \vec{r}_1) D_{m_1 n_1}^{l_1} (L \rightarrow 1) f_{12} \left( \frac{2l_2+1}{8\pi^2} \right)^{1/2} \exp(-i\vec{e}_2 \cdot \vec{r}_2) \\
 &\quad \times D_{m_2 n_2}^{l_2*} (L \rightarrow 2) d(L \rightarrow 1) d(l \rightarrow 2) d\vec{r} \\
 &= \frac{\{(2l_1+1)(2l_2+1)\}^{1/2}}{8\pi^2} \int_{\text{cube}} f_{12} \exp(-i\vec{e} \cdot (\vec{r}_2 - \vec{r}_1)) D_{m_1 n_1}^{l_1} (L \rightarrow 1) D_{m_2 n_2}^{l_2*} (L \rightarrow 2) \\
 &\quad \times d(L \rightarrow 1) d(L \rightarrow 2) d\vec{r} \\
 &= \frac{\{(2l_1+1)(2l_2+1)\}^{1/2}}{8\pi^2} \int_{\text{cube}} f_{12} \exp(-i\vec{e} \cdot \vec{r}) D_{m_1 n_1}^{l_1} (L \rightarrow 1) D_{m_2 n_2}^{l_2*} (L \rightarrow 2) d(L \rightarrow 1) \\
 &\quad d(L \rightarrow 2) d\vec{r} \tag{43}
 \end{aligned}$$

when  $\vec{e} = \vec{e}_1 = \vec{e}_2$ ,  $\vec{r} = \vec{r}_2 - \vec{r}_1$

If we use the expression for  $f_{12}$  in terms of  $\tilde{f}_{12}$  from equation (25) with the S coordinate system to coincide with the L coordinate system, then

$$\begin{aligned}
 f_{12} &= \sum_{\substack{l_1 l_2 l \\ m_1 m_2 r \\ n_1 n_2 n}} \tilde{f}_{12} \begin{pmatrix} l_1 & l_2 & l \\ m_1 & m_2 & r \end{pmatrix} (-)^{n_1} \begin{bmatrix} l_1 & l_2 & l \\ -n_1 & n_2 & n \end{bmatrix} D_{m_1 n_1}^{l_1*} (L \rightarrow 1) D_{m_2 n_2}^{l_2} (L \rightarrow 2) \\
 &\quad \times D_{on}^l (L \rightarrow r) \tag{44}
 \end{aligned}$$

The function  $\exp(i\vec{e} \cdot \vec{r})$  is expanded in the following way

$$\exp(i\vec{e} \cdot \vec{r}) = \sum_l (-i)^l [(2l+1)] j_l(rt) D_{00}^l (r \rightarrow t) \tag{45}$$

$$\bar{q}_{XY}(f) = \bar{f}_{XY} + \sum_{\nu \geq 1} c' \nu \bar{p}_{XY}(\nu f) \quad (62)$$

and its full transform

$$\tilde{q}_{XY}(f) = \tilde{f}_{XY} + \sum_{\nu \geq 1} c' \nu \tilde{p}_{XY}(\nu f) \quad (63)$$

#### MAYER'S Rearrangement

The cluster function  $\gamma(\{i\}, \{j\})$ , is defined as

$$\gamma(\{i\}, \{j\}) = \exp \left[ -\beta u(\{i\}, \{j\}) \right] - 1 \quad (64)$$

and is a pairwise invariant function.

The graphs occurring in the expansion of potential of average force described in the definition of  $S(X, Y, :n)$  contains chains and rings of  $\gamma$ -bonds and they can be integrated the same way as above if the mathematical operations leading to find the transform of  $\gamma$ -bond can be carried out successfully. This is possible if the expansion of  $\gamma$  given in equation (26) can be terminated after finite number of terms without any error. However, the long range nature of the angle dependent force makes it possible to sum over infinite set of graphs. This is done by following Mayer's procedure which applies cluster theory to ionic solution. The only difference is that here the convolution theorem for angle dependent forces is used instead of that for central forces.

Here the pairwise potential is divided into two parts:

- (i) One is the potential at long range. This is denoted as  $u_{12}^C$  and is the potential of interaction of the two nonoverlapping charge distribution having the same net charge, dipole and quadrupole moment as molecule 1 and 2. This is defined in such a way that  $u_{12}^C$  vanishes for  $r_{12} < a_{12}$ , where  $a_{12}$  is the cutoff distance where the two charge

the transmitted and reflected waves are affected; a factor of  $1/\epsilon_s^2(i\omega_n)$  appears in Eq. (4). Also, the polarizability now carries an asterisk.  $\alpha^*$  is an excess polarizability of the particle over that of the medium.  $\alpha^*$  can be zero or can have either sign. Whereas for atoms in vacuum  $\alpha$  is the polarizability of the particle alone (the polarizability of vacuum is zero), the  $\alpha^*$  that appears in Eq. (4) and (6) depend on the polarizability of the solvent also.  $\alpha^*$  for the same particle is different in different solvent media. The retarded energy sets in at shorter distances, since light is slowed down by the medium by a factor  $\sqrt{\epsilon_3}$ .

For a small isotropic particle interacting with a single interface from which it is separated by a medium 3, the nonretarded free energy is given by (15,16)

$$G = - \frac{kT}{2r^3} \sum_{n=0}^{\infty} ' \alpha_1^* (i\omega_n) \Delta_{23}/\epsilon_3 (i\omega_n) \quad (7)$$

where

$$\Delta_{23} = \frac{\epsilon_2(i\omega_n) - \epsilon_3(i\omega_n)}{\epsilon_2(i\omega_n) + \epsilon_3(i\omega_n)}$$

Prime has the same meaning as in Eq. (2) and  $r$  is the distance between the particle and the interface. This expression, which applies to a body with small dimensions compared with  $r$ , contains a term with  $n=0$  that is very small for nonpolar molecules and for polar molecules depends on the permanent dipole moment

primarily. Terms with  $n > 0$  give the dispersion energy since they are the terms that arise from  $\omega_n \neq 0$ , that is from fluctuations. The application of the formula requires a determination of  $\alpha_1^*$ , the excess permeability of the particle in the medium. For small spherical particles, for example large macromolecules, macromolecular assemblies viz. cells, organelles, membrane vesicles, which can be approximated as a continuous medium of permeability  $\epsilon_1$ , expressions for  $\alpha_1^*$  have been derived (17) and lead to the following formula for the nonretarded energies of interaction with an interface (R is the radius of the particle)

$$G = - \frac{\hbar R^3}{4\pi r^3} \int_0^\infty \frac{\epsilon_1 - \epsilon_3}{\epsilon_1 + 2\epsilon_3} \times \frac{\epsilon_2 - \epsilon_3}{\epsilon_2 + \epsilon_3} d\omega \quad (8)$$

for particle 1 in medium 3 and

$$G = - \frac{\hbar R^3}{4\pi r^3} \int_0^\infty \frac{\epsilon_1 - \epsilon_2}{\epsilon_1 + 2\epsilon_2} \times \frac{\epsilon_3 - \epsilon_2}{\epsilon_3 + \epsilon_2} d\omega \quad (9)$$

for particle 1 in medium 2. In these formulas  $\epsilon_n = \epsilon_n(i\omega)$ . Since,  $F(r) = -\partial G/\partial r$ , the particle is attracted to the interface if the integral in equation (8) is positive at a certain distance. If  $\epsilon_2 = \epsilon_3$ , the interaction disappears, obviously because the interface disappears. The particle is then an isolated particle in an infinite homogeneous medium. The interaction disappears if  $\epsilon_1 = \epsilon_3$ . The interaction arises because of polarization and only at the interface, differential



The values of  $\tilde{h}_{1_1 1_2}(t, n)$  are evaluated according to eqn.(76) and are given in the Appendix.

Calculation of  $\tilde{q}_{XY}(t)$  needs calculation of the matrix elements of the matrix  $H (I - C_+ M_+ H - C_- M_- H - C_m M_m H)^{-1}$

$$\begin{aligned} C_+ M_+ H &= C_+ \begin{bmatrix} q_+^2 & 0 \\ 0 & 0 \end{bmatrix} \begin{bmatrix} \tilde{h}_{00} & \tilde{h}_{01} \\ \tilde{h}_{10} & \tilde{h}_{11} \end{bmatrix} \\ &= \begin{bmatrix} C_+ q_+^2 \tilde{h}_{00} & C_+ q_+^2 \tilde{h}_{01} \\ 0 & 0 \end{bmatrix} \end{aligned} \quad (94)$$

$$\begin{aligned} C_- M_- H &= C_- \begin{bmatrix} q_-^2 & 0 \\ 0 & 0 \end{bmatrix} \begin{bmatrix} \tilde{h}_{00} & \tilde{h}_{01} \\ \tilde{h}_{10} & \tilde{h}_{11} \end{bmatrix} \\ &= \begin{bmatrix} C_- q_-^2 \tilde{h}_{00} & C_- q_-^2 \tilde{h}_{01} \\ 0 & 0 \end{bmatrix} \end{aligned} \quad (95)$$

$$\begin{aligned} C_m M_m H &= C_m \begin{bmatrix} q_m^2 & 0 \\ 0 & \mu_m^2 \end{bmatrix} \begin{bmatrix} \tilde{h}_{00} & \tilde{h}_{01} \\ \tilde{h}_{10} & \tilde{h}_{11} \end{bmatrix} \\ &= \begin{bmatrix} C_m q_m^2 \tilde{h}_{00} & C_m q_m^2 \tilde{h}_{01} \\ C_m \mu_m^2 \tilde{h}_{10} & C_m \mu_m^2 \tilde{h}_{11} \end{bmatrix} \end{aligned} \quad (96)$$

$$(I - C_+ M_+ H - C_- M_- H - C_m M_m H)$$

$$= \left[ \begin{array}{c|c} (1 - C_+ q_+^2 \tilde{h}_{00} - C_- q_-^2 \tilde{h}_{00} - C_m q_m^2 \tilde{h}_{00}) & (-C_+ q_+^2 \tilde{h}_{01} - C_- q_-^2 \tilde{h}_{01} - C_m q_m^2 \tilde{h}_{01}) \\ \hline -C_m \mu_m^2 \tilde{h}_{10} & 1 - C_m \mu_m^2 \tilde{h}_{11} \end{array} \right]$$

$$= \frac{i \times 3\sqrt{3}}{16\pi^4} \times \left(-\frac{1}{\sqrt{3}}\right) \times q_+ \mu_m \int_0^\infty P_{21} (n=0) j_1 (r_{m+}t) t^2 dt$$

$$= -\frac{3i}{16\pi^4} \times q_+ \mu_m \int_0^\infty i P \left( \frac{\sin (r_{m+}t)}{r_{m+}^2 t^2} - \frac{\cos (r_{m+}t)}{r_{m+}t} \right) t^2 dt$$

$$= \frac{3}{16\pi^4} \times q_+ \mu_m \left[ \frac{1}{r_{m+}^2} \int_0^\infty P \sin(r_{m+}t) dt - \frac{1}{r_{m+}} \int_0^\infty P t \cos(r_{m+}t) dt \right]$$

$$\bar{q}_{m-} \begin{pmatrix} 1 & 0 & 1 \\ 0 & 0 & r_{m-} \end{pmatrix}$$

$$= \frac{3}{16\pi^4} \times q_- \mu_m \left[ \frac{1}{r_{m-}^2} \int_0^\infty P \sin(r_{m-}t) dt - \frac{1}{r_{m-}} \int_0^\infty P \cos(r_{m-}t) dt \right]$$

$$\bar{q}_{mm} \begin{pmatrix} 0 & 0 & 0 \\ 0 & 0 & r_{mm} \end{pmatrix}$$

$$= \frac{1}{16\pi^4} \times (i)^0 \times (-)^0 \times \begin{bmatrix} 0 & 0 & 0 \\ 0 & 0 & 0 \end{bmatrix}_{3j} \int_0^\infty \tilde{q}_{mm} \begin{pmatrix} 0 & 0 & t \\ 0 & 0 & 0 \end{pmatrix} j_0(r_{mm}t) t^2 dt$$

$$= \frac{1}{16\pi^4} \times \frac{q_{mm}^2}{r_{mm}} \int_0^\infty P_{11} (n=0) t \sin (r_{mm}t) dt$$

$$\bar{q}_{mm} \begin{pmatrix} 0 & 1 & 1 \\ 0 & 0 & r_{mm} \end{pmatrix}$$

$$= \frac{1}{16\pi^4} \times (i) \times 3\sqrt{3} \times (-)^0 \times \begin{bmatrix} 0 & 1 & 1 \\ 0 & 0 & 0 \end{bmatrix}_{3j} \int_0^\infty \tilde{q}_{mm} \begin{pmatrix} 0 & 1 & t \\ 0 & 0 & r_{mm} \end{pmatrix} j_1(r_{m+}t) t^2 dt$$

$$= \frac{3\sqrt{3} i}{16\pi^4} \times \left(-\frac{1}{\sqrt{3}}\right) \times q_m \mu_m \int P_{12} (n=0) j_1 (r_{mm}t) t^2 dt$$

$$= -\frac{3 i}{16\pi^4} \times q_m \mu_m \int_0^\infty (-i) P \left( \frac{\sin (r_{mm}t)}{r_{mm}^2 t^2} - \frac{\cos (r_{mm}t)}{r_{mm}t} \right) t^2 dt$$

polarization leads to accumulation of net charge, because of uncancelled induced electric moments. Silver in a highly readable account of forces in membrane systems given in his book (2), calls the disappearance of interaction with  $\epsilon_1 = \epsilon_3$  as the dielectric analog of Archimedes Principle, the disappearance of force of buoyancy on a particle immersed in a medium having the same specific gravity as that of the medium. It is interesting that if the particle with  $\epsilon_1 = \epsilon_3$  is placed in the medium with dielectric permittivity  $\epsilon_2$ , the particle-interface force is not zero, even though, as noted above it is zero if it is in medium with dielectric permittivity  $\epsilon_3$ . There is no unique particle-interface interaction. It depends on which side of the interface the particle is located. Also, for,  $\epsilon_1 > \epsilon_3 > \epsilon_2$  over the whole range of frequency,  $G$  of Eq. (8) is negative and that of Eq. (9) is positive. This means that a particle originally placed in medium 2 will be attracted toward the interface and if its momentum carries it through to medium 3, it will be repelled from the interface. We thus can have repulsive Vander Waals force, in addition to the more well known Vander Waals attractive force. It all depends on the relative magnitudes of dielectric permittivity of the particles (and/or interfaces) and the medium over the whole range of frequency. The inequality conditions on the values of relative permittivity given above need not hold over the whole range of frequency. These are written in this way, only for purposes of convenience of expression. The important

is zero, but we have not done so. Integrals in Eq. 114(a) and (b) yield  $\delta$ -functions at  $r=0$  because  $P_{22}(n=1,-1)$  spread indefinitely along the  $t$ -axis as  $a \rightarrow 0$ . All other integrals do not contribute for identical reasons.

Once we get  $\bar{q}$ , we use eqn. (26) to calculate  $q$ . Below we give the expressions for  $q$ .

$$q_{++} = \bar{q}_{++} \begin{pmatrix} 0 & 0 & 0 \\ 0 & 0 & r_{++} \end{pmatrix} \begin{bmatrix} 0 & 0 & 0 \\ 0 & 0 & 0 \end{bmatrix}_{3j} (-)^0 D_{00}^{0*}(r_{++} \rightarrow +) D_{00}^0(r_{++} \rightarrow +) \\ = \bar{q}_{++} \begin{pmatrix} 0 & 0 & 0 \\ 0 & 0 & r_{++} \end{pmatrix}$$

$$q_{+-} = \bar{q}_{+-} \begin{pmatrix} 0 & 0 & 0 \\ 0 & 0 & r_{+-} \end{pmatrix} \begin{bmatrix} 0 & 0 & 0 \\ 0 & 0 & 0 \end{bmatrix}_{3j} (-)^0 D_{00}^{0*}(r_{+-} \rightarrow +) D_{00}^0(r_{+-} \rightarrow -) \\ = \bar{q}_{+-} \begin{pmatrix} 0 & 0 & 0 \\ 0 & 0 & r_{+-} \end{pmatrix}$$

$$q_{+m} = \bar{q}_{+m} \begin{pmatrix} 0 & 0 & 0 \\ 0 & 0 & r_{+m} \end{pmatrix} \begin{bmatrix} 0 & 0 & 0 \\ 0 & 0 & 0 \end{bmatrix}_{3j} (-)^0 D_{00}^{0*}(r_{+m} \rightarrow +) D_{00}^0(r_{+m} \rightarrow m) \\ + \bar{q}_{+-} \begin{pmatrix} 0 & 1 & 1 \\ 0 & 0 & r_{+m} \end{pmatrix} \begin{bmatrix} 0 & 1 & 1 \\ 0 & 0 & 0 \end{bmatrix}_{3j} (-)^0 D_{00}^{0*}(r_{+m} \rightarrow +) D_{00}^1(r_{+m} \rightarrow m) \\ = \bar{q}_{+m} \begin{pmatrix} 0 & 0 & 0 \\ 0 & 0 & r_{+m} \end{pmatrix} - \frac{1}{\sqrt{3}} \bar{q}_{+-} \begin{pmatrix} 0 & 1 & 1 \\ 0 & 0 & r_{+m} \end{pmatrix} \cos \beta_1$$

$$q_{-+} = \bar{q}_{-+} \begin{pmatrix} 0 & 0 & 0 \\ 0 & 0 & r_{-+} \end{pmatrix} \begin{bmatrix} 0 & 0 & 0 \\ 0 & 0 & 0 \end{bmatrix}_{3j} (-)^0 D_{00}^{0*}(r_{-+} \rightarrow -) D_{00}^0(r_{-+} \rightarrow +) \\ = \bar{q}_{-+} \begin{pmatrix} 0 & 0 & 0 \\ 0 & 0 & r_{-+} \end{pmatrix}$$

$$q_{--} = \bar{q}_{--} \begin{pmatrix} 0 & 0 & 0 \\ 0 & 0 & r_{--} \end{pmatrix} \begin{bmatrix} 0 & 0 & 0 \\ 0 & 0 & 0 \end{bmatrix}_{3j} (-)^0 D_{00}^{0*}(r_{--} \rightarrow -) D_{00}^0(r_{--} \rightarrow -)$$

quantity is the value of the integral of Eqs.(8) or (9), which depend on relative values of permittivity over the whole range of frequency. Similar expressions exist for interaction between two planar membrane surfaces (18-20).

The interesting phenomenon mentioned above that the same particle senses different forces on two sides of an interface is known in simpler systems, viz. an ion interacting with an infinite planar membrane because of static polarization induced in the membrane dielectric by the charge. The effect of polarization is manifested as an induced charge at the interface. The field outside a polarized dielectric is equivalent to that due to surface charge  $(\vec{P} \cdot \vec{n})$  and volume charge  $(-\vec{\nabla} \cdot \vec{P})$ , where  $\vec{n}$  is the unit vector along the normal at the interface and  $\vec{P}$  is polarization density. Here the planar dielectric is polarized by the ion and the ion interacts with the surface charge at the interface  $(\vec{P} \cdot \vec{n})$  since  $\vec{\nabla} \cdot \vec{P} = 0$  in a homogeneous dielectric. This interaction is equivalent to that between the source charge and image charge on the other side of the dielectric. The magnitude of the image charge is (2)

$$Q_{\text{image}} = \frac{\epsilon_2 - \epsilon_3}{\epsilon_2 + \epsilon_3} Q,$$

where point charge  $Q$  is in a medium of dielectric permittivity  $\epsilon_3$  and that of the other side of the interface is  $\epsilon_2$ . If  $Q$  is positive  $Q_{\text{image}}$  is positive if  $\epsilon_2 > \epsilon_3$ , but it is negative if  $\epsilon_2 < \epsilon_3$ . The energy of interaction is repulsive if the ion is in

the aqueous phase and is attractive if it is in the membrane phase. We also come across this phenomenon in Chapter II. The similarity exists because both the image force and the Vander Waal's force owe their origin to polarization, the former considers the polarization due to static fields only.

Dispersive forces play an important role in structural organization of macromolecular assemblies. It has been shown that the interaction between rods tend to align themselves so that they are adjacent and parallel. This result has been used as the basis for one theoretic approach to the behaviour of the lipid chains in the liquid crystal state of hydrated bilayers (21).

In this thesis, we have not studied dispersive forces, but have studied (Chapter II) the effect of static polarization of macroionic dielectric by ions in solution. Our interest in polarization effects started with an original interest in dispersive forces, inspired by McLachlan's papers (12,13). The review given above is a reflection of this early interest in a subject, which is extremely important in Biophysical Chemistry, but has not yet received the attention it deserves.

#### **1.4 Measurement of Dispersive and Inductive Forces: Role of Theory**

The recent cell fusion experiments focus on the importance of measurement of dispersive and inductive forces. These forces are operative mostly at short distances and cell fusion also

we get the value of  $\phi_{13} * \phi_{31}$  as a function of  $r_{11}$ .

Other integrals in this section are evaluated in the same way.

(iii) The integrals given in (iii) are evaluated as follows :

$$\phi_{11} * \phi_{13} = \int \phi_{11}(\vec{r}_{11}) \phi_{13}(\vec{r}_{13}, \beta_3) d\{1\} d\Gamma_1$$

For each value of  $\beta_3$ , the integral is independent of  $\beta_3$  and is only dependent on  $\vec{r}_{13}$ . Hence it can be evaluated as the integrals in (i). This procedure is repeated for all the values of  $\beta_3$ . Thus the resulting function obtained on integration becomes a function of  $r_{11}$  and  $\beta_3$ . Multiplication by  $8\pi^2$  arises from integration over  $d\Gamma$ .

Other integrals in this section are evaluated in the same way.

(iv) The integrals given in (iv) are evaluated as follows :

$$\phi_{13} * \phi_{3,3''} = \int \phi_{13}(\vec{r}_{13}, \beta_3) \phi_{3,3''}(\vec{r}_{3,3''}, \beta_3, \beta_{3''}, \alpha_3, -\alpha_{3''}) d\{3'\} d\alpha_3, \sin\beta_3, d\beta_{3''} d\gamma_{3''}$$

$$= \int_0^{2\pi} d\gamma_3, \int_0^\infty \int_0^\pi \sin\beta_3, d\beta_3, d\{3'\} \phi_{13}(\vec{r}_{13}, \beta_3)$$

$$\times \int_0^{2\pi} \phi_{3,3''}(\vec{r}_{3,3''}, \beta_3, \beta_{3''}, \alpha_3, -\alpha_{3''}) d\alpha_3,$$

We have values of  $\phi_{3,3''}$  with  $\alpha_3, -\alpha_{3''}$  varying from  $-2\pi$  to  $+2\pi$

$$\int_0^{2\pi} \phi_{3,3''}(\vec{r}_{3,3''}, \beta_3, \beta_{3''}, \alpha_3, -\alpha_{3''}) d\alpha_3,$$

occurs only when particles come close. The cells or vesicles are usually charged. Thus electrostatic forces screened by electrolytes present in solution, dominate. Dispersive and inductive forces are difficult to measure directly in the presence of stronger electrostatic forces. In these systems, one therefore has to calculate (and not measure directly) dispersive and inductive forces. Direct measurements are possible only with neutral systems or with systems with low charge density. The measurement of hydration forces between charged bilayers by osmotic stress technique of Parsegian is also difficult (8). This is one of those situation where theory is useful because one is able to theoretically calculate a quantity (from experimental data of different kinds) which one cannot measure experimentally. The focus is therefore on the effect of dielectric permittivity (static and frequency dependent) of macromolecular particles in solution on observable properties. Macromolecules isolated from the solvent are not amenable to experimental investigation. Their dielectric permittivity must be obtained from the measurements on properties of suspensions. Since experimentally measured quantities are expressed in terms of correlation functions defined in Statistical Mechanics it is important to investigate the interactions that depend on dielectric permittivity of suspended particles. These interactions, through the already known theoretical framework will influence correlation functions.



$$= \int d\{3\} d\Gamma_3 q_{13} (xh)_{312} = (qxh)_{1312}$$

$$\begin{aligned} \int q_{13} x_{32} h_{22} d\{3\} d\Gamma_3 d\{2\} d\Gamma_2 &= \int d\{3\} d\Gamma_3 q_{13} \int x_{32} h_{22} d\{2\} d\Gamma_2 \\ &= \int d\{3\} d\Gamma_3 q_{13} (xh)_{322} = (qxh)_{1322} \end{aligned}$$

$(xh)_{312}$  ,  $(xh)_{322}$  are evaluated as  $\phi_{31} * \phi_{11}$  and  $(qxh)_{1312}$ ,  $(qxh)_{1322}$  are also evaluated as  $\phi_{13} * \phi_{31}$  in 4.3 above.

$$\begin{aligned} \int q_{13} x_{33, h_{3,2}} d\{3\} d\Gamma_3 d\{3'\} d\Gamma_3, &= \int d\{3\} d\Gamma_3 q_{13} \int x_{33, h_{3,2}} d\{3'\} d\Gamma_3, \\ &= \int d\{3\} d\Gamma_3 q_{13} (xh)_{33,2} = (qxh)_{133,2} \end{aligned}$$

$(xh)_{33,2}$  is evaluated the same way as  $\phi_{33} * \phi_{31}$  and  $(qxh)_{133,2}$  is evaluated the same way as  $\phi_{13} * \phi_{31}$  in 4.3 above.

(iii) Calculation of  $\tau_{13}$

$$\tau_{13} = \sum_{i=1}^3 x_{1i} * h_{i3} + \sum_{i=1}^3 q_{1i} * x_{i3} + \sum_{i,j=1}^3 q_{1i} * x_{ij} * h_{j3}$$

Consider the first term:

$$\begin{aligned} \sum_{i=1}^3 x_{1i} * h_{i3} &= c_1 \int x_{11} h_{13} d\{1\} d\Gamma_1 + c_2 \int x_{12} h_{23} d\{2\} d\Gamma_2 \\ &+ c_3 \int x_{13, h_{3,3}} d\{3'\} d\Gamma_3, \end{aligned}$$

The first two integrals are evaluated the same way as  $\phi_{11} * \phi_{13}$  and  $\int x_{13, h_{3,3}} d\{3'\} d\Gamma_3$ , is evaluated the same way as  $\phi_{13} * \phi_{33}$  in 4.3 above.

The second term

$$\sum_i q_{1i} * x_{i3} \text{ is evaluated as } \sum_i x_{1i} * h_{i3}$$

Finally consider the third term,

## 1.5 Particle Size, Polarization Effects, Dipolar Interaction

Size, shape, curvature and packing considerations in physical organization of membrane assemblies have been of considerable interest to physical chemists (22). The thermodynamics of small systems has been an interesting area of investigation (23). Fusion characteristics (24-27) and phase transition characteristics (28,29) of membrane vesicles are known to be dependent on size. Macromolecules, proteins, lipid vesicles, cellular particles and cells carry significant permanent dipole moment (30,31). There exists significant contributions from peptide units in proteins, oriented acyl chains in lipids, oriented water of hydration at the macromolecule-solvent interface, partially dissociated ionizable groups distributed on the surface. The magnitude of permanent dipole moment will in general increase with size. In addition, dipole moments can be induced by external electric field. The solution of the electrostatic problem of a dielectric particle suspended in a solvent of a different dielectric constant in the presence of an uniform electric field is derived in text books (32). The values of the polarizabilities depend on the size of the macroion as well as its dielectric permittivity. Thus external electric field turns on interactions that depend on size and on relative permittivity of the macromolecular particles. The ionic interactions in solution that polarizes the macroionic dielectric also turn on interactions that depend on the size and

$$= \int d\{1\} d\Gamma_1 q_{31} (xh)_{113}, = (qxh)_{3113},$$

$$\int q_{31} x_{12} h_{23}, d\{1\} d\Gamma_1 d\{2\} d\Gamma_2 = \int d\{1\} d\Gamma_1 q_{31} \int x_{12} h_{23}, d\{2\} d\Gamma_2$$

$$= \int d\{1\} d\Gamma_1 q_{31} (xh)_{123}, = (qxh)_{3123},$$

$$\int q_{32} x_{21} h_{13}, d\{2\} d\Gamma_2 d\{1\} d\Gamma_1 = \int d\{2\} d\Gamma_2 q_{32} \int x_{21} h_{13}, d\{1\} d\Gamma_1$$

$$= \int d\{2\} d\Gamma_2 q_{32} (xh)_{213}, = (qxh)_{3213},$$

$$\int q_{32} x_{22} h_{23}, d\{2\} d\Gamma_2 d\{2\} d\Gamma_2 = \int d\{2\} d\Gamma_2 q_{32} \int x_{22} h_{23}, d\{2\} d\Gamma_2$$

$$= \int d\{2\} d\Gamma_2 q_{32} (xh)_{223}, = (qxh)_{3223},$$

$(xh)_{113}, (xh)_{123}, (xh)_{213}, (xh)_{223},$  are evaluated the same way as  $\phi_{11} * \phi_{13}$  in 4.3 above.

$(qxh)_{3113}, (qxh)_{3123}, (qxh)_{3213}, (qxh)_{3223},$  are evaluated the same way as  $\phi_{31} * \phi_{13}$  in 4.3 above.

$$\int q_{31} x_{13''} h_{3''3}, d\{1\} d\Gamma_1 d\{3''\} d\Gamma_{3''} = \int d\{1\} d\Gamma_1 q_{31} \int x_{13''} h_{3''3}, d\{3''\} d\Gamma_{3''}$$

$$= \int d\{1\} d\Gamma_1 q_{31} (xh)_{13''3}, = (qxh)_{313''3},$$

$$\int q_{32} x_{23''} h_{3''3}, d\{2\} d\Gamma_2 d\{3''\} d\Gamma_{3''} = \int d\{2\} d\Gamma_2 q_{32} \int x_{23''} h_{3''3}, d\{3''\} d\Gamma_{3''}$$

dielectric permittivity of the particles. This is discussed in Chapter II. The effects of these interactions on correlation function are not linearly superposable. The interaction between permanent dipoles, ions and permanent dipoles, ions and induced dipoles, induced dipoles and induced dipoles through their interplay will determine the correlation function from which all measured properties can be calculated. The correlation function (static and time dependent) depends on permittivity (static and frequency dependent) of these particles. So, these permittivities become calculable. The dielectric constant of these suspensions over a range of frequency can be one of the experimentally measured quantities from which one may calculate dielectric permittivity of the particles. Friedman (33) has expressed static dielectric constant of solutions in terms of correlation functions. Light scattering and small angle neutron scattering has been used in conjunction with theories of correlation function to measure properties, in particular, the charge of micellar particles in suspensions. These are discussed later in this chapter. We have mentioned earlier that angle-dependent interactions can play an important role in molecular recognition at a distance larger than that at which valence forces operate and can determine trajectories of bimolecules that land them on specific sites.

$$= \left[ \frac{4\pi}{2\ell+1} \right]^{1/2} Y_{\ell m}^* (\beta, \alpha)$$

$$D_{0-m}^{\ell*} (\alpha, \beta, \gamma) = (-)^m D_{0m}^{\ell} (\alpha, \beta, \gamma)$$

$$= (-)^m (-)^m \left( \frac{4\pi}{2\ell+1} \right)^{1/2} Y_{\ell m} (\beta, \alpha)$$

$$= \left( \frac{4\pi}{2\ell+1} \right)^{1/2} Y_{\ell m} (\beta, \alpha)$$

$Y_{\ell, m}(\beta, \alpha)$  are spherical harmonics

$$D_{01}^1 (\alpha, \beta, \gamma) = - \left( \frac{4\pi}{3} \right)^{1/2} Y_{11} (\beta, \alpha)$$

$$= \frac{1}{\sqrt{2}} \sin\beta e^{i\alpha}$$

$$D_{01}^{1*} (\alpha, \beta, \gamma) = \frac{1}{\sqrt{2}} \sin\beta e^{-i\alpha}$$

$$D_{0-1}^1 (\alpha, \beta, \gamma) = \left( \frac{4\pi}{3} \right)^{1/2} Y_{11}^* (\beta, \alpha)$$

$$= - \frac{1}{\sqrt{2}} \sin\beta e^{-i\alpha}$$

$$D_{0-1}^{1*} (\alpha, \beta, \gamma) = - \frac{1}{\sqrt{2}} \sin\beta e^{i\alpha}$$

4. Integration of  $\int_0^\infty \frac{1}{t^2+k^2} \cos(rt) dt$  :

$$\left( \frac{1}{2\pi} \right)^{1/2} \int_{-\infty}^{\infty} e^{irt} F(t) dt = f(r)$$

## 1.6 Macromolecular Suspension as an Inhomogeneous Dielectric

A suspension of dielectric particles in a dielectric continuum can be viewed as an ionic solution or as an inhomogeneous but uniform mixtures of dielectrics. The principal aim of the theory of uniform dielectric mixtures is to calculate an effective dielectric permittivity ( $\epsilon_{\text{eff}}$ ), a quantity that can be defined as the ratio of the capacitance of a capacitor that contains the mixture in between the plates to that with no material contained in it (32). The  $\epsilon_{\text{eff}}$  of an uniform suspension of concentric spheres of different dielectric permittivity of the inner and the outer sphere, embedded in a dielectric continuum, has been calculated by Wagner, using Maxwell's method for calculating effective conductivity of the same system. The system is identical to suspension of membrane vesicles in aqueous medium. Rayleigh has discussed  $\epsilon_{\text{eff}}$  of simple cubic arrangement of dielectric spheres in a dielectric continuum (32). Lam has given an improved theory recently (34). Generalization of Rayleigh's theory to a disordered arrangement of identical dielectric spheres in a dielectric continuum has been given by Günther and Heinrich (35). There are recent papers on cluster theory of effective dielectric constant of a polarizable suspension (36,37), bounds on the values of effective dielectric constant (38,39), effective dielectric constant of a dispersion of spheres (40) and on dielectric constant of a suspension of spherical inclusion (41). Effect of double layers in

$$\begin{aligned}
S_1 &= \frac{1}{\sqrt{N}} \sum_{j=0}^{N/2} = \frac{1}{\sqrt{N}} \sum_{j'=0}^{N/2} f_{j'}, \exp(-(2\pi i j' k)/N) \\
&= \frac{1}{\sqrt{N}} f_0 + \frac{1}{\sqrt{N}} \sum_{j'=1}^{(N/2)} f_{j'}, \exp(-(2\pi i j' k)/N) \\
&= \frac{1}{\sqrt{N}} f_0 + \frac{1}{\sqrt{N}} f_{N/2} \exp(-\pi i k) + \frac{1}{\sqrt{N}} \sum_{j'=1}^{(N/2)-1} f_{j'}, \exp((-2\pi i j' k)/N)
\end{aligned}$$

$$S_2 = \frac{1}{\sqrt{N}} \sum_{j=(N/2)+1}^{N-1} = \frac{1}{\sqrt{N}} \sum_{j'=(N/2)+1}^{N-1} f_{j'}, \exp(-(2\pi i j' k)/N)$$

We note  $j' = N - j''$ , hence  $f_{j'} = f_{N-j''}$ ; also,  $f_{j'} = \pm f_{j''}$  (if  $j' = j''$ , symmetry or antisymmetry),

$$\begin{aligned}
\therefore S_2 &= \pm \frac{1}{\sqrt{N}} \sum_{j''=1}^{(N/2)-1} f_{j''} \exp(-(2\pi i (N-j'') k)/N) \\
&= \pm \frac{1}{\sqrt{N}} \sum_{j''=1}^{(N/2)-1} f_{j''} \exp(+ (2\pi i j'' k)/N)
\end{aligned}$$

(noting  $\exp(-2\pi i k) = 1$ , since  $k$  is an integer)

$$\begin{aligned}
\therefore S &= S_1 + S_2 = \frac{1}{\sqrt{N}} f_0 + \frac{1}{\sqrt{N}} f_{N/2} \exp(-\pi i k) \\
&\quad + \frac{1}{\sqrt{N}} \sum_{j'=1}^{(N/2)-1} f_{j'} \left\{ \exp((-2\pi i j' k)/N) \pm \exp(+2\pi i j' k/N) \right\} \\
&\quad \text{(combining terms } j' = j'')
\end{aligned}$$

$$= \frac{1}{\sqrt{N}} f_0 + \frac{1}{\sqrt{N}} f_{N/2} \exp(-\pi i k)$$

$$+ \frac{1}{\sqrt{N}} \sum_{j'=1}^{(N/2)-1} f_{j'} \left\{ 2 \cos((2\pi j' k)/N) \right\} \text{ if the set is symmetrized}$$

heterogeneous systems is given by Dukhin and Shilov (42). Attempts to calculate electrical properties of suspended particles from those of suspensions have been made (43). The theory has been admirably summarized by Scaife (32). These theories are developed for uncharged dielectrics and the solution does not contain ions. We were initially interested in these line of research, in relation to our problem, but did not eventually pursue them in this thesis.

Now, we discuss a macroionic solution as an ionic solution.

### 1.7 Integral Equation Theories:

The theory of ionic solution and that of electrical double layer has undergone significant change in the last three decades under the influence of the development of statistical mechanics of liquids, particularly the methods of computer simulation and integral equation theories (44-54). A development of the cluster theory of ionic solution leading to Allnatt's HNC integral equation for calculation of correlation function is given in Chapter III. Even though the integral equations viz. Hypernetted chain (HNC) and Percus Yevick (PY) equations were first derived from cluster theory they have been derived later by functional differentiation methods (46). The former derivation has difficult questions about range of validity, depending on convergence of series summation. They do not remain valid for dipoles at liquid densities. The latter derivation holds even at



#### 5.4 Features of the $g(r)$ versus $r$ Plots (Figs. 5.1-5.73)

The objective of a detailed study of  $g(r)$  vs.  $r$  graphs as a function of macroion size, charge density, macroion concentration and ionic strength is to be able to think of the macroion gas as an one-component interacting system. This is necessary for an easy intuitive access to their behaviour. Several attempts have been made to obtain expressions of  $v^{\text{eff}}(r)$  (6,21,22). An examination of these, particularly that of Belloni (22) shows a complicated nonmonotonic dependence on all parameters, size, charge density and concentration of macroion and background electrolyte. We also observe quite complicated affects and summarize qualitative features below:

##### Effect of Macroion Concentration and Ionic Strength:

(i)  $r_m = 300$ ,  $cdnst = 4800$  (Figs.5.1-5.6).

Consider  $r_m = 300$ ,  $cdnst = 4800$ ,  $c_m = 1 \times 10^{-6}$ ,  $c_- = 1 \times 10^{-5}$  (Fig. 5.2). This system gives a highly attractive  $g(r)$  at small  $d_r$ , which becomes weakly repulsive at  $d_r \sim 2.2$  and then slowly levels off to  $g(r) = 1$  at  $d_r \sim 3$ . In contrast, at  $c_m = 1 \times 10^{-7}$ ,  $g(r)$  is highly repulsive at all  $d_r$  upto 3.20, only to level off to  $g(r) = 1$  at  $d_r \sim 3.33$ , i.e.,  $r = 1000 \text{ \AA}^0$ . The range of interaction is roughly the same in the two cases ( $\sim 1000 \text{ \AA}^0$ ), but there is significant difference in features, the attractive region being totally absent at lower  $c_m$  and being predominant at higher  $c_m$ . When  $c_m$  is reduced to  $1 \times 10^{-8}$ ,  $g(r)$  is even more repulsive and stays near 0.0 over the whole range of  $r=0$  to  $1000 \text{ \AA}^0$  (this graph is not plotted). The trend shown in going from  $c_m = 1 \times 10^{-6}$  to  $1 \times 10^{-7}$  accentuates at  $c_m = 1 \times 10^{-8}$ . When  $c_-$  is raised to  $1 \times 10^{-4}$  (Fig.5.3) the qualitative nature of the dependence of

repulsion, a little more so compared to  $r_m = 200$  at large distances. The values of  $g$  at the maximum of  $r_m = 300$  system falls as  $c^-$  increases, otherwise the shapes remain unaltered. Figs. 5.61-5.63 share the parameters of 5.58 to 5.60 except that  $cdnst = 19200$ . At this lower charge density  $r_m = 200$  graph shows less repulsive correlation than  $r_m = 300$  at all  $r$  values. Effects of size at  $c_m = 1 \times 10^{-7}$  are shown in Figs. 5.64 to 5.67 at  $cdnst = 4800$ ,  $c^- = 0$  (Fig. 5.64),  $10^{-5}$  (Fig. 5.65),  $10^{-4}$  (Fig. 5.66).  $r_m = 200$  shows less repulsive feature compared to  $r_m = 300$  in all of the graphs. The repulsive correlation decrease and distinction between the two sizes increase as  $c^-$  increases. At  $c^- = 1 \times 10^{-3}$  (Fig. 5.67),  $r_m = 300$  shows a large attractive peak in sharp contrast to a predominantly repulsive correlation at  $r_m = 200$ . The distinction between the two sizes is very clear in this case. We note that  $g = 88$  is equivalent to  $w \approx -4.606$  kT. Similar trends are seen in Figs. 5.68 to 5.70, for which  $c_m = 1 \times 10^{-7}$ ,  $cdnst = 19200$ ,  $c^- = 0.0, 10^{-4}, 10^{-3}$ . At lower  $c^-$  values,  $r_m = 200$  shows less repulsive correlation than  $r_m = 300$  at lower values of  $c^-$  ( $0, 10^{-4}$ ) but at  $c^- = 10^{-3}$ ,  $r_m = 300$  shows attractive correlation at larger  $r$  and the graphs pushes itself above that of  $r_m = 200$ , which shows repulsive correlation at all  $r$ . Fig. 5.71 to Fig. 5.73 show macroionic size dependence at  $c_m = 1 \times 10^{-7}$ ,  $cdnst = 600$ ,  $c^- = 0, 10^{-4}, 10^{-3}$ .  $r_m = 300$  shows a graph with attractive correlation at hard sphere contact, which has a slightly repulsive dip before levelling off to  $g=1$ .  $r_m = 200$  graphs show weakly attractive peaks at  $c^- = 0, 10^{-4}$  (nearly equal, with small shift towards hard sphere contact at  $10^{-4}$  M) and a larger attractive peak, closer to hard sphere contact at  $c^-$

liquid densities and show the generality of the results obtained under more restrictive conditions. Powerful algorithms exist for solving the HNC equation (55-57). A slightly older review provides a systematic introduction to numerical methods of integral equation solving (58). Comparison of different methods is given in a recent paper (59). These methods directly solve the integral equation and does not require the cluster theoretic development or the  $g$  bond sums (introduced in Chapter III), and converge without much problem at liquid densities, virtually independent of the guess value. The problem of long range of coulombic interaction is handled in cluster theory by summation of diagram to obtain screened potentials of shorter range. The problem of long range of potential is handled numerically in the methods that do not use diagram summation techniques (55-57). Of the various integral equations, HNC equation has been most successful in the treatment of ionic solutions. The Mean Spherical Approximation (MSA), though not as successful as HNC theory can be analytically solved and for this reason has received significant attention, HNC calculations on 1:1 electrolytes have been highly successful (60-65). Problems with numerical methods arise for weakly screened ionic systems, i.e., at low ionic strengths, but these problems have been solved (70). The calculated distribution function perhaps underestimates repulsion between like charges at short distances, and overestimates the number of ion pairs with same charge (71,72). It

has been pointed out that this overestimate arises from the approximations inherent in HNC theory, i.e., neglect of some highly connected diagrams in the cluster expansion (71,73). These diagrams called the bridge diagrams were ignored only because of the difficulty in calculating them. Recent developments make it possible to incorporate them (74,75) and the modified theory is called RHNC or MHNC theory. Incorporation of these diagrams should introduce additional short range repulsion. This aspect is discussed in greater detail later. Some attempts have been made to incorporate these diagrams in calculation of macromolecular systems (71,76). They suggest that indeed, short range repulsive forces enter and the problem of overestimate of like charge pairs at short distances disappears. There are also reports where the theory has not been very successful (77,78) in interpreting properties, e.g. in calculating X-ray scattering functions for models of aqueous  $\text{Ph}_4\text{AsCl}$  which fit the osmotic coefficient data.

### 1.8 Highly Asymmetrical Electrolytes: Polarizable Ions

Macroionic solutions are different from solutions of symmetrical electrolytes of ions of comparable and small size and charge (viz.  $\text{NaCl}$  or  $\text{CaSO}_4$ ) on two counts. Firstly, there is a huge asymmetry in charge and in size between the macroion and the small ion. This asymmetry has made the techniques of computer simulation of polyelectrolytes difficult and

difference. The graph in this case calculates an average of  $g$  over all angles to obtain  $g$  as a function of  $r$  only. This system could not be studied further because of long computer time needed. That is why only one iteration was done only to check that the programme works. Detailed study is now being undertaken.

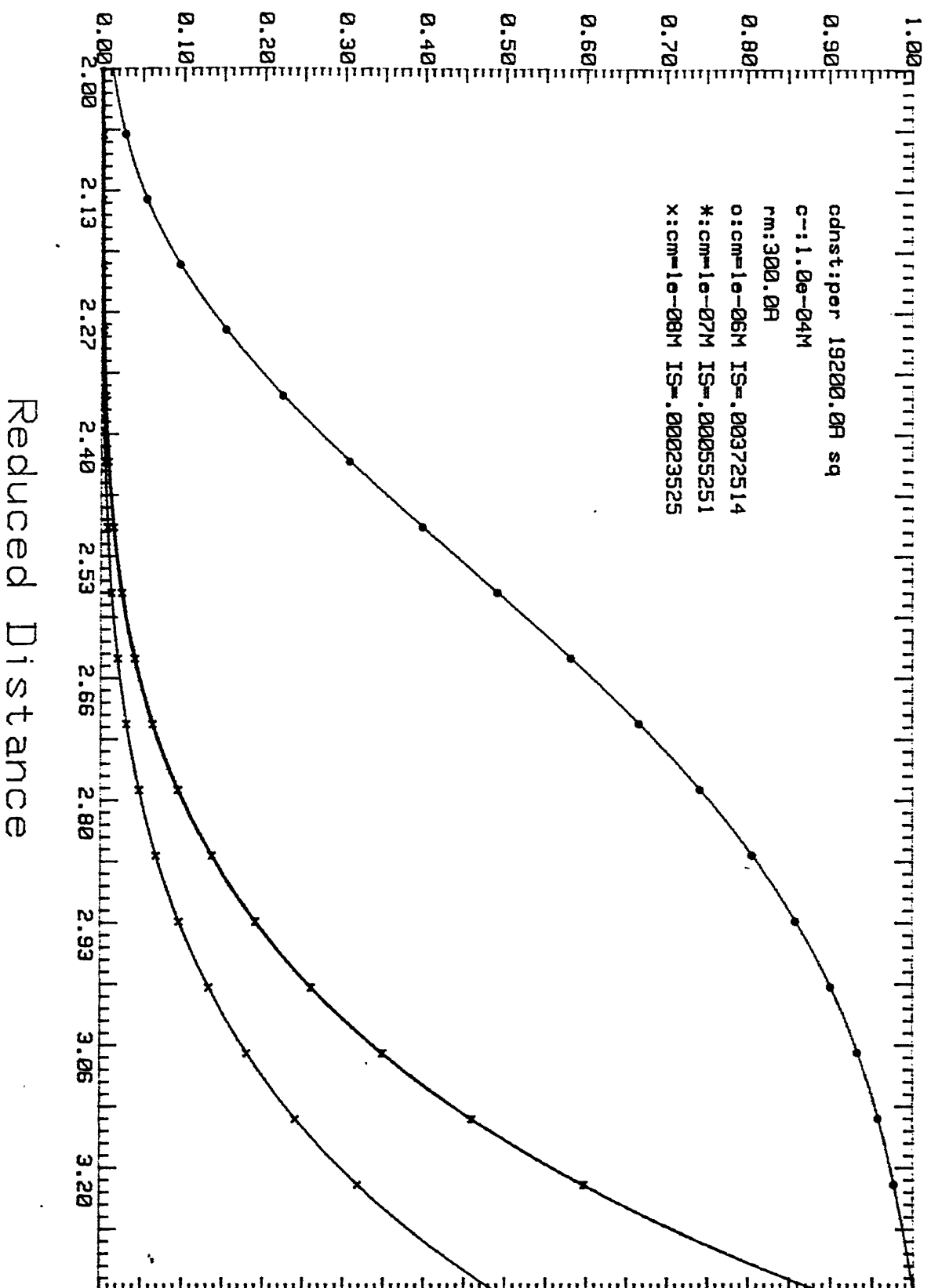
error-prones. The theoretical techniques e.g. integral equation methods, also require considerable development beyond those used for symmetrical electrolytes, to handle these highly asymmetric system. We discuss these problems later in this chapter. Secondly macroions produce a dielectric heterogeneity of a significant size in solution. A sphere of several hundred Angström radius of dielectric permittivity of 2-30 (30) suspended in a dielectric continuum of relative permittivity of 80 has significant polarizability. Ions in solution produce electric fields that induce multipole moments in the macroion. This effect has been considered in developing theory of electrolytes near a planar dielectric wall. The recent papers related to this effect are summarized in Section 1 of Chapter II.

### 1.9 Effect of Long Range Correlation in Charged Micelles

Due to repulsive Coulombic interaction, charged macromolecules exhibit long range order considerably greater than particle diameter. For sufficiently long range interactions, solid-like structures can be formed, where each particle is constrained by interparticle forces to a particular lattice site. Such structures have been observed with Tipula Iridescent virus (79) and certain polymer colloids (80-81). More recently Schaefer and Berne (82) using photon correlation spectroscopy studied a solution of R-17 virus at low ionic strength. When these data are normalized with respect to those at

# Correlation Function Vs. Distance F-5.9

Macro Ion-Macro Ion Correlation;  $g(r)$

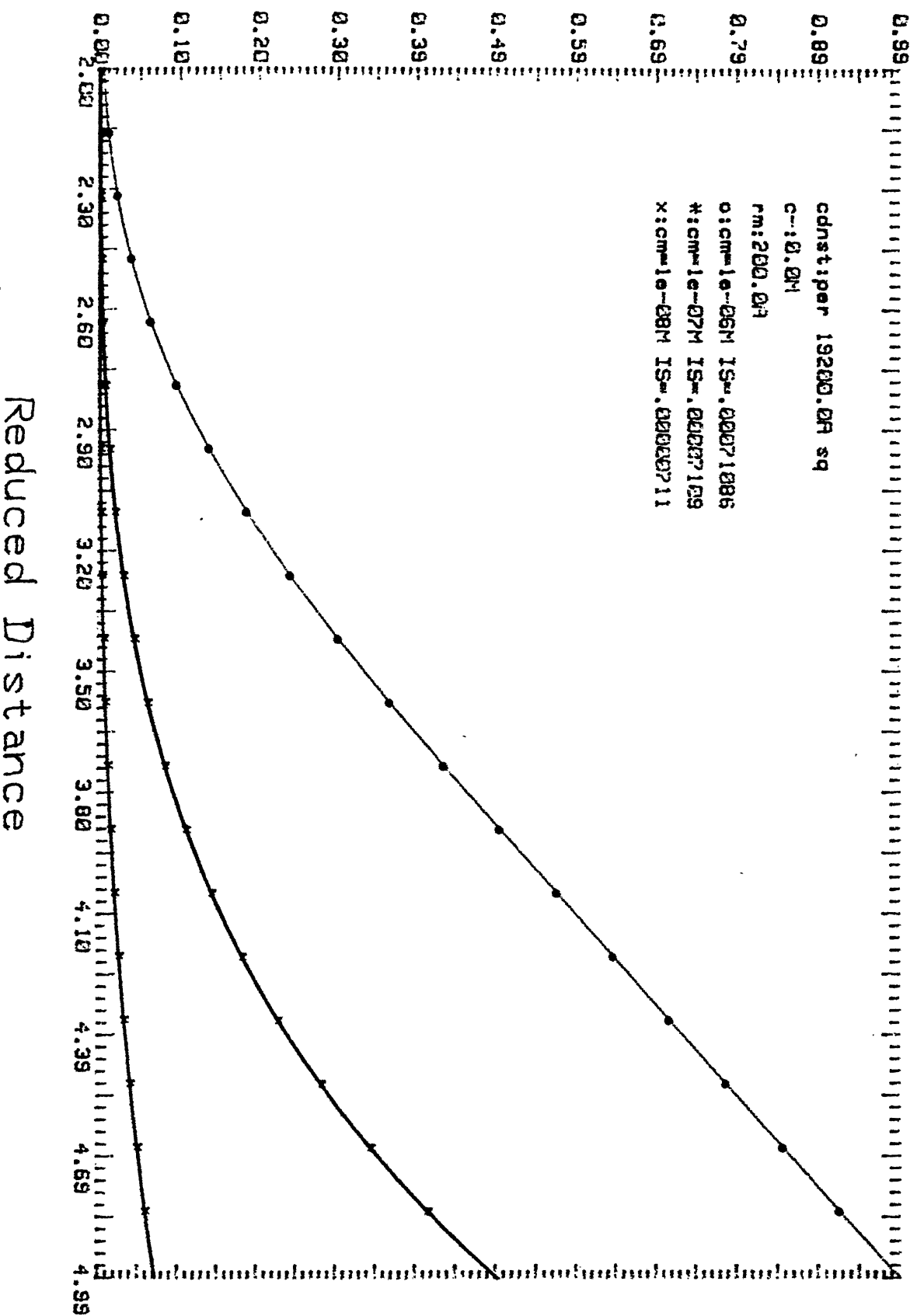


high ionic strength, where the charge is shielded, they find that the scattered intensity and the decay rate of field correlation function show a strong dependence on angle, indicating incipient translational ordering. The range of interparticle interaction is about half of the mean interparticle distance. Schaefer and Ackerson (83) study using inelastic light scattering a suspension of polystyrene particles so highly charged that the repulsive forces between the particles lead to a transition between liquid-like to solid-like structures. The system displays features analogous to melting of atomic crystals, but it is unique in that the structure results from repulsive forces and the interparticle spacing is such that the structure can be probed by visible light sources. They confirm the earlier observation of Williams and Crandell (84) that the suspension is ordered into a cubic lattice structure. The inelastic light scattering studies give information about particle motion near the freezing transition. Clark et al (85) developed methods for growing colloid crystals and point out that they offer unique opportunity for the study of the collective static and dynamic behaviour of strongly interacting spherical particles whose structure is well defined, rather than statistically defined structures of atomic solids and liquids. The distinct theoretical and experimental advantages of studying them over atomic solids and liquids for testing theoretical models is given. Williams (84) measure the melting temperatures of

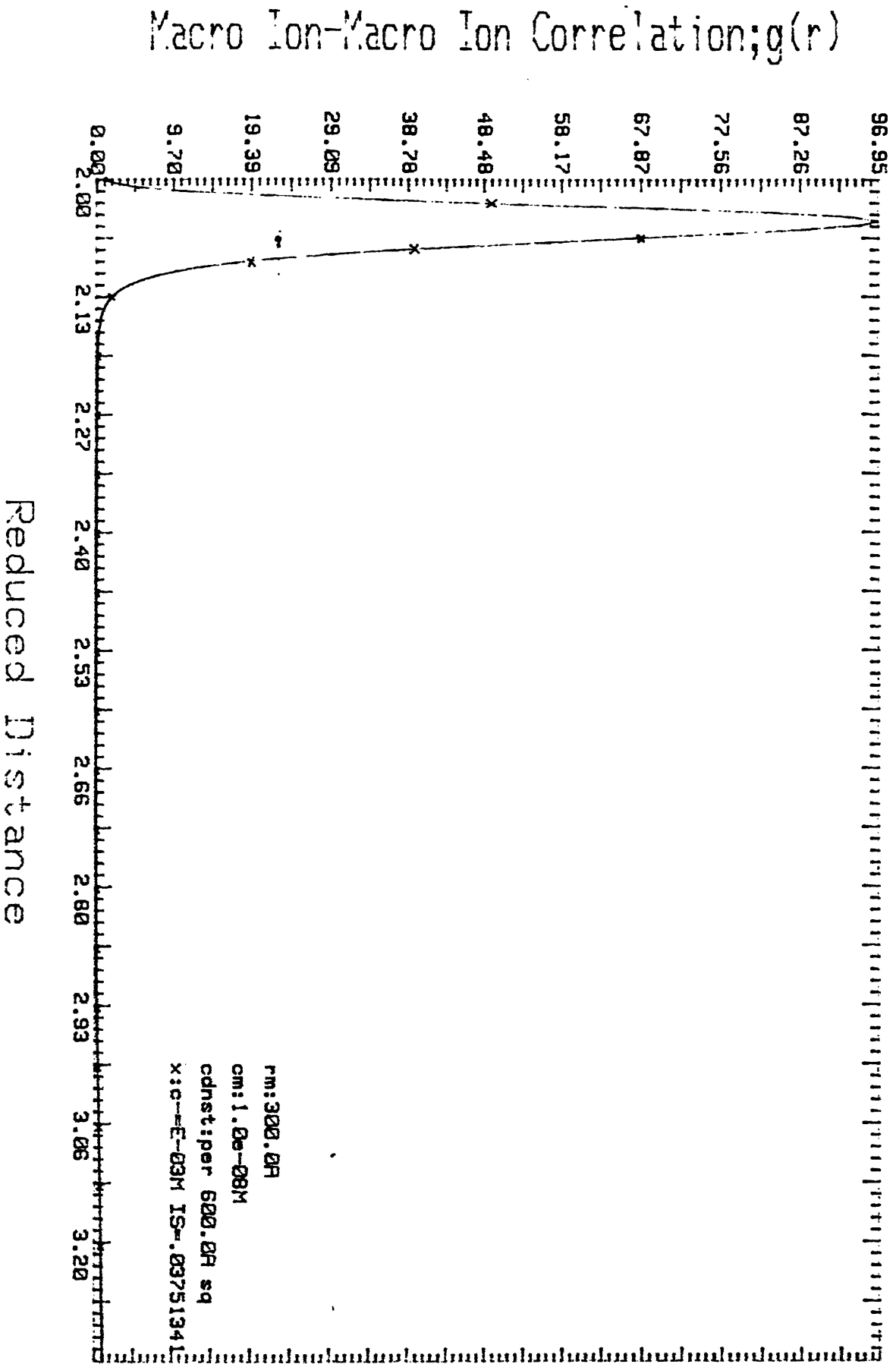


# Correlation Function Vs. Distance

F-5.1



# Correlation Function Vs. Distance F-5.29



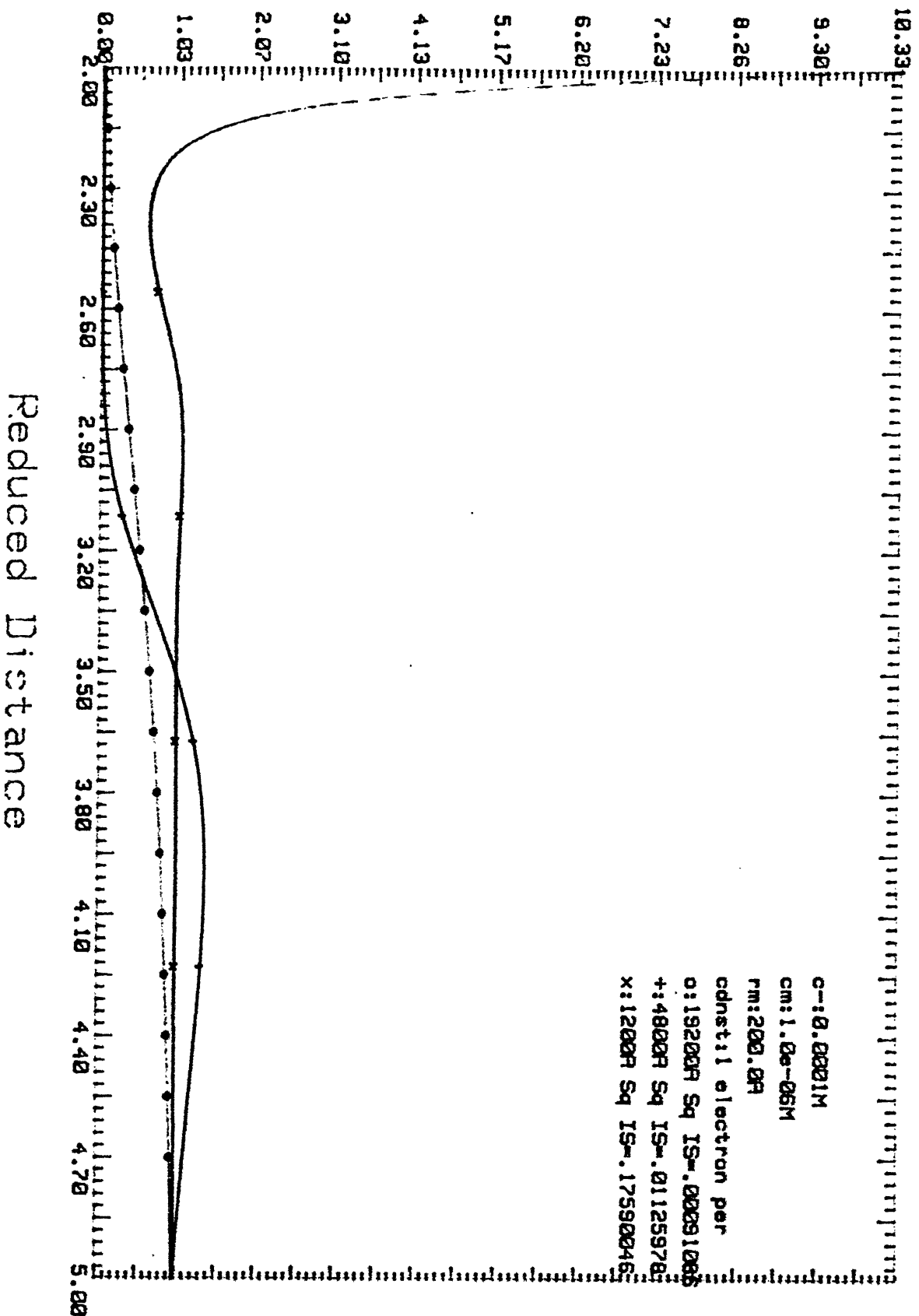
crystallized suspensions of polystyrene spheres as a function of concentration. In a colloidal crystal, interaction between charged colloidal particles with sufficient strength to cause crystallization is describable by Debye-Hückel theory but with a renormalized charge, which is a parameter of the theory. The relation between renormalized charge and actual charge is obtained by solving Poisson-Boltzmann equation, numerically in Wigner-Seitz cell (86). This relationship is not yet fully understood for colloidal suspensions. Lindsay and Chaiken (87) report the phenomenon of glass transition in these systems. Recent reviews of interest are by Pieranski (88) and Pusey (89). Clark and Ackerson (90, 91) report experimental results on the coupling of concentration fluctuations to steady state shear flow in a colloidal system of strongly coupled charged plastic spheres.

When interparticle interaction is weak, long range order is destroyed but considerable short range order persists to give a liquid like structure. Various biological materials which show such effects have been studied by X-ray scattering (92-94) and light scattering (95). Aqueous dispersion of AgI particles at low ionic strength show a definite maximum in measurements of scattered light intensity as a function of scattering angle. These maxima indicate a well defined first co-ordination shell of particles of AgI at a distance of at least 10 particle diameters. Brown (96) use conventional light scattering and photon

correlation spectroscopy of aqueous dispersions of charged spherical polystyrene particles (radius  $\sim 250 \text{ \AA}$ ) at low ionic strength. A first and sometimes a second diffraction maxima are found. Considerable liquid like structure is maintained at a distance of  $\sim 10^4 \text{ \AA}$ , about 20 times the diameter. Schaefer (97) studied dilute suspensions of polystyrene spheres (radius  $436 \text{ \AA}$ ) by light scattering to obtain similar results. Apart from light scattering, small angle neutron scattering has also been used in studying micelles, a subclass of macroions. The experiments show that long-range interparticle interaction plays a dominant role in determining the equilibrium properties of these systems (98-102). The intensity of radiation scattered from micellar solution may be written as  $I(Q) = P(Q) S(Q)$ , where  $S(Q)$  is the intermicellar structure factor describing intermicellar correlation and  $P(Q)$  is the intramicellar structure factor where  $Q$  is the Bragg number. Methods of obtaining  $P(Q)$  in protein solutions and micellar solution, experimentally and assuming models is discussed by Bendedouch et al (100).  $S(Q)$  can be calculated from statistical mechanical theory, given the interaction potential between macroions. It has been possible to obtain and fit scattering data with only two variable parameters of a simple theory (discussed below), the micellar aggregation number and the effective charge of the micelle (98-102). The development of methods for calculation of correlation function in macromolecular systems is thus necessary for extracting molecular

# Correlation Function Vs. Distance F-5.39

Macro Ion-Macro Ion Correlation;g(r)



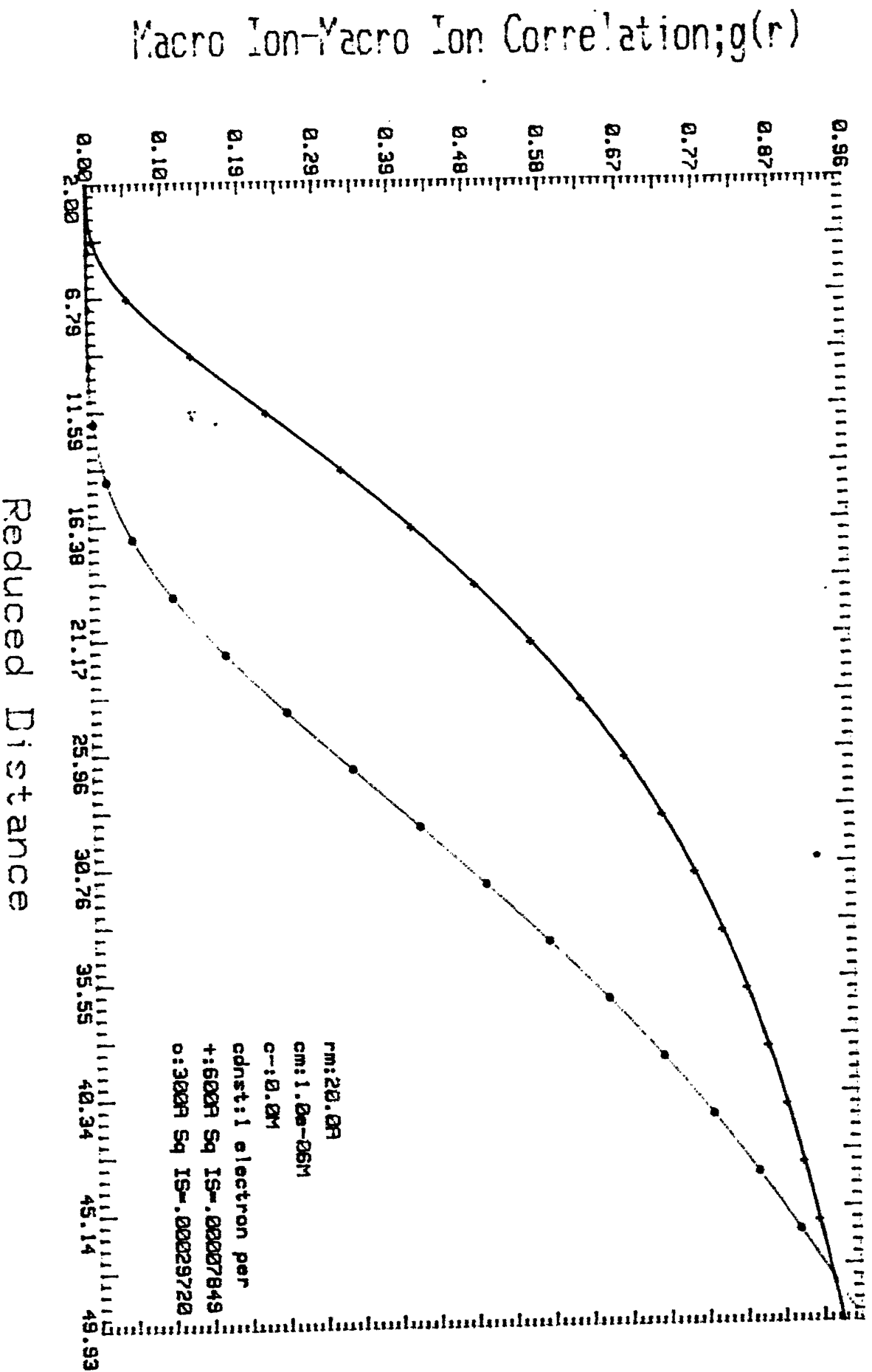
Reduced Distance

information on micelles.

### 1.10 Correlation Function Calculations: Models

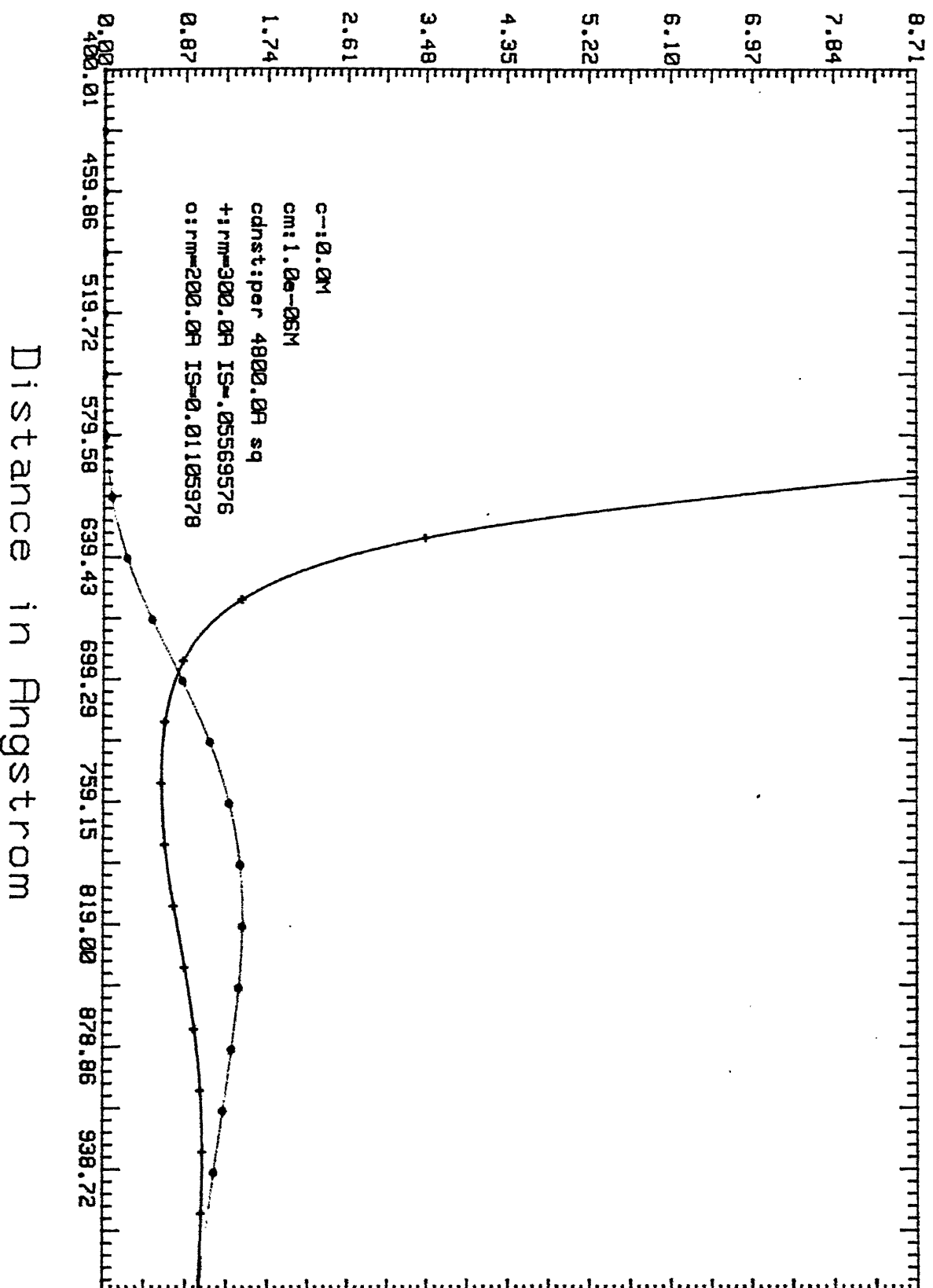
In order to calculate correlation function, the input needed is potential energy between particles. A full theory would have to include, macroion-macroion, macroion-small ion, small ion-small ion interaction potentials, as well as interaction potential between solvent molecule and each of these ions. This is too tall an order. A widely used approximation is not to explicitly recognise solvent structure on a molecular level. Their effect shows up only through the presence of static dielectric constant as the screening constant of electrostatic interaction. This reduction in complexity is reasonable because of the small size of the solvent molecules compared to that of macroions and to the Debye screening length of the microscopic ions. The adiabatic approximation which in Quantum theory of molecules is known as Born-Oppenheimer approximation is used here. This adiabatic model of solution is called the McMillan-Mayer model . A further reduction of the initially many component system may be achieved by taking advantage of the large asymmetry of size to eliminate the degrees of freedom of microscopic ions and derive effective interaction between "dressed"macroions. The interaction potential, then includes interaction between double layers. The most widely used dressed macroion potential is the Derjaguin-Landau-Verwey-Over-

# Correlation Function Vs. Distance F-5.49



# Correlation Function Vs. Distance F-5.59

Macro Ion-Macro Ion Correlation;  $g(r)$





beek (DLVO) potential (103). The parameters of this potential are Debye screening parameter  $\kappa$ , a surface charge  $Z^*$  and macroion size  $\sigma$ . This potential also includes Vander Waal's interactions between colloidal particles. Recently, several authors have reported studies using integral equation theories to calculate correlation functions with DLVO potential. Such attempts treat the macromolecular suspension as an one-component system with electrolyte and solvent "smeared out" and appearing as parameters in the effective potential between macroions, the only constituent of the one component model (OCM) system. Since macroions are charged, the one component system is a plasma. One may also consider the small counter-ions explicitly. Then, DLVO potential is not used. The unscreened Coulombic potential is used instead. The screening of the DLVO potential arises as a result of correlation function calculation, which takes the effect of all constituent ions. The solvent is still in the background, showing up only through its dielectric constant appearing as the screening constant. If the counterion of the macroion is the only other ion present, then it is a two component model system. In the presence of an added electrolyte, which shares the counterion of the macroion, we obtain a three component system. In this thesis, we have studied a three component system.

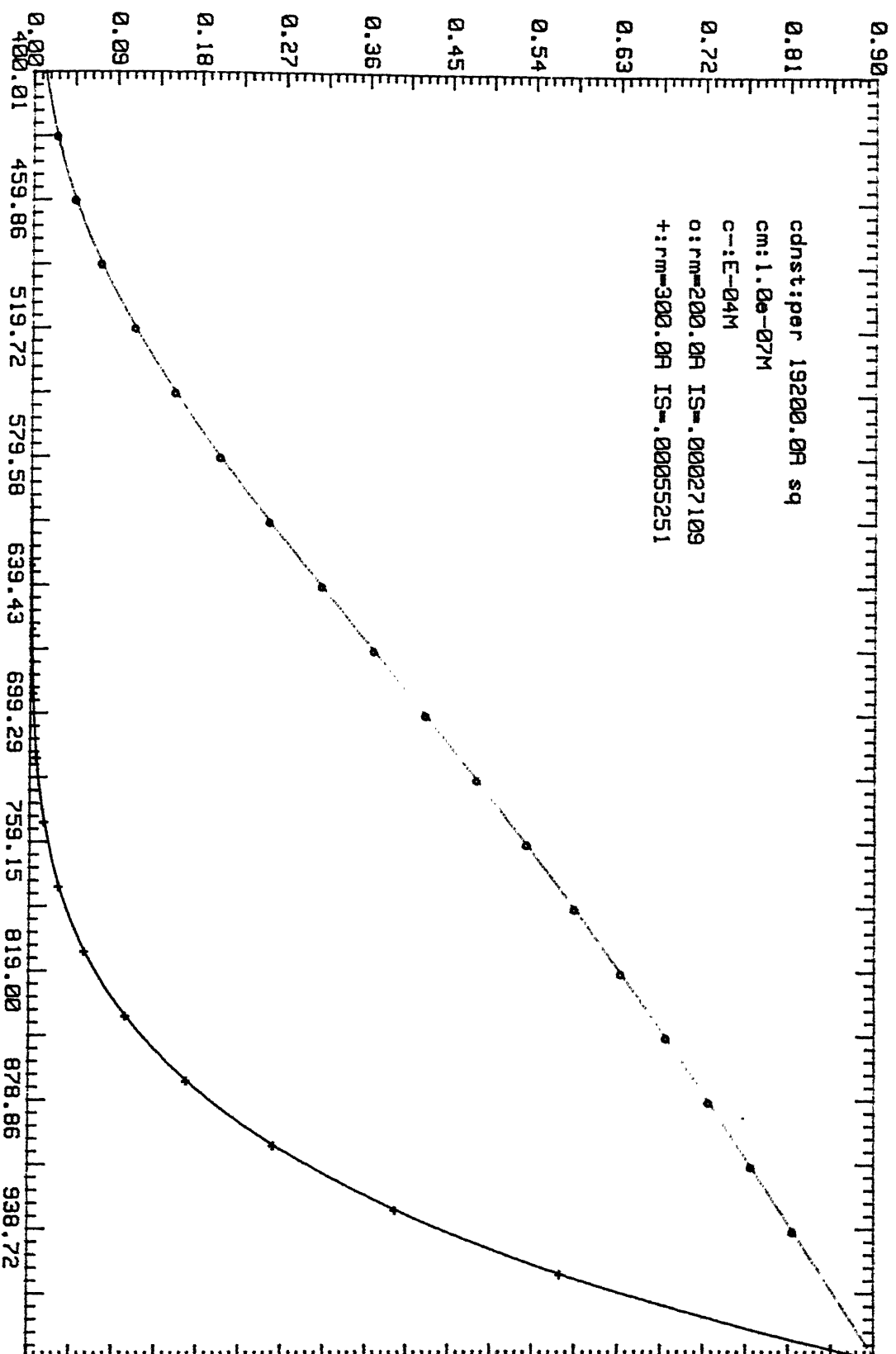
### 1.11 Essential Role of Integral Equation Theories

As noted earlier, in the study of macroionic solutions, the integral equation theory has an essential role. In systems with symmetric electrolyte with small charges, the computer simulation results are highly accurate. The results obtained from the integral equation theories are easier to obtain and are usually verified for correctness against the simulation results. For highly charged asymmetric electrolytes, that treat all ions on equal footing, computer simulation is difficult because there must be a relatively large total number of ions in the basic cell in order to have enough polyions so that polyion-polyion correlation is not destroyed by boundary effects (104). A minimum of 50 polyions is needed for simulation studies. If charge dissymmetry is 100, electroneutrality demands the presence of about 5000 ions (polyions + counterions). In addition, the small and large particles move on very different time scales, necessitating too large a number of elementary steps (105). The attainment of convergence in simulation studies irrespective of simulation technique is slow. In Monte Carlo (MC) simulation, a low acceptance is obtained for attempted moves of a colloid due to accumulation of counterions close to it. Similarly, in molecular dynamics (MD) and Brownian dynamics (BD), the counterions generate a narrow and deep potential well in which the colloid is trapped, resulting in a low diffusional motion. This is a physically correct effect, but it hampers the

# Correlation Function Vs. Distance F-5.69

Macro Ion-Macro Ion Correlation;  $g(r)$

cdnst:per 19200.00 sq  
cm:1.0e-07M  
c:-E-04M  
o:rm=200.00 IS=.00027109  
+irm=300.00 IS=.00055251



Distance in Angstrom

convergence of the simulation. The problems in simulation arising from long ranged Coulombic force also causes partly unresolved methodological problems. Simulation studies in these systems are more difficult and more error-prone than in solution of small ions.

#### 1.12 MSA: Measure of Macroion Charge

Amongst the various integral equation theories the mean spherical approximation (MSA) has attracted attention before others because analytic solutions to these models are known. MSA applied to ionic systems has the following properties (104) (i) in the high charge high density limit, it becomes identical to the HNC approximation and (ii) the long range ( $r \rightarrow \infty$ ) part of the direct correlation functions is asymptotically correct. However, when the charges are not too high and the concentration is low, as in micellar systems, the MSA pair correlation functions become increasingly inaccurate at small interionic separation. For the case of ionic colloids, a simple way to correct this deficiency is to redefine the polyion diameter and charge. The model takes into account the fact that because of strong repulsion, the spheres repel so strongly that the effective diameter is larger than the actual diameter. The renormalized charges, i.e., the redefined charges are different from the actual charges because of screening by ions that are so effectively shielding the polyion that they can be considered as part of the polyion, i.e.,

```

c(1,1)=(e2/e1)*c(2,2)+(e3/e1)*c(3,3)
nnn=nn+1
xn=dfloat(n)
sum=0.0
do i=1,m
do j=1,l
sum=sum+(c(i,j)*(e(j)**2))
end do
end do
kp=sqrt((4.0d0*3.14d0*sum)/(dc*bc*temp))
write(6,*)kp
rng=2.0d0*(tmax-tmin)
tbn=rng/xn
do i=1,l
do j=1,m
r(i,j,1)=tmin
end do
end do

```

```

C*****
c CALCULATION OF q and phi FUNCTIONS
C*****
do i=1,l
do j=1,m
do k=1,nn
q(i,j,k)=(-e(i)*e(j)*dexp(-kp*r(i,j,k)))/(dc*r(i,j,k)*bc*temp)
if((i.ne.3).and.(j.ne.3))then
if(i.ne.j)then
if(r(i,j,k).le.(r1+r2))then
phi(i,j,k)=-1.0
else
phi(i,j,k)=dexp(q(i,j,k))-1.0d0
end if

```

```

end do
end do
jd=jd+1
write(6,*)jd
c  CALCULATION OF THE CONVOLUTION INTEGRAL q*x , x*h , q*x*h
c*****
do i=1,l
do j=1,m
do k=1,nn
xh(i,j,k)=h(i,j,k)*r(i,j,k)
yh(i,j,k)=0.0d0
xx(i,j,k)=x(i,j,k)*r(i,j,k)
yx(i,j,k)=0.0d0
hh(k)=h(i,j,k)*(r(i,j,k)**2)
xxd(k)=x(i,j,k)*(r(i,j,k)**2)
rd(k)=r(i,j,k)
end do
ifail=1
call d01gaf(rd,hh,nn,ad,error,ifail)
ansh(i,j)=ad
call d01gaf(rd,xxd,nn,ad,error,ifail)
ansx(i,j)=ad
end do
end do
do k=nnn,n
do i=1,l
do j=1,m
xh(i,j,k)=-xh(i,j,(n+2-k))
yh(i,j,k)=0.0d0
xx(i,j,k)=-xx(i,j,(n+2-k))
yx(i,j,k)=0.0d0
end do
end do
end do
do i=1,l
do j=1,m

```

may be considered to be bound by the polyion. Thus the renormalized charges of the MSA can be interpreted to distinguish between charges "bound" to the polyion and those that are "loose" in the diffuse layer. This model is called the rescaled MSA or RMSA. Medina-Noyola and McQuarrie (106) have treated a three component system of macroion, its counterion and the coion with well defined hard sphere radii, in a dielectric continuum (the primitive model) and have solved the Ornstein-Zernike equation under MSA closure. They show that in the limit where diameters of the counterions and coions are negligible compared to that of the macroionic particles (the Debye-Hückel limit), the primitive model is reduced to an one component problem with effective screened interaction between "dressed" macroions. In the limit of low concentration of macroions the DLVO potential is recovered. This result shows that if any integral equation theory with DLVO potential is used to calculate  $S(Q)$ , the parameters of fit, in particular the "charge of the macroion" that appears in the DLVO potential will be affected by the finite size of small ions and by the macroion concentration. The calculated charge is the actual charge only in the limit of zero size of small ions and infinite dilution of macroions. The  $Z^*$  of DLVO potential is thus a parameter of fit and its physical meaning is related to the actual charge in a complicated way. The charge that appears in RMSA theory that treats coions and counterions explicitly has more direct physical meaning, as pointed out above. It appears

in theory in the expression of unscreened Coulombic interaction of the macroion with other ions. This renormalized charge is not the actual charge that the macroion would have had if counterions and coions were absent. Thus this charge will depend on nature of coions and counterions, temperature, charge of the macroion, nature of binding sites etc. It is however a physically interpretable parameter of considerable information content. As will be mentioned later, when both one component model with DLVO potential and multicomponent model in the RMSA theory have also been used in data analysis, the charge of the one component model is either less or equal to that obtained from multicomponent model (107-109). The charge of the RMSA multicomponent model agrees with that estimated from other theories of micelles (110). The aggregation number, the other parameter calculated, is however the same in results obtained from both models.

The MSA for a system of charged hard spheres, has been solved by Waisman and Lebowitz (111, 112). The solution for an arbitrary mixture of hard spheres of arbitrary size and charge, the model of an ionic mixtures has been solved by Blum(113) and Blum and Hoyer (114). A note by Hiroike (115) is a supplement to Blum's theory (113). MSA for DLVO (Yukawa) potential has been solved by Waisman (116) for a monodisperse solution. The corresponding solution for a polydisperse solution was given by Blum and Hoyer (117) and Blum (118). The solution for a binary mixture of charged hard spheres and point ions has been treated



```

xq2t(i)=q2t(i)*td(i)*sin(r(1,1,j)*td(i))
xq3t(i)=q3t(i)*td(i)*sin(r(1,1,j)*td(i))
xq11t(i)=q11t(i)*td(i)*sin(r(1,1,j)*td(i))
xq21t(i)=q21t(i)*td(i)*sin(r(1,1,j)*td(i))
xq31t(i)=q31t(i)*td(i)*sin(r(1,1,j)*td(i))
end do

C*****
c  CALCULATION OF q(r) FROM q(t) BY NUMERICAL INTEGRATION
C*****

  ifail=1
  call d01gaf(td,xq1t,nn,ad,error,ifail)
  yq1t(j)=epc*fp*ad*(1.0/r(1,1,j))
  ifail=1
  call d01gaf(td,xq2t,nn,ad,error,ifail)
  yq2t(j)=epc*fp*ad*(1.0/r(1,1,j))
  ifail=1
  call d01gaf(td,xq3t,nn,ad,error,ifail)
  yq3t(j)=epc*fp*ad*(1.0/r(1,1,j))
  ifail=1
  call d01gaf(td,xq11t,nn,ad,error,ifail)
  yq11t(j)=epc*fp*ad*(1.0/r(1,1,j))
  ifail=1
  call d01gaf(td,xq21t,nn,ad,error,ifail)
  yq21t(j)=epc*fp*ad*(1.0/r(1,1,j))
  ifail=1
  call d01gaf(td,xq31t,nn,ad,error,ifail)
  yq31t(j)=epc*fp*ad*(1.0/r(1,1,j))
end do

do i=1,nn
  q(1,1,i)=e(1)*e(1)*yq1t(i)
  q(1,2,i)=e(1)*e(2)*yq2t(i)
  q(2,1,i)=e(2)*e(1)*yq1t(i)
  q(2,2,i)=e(2)*e(2)*yq2t(i)
  q(1,3,i)=e(1)*e(3)*yq3t(i)
  q(2,3,i)=e(2)*e(3)*yq3t(i)
  q(3,1,i)=e(3)*e(1)*yq11t(i)

```

```

if(r(i,j,k).le.(r1+rm))then
h(i,j,k)=-1.0
else
h(i,j,k)=exp(q(i,j,k)+ytao(i,j,k))-1.0d0
endif
endif
if((i.eq.3).and.(j.eq.2)) then
if(r(i,j,k).le.(r2+rm))then
h(i,j,k)=-1.0
else
h(i,j,k)=exp(q(i,j,k)+ytao(i,j,k))-1.0d0
endif
endif
x(i,j,k)=h(i,j,k)-q(i,j,k)-ytao(i,j,k)
end do
end do
end do

C*****
C  CALCULATION OF THE CONVOLUTION INTEGRAL q*x , x*h , q*h*x
C*****
jd=jd+1
write(6,*)jd
do i=1,l
do j=1,m
do k=1,nn
xh(i,j,k)=h(i,j,k)*r(i,j,k)
yh(i,j,k)=0.0d0
xx(i,j,k)=x(i,j,k)*r(i,j,k)
yx(i,j,k)=0.0d0
hh(k)=h(i,j,k)*(r(i,j,k)**2)
xxd(k)=x(i,j,k)*(r(i,j,k)**2)
rd(k)=r(i,j,k)
end do
ifail=1
call d0lgaf(rd,hh,nn,ad,error,ifail)
ansh(i,j)=ad

```

by Gillan et al (119). Waisman's solution (116) was simplified by Hoyer and Stell (120), Hoyer and Blum (121) and by Cummins and Smith (122). The solution was used by Hayter and Penfold (123) to describe the structure factor of a macroion solution. The solution of MSA for a sum of two Yukawa potential terms has been given by Hoyer et al (124). The Hayter-Penfold solution (123) has been obtained in a slightly different form by Pastore et al (125). In the limit of no screening an analytic solution of MSA is given by Palmer and Weeks (126).

The MSA solution of Hayter and Penfold (123) has been used to interpret their own experimental neutron scattering results on a micellar solution (98). The calculated structure factor enabled them to obtain micellar charge and aggregation number. This and other early reports on analysis of neutron scattering data are done in the one component model (OCM) (99-101). The Hayter-Penfold MSA solutions are extended to arbitrarily low densities of highly charged colloids using a rescaling argument by Hansen and Hayter (127,128). Triolo et al (102) use the rescaled theory as well as the Hayter-Penfold theory to analyse their neutron scattering data on micelles. The OCM analysis suffers from the fact that only small ions are counted in calculating Debye screening length. This becomes increasingly unacceptable at high concentrations of micelles used in micellar experiments. This is, in addition to the difficulty in interpreting the calculated charge parameter. These problems

inspired workers to consider the macroions and small ions on an equal footing, the solvent still remaining in the background. This is the so-called primitive model (PM) and is explicitly multicomponent. Belloni (129) and Beresford-Smith et al (130) consider a multicomponent PM and then construct an OCM whose equations incorporate the terms of the multicomponent model. Such a transformation, say in the MSA leads to an expression of the direct correlation function of the OCM;  $c^{eff}(r)$  in terms of the  $C_{ij}$ 's, ion sizes, charges and concentrations of the multicomponent PM. The  $V(r)$  of the one component MSA theory, in reality an effective  $V(r)$ , called  $v^{eff}(r)$  is related naturally to  $c^{eff}(r)$  by the MSA closure  $-\beta v^{eff}(r) = c^{eff}(r)$  ( $\beta = 1/kT$ ). Belloni (129) derives, for example,

$$\beta v^{eff}(r) = Z_o^2 L_B x^2 \frac{e^{-\kappa r}}{r}, \quad r > \sigma_o$$

where  $\sigma_o$  is twice the macroion radius; index o refers to polyion; index 1 and greater than 1 to small ions;  $Z_o$  is charge on polyion;  $L_B = e^2/4\pi\epsilon_o\epsilon kT$ ,

$\kappa = (4\pi L_B \sum_{i=1} \rho_i Z_i^2)^{1/2}$ , the Debye screening parameter calculated from small ions only;  $\rho_i$ 's are number densities,

$X = \text{ch}(\kappa a) + U (\kappa a \text{ch}(\kappa a) - \text{sh}(\kappa a))$  and  $U = (Z/(\kappa a)^3) - (\gamma/\kappa a)$ ,  $\text{ch}$  and  $\text{sh}$  are hyperbolic cosine and sine functions;  $a = \sigma_o/2$ , the macroion radius.  $\gamma = (\Gamma a + Z)/(1 + \Gamma a + Z)$ , where  $Z = 3\phi/(1-\phi)$ ,  $\phi = \pi\rho_o\sigma_o^3/6$ , the volume fraction of macroion;  $\Gamma$ , the MSA screening parameter is given by

```

double precision yxh333(mmd,n,n,nd),y1333(mmd,n),
1 y2333(mmd,n),yqx333(mmd,n,n,nd),y3313(mmd,n,n,nd),
1 y3323(mmd,n,n,nd),y3333(mmd,n,n,nd)
double precision yxh313(mmd,n,n,nd),yxh323(mmd,n,n,nd),
1 yqx313(mmd,n,n),yqx323(mmd,n,n),y1313(mmd,n),y1323
1 (mmd,n),y2313(mmd,n),y2323(mmd,n)
double precision y1312(mmd),y1322(mmd),y1332(mmd),
1 y2312(mmd),y2322(mmd),y2332(mmd)
double precision yxh312(mmd,n),yxh322(mmd,n),yxh332(mmd,n),
1 yqx312(mmd,n),yqx322(mmd,n),yqx332(mmd,n),y3312(mmd,n),
1 y3322(mmd,n),y3332(mmd,n)
double precision y1311(mmd),y1321(mmd),y1331(mmd),
1 y2311(mmd),y2321(mmd),y2331(mmd)
double precision yxh311(mmd,n),yxh321(mmd,n),yxh331(mmd,n),
1 yqx311(mmd,n),yqx321(mmd,n),yqx331(mmd,n),y3311(mmd,n),
1 y3321(mmd,n),y3331(mmd,n)
double precision yxh213(mmd,n),yxh223(mmd,n),yxh233(mmd,n),
1 yqx213(mmd,n),yqx223(mmd,n),yqx233(mmd,n),y1213(mmd,n),
1 y1223(mmd,n),y1233(mmd,n),y2213(mmd,n),y2223(mmd,n)
1 ,y2233(mmd,n),y3213(mmd,n,n),y3223(mmd,n,n),
1 y3233(mmd,n,n)
double precision y1212(md),y1222(md),y1232(md),
1 y2212(md),y2222(md),y2232(md),y3212(mmd,n),
1 y3222(mmd,n),y3232(mmd,n)
double precision yxh212(md),yxh222(md),yxh232(mmd),yqx212(md),
1 yqx222(md),yqx232(mmd)
double precision y1211(md),y1221(md),y1231(md),
1 y2211(md),y2221(md),y2231(md)
double precision yxh211(md),yxh221(md),yxh231(mmd),yqx211(md),
1 yqx221(md),yqx231(mmd),y3211(mmd,n),y3221(mmd,n),
1 y3231(mmd,n)
double precision yxh113(mmd,n),yxh123(mmd,n),yxh133(mmd,n),
1 yqx113(mmd,n),yqx123(mmd,n),yqx133(mmd,n),y1113(mmd,n),
1 y1123(mmd,n),y1133(mmd,n),y2113(mmd,n),
1 y2123(mmd,n),y2133(mmd,n),y3113(mmd,n,n),y3123
1 (mmd,n,n),y3133(mmd,n,n)

```

$$\Gamma^2 = \kappa^2 + \frac{q_o^2}{(1 + \Gamma a + Z)^2}$$

where  $q_o = (4\pi L_B \rho_o)^{1/2} z_o$ . This is derived using MSA with point-like ions. Belloni also treats MSA with finite ion size and RMSA. In the limit of infinite dilution, DLVO potentials are recovered. Use of these OCM potentials in the RMSA, obtains polyion-polyion structure factors nearly identical to those obtained in TCM (PM) in MSA. The effective potential presents a larger electrostatic repulsion than the classical DLVO potential. This means that the use of DLVO induces an overestimate of the colloidal charge. The HNC integral equation in the PM compared to the RMSA equation, produces a larger accumulation of counterions on the colloidal surface and thus a lower effective repulsion between macroions. Beresford-Smith et al (130) consider a less complete model to calculate  $v^{eff}(r)$ . The ion-ion direct correlation functions that appear in  $v^{eff}(r)$  are treated by Debye-Hückel theory and the polyion-ion direct correlation function is calculated in the "jellium" approximation, which assumes that the distribution of colloids is uniform.

Medina-Noyola (131) studied MSA in the primitive model of an asymmetric two-component electrolyte in the limit of negligible size of the latter. The explicit calculations in the limit of negligible charge ratio show that the simple theory reproduces the main features of the liquid like structure obtained from scattering experiments. Nagele et al (132) study the primitive

```

call iim(phi13,phi12,yph213,r,k,tbn3,tbn4,w,lw,mmd,n,md,
1 xtemp1,ytemp1,ytemp2,xijkdd,eps)
call iim(phi23,phi22,yph223,r,k,tbn3,tbn4,w,lw,mmd,n,md,
1 xtemp1,ytemp1,ytemp2,xijkdd,eps)
call iim(phi31,phi11,yph311,r,k,tbn3,tbn4,w,lw,mmd,n,md,
1 xtemp1,ytemp1,ytemp2,xijkdd,eps)
call iim(phi32,phi12,yph321,r,k,tbn3,tbn4,w,lw,mmd,n,md,
1 xtemp1,ytemp1,ytemp2,xijkdd,eps)
call iim(phi31,phi12,yph312,r,k,tbn3,tbn4,w,lw,mmd,n,md,
1 xtemp1,ytemp1,ytemp2,xijkdd,eps)
call iim(phi32,phi22,yph322,r,k,tbn3,tbn4,w,lw,mmd,n,md,
1 xtemp1,ytemp1,ytemp2,xijkdd,eps)

```

```

C-----
call xint2(q33,alpha,mmd,n,nd,f33,xx,ans,error,al)
call imm(q13,f33,yq133,beta,r,k,tbn3,tbn4,w,lw,mmd,n,md,
1 xtemp1,ytemp1,ytemp2,xijkdd,xijkd,tmp,ans,error)
call imm(q23,f33,yq233,beta,r,k,tbn3,tbn4,w,lw,mmd,n,md,
1 xtemp1,ytemp1,ytemp2,xijkdd,xijkd,tmp,ans,error)
call xint1(q33,alpha,mmd,n,nd,f33,xx,ans,error,al)
call imm(q31,f33,yq331,beta,r,k,tbn3,tbn4,w,lw,mmd,n,md,
1 xtemp1,ytemp1,ytemp2,xijkdd,xijkd,tmp,ans,error)
call imm(q32,f33,yq332,beta,r,k,tbn3,tbn4,w,lw,mmd,n,md,
1 xtemp1,ytemp1,ytemp2,xijkdd,xijkd,tmp,ans,error)

```

```

C-----
call xint2(phi33,alpha,mmd,n,nd,f33,xx,ans,error,al)
call imm(phi13,f33,yph133,beta,r,k,tbn3,tbn4,w,lw,mmd,n,md,
1 xtemp1,ytemp1,ytemp2,xijkdd,xijkd,tmp,ans,error)
call imm(phi23,f33,yph233,beta,r,k,tbn3,tbn4,w,lw,mmd,n,md,
1 xtemp1,ytemp1,ytemp2,xijkdd,xijkd,tmp,ans,error)
call xint1(phi33,alpha,mmd,n,nd,f33,xx,ans,error,al)
call imm(phi31,f33,yph331,beta,r,k,tbn3,tbn4,w,lw,mmd,n,md,
1 xtemp1,ytemp1,ytemp2,xijkdd,xijkd,tmp,ans,error)
call imm(phi32,f33,yph332,beta,r,k,tbn3,tbn4,w,lw,mmd,n,md,
1 xtemp1,ytemp1,ytemp2,xijkdd,xijkd,tmp,ans,error)

```

```

C-----
call mim(q31,q13,yq313,r,k,tbn3,tbn4,w,lw,mmd,n,md,xtemp1,

```

```

call imi(q13,yxh311,y1311,beta,r,k,tbn3,tbn4,w,lw,mmd,n,md,
1  xtemp1,ytemp1,ytemp2,xijkdd,yxijkd,tmp,ans,error)
call imi(q13,yxh321,y1321,beta,r,k,tbn3,tbn4,w,lw,mmd,n,md,
1  xtemp1,ytemp1,ytemp2,xijkdd,yxijkd,tmp,ans,error)
call imi(q13,yxh331,y1331,beta,r,k,tbn3,tbn4,w,lw,mmd,n,md,
1  xtemp1,ytemp1,ytemp2,xijkdd,yxijkd,tmp,ans,error)
c-----
do i=1,mmd
temp1=(c1*yxh111(i))+(c2*yxh121(i))+(c3*fps*yxh131(i))
temp3=(c1*c1*y1111(i))+(c1*c2*y1121(i))+(c1*c3*
1  fps*y1131(i))+(c2*c1*y1211(i))+(c2*c2*y1221
1  (i))+(c2*c3*fps*y1231(i))+(c3*c1*fps*y1311(i))+(c3*c2*
1  fps*y1321(i))+(c3*c3*epc*y1331(i))
tao11=temp1+qx11(i)+temp3
if(r(i).le.(2.0*r1)) then
h11(i)=-1.0
else
h11(i)=dexp(q11(i)+tao11)-1.0d0
end if
x11(i)=h11(i)-q11(i)-tao11
end do
c-----
call iii(q11,yxh112,y1112,yxij,yxjk,r,k,tbn3,tbn4,md,mmd,w,
1  lw,xtemp1,eps)
call iii(q11,yxh122,y1122,yxij,yxjk,r,k,tbn3,tbn4,md,mmd,w,
1  lw,xtemp1,eps)
call iii(q11,yxh132,y1132,yxij,yxjk,r,k,tbn3,tbn4,md,mmd,w,
1  lw,xtemp1,eps)
call iii(q12,yxh212,y1212,yxij,yxjk,r,k,tbn3,tbn4,md,mmd,w,
1  lw,xtemp1,eps)
call iii(q12,yxh222,y1222,yxij,yxjk,r,k,tbn3,tbn4,md,mmd,w,
1  lw,xtemp1,eps)
call iii(q12,yxh232,y1232,yxij,yxjk,r,k,tbn3,tbn4,md,mmd,w,
1  lw,xtemp1,eps)
call imi(q13,yxh312,y1312,beta,r,k,tbn3,tbn4,w,lw,mmd,n,md,
1  xtemp1,ytemp1,ytemp2,xijkdd,yxijkd,tmp,ans,error)

```



model in the MSA with nonvanishing size of the ions of the electrolyte. The effect of this size is studied particularly at high ionic strength by comparison with the results of an one component model. The calculated macroion charge in the two component model differ from that in the one component model. The double layer is also different in the two models. It is pointed out that the one component model assumes Debye-Hückel distribution around macroion, which is assumed to remain unchanged even as other macroions approach. This is certainly not the case. The primitive model does not make this assumption and calculates macroion-small ion correlation explicitly in the presence of other macroions. It is found that macroion-coion distribution does not obey Debye-Hückel distribution. Senatore and Blum (178) treat a polydisperse micellar system in the primitive multicomponent ionic fluid model in the MSA.

### 1.13 HNC Calculations on Polyelectrolytes

Patey (72) carried out the first HNC calculations on spherical macroions, at infinite dilution in the presence of coions and counter ions in a dielectric continuum. He treats all ions on an equal footing. He reports data on macroion-macroion potential of mean force and finds significant dependence on macroion size and charge density. He observes, for certain values of parameters, a peak in the macroion-macroion correlation function ( $g_{mm} > 1$ ), i.e., finds an attractive force between

```

end do
C*****
c FINAL VALUE OF tao AND SUBSEQUENT VALUES OF h AND x FUNCTION
c ARE CALCULATED.
C*****
  if(nitr.ne.nu)go to 300
  continue
C-----
C*****
c CALCULATIN OF THE h VALUES AVERAGED OVER THE ANGLES.
C*****
  do i=1,mmd
    if(r(i).le.(2.0*r1))h11(i)=-1.0
    if(r(i).le.(2.0*r2))h22(i)=-1.0
    if(r(i).le.(r1+r2))h12(i)=-1.0
    if(r(i).le.(r1+r2))h21(i)=-1.0
  end do
  do i=1,mmd
    if(r(i).le.(r1+r3))then
      h13d(i)=-1.0
    else
      do j=1,n
        tmp(j)=h13(i,j)*sin(beta(j))
      end do
      ifail=1
      call d01gaf(beta,tmp,n,h13d(i),error,ifail)
      h13d(i)=0.5*h13d(i)
    end if
  end do
  do i=1,mmd
    if(r(i).le.(r2+r3))then
      h23d(i)=-1.0
    else
      do j=1,n
        tmp(j)=h23(i,j)*sin(beta(j))
      end do
    end if
  end do

```

similarly charged macroions, which is contrary to the usual belief in colloid chemistry that the forces are repulsive at all distances. He interprets it as a macroion dimer held together by piled up counterion density. This attractive force has been observed by later workers also, in integral equation studies as well as in computer simulation studies. Teubner (73) uses analytic methods to calculate potential of average force between colloidal particles in the HNC approximation in the two limiting cases (i) small potentials and (ii) limiting case of large spheres with arbitrary charges. The maxima in  $g$  versus  $r$  plot is obtained as in numerical studies of Patey. An expression of the force between two identical charged spherical particles has been derived by Bell and Levine, (177) and the force is always repulsive. The assumptions on which this result is based are no more than those inherent in the classical model for the mobile ions and their interaction with charged particles, i.e., point-like ions with Debye-Hückel interaction, Poisson-Boltzmann theory for ion-colloid correlation. In particular, no assumption is made for interaction of colloid particles with themselves. Instead, their free energy is obtained rigorously by a charging process. Thus the classical theory equivalent to HNC theory for ion-colloid interaction circumvents the approximations of HNC theory to study colloid-colloid interaction and provides a direct test of the latter. On the basis of this argument, Teubner concludes that the attraction shown in HNC calculations is an

```

      call fft(r,k,tbn3,xtemp1,ytemp1,md,mmd,w,lw)
      do i=1,mmd
        x1(i,1)=ytemp1(i)
      end do
    end do
  do jdd=1,n
    do l=1,nd
      do i=1,mmd
ytemp2(i)=xjk(i,jd,jdd,l)
      end do
      call fft(r,k,tbn3,xtemp1,ytemp2,md,mmd,w,lw)
      do i=1,mmd
        x2(i,1)=ytemp2(i)
      end do
    end do
    do i=1,mmd
      do l=1,nd
        xtmpr1(l)=x1(i,1)
        ytmpr1(l)=0.0
        xtmpr2(l)=x2(i,1)
        ytmpr2(l)=0.0
      end do
c      do l=(nd/2)+1,nd
c        xtmpr1(l)=0.0
c        ytmpr1(l)=0.0
c        xtmpr2(l)=0.0
c        ytmpr2(l)=0.0
c      end do
      ndfn(ndim)=nd
      nfn=ndfn(ndim)
      ifail=0
      call c06fjf(ndim,ndfn,nfn,xtmpr1,ytmpr1,w1,lw1,ifail)
      ndfn(ndim)=nd
      nfn=ndfn(ndim)
      ifail=0
      call c06fjf(ndim,ndfn,nfn,xtmpr2,ytmpr2,w1,lw1,ifail)

```

artifact of the approximations made in assuming HNC closure, i.e., neglect of highly connected bridge diagrams.

Rosenfeld and Ashcroft (74) showed that within the accuracy of present day computer simulation studies, bridge functions constitute the same universal family of curves, irrespective of the assumed pair potential. Since computer simulation results for hard spheres are known accurately, these results can be used to handle any potential. The authors suggest that a modified HNC equation be solved with one parameter bridge function family appropriate to hard spheres and the single parameter (the hard sphere packing fraction) can be determined by appealing to the requirement of thermodynamic consistency. The assertion of universality is demonstrated via the application of this new method to a wide class of different potentials including Coulomb and Yukawa potential of importance in this thesis. Malihevsky and Labik (75) have now carried out this parameterization and provided an easy to use formula  $B(r)$ , which has to be merely added to the interaction potential. Teubner (73) points out on the basis of the work of Rosenfeld and Ashcroft (74) that the addition of bridge functions is equivalent to adding short range repulsive forces and it will nullify the "spurious" short range attractive forces. Rössky et al (71) have made similar observations in their study of 2:2 electrolytes.

Khan et al (133) used HNC approximation for macroion-macroion correlations and MSA for macro ion-small ion

and small ion-small ion correlations. The point ion limit of the counter-ions yield an analytic solution for the counter-ion part of the problem. This maps the macroion part of the problem onto an one-component problem where the macroion interacts via a screened Coulomb potential with Guoy-Chapman form of screening length and an effective charge that depends on the macroion-macroion pair correlations. Khan et al. are constructing an one-component model very much the way it is done in the MSA in Refs. 129 and 130, excepting that here macroion-macroion correlation is treated in the HNC and the rest in the MSA. Numerical solutions of the effective one component equation in the HNC approximation are presented and in particular the effects of macroion charge, non additive core diameters, and added electrolyte are examined. There is a strong renormalization of the effective macroion charge. At very high charge a second melting of colloidal crystals is predicted. A colloidal particle of total charge 11000 e ( $e$  = electronic charge) has been studied. This is the highest charged colloid studied so far. Studies on highly charged electrolytes with all ions treated on equal footing in the HNC approximation have also been reported. Elkoubi et al (134) have applied the HNC theory to asymmetric electrolytes (charge ratio -6:+1, size ratio 2:1) to obtain information about correlation function and number of ion pairs. The study presumably also tests the applicability of the full HNC treatment to polyelectrolytes. Rogers (135) study systems with

ions of the same size and charge asymmetry upto 20:1. Beresford-Smith and Chan (136) treat a dilute but strongly interacting colloidal system as an asymmetric electrolyte (radius  $500 \text{ \AA}$ , charge ratio -120: +1) in the HNC approximation and obtain an effective pair potential between macroions which depend on the density of the macroion. This is in a spirit similar to Refs. 129-130. The colloid-colloid radial distribution function can be fitted by an one component model provided the charge is treated as an adjustable parameter. The concentration dependence is consistent with the presence of many body effects. Logarithmic distribution of points in the Fourier transform algorithm as used by Rosky and Friedman (70) has been tried, but gives no difference from those obtained using the usual even spacing of points. Belloni (137) treats a charge asymmetry of 1: -40 and size asymmetry of  $5:50 \text{ \AA}$  in the full HNC formulation. The value of effective charge is obtained by comparing the solution of the full system and the polyion-polyion structure factor of the equivalent effective one component system. The charge parameter of the dressed macroion model, that gives the best fit is the effective charge. A three component system is studied by addition of salt to show the effects of screening. The +2:-20 electrolyte is also studied briefly, Bratko et al (138,104) study colloidal suspensions as asymmetric electrolyte in the primitive model and solve Ornstein-Zernike equation mostly with the conventional HNC closure as well as with HNC-PY closure

(HNC for macroion-macroion, PY for the rest). A macroion charge as large as 40 and 64 have been studied. Agreement with Monte Carlo simulation result is good. The correlation function between two macroions show a peak at a distance of 4-5 nm for a macroion radius of 1 nm. The conventional HNC closure gives results similar to HNC-PY closure, but the convergence is obtained with HNC-PY closure in systems, where HNC closure did not give convergence. An important difficulty in treating asymmetric electrolytes in the HNC approximation is the difficulty of obtaining convergence by the usual method, if one uses the two component model in the PM. The choice of the closure may improve matters, as it seems to do if HNC-PY closure is used. This important difficulty is reported in our work in Chapter V, as well as by other workers (56,137,138). Abernethy and Gillan (56) use a potential of the form  $\phi_{\lambda\nu}(r) = \frac{z_\lambda z_\nu e^2}{\epsilon r} + \phi_o(r_o/r)^n$ ,  $\phi_o$ ,  $r_o$ ,  $n$  are constants, in particular  $n = 9$ . They define two parameters  $\eta = \frac{1}{6} \pi \rho r_o^3 (\phi_o/K_B T)^{3/n}$  and  $\Gamma = Z^2 e^2 / a_o \epsilon K_B T$ ,  $\rho$  is the total ion density and  $a_o$  is the ion sphere radius,  $a_o = (3/4\pi\rho)^{1/3}$ . They solve HNC equation for ionic mixtures, according to Gillan's algorithm (55), developed for single component neutral liquid and find that there is a boundary in the  $\eta, \Gamma$  plane, i.e., a region of high density and high charges (low temperature) in which solutions to the HNC equations cannot be obtained. Linse and Jonsson (139) have done Monte Carlo and HNC calculations on micelles at a charge density of  $1e/100 \text{ \AA}^2$ ,



micellar radius  $10\text{\AA}$ , i.e., net charge on the micelle is  $\sim 12$  electronic charges, counterion radius  $1\text{\AA}$ . Both Monte Carlo and HNC results show similar features in plots of correlation function versus  $r$ . In calculation of properties HNC, MSA and Poisson Boltzmann theories give about the same error. The authors conclude that the additional effort needed for HNC theory is not really very meaningful.

Linse (140, 141) study a two component asymmetric electrolyte (1:20) by HNC theory in the two component primitive model (TCM) and molecular dynamics simulation. He demonstrates that the inherent approximations of MSA and HNC theories make the micellar charge values calculated from experimental neutron scattering data using these theories less than their nominal values. He points out that a smaller value does not indicate incomplete ionization. The calculated charge is merely a fitting parameter. The HNC theoretic values improves upon the MSA theoretic value but are still not correct. Like other workers, Linse also explores the possibility of working out an one-component potential. One approach is to calculate correlation function from OCM using DLVO potential, with variable parameters  $A$  and  $B$  ( $u(r) = A \exp(-r/B)/r$ , at  $r$  greater than hard sphere diameter), and accept those  $A$  and  $B$  which generates a correlation function (in OCM) that fit the TCM data best. The other approach, is to fit the TCM data directly with an one component O-Z equation with an HNC closure using effective direct

correlation function and an effective potential appearing in place of  $C(r)$  and  $U(r)$ , in the same way Belloni (129) and Beresford-Smith et al (130) have done in MSA theories and Beresford-Smith and Chan (136) in HNC theory. Linse adopts the second approach. The  $v^{\text{eff}}(r)$  differs from the screened Coulomb DLVO potential. The experimental data is to be fitted with parameters of the theory either in OCM or in TCM and the optimized parameters of fit are the macroion charge ( $Z_M$ ) and micellar aggregation number ( $n$ ) (number of micellar particles being equal to (concentration of the salt minus critical micelles concentration) divided by  $n$ ). As in the case of MSA theories  $Z_M$  of TCM is physically more meaningful and is different in magnitude from that of OCM. Rogers-Young closure is studied and is found to give the most accurate structure factor in OCM. On comparison with simulation data, HNC theory is found to overestimate micelle-ion and ion-ion correlation which results in too weak an effective micelle-micelle repulsion. Linse (142) uses the effective potentials of OCM and the TCM in PM for computer simulation to obtain triplet correlations and find that effective potentials underestimate triplet correlation at small distances.

The central problem that makes the use of TCM in the HNC closure a difficult proposition is that convergence of the usual iterative scheme fails at high particle density and charge of the polyion. One possible solution of this problem is to use

alternative closures for the solution of O-Z equation. Belloni (105) applies mixed integral equation proposed by Zerah and Hansen (ZH) a closure that interpolates continuously between the Percus-Yevick (PY) and HNC closures for charges of the same sign and between HNC and MSA for charges of opposite sign. The thermodynamic consistency between the virial and compressibility equations of state is obtained by varying the single parameter in the switching function. Several methods of choosing this parameter are discussed. In weakly screened and highly charged suspensions, the ZH equation improves appreciably the HNC results. Convergent solutions are obtained at polyion charge inaccessible in the usual HNC theory. The region of divergent solutions now shifts to higher charge. In the absence of simulation data ZH equation is useful in quantifying the accuracy of HNC closure. Fushiki (143) attempts to remove the instability of the ordinary iterative method by modifying the iteration process. They use a certain distribution of colloids (instead of Jellium approximation used in Ref. 130) and calculate  $C_{ij}(r)$  ( $i \neq 0$ , index 0 is for polyion). On the other hand, the colloidal distribution is determined from the effective potential constructed from  $C_{ij}(r)$  ( $i \neq 0$ ). When both calculations are performed with the HNC approximation, it becomes simply the multicomponent HNC approximation separated into two parts. In each part, one of the two groups of correlation functions namely (a) the colloid-colloid correlation function or (b) the

colloid-ion and ion-ion correlation functions, are iterated, when those of the other group are fixed. The separative method removes the instability of an ordinary iterative method to some extent. Moreover, it shows that the colloid-colloid correlation function is slowly convergent. Fushiki applies Newton-Raphson (NR) method to improve the convergence. The separative NR method successfully enhances the convergence rate in the large charge region. Very much in the spirit of Refs. 129, 130, 136, 140, Fushiki derives a  $v^{\text{eff}}(r)$  in the one component HNC theory. Henderson and Lozada-Cassou (188) have solved the MSA for large hard macroions in a hard sphere dipolar solvent in a dielectric continuum whose dielectric constant equals that of the solvent. This result shows oscillations in force as a function of distance, as has been seen in the direct force measurements between mica surfaces by Israelachvili and his group (2). Lowen et al (143) have recently proposed that MD for the macroions be combined with density functional description of the microscopic ions.

#### 1.14 Ion-dipole mixture:

The primitive model which treats the ions explicitly but ignores the discrete molecular structure of the solvent, including its effect only through the appearance of the solvent dielectric constant as the screening constant of Coulombic interaction, is clearly an oversimplified model. Friedman and his

group have made systematic efforts to improve upon the primitive model (62,63,66-69) by considerations of classical electrostatics in terms of cavity and Gurney terms. The first and a remarkably thorough investigation that attempts to consider dipoles explicitly by methods of statistical mechanics is due to Jepsen and Friedman (145). It aims to modify the primitive model. It also develops the techniques of handling angle-dependent potential. We have made extensive use of the Jepsen-Friedman method in this thesis. Jepsen and Friedman develop methods for calculating the sums of g-bond chain diagrams and thus makes it possible to solve HNC equation of an ion-dipole mixture. We describe the results in Chapter IV.

Of the various integral equation theories, MSA received a lot of early attention because an analytic solution is possible. Wertheim solved MSA for pure fluids of hard spheres with embedded dipoles (146). Adelman and Deutsch (147) extended Wertheim's method to solve MSA for simple polar mixtures and for mixtures of polar and nonpolar molecules. Blum and Torruella (148) developed methods of invariant expansion of two body statistical correlation functions, which has been extensively used in later work on angle-dependent potential. Blum (149,150) extended Wertheim's method of hard spheres with embedded point dipole to an arbitrary charge distribution. Adelman and Deutsch (151), Blum (152-154), Chan et al (155) solve MSA for a mixture of ions and dipoles. Hoyer et al.(156) solved generalized MSA for polar and

ionic fluids. Stell (157) has reviewed this method. Patey (158) summarize the contributions of MSA, but points out that quantitatively it is a poor description of the structural and thermodynamic properties. The basis for this conclusion is the poor agreement of the MSA results with the results of Monte Carlo simulation. Patey used the linearized and quadratic hypernetted chain approximation (LHNC, QHNC) to solve the Ornstein-Zernicke equation for hard spheres with pure dipoles (158,159) and those with pure linear quadrupoles (160) and obtained good agreement with Monte-Carlo results. When fluids with both dipoles and quadrupoles embedded in the same sphere were studied, the agreement with Monte Carlo results was not so good (161). Patey et al (159) solved LHNC and QHNC approximations for fluids of dipolar hard spheres and Stockmayer particles. Dependence of pair correlation functions and dielectric constant on density and dipole moment is studied. The LHNC theory is found to be poor, whereas the QHNC theory is found to be excellent. A nonlinear truncated HNC (THNC) approximation for dipolar fluids has been considered by Chan and Walker (162). Levesque et al (163) have studied ion-dipole mixtures in LHNC and QHNC approximation and find features in ion-ion correlation not found in the primitive model. Solvent separated ion-pairs are found to be important in some solutions. Patey et al (164) calculate potential of mean force between ions embedded in a dipolar solvent by LHNC approximation. The results are in good agreement with Monte

Carlo results. The MSA results are poor and unphysical at low concentration and small  $r$ . The full HNC and RHNC theory for systems with angle-dependent potential have been developed by Fries and Patey (165). These theories solve the integral equation without using cluster theoretic diagram summations. It improves upon RLHNC and RQHNC methods for both dipolar hard sphere (165) and Stockmayer (dipolar-Lennard Jones) fluids (166). This is particularly true of static dielectric constant for which an accurate theory is difficult to obtain. Perkyns et al (167) have applied the RHNC theory to hard spheres with dipoles and axially symmetrical quadrupoles and compare the results with Monte Carlo results and find significant improvement over RLHNC and RQHNC results.

Caillol et al, (168) apply RHNC and RLHNC theory to 1:1 electrolyte solutions (ion-dipole mixture) and compare the results with molecular dynamics simulation results. It is shown that the theoretical results and molecular dynamics calculations are generally in good agreement for the solvent-solvent and ion-solvent correlation functions. The RHNC theory gives much better results compared to RLHNC theory for ion-solvent correlations and dielectric constant. Unambiguous evaluation of ion-ion structure is not possible because of convergence difficulties in the molecular dynamics simulations.

Kusalik and Patey (169-171) apply RHNC theory to ion-dipole mixtures. They find that in univalent ions in water like dipolar

solvent, inclusion of octupole moment of water affects properties, ion solvation and ion-ion and ion-solvent distribution functions. Polarizable dipole-tetrahedral quadrupole solvent molecules in mixture with ions are studied. Solvent polarizability affects properties significantly. Patey's group, equipped with the experience gained on RHNC theory of mixtures of small ions and dipoles, have treated macroionic solution as an ion-dipole mixture in the RHNC theory (172-175). Large sizes could not be handled. In the first study (172) with only the macroion and the dipole, the solvent structure was found resistant to alteration due to surface charge. Oscillatory behaviour of polarization density and mean electrostatic potential is observed. In the second paper of this series, counter ion response to macroion surface charge (173) is studied and significant size effect is observed. The relationship that potential of mean force equals charge multiplied by mean electrostatic potential is found to be nowhere near the calculated values. Calculated potential of mean force shows oscillatory behaviour as a function of distance. Patey and his group then proceed (174) to study a mixture of macroion, counterion, coion and solvent dipoles (Macroion, KCl, H<sub>2</sub>O) as a function of size and surface charge density (largest charge density 91 Å<sup>02</sup>/electronic charge) and obtain results on ion and dipole distribution around macroions. Torrie et al (175) extend these studies on KCl solution to NaCl solution. The



solvent structure around macroion surface is very different from that near a planar surface. The ice-like ordering known to occur near flat surfaces is seen around macroion surface also, once the size exceeds a critical value. All these four papers from Patey's group study an infinitely dilute macroion solution and do not study macroion-macroion correlation function. Non spherical macroion shape has also been studied in RHNC theory of ion-dipole mixture (176).

### 1.15 Bridge Functions

It has been mentioned earlier that HNC theory has assumed central importance in the theory of asymmetric electrolytes because of the difficulty of carrying out simulation studies. Efforts to take into account the bridge diagrams (set equal to zero in the HNC closure) and improve the HNC theory have gained momentum in recent years. The suggestion of Rosenfeld and Ashcroft (74) that bridge diagrams evaluated from hard sphere simulation results will apply universally, if true, makes it a simple matter to incorporate bridge diagrams (75). This modification is the basis of the so called RHNC (R for Reference) or MHNC (M for modified) theories. It gives excellent results for simple concentrated systems which are close to hard sphere system, but its extension to charged mixtures is not considered to be straightforward. Belloni (105) has obtained poor results with MHNC in charged mixtures. Good results have also been

obtained in several studies (168-171,179). Recent papers have appeared that try to include bridge functions, in description of ionic systems (180-185). A recent modification of the HNC theory, called the three point extension of HNC theory has been developed by Lozada-Cassou and his colleagues (186,187,76). In this theory, one considers two particles of an one species bulk fluid to be joined by an imaginary rigid bar, hence forming a dumb bell. This diatomic particle is considered to be one species in a two species system, where the other species is a monatomic particle. A two particle correlation function between these two different particles is calculated as a function of the length of the dumb bell, to obtain three particle distribution function, which yields through exact Born-Green -Yvon equation the two particle distribution function. The two particle distribution function so calculated is different from its counter part calculated by the usual method because the bridge diagrams for the interaction of the two particles joined by the dumb bell are taken into account. This is therefore an improved correlation function. Some recent reports (188-192) have appeared on theoretical calculation of force between macroions in an electrolyte using specific models of solvent, which reproduce oscillations in force as a function of distance between macroions, as observed experimentally by Israelachvili and his group (2).

### 1.16 Integral Equation in Treatment of External Field and Planar Interface

In statistical mechanics of fluids, a set of particles can be taken as a source of an external field. Thus if a spherical particle in the fluid is taken as a source of an external field, then by taking the limit of infinite radius of this particle, in an integral equation theory of a bulk fluid, one obtains the corresponding theory for a fluid in an external field of planar geometry. HNC theory has been modified in this way to study the structure of electrolytes near a planar interface, i.e., that of the double layer by Henderson and others. The subject has recently been reviewed by Henderson and Blum in Chapter 6 of Ref. 53. HNC theory has not been as successful in handling double layer as it has been in the treatment of bulk electrolytes indicating need for caution and need for all possible improvements in its application to macroionic solutions. If a particle can be treated as an external field, the external field can also be treated as a particle in the fluid. This approach has been used in the treatment of a fluid in an external field of planar, cylindrical and spherical geometries (193-196). Treatment of external field and older references are also given by Percus (48) and Stell (49).

### 1.17 Molecular Recognition at a Distance

There are several recent reports in the literature that study the orientation of polypeptide hormones directed towards a

charged membrane interface. The molecular conformation is found to be simultaneously modified and adapted to the receptor site. The technique used is Monte Carlo simulation (197,198). These effects are basic to molecular recognition at longer range than that at which valence forces operate, a theme referred to earlier.

### 1.18 Structure of this Thesis

In this background, we describe our investigations in this area in the chapters that follow. Chapter II considers Coulombic interactions arising from polarization of the macroion dielectric in a macroionic solution. We find that the effect will be significant only if the charge on the macroion is small, otherwise interaction between permanent charges dominate and more importantly, if the macroion is nonspherical, then polarization effects will show up even if interaction between permanent charges are present. Chapter III presents the cluster theoretic approach to HNC equation, which results in Allnatt's integral equation. This equation differs from the usual HNC equation in a subtle way. The summation of g-bond chains are carried out to obtain convergent sums before highly connected bridge diagrams are ignored in the HNC closure. The equation of closure is different from that in the general HNC theory developed for non-ionic fluids. Since, the indication in the literature (104,105,133,138,143) is that the choice of suitable closure may

reduce the problem of not obtaining convergence in solution of HNC equation, we were prompted to investigate if the use of Allnatt's equation will reduce problem of convergence. All existing literature reports (viz. 104,105,133,138,140,141,143) solve the more general HNC equation (not Allnatt equation) using powerful numerical algorithms (55,56), which handle the problem of long range forces numerically rather than by diagrammatic summation. We have solved Allnatt's integral equation numerically following standard methods developed by other workers, in Chapter V and find that the range of macroionic charge over which convergent solution of HNC equation is not obtained shifts and macroions of higher charge can be handled. The problem does not disappear but becomes less intense. In chapter III, we also modify cluster theory of g-bond summation in electrolytes and obtain expression of q-bond in systems that have substantial effect arising from polarization of macroion dielectric by other ions present in solution, small ions and macroions. In Chapter IV, we obtain expressions of g-bond sums for ion-dipole mixture following the method of Jepsen and Friedman (145) and use them to numerically solve Allnatt's equation for ion-dipole mixture. The theory holds for solutes that carry charge and dipole moment both and is easier to program compared to RHNC theory of Patey and his group, described above (158-176). It does not hold at liquid densities (however, see chapter IV section 6) and therefore can be applied only to

solution in the primitive model, i.e., solvent has to be treated as a continuum. In Chapter V, we describe numerical methods used and the results of numerical calculation. The effect of macroion dipole moment, not reported yet, in the literature is found to be significant. We could not however obtain extensive numerical data on ion-dipole mixtures, because of very long computation time. This work is now being carried out.

## REFERENCES

1. Wilschut, J. and Hoekstra, D., Membrane Fusion, Marcel Dekker, New York, 1991.
2. Silver, B., Physical Chemistry of Membranes, Allen and Unwin, Boston, London, Sydney and The Solomon Press, New York, 1985.
3. Rau, D.C. and Parsegian, V.A., Biophys. J., 61, 246, 1992.
4. Rau, D.C. and Parsegian, V.A., Biophys. J., 61, 260, 1992.
5. Rau, D.C. and Parsegian, V.A., Science, 249, 1278, 1990.
6. Israelachvili, J.W. and Wennerstrom, H., Langmuir, 6, 873, 1990.
7. Parsegian, V.A. and Rand, R.A., Langmuir, 7, 1299, 1991.
8. Rand, R.P. and Parsegian, V.A., Biochimica et Biophysica Acta, 988, 351, 1989.
9. Mahanty, J. and Ninham, B., Dispersion Forces, Academic Press, London, 1976.
10. Israelachvili, J.N., Q. Rev. Biophys., 6, 341, 1974.
11. Lifshitz, E.M., Sov. Phys., J.E.T.P., 2, 73, 1956.
12. McLachlan, A.D., Proc. Roy. Soc. London, A271, 387, 1963.
13. McLachlan, A.D., Proc. Roy. Soc. London, A274, 80, 1963.
14. Casimir, H.B.G. and Polder, D., Phys. Rev. 73, 360, 1948.

15. Israelachvili, J.N., Proc. Roy. Soc., London, A331, 39, 1972.
16. Imura, H. and Okano, K., J. Chem. Phys., 58, 2763, 1973.
17. McLachlan, A.D., Disc. Farad. Soc., 40, 239, 1965.
18. Israelachvili, J.N. and Tabor, D., Proc. Roy. Soc., A331, 19, 1972.
19. Haydon, D.A. and Taylor, J.L., Nature (London), 217, 739, 1968.
20. Parsegian, V.A., Ann. Rev. Biophys. Bioeng., 2, 221, 1973.
21. Marcelja, S., Biochim. Biophys. Acta, 367, 165, 1974.
22. Israelachvili, J.N., Marcelja, S. and Horn, R.G., Quart. Rev. Biophys., 13, 121, 1980.
23. Hill, T.L., Thermodynamics of Small Systems, Vols. 1&2, W.A. Benjamin Inc., New York, 1963,
24. Bentz, J. and Düzgünes, N., Biochemistry, 24, 5436, 1985.
25. Cornell, B.A., Middlehurst, T. and Separovic, F., Biochem. Biophys. Acta, 598, 405, 1980.
26. Hallen, R.M., Ph.D. Thesis, IIT Kanpur, 1981.
27. T.K. Khan, IIT Kanpur, personal communication.
28. Sheetz, M.P. and Chan, S.I., Biochemistry, 11, 4573, 1972.
29. Lichtenberg, D., Peterson, N.O., Girardet, J., Kainosho, M., Kroon, P.A., Seiter, C.H.A., Feigenson, G.W. and Chan, S.I., Biochim. Biophys. Acta, 382, 10, 1975.
30. Gennes, R.B., Biomembranes: Molecular Structure & Function, Springer-Verlag, New York, Berlin, Heidelberg, 1989, Chapter 7.
31. Grant, E.H., Sheppard, R.J. and South, G.P., Dielectric Behaviour of Biological Molecules in Solution, Clarendon Press, Oxford, 1978, Chapter 6.
32. Scaife, B.K.P., Theory of Dielectric, Clarendon Press, Oxford, 1989.
33. Friedman, H.L., J. Chem. Phys., 76, 1092, 1982.

34. Lam, J., J. Applied Physics, 60, 4230, 1986.
35. Günther, K. and Heinrich, D., Zeitschrift für Physik, 185, 345, 1965.
36. Felderhof, B.U., Ford, G.W. and Cohen, E.G.D., J. Stat. Phys., 28, 135, 1982.
37. Felderhof, B.U., Ford, G.W. and Cohen, E.G.D., J. Stat. Phys., 28, 649, 1982.
38. Felderhof, B.U., J. Phys. C, 15, 3943, 1982.
39. Felderhof, B.U., J. Phys. C, 15, 3953, 1982.
40. Geigenmüller, U. and Mazur, P., Physica, 136A, 316, 1986.
41. Felderhof, B.U., Ford, G.W. and Cohen, E.G.D., J. Stat. Phys., 33, 241, 1983.
42. Dukhin, S.S. and Shilov, V.N., Dielectric phenomena and the double layer in disperse systems and polyelectrolytes. Halsted Press, Wiley, New York, 1974.
43. Fricke, H., Phys. Rev., 24, 575, 1924.
44. Hansen, J. and McDonald, I.R., Theory of Simple Fluids, Academic Press, 1986.
45. Gray, C.G. and Gubbins, K.E., Theory of Molecular Fluids, Vol. 1, Oxford University Press, 1984.
46. Friedman, H.L., A Course in Statistical Mechanics, Prentice Hall, 1985.
47. Friedman, H.L. and Dale, W.D.T. in Modern Theoretical Chemistry, Volume 5A, B.J. Berne Ed., Plenum Press, New York, London, 1977, p. 85.
48. Percus, J.K. in Equilibrium Theory of Classical Fluids, Ed. Stell, G. and Lebowitz, J.L., Benjamin Inc., 1964.
49. Stell, G. in Equilibrium Theory of Classical Fluids, Ed. Stell, G. and Labowitz, J.L., Benjamin Inc., 1964.
50. Friedman, H.L., Ionic Solution Theory, Wiley Interscience, 1962.
51. Carnie, S.L. and Patey, G.N., Adv. in Chem. Phys., 56, 141, 1984.



52. Blum, L., Adv. in Chem. Phys., 78, 171, 1990.
53. Henderson, D. (Ed.), Fundamentals of Inhomogeneous Fluids, Marcel Dekker Inc., 1992.
54. Allen, M.P. and Tildesley, D.J., Computer Simulation of Liquids, Clarendon, Oxford, 1989.
55. Gillan, M.J., Mol. Phys., 38, 1781, 1979.
56. Abernethy, G.M. and Gillan, M.J., Mol. Phys., 39, 839, 1980.
57. Labik, S., Malijevsky, A. and Vonka, P., Mol. Phys., 56, 709, 1985.
58. Watts, R.O., Statistical Mechanics, Vol. 1, Specialist Periodical Report ed. by K. Singer (The Chemical Society, London), 1973, p.1.
59. Teran, L.M., Diaz-Herrera, E., Lozada Casou, M. & Saavedra-Barrera, R., J. Comp. Phys., 84, 326, 1989.
60. Rasaiah, J.C. and Friedman, H.L., J. Chem. Phys., 48, 2742, 1968.
61. Rasaiah, J.C. and Friedman, H.L., ibid, 50, 3965, 1965.
62. Ramanathan, P.S., Krishnan, C.V. and Friedman, H.L., J. Solution Chem., 1, 237, 1972.
63. Ramanathan, P.S. and Friedman, H.L., J. Chem. Phys., 54, 1086, 1971.
64. Larsen, B., J. Chem. Phys., 68, 4511, 1978.
65. Rasaiah, J.C., ibid, 56, 3071, 1972.
66. Friedman, H.L. and Krishnan, C.V., J. Phys. Chem., 78, 1927, 1974.
67. Friedman, H.L. and Ramanathan, P.S., ibid, 74, 3756, 1970.
68. Krishnan, C.V. and Friedman, H.L., J. Solution Chem., 3, 727, 1974.
69. Rasaiah, J.C., J. Solution Chem., 2, 301, 1973.
70. Rossky, P.J. and Friedman, H.L., J. Chem. Phys., 72, 5694, 1980.

71. Rossky, P.J., Judowicz, J.B., Tembe, B.L. and Friedman, H.L., *ibid*, 73, 3372, 1980.
72. Patey, G.N., *J.Chem. Phys.*, 72, 5763, 1980.
73. Teubner, M., *ibid*, 75, 1907, 1981.
74. Rosenfeld, Y. and Ashcroft, N.W., *Phys. Rev. A*, 20, 1208, 1979.
75. Malijevsky, A. and Labik, S., *Mol. Phys.*, 60, 663, 1987.
76. Sanchez, J. and Lozada-Cassou, M., *Chem. Phys. Lett.*, 190, 22, 1992.
77. Friedman, H.L., Zebolsky, D.M. and Kalman, E., *J. Solution Chem.*, 5, 853, 1976.
78. Friedman, H.L. and Krishnan, C.V., *J. Phys. Chem.*, 78, 1927, 1974.
79. Klug, A., Franklin, R.F. and Humphrey-Owens, S.P.F., *Biochim. Biophys. Acta*, 32, 203, 1959.
80. Hiltner, P. and Kriger, I.M., *J. Phys. Chem.*, 73, 2386, 1969.
81. Barday, L. Harrington, A. and Ottewill, R.H., *Koll. Ze Z. Polym.* 250, 655, 1972.
82. Schaefer, D.W. and Berne, B.J., *Phys. Rev. Lett.*, 32, 1110, 1974.
83. Schaefer, D.W. and Ackerson, B.J., *Phys. Rev. Lett.*, 35, 1448, 1975.
84. Williams, R., Crandell, R.S. and Wojtowitz, P.J., *ibid*, 37, 348, 1976.
85. Clark, N.A., Hurd, A.J. and Ackerson, B.J., *Nature* 281, 58, 1979.
86. Alexander, S., Chaikin, Grant, P., Morales, G.J. and Pincus, P., *J. Chem. Phys.*, 80, 3776, 1984.
87. Lindsay, H.M. and Chaiken, P., *J. Chem. Phys.*, 76, 3774, 1982.
88. Pieranski, P., *Contemp. Phys.*, 24, 25, 1983.
89. Pusey, P.N. in *Liquids, Freezing and the Glass Tranmsition*.

Hanse, J.P., Levesque, D. and Zinn-Justin, J., Eds. North Holland, Amsterdam, 1991.

90. Clark, N.A. and Ackerson, B.J., Phys. Rev. Lett., 44, 1005, 1980.
91. Clark, N.A. and Ackerson, B.J., Physica (utrecht) 118A, 221, 1983.
92. Bernal, J.D. and King, S.V., in Physics of Simple Liquids, H.N.V. Temperley, Rowlinson, J.S. and Rushbrooke, G.S., North Holland, Amsterdam, 1968.
93. Riley, D.P. and Oster, Discuss. Faraday. Soc., 11, 107, 1951.
94. Doty, P. and Steiner, R.F., J. Chem. Phys., 20, 85, 1951.
95. Steiner, R.F., Ph.D. Thesis, Harvard University, 1950.
96. Brown, J.C., Pusey, P.N., Goodwin, J.W. and Ottewill, R.H., J. Phys. A 8, 664, 1978.
97. Schaefer, D.W., J. Chem. Phys., 66, 3980, 1977.
98. Hayter, H.B. and Penfold, J., J. Chem. Soc. Faraday Trans. I, 77, 1851, 1981.
99. Hayter, J.B. and Zemb, T., Chem. Phys. Lett., 93, 91, 1982.
100. Bendedouch, D., Chen, S.H. and Koehler, W.C., J. Phys. Chem., 87, 2621, 1983.
101. Bendedouch, D. and Chen, S.H., J. Phys. Chem., 87, 1653, 1983.
102. Triolo, R., Hayter, J.B., Magid, L.J., Johnson Jr. J.S., J. Chem. Phys., 1983, 79, 1977.
103. Veerway, E.W. and Overbeek, J.Th.G. Theory of the Stability of Lyophilic Colloids, Elsevier, New York, 1948.
104. Bratko, D., Friedman, H.L. and Zhong, E.C., J. Chem. Phys., 85, 377, 1986.
105. Belloni, L., J. Chem. Phys., 88, 5143, 1988.
106. Medina-Noyola, M., and McQuarrie, D.A., ibid, 73, 6279, 1980.
107. Sheu, E.Y., Wu, C.F., Chen, S.H. and Blum, L., Phys. Rev.,

A32, 3807, 1985.

108. Chao, Y.S., Sheu, E.Y. and Chen, S.H., J. Phys. Chem., 89, 4395, 4862, 1985.
109. Sheu, E.Y., Wu, C.F. and Chen, S.H., J. Phys. Chem., 90, 4179, 1986.
110. Evans, D.F., Mitchell, D.J. and Ninham, B.W., J. Phys. Chem., 88, 6344, 1984.
111. Waisman, E. and Lebowitz, J.L., J. Chem. Phys., 56, 3086, 1972.
112. Waisman, E. and Labowitz, J.L., J. Chem. Phys., 56, 3093, 1972.
113. Blum, L., Mol. Phys., 30, 1529, 1975.
114. Blum, L. and Hoyer, J.S., J. Phys. Chem., 81, 1311, 1977.
115. Hiroike, K., Mol. Phys. 33, 1195, 1977.
116. Waisman, E., Mol. Phys. 25, 45, 1973.
117. Hoyer, J.S. and Blum, L., J. Stat. Phys., 19, 317, 1978.
118. Blum, L., J. Stat. Phys., 22, 661, 1980.
119. Gillan, M., Larsen, B., Tosi, M.P. and March, N.H., J. Phys. C., 9, 889, 1976.
120. Hoyer, J.S. and Stell, G., Mol. Phys., 32, 195, 1976.
121. Hoyer, J.S. and Blum, L., J. Stat. Phys., 16, 399, 1977.
122. Cummins, P.T. and Smith, E.R., Mol. Phys., 38, 997, 1979.
123. Hayter, J.B. and Penfold, J., Mol. Phys., 42, 109, 1981.
124. Hoyer, J.S., Stell, G. and Waisman, E., Mol. Phys., 32, 209, 1976.
125. Pastore, G., Nappi, C., De Angelis, U. and Forlani, A., Phys. Lett., A 78, 75, 1980.
126. Palmer, R.G. and Weeks, J.D., J. Chem. Phys., 58, 4171, 1973.
127. Hansen, J.P. and Hayter, J.B., Mol. Phys., 46, 651, 1982.

128. Hayter, J.B., Faraday Discuss, Chem. Soc., 76, 7, 1983.
129. Belloni, L., J. Chem. Phys., 85, 519, 1986.
130. Beresford-Smith, B., Chan, D.Y.C. and Mitchell, D.J., J. Colloid Interface Sci., 105, 216, 1985.
131. Medina-Noyola, M., J. Chem. Phys., 77, 1428, 1982.
132. Nagele, G., Klein, R. and Medina-Noyola, M., J. Chem. Phys., 83, 2560, 1985.
133. Khan, S., Morton, T.L. and Ronis, D., Phys. Rev. A 35, 4295, 1987.
134. Elkoubi, D., Turq, D. and Hansen, J.P., Chem. Phys. Lett., 52, 493, 1977.
135. Rogers, F.J., J. Chem. Phys., 73, 6272, 1980.
136. Beresford-Smith, B. and Chan, D.Y.C., Chem. Phys. Lett., 92, 474, 1982.
137. Belloni, L., Chem. Phys., 99, 43, 1985.
138. Bratko, D., Friedman, H.L., Chen, S.H. and Blum, L., Phys. Rev. A34, 2215, 1986.
139. Linse, P. and Jonsson, B., J. Chem. Phys., 78, 3167, 1983.
140. Linse, P., J. Chem. Phys., 93, 1376, 1990.
141. Linse, P., J. Chem. Phys., 94, 3817, 1991.
142. Linse, P., *ibid*, 94, 8227, 1991.
143. Fushiki, M., J. Chem. Phys., 89, 7445, 1988.
144. Lowen, H., Hansen, J.P. and Madden, P.A., J. Chem. Phys., 98, 3275, 1993.
145. Jepsen, D.W. and Friedman, H.L., J. Chem. Phys., 38, 846, 1963.
146. Wertheim, M.S., J. Chem. Phys., 55, 4291, 1971.
147. Adelman, S.A. and Deutsch, J.M., J. Chem. Phys., 59, 3971, 1973.
148. Blum, L. and Toruella, A.J., J. Chem. Phys., 56, 303, 1972.

149. Blum, L., *ibid*, 57, 1862, 1972.
150. Blum, L., *ibid*, 58, 3295, 1973.
151. Adelman, S.A. and Deutsch, J.M., *ibid*, 60, 3935, 1974.
152. Blum, L., *ibid*, 61, 2129, 1974.
153. Blum, L., *Chem. Phys. Lett.*, 26, 200, 1974.
154. Blum, L., *J. Stat. Phys.*, 18, 451, 1978.
155. Chan, D.Y.C., Mitchell, D.J. and Ninham, B.W., *J. Chem. Phys.*, 70, 2946, 1979.
156. Hoyer, J.S., Lebowitz, J.L. and Stell, G., *J. Chem. Phys.*, 61, 3253, 1974.
157. Stell, G. in *Modern Theoretical Chemistry*, Vol. 5A, B.J. Berne Ed., Plenum Press, 1977.
158. Patey, G.N., *Mol. Phys.*, 34, 427, 1977.
159. Patey, G.N., Levesque, D. and Weis, J.J., *ibid*, 38, 219, 1979.
160. Patey, G.N., *ibid*, 35, 1413, 1978.
161. Patey, G.N., Levesque, D. and Weis, J.J., *Mol. Phys.*, 38, 1635, 1979.
162. Chan, D.Y.C. and Walker, G.R. *Mol. Phys.*, 47, 881, 1982.
163. Levesque, D., Weis, J.J. and Patey, G.N., *J. Chem. Phys.*, 72, 1887, 1980.
164. Patey, G.N., Levesque, D. and Weis J.J., *Phys. Lett. A* 66, 115, 1979.
165. Patey, G.N. and Fries, P.H., *J. Chem. Phys.*, 82, 429, 1985.
166. Lee, L.Y., Fries, P.H. and Patey, G.N., *Mol. Phys.*, 55, 751, 1985.
167. Perkyns, J.S., Fries, P.H. and Patey, G.N., *Mol. Phys.*, 57, 529, 1986.
168. Caillol, J.M., Levesque, D., Weis, J.J., Kusalik, P.G. and Patey, G.N., *ibid*, 62, 461, 1987.
169. Kusalik, P.G. and Patey, G.N., *J. Chem. Phys.*, 88, 7715,

1988.

170. Kusalik, P.G. and Patey, G.N., *ibid*, 89, 5843, 1988.
171. Kusalik, P.G. and Patey, G.N., *ibid*, 92, 1345, 1990.
172. Torrie, G.M., Kusalik, P.G. and Patey, G.N., *ibid*, 88, 7826, 1988.
173. Torrie, G.M., Kausalik, P.G. and Patey, G.N., *ibid*, 89, 3285, 1988.
174. Torrie, G.M., Kusalik, P.G. and Patey, G.N., *ibid*, 90, 4573, 1989.
175. Torrie, G.M., Kusalik, P.G. and Patey, G.N., *ibid*, 91, 6367, 1989.
176. Perera, A. and Patey, G.N., *ibid.*, 91, 5316, 1989.
177. Bell, G.M. and Levine, S., *Trans. Farad. Soc.*, 54, 785, 1958.
178. Senatore, G. and Blum, L., *J. Phys. Chem.*, 89, 2676, 1985.
179. Vlachy, V., Pohar, C. and Haymet, A.D.J., *J. Chem. Phys.*, 88, 2066, 1988.
180. Ichiye, T. and Haymet, A.D.J., *J. Chem. Phys.*, 89, 4315, 1988.
181. Ichiye, T. and Haymet, A.D.J., *ibid*, 93, 8954, 1990.
182. Vlachy, V., Ichiye, T. and Haymet, A.D.J., *J. Amer. Chem. Soc.*, 113, 1077, 1991.
183. Foiles, S.M., Aschroft, N.W. and Reatto, J. *Chem. Phys.*, 80, 4441, 1984.
184. Attard, P. and Patey, G.N., *J. Chem. Phys.*, 92, 4970, 1990.
185. Duh, D.M. and Haymet, A.D.J., *ibid*, 97, 7716, 1992.
186. Lozada-Cassou, M. and Diaz-Herrera, E., *Chem. Phys. Lett.* 127, 392, 1986.
187. Lozada-Cassou, M. and Diaz-Herrera, E., *J. Chem. Phys.*, 93, 1386, 1990.
188. Lozada-Cassou, M. and Henderson, D., *J. Colloid. Interface Sci.*, 114, 180, 1986.

189. Bratko, D., Blum, L. and Luzar, A., J. Chem. Phys., 83, 6367, 1985.
190. Cummins, P.T. and Blum, L., *ibid*, 84, 1833, 1986.
191. Blum, L., Cummins, P.T. and Bratko, D., *ibid*, 92, 3741, 1990.
192. Luzar, A., Bratko, D. and Blum, L., *ibid*, 86, 2995, 1986.
193. Lozada-Cassou, M., J. Chem. Phys., 75, 1412, 1981.
194. Lozada-Cassou, M., *ibid*, 77, 5258, 1982.
195. Lozada-Coussou, M., J. Phys. Chem., 87, 3279, 1983.
196. Gonzales-Tovar, E. and Lozada-Cassou, M., J. Phys. Chem., 93, 3761, 1989.
197. Elhebil, F. and Premilat, S., Biophys. Chem., 42, 195, 1992.
198. Premilat, S. and Elhebil, F., J. Chem. Phys., 96, 9034, 1993.



## CHAPTER II

### COULOMBIC INTERACTION IN MACROIONIC SOLUTION **EFFECT OF POLARIZATION OF MACROION DIELECTRIC**

## 2.1 Introduction

When an ion approaches a dielectric discontinuity as is present on the interface between a macroion and the solvent, it induces bound charge at the interface. The ion differentially polarizes the two media, because their dielectric constant and polarizability are different. The different density of induced dipole moments do not cancel off at the interface. The interaction between the point charge and the bound charge on the macroion-solvent interface gives rise to terms in the energy of interaction which are absent in the expression of interaction between two point charges. These interactions can also be thought of as arising due to the presence of fictitious charges called image charges that lie inside in the macroion dielectric, while the point ion lies in the solvent medium outside the macroion. The formula of energy of a charge distribution near a dielectric is a standard problem in electrostatics, yet a closer examination of the textbook presentations suggest need for further clarification of the physics behind the mathematical equations (1-5). The statistical mechanics of ions near a dielectric discontinuity provided by a planar dielectric surface has been considered by several authors (6-23). The problem is of interest in the theory of surface tension of electrolytes (6,7). An ion senses a repulsive force due to the image charge located in air, when it approaches the air water interface from the aqueous solvent side. The force would have been attractive if

the ion was approaching from the air side of the interface. This repulsion decreases ionic concentration at the interface and increases surface tension. The planar geometry is also the geometry of choice when dielectric constant of macromolecular media have been taken into account in theory because of its simplicity. The experiments on forces between bilayers has also inspired these theoretical estimates, which makes a realistic calculation of forces between bilayers possible. In calculations on macromolecular spheres, the image charge has been ignored (24).

The problem of taking image charges into account is a difficult one. An ion induces polarized bound charges in the dielectric. The potential arising from the bound charges is proportional to the charge of the ion and is a function of the spatial co-ordinates. In the case of the planar dielectric, cylindrical co-ordinate is used. The distance  $z$  from the surface and the  $(r, \theta)$  on the  $xy$  plane at  $z = z_0$  ( $z$ -axis being the line perpendicular to the surface passing through the location of the point ion) are used to specify potential arising from bound charges. The process of polarization by the point ion does not create any net charge, by the principle of conservation of charge, but reorganizes charge, i.e., creates induced multipole moments, whose potential is angle dependent. The polarising charge ( $Q$ ) senses the potential created by virtue of its own polarization giving rise to terms in potential energy

proportional to  $Q^2$ . It also senses the potential created by polarization by other charges ( $Q'$ ), giving rise to terms in proportional to  $QQ'$ . The potential energy of a system of ions near two closely spaced dielectric interface is given by (10)

$$U_N = \frac{1}{2} \sum_{\substack{\nu, \lambda=1 \\ \nu \neq \lambda}}^N \left[ \frac{q_\nu q_\lambda}{\epsilon_1 |\bar{R}_\nu - \bar{R}_\lambda|} + u_{\nu\lambda}^{\text{core}} (|\bar{R}_\nu - \bar{R}_\lambda|) \right] \\ + \frac{1}{2} \sum_{\nu, \lambda=1}^N q_\nu q_\lambda \phi^{\text{im}} (\bar{R}_\nu, \bar{R}_\lambda) + \sum_{\nu=1}^N v_\nu^{\text{ext}}(z_\nu) + v^{\text{S-S}} \quad (1)$$

where

$u_{\nu\lambda}^{\text{core}}$  is the ion-ion core potential.

$\phi^{\text{im}} (\bar{R}_\nu, \bar{R}_\lambda)$  is the potential at  $\bar{R}_\nu$  created by image effects associated with a unit charge at  $\bar{R}_\lambda$ .  $\epsilon_1$  is the dielectric permittivity of the solvent.

$v_\nu^{\text{ext}} (z_\nu)$  contains the short range wall potentials ( $v_\nu^{\text{sh}}$ ) and (if present) the interaction with the uniform surface charge or the homogeneous background charge and  $v^{\text{S-S}}$  is the direct interaction between two surfaces. Kjellander and Marcelja (10-12) prefer to use image potentials, i.e., potential due to bound charges, rather than explicitly considering image charges. The potential at a point  $(\bar{r}_\nu, z_\nu)$  due to a unit point charge located at  $(\bar{r}_\lambda, z_\lambda)$  and the associated induced surface charge at the plane of dielectric discontinuity

$$\phi (r_{\nu\lambda}, z_{\nu}, z_{\lambda}) = \frac{1}{\epsilon_1 R_{\nu\lambda}} + \phi^{\text{im}}$$

The second term in the expression of  $U_N$  given above can be split into two parts, the self-image interactions

$$\frac{1}{2} \sum_{\nu=1}^N u_{\nu\nu}^{\text{im}} (0, z_{\nu}, z_{\nu}) \quad \text{and the}$$

pairwise interactions

$$\sum_{\nu>\lambda=1}^N u_{\nu\lambda}^{\text{im}} (r_{\nu\lambda}, z_{\nu}, z_{\lambda}). \quad \text{The factor of half in the}$$

expression of self image potential is to be noted and will be discussed in detail in section 2.3. The self image term is the term proportional to  $Q^2$  referred to above and the pairwise term have been called the term proportional to  $QQ'$  above. In the case of ions near a wall, the self image term is a function only of the  $z$ -coordinate of the ion. Thus it is natural to consider it as arising from the surface. The surface is not part of the system of ions and this potential "due to the surface" is called  $V^{\text{ext}}(z_{\nu})$ . The term  $u_{\nu\lambda}^{\text{im}}(r_{\nu\lambda}, z_{\nu}, z_{\lambda})$  when grouped with the direct charge-charge interaction potential gives rise to a term that is dependent on  $r_{\nu\lambda}$  and therefore is called net interaction potential. Unlike the usual pairwise additive Coulomb potential in the absence of a surface, this potential although pairwise additive for a given configuration of ions, is dependent on  $z_{\nu}$  and  $z_{\lambda}$ , i.e., are not translationally invariant. The two terms

both arise because of image potential and are therefore coupled.  $r_{\nu\lambda}, z_{\nu}, z_{\lambda}$  cannot be independently varied. The difficulty of handling image effect arises here. Much of liquid state physics formalism has been developed assuming that the external potential and the internal many body potentials can be varied independently and that the latter are translationally invariant.

In our system of a macroion and point ions (with size) in a dielectric continuum, the macroion is, in a natural way, a component, part of the system. We therefore have no external potential, as is found in the treatment of planar dielectrics. For a system of a macroion and two ions the potential energy of interaction is a sum of (a) three two particle charge-charge pair potentials  $(\frac{Q_m Q_1}{r_{1m}} + \frac{Q_m Q_2}{r_{2m}} + \frac{Q_1 Q_2}{r_{12}})$  which depend on the distance between three pairs, (b) image charge interactions of  $Q_1$  and  $Q_2$  with their own respective image potentials (due to bound charges polarized by itself) and (c) with image potentials due to the other charge  $(Q_1^2 \phi_{im}^{(1)} + Q_1 Q_2 \phi_{im}^{(1)} + Q_1 Q_2 \phi_{im}^{(2)} + Q_2^2 \phi_{im}^{(2)})$ .  $\phi_{im}^{(1)}$  and  $\phi_{im}^{(2)}$  are potentials generated by an unit charge that depend on coordinates of particles 1 and particle 2. It is shown in section 3, that the terms  $Q_1^2 \phi_{im}^{(1)}$  and  $Q_2^2 \phi_{im}^{(2)}$  contain terms inversely proportional to integral powers of distance between the charge and the macroion. These terms can be added to the  $Q_1 Q_2 / \epsilon_s r_{12}$  (where  $\epsilon_s$  is the static relative permittivity of the solvent term) give an expression  $Q_1 Q_2 / \epsilon(r_{12}) r_{12}$ . The terms  $Q_1 Q_2 \phi_{im}^{(1)}$  and  $Q_1 Q_2 \phi_{im}^{(2)}$  depend on  $(\vec{r}_{1m})$  and  $(\vec{r}_{2m})$  where the

origin is the center of the macroion. A similar situation exists in interaction with a planar dielectric where  $u_{\nu\lambda}$  is a function of  $r_{\nu\lambda}$ ,  $z_\nu$ ,  $z_\lambda$ . We can write it as  $Q_1 Q_2 f(\vec{r}_1, \vec{r}_2)$ . Similar terms depending on co-ordinates of three particles exist for all other pairs. A system of two macroions and one point ion will have the added complication of interaction between the polarized bound charge distributions on the two macroions. This is in addition to the usual charge-charge interaction between the three pairs formed by the ion and the two macroions, the interaction between ion and the bound charges on the two macroions and the interaction between one macroion and the induced bound charge on the other. The interaction between the polarized charges is called in the image charge language formation of multiple images. Further if we ignore these, the potential energy of a system of two ions and two macroions will have  $Q_1 Q_2$  terms multiplied by a function of  $\vec{r}_m$  of one macroion in a coordinate system fixed at the origin of the other as well as  $(\vec{r}_1, \vec{r}_2)$ . In more complex configurations with more macroions, the number of co-ordinates increase. It is, a complex many body problem.

Kjellander and Marcelja (13,14), for a system of ions near a planar interface and between two planar interfaces show that the grand canonical partition function and the distribution function of the system is equivalent to that of a two dimensional M component mixture. A particular layer, i.e., a particular value of the co-ordinate  $z$  corresponds to a particular "species" in a

two dimensional mixture. The theory of an inhomogeneous three dimensional fluid near a planar wall can be strictly mapped onto the theory for a two dimensional multicomponent homogeneous fluid. They have applied this theory to several systems (15-18) with excellent results. This mapping has become possible because of the geometry of the system. At a given  $z$ , the wall potential, which includes charge-self image interaction ( $Q^2$  terms), depends only on  $z$  and the potential between a pair of ions has translational invariance on a X-Y plane.

In some studies (19-21), the interaction energy between a charge and the bound charge polarized by all other ions, which depends on the coordinates of all ions in solution is replaced by an effective potential energy dependent on the coordinate of only this particular charge. The expression of the effective potential energy was first given by Onsager and Samaras (6) (hereafter called OS potential) and later has been rederived in different contexts by other authors (7-12). It is the charge-image interaction energy multiplied by a screening term due to the presence of all other charges, the screening term being  $e^{-2\kappa x}$ , where  $x$  is the distance of the ion from the interface and  $\kappa$  is the well known Debye screening constant, calculated from bulk ion densities. It is easy to handle this term, since it depends only on the coordinate of a single ion, effectively an external field due to the wall. The potential has been used in Monte Carlo calculations (19,20), HNC, as well as in



Born-Green-Yvon (BGY) theory (21). The agreement of HNC calculation with OS potential with simulation results, that use OS potential and that consider the system of all image charges explicitly is good according Torrie et al (19,20) but is not found to be satisfactory by Croxton et al (21).

Nicholls and Pratt (7) in their studies on surface tension of ionic solutions have treated the system of charge and image charges as an interacting system of charges ( $U_{ir}$  is the charge-image charge interaction potential, i.e., unscreened OS potential,  $U_{rr}$  is the usual Coulomb potential;  $i$  = image-charge,  $r$  = real-charge) have used cluster theory under low ionic strength limiting condition to derive integral equations applicable near a surface and rederive Onsager-Samaras equation as the potential of mean force, the screening resulting from interaction in the system of image-charges and real charges. In contrast to Kjellander and Marcelja (13,14) they use image-charges explicitly.

Another approach to handling image charges has been the use of Modified Poisson-Boltzmann equation (22,23). This theory arose out of Kirkwood's early work (25). Outhwaite has applied lowest order Born-Green-Yvon integral equation to the double layer problem and has derived a modified Poisson-Boltzmann equation (26). In this approach, a fluctuation potential describes the electrostatic potential in the presence of a fixed ion and the mean potential that arises from the solution of the

Poisson-Boltzmann equation. It has been possible to include image forces in the fluctuation potential (22,23). Torrie et al (19) find excellent agreement between Monte Carlo calculation that includes all image charges explicitly and the prediction of modified Poisson-Boltzmann theory and call this theory an unqualified success. In all these calculations, only planar geometry has been handled.

In the theory of dielectric constant of a system of polarizable molecular spheres, the effect of polarizability has been considered by many workers (27-33). Wertheim (28-30), in particular has developed graph theoretical analysis using topological reduction and resummation to obtain expressions of correlation function in a system of polarizable molecules. We have not worked out the relationship of these techniques to the topological reduction and resummation methods discussed in Chapter III. They are apparently different. It is possible that Wertheim's methods can be used in this problem also. The system studied by them are not charged. Wertheim's method (28-30) and that of Høye and Stell (31) replace the many body forces by effective two body angle-dependent forces. Computer experiments (34,35) show that such replacements give correct results. Polarization effects in ionic systems, with specific reference to computer simulation studies are discussed in a recent paper by Wilson and Madden (36).

In order to understand effects of polarization of the macroion dielectric by a point ion in solution, we found it necessary to understand certain standard text book material from first principles. This is given in sections 2.2 and 2.3. .

## 2.2 Screening Constant of a System of Two Point Ions

A standard book theorem (1-5) in electrostatics states that the field due to a polarized dielectric, outside as well as inside a dielectric is given by the field due to a bound surface charge density  $\vec{P} \cdot \vec{n}$  (where  $\vec{n}$  is the outward normal to the surface) and a bound volume charge density  $-\vec{\nabla} \cdot \vec{P}$ , where  $\vec{P}$  is the polarization density, i.e., dipole moment per unit volume. The field due to the charges that cause polarization has to be superimposed on it to obtain the total field. A standard solved example in textbooks (3) is that of a point charge at the center of a spherical dielectric of relative dielectric permittivity  $\epsilon_s$  and radius  $R$ . The polarization on the surface (the direction of the polarization vector is the same as that of the outward pointing normal) is given by

$$\frac{Q}{4\pi R^2} \left(1 - \frac{1}{\epsilon_s}\right) \hat{n}, \text{ since } \vec{D} = \frac{Q}{R^2} \hat{n} \text{ (by Gauss's law using spherical symmetry)}$$

and using  $\vec{D} = \epsilon_s \vec{E}$ ,  $\vec{E} = \frac{Q}{\epsilon_s R^2}$ , we obtain  $\vec{P} \cdot \vec{n} = \frac{Q}{4\pi R^2} \left(\frac{\epsilon_s - 1}{\epsilon_s}\right)$  at all points on the surface. The total surface charge is

$$Q = \int_S \vec{P} \cdot \hat{n} \, d\vec{a} = Q \left( \frac{\epsilon_s^{-1}}{\epsilon_s} \right) \left( \int_S d\vec{a} = 4\pi R^2 \right). \quad \text{It is obvious that this}$$

result holds even if the surface is not spherical. By divergence theorem, for any vector  $\vec{P}$ , we have  $\int_S \vec{P} \cdot \hat{n} \, d\vec{a} = \int_V \text{div } \vec{P} \, dv$

where  $V$  is the volume enclosed by the surface. The enclosed dielectric is homogeneous, i.e.,  $\text{div } \vec{P}$  is zero everywhere excepting the origin where the free point charge is located (3).

This follows from

$$\vec{P} = \frac{\vec{D} - \vec{E}}{4\pi} = \frac{\vec{D}}{4\pi} \left\{ (\epsilon_s - 1) / \epsilon_s \right\}$$

In a homogeneous dielectric  $\epsilon_s$  is not a function of position

$$\begin{aligned} \therefore \text{div } \vec{P} &= \frac{\epsilon_s^{-1}}{4\pi\epsilon_s} \text{div } \vec{D} \\ &= \frac{\epsilon_s^{-1}}{\epsilon_s} \rho_{\text{free}} \\ \rho_{\text{bound}} &= -\text{div } \vec{P} \quad \therefore \quad \rho_{\text{bound}} = \frac{-(\epsilon_s - 1)}{\epsilon_s} \cdot \rho_{\text{free}} \end{aligned}$$

in a homogeneous dielectric. In addition using spherical symmetry of  $\vec{D}, \vec{E}, \vec{P}$ ,

$$\text{div } \vec{P} = \frac{1}{r} \frac{d}{dr} r^2 P = 0$$

since  $\epsilon_s$  is constant,  $P$  is a function of  $r^2$  alone and  $r^2 P$  is independent of  $r$ . The volume integral of  $\text{div } \vec{P}$  located at the origin is calculated by considering a sphere of radius  $\delta$  (no material inside) around  $Q$ , calculate  $\int_S \vec{P} \cdot \hat{n} \, d\vec{a}$  for this sphere

(now the  $\vec{n}'$  vectors are opposite to  $\hat{n}$  at the outer surface,  $S'$  is the surface of the sphere of radius  $\delta$ ) and let  $\delta \rightarrow 0$ . For the inner surface,  $\int_{S'} \vec{P} \cdot \vec{n}' d\vec{a} = -Q \left( \frac{\epsilon_s^{-1}}{\epsilon_s} \right)$  (negative sign arises

because  $\vec{P}$  due to the charge is still pointing radially outward and  $\vec{n}'$  points radially inward).  $\int_{S+S'} \vec{P} \cdot \vec{n} d\vec{a} = 0$  as it should be,

because the enclosed dielectric is homogeneous and no point charge is embedded in the dielectric ( $\vec{\nabla} \cdot \vec{P} = 0$  everywhere in the enclosed volume). As  $\delta \rightarrow 0$ ,  $\int_{S'} \vec{P} \cdot \vec{n}' da'$  becomes  $\int_V \text{div } \vec{P} dv$ ,

because the inner surface now becomes a point, the origin where  $Q$  is located. Thus the charge on the inner surface becomes a concentrated volume charge at the center of a magnitude

$-Q \left( \frac{\epsilon_s^{-1}}{\epsilon_s} \right)$ . The net charge at the origin is  $Q_{\text{net}} = Q - Q \left( \frac{\epsilon_s^{-1}}{\epsilon_s} \right) = \frac{Q}{\epsilon_s}$ .

The dielectric is then replaced by a polarized point charge  $-Q \left( \frac{\epsilon_s^{-1}}{\epsilon_s} \right)$  at the origin and a distributed total surface charge  $+Q \left( \frac{\epsilon_s^{-1}}{\epsilon_s} \right)$  at the surface. The original field generating charge  $Q$  is also at the origin. The field inside the dielectric is due to a net charge  $Q_{\text{net}} = Q - Q \left( \frac{\epsilon_s^{-1}}{\epsilon_s} \right) = \frac{Q}{\epsilon_s}$  at the origin, if the surface is sufficiently far away to make the effect of surface charge inconsequential. Now that the dielectric has been replaced by only polarized charges there is no material left to

worry about. Now we bring a second point charge from infinity to a point at a distance,  $r$  from the origin. The potential energy of interaction is given by  $V(r) = \frac{QQ'}{\epsilon_s r}$ . The charge that comes in does not cause any additional polarization, because there is no matter to polarize. In addition we note that the field generating charge is held fixed. The work done on it by the charge being brought is not counted, because even though  $\vec{F} \neq 0$ , there is no displacement. One requires external agency to hold it in position. But work done by them is not counted as electrostatic energy.

## 2.3 Energy of a system of charges in the presence of a dielectric

It is a standard textbook result (1,2) that the work done in assembling a system of fixed charges in the presence of a dielectric, that they polarize is given by

$$W = \frac{1}{8\pi} \int \vec{E} \cdot \vec{D} \, dv, \text{ where the integration runs over all space.}$$

It is easily shown (3) that this expression equals  $\frac{1}{2} \int \rho_f V \, dv$ , where the integration has to go over the location of the free charge distribution. The  $V$  of this expression arises from free charges and polarized bound charges. The formula looks similar to that of a system of free charges in the absence of the dielectric, but it cannot be taken over in the treatment in the presence of a dielectric without further justification, because, for one, the work done on the polarized body to bring it from an unpolarized to a polarized state has to be taken into account.

The energy of a system of free charges in the presence of dielectrics is at first sight given by

$$U = \frac{1}{2} \int \rho_f V_f dv + \int \rho_f V_b dv,$$

where  $V_f$  is the potential at the location of a free charge due to other free charges and  $V_b$  is the potential due to polarized bound charges. The factor of a 1/2 in front of the first term is to avoid double counting. The second term has no such factor. However, the above equation is not quite correct since it holds if the dielectric is already polarized. Evidently we must consider the energy spent by the system of free charges in polarizing the dielectric. The energy of a dielectric body placed in an electric field whose sources are located in vacuum and are held fixed is given in textbooks (1,2). It is this energy that we must subtract from the expression of  $U$  given above to obtain total energy of the system of free charges. This expression of energy of a dielectric body in vacuum in the field of fixed charges is  $-\frac{1}{2} \int_V \vec{P} \cdot \vec{E}_0 dv$ , where  $\vec{P}$  is the polarisation of the dielectric body and  $\vec{E}_0$  is the electric field due to fixed charges only, in the absence of dielectric (the polarized dielectric modifies this field to  $\vec{E}$ , but we have only  $\vec{E}_0$  in the formula). The integral goes only over the volume of the body, because  $\vec{P} = 0$  outside the body. It is easily shown that  $-\frac{1}{2} \int_V \vec{P} \cdot \vec{E}_0 dv = +\frac{1}{2} \int \rho_f V_b dv$ . This is the work done by the fixed electric charges on the dielectric. The charge distribution does work on the dielectric by separating charges in the dielectric and

thereby reduces their own energy by  $\frac{1}{2} \int \rho_f V_b dv$ . Thus, the energy of the system of free charges (held fixed) in presence of a dielectric is given by

$$\begin{aligned} U_{\text{total}} &= \frac{1}{2} \int_V \rho_f V_f dv + \int_V \rho_f V_b dv - \frac{1}{2} \int_V \rho_f V_b dv \\ &= \frac{1}{2} \int_V \rho_f (V_f + V_b) dv = \frac{1}{2} \int_V \rho_f V dv; \end{aligned}$$

in textbooks (3) starting from  $-\frac{1}{8\pi} \int \vec{E} \cdot \vec{D} dv$ .

We now sketch the equivalence used above,

$$\begin{aligned} -\frac{1}{2} \int_V \vec{P} \cdot \vec{E}_0 dv &= -\frac{1}{2} \int_{\text{all space}} \vec{P} \cdot \vec{E}_0 dv \quad (\vec{P} = 0 \text{ outside } V) \\ &= +\frac{1}{2} \int_V \vec{P} \cdot \vec{\nabla} V_f dv = +\frac{1}{2} \int_V (\vec{\nabla} \cdot V_f \vec{P}) dv - \frac{1}{2} \int_V (\vec{\nabla} \cdot \vec{P}) V_f dv \\ &= +\frac{1}{2} \int_S (V_f \vec{P}) \cdot \vec{n} da + \frac{1}{2} \int_{\text{all space}} \rho_b V_f dv \quad (\text{we recall } -\vec{\nabla} \cdot \vec{P} = \rho_{\text{bound}} = \rho_b) \\ &\quad \text{at infinity} \\ &= 0 + \frac{1}{2} \int_V \rho_b V_f dv. \quad (\text{Since } \rho_b \text{ and } \vec{P} \text{ are zero outside } V). \\ &= +\frac{1}{2} \int_V \rho_b V_f dv + \frac{1}{2} \int_V \rho_f V_b dv \end{aligned}$$

(since it is immaterial, whether the free charges are considered as field generating and bound charges as field sensing or vice versa).

The formula of the energy of the polarized body is obtained in the presence of fixed charges. When the dielectric is introduced in the presence of already assembled charges, work is done on the dielectric to bring it to a state of polarization.



The polarized body exerts force on the fixed charges, but no work is done on them because the source charges are kept in fixed location, with the aid of external agencies. The difference in energy in the presence and in the absence of the dielectric (i.e. change in  $\frac{1}{8\pi} \int_V \vec{E} \cdot \vec{D} dv$ ) is thus solely due to work done on the dielectric to separate the charges, i.e., to polarize it and this term for a dielectric in a vacuum is  $-\frac{1}{2} \int \vec{P} \cdot \vec{E}_0 dv$ . If the dielectric is not in vacuum, but is embedded in another dielectric of different permittivity,  $\vec{P}$  is not the polarization, but the difference in polarization. This is all about the energy stored in the bound charges in the dielectric. However, as the bound charges get created, they interact with the sources that produce them. This interaction can be equivalently viewed from two different angles. In one view, we assemble the source charges in the presence of already polarized dielectric. (To assume that the dielectric is already polarized is in keeping with the spirit of electrostatics, where all field generating charges, must be held fixed). In the other equivalent view, the source charges are held fixed. The bound charges, when absent, i.e., before polarization, can be thought to be at infinity. Polarization process "assembles" them at their final location, in the field of the fixed source charges. The energy of this interaction is thus  $\int \rho_f V_b dv$  and equivalently  $\int \rho_b V_f dv$ .

In the presentation given above, we assemble the free charges in the presence of an already polarized dielectric ( $U = \frac{1}{2} \int \rho_f V_f dv + \int \rho_f V_b dv$ ) and then again polarize the dielectric in the presence of already assembled free charges ( $U = - \frac{1}{2} \int \rho_f V_b dv$ ). This sequence is a little complex since it is not clear whether free charges are assembled first or the dielectric is polarized first.

An equivalent simpler way to assemble the configuration of free charges and the dielectric is to first assemble the free charges, work done by the external agency being  $\frac{1}{2} \int \rho_f V_f dv$ , then one inserts the dielectric keeping the free charges fixed. In doing so, the free charges spend an energy  $\frac{1}{2} \int \rho_f V_b dv$ : the external agency replenishes this to keep the free charges fixed. Total work done by the external agency =  $\frac{1}{2} \int \rho_f V dv$ , where  $V = V_f + V_b$ . This is the total energy of the system of free charges in the presence of a dielectric.

The result obtained by a mathematical transformation of  $\frac{1}{8\pi} \int \vec{E} \cdot \vec{D} dv$  to  $\frac{1}{2} \int \rho_f V dv$  is the same as that obtained above, but the identification of different contributions to  $\frac{1}{2} \int \rho_f V dv$  makes the physics clearer. Amongst textbooks Jackson (1) mentions the mathematical equivalence of the two, Corson and Lorrain (3) assumes that the energy is  $\frac{1}{2} \int \rho_f V dv$  without justification and Griffiths (4) identifies  $W_{\text{Total}} = W_{\text{free}} + W_{\text{bound}} + W_{\text{spring}}$ . His  $W_{\text{spring}}$  is the energy stored in the dielectric. But he states, without proof that  $W_{\text{bound}}$  cancels

$W_{\text{spring}}$ , a statement, which as we understand, is incorrect.

The problem of the calculation of energy of two interacting point charges in a dielectric medium (section 2.2) is more easily handled using this formula. The Poisson's equation of a point ion  $Q$  in a dielectric ( $\epsilon_s$ ) is  $\epsilon_s \nabla^2 \phi = Q$ . This is equivalent to  $\nabla^2 \phi = Q/\epsilon_s$ , i.e. the mathematical equivalent of being able to replace the dielectric, by merely reducing the charge by a factor of  $1/\epsilon_s$  to get the effect of the dielectric polarization. A bound charge  $-Q(\frac{\epsilon_s - 1}{\epsilon_s})$  is thus created at the location of the point ion. Two ions of charge  $Q_1, Q_2$  at a distance  $r$  in the dielectric, are both replaced by  $Q_1/\epsilon_s$  and  $Q_2/\epsilon_s$  in vacuum. Energy calculation uses the formula  $\frac{1}{2} \int_V \rho_f V dv = \frac{1}{2} \left\{ Q_1 \frac{Q_2}{\epsilon_s r} + Q_2 \frac{Q_1}{\epsilon_s r} \right\} = \frac{Q_1 Q_2}{\epsilon_s r}$ .

## 2.4 Screening Constant of a System of an Ion and a Macroion

Let us now consider a system of a point ion and a macroion (surface charge density  $\sigma$ , radius  $r_0$ , relative dielectric permittivity  $\epsilon_1$ ), embedded in the solvent dielectric (of infinite extent) of relative dielectric permittivity  $\epsilon_s$ . (The following development on electrostatics follows Landau and Lifshitz (2)).

We combine three equations  $\vec{D} = \epsilon \vec{E}$ ,  $\text{div} \vec{D} = 0$ ,  $\vec{E} = -\nabla \phi$ , to obtain

$$\text{div} (\epsilon \nabla \phi) = 0$$

The equation becomes the ordinary Laplace's equation only in a homogeneous dielectric medium. The boundary conditions on the

surface separating two isotropic dielectrics written in terms of potential are  $\phi_1 = \phi_2$ ,  $\epsilon_1 \left( \frac{\partial \phi_1}{\partial n} \right) = \epsilon_2 \left( \frac{\partial \phi_2}{\partial n} \right) + 4\pi\sigma$ , where  $\partial\phi/\partial n$  is the component of  $\nabla\phi$  in the direction outward normal, to the interface between 1 and 2, pointing from 1 to 2 and  $\sigma$  is the charge density at the interface. This equation becomes the ordinary Laplace's equation  $\nabla^2\phi = 0$ , if  $\epsilon$  is not a function of position, i.e., if the dielectric is homogeneous. If a dielectric medium is piecewise homogeneous, then it reduces to  $\nabla^2\phi = 0$  in each homogeneous region, so that the dielectric permeability appears only through the boundary conditions and in the Poisson's equation that holds at the location of the point charge. The charge  $Q$  is located in the homogeneous dielectric continuum of permittivity  $\epsilon_s$ . So Poisson's equation is  $\epsilon_s \nabla^2\phi = Q$  or,  $\nabla^2\phi = Q/\epsilon_s$ . The boundary conditions, as is easily seen above, involve only the ratio of the dielectric permeabilities of the two adjoining media. In particular, the boundary condition of an electrostatic problem for a dielectric body of permeability  $\epsilon_2$  surrounded by a medium of permeability  $\epsilon_1$  (with charge density  $\sigma$  at the interface) is the same as for a body of permeability  $\epsilon_2/\epsilon_1$  surrounded by a vacuum with a charge density  $\sigma/\epsilon_1$  at the interface. The real system under consideration by us is a dielectric sphere of radius  $r_0$  of dielectric constant  $\epsilon_1$  and charge density  $\sigma$  embedded in a dielectric continuum of dielectric constant  $\epsilon_s$  with a polarizing charge of magnitude  $Q$  at a distance  $d_0$  from the center of the sphere. The equivalent simpler

system is a sphere of radius  $r_0$ , dielectric permittivity  $\epsilon_1/\epsilon_s$  and surface charge density  $\sigma/\epsilon_s$  placed in vacuum at a distance  $d_0$  from the point charge which now has a magnitude  $Q/\epsilon_s$ . There is only one dielectric discontinuity, i.e., at the surface of the sphere. We will therefore have polarized bound charge at the interface. In the real system the point ion differentially polarizes the solvent and the macroion dielectric resulting in a surface charge along the interface of the macroion and solvent. In the simpler model system, the vacuum is not polarized, the medium in the sphere (dielectric permittivity  $\epsilon_1/\epsilon_s$ ) is polarized, to result in induced surface charge density. Since relative permittivity undergoes a step change at the macroion surface, we obtain a nonzero value of  $-\vec{\nabla} \cdot \vec{P}$ , which in this case is the surface charge  $\left( \frac{1}{r} \frac{\partial}{\partial r} (r^2 P) \right)$  is a delta function at  $r = r_0$ , since  $r^2 P$  undergoes a step change at  $r = r_0$ , this  $\delta(r-r_0)$  converts the volume charge to a surface charge. The energy of interaction is calculated from the expression  $\frac{1}{2} \int_V \rho_f V dv$  where  $V$  arises from both free and bound charges. Thus, to calculate energy, we require the magnitude of electrical potential at the location of free charges. This is done by solving Laplace's Equation. We solve Laplace's equation for the simpler equivalent problem of a sphere of dielectric permittivity  $\epsilon_1/\epsilon_s$ , radius  $r_0$  and surface charge density  $\sigma/\epsilon_s$  embedded in vacuum with a charge of magnitude  $Q/\epsilon_s$  at a distance  $d_0$  from the center to obtain values of  $V$  at all points in space, in particular at the location

of free charges to be able to compute  $\frac{1}{2} \int \rho_f V d\tau$ . Since the net induced charge on the surface of dielectric discontinuity is zero, by principle of conservation of charge, the potential energy of interaction between the spherical surface charge of macroionic sphere (permanent and glued to the surface) and the nonspherical induced charge distribution turns out to be zero. If we consider the permanent surface charge distribution to lie inside the induced charge distribution on the same surface (the energy is invariant to whether it is considered to be inside or outside, so long as they are both very close to the surface), we can, by using Gauss's Law replace the spherically symmetric permanent surface charge distribution by a point charge at the center. The interaction of this point charge ( $Q_1$ ) with the nonspherical induced charge distribution ( $\sigma(\theta)$ , azimuthal symmetry)

$$U = \int \int Q_1 \frac{\sigma(\theta)}{r_o^2} r_o^2 \sin\theta \, d\theta \, d\phi = Q_1 \iint \sigma(\theta) \sin\theta \, d\theta \, d\phi \quad (2)$$

The integral is proportional to the net induced charge and its magnitude is zero; making  $U = 0$ .

We only require  $V$  at the location of the point charge  $Q$  to calculate  $(\frac{1}{2}) \int \rho_f V \, dv$ . In the following, we solve Laplace's equation.

The general form of the solution of Laplace's equation is given by:

$$\phi_1 = \sum_{n=0}^{\infty} a_n r^n P_n(\mu) \quad \mu = \cos\theta \quad (3)$$

$0 < r < r_0$

$$\phi_2 = \frac{Q}{\epsilon_s d_0} \sum_{n=0}^{\infty} \left( \frac{r}{d_0} \right)^n P_n(\mu) + \sum_{n=0}^{\infty} B_n r^{-n-1} P_n(\mu) \quad (4)$$

$r_0 < r < d_0$

$$\phi_3 = \frac{Q}{\epsilon_s r} \sum_{n=0}^{\infty} \left( \frac{d_0}{r} \right)^n P_n(\mu) + \sum_{n=0}^{\infty} B_n r^{-n-1} P_n(\mu) \quad (5)$$

$d_0 < r < \infty$

Boundary Conditions are:

- (1) (a)  $\phi_1 = \phi_2$  at  $r = r_0$ ;  
 (b)  $\phi_2 = \phi_3$  at  $r = d_0$  is automatically satisfied  
 by virtue of the form of Eqs. (2) and (3),
- (2) (a)  $\hat{n} \cdot (\vec{\nabla} \phi_2 - (\epsilon_1/\epsilon_s) \vec{\nabla} \phi_1) = -4\pi(\sigma/\epsilon_s)$  at  $r = r_0$   
 or  $\frac{\partial \phi_2}{\partial r} - \left( \epsilon_1/\epsilon_s \right) \frac{\partial \phi_1}{\partial r} = -4\pi (\sigma/\epsilon_s)$  at  $r = r_0$

(b) This condition is automatically fulfilled at  $r = d_0$ .

From boundary condition 2(a), we obtain

$$\begin{aligned} & \frac{Q}{\epsilon_s d_0} \sum_{n=0}^{\infty} n \cdot \frac{r_0^{n-1}}{d_0^n} P_n(\mu) + \sum_{n=0}^{\infty} B_n (-n-1) r_0^{-n-2} P_n(\mu) \\ & - (\epsilon_1/\epsilon_s) \left[ \sum_{n=0}^{\infty} a_n n \cdot r_0^{n-1} P_n(\mu) \right] = -4\pi (\sigma/\epsilon_s) \end{aligned} \quad (6)$$

We now equate terms of the same  $n$  on both sides of the equation.

This is possible because the equations hold at the same  $r$  for all  $\theta$  and because of the orthonormality of the Legendre Polynomials. We then obtain for the  $n = 0$  term

$$-B_0 r_0^{-2} = -4\pi(\sigma/\epsilon_s) \quad \text{or, } B_0 = \frac{4\pi\sigma r_0^2}{\epsilon_s}$$

We define total charge on the macroion  $Q_m = (4\pi r_0^2)\sigma$

$$\therefore B_0 = \frac{Q_m}{\epsilon_s}$$

The  $n = 0$  term is the contribution of the net charge of the macroion to the field outside the sphere at  $r = d_0$

$$(\phi_2) = \frac{Q_m}{\epsilon_s d_0} + \frac{Q}{\epsilon_s d_0} \quad (7)$$

The formula  $U = \frac{1}{2} \int \rho \phi_V dv$  gives rise to the well known screened charge-charge interaction term

$$U = \frac{1}{2} \left\{ \frac{Q}{\epsilon_s d_0} \cdot Q_m + Q \cdot \frac{Q_m}{\epsilon_s d_0} \right\} = \frac{QQ_m}{\epsilon_s d_0} \quad (8)$$

The term  $Q^2/\epsilon_s d_0$  is not part of energy of interaction. It is however part of total energy. Terms with  $n \neq 0$ ; similarly give

$$\frac{Q}{\epsilon_s d_0} n \frac{r_0^{n-1}}{d_0^n} - B_{n_0}^{(n+1)} r_0^{-n-1} - (\epsilon_1/\epsilon_s) a_n n r_0^{n-1} = 0 \quad (9)$$

From boundary condition 1(a), we have



$$\sum_{n=0}^{\infty} a_n r_o^n P_n(\mu) = \frac{Q}{\epsilon_s d_o} \sum_{n=0}^{\infty} \left( \frac{r_o}{d_o} \right)^n P_n(\mu) + \sum_{n=0}^{\infty} B_n r_o^{-(n+1)} P_n(\mu) \quad (10)$$

Equating coefficients of  $P_n(\mu)$  for each  $n$ , we obtain for  $n = 0$ ,

$$a_o = \frac{Q}{\epsilon_s d_o} + \frac{B_o}{r_o} = \frac{Q}{\epsilon_s d_o} + \frac{Q_m}{\epsilon_s r_o} \quad (11)$$

and for  $n \neq 0$

$$a_n r_o^n = \frac{Q}{\epsilon_s d_o} \left( \frac{r_o}{d_o} \right)^n + B_n \cdot r_o^{-(n+1)} \quad (12)$$

Rearranging Eq. (6) we obtain

$$(\epsilon_1/\epsilon_s) a_n n \cdot r_o^{n-1} = \frac{Q}{\epsilon_s d_o} n \frac{r_o^{n-1}}{d_o^n} - B_n (n+1) r_o^{-n-2}$$

$$\text{or, } a_n r_o^{n-1} = \frac{Q}{\epsilon_1 d_o} \frac{r_o^{n-1}}{d_o^n} - \frac{\epsilon_s}{\epsilon_1} B_n \cdot \frac{n+1}{n} \cdot r_o^{-n-2}$$

$$\text{or, } a_n r_o^n = \frac{Q}{\epsilon_1 d_o} \frac{r_o^n}{d_o^n} - \frac{\epsilon_s}{\epsilon_1} B_n \cdot \frac{n+1}{n} \cdot r_o^{-n-1}$$

Equating R.H.S. of Eqs. (9) and (10) we obtain

$$\begin{aligned} \frac{Q}{\epsilon_s d_o} \left( \frac{r_o}{d_o} \right)^n + B_n r_o^{-(n+1)} &= \left( \frac{\epsilon_s}{\epsilon_1} \right) \left( \frac{Q}{\epsilon_s d_o} \right) \left( \frac{r_o}{d_o} \right)^n \\ &- \left( \frac{\epsilon_s}{\epsilon_1} \right) B_n \left( \frac{n+1}{n} \right) r_o^{-(n+1)} \end{aligned}$$

or,

$$B_n r_o^{-(n+1)} \left\{ \left( \frac{n+1}{n} \right) \left( \frac{\epsilon_s}{\epsilon_1} \right) + 1 \right\} = \frac{Q}{\epsilon_s d_o} \left( \frac{r_o}{d_o} \right)^n \left( \frac{\epsilon_s}{\epsilon_1} - 1 \right)$$

or,

$$B_n = \frac{Q}{\epsilon_s d_o} \left( \frac{r_o}{d_o} \right)^n \frac{1}{1 + \left( \frac{n+1}{n} \right) \left( \frac{\epsilon_s}{\epsilon_1} \right)} r_o^{n+1} \left( \frac{\epsilon_s}{\epsilon_1} - 1 \right) \quad (13)$$

where  $n \neq 0$ .

The potential outside the sphere due to the  $n$ th induced multipole on the sphere is given by  $B_n r^{-(n+1)} P_n(\mu)$ . The point charge that senses the field lies on the  $z$ -axis, i.e.,  $\mu = \cos\theta = 1 \therefore P_n(\mu) = 1$  for all  $n$ . We then obtain

$$V_n(r=d_o) = B_n d_o^{-(n+1)} = \frac{Q}{\epsilon_s d_o} \left( \frac{r_o}{d_o} \right)^n \frac{1}{1 + \left( \frac{n+1}{n} \right) \left( \frac{\epsilon_s}{\epsilon_1} \right)} \left( \frac{\epsilon_s}{\epsilon_1} - 1 \right) \left( \frac{r_o}{d_o} \right)^{n+1} \quad (14)$$

We recall that the energy is calculated by taking the energy of the free charges in the field of free and bound charges. The free point charge has a magnitude  $Q$ . The interaction energy between the charge  $Q$  and the potential due to the  $n$ th ( $n \geq 1$ ) induced multipole (with a factor  $1/2$ ) is

$$E^{(n)} = \frac{1}{2} Q V^{(n)} = \frac{Q^2}{2\epsilon_s d_o} \left( \frac{r_o}{d_o} \right)^{2n+1} \frac{1}{1 + \left( \frac{n+1}{n} \right) \left( \frac{\epsilon_s}{\epsilon_1} \right)} \left( \frac{\epsilon_s}{\epsilon_1} - 1 \right) \quad (15)$$

The leading term  $n = 1$ , the dipolar term is

$$E^{(1)} = \frac{Q^2}{2\epsilon_s d_o} \left(\frac{r_o}{d_o}\right)^3 \cdot \frac{1}{1 + 2 \left(\frac{\epsilon_s}{\epsilon_1}\right)} \left(\frac{\epsilon_s}{\epsilon_1} - 1\right)$$

The  $n = 0$  term contributes in the expression of interaction energy.

$$E_o = \frac{Q_m Q}{\epsilon_s d_o}, \text{ as obtained in Eq. (8)}$$

Setting  $Q = \alpha Q_m$ , we obtain

$$E = E_o + E_1 = \frac{QQ_m}{\epsilon_s d_o} \left[ 1 + \frac{\alpha}{2(1+2(\epsilon_s/\epsilon_1))} \left(\frac{r_o}{d_o}\right)^3 \left(\frac{\epsilon_s}{\epsilon_1} - 1\right) \right] \quad (16)$$

Summing over terms involving multipoles higher than dipole

$$E = \frac{QQ_m}{\epsilon_s d_o} \left[ 1 + \frac{\alpha}{2} \sum_n \frac{1}{1 + \left(\frac{n+1}{n}\right) \left(\frac{\epsilon_s}{\epsilon_1}\right)} \left(\frac{r_o}{d_o}\right)^{2n+1} \left(\frac{\epsilon_s}{\epsilon_1} - 1\right) \right] \quad (17)$$

The term in the bracket multiplied by  $\frac{1}{\epsilon_s}$  is called  $\frac{1}{\epsilon_{eff}}$ , the inverse of the effective screening constant of the charge-charge interaction term. In the limit  $\epsilon_1 = \epsilon_s$ , and in the limit  $d_o \gg r_o$ , it reduces to  $\frac{1}{\epsilon_s}$ .

We may now verify that the potential energy of the permanent charge distribution on the macroionic surface due to interaction with bound polarized surface charge is zero. The energy of  $\rho_f$  is given by

$$\begin{aligned}
U &= \int \rho_f \phi_1 (r = r_o) da \\
&= \int_s \rho_f \sum_n a_n r_o^n P_n (\cos\theta) da \\
&= \sum_n a_n \int_s \rho_f P_n (\cos\theta) da \\
&= \sum_n a_n \rho_f \int_s P_n (\cos\theta) r_o^2 \sin\theta d\theta d\phi \\
&\quad \text{(since } \rho_f \text{ is constant on the surface)} \\
&= \sum_n a_n \rho_f 2\pi r_o^2 \int_0^\pi P_n (\cos\theta) \sin\theta d\theta
\end{aligned}$$

The term with  $n \neq 0$  go to zero, since  $\int_{-1}^{+1} P_n(x) dx = \int_{-1}^{+1} P_n(x) P_0(x) dx = \delta_{no}$

$\therefore U = a_o \rho_f 4\pi r_o^2$  (we note  $\rho_f = \frac{\sigma_s}{\epsilon_s}$ , where  $\rho_f$  is the surface charge density of the model problem and  $\sigma_s$  is the actual surface charge density)

$$\begin{aligned}
&= \frac{Q}{\epsilon_s d_o} (\rho_f 4\pi r_o^2) + \frac{Q_m}{\epsilon_s r_o} (\rho_f \cdot 4\pi r_o^2) \\
&= \frac{QQ_m}{\epsilon_s d_o} + \frac{Q_m^2}{\epsilon_s r_o} \tag{18}
\end{aligned}$$

This first term has already been counted. The second term is the

self energy term of the macroion charge. It is not counted as energy of interaction. Thus macroionic surface charge gives zero interaction energy with bound polarized charge.

## 2.5 Point ion-Macroion Interaction, Viewed from the Macroion and the point ion

An apparent dichotomy arises if we look at point-ion macroion interaction, treating macroion in the field of point ion and the charges polarized by it in the dielectrics or in the reverse order, treating point ion in the field of macroion and the charges polarized by it in the dielectrics. The dielectric is an infinite solvent dielectric ( $\epsilon_s$ ) with a macroion dielectric ( $\epsilon_1$ ) embedded in it. If point ion (Q) is the polarizing charge, it induces  $+Q(\frac{\epsilon_s - 1}{\epsilon_s})$  on the surface, which is far away and  $-Q(\frac{\epsilon_s - 1}{\epsilon_s})$ , the cavity charge, which lies at the location of point ion Q. It also induces a charge distribution with a net charge zero (principle of conservation of charge) on the surface of the macroion. This induction takes away the spherical symmetry of the problem. We are no longer allowed to write the following equality, which we did for a point charge in the absence of the dielectric

$$\int_s \vec{D} \cdot \vec{n} \, da = 4\pi R^2 D_n \text{ (or its equivalent for } \vec{E})$$

Therefore we cannot write  $D_n = \frac{Q}{R^2}$  and  $P_n = (\frac{\epsilon_s - 1}{\epsilon_s}) \frac{Q}{4\pi R^2}$ . But

$\int_s P_n da = Q(\frac{\epsilon_s - 1}{\epsilon_s})$  still holds, since the net charge in the dielectric is still  $Q$ . Thus the total charge  $Q(\frac{\epsilon_s - 1}{\epsilon_s})$  is distributed non-spherically on the surface. The magnitude of the cavity charge, by principle of conservation of charge is its negative. Now that the dielectric is polarized, it can be replaced by the induced surface charges. We can now place the macroion surface charge of density  $\sigma$ . It interacts with the point charge  $Q$ , and the induced charge  $-Q(\frac{\epsilon_s - 1}{\epsilon_s})$  lying at the identical location, i.e., with a net charge  $Q/\epsilon_s$ . This term is  $QQ_m/\epsilon_s$ . The energy of interaction of macroion surface charge with the induced charge on the macroion surface is zero as shown in section 2.4. The energy of interaction of  $Q$  with the surface charges induced by it is calculated in section 2.4. The energy of the polarized dielectric in the presence of the free charges has also been included there.

Let us now consider the problem in the reverse order. Let the macroion be the field-generating charge. The interaction energy is to be calculated as a sum of interaction energy of the point charge with the macroion and the charges induced by polarization due to the macroion. Let us first consider the macroion  $(r_o, \epsilon_1)$  located inside a spherical solvent dielectric  $(R, \epsilon_s)$ , the center of the macroion coinciding with that of the

spherical dielectric. The field due to the macroion at the dielectric surface is unaffected by  $\epsilon_1$  and therefore  $\int_S \vec{P} \cdot \vec{n} \, da$  at

the surface of the dielectric is given by  $Q' \left( \frac{\epsilon_s - 1}{\epsilon_s} \right)$ , where

$Q' = 4\pi r_0^2 \sigma$ . As seen earlier  $\int_S \vec{P} \cdot \vec{n} \, da$  is the net surface charge

on the dielectric surface. The induced volume charge  $(\text{div} \vec{P})$  is localised on the macroion surface because  $\rho_f \neq 0$  on this surface. The principle of conservation of charge dictates

that the net induced charge on the interface is  $-Q' \left( \frac{\epsilon_s - 1}{\epsilon_s} \right)$ . To

this we add macroion charge density  $\sigma$  ( $Q' = 4\pi r_0^2 \sigma$ ). Then the dielectric is removed. Only the charges, induced and permanent remain. The net charge inside the Gaussian sphere that encloses the macroion at the center and has the point ion on its surface, is  $\frac{Q'}{\epsilon_s}$ . The interaction energy is then  $\frac{QQ'}{\epsilon_s}$ . It appears, as

though, a difference is arising from the results of the analysis, which treats the point charge as the field generating charge. In the problem of a point ion in a spherical dielectric, the induced charge is a point charge, in contrast to the problem of a macroion where the induced charge is a distribution of charge on the interface. Whereas the point charge is not polarizable, the induced charge distribution is polarizable. The net charge of the distribution remains unaltered as a point charge is placed at a finite distance  $d_0$  but the distribution is polarized. The

resulting field is no longer given by the total charge on the macroion surface alone. The dipole and the higher multipole moments have to be considered. The polarizability of this induced charge distribution depends on  $\epsilon_1$  and  $\epsilon_s$  and is calculated by solving Laplace's equations. The magnitude of the induced charge as well as the polarizabilities of the distribution owe their origin to the different dielectric constant of the macroion dielectric and the solvent dielectric when the dielectrics are replaced by induced charges. The "memory" of the dielectrics remain not only in the magnitude of the charge, but also in the polarizability of the distribution. The text book example of induced charge is a point charge, which has no polarizability. If these polarizabilities are taken into account, then the point charge at a distance  $d_0$ , will induce moments, dipole as well as higher multipoles and the interaction energy will include, interaction energies between macroion charge and multipoles induced at the interface by the point charge. Once we take the polarizabilities of the induced charge distribution into account, it ceases to matter whether we take the macroion or the point ion as the charge generating object. The polarization by the point charge (which in this analysis occurs in vacuum) alters interactions of the macroion charge and polarized charges at the interface, i.e., modifies the self energy of the field generating charge. This 'self energy' is part of the interaction energy, because it disappears if the



magnitude of the point charge is set equal to zero or if it is shifted to infinity.

We may note that the simpler equivalent dielectric problem, of a dielectric sphere ( $r_0$ ,  $\epsilon_1/\epsilon_s$ ,  $\sigma/\epsilon_s$ ) in vacuum (section 2.4), introduces the effect of the cavity charge by replacing  $\sigma$  by  $\sigma/\epsilon_s$  right at the outset. It is not embedded in a solvent dielectric of permittivity  $\epsilon_s$  and therefore formally does not have a cavity or a cavity charge. The polarized bound charges at the interface is the same in the simplified model problem as in the original problem, as shown in section 2.4.

None of this dichotomy or confusion arises if one formally solves the Boundary value problem.

## 2.6 Screening Constant of a System of Two Interacting Macroions

Macroion 1 will interact with the charges it polarizes on the surface of macroion 2 and vice versa. The interaction energy can be calculated, after the dielectrics are replaced by replacing the permanent surface charge distribution by an equivalent point charge at the center. The interaction energy is

$$U = \frac{QQ'}{\epsilon_{\text{eff}} d_0} = \frac{QQ'}{\epsilon_s d_0} + \frac{QQ'}{d_0} \left( \frac{1}{\epsilon_{\text{eff}}} - \frac{1}{\epsilon_s} \right) \quad (19)$$

The treatment of point ion-macroion interaction takes the interaction between point ion and the total induced charge distribution into account, i.e. between point ion and all the induced multipoles. While treating the system of two macroions,

we have not calculated interaction between the two induced charge distributions, as well as interactions arising from moments induced by the induced multipole moments. These interactions are of higher order, but will contribute significantly at short distances. For a system of two interacting macroions, we obtain,

$$U = \frac{QQ'}{d_o} \left[ \frac{1}{\epsilon_s} + 2 \left( \frac{1}{\epsilon_{eff}} - \frac{1}{\epsilon_s} \right) \right]$$

The term within the [ ] is called  $1/\epsilon_{eff}$  for macroion-macroion interaction. In the limit  $\epsilon_s = \epsilon_1$  and in the limit  $d_o \gg r_o$ , it reduces to  $\frac{1}{\epsilon_s}$ .

## 2.7 Numerical Estimates of Effective Screening Constant: Significant Modification of the Screening Constant for a Nonspherical Particle

The leading term in the summation of Eq. (16) with  $n=1$ , (the dipolar term) and with  $\epsilon_s = 80$ ,  $\epsilon_1 = 5$ , gives at  $r_o = d_o$  a value of about  $\frac{1}{2}$ ; the limiting value for  $\epsilon_s \gg \epsilon_1$ . If the macroion charge is very low, such that  $\alpha = 1$ , then it is a significant interaction. Then,  $\epsilon_{eff} \approx 64$ . But even in system of moderate charge density on macroion surface (net charge  $\approx 25$  electronic charges) the interaction of the polarized charge distribution with the polarizing charge is negligible. Eq. (16) only incorporates a two-body interaction. The interaction of the system of a charge and its image charge, with other charges and of the charge with the image-charges due to other charges leads to a screening, represented by Onsager-Samaras potential for a planar surface. Irrespective of the form of the screening term

for a spherical surface, (the screening in any case only reduces the interaction) the image interaction will not be significant unless the macroion is virtually uncharged. The macroion-macroion interaction potential does not have the problem of having an  $\alpha \ll 1$  (Eq. 16). For two equally charged macroions  $\alpha = 1$ . But then the distance of closest approach is  $d_0 = 2r_0$ . In the  $n = 1$  term the term that adds to 1 in the bracketted expression of Eq. (16) is  $\frac{1}{32}$ . In the macroion-macroion interaction of Eq. (18), this gets multiplied by 2. The value of  $\epsilon_{\text{eff}}$  at the distance of shortest approach is  $\sim 76$  and approaches 80 at larger distances. Thus, we are justified in leaving out the image interactions altogether in calculations in Chapter III. However, the following consideration shows that the effect will be significant if the macroion deviates from spherical symmetry.

The zero interaction energy between the permanent surface charge and the induced surface charge owes its origin to the spherical symmetry of the macroion. For non-spherical particles, this interaction will not be zero.

The energy of interaction between a fixed charge distribution and an induced charge distribution on the macroion surface is given by

$$U = \frac{1}{2} \int da \int da' \frac{\sigma_{\text{fixed}}(\theta, \phi) \sigma_{\text{induced}}(\theta', \phi')}{|\vec{r} - \vec{r}'|}$$

where  $da$  and  $da'$  are located at  $\vec{r}(= r, \theta, \phi)$  and  $\vec{r}'(= r', \theta', \phi')$  respectively. In general this integral cannot vanish.

The point ion-macroion polarization effect turned out to be negligible only because  $Q^2 \ll QQ'$  ( $\alpha \ll 1$ ). But if the macroion is not spherical, the polarization effect will yield terms proportional to  $QQ'$  since  $Q' = 4\pi r_o^2 \sigma_{\text{fixed}}$  and  $\sigma_{\text{induced}}$  is proportional to  $Q$ . Thus  $\alpha$  being  $\ll 1$  will not matter. This effect will no longer be negligible. Since this term is proportional  $QQ'$ , it can be formally said to modify the screening constant (unlike terms proportional to  $Q^2$  which are included to modify screening constant for purposes of calculation only). Presence of a permanent dipole moment on the macroion will also introduce terms representing interaction with polarized charges, for spherical as well as nonspherical macroion. For macroion-macroion interaction,  $\alpha = 1$ . The distance of shortest approach is  $d_o(\text{min}) = 2r_o$ , where  $r_o$  is the macroion radius. As compared to a point ion, the polarizing macroion will be further off from the macroion being polarized, but its charge being larger, the induced charge on its surface will be significant. The interaction energy of the charge of the macroion being polarized with the polarized charges on its own surface is going to be substantial.

Presence of OS-type screening constant (the form may or may not remain  $e^{-2\kappa x}$ , where  $x$  is distance from macroion center) will modify this interaction energy, but at not too high a  $\kappa$ , (viz.  $\sim 10^6$ ), the screening will not lower the interaction by an order of magnitude.

## 2.8 Polarized Charge Distribution at the Macroion Surface

The model problem treated in 2.4 has vacuum in the exterior and dielectric permittivity  $\epsilon_1/\epsilon_s$  in the interior. The  $\vec{P} \cdot \vec{n}$  can therefore be calculated by considering only the polarization on the internal surface. The magnitude of  $\vec{P} \cdot \vec{n}$  (using  $\vec{P} = \frac{1}{4\pi} \vec{\nabla}(\vec{D} - \vec{E})$ )

$$\begin{aligned} & \frac{1}{4\pi} \left\{ (\epsilon_1/\epsilon_s) - 1 \right\} \left( - \frac{\partial \phi}{\partial r} \right) \Big|_{r=r_o} \\ &= - \frac{1}{4\pi} \frac{\epsilon_1 - \epsilon_s}{\epsilon_s} \sum_{n=0}^{\infty} A_n r_o^{n-1} P_n(\mu) \end{aligned}$$

We first note that  $n=0$  term does not contribute to the angular dependence of  $\vec{P} \cdot \vec{n}$ , which is given by  $P_n(\mu)$  for each term. We note  $A_n$  is positive, if  $Q$  is positive and vice versa. For the dipole term  $P_1(\mu) = \cos\theta$ . At  $\theta = 0$ ,  $P_1(\mu) = 1$ ,  $\epsilon_1 < \epsilon_s$  therefore the induced charge is positive if  $Q$  is positive and vice versa. Maximum value of  $P_1(\mu)$  is 1. Therefore the maximum density of induced charge is at  $\theta=0^\circ$ . At  $\theta = 90^\circ$ ,  $P_1(\mu) = 0$  and it is negative at  $\theta > 90^\circ$ . The equatorial charge density is zero. The hemisphere closer to the point charge carries the same sign as that of the point charge. The reverse is true for the other hemisphere. The net interaction is repulsive. The same is true for charge-planar dielectric systems (11,12). The net induced charge is zero, because

$$\begin{aligned} \int_S P_n(\cos\theta) da &= 2\pi r_o^2 \int_0^\pi P_n(\cos\theta) \sin\theta d\theta \\ &= 0, \quad \left( \text{using} \int_{-1}^{+1} P_n(x) P_o(x) dx = \delta_{no} \right) \end{aligned}$$

## REFERENCES

1. Jackson, J.D., Classical Electrodynamics, John Wiley, 2nd Edition, 1975, 10th Wiley Eastern Reprint, June, 1993, Chapter 4.
2. Landau, L.D. and E.M. Lifshitz, Electrodynamics of Continuous Media, Section 10, 11, Pergamon Press, 1963.
3. Corson, D. and Lorrain, P., Electromagnetic Fields and Waves, Chapter 3, W.H. Freeman and Company, San Fransisco, 1970.
4. Griffiths, D.J., Introduction to Electrodynamics, Prentice Hall, 2nd Edition, 8th Printing, Prentice Hall India, 1993, Chapter 4.
5. Panofsky, W. and Phillips, M., Classical Electricity and Magnetism, Addison-Wesley, 1962.
6. Onsager, L. and Samaras, N.N.T., J. Chem. Phys., 2, 528, 1934.
7. Nicholls, A.L. and Pratt, L.R., *ibid*, 76, 3782, 1981.
8. Guernsey, R.L., Phys. Fluids, 13, 2089, 1970.
9. Buff, F.P. and Stillinger, F.H., J. Chem. Phys., 25, 312, 1956.
10. Jancovici, B., J. Stat. Phys., 28, 43, 1982.
11. Carnie, S.L. and D.Y.C., Mol. Phys., 51, 1047, 1984.
12. Mitchell, D.J. and Richmond, P., J. Colloid and Interface Science, 46, 118, 1974.
13. Kjellander, R. and Marcelja, S., J. Chem. Phys. 82, 2122, 1985.
14. Kjellander, R. and Marcelja, S., *ibid*, 82, 7129, 1985.
15. Kjellander, R. and Marcelja, S., *ibid*, 88, 7138, 1988.
16. Kjellander, R. and Marcelja, S., J. Phys. Chem., 90, 1230, 1986.
17. Kjellander, R. and Marcelja, S., Chem. Phys. Lett., 127, 402, 1986.

18. Kjellander R. and Marcelja, S., Chem. Phys. Lett., 142, 485, 1987.
19. Torrie, G.M., Valleau, J.P. and Patey, G.N., J. Chem. Phys., 76, 4615, 1982.
20. Torrie, G.M. and Valleau, J.P., J. Phys. Chem., 86, 3251, 1982.
21. Croxton, T.L., McQuarrie, D.A., Torrie, G.M., Valleau, J.P. and Patey, G.N., Can. J. Chem., 59, 1998, 1981.
22. Bell, G.M. and Rangecroft, P.D., Mol. Phys. 24, 255, 1972.
23. Outhwaite, C.W., Bhuiyan, L.P. and Levine, S., J. Chem. Soc., Farad. Trans. II, 76, 1388, 1980.
24. Sanchez, J. and Lozada-Cassou, M., Chem. Phys. Lett., 190, 22, 1992.
25. Kirkwood, J.G., J. Chem. Phys. 2, 767, 1934.
26. Outhwaite, C.W., J. Chem. Soc. Faraday Trans. II, 74, 1214, 1978.
27. Scaife, B.K.P., Theory of Dielectrics, Oxford University Press, 1989.
28. Wertheim, M., Mol. Phys., 25, 211, 1973.
29. Wertheim, M., ibid, 26, 1425, 1973.
30. Wertheim, M., ibid, 33, 95, 1977.
31. Wertheim, M., ibid, 34, 409, 1977.
32. Hoye, J.S. and Stell, G., J. Chem. Phys., 73, 461, 1980.
33. Carnie, S.L. and Patey, G.N., Mol. Phys., 47, 1129, 1982.
34. Patey, G.N., Torrie, G.M. and Valleau, J.P., J. Chem. Phys., 71, 96, 1979.
35. Pollock, E.L., Torrie, G.M. and Valleau, J.P., J. Chem. Phys., 71, 96, 1976.
36. Wilson, M. and Madden, P.A., J. Phys., Condens. Matter, 5, 2687, 1993.

### CHAPTER III

## HNC THEORY OF MACROMOLECULES INTERACTING THROUGH CENTRAL POTENTIAL



## Introduction

In this chapter, we describe the method used by us to calculate correlation function of macroionic particles in solution. This method has been developed by Mayer, Meeron, Allnatt and has been used in calculating correlation function of ionic solution by Rasaiah and Friedman. The method has been described from first principles. The computer implementation are discussed in Chapter 5. In section 3.9, we describe a modification of the method, developed by us, in order to treat Coulombic systems, whose screening constant is a function of interparticle distance. In Chapter 2, we have seen how such a situation arises because of polarization of macroionic particles.

### 3.1 STATISTICAL MECHANICAL PRELIMINARIES

In statistical mechanics, one is interested in calculating properties of a system of many interacting particles. The mechanical state of the system is not completely specified. The preparation of the system places only gross constraints, such as specification of energy, and volume, but does not specify the position and velocity of an Avogadro number of particles. Thus the system has a range of accessible mechanical states in phase space, rather than an unique mechanical state. In geometrical language, a volume in phase space, rather than a single point is necessary to characterize its state. Specification of a mechanical state would require a single point. For calculation of properties, one assigns weight factors to every point in the accessible region in phase space. The measured equilibrium property of the system is identified as (for mechanical

properties) the average of the mechanical property defined at each point in phase space over the accessible region, duly weighted by the appropriate weight factor. Properties like entropy which have no mechanical counterpart are also calculated from these weight factors. The specification of the range of accessible states defines an ensemble. If the system is in a heat bath at temperature  $T$  and is enclosed in an impermeable container, then states of all energies (not exceeding that of the heat bath) are accessible to the system, the number of particles remaining fixed. This collection of accessible states is called a canonical ensemble. The weight factor of a mechanical state with particle 1 at  $\vec{r}_1$ , and having momentum  $\vec{p}_1$ , particle 2 at  $\vec{r}_2$  and having momentum  $\vec{p}_2$  and particle  $N$  at  $\vec{r}_N$  having an energy  $E$  ( $= T+V$ ) (the temperature of the bath being  $T$ ) is given, in the canonical ensemble, as

$$P(\vec{r}_1 \dots \vec{r}_N) = \frac{\exp(-E/kT) dp_1 \dots dp_{3N} dr_1 \dots dr_{3N}}{Z} \dots \quad (1)$$

where  $Z$ , the partition function is  $\int \exp(-E/kT) dp_1 \dots dp_{3N} dr_1 \dots dr_{3N}$ . In a more general ensemble, called the Grand Canonical ensemble, the number of particles can also vary in addition to energy, in going from one accessible state to another. The mechanical states are characterized by both. The energy is denoted by  $E_N(\vec{r}, \vec{p})$  where  $N$  is a set that specifies composition of the particle set  $N_1 \dots r$ ,  $\vec{r}$  is a set  $\vec{r}_1, \vec{r}_2 \dots \vec{r}_N$  and so is  $\vec{p}$ . The weight factor in the grand canonical ensemble of a state with (i) particle 1 at  $\vec{r}_1$  and having momentum  $\vec{p}_1$ , particle 2 at  $\vec{r}_2 \dots$  particle  $N$  at  $\vec{r}_N$  and having momentum  $\vec{p}_N$  (ii) the energy of

the system being E, (iii) the chemical potential of the bath being  $\mu$  and (iv) its temperature being T, is given by

$$P_N(\vec{r}_1, \dots, \vec{r}_N) = \exp(-E/kT) \exp(\vec{N} \cdot \vec{\mu}/kT) / \theta \dots \quad (2)$$

where  $\theta$  the grand canonical partition function given  $\theta = \sum_N \exp(\vec{N} \cdot \vec{\mu}/kT) Z_N$ ;  $\vec{N} \cdot \vec{\mu} = \sum_i N_i \mu_i$ ; and  $Z_N$  is the canonical partition function of a N particle system.

### 3.2 DISTRIBUTION FUNCTION

In the development of the theory, sums of these weight factors play an important role. One such is n-particle distribution function  $\rho_n(\vec{r}_1, \dots, \vec{r}_n)$  which is the sum of weight factors of all states which have position coordinates of any set of n particles, 1, 2, ..., n, at  $\vec{r}_1, \vec{r}_2, \dots, \vec{r}_n$  but have varying momenta of all particles and varying coordinates of particles n+1, ..., N (all particles unlabelled). The expression of  $\rho_n$  in the canonical ensemble is

$$\rho^{(n)}(\vec{r}_1, \dots, \vec{r}_n) = \frac{N!}{(N-n)!} \frac{\int \exp(-u_N(\vec{r}_1, \dots, \vec{r}_N)/kT) d\vec{r}_{n+1} \dots d\vec{r}_N}{\int \exp(-u_N(\vec{r}_1, \dots, \vec{r}_N)/kT) d\vec{r}_1 \dots d\vec{r}_N} \dots \quad (3)$$

where the factor  $\frac{N!}{(N-n)!}$  arises out of the fact that we are considering unlabelled particles. We note that

$$\int_V \dots \int \rho^{(n)}(\vec{r}_1, \vec{r}_2, \dots, \vec{r}_n) d\vec{r}_1 \dots d\vec{r}_n = \frac{N!}{(N-n)!} \dots \quad (4)$$

$\rho^{(n)}$  is more specifically called the generic distribution function in contrast to the specific distribution function  $P^n(\vec{r}_1, \dots, \vec{r}_n)$ , whose expression is identical, except that  $N!/(N-n)!$  is left out. The simplest distribution function  $\rho^{(n)}$  is  $\rho^{(1)}(\vec{r}_1)$ . The quantity  $\rho^{(1)}(\vec{r}_1)d\vec{r}_1$  is the sum of the weight factors of all states that share the common property of having any one of the particles, in an infinitesimal volume element around  $\vec{r}_1$ . In a homogeneous fluid  $\rho_1^{(1)}(\vec{r}_1)$  is independent of  $\vec{r}_1$  and we obtain

$$\frac{1}{V} \int \rho^{(1)}(\vec{r}_1) d\vec{r}_1 = \rho^{(1)} = \frac{1}{V} \left\{ \frac{N!}{(N-1)!} \right\} = \frac{N}{V} = \rho, \text{ the density.}$$

The quantity  $\rho^{(2)}(\vec{r}_1, \vec{r}_2) d\vec{r}_1 d\vec{r}_2$  is sum of weight factors of all states that share the common property that any one particle (unlabelled) is located within an infinitesimal volume element around  $\vec{r}_1$  and another particle is located within an infinitesimal volume element around  $\vec{r}_2$ . In the more usual language, it is the probability that one molecule is found within  $d\vec{r}_1$  around  $\vec{r}_1$  and another in  $d\vec{r}_2$  at  $\vec{r}_2$ . In a fluid without an external field,  $\rho^{(2)}$  depends only on interparticle separation

$$\rho^{(2)}(\vec{r}_1, \vec{r}_2) = \rho^{(2)}(r_{12}).$$

The independence of  $\rho^{(2)}$  of absolute location in space allows us to write,

$$\int_V \int_V \rho^{(2)}(r_{12}) d\vec{r}_1 d\vec{r}_2 = \int_V \int_V \rho^{(2)}(r_{12}) d\vec{r}_{12} d\vec{r}_1 = \int_V d\vec{r}_1 \int_V \rho^{(2)}(r_{12}) d\vec{r}_{12}$$

$$= V \int_V \rho^{(2)}(r_{12}) d\vec{r}_{12} = \frac{N!}{(N-2)!} = N(N-1) \text{ (using Eq. (4))}. \text{ If the}$$
 distribution is completely random, the distribution function  $\rho^{(n)}$  becomes

$$\rho^{(n)}(\vec{r}_1, \dots, \vec{r}_n) d\vec{r}_1, \dots, d\vec{r}_n = \frac{N!}{(N-n)!} \frac{d\vec{r}_1}{V} \cdot \frac{d\vec{r}_2}{V} \dots \frac{d\vec{r}_n}{V},$$
 since the probability (or the weight factor) is uniform. We obtain
 
$$\rho^{(n)} = \frac{N!}{V^N (N-n)!}.$$
 However, in all real systems of interacting particles, the distribution deviates from random, and a measure of this deviation is called correlation function. It is defined by the relation

$$\rho^{(n)}(\vec{r}_1, \dots, \vec{r}_n) = \rho^{(1)}(\vec{r}_1) \dots \rho^{(1)}(\vec{r}_n) g_n(\vec{r}_1, \dots, \vec{r}_n)$$

In a system of non-interacting particles,  $\rho^{(1)} = \frac{N}{V}$  and we obtain
 
$$g^{(n)} = \frac{1}{N^n} \frac{N!}{(N-n)!} = 1 + O\left(\frac{1}{N}\right).$$
 Thus  $g^{(n)} = 1$  only in the limit  $N \longrightarrow \infty$ . In a fluid,  $g^{(n)}$  has the following properties.

$$\rho^{(n)}(\vec{r}_1, \dots, \vec{r}_n) = \rho^n g^{(n)}(\vec{r}_1, \dots, \vec{r}_n)$$

From the expression of  $\rho^{(n)}$ , we obtain,

$$g^{(n)}(\vec{r}_1, \dots, \vec{r}_n) = \frac{V^n}{N^n} \cdot \frac{N!}{(N-n)!} \frac{\int \dots \int_V \exp(-u(\vec{r}_1, \dots, \vec{r}_n)/kT) d\vec{r}_{n+1} \dots d\vec{r}_N}{Z}$$

Noting that  $\frac{1}{N^n} \frac{N!}{(N-n)!} = 1 + O\left(\frac{1}{N}\right)$ , and ignoring the term  $O\left(\frac{1}{N}\right)$ , we have

$$g^{(n)}(\vec{r}_1 \dots \vec{r}_n) = \frac{v^n \int \dots \int \exp(-u(r_1 \dots r_N)/kT) d\vec{r}_{n+1} \dots d\vec{r}_N}{Z}$$

The normalization of  $g^{(n)}$  is given by

$$\frac{1}{v^n} \int \dots \int_V g^{(n)}(\vec{r}_1 \dots \vec{r}_n) d\vec{r}_1 \dots d\vec{r}_n = \frac{N!}{N^n(N-n)!} = 1 + O\left(\frac{1}{N}\right)$$

A two particle correlation function in a fluid without an external field has the property of  $g^{(2)}(\vec{r}_1, \vec{r}_2) = g^{(2)}(\vec{r}_{12})$ . If the interparticle potential is not angle dependent as in the case of forces between ions,  $g^{(2)}$  is dependent only on interparticle distance  $r_{12}$ . Normalization of  $g^{(2)}$  is given by

$$\begin{aligned} \frac{1}{v^2} \int \int_V g^{(2)}(\vec{r}_{12}) d\vec{r}_1 d\vec{r}_2 &= \frac{1}{v^2} \int \int_2 g^{(2)}(\vec{r}_{12}) d\vec{r}_1 d\vec{r}_{12} \\ &= \frac{1}{v^2} \int_V d\vec{r}_1 \int g^{(2)}(\vec{r}_{12}) d\vec{r}_{12} \\ &= \frac{1}{v} \int_V g^{(2)}(\vec{r}_{12}) d\vec{r}_{12} = \frac{N(N-1)}{N^2} \\ &= \frac{N-1}{N} = 1 - \frac{1}{N} \end{aligned}$$

The term  $O\left(\frac{1}{N}\right) = \frac{1}{N}$ .

The relationships between thermodynamic properties of a fluid and  $g^{(2)}(\vec{r}_{12})$  are given in standard text books, viz. Hill [1]. A few are given below :

(i) Internal energy  $E$

$$\frac{E}{NkT} = \frac{3}{2} + \frac{\rho}{2kT} \int_0^\infty u(r) g(r) 4\pi r^2 dr$$

where  $u(r)$  is the angle independent interaction potential between two particles and  $g(r)$  is  $g^{(2)}(r_{12})$ , also independent of orientation of  $\vec{r}_{12}$ .

(ii) Pressure  $P$

$$P = \frac{NkT}{V} - \frac{N}{6} \rho \int_0^{\infty} r \frac{du(r)}{dr} g(r) 4\pi r^2 dr$$

(iii) Chemical potential

$$\mu = kT \ln \rho \Lambda^3 + \rho \int_0^1 \int_0^{\infty} u(r) g(r, \xi) 4\pi r^2 d\xi dr$$

where  $\xi$  is the coupling parameter and it has a value 1 for a real fluid.

### 3.3 POTENTIAL OF AVERAGE FORCE

In statistical mechanics, one calculates the ensemble average of mechanical quantities and identifies the average with the corresponding quantities in thermodynamic systems in thermal equilibrium. For example, internal energy of a thermodynamic system in thermal equilibrium, which is necessarily, in an incompletely specified dynamical state is identified with the ensemble average of mechanical energy of the system. Force between two particles is another mechanical quantity. In a thermodynamic system, the corresponding quantity is average force. Let  $u_N(\vec{r}_1, \dots, \vec{r}_N)$  be the potential energy of a system of  $N$  particles. The force on particle  $\alpha$  is defined as  $F_\alpha = \nabla_\alpha u(N)$ .

If we are calculating force on particle 1 in a given fixed configuration of two particles positioned at a given location and orientation we calculate an average of force over all mechanical

states, which share the same value of  $\vec{r}_1$  and  $\vec{r}_2$ , but differ in  $\vec{r}_3$  to  $\vec{r}_N$  and  $\vec{p}_1$  to  $\vec{p}_N$ . The desired average is

$$\begin{aligned} \therefore \bar{F}_1 &= \frac{\int_{\text{V phase space}} \dots \dots \dots \exp(-E(\vec{r}_N, \vec{p}_N)/kT) \nabla_1 u^{(N)} d\vec{r}_3 \dots d\vec{r}_N d\vec{p}_1 \dots d\vec{p}_N}{\int_{\text{V phase space}} \dots \dots \int \exp(-E(\vec{r}_N, \vec{p}_N)/kT) d\vec{r}_1 \dots d\vec{r}_N d\vec{p}_1 \dots d\vec{p}_N} \\ &= \frac{\int \dots \dots \int e^{-u(\vec{r}_N)/kT} \nabla_1 u^{(N)} d\vec{r}_3 \dots d\vec{r}_N}{(\text{Configuration space})} \\ &= \int \dots \dots \int_{\text{V}} e^{-u(\vec{r}_N)/kT} d\vec{r}_3 \dots d\vec{r}_N \\ &\quad (\text{Configuration space}) \end{aligned}$$

Potential of average force is related to average force defined above by the relation

$$\bar{F}_1 = - \nabla_1 \omega^{(2)}(\vec{r}_1, \vec{r}_2)$$

Usually  $\omega^{(2)}(\vec{r}_1, \vec{r}_2) = \omega^{(2)}(\vec{r}_{12})$ . It is shown in standard textbooks, e.g. Hill [1] that the relation between  $g^{(2)}(\vec{r}_{12})$  and  $\omega^{(2)}(\vec{r}_{12})$  for a fluid is

$$\omega^{(2)} = -kT \ln g^{(2)}.$$

Unlike mechanical potential energy which is pairwise additive in most cases,  $\omega^{(n)}$  is not pairwise additive. An approximation that treats  $\omega^{(n)}$  as pairwise additive was introduced into statistical physics by Kirkwood. Corresponding definitions in the Grand canonical ensemble are given in Hill [1].

### 3.4 CLUSTERS

Cluster integrals play an important role in the problems attempted in this thesis. They make their first appearance in statistical mechanics in the theory of imperfect gas. The



partition function in the canonical ensemble is given by

$$Q = \frac{1}{h^{3N} N!} \int \dots \int e^{-\mathcal{H}/kT} d\vec{p}_1 \dots d\vec{p}_N d\vec{r}_1 \dots d\vec{r}_N$$

$$\mathcal{H} = \sum_{i=1}^N \frac{1}{2m} (p_{xi}^2 + p_{yi}^2 + p_{zi}^2) + U(\vec{r}_1, \dots, \vec{r}_N)$$

Substituting this expression of  $\mathcal{H}$  in the formula for  $Q$  and having carried out momentum integrations, we obtain

$$Q = \frac{Z}{N! \Lambda^{3N}}, \text{ where } \Lambda = \frac{h}{(2\pi mkT)^{1/2}}$$

and  $Z = \int_V \dots \int e^{-U/kT} dr_1 \dots dr_N,$

is the configuration integral. The integration is over the whole of configuration space. The integral is over a  $\sim 10^{20}$  dimensional space for a macroscopic system and a direct integration cannot be carried out. The method of cluster expansion allows us to handle this complicated integral. One assumes  $U(\vec{r}_1, \dots, \vec{r}_N) = \sum_{1 \leq i < j \leq N} u(r_{ij})$ , i.e., pairwise additivity of intermolecular potential, an assumption that is true for a large variety of potentials. Then we obtain

$$e^{-U/kT} = e^{-\sum_{1 \leq i < j \leq N} u(r_{ij})/kT} = \prod_{1 \leq i < j \leq N} e^{-u(r_{ij})/kT}$$

$$= \prod_{1 \leq i < j \leq N} (1 + \gamma_{ij})$$

where  $\gamma_{ij} = e^{-u(r_{ij})/kT} - 1.$

An expansion of the product of  $(1 + \gamma_{ij})$  terms give

$$e^{-U/kT} = 1 + \sum \gamma_{ij} + \sum \gamma_{ij} \gamma_{kl} + \dots$$

The order of integration and summation being interchangeable, the configuration integral equals sum of cluster integrals. In the absence of intermolecular forces all  $\gamma_{ij}$ 's are zero,  $e^{-U/kT} = 1$  and  $Z = V^N$ . The expansion of  $e^{-U/kT}$  has terms arising out of all possible combinations from zero to all the  $N(N-1)/2$   $\gamma$  functions. Any such term may be represented by a diagram consisting of circles for the molecules and a line segment between the  $i$ th and  $j$ th molecule for each factor  $\gamma_{ij}$  which occurs in the term. For each of the terms there is one such diagram and for each diagram, there is one term. For any particular diagram molecules which are connected together directly or indirectly by lines are said to form a "cluster". Analogous to  $\gamma_{ij}$ , one can define  $\gamma_m \{m\}$ , the cluster function for the set  $m$  of molecules at co-ordinate  $\{m\}$  by

$$\gamma_m \{m\} = \exp \left[ - u_m \{m\} / kT \right] - 1$$

where  $u_m$  is the potential energy of  $m$  particle interaction, viz.  
 $u_3 \{i,j,k\} = u_{ijk} \{i,j,k\} - u_{ij} \{i,j\} - u_{jk} \{j,k\} - u_{ik} \{i,k\}$ ,  
 where  $u_{ijk} \{i,j,k\}$  is the potential energy of a system of three particles and  $u_{ij}$ ,  $u_{jk}$  and  $u_{ik}$  are potential energies of the three two particle subsystems. Since  $\gamma_{ij}$  depends only on the co-ordinates of  $i$ th and  $j$ th particles only, in an one-component system all cluster integrals  $\int \gamma_{ij} d\{i,j\}$  are equal, independent of  $i$  and  $j$ . This leads to simplification. The combinatorial problem in calculating the number of different terms that give

the same result on integration is formidable and the necessary expressions are given in standard textbooks, viz. Hill (1) and Friedman (2).

### 3.5 Topological Classification

In the above discussion, we classify clusters on the basis of the criteria of number of particles, whose co-ordinates are being integrated over in the cluster integral. One can also classify them on topological criteria, i.e. based on their connectivity. The topological classification has been important in many developments in statistical mechanics.

A cluster is called at least singly connected (ALSC) if each of the  $n(n-1)/2$  pairs of vertices are either directly connected by a bond or are connected by a sequence of bonds that join other intermediate vertices along the path between indirectly connected vertices. A cluster is called at least doubly connected (ALDC) if there are at least two entirely independent paths which do not cross at any vertex, between each pair of molecules in the diagram. An ALSC cluster can be decomposed into a product of ALDC clusters. This is why ALSC clusters are called reducible and ALDC clusters are called irreducible. Fig.1 shows irreducible clusters for  $j = 2, 3, 4$ . After one has grouped together the terms in the cluster expansion of configuration integral, which gives identical value, one obtains

$$Z = N! \sum_n \prod_{j=1}^N \frac{(V b_j)^{m_j}}{m_j!} \left( \sum_{j=1}^N j m_j = N \right)$$

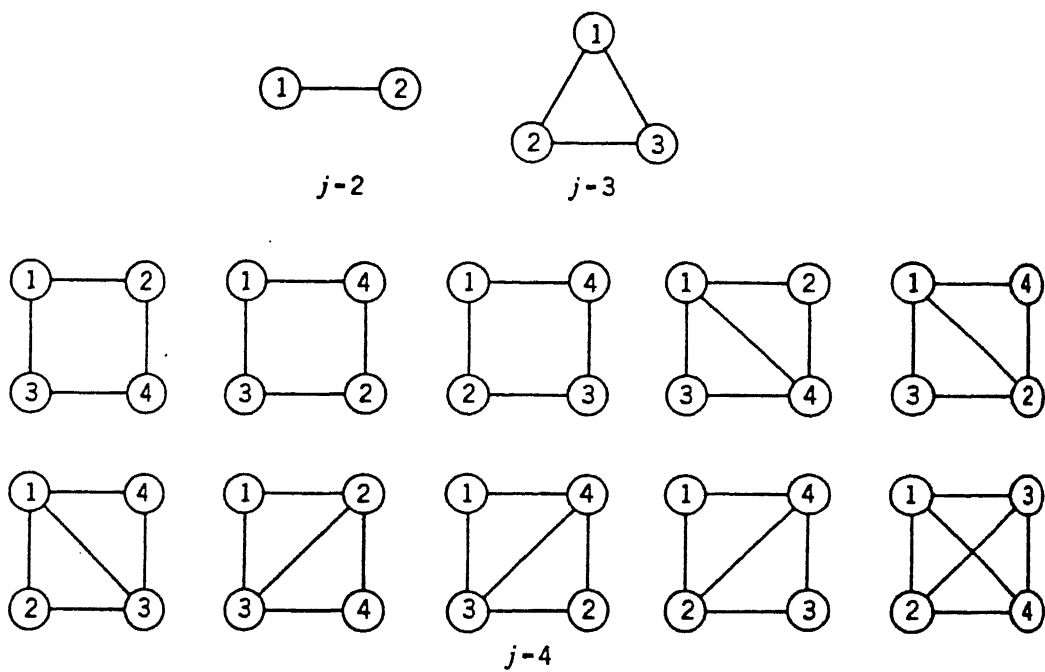


Figure 3.1: Irreducible cluster for  $j=2,3,4$ .

$$\text{where } b_j = \frac{1}{j! V} \int \dots \int_V S_{1,2,\dots,j} d\vec{r}_1 \dots d\vec{r}_j$$

is the cluster integral where  $S_{1,2,\dots,j}$  is the cluster sum, e.g., if  $j=3$ .  $S_{1,2,3} = \gamma_{12}\gamma_{23} + \gamma_{12}\gamma_{13} + \gamma_{13}\gamma_{23} + \gamma_{12}\gamma_{13}\gamma_{23}$ , i.e., sum of all terms which connect in a cluster each of the molecules  $1,2,\dots,j$ , no other molecules being connected to this cluster.  $b_j$  is in general reducible and can be expressed as product of irreducible integrals  $\beta_k$ , defined by

$$\beta_k = \frac{1}{k! V} \int \dots \int_V S'_{1,2,\dots,k+1} d\vec{r}_1 \dots d\vec{r}_{k+1}$$

$S'_{12} = \gamma_{12}$ ,  $S'_{1,2,3} = \gamma_{12}\gamma_{13}\gamma_{23}$ .  $S'_{1,2,3,4}$  is a sum of ten terms corresponding to the irreducible clusters shown in Fig. 1 for  $j = 4$ . The relationship is

$$b_j = \frac{1}{j^2} \sum_n \prod_{k=1}^{j-1} \frac{(j \beta_k)^{n_k}}{n_k!}, \text{ where the } \sum_{k=1}^{j-1} k n_k = j-1$$

Summation is over all sets  $n$  consistent with  $\sum_{k=1}^{j-1} k n_k = j-1$ . The irreducible cluster integrals are directly related to the virial coefficients of imperfect gas theory by the equation

$$B_n = - \frac{n-1}{n} \beta_{n-1}$$

The cluster integrals appear in the expression of partition function and configuration integral and therefore appear in the expression of all properties of a system of interacting particles, the imperfect gas or an ionic solution. The two statistical mechanical quantities of interest to us in this thesis, the correlation function  $g_2$  and the potential of average force  $\omega_2$  have been expanded in terms of cluster integrals (3,4).

### 3.6 Theory of Ionic Solution

McMillan and Mayer (5) developed a theory of solution in which the solution is shown to be equivalent to a gas of solute particles interacting with each other with potential of average force at infinite dilution. Mayer (6) treated the system of the McMillan-Mayer ionic gas by cluster theory. The pressure of this gas is the osmotic pressure of the solution and its virial coefficients are those that appear in fitting the concentration dependence of the osmotic pressure. The potential of average force at infinite dilution is taken to be pairwise additive and its expression is written as:

$$\omega_{12} = \frac{z_1 z_2 \epsilon^2}{D r_{12}} + \omega_{12}^* ,$$

where  $\epsilon$  is electronic charge,  $z_{1,2}$  are charges on ions 1 and 2 in units of electronic charge,  $D$  is the dielectric constant of the solvent,  $r_{12}$  is interparticle distance and  $\omega_{12}^*$  is hard sphere potential

$$\begin{aligned} \omega_{12}^* &= \infty \text{ where } r_{12} \leq a_1 + a_2 \\ &= 0 \text{ when } r_{12} > a_1 + a_2 \end{aligned}$$

where  $a_1$  and  $a_2$  are hard sphere radii of particle 1 and 2. Appearance of  $\frac{1}{D}$  in the expression of  $\omega_{12}$  as a screening constant takes into account the effect of the solvent molecules, which are thereafter ignored. This expression of  $\omega_{12}$  is taken as  $u_{12}$  of the gas of ionic solute and Mayer then calculates the virial coefficients of this gas. Thus the solvent as well as ions other than the two ions, whose interaction is under study

have been taken into account. When this expression of  $\omega_{12}$  is used in evaluation of integrals  $B_n$ , one runs into divergent integrals. For example,

$$\begin{aligned} 2B_2 &= \lim_{V \rightarrow \infty} (1/V) \int_V \gamma_{ij} d\{ij\} \\ &= \lim_{V \rightarrow \infty} \int_0^R \gamma(r) 4\pi r^2 dr \end{aligned}$$

(where  $R$  is the radius of the containing vessel, assumed to be spherical)

$$= \lim_{R \rightarrow \infty} \int_0^R \left( e^{-z_1 z_2 \epsilon^2 / DrkT} - 1 \right) 4\pi r^2 dr$$

The convergence of this integral can be examined by expanding the exponential.

$$\text{Let } \lambda = 4\pi \frac{z_1 z_2 \epsilon^2}{kT}$$

Then,

$$2B_2 = \sum_{n \geq 1} (-\lambda)^n \lim_{R \rightarrow \infty} \int_0^R (4\pi r)^{1-n} r dr / n!$$

The terms with  $n < 4$  lead to divergence of the sum as  $R \rightarrow \infty$ . The integrals on terms for  $n \geq 3$  also diverge at the lower limit even for finite  $R$ . However the integrand  $(e^{-\lambda/4\pi r} - 1)4\pi r^2$  does not diverge at  $r=0$ , so the effect of this divergence of the integral must cancel in the summation. One suspects that by appropriate summation, the divergences at  $R \rightarrow \infty$  may be shown to cancel too. Mayer devised a summation procedure to handle this divergence. The basic technique is to classify cluster diagrams on the basis of topological criterion and then sum them.

The topological classification used by Mayer is not what distinguishes the reducible from the irreducible integrals. We describe the procedure below. Firstly, Mayer used the following

expression for  $\omega_{12}$

$$\omega_{12} = \frac{z_1 z_2 \epsilon^2}{Dr_{12}} e^{-\alpha r_{12}} + \omega_{12}^* \quad (5)$$

where  $\omega_{12}^* = 0$  if  $r_{12} > a_{12}$ , hard sphere radius and  $\omega_{12}^* = \infty$ , otherwise, the factor  $e^{-\alpha r_{12}}$  is introduced to handle divergence.

The expression of osmotic pressure of the solution (or the pressure of the McMillan Mayer gas of ionic solute) is

$$P/kT = \sum_{S=1}^{\sigma} C_S - \sum_{n \geq 2} (\sum n_S - 1) B_n c^n$$

$B_n$  is expressible in terms of irreducible cluster integrals for a set of  $n$  molecules. Thus  $B_n$  is a sum of products. In the expression of  $P/kT$ , the order of summation is implicitly specified, namely, that one sums over all products in the integrand of a specific  $B_n$  and then over all values of  $n$ . As long as the integrals converge, it is of course equally legitimate to sum first over all values of  $n$  for some specified type of product in the integrand and then later over all type of products. If this is done in a particular way the sum over  $n$  of certain types of products of the integrands can be seen to converge in the limit that  $\alpha$  approaches zero. In this case, one therefore has computed the properties of the solution for which the potentials of average force between solute molecules is given by Eq. 5 above. Mayer expands the expression  $\gamma_{rs} = e^{w_{rs}/kT} - 1$ , with  $w_{rs}$  given by Eq. 5, as



$$\gamma_{rs} = k_{rs}^{**}(R) + \sum_{n \geq 1} \frac{1}{n!} \left[ -\lambda z_s z_r g(R) \right]^n \left[ k_{sr}^* + 1 \right]$$

where  $\lambda = 4\pi\epsilon/D kT$   $g(R) = e^{-\alpha R/4\pi R}$ .

$$k_{rs}^{**} = e^{-\omega_{rs}^*/kT} - 1. \quad \text{At small values of } R, \text{ below the}$$

sum of hard sphere radii of  $r$  and  $s$ ,  $k_{rs}^{**} = -1$ . At larger  $R$ ,  $k_{rs}^{**} = 0$ .

$B_n$ , the  $n$ th virial coefficient is defined as

$$B_n = B_{n_1, n_2, \dots, n_r, \dots, n_\sigma}$$

$$= \left[ \prod_{\sigma} n_s \right]^{-1} \iint \dots \int \sum \prod \gamma_{rs} d\tau_{n-1}$$

where the integration is extended over the coordinates of all but one of the particles and the integrand is a sum of products of functions  $\gamma_{rs}$  of the distance between the constituent molecules of the set  $n$ .

Now the product of functions, of  $\gamma_{rs}$  are sums of product of function of  $k_{rs}^{**}$  and  $(-\lambda z_s z_r g(R))$ . The functions are represented by lines on the graph. The lines are called bonds. A line representative  $k_{rs}^{**}$  is called the  $k$ -bond and that representing  $-\lambda z_s z_r g(R)$  is called the  $g$  bond. The distinction can be made by using dotted line for  $k$  bond and solid line for  $g$  bonds. More than one solid line between two points on a graph (two atoms) means more than one  $g$ -bond. Thus each original graph formed from  $\gamma$  bonds break up as sum of diagrams involving  $g$  bonds and  $k$  bonds. This is illustrated in Figure 2. Apart from graphs with  $n=2$ , all other graphs are ALDC graphs. For  $n = 2$ , the two particles are connected either by a  $g$ -bond ( $sr, l$ ) or by a  $k$  bond ( $sr, k$ ). Among ALDC graphs, one identifies cyclic graphs (shown in Fig. 2, type c

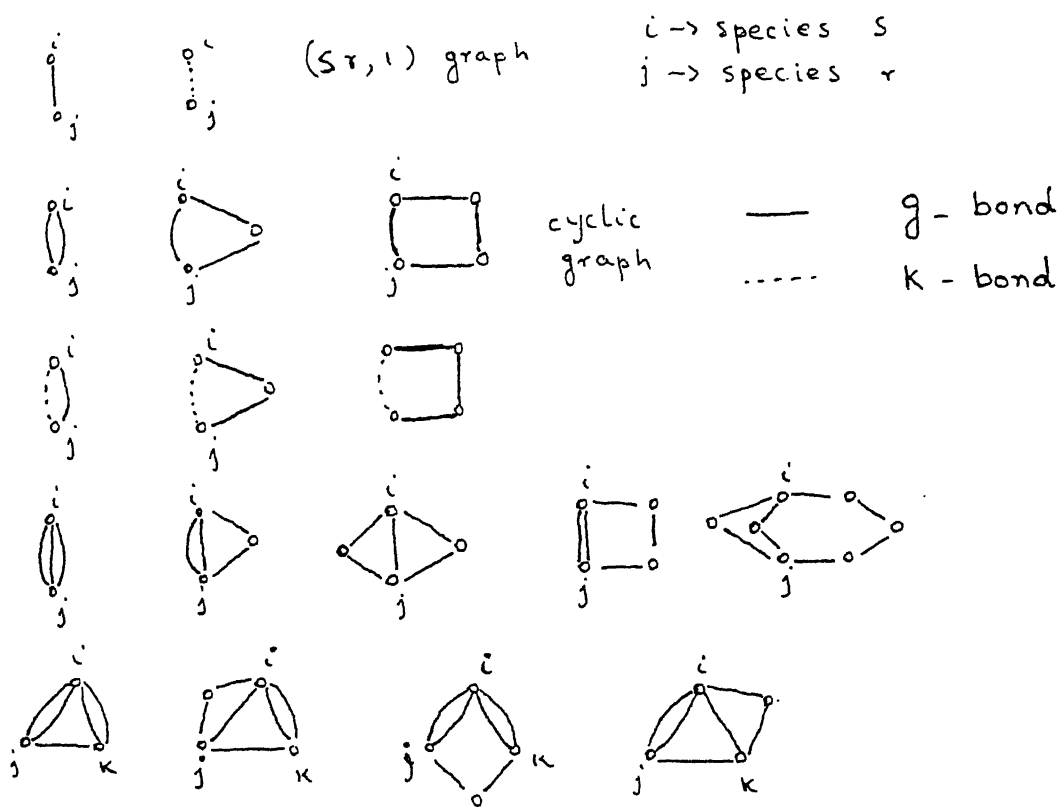


Figure 3.2: Some graphs of g-bonds and g-bond chains and k-bond

(g bond only)) made of only bonds called cycles. Other classes of cyclic graphs have k bonds instead of g. The contribution of singly connected graphs (sr, l) graphs is shown to be zero and that due to cyclic graphs is shown to be  $\kappa^3/12\pi$ , where  $\kappa^2 = \frac{4\pi\epsilon^2}{D kT} \sum_s C_s z_s^2$ . Our interest lies in the method of topological classification and subsequent summation of the remaining graphs. In these graphs, there are some particles which are unique in that they are either connected together directly by k bonds or are more than doubly connected, whereas the remaining particles are in g bonds chains which connect members of this unique set. For a given type (t, m) the set m of the unique particles and the structure by which they are connected by k bonds or by chains of g bonds is fixed but the number of members in the various g bond chains vary. Each type (t, m) is called a prototype graph, and each graph has a parent prototype graph. Conversely, if in any graph there is either a direct g bond between two particles, which are either connected by k bonds or are triply or more connected or if there is a g bond chain between these two particles, then there exist an infinite number of other graphs differing from the first only in the length, and the constituent kinds of ions of this g bond chain. The summation is carried out for one prototype at a time and then over the prototypes.

One first defines and evaluates an integral

$$q_n(R_{ij}) = \iiint \dots \int g(R_{i1}) g(R_{12}) \dots g(R_{n-1,n}) g(R_{n,j}) d\tau_n$$

which is the integral over the intermediate particles of a chain of g bonds having n intermediate vertices. One decides to work in Fourier space and uses the convolution theorem. The Fourier

transform in three dimensions of a function  $g(R)$  dependent on  $R$ , the distance only, is easily shown to be

$$G(t) = 4\pi \int_0^{\infty} g(R) \cdot R^2 \cdot \frac{\sin tR}{tR} dR$$

The inverse of this relation is

$$g(R) = \frac{1}{2\pi^2} \int_0^{\infty} t^2 G(t) \frac{\sin tR}{tR} dt$$

By convolution theorem, one obtains the Fourier transform of  $q_n(R_{ij})$  to be  $Q_n(t) = G(t)^{n+1}$ . The relationship between  $q_n(R)$  and  $Q_n(t)$  is exactly the same as that of  $g(R)$  and  $G(t)$ . If  $g(R)$  is defined as  $e^{-\alpha R}/4\pi R$ , one will have to take into the factor  $Z_s^2$  for each particle  $s$  in the chain. Eventually there is a multiplication by  $C_s$  and a summation over  $s$ . This gives rise to a factor  $\kappa^2 = \lambda \sum_s C_s Z_s^2$  (recall the  $g$  bond stands for  $-\lambda Z_s Z_r g(R)$ ). If there are  $n$  intermediate points in the chain, one obtains  $(-\kappa^2)^n$ . Thus,

$$\begin{aligned} Q(t) &= \sum_n (-\kappa^2)^n Q_n(t) = \sum_n (-\kappa^2)^n [G(t)]^{n+1} \\ &= \frac{1}{\kappa^2 + [G(t)]^{-1}} \end{aligned} \quad (6a)$$

If  $g(R)$  is  $e^{-\alpha R}/4\pi R$ , then  $G(t) = \frac{1}{\alpha^2 + t^2}$ , and  $Q(t) = \frac{1}{\kappa^2 + \alpha^2 + t^2}$  provided the series converges. The question of convergence and the choice of  $e^{-\alpha R}$  as the convergence factor is considered separately. In the limit  $\alpha \rightarrow 0$ , we obtain

$$Q(t) = (\kappa^2 + t^2)^{-1}$$

and

$$q(R) = e^{-\kappa R}/4\pi R$$

We note  $q(R)$  differs from  $g(R)$  only in the replacement of  $\alpha$  in  $g$

by  $\kappa$  in  $q$ . The sum of all diagrams of type  $(t,m)$  in which  $g$  bond chains of all lengths and all ordered arrangement of atoms have been summed between two atoms  $r$  and  $s$ , one obtains (as a result of summation) a  $q$ -bond between  $r$  and  $s$ . The summation over all  $g$  bond chains is carried out over all pairs of points  $r$  and  $s$  in the prototype. Thus, we end up with prototype diagrams connected by  $q$  bonds only. This is illustrated in Figure 3. The job of summing over prototypes now remains. We started off with  $g$  bonds of the form  $e^{-\alpha R}/4\pi R$  to avoid divergence of cluster integrals and in the limit  $\alpha \rightarrow 0$ , have ended up with  $q$  bonds of the form  $e^{-\kappa R}/4\pi R$ . The problem of divergence of cluster integrals has disappeared as a result of summation.

### 3.7 Cluster Summation of Potential of Average Force and Radial Distribution function.

The radial distribution function can be expanded in powers of particle number density. The expression for an one component system is given by Mayer and Montroll (3). The coefficient of the  $m$ th power of particle number density in the expansion of the distribution function of  $n$  particles is  $\frac{1}{m!}$  multiplied by an integral over the coordinate of  $m$  particles. The integrand is the sum of all possible products of the Mayer cluster function  $\gamma_{ij}$  of the distance between particles  $i$  and  $j$ . In these products each particle of the set  $m$  is connected to at least two of the set of  $n$ -particles by independent paths. An extension to multicomponent systems has been made by Meeron (4). For this, he used the notation used by Mayer & McMillan (5) for a multicomponent system in a slightly extended form. The



simplicity of this notation lies in the fact that the expression for one-component system can be extended to that of the multicomponent system by simple transcription.

$$\bar{n} = \text{The set of } \bar{n} \text{ particles of } \sigma \text{ kinds} = (n_1, n_2, \dots, n_i, \dots, n_\sigma) \quad (6)$$

$$n_i = \text{The number of particles of } i^{\text{th}} \text{ kind}$$

$$n = \sum_i n_i \quad (7)$$

$$\bar{\rho} = \text{The set of number densities} = (\rho_1, \rho_2, \dots, \rho_i, \dots, \rho_\sigma) \quad (8)$$

$$\bar{n}! = n_1! \ n_2! \ \dots n_i! \ \dots n_\sigma! \quad (9)$$

$$\bar{x}^{\bar{n}} = x_1^{n_1} \ x_2^{n_2} \ \dots x_i^{n_i} \ \dots x_\sigma^{n_\sigma} \quad (10)$$

$$\frac{\partial \bar{n}}{\partial \bar{x}^{\bar{n}}} = \frac{\partial^{n_1}}{\partial x_1^{n_1}} \ \frac{\partial^{n_2}}{\partial x_2^{n_2}} \ \dots \frac{\partial^{n_i}}{\partial x_i^{n_i}} \ \dots \frac{\partial^{n_\sigma}}{\partial x_\sigma^{n_\sigma}} \quad (11)$$

$$\int f(\bar{n}) \ d(\bar{n}) = \int \dots \int f(\bar{n}) \prod_{j=1}^{n_1} d\tau_{1j} \prod_{j=1}^{n_2} d\tau_{2j} \dots \prod_{j=1}^{n_\sigma} d\tau_{\sigma j} \quad (12)$$

$$\text{where } \prod_{j=1}^{n_\sigma} d\tau_{\sigma j} = d\tau_1 \ d\tau_2 \ \dots d\tau_{n_\sigma} \text{ of the } \sigma\text{th species} \quad (13)$$

Meeron proved that the n-particle distribution function can be expressed as

$$g(\bar{n}) = \sum_{\bar{v} \geq 0} \frac{\rho^{\bar{v}}}{\bar{v}!} \ g_{\bar{v}}(\bar{n}) \quad (14)$$

$$\text{where } g_{\bar{v}}(\bar{n}) = \exp \left[ - \frac{U(\bar{n})}{kT} \right] \int P(\bar{n}; \bar{v}) \ d(\bar{v}) \quad (15)$$

$$P(\bar{n}, \bar{v}) : \text{The sum of all possible products of } \gamma_{ij} \text{ in which each particle of the set } \bar{v} \text{ is independently connected to at least two particles of the set } \bar{n}. \quad (16)$$

Also the potential of average force acting in the set  $\bar{n}$  is

expressed as

$$\omega(\bar{n}) = \sum_{\bar{v} \geq 0} \frac{\bar{\rho}^{\bar{v}}}{\bar{v}!} \omega_{\bar{v}}(\bar{n}) \quad (17)$$

where

$$\omega(\bar{n}) = -kT \ln g(\bar{n}) \quad (18)$$

and

$$\omega_{\bar{v}}(\bar{n}) = -kT \int Q(\bar{n}; \bar{v}) d(\bar{v}) \quad (19)$$

$Q(\bar{n}; \bar{v})$  : The sum of all possible products of  $\gamma_{ij}$  in which each particle of the set  $\bar{v}$  is independently connected to at least two particles of  $\bar{n}$  and in which all particles  $\bar{v}$  are connected among themselves independent of those of the set  $\bar{n}$ . (20)

Our interest lies in the radial distribution function,  $g(ij)$ , of two particles of kind  $i$  and  $j$  and the potential of average force  $\omega(ij)$  acting in the set of same particles

$$\begin{aligned} g(ij) &= \sum_{\bar{v} \geq 0} \sum_{v_1} \dots \sum_{v_\sigma} \frac{\rho_1^{v_1} \rho_2^{v_2} \dots \rho_\sigma^{v_\sigma}}{v_1! v_2! \dots v_\sigma!} g_{v_1 v_2 \dots v_\sigma}(i, j) = \\ &= \sum_{\bar{v} \geq 0} \frac{\bar{\rho}^{\bar{v}}}{\bar{v}!} g_{\bar{v}}(ij) \end{aligned} \quad (21)$$

$$g_{\bar{v}}(ij) = \exp \left[ -\frac{U(ij)}{kT} \right] \int P(ij, \bar{v}) d\bar{v} \quad (22)$$

$P(ij, \bar{v})$  = The sum of all possible products of  $\gamma$  functions in which each particle of the set  $\bar{v}$  is connected independently to  $i$  and  $j$ . (23)

$$\omega(ij) = \sum_{\bar{v} \geq 0} \sum_{v_1} \sum_{v_2} \dots \sum_{v_\sigma} \frac{\rho_1^{v_1} \rho_2^{v_2} \dots \rho_\sigma^{v_\sigma}}{v_1! v_2! \dots v_\sigma!} \omega_{v_1 v_2 \dots v_\sigma}(ij) =$$



$$= \sum_{\bar{\nu} \geq 0} \frac{\bar{\rho}^{\bar{\nu}}}{\bar{\nu}!} \omega_{\bar{\nu}}(ij) \quad (24)$$

$$\omega_{\bar{\nu}}(ij) = -kT \int Q(ij, \bar{\nu}) d(\bar{\nu}) \quad (25)$$

$Q(ij, \bar{\nu})$  : The sum of all possible products of  $\gamma$  functions in which each particle of  $\bar{\nu}$  is independently connected to  $i$  and  $j$  and particles of  $\bar{\nu}$  are connected to each other independently of  $i$  and  $j$ . (26)

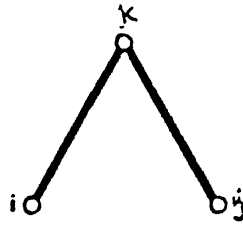
The above products are represented in terms of the diagrams in which the particles are represented by circles and  $\gamma$  functions by lines. The diagrams are shown in Fig. 4. The meaning of a particle being independently connected to  $i$  and  $j$  means that the paths through which it is connected to  $i$  and  $j$  contain mutually exclusive sets of particles.

With increase in the number of particles, the number and complexity of the diagrams increase. Thus we see that the evaluation of  $g(ij)$  and  $\omega(ij)$  means summation of an infinite number of diagrams. Evaluation of a single diagram becomes difficult as the integrals diverge for Coulombic potential. This has been shown in the previous section. Hence the evaluation is done the same way as Mayer did for evaluation of virial coefficient. This method elucidated by Meeron (7) consists of multiplying the Coulombic part by  $e^{-\alpha r}$ , expanding the exponential in the function  $\gamma_{kl}$ , collecting all the diagrams of a given type for all values of  $n$  and summing them, and letting  $\alpha \longrightarrow 0$  in the final result.

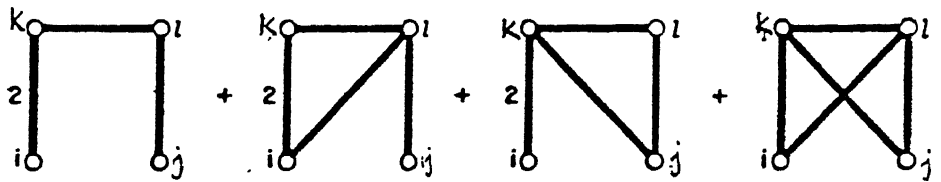
The pair potential of average force at infinite dilution is given the same way as Mayer as the sum of a short-range and of a

$$Q(ij;k) =$$

$$P(ij;k) =$$



$$Q(ij;kl) =$$



$$P(ij;kl) =$$

$$Q(ij;kl)$$

+

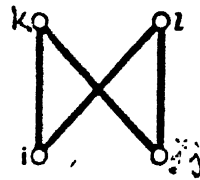


Figure 3.4: Diagrammatic representation of  $Q(ij;k)$ ,  $P(ij;k)$ ,  $Q(ij;kl)$  and  $P(ij;kl)$ .

Coulomb part multiplied by  $e^{-\alpha r}$ .

$$U(kl) = U^*(kl) + Z_k Z_l \frac{\epsilon^2 e^{-\alpha r}}{Dr} \quad (27)$$

$$\begin{aligned} U^*(kl) &= +\infty \text{ for } r_{kl} < a_{kl}; a_{kl} \text{ is a small distance} \\ &= \text{ for } r_{kl} > a_{kl} \end{aligned} \quad (28)$$

$Z_k, Z_l \longrightarrow$  Algebraic charges on ions of kinds  $k$  and  $l$

$\epsilon \longrightarrow$  Unit of electronic charge

$D \longrightarrow$  the Macroscopic dielectric constant of the solution

$$\text{Let } \lambda = \frac{\epsilon^2}{DkT} \quad (29)$$

$$g(r) = \frac{e^{-\alpha r}}{r} \quad (30)$$

$$\exp \left[ \frac{-U^*(kl)}{kT} \right] = 1 + \gamma_{kl}^* \quad (31)$$

$$\text{Hence } \gamma_{kl} = \gamma_{kl}^* + \sum_{n \geq 1} \frac{1}{n!} [-Z_k Z_l \lambda g(r)]^n (1 + \gamma_{kl}^*) \quad (32)$$

Each bond  $\gamma_{kl}$  can be represented by a sum of  $\gamma_{kl}^*$  bond and  $[-Z_k Z_l \lambda g(r)]^n$ , with  $1 \leq n \leq \infty$  and the products in diagram is further broken into sums of products of  $\gamma^*$ -bond and  $g$ -bond. A  $\gamma^*$  bond is the function  $\gamma^*(r)$  and a  $g$ -bond is  $[-Z_k Z_l \lambda g(r_{kl})]$ . In the original product of  $Q$ , there can be at most one  $\gamma^*$ -bond and any number of  $g$ -bond between two vertices. The number and location of bonds in a product involving the set  $\bar{N}+ij$  of ions are described by the symbol  $t_{\bar{N}}$ , the given pattern.  $Q(ij, \bar{N})$  is given by the sum of  $Q(ij, t_{\bar{N}})$  over all possible patterns  $t_{\bar{N}}$ . For all  $\bar{N}$ , all the  $t_{\bar{N}}$ 's form a class. In any diagram, there are rows of ions in which each is connected to the preceding and the following by a single  $g$ -bond and this is called  $g$ -bond chain. There is a subclass  $s_{\bar{m}}$  of the class  $t_{\bar{N}}$ , which contains only those patterns without a  $g$ -bond

chain in any of them. The pattern  $s_{\bar{m}}$  and the set  $\bar{m}$  are prototype pattern and prototype set respectively. Any other pattern of  $t_{\bar{N}}$  can be derived from a particular pattern of  $s_{\bar{m}}$  by replacing any g-bond by a g-bond chain of varying length. (Fig. 5 and 6). Let us consider a prototype pattern with  $\nu$  g-bonds. Each g-bond can be replaced by a g-bond chain with  $\bar{n}_i$  number of particles. A diagram can be derived from this prototype with  $\nu$  g-bond chains with  $\bar{n}_1, \bar{n}_2, \dots, \bar{n}_\nu$  number of particles in the chains. Other diagrams also can be derived from this with the number and composition of particles varying in the g-bond chains. All these diagrams can be grouped together and can be summed by following the method elucidated earlier by Mayer (6). This is shown as follows.

Let us consider the diagram with  $\nu$  g-bond chain with  $\bar{n}_1, \bar{n}_2, \dots, \bar{n}_1, \dots, \bar{n}_\nu$  particles in the respective g-bond chains. This constitutes a product in  $Q(ij, t_{\bar{m}+\bar{n}})$  and can be represented by the symbol  $Q(ij, \bar{n}_1, \dots, \bar{n}_\nu, s_{\bar{m}})$ . If this is integrated over the coordinates of the particles of  $\bar{n} = \bar{n}_1 + \dots, \bar{n}_\nu$ , then we get the following:

$$\int Q(ij, \bar{n}_1, \dots, \bar{n}_\nu, s_{\bar{m}}) d(\bar{n}) = (-\lambda)^\nu \left[ \prod_{k,l}^{m+\bar{i}j} (\nu_{kl}^o!)^{-1/2} (z_k z_l)^{\nu_{kl}/2} \right]$$

$$\prod_{s=1}^{\nu} (-\lambda)^{n_s} \bar{z}^{2\bar{n}_s} I_s(\gamma_{kl}) f(s_{\bar{m}})$$

The above expression is obtained because the algebraic expression of the g-bond is  $[-z_i z_j \lambda g(\gamma_{ij})]$ . The term  $\nu_{kl}^o$  is the number of direct g-bonds in the prototype consisting of  $\bar{m} + ij$

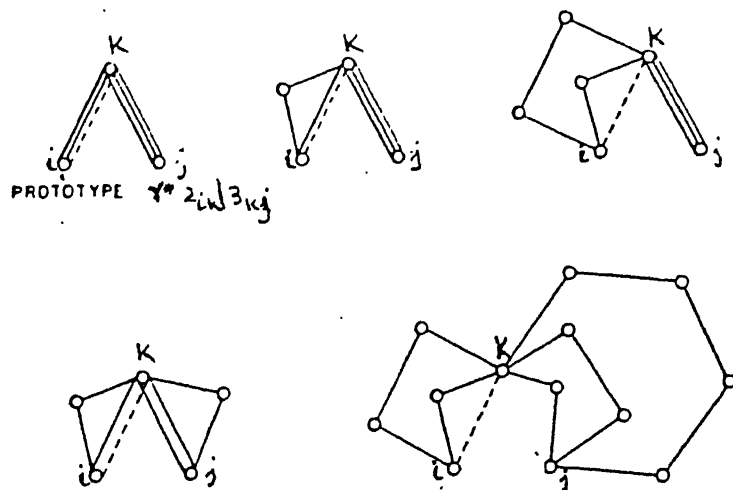


Figure 3.5: Diagrammatic representation of the prototype  $\gamma^{*2}_{ik}/^3_{kj}$  and some patterns derivable from it.

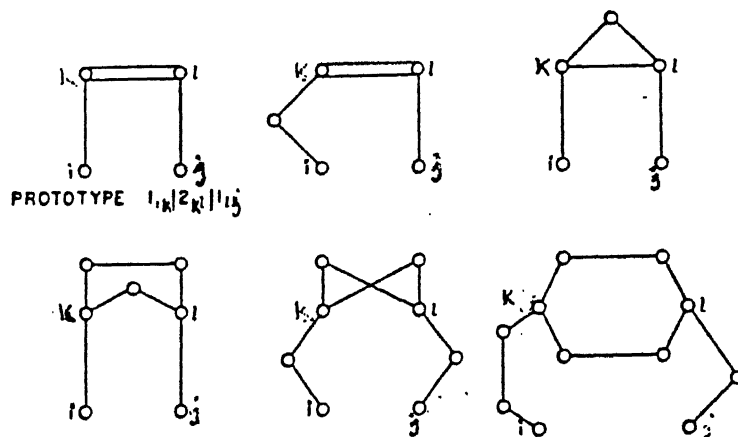


Figure 3.6: Diagrammatic representation of the prototype and some patterns derivable from it.

between  $k$  and  $l$ .  $\nu_{kl}$  is the sum of  $\nu_{kl}^0$  and the number of  $g$ -bond chains between  $k$  and  $l$  of the prototype.

$\prod_{s=1}^{\nu}$  represents multiplication over all the  $\nu$   $g$ -bond chains  $f(s_m) \longrightarrow$  product of  $\gamma^*$  bonds corresponding to the prototype  $s_m$ .

$$I_s(r_{kl}) = \int g(r_{kl}) g(r_{12}) \dots g(r_{n_s-1, n_s}) g(r_{n_s, l}) d(\bar{n}_s) \quad (33)$$

The number of times;  $M_n(s_m)$ , the product  $Q(ij, \bar{n}_1, \dots, \bar{n}_\nu, s_m)$  appears in the sum  $Q(ij, \bar{m} + \bar{n})$  is the product of following three factors:

- (i) The number of ways of choosing the sets  $\bar{m}$  and  $\bar{n}_1, \dots, \bar{n}_\nu$  from the set  $\bar{m} + \bar{n}$ . This is equal to  $\frac{(\bar{m} + \bar{n})!}{\bar{m}! \prod_{s=1}^{\nu} \bar{n}_s!}$
- (ii) The product of the number of ways in which each set of particles,  $\bar{n}_s$  can be ordered in the corresponding chain. This is equal to  $\prod_{s=1}^{\nu} n_s!$ .
- (iii)  $M(s_m)$ , the number of times that the prototype diagram,  $s_m$  occurs in the sum  $Q(ij, \bar{m})$ .

Hence,

$$M_n(s_m) = M(s_m) \frac{(\bar{m} + \bar{n})!}{\bar{m}!} \prod_{s=1}^{\nu} \frac{n_s!}{\bar{n}_s!} \quad (34)$$

The sum  $S(ij, s_m)$  is defined in such a way that  $M(s_m) \frac{\bar{\rho}^{\bar{m}}}{\bar{m}!}$   $S(ij, s_m)$  is the sum of all the integrals of  $Q(ij, \bar{n}_1, \dots, \bar{n}_\nu, s_m)$  multiplied by appropriate factors for  $n$  varying from zero to infinity.

Hence,

$$M(s_m) \frac{\bar{\rho}}{\bar{m}!} S(ij, s_m) = \lim_{\alpha \rightarrow 0} \left[ \sum_{n \geq 0} M_n(s_m) \frac{\bar{\rho}}{(\bar{m} + \bar{n})!} \int Q(ij, \bar{n}_1, \dots, \bar{n}_\nu, s_m) d(\bar{n}) \right] \quad (35)$$

If the above equation is integrated over the coordinates of the particles of the set  $\bar{m}$ , then we get the contribution of the integrals over chains of g-bonds of all products belonging to the prototype  $Q(ij, s_m)$  and summed over all chain lengths from zero to infinity, and over all possible combination of particle species and arrangements on a given combination of chain lengths to  $-W(ij)/kT$ . The limit  $\alpha \rightarrow 0$  is taken in order to get the value for Coulombic pair potential of average force at infinite dilution.

Evaluation of  $S$  involves evaluating the integral in eq.(33) and that is done by three-dimensional Fourier transform and

$$I_s(r_{kl}) = 8 \frac{(4\pi)^{n_s-1}}{r_{kl}} \int_0^\infty \frac{t}{(\alpha^2 + t^2)^{n_s+1}} \sin(r_{kl} t) dt \quad (36)$$

Using eq. (30) in the expression of  $S(ij, s_m)$  and after further mathematical manipulation,

$$S(ij, s_m) = f(s_m) \prod_{k,l}^{\bar{m}+ij} \frac{1}{(\nu_{kl})!^{1/2}} (q_{kl})^{1/2} \nu_{kl} \quad (37)$$

where,

$$q_{kl} = - \frac{Z_k Z_l \lambda e^{-\kappa r}}{r} \quad (38)$$

and

$$\kappa^2 = 4\pi\lambda \sum_{j=1}^{\sigma} \rho_j z_j^2 \quad (39)$$

Hence the products  $S(ij, s_m)$  can be represented by the same diagram as the corresponding prototype products  $Q(ij, s_m)$  with the same pattern  $s_m$  and the same prototype set  $\bar{m}$  of ions, where each bond is a q-bond instead of a g-bond.  $\nu_{kl}$  denotes the number of q-bonds between  $k$  and  $l$ . The problem of divergence of cluster integrals has disappeared.

Each q-bond represents the function  $-\frac{z_k z_l e^{-\kappa r}}{r}$  instead of  $\frac{-z_k z_l e^{-\alpha r}}{r}$ . Even though the products of type  $Q(ij, s_m)$  are independent of ion number densities, the products of the type  $S(ij, s_m)$  depend on the densities to all orders through the parameter  $\kappa$ . According to the definition of a prototype pattern, there can be no q-bond chain in  $S(ij, s_m)$ .

The  $Q$  diagrams which involve only g-bond chains of varying length give rise to  $\frac{-z_i z_j^2 e^{-\kappa r}}{r}$ , the Debye-Huckel potential of average force.

Thus the expansion in eq. (24) is written as

$$\omega(ij) = U^*(ij) + \frac{z_i z_j^2 e^{-\kappa r}}{r} - kT \sum_{\bar{m} \geq 1} \frac{\bar{\rho}^{\bar{m}}}{\bar{m}!} \int \sum_{\bar{s}_m} M(s_m) S(ij, s_m) d(\bar{m}) \quad (40)$$

Since  $S(ij, s_m)$  are the same diagrams as  $Q(ij, s_m)$  with q-bond replacing g-bond, and  $\gamma^*$ -bond; then for a fixed  $\bar{m}$ , there are infinite number of diagrams, with number of bonds between any two particles varying from one to infinity.



If  $\bar{m} = 1$ , i.e., we have one particle of species 1 apart from i and j, then a typical pattern will have  $\nu_{il}$  bonds between i and l and  $\nu_{lj}$  bonds between l and j and

$$S(ij ; \nu_{il} | \nu_{lj}) = \frac{1}{\nu_{il}! \nu_{lj}!} (q_{il})^{\nu_{il}} (q_{lj})^{\nu_{lj}} \quad (41)$$

If all the S products are summed for all  $\nu$  values, then we get

$$\sum_{s_1} M(s_1) S(ij; s_1) = F_{il} F_{lj} - q_{il} q_{lj} \quad (42)$$

where

$$F_{il} = \exp \left[ -\frac{1}{kT} \left( U^*(il) + z_i z_l \frac{\epsilon^2}{Dr} e^{-kr} \right) \right] - 1 \quad (43)$$

Similar summation will have to be carried out with higher patterns, i.e. with  $\bar{s}_m$  with  $\bar{m} = 2, 3, \dots$

This gives

$$\sum_{s_m} M(\bar{s}_m) S(ij, \bar{s}_m) = \theta(ij, \bar{m}) \quad (44)$$

$\theta(ij, \bar{m})$  are sums of all possible products of function  $q_{kl}$  and of  $\phi_{kl}$  where

$$\phi_{kl} = \exp \left[ -\frac{1}{kT} \left[ U^*(kl) + z_k z_l \frac{\epsilon^2}{Dr} e^{-kr} \right] \right] - 1 - q_{kl} \quad (45)$$

This sum is defined exactly the same way as the sum  $Q(ij, \bar{m})$ . The only difference is that instead of g-bonds, these diagrams will have connection made through all possible combination of  $\phi$ -bonds and q-bonds. The restriction in these connection is that there should be no two successive q-bonds. If so, we will get a q-bond chain which has already been summed.

In Fig. (7) diagrammatic representation of products of  $\phi$ -bonds and  $q$ -bond corresponding to  $\theta(ij, kl)$  are given.

Thus eq. (40) reduces further to

$$\omega(ij) = U^*(ij) + z_i z_j \epsilon^2 \frac{e^{-\kappa r}}{Dr} - kT \sum_{\bar{m} \geq 1} \frac{\bar{\rho}^{\bar{m}}}{\bar{m}!} \int \theta(ij, \bar{m}) d(\bar{m}) \quad (46)$$

In the above description, the  $\gamma$ -bonds are broken into  $g$ -bonds are  $\gamma^*$  bonds. In a later development Meeron (8,9) carried out the summation of cluster integrals to express potential of average force for one-component systems with no long-range order which involve diagrams with  $\gamma$ -bonds. No break up into  $g$ -bond and  $\gamma^*$ -bond is made. The topological classification is done in terms of the order of nodes. Hence the expansion is termed as Nodal Expansion. The order of a node is the number of particles to which the particle corresponding to the node is connected. A row of nodes of second order is called a  $\gamma$ -bond chain. The set of particles which form nodes of third or higher order constitute the prototype pattern. The diagrams over which summation takes place are the  $Q$ -diagrams defined in equation (21) and Fig. 4. The summation procedure is the same as that of above. Hence,

$$W(ij) = U(ij) + w(ij) - kT \sum_{m \geq 1} \sum_{s_m} \frac{\rho^m}{m!} \int k_o(s_m) P_\gamma(s_m) \prod_{m+i,j} \frac{1}{v_{kl}!} \\ \times \left[ - \frac{w(r_{kl})}{kT} \right]^{v_{kl}} d(m) \quad (47)$$

$U(ij)$  is the direct interaction potential between particle  $i$  and  $j$ .

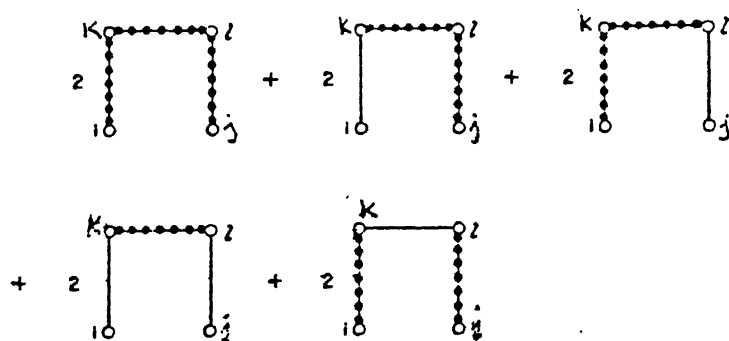


Figure 3.7: Diagrammatic representation of first  $\Theta$  diagram.  $\Theta(ij;kl)$ . Dotted lines denote  $\Psi$  bonds.

$w(ij)$  is the summation over the integrals corresponding to  $\gamma$ -bond chains of all length.

$m$  is the number of particles in the prototype pattern  $s_m$ .

The second summation is over all the prototype patterns for  $m$ .

$K_O(s_m)$  is the number of times the prototype pattern  $s_m$  appears.

$P_\gamma(s_m)$  is the product of direct  $\gamma$ -bonds between pairs of particles in the pattern  $s_m$ .

$\nu_{kl}$  is the number of  $\gamma$ -bond chains between pairs of particles in the prototype. After the first summation the diagrams representing  $W(ij)$  are the prototype patterns. With a given pattern there can be  $\nu$  number of  $\omega$ -bonds with  $\nu$  varying from zero to infinity. Thus all patterns  $s_m$  for the same  $m$  and in which the same pairs of particles are connected by any combination and number of bonds can be added together. Thus,

$$W(ij) = U(ij) + w(ij) - kT \sum_{m \geq 1} \frac{\rho^m}{m!} \int \theta(ij; m) d(m) \quad (48)$$

Here the functions  $\theta(ij, m)$  are sums of products defined exactly in a similar way for  $Q(ij; N)$  defined in eq. (20), with the connections made by all possible combination of  $\psi$ -bonds and  $w$ -bonds; with the bonds defined below:

$$w'_1(r_{12}) = \gamma(r_{12}) - \frac{w(r_{12})}{kT} \quad (49)$$

$$\Psi(r_{12}) = \exp \left\{ - \frac{1}{kT} \left[ U(r_{12}) + \omega(r_{12}) \right] \right\} - 1 - w'_1(r_{12}) \quad (50)$$

The restriction in the connectivity is that there should be no  $w'_1$ -bond chains.

Now we have diagrams with the same topology as  $Q(ij, N)$ . But the bonds are  $w'_1$ -bond and  $\Psi$ -bond instead of  $\gamma$ -bonds. Let these bonds be denoted by  $w'_1$  and  $\Psi_1$  respectively. Now we have diagrams with prototype patterns as well as chains with all possible combination of  $w'_1$  and  $\Psi_1$  bonds. Summation over chains of all possible combination of  $w'_1$  and  $\Psi_1$  over all possible length can be carried out as summation over  $\gamma$ -bond chains of all possible lengths are carried out. This is given as below:

The chain integral  $f_m(ij)$  is defined as

$$f_m(\vec{r}_{ij}) = -\frac{\rho^m}{m!} \sum_{\text{comb.}} \int G(r_{i1}) G(r_{12}) G(r_{23}) \dots G(r_{m-1,m}) G(r_{mk}) d(\vec{m}) \quad (51)$$

Each function  $G(r_{kl})$  in equation (51) represents either a  $\Psi_1$ -bond or a  $w'_1$ -bond and the summation is carried out over all possible combination of these bonds in the chain of  $m$  intermediate particles between particles  $i$  and  $j$ , and all permutation of the  $m$  particles in this chain. The integral in equation (51) is an  $m$ -fold convolution which is evaluated by Fourier transform techniques, as discussed earlier. By appropriate mathematical manipulations, we get

$$\begin{aligned} w_2(r_{ij}) &= -kT \sum_{m \geq 1} f_m(ij) \\ &= -\frac{kT}{(2\pi)^3} \int S_2(t) \exp(i \vec{r}_{ij} \cdot \vec{t}) d\vec{t} \end{aligned} \quad (52)$$

$$\text{where } S_2(t) = \sum_{m \geq 1} \sigma_m(t) \quad (53)$$

$$\text{where } \sigma_m(t) = \int f_m(\vec{r}_{ij}) \exp(i \vec{t} \cdot \vec{r}_{ij}) d\vec{r}_{ij} \quad (54)$$

Thus by summation over side chains, we get diagrams which have  $w_2(\vec{r})$  bonds and  $\Psi_1$  and/or  $w_1$  bonds between two particles in the prototype pattern. Then summation over all diagrams with number of bonds between two particles in the prototype pattern varying from one to infinity is carried out and we get  $\theta_2$  diagrams which define the potential of average force in the following way:

$$W(r_{ij}) = U(r_{ij}) + w_1(r_{ij}) + w_2(r_{ij}) - kT \sum_{m \geq 1} \frac{\rho^m}{m!} \int \theta_2(ij, m) d(\vec{m}) \quad (55)$$

$\theta_2(ij, m)$  are diagrams defined the same way as  $\theta_1(ij, m)$  with  $\Psi_2$  and  $w'_2$  bonds replacing  $\Psi_1$  and  $w'_1$  bonds with  $\Psi_2$  and  $w'_2$ -bonds defined as

$$w'_2(\vec{r}) = \exp \left\{ -(U(r) + \omega_1(r))/kT \right\} - 1 - \frac{w_2(r)}{kT} \quad (56)$$

$$\Psi_2(\vec{r}) = \exp \left\{ -[U(\vec{r}) + w_1(\vec{r}) + w_2(\vec{r})]/kT \right\} - 1 - w'_2(\vec{r}) \quad (57)$$

The above procedure can be applied to chains involving  $\Psi_2$  and  $w'_2$ -bonds and the procedure can be repeated indefinitely yielding third, fourth, ....nth chain potential, with each potential given in terms of the preceding ones. Thus after nth nodal expansion the potential of average force is written as

$$W(\vec{r}_{ij}) = U(\vec{r}_{ij}) + w_n(\vec{r}_{ij}) - kT \sum_{m \geq 1} \frac{\rho^m}{m!} \int \theta_n(ij, m) d(\vec{m}) \quad (58)$$

In a similar way nodal expansion can be carried out to get  $g(\vec{r}_{ij})$ , the distribution function. If we calculate  $W(\vec{r}_{ij})$  by

truncating the  $m$ th term in the  $n$ th nodal expansion, then we evaluate and sum over infinite number of diagrams in the original  $Q$  expansions. Hence we get a well defined approximation to the function.

The function  $w_n(\vec{r}_{ij})$  in equation (57) is given by the following expression

$$w_n(\vec{r}_{ij}) = w_1(\vec{r}_{ij}) + w_2(\vec{r}_{ij}) + \dots + w_n(\vec{r}_{ij}) = \sum_{\nu=1}^n w_{\nu}(\vec{r}_{ij}) \quad (59)$$

From the method by which the above series for  $w_n(\vec{r}_{ij})$  is obtained, it appears probable that the series should converge to a limit as  $n \rightarrow \infty$  since the successive terms involve integrals of products with rapidly increasing degree of connectivity. Hence these integrals will be nonzero over a decreasing part of configuration space of the particles involved. Hence we can write

$$w(\vec{r}_{ij}) = \lim_{n \rightarrow \infty} w_n(\vec{r}_{ij}) \quad (60)$$

Also  $\omega(\vec{r}_{ij})$  can be evaluated by solving an integral equation. Thus the repeated summation of certain well defined classes of graphs in the density expansion of potential of average force and pair distribution function results, in the limit, in an integral equation, which permits a formally exact treatment of a many body system. This integral equation is derived by Meeron (10). An equivalent derivation is given by van Leeuwen, Groeneveld and de Boer (11). The derivation by Meeron follows from topological analysis of the structure of the cluster coefficients in the density expansion of the potential of average

force. The resulting rigorous integral equation involves only pair distribution function and hence is formally closed. But it contains a term given by an infinite series of finite-density cluster integrals. This necessitates an approximation of some form. The approximation is called HNC approximation which will be discussed later. The derivation of the integral equation is given below. This derivation is done for an one component system. Later this is extended to multicomponent system by Allnatt (12).

Let us consider all the diagrams defined as  $Q(ij, n)$  in equation (26). All the diagrams belonging to this can be divided into two groups depending on whether they have cutting points or not. Cutting points (also called articulation points) are points at which each group can be separated into two or more parts. The examples are given in Fig.8. In the  $Q$ -sum, the two types of graphs are separated and each type is put in a separate integral. The sum of the integrals of all graphs containing cutting points with each integral multiplied by the appropriate factor  $\frac{\rho^n}{n!}$  is denoted by  $\tau(\vec{r}_{ij})$  and is called  $\tau$ -sum. The corresponding sum of all integrals of graphs containing no cutting points is denoted  $\zeta(\vec{r}_{ij})$ . Hence formally, the  $Q$ -sums can be written as

$$Q(\vec{r}_{ij}) = \tau(\vec{r}_{ij}) + \zeta(\vec{r}_{ij}) \quad (61)$$

In the  $\tau$ -diagram, there are adjacent cutting points defined by the fact that there are no other cutting points between them. Between these two cutting points, we can have any subgraph, the only constraint being that there be no cutting points in that subgraph. These subgraphs can contain graphs of any of the



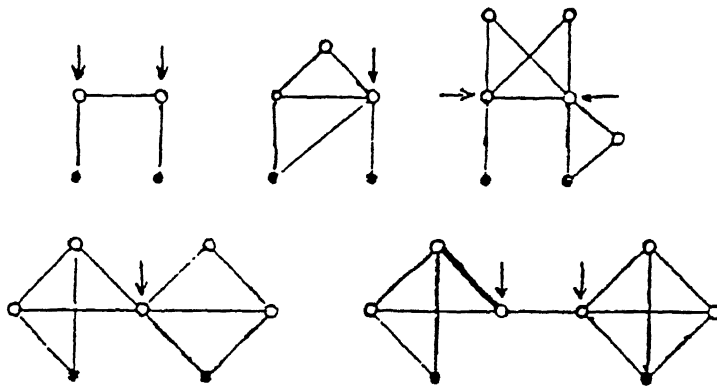


Figure 3.8(a): Diagrammatic representation of  $\tau(r)$ . The arrows indicate cutting point

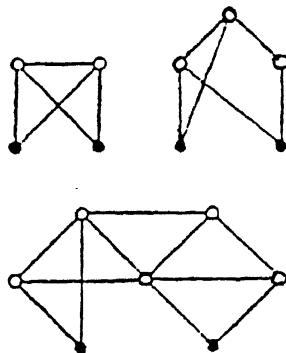


Figure 3.8(b): Diagrammatic representation of  $\zeta(r)$ , graphs with no cutting points.

following type:

- (i) Graphs from  $\zeta$ -sum,
- (ii) Products of graphs from  $\zeta$ -sum
- (iii) Products of graphs from  $\tau$ -sum
- (iv) A direct f-bond.

In a particular  $\tau$ -diagram, all the subgraphs which can be joined to a pair of specific adjacent cutting points are connected to the rest part of the main  $\tau$ -diagram via this specific pair. Hence all the subgraphs can be grouped together in a subset and we can sum over all possible subsets and all possible connections between the specific pair of adjacent cutting points. Then we get an expression which is a function of only the relative coordinates of the pair of adjacent cutting points. This is called  $h(\vec{r}_{kl})$ , where  $K$  and  $l$  are the specific pair of adjacent cutting points. The mathematical expression for  $h(\vec{r}_{kl})$  is

$$h(\vec{r}_{kl}) = \left\{ 1 + \gamma(\vec{r}_{kl}) \right\} \exp \left[ Q(\vec{r}_{kl}) \right] - 1 = g(\vec{r}_{kl}) - 1 \quad (62)$$

In obtaining equation (62), we have considered all single  $Q$ -graphs which include those with cutting points, i.e. it contains the entire  $\tau$ -sum. These are to be excluded from the allowable subgraphs connecting any pair of adjacent cutting points. Thus we get another function  $c(\vec{r}_{kl})$  given as

$$c(\vec{r}_{kl}) = h(\vec{r}_{kl}) - \tau(\vec{r}_{kl}) \quad (63)$$

By looking at graphs and combinatorial theory, we obtain

$$\tau(\vec{r}_{ij}) = \sum_{n \geq 1} \rho^n \int c(\vec{r}_{ij}) c(\vec{r}_{12}) \dots c(\vec{r}_{n-1,n}) c(\vec{r}_{nj}) d(\vec{n}) \quad (64)$$

The function  $c(\vec{r})$  is the Ornstein-Zernike direct correlation function. By Fourier Transformation techniques and mathematical rearrangement, we get

$$\tau(\vec{r}_{ij}) = \rho \int h(\vec{r}_{ij} - \vec{r}_{j1}) \left[ h(\vec{r}_{j1}) - Q(\vec{r}_{j1}) + \zeta(\vec{r}_{j1}) \right] d\vec{r}_{j1} \quad (65)$$

$$Q(\vec{r}_{ij}) = \rho \int h(\vec{r}_{ij} - \vec{r}_{j1}) \left[ h(\vec{r}_{j1}) - Q(\vec{r}_{j1}) + \zeta(\vec{r}_{j1}) \right] d\vec{r}_{j1} + \zeta(\vec{r}_{ij}) \quad (66)$$

From equation (66) we see that  $h(\vec{r}_{ij})$  is given in terms of  $Q(\vec{r}_{ij})$  and we have an integral equation involving two unknown functions.

In order to solve the integral equation in (65,66), we have to look at the graphs included in  $\zeta(\vec{r}_{ij})$ . These  $\zeta$ -graphs can also be classified into two groups, i.e. graphs with bifocal points and graphs without bifocal points. Bifocal points are pair of points where the graph separates into two or more parts, and each part contains at least one particle. In Figures 9 and 10, we show graphs with bifocal points and without bifocal points respectively. The graphs without bifocal points are called prototypes and we get a graph with bifocal points by replacing the  $\gamma$ -bond by a diagram in the prototype. This is shown in Fig. 11. Thus we can take a specific prototype and replace the  $\gamma$ -bond by all possible diagrams in all possible combination. Summing over all these graphs we get a diagram whose topology is equivalent to that of the prototype, but the  $\gamma$ -bonds

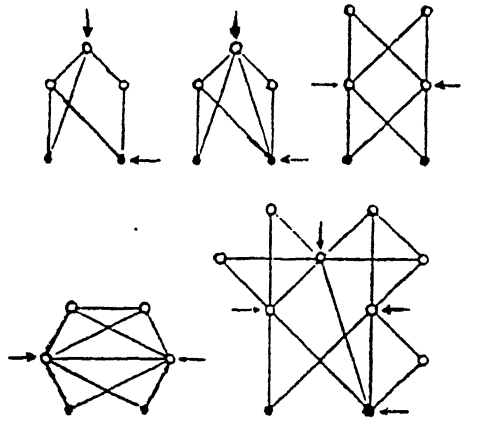


Figure 3.9:  $\zeta$  graphs containing bifocal points(indicated by arrows).

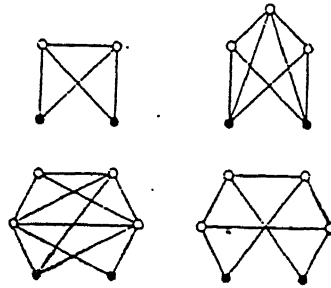


Figure 3.10:  $\zeta$  graphs with no bifocal points. These are the prototypes.

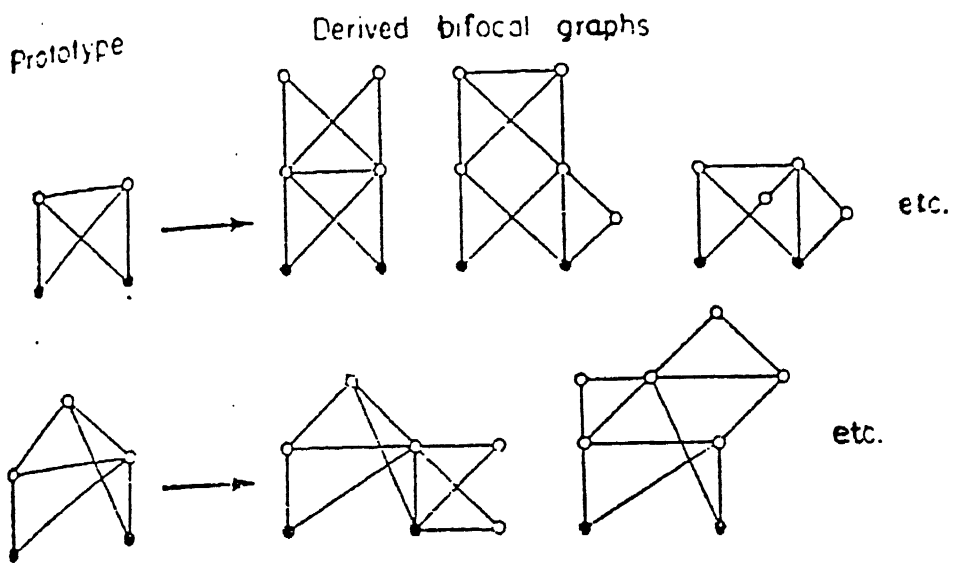


Figure 3.11: Derivation of graphs containing bifocal points from prototypes.

are replaced by h-bonds. Hence

$$\zeta(\vec{r}_{ij}) = \sum_{n \geq 2} \frac{\rho^n}{n!} \int Z(ij, n) d(\vec{n}) \quad (67)$$

Here  $Z(ij, n)$  are sums of all possible products of function  $h(\vec{r}_{kl})$  connecting the particles of the set  $ij+n$  in prototype pattern. Thus equation (66) and (67) provide a set of equations closed in pair space whose solution would yield values of the pair potential of average force, pair distribution function, the total correlation function and the direct correlation function.

Now the prototype expansion of  $\zeta(\vec{r}_{ij})$  in equation (67) is an infinite series of extremely complicated cluster integrals involving the unknown functions  $h(\vec{r}_{kl})$  and these functions are to be determined from the solution. Inclusion of only the first term, i.e.,  $n = 2$ , in  $\zeta(\vec{r}_{ij})$ , gives an integral equation for  $Q(ij)$  which becomes very difficult to evaluate. Thus an approximation is made and it results from the assumption that  $\zeta(\vec{r}_{ij}) = 0$ . By putting this in equation (66) we see that we get a simple closed convolution equation

$$\tau(\vec{r}_{ij}) = \rho \int h(\vec{r}_{ij} - \vec{r}_{j1}) \left[ h(\vec{r}_{j1}) - \tau(\vec{r}_{j1}) \right] d\vec{r}_{j1} \quad (68)$$

This convolution approximation represents the limit of the nodal expansion sequence described above (9,13).

The account given above for derivation of an integral equation considers a system of single component with a general interaction potential. Allnatt (12) has adapted this to derive an integral equation for an ionic solution with central Coulomb forces (charge-charge only). He has done this to put the Mayer ionic solution theory into the form of a set of integral equations for the radial distribution function by starting from

the series expansions for ionic solutions given by Meeron (7). The pairwise potential of average force at infinite dilution for two solute particles of species i and j a distance  $R_{ij}$  apart will be written as the sum of an ideal Coulomb part and an unspecified short range part.

$$U_{ij} = U_{ij}^* + z_i z_j \epsilon^2 / D R_{ij} \quad (69)$$

$D \longrightarrow$  the macroscopic dielectric constant of pure solvent in the reference state

$z_i, z_j \longrightarrow$  Algebraic charges on the ions of species i and j respectively

$\epsilon \longrightarrow$  The magnitude of electronic charge.

The pair distribution function for a pair of ions of species i and j is given by

$$g_{ij} = \exp \left( - \frac{\omega_{ij}}{kT} \right) \quad (70)$$

$\omega_{ij}$  given by Meeron is shown in equation (46).

$$\text{Hence } g_{ij} = \exp (q_{ij} - \beta U_{ij}^* + \alpha_{ij}) \quad (71)$$

where

$$q_{ij} = - \frac{-z_i z_j \epsilon^2 \exp(-\kappa R_{ij})}{D R_{ij} kT} \quad (72)$$

$$\alpha_{ij} = \sum_{m \leq 1}^{\sigma} \frac{\bar{\rho}^{\bar{m}}}{\bar{m}!} \int \theta (ij, \bar{m}) d(\bar{m}) \quad (73)$$

The integral refers to that in a multicomponent system.  $\theta(ij, \bar{m})$  are sums of products of  $q$  and  $\phi$ -bonds where  $\phi$  is defined from equation (45) as

$$\phi_{ij} = \exp(q_{ij} - \beta U_{ij}^*) - 1 - q_{ij} \quad (74)$$

The diagrams represented by  $\theta$  have the same topology as  $Q$  defined in equation (26). They can be redefined as follows.

$\theta(ij, \bar{m})$  is the sum of all products of  $q$  and  $\phi$  functions.

- a) Every node of set  $\bar{m}$  is connected to both  $i$  and  $j$  either directly or by two or more independent paths.
- b) all nodes of set  $\bar{m}$  are connected among themselves.
- c) There is no direct bond between  $i$  and  $j$ .
- d) Only isolated  $q$ -bonds appear.

The method for the derivation of the integral equation is similar to that of Meeron (10) to derive the exact integral equation for monoatomic fluid. He used diagrams with  $\gamma$ -bonds only. Here the diagrams used consist of two types of bonds. These diagrams are also divided into two groups according to the fact that they are with cutting points or without cutting points. Hence

$$\alpha(\vec{r}_{ij}) = \tau(\vec{r}_{ij}) + \zeta(\vec{r}_{ij}) \quad (75)$$

As explained above,  $\tau(\vec{r}_{ij})$  is the sum of all contributions in which the corresponding diagrams have cutting point.  $\zeta(\vec{r}_{ij})$  is the sum of all contributions without cutting points. In a similar way adjacent cutting points are defined in  $\tau$  diagrams. These adjacent cutting points can be joined by a single bond or a subdiagram. The subdiagrams between adjacent cutting points  $k$  and  $l$  can be made up of

- i) Diagrams of  $\zeta(\vec{r}_{kl})$  or their products
- ii) Products of  $\tau(\vec{r}_{kl})$  diagrams
- iii) Products of  $\tau(\vec{r}_{kl})$  and  $\zeta(\vec{r}_{kl})$  diagrams
- iv) Any of the diagrams in (i), (ii), (iii) with an extra  $q$ -bond or  $\phi$ -bond
- v) A single  $\phi$ -bond.



As the nodes in the subdiagrams between adjacent cutting points are connected to the rest of the diagram through this pair of cutting points, we can integrate over the coordinates of the subset of nodes in the subdiagram and the integral is a function of the relative coordinates of adjacent cutting points. Hence it is possible to sum over all diagrams differing only in the subdiagram connecting the adjacent cutting points and as a result of summation we get a modified bond between  $k$  and  $l$  called  $X(\vec{r}_{kl})$ . By mathematical manipulation we find

$$X(\vec{r}_{kl}) = h(\vec{r}_{kl}) - \tau(\vec{r}_{kl}) - q(\vec{r}_{kl}) \quad (76)$$

where

$$h(\vec{r}_{kl}) = g(\vec{r}_{kl}) - 1 \quad (77)$$

Let us consider terms in  $\tau(\vec{r}_{ij})$  with composition  $(i+j+\bar{M})$  and  $n$  cutting points of composition  $\bar{n}$ . The set  $(\bar{M} - \bar{n})$  is divided into  $(n+1)$  subsets of compositions  $\bar{a}_1, \bar{a}_2, \dots, \bar{a}_{n+1}$ . The set  $\bar{M}$  can be divided up into  $(n+2)$  sub-sets in  $\bar{M}!/\bar{n}!\bar{a}_1! \bar{a}_2! \dots \bar{a}_{n+1}!$  ways. The  $\bar{M}!$  cancels with the  $\frac{1}{\bar{M}!}$  of  $\frac{\rho^{\bar{M}}}{\bar{M}!}$ . The  $n$ -cutting points can be arranged in  $\bar{n}!$  different ways to give that many diagrams with the same set of points. Hence this cancels with the  $\bar{n}!$  in the  $\bar{M}!/\bar{n}!\bar{a}_1! \dots \bar{a}_{n+1}!$  term. Thus it is left with  $\frac{1}{\bar{a}_1! \bar{a}_2! \dots \bar{a}_{n+1}!}$  and each of them with corresponding  $\rho^{a_m}$  gets absorbed with the appropriate  $X$ -bond.

$$\text{Hence } \tau(\vec{r}_{ij}) = \sum_{n \geq 1} \rho^{\bar{n}} \int T(ij, \bar{n}) d(\bar{n}) \quad (78)$$

where  $T(ij, \bar{n})$  is the sum of all distinguishable chains of  $X$ -bonds and isolated  $q$ -bonds in which intermediate nodes between  $i$  and  $j$  have composition  $\bar{n}$  and particles of the same species are

counted as indistinguishable but particle of different species are distinguishable.

Now we can divide the  $\tau$ -diagrams further into two groups:  $A(\vec{r}_{ij})$  and  $B(\vec{r}_{ij})$ .  $A(\vec{r}_{ij})$  is sum of all contribution to  $\tau(\vec{r}_{ij})$  in which the bond connected to  $i$  is an X-bond and  $B(\vec{r}_{ij})$  is the sum of all contribution to  $\tau(\vec{r}_{ij})$  in which the bond connected to 'i' is a q-bond. Hence

$$\tau(\vec{r}_{ij}) = A(\vec{r}_{ij}) + B(\vec{r}_{ij}) \quad (79)$$

$$\begin{aligned} A(\vec{r}_{ij}) &= \sum_{k=1}^{\sigma} c_k \int X(\vec{r}_{ik}) \left[ X(\vec{r}_{kj}) + q(\vec{r}_{kj}) + \tau(\vec{r}_{kj}) \right] dk \\ &= \sum_{k=1}^{\sigma} c_k \int X(\vec{r}_{ik}) h(\vec{r}_{kj}) dk \end{aligned} \quad (80)$$

$$\begin{aligned} B(\vec{r}_{ij}) &= \sum_{k=1}^{\sigma} c_k \int q(\vec{r}_{ik}) \left[ X(\vec{r}_{kj}) + A(\vec{r}_{kj}) \right] dk \\ &= \sum_{k=1}^{\sigma} c_k \int q(\vec{r}_{ik}) \left[ X(\vec{r}_{kj}) + \sum_{l=1}^{\sigma} c_l \int X(\vec{r}_{kl}) h(\vec{r}_{lj}) dl \right] dk \\ &= \sum_{k=1}^{\sigma} c_k \int q(\vec{r}_{ik}) X(\vec{r}_{kj}) dk + \sum_{k=1}^{\sigma} \sum_{l=1}^{\sigma} c_k c_l \iint q(\vec{r}_{ik}) X(\vec{r}_{kl}) h(\vec{r}_{lj}) dk dl \end{aligned} \quad (81)$$

$$\begin{aligned} \tau(\vec{r}_{ij}) &= A(\vec{r}_{ij}) + B(\vec{r}_{ij}) = \sum_{k=1}^{\sigma} c_k \int X(\vec{r}_{ik}) h(\vec{r}_{kj}) dk + \sum_{k=1}^{\sigma} c_k \int q(\vec{r}_{ik}) X(\vec{r}_{kj}) dk \\ &+ \sum_{k=1}^{\sigma} \sum_{l=1}^{\sigma} c_k c_l \iint q(\vec{r}_{ik}) X(\vec{r}_{kl}) h(\vec{r}_{lj}) dk dl \end{aligned} \quad (82)$$

From equation (71) we have the expression for the pair distribution function as

$$\log g(\vec{r}_{ij}) + \beta U(\vec{r}_{ij})^* - q(\vec{r}_{ij}) = \tau(\vec{r}_{ij}) + \zeta(\vec{r}_{ij}) \quad (83)$$

and the integral equation for the pair distribution function is found by eliminating  $\tau$  from equation (78). The term  $\zeta(\vec{r}_{ij})$  is evaluated as that by Meeron (10) and

$$\zeta(\vec{r}_{ij}) = \sum_{n \geq 2} \frac{\bar{c}^{\bar{n}}}{\bar{n}!} \int z(ij, \bar{n}) d(\bar{n}) \quad (84)$$

where  $Z(ij, \bar{n})$  is the sum of all possible products of functions  $h$  connecting the nodes of set  $(i + j + \bar{n})$  in prototype patterns. (A prototype pattern is a diagram belonging to the subset of diagrams of set  $\zeta(\vec{r}_{ij})$  with no bifocal points. (Bifocal points are pair of points through which the diagram can be separated).)

As Meeron (10) has shown, the integral equation is solved by making the approximation  $\zeta = 0$ . We then get the HNC approximation. In this present equation a relationship to the Mayer Ionic Solution Theory is presented. The integral equation can be solved by iteration procedure. An initial approximation for  $\tau(\vec{r}_{ij})$  is made which leads to the calculation of  $h(\vec{r}_{ij})$ . This can give the value of  $X(\vec{r}_{ij})$ . Then we calculate improved values of  $\tau(\vec{r}_{ij})$  from equation (82). If the initial approximation of  $\tau$  is zero, then  $X(\vec{r}_{ij}) = \phi(\vec{r}_{ij})$  and  $\tau^{(1)}(\vec{r}_{ij})$  becomes equal to the contributions of all chains of  $\phi$ -bonds and isolated  $q$ -bonds. Successive iterations adds series and parallel combination of such chains. Van Leeuwen et al. (11) have done a parallel development of the HNC approximation. There they have shown explicitly how more and more diagrams are included in the evaluation by series and parallel combinations of chains in successive iteration. Thus if the process is iterated for sufficient number of times such that the values converge, then we

have summed over a very large number of diagrams of significant numerical magnitude. The convergence indicates that one has now reached very highly connected diagrams, whose values are small, because the integrand is nonzero only over a limited region of configuration space.

We note that the Allnatt equation deduced above differs from the original HNC equation derived for nonionic fluids in that the shielded potential  $q_{ij}$  and short range potential  $U_{ij}^*$  appear instead of the total direct potential  $U_{ij}$ . The equation ( 82 ) being solved is the same as Ornstein-Zernicke equation  $\tau_{ij}^{(r)}$  of Eq. ( 82 ) is  $h_{ij}(r) - c_{ij}(r)(E_0)$ . The diagrams of class A and B represent the convolution integral  $\int h_{ik} c_{kj} dk$ . However the closure is different. Whereas the closure of the usual HNC theory of nonionic fluids is (Eq 5.19 of Ref. 17 of 4. 7)

$$c(r) = -\beta U(r) + h(r) - \log (h(r) + 1)$$

$$\text{or, } \beta U_{ij}(r) = \left\{ h_{ij}(r) - c_{ij}(r) \right\} - \log (h_{ij}(r) + 1)$$

$$\text{or, } \beta U_{ij}(r) = \tau_{ij}(r) - \log (h_{ij}(r) + 1)$$

$$\text{or, } \beta U_{ij}^*(r) - g_{ij}(r) = \tau_{ij} - \log (h_{ij}(r) + 1)$$

The closure for Allnatt equation is (Eq. 83 with  $\xi=0$ )

$$\log (1 + h_{ij}(r) + \beta U_{ij}^*(r) - q_{ij}(r)) = \tau_{ij}(r)$$

$$\text{or, } \beta U_{ij}^*(r) - q_{ij}(r) = \tau_{ij}(r) - \log (1 + h_{ij}(r))$$

The difference is that a g-bond in the closure of the HNC equation of nonionic fluids is replaced by a q-bond in the closure of the Allnatt equation.

### 3.8 Solution of Integral Equation

The method for this is developed by Rasaiah and Friedman (14). From equation (82) we see that the terms used to describe  $\tau$  are integrals of type

$$\sum_{k=1}^{\sigma} c_k \int a(\vec{r}_{ik}) b(\vec{r}_{kj}) d\{K\} \quad \text{and it can be written as}$$

$$\sum_{k=1}^{\sigma} c_k \int a(\vec{r}_{ik}) b(\vec{r}_{kj}) d\{K\} = a_{ik} * b_{kj} \quad (85)$$

Here  $K$  is the species of the molecule at the cutting point nearest to  $i$  and  $\{K\}$  is its spatial coordinate. The notation  $*$  indicates sum over the species at the cutting point and the integral is a convolution integral. Now  $i$  and  $j$  can be varied to get each pair of species and there will be in total  $\sigma^2$  terms like equation (85). Then the notation can be made compact as  $a*b$  which represents all the  $\sigma^2$  terms. If we consider all the pairs of species, then all the above expressions for  $\tau$ ,  $X$ ,  $h$ ,  $q$  etc. reduce to a matrix notation as follows:

$$X = h - q - \tau \quad (86)$$

$$h = g - 1 \quad (87)$$

$$\tau = A + B \quad (88)$$

$$\tau = X * h + q * X + q * X * h \quad (89)$$

From equation (71), we find,

$$g(\vec{r}_{ij}) = \exp\left(-\frac{U^*(\vec{r}_{ij})}{kT}\right) \exp\left[q(\vec{r}_{ij}) + \tau(\vec{r}_{ij}) + \zeta(\vec{r}_{ij})\right]$$

Here  $U^*(\vec{r}_{ij})$  is the hard sphere potential defined as

$$U^* = \begin{cases} \infty & , \vec{r}_{ij} < a_{ij} \\ 0 & , \vec{r}_{ij} > a_{ij} \end{cases} \quad (90)$$

hence

$$\exp \left[ - \frac{U^*(\vec{r}_{ij})}{kT} \right] = \begin{cases} \exp(-\infty) = 0 & , r < a_{ij} \\ \exp(0) = 1 & , r > a_{ij} \end{cases} \quad (91)$$

hence

$$\begin{aligned} 1 + h(\vec{r}_{ij}) &= 0, r < a_{ij} \\ 1 + h(\vec{r}_{ij}) &= \exp \left[ q(\vec{r}_{ij}) + \tau(\vec{r}_{ij}) + \zeta(\vec{r}_{ij}) \right], r > a_{ij} \end{aligned} \quad (92)$$

In the HNC approximation  $\zeta(\vec{r}_{ij}) = 0$

$$\text{Hence } 1 + h(\vec{r}_{ij}) = \exp \left[ q(\vec{r}_{ij}) + \tau(\vec{r}_{ij}) \right] \quad (93)$$

The procedure to solve the above equations to get pair distribution function involves following steps.

(i) We take an initial approximate  $\tau$ . The approximation is evaluation of equation (73) with  $m = 1$ . With  $m = 1$  we get diagrams with cutting points only. So we include all the diagrams consisting of  $\phi$ -bonds and  $q$ -bonds, but no  $q$ -bond chain. Thus from the consideration of all the diagrams given in Fig.(12) we see that

$$\tau_0 = \phi * \phi + \phi * q + q * \phi \quad (94)$$

Let us define a function  $\phi' = \phi + q$ .

$$\begin{aligned} \text{Hence } \tau_0 &= (\phi' - q) * (\phi' - q) + (\phi' - q) * q + q * (\phi' - q) \\ &= \phi' * \phi' - q * q \end{aligned} \quad (95)$$

From equation (74)

$$\begin{aligned} \phi' &= \phi + q \\ &= \exp \left( - \frac{U^*}{kT} \right) \exp(q(\vec{r}_{ij})) - 1 \end{aligned}$$

$$Q(ij; 1) = \begin{array}{c} \circ \\ \diagup \quad \diagdown \\ \circ \quad \circ \end{array} + \begin{array}{c} \circ \\ \diagup \quad \text{---} \diagdown \\ \circ \quad \circ \end{array} + \begin{array}{c} \circ \\ \text{---} \diagup \quad \diagdown \\ \circ \quad \circ \end{array}$$

Fig-3.12 The diagrams used in the calculation of initial  $\tau$ .

— :  $\phi$  - bond

--- :  $q$  - bond

$$\left. \begin{aligned} &= -1, \quad r < a_{ij} \\ &= \exp(q(\vec{r}_{ij})) - 1, r > a_{ij} \end{aligned} \right\} \quad (96)$$

Clearly  $\phi'$  is calculated from  $q$ . Now  $q$  is calculated from equation (72). We get this expression for  $q$  when we consider the dielectric constant of the medium (solvent containing the solute particles which constitute a McMillan-Mayer gas) to be uniform. In Chapter 2, we have shown that dielectric constant can vary as a function of distance in the presence of macroion and hence the expression for  $q$  will be modified. This we will show in a section below (Section 3.9).

- (ii) Once  $\tau$  is calculated, we use this to calculate  $h$  using equation (92).
- (iii) Then we calculate  $X$  using equation (86)
- (iv) Now that we have initial round values for  $h$ , and  $X$  and we know the value of  $q$ , we can calculate an improved value of  $\tau$  using equation (89).

Once we get an improved value of  $\tau$ , we can repeat step (ii), (iii) and (iv) to get further improved  $\tau$  and this process is carried out till there is no longer a change in the values. Then we calculate final value of  $h$  which gives us  $g$ , pair distribution function.

### 3.9 Calculation of $q$ function for an ionic system with distance dependent screening constant : Derivation of a modified Meeron formula of $q$ bond

The theory for calculation of  $\omega(r)$  in charged macromolecular systems where screening constant for Coulombic interaction is a function of intermolecular distance requires modification of the



method of Meeron, described above, for calculation of  $\omega(r)$  of an ionic solution. The first point in Meeron's method, where a departure has to be made is in Eq. 27, 29, 30 where Coulomb potential (including the convergence factor)  $z_r z_l \frac{\epsilon^2 e^{-\alpha r}}{Dr}$  is expressed as a product of two factors  $\lambda = \frac{\epsilon^2}{D kT}$  and  $g(r) = \frac{e^{-\alpha r}}{r}$ .  $D$  is no longer a constant, but is a function of  $r$  and should be shifted to  $g(r)$ . Thus, redefined  $\lambda$  and  $g(r)$  called  $\lambda'$  and  $g'(r)$  are given by:

$$\lambda' = \frac{\epsilon^2}{kT} \quad \text{and} \quad g'(r) = \frac{e^{-\alpha r}}{D(r)r} . \quad (97)$$

The additional complication is that  $D(r)$  depends on the particle pair, whose Coulombic interaction is being screened. We therefore must introduce

$$g'_{mn}(r) = \frac{e^{-\alpha r_{mn}}}{D_{mn}(r_{mn})r_{mn}} ,$$

a modified  $g$  function between particles  $m$  and  $n$ . A modified  $g'$  bond is  $= -Z_m Z_n \lambda' g'_{mn}(r)$ . The integral over  $g'$  bond chains, the equivalent of Eq. 33, is written as

$$I_s(r_{kl}) = \int g'_{k1}(r_{k1}) g'_{12}(r_{12}) \dots g'_{ns,1}(r_{ns,1}) d\{\bar{n}_s\} \quad (98)$$

Whereas in Meeron's method all  $g$  bonds, irrespective of which pair of particles they connect are identical, we have a situation in which the  $g'$  bonds are not identical.

Even if the composition set of intermediate particles is the same, their order of arrangement makes a difference to the value of the integral. Meeron takes advantage of the fact that  $I_s$  in his case, is independent of the order of arrangement of intermediate particles and is therefore multiplied by a

combinatorial factor given in Eq. (34) and a further summation is carried out over all composition sets of the intermediate particles in Eq. (35) to obtain a sum of all chains between two particles. This sum is the  $q$  bond and one obtains expression for  $q$  bond between all pairs of particles in Eq. (38). The expression depends on the specific nature of the terminal points (between which one builds chains) only through the values of their charge (viz.  $Z_k, Z_l$ ). In the case under consideration, this method is inapplicable, because  $I_s$  depends on the specific order of intermediate particles in the chain. The method, we have adopted is based on that used by Friedman and Jepsen (15) in the theory of calculation of  $q$  bond in systems with angle dependent potential. The details of this method is given in section 4.1. The method, as applied to our specific problem, is described below.

Let us consider a chain of length 4 with macroions at the two terminals. The two intermediate particles can be all possible combinations, of positive ion, negative ion and macroion, a total of nine possibilities. Each of these combinations give rise to a  $g'$  bond chain, whose expression is typically

$$(-\lambda Z_m g'_{m+} Z_+) (-\lambda Z_+ g'_+ - Z_-) (-\lambda Z_- g'_{-m} Z_m)$$

(the chain is  $\overset{m}{\circ} \xrightarrow{g'_{m+}} \overset{+}{\circ} \xrightarrow{g'_+ -} \overset{-}{\circ} \xrightarrow{g'_{-m}} \overset{m}{\circ}$  )

which simplifies to  $(-\lambda)^3 (Z_m g'_{m+} (r_{m+}) Z_+^2 g'_+ - (r_+ -) Z_-^2 g'_{-m} (r_{-m}) Z_m)$

The integral to be evaluated is

$$I_S(r_{mm}) = (-\lambda)^3 \int_{-\infty}^{+\infty} z_m g'_{m+}(r_{m+}) z_+^2 g'_{+ -}(r_{+ -}) z_-^2 g_{-m}(r_{-m}) z_m d\vec{r}_+ d\vec{r}_-$$

It is evaluated in the Fourier domain. The three dimensional Fourier transform of  $I_S(r_{mm})$  is

$$\begin{aligned} \hat{I}(t) &= (-\lambda)^3 \int_{-\infty}^{+\infty} d\vec{r}_{mm} e^{-i\vec{t} \cdot \vec{r}_{mm}} \int_{-\infty}^{+\infty} d\vec{r}_+ d\vec{r}_- z_m g'_{m+}(r_{m+}) z_+^2 g'_{+ -}(r_{+ -}) \\ &\quad z_-^2 g_{-m}(r_{-m}) z_m \\ &= (-\lambda)^3 \int z_m g'_{m+}(r_{m+}) z_+^2 g'_{+ -}(r_{+ -}) z_-^2 g_{-m}(r_{-m}) z_m \\ &\quad e^{-i\vec{t} \cdot (\vec{r}_{m+} + \vec{r}_{+ -} + \vec{r}_{-m})} d\vec{r}_+ d\vec{r}_- d\vec{r}_m \\ &= (-\lambda)^3 z_m \int g'_{m+}(r_{m+}) e^{-it \cdot \vec{r}_{m+}} d\vec{r}_{m+} \int g'_{+ -}(r_{+ -}) e^{-it \cdot \vec{r}_{+ -}} d\vec{r}_{+ -} \\ &\quad \times \int z_-^2 g_{-m}(r_{-m}) e^{-i\vec{t} \cdot \vec{r}_{-m}} d\vec{r}_{-m} \end{aligned}$$

(noting  $d\vec{r}_+ = d\vec{r}_{m+}$ ,  $d\vec{r}_- = d\vec{r}_{-m}$ , and Jacobian of transformation  $d\vec{r}_{m+} d\vec{r}_{-m} d\vec{r}_{mm}$  to  $d\vec{r}_{m+} d\vec{r}_{+ -} d\vec{r}_{-m}$  is unity).

$$= (-\lambda)^3 z_m \tilde{g}_{m+}(t) z_+^2 \tilde{g}_{+ -}(t) z_-^2 \tilde{g}_{-m}(t) z_m, \quad (99)$$

where

$$\begin{aligned} \tilde{g}_{m+}(t) &= \int g'_{m+}(r_{m+}) e^{-i\vec{t} \cdot \vec{r}_{m+}} d\vec{r}_{m+} \\ &= \frac{4\pi}{t} \int g'_{m+}(r_{m+}) r_{m+} \sin tr_{m+} dr_{m+} \end{aligned}$$

(This is an well known identity (7). It has been derived explicitly in Chapter 5).

The sum of nine such terms  $\tilde{p}_{mm}(t)$  can be written in the following form

$$\tilde{p}_{mm}^{(4)}(t) = (-\lambda)^3 z_m z_m \sum_{n,l} \tilde{g}'_{mn}(t) z_n^2 \tilde{g}'_{nl}(t) z_l^2 \tilde{g}'_{lm}(t)$$

(where n and l run over the indices m, + and -)

$$= (-\lambda)^3 z_m z_m \sum_{\substack{n,l, \\ p,q}} \tilde{g}'_{mn}(t) (z_n z_p \delta_{np}) \tilde{g}'_{pq}(t) (z_q z_l \delta_{ql}) \tilde{g}'_{lm}(t)$$

(where n,l,p,q run over indices m, + and -)

$$= (-\lambda)^3 z_m z_m (H' Z H' Z H')_{mm} \quad (100)$$

where  $H'$  is a matrix, whose elements are  $(H')_{mn} = \tilde{g}'_{mn}(t)$   
 $Z$  is a matrix, whose elements are  $(Z)_{mn} = z_m z_n \delta_{mn}$

As the terminal particles change, the matrix element of  $(H' Z H' Z H')$  change accordingly, viz. if the terminal particles are a positive ion and a negative ion, then

$$\tilde{p}_{+-}^{(n+2)}(t) = (-\lambda)^{n+1} z_+ z_- (H' (Z H')_n)_{+-} \quad (101)$$

The quantity of interest to us is  $q_{XY}(r)$  which is related to  $p_{XY}(r)$  derived above (Eq. 100 and Eq.101) by the equation

$$q_{XY}(r) = g_{XY}(r) + \sum_{\nu > 1} \bar{\rho}^{\bar{\nu}} p_{XY}(r), \quad (102)$$

where the bars over  $\rho$  and  $\nu$  stand for a composition set,  $\rho$  is the number density. In Fourier space, the equation is

$$\tilde{q}_{XY}(t) = \tilde{g}_{XY}(t) + \sum_{\nu > 1} \bar{\rho}^{\bar{\nu}} \tilde{p}_{XY}(t) \quad (103)$$

The multiplicative factor with number densities arise from Eq.(17), the cluster expansion of  $\omega(r)$ . The integral over the Q diagrams are multiplied by  $\bar{\rho}^{\bar{\nu}}$ . The factor  $\bar{\rho}$  can be shifted to

the vertices of the Q diagram that multiplies  $\frac{\bar{\rho}^\nu}{\bar{\nu}!}$ . Thus g-bond chains that connect the vertices X and Y on a Q diagram (resulting from the expansion of  $\gamma$  bonds of the Q diagram in terms of g-bond chains) carry the corresponding number density on each of the vertices of the g-bond chain. In evaluating  $p_{XY}(r)$  we left out the number density terms. Now in the final summation to obtain the convergent g bonds, we include them.  $g_{XY}(r)$  is a single direct g-bond between X and Y without any particle in between, i.e., the chain length is zero.

For the system under consideration, we obtain

$$\therefore \tilde{q}_{XY}(t) = \tilde{g}'_{XY}(t) + \sum_{\nu>1} \bar{\rho}^\nu (-\lambda)^{\nu+1} Z_X Z_Y (H' (ZH')_\nu)_{XY} \quad (103)$$

We include  $\lambda$  in the  $H'$  matrices both of which are  $\nu+1$  in number

$$\tilde{q}_{XY}(t) = \sum_{\nu>1} \bar{\rho}^\nu Z_X Z_Y (H' (ZH')_\nu)_{XY} \quad (104)$$

The matrix  $Z$  is diagonal and has square of charges of individual species along its diagonal, i.e.,  $Z$  matrix of our system is given below:

$$Z = \begin{matrix} & \begin{matrix} + & - & m \end{matrix} \\ \begin{matrix} + \\ - \\ m \end{matrix} & \begin{bmatrix} Z_+^2 & 0 & 0 \\ 0 & Z_-^2 & 0 \\ 0 & 0 & Z_m^2 \end{bmatrix} \end{matrix} \quad (105)$$

We can easily include  $\bar{\rho}^\nu$  in this matrix and obtain another diagonal matrix, which we call  $Z'$

$$Z' = \begin{matrix} & + & - & m \\ + & \rho_+ Z_+^2 & 0 & 0 \\ - & 0 & \rho_- Z_-^2 & 0 \\ m & 0 & 0 & \rho_m Z_m^2 \end{matrix} \quad (106)$$

Further summation over all possible values of chain length  $\nu+1$ , gives

$$\tilde{q}_{XY}(t) = \tilde{g}_{XY}(t) + Z_X \left\{ (-\lambda H') \left[ I - Z'(-\lambda H') \right]^{-1} Z' (-\lambda H') \right\}_{XY} \quad (107)$$

$\tilde{g}_{XY}(t)$  connects X and Y with one  $\tilde{g}'$  "Connector".

The term  $Z' (-\lambda H')$  (following  $\left[ I - Z'(-\lambda H') \right]^{-1}$  is needed because the first term in the expansion of  $\left[ I - Z'(\lambda H') \right]^{-1}$  is I and it generates a connection between X and Y through two  $\tilde{g}'$  "connectors". This term is linear in  $\rho$  (since only one  $Z'$  is present), whereas  $\tilde{g}_{XY}(t)$  is independent of  $\rho$ . The power of  $\rho$  equals the number of intermediate vertices between X and Y. Thus if there is one intermediate vertex, there are three particles altogether (X, Y and the intermediate particle) and two connectors are needed. The first term  $\tilde{g}_{XY}(t)$  has no intermediate particles and thus only one  $\tilde{g}'$  connector is needed.

We can simplify the above expression to write

$$\tilde{q}_{XY}(t) = Z_X \left[ (-\lambda H') \left[ I - Z'(-\lambda H') \right]^{-1} \right]_{XY} Z_Y \quad (108)$$

The expansion of this expression will have a first term which contains a single  $\tilde{g}'$  function, which is  $\tilde{g}_{XY}(t)$ . Thus  $\tilde{g}_{XY}(t)$  is no longer needed as a separate term. We now explicitly write the expressions for  $Z'$ ,  $\lambda H'$  and  $[I - Z'(-\lambda H')]$

$$Z' = - \begin{matrix} & + & - & m \\ \begin{bmatrix} \rho_+ Z_+^2 & 0 & 0 \\ 0 & \rho_- Z_-^2 & 0 \\ 0 & 0 & \rho_m Z_m^2 \end{bmatrix} \end{matrix} \quad (109)$$

$$\begin{matrix} & + & - & m \\ \begin{bmatrix} -\lambda \tilde{g}'_{++} & -\lambda \tilde{g}'_{+-} & -\lambda \tilde{g}'_{+m} \\ -\lambda \tilde{g}'_{-+} & -\lambda \tilde{g}'_{--} & -\lambda \tilde{g}'_{-m} \\ -\lambda \tilde{g}'_{m+} & -\lambda \tilde{g}'_{m-} & -\lambda \tilde{g}'_{mm} \end{bmatrix} \end{matrix} \quad (110)$$

$$[I - Z' (-\lambda H')]$$

$$\begin{bmatrix} (1 + \rho_+ Z_+^2 \lambda \tilde{g}'_{++}) & (\rho_+ Z_+^2 \lambda \tilde{g}'_{+-}) & (\rho_+ \lambda Z_+^2 \tilde{g}'_{+m}) \\ (\rho_- Z_-^2 \lambda \tilde{g}'_{-+}) & (1 + \rho_- Z_-^2 \lambda \tilde{g}'_{--}) & (\rho_- Z_-^2 \lambda \tilde{g}'_{-m}) \\ (\rho_m Z_m^2 \lambda \tilde{g}'_{m+}) & (\rho_m Z_m^2 \lambda \tilde{g}'_{m-}) & (1 + \rho_m Z_m^2 \lambda \tilde{g}'_{mm}) \end{bmatrix} \quad (111)$$

The inverse of this matrix needed for calculation  $\tilde{q}_{XY}(t)$  has to be computed in the usual manner:

$$(A)^{-1} = \frac{A_C^T}{\det(A)} \quad (112)$$

(where  $A_C^T$  is the transpose of the cofactor matrix of A.

$\det(A)$  is the determinant of the matrix A).

In the general case, no further simplification is possible.

However, in the system of +ve ion, -ve ion and macroion,  $\tilde{g}'_{++}$ ,  $\tilde{g}'_{+-}$ ,  $\tilde{g}'_{-+}$ ,  $\tilde{g}'_{--}$  have the simple form

$$\tilde{g}'_{pq} = \lim_{\alpha \rightarrow 0} \int \int \int_0^\infty \frac{e^{-\alpha r}}{r \cdot D} e^{-i\vec{r} \cdot \vec{r}} d\vec{r} (D \text{ is not a function of } r)$$

$$\begin{aligned}
&= \begin{bmatrix} -\frac{\delta}{t^2} & -\frac{\delta}{t^2} & -\lambda\tilde{g}'_{+m} \\ -\frac{\delta}{t^2} & -\frac{\delta}{t^2} & -\lambda\tilde{g}'_{-m} \\ -\lambda\tilde{g}'_{m+} & -\lambda\tilde{g}'_{m-} & -\lambda\tilde{g}'_{mm} \end{bmatrix} \times \begin{bmatrix} \frac{1}{\det} \rho_{11} & \frac{1}{\det} \rho_{12} & \frac{1}{\det} \rho_{13} \\ \frac{1}{\det} \rho_{21} & \frac{1}{\det} \rho_{22} & \frac{1}{\det} \rho_{23} \\ \frac{1}{\det} \rho_{31} & \frac{1}{\det} \rho_{32} & \frac{1}{\det} \rho_{33} \end{bmatrix} \\
&= \frac{1}{\det} \begin{bmatrix} -\frac{\delta}{t^2} (\rho_{11}+\rho_{21}) & -\frac{\delta}{t^2} (\rho_{12}+\rho_{22}) & -\frac{\delta}{t^2} (\rho_{13}+\rho_{23}) \\ -\lambda\tilde{g}'_{+m} (\rho_{31}) & -\lambda\tilde{g}'_{+m} (\rho_{32}) & -\lambda\tilde{g}'_{+m} (\rho_{33}) \\ -\frac{\delta}{t^2} (\rho_{11}+\rho_{21}) & -\frac{\delta}{t^2} (\rho_{12}+\rho_{22}) & -\frac{\delta}{t^2} (\rho_{13}+\rho_{23}) \\ -\lambda\tilde{g}'_{-m} (\rho_{31}) & -\lambda\tilde{g}'_{-m} (\rho_{32}) & -\lambda\tilde{g}'_{-m} (\rho_{33}) \\ -\frac{\delta}{t^2} (\rho_{11}+\rho_{21}) & -\frac{\delta}{t^2} (\rho_{12}+\rho_{22}) & -\frac{\delta}{t^2} (\rho_{13}+\rho_{23}) \\ -\lambda\tilde{g}'_{mm} (\rho_{31}) & -\lambda\tilde{g}'_{mm} (\rho_{32}) & -\lambda\tilde{g}'_{mm} (\rho_{33}) \end{bmatrix}
\end{aligned}$$

The  $ij$ -th term in the above matrix gives us  $\tilde{q}_{ij}(t)$ . In the limit, when the screening constant is not a function of  $r$ , then  $\lambda\tilde{g}'_{mm}, \lambda\tilde{g}'_{m+}, \lambda\tilde{g}'_{m-}, \lambda\tilde{g}'_{+m}, \lambda\tilde{g}'_{-m}$  becomes  $\frac{\delta}{t^2}$  as shown in equation (113). If we look at  $\tilde{q}_{XY}(t)$  term in the matrix, we find

$$\begin{aligned}
\tilde{q}_{++}(t) &= \tilde{q}_{+-}(t) = \tilde{q}_{+m}(t) = \tilde{q}_{-+}(t) = \tilde{q}_{--}(t) = \\
\tilde{q}_{-m}(t) &= \tilde{q}_{m+}(t) = \tilde{q}_{m-}(t) = \tilde{q}_{mm}(t) = -\frac{\delta}{t^2} \times \frac{1}{\det}
\end{aligned}$$

$$\det = 1 + \frac{\delta}{t^2} (\rho_+ z_+^2 + \rho_- z_-^2 + \rho_m z_m^2)$$



$$= 1 + \frac{4\pi\epsilon^2}{D kTt^2} (\sum_i \rho_i z_i^2)$$

$$= 1 + \frac{1}{t^2} \times \frac{4\pi\epsilon^2}{D kT} (\sum_i \rho_i z_i^2)$$

$$= 1 + \frac{\kappa^2}{t^2} = \frac{t^2 + \kappa^2}{t^2}$$

$$\therefore \tilde{q}_{++}(t) = \tilde{q}_{+-}(t) = \tilde{q}_{+m}(t) = \tilde{q}_{-+}(t) = \tilde{q}_{--}(t) = \tilde{q}_{-m}(t) = \tilde{q}_{m+}(t) \\ = \tilde{q}_{m-}(t) = \tilde{q}_{mm}(t) = - \frac{t^2 x(\delta/t^2)}{t^2 + \kappa^2}$$

This when Fourier Transformed back, gives

$$- \frac{1}{8\pi^3} \times \delta \int_0^\infty \frac{1}{t^2 + \kappa^2} \frac{\sin tr}{tr} 4\pi t \, dr \\ = - \frac{1}{2\pi^2} \cdot \frac{4\pi\epsilon^2}{D kT} \int \frac{t}{t^2 + \kappa^2} \sin tr \, dt \\ = - \frac{2}{\pi} \cdot \frac{\lambda}{D} \cdot \frac{\pi}{2} \frac{e^{-\kappa r}}{r} \\ = - \frac{\lambda e^{-\kappa r}}{Dr}$$

This value when multiplied by appropriate Z values gives the q value derived by Meeron with the usual distance independent screening constant.

$$\therefore q_{++}(r) = - \frac{z_+^2 \epsilon^2}{DkT} \cdot \frac{e^{-\kappa r}}{r} \\ q_{+-}(r) = - \frac{z_+ z_- \epsilon^2}{DkT} \cdot \frac{e^{-\kappa r}}{r} \\ q_{+m}(r) = - \frac{z_+ z_m \epsilon^2}{DkT} \cdot \frac{e^{-\kappa r}}{r} \text{ etc.}$$

The relationship of this method to that of Jepsen and Friedman (15), is discussed in Chapter 4, where we also describe their

method in detail.

### 3.10 The Question of Convergence

In Mayer's theory (Eq. 6(a)) and in Meeron theory (Eq.36 to Eq. 39), a series summation is carried out. This is explicitly seen in Eq. (6a) and once again is given below:

$$\begin{aligned}
 & \sum_n (-\kappa^2)^n [G(t)]^{n+1} \\
 &= G(t) \sum_n (-\kappa^2)^n [G(t)]^n \\
 &= G(t) \left\{ 1 - \kappa^2 G(t) + (\kappa^2 G(t))^2 - (\kappa^2 G(t))^3 + \dots \right\} \\
 &= G(t) \left\{ 1 + \kappa^2 G(t) \right\}^{-1} \\
 &= \frac{G(t)}{1 + \kappa^2 G(t)} \\
 &= \frac{1}{G(t)^{-1} + \kappa^2}
 \end{aligned}$$

The series summation involved is

$$1 - x + x^2 - \dots = (1 + x)^{-1}, \text{ where } x = \kappa^2 G(t)$$

The series converges only if  $|x| < 1$ . This restriction would restrict the utility of the theory.  $|x| < 1$  means  $|\kappa^2 G(t)| < 1$ .  $G(t) = 1/t^2$ ,  $t$  ranges from 0 to  $\infty$ ,  $\kappa^2 G(t)$  therefore is always positive.  $\kappa^2 G(t) = (\kappa^2/t^2) < 1$  implies  $t^2 > \kappa^2$ . For Fourier inversion, one requires the expression  $(1 + x)^{-1}$  to be valid over the whole range of  $t$  from 0 to  $\infty$ . This would be true only in the limit  $\kappa^2 \rightarrow 0$ , i.e., in the limit of an infinitely dilute solution. However, the method of analytic continuation extends

the validity of the equation in the range  $t^2 < \kappa^2$  also (2). Let us discuss briefly how  $1 - x + x^2 - \dots = (1 + x)^{-1}$  can hold outside its traditional radius of convergence. Our presentation follows that of Dennery and Krzywicki (16). Let us consider two functions  $f_1(z)$  and  $f_2(z)$  which have different functional forms and are analytic within regions  $D_1$  and  $D_2$  respectively, which overlap. If  $f_1(z)$  and  $f_2(z)$  are identical within the intersection  $D_1 \cap D_2$  of the two regions, the results of the analytic continuation of  $f_1(z)$  in  $D_2$  (which is unique, by virtue of a theorem proved in Ref. 16) must be identical with  $f_2(z)$  and the result of the analytic continuation of  $f_2(z)$  in  $D_1$  must coincide with  $f_1(z)$ . Thus, we may regard  $f_1(z)$  and  $f_2(z)$  as corresponding to a unique function  $f(z)$ .

$$f(z) = \begin{cases} f_1(z), & z \in D_1 \\ f_2(z), & z \in D_2 \end{cases}$$

which is analytic throughout the union  $D_1 + D_2$  of the regions  $D_1$  and  $D_2$  and is uniquely determined by  $f_1(z)$  or  $f_2(z)$  for  $z \in D_1 \cap D_2$ . We take, as an illustration

$$f_1(z) = 1 + z + z^2 +$$

which is defined for

$$|z| < 1,$$

where the series is convergent and

$$f_2(z) = \frac{2}{3} + \left(\frac{2}{3}\right)^2 \left(z + \frac{1}{2}\right) + \left(\frac{2}{3}\right)^3 \left(z + \frac{1}{2}\right)^2 + \dots$$

which is defined for

$$\left|z + \frac{1}{2}\right| < 1$$

where  $f_2(z)$  converges.

The series can be summed as

$$f_1(z) = \frac{1}{1-z} = 1 + z + z^2 + \dots \text{ for } |z| < 1$$

and

$$\begin{aligned} f_2(z) &= \frac{2}{3} \left\{ 1 + \frac{2}{3} \left(z + \frac{1}{2}\right) + \left(\frac{2}{3}\right)^2 \left(z + \frac{1}{2}\right)^2 + \dots \right\} \\ &= \frac{2}{3} \left\{ 1 + z' + z'^2 + \dots \right\} \end{aligned}$$

$$\left( \text{where, } z' = \frac{2}{3} \left(z + \frac{1}{2}\right) \text{ and since } \left|z + \frac{1}{2}\right| < 1, \text{ we have } |z'| < 1 \right).$$

Using  $|z'| < 1$ , we obtain the expression given below:

$$\begin{aligned} f_2(z) &= \frac{2}{3} \cdot \frac{1}{1-z'} \\ &= \frac{2}{3} \cdot \frac{1}{1 - \frac{2}{3} \left(z + \frac{1}{2}\right)} \\ &= \frac{1}{\frac{3}{2} - \left(z + \frac{1}{2}\right)} \quad \begin{array}{l} \text{(Multiplying Numerator and} \\ \text{Denominator by } \frac{3}{2}) \end{array} \\ &= \frac{1}{1 - z}, \text{ once again.} \end{aligned}$$

We see that  $f_1(z)$  and  $f_2(z)$ , the two series sum mentioned above have different functional forms, which converge in the two overlapping regions defined by inequalities  $|z| < 1$  and  $|z + \frac{1}{2}| < 1$ , respectively represent in fact the same analytic function

$$f(z) = \frac{1}{1-z}.$$

The region  $|z + \frac{1}{2}| < 1$  means  $z$  can be on the real axis range from  $\frac{1}{2}$  to  $-\frac{3}{2}$ . On the positive axis, the range has not been extended beyond what is covered by  $|z| < 1$ , but on the negative axis, it is extended beyond the range of  $|z| < 1$ . Clearly the same

argument can extend the range all the way to  $-\infty$  on the negative axis. Similarly, if we take

$$f_1(z) = 1 - z + z^2 - z^3 + \dots$$

which is defined for

$$|z| < 1, \text{ where the series is convergent}$$

and

$$f_2(z) = \frac{2}{3} - \left(\frac{2}{3}\right)^2 \left(z - \frac{1}{2}\right) + \left(\frac{2}{3}\right)^2 \left(z - \frac{1}{2}\right)^3$$

which is defined for

$$\left| z - \frac{1}{2} \right| < 1, \text{ where it converges.}$$

We find that

$$f_1(z) = \frac{1}{1+z} \text{ for } |z| < 1$$

and

$$\begin{aligned} f_2(z) &= \frac{2}{3} \left\{ 1 - \frac{2}{3} \left(z - \frac{1}{2}\right) + \left(\frac{2}{3}\right)^2 \left(z - \frac{1}{2}\right)^2 - \dots \right\} \\ &= \frac{1}{\frac{3}{2} - z - \frac{1}{2}} = \frac{1}{1+z} \text{ for } \left| z - \frac{1}{2} \right| < 1 \end{aligned}$$

The range  $\left| z - \frac{1}{2} \right| < 1$  implies  $z < \frac{3}{2}$  on the positive axis to  $z > -\frac{1}{2}$  on the negative axis. In this way, one can go all the way along the positive axis. In these two examples it was possible to find unique expressions  $\frac{1}{1-z}$  and  $\frac{1}{1+z}$ , which remained valid in two circular regions considered (viz.  $|z| < 1$  and  $\left| z + \frac{1}{2} \right| < 1$ ). It is in general not possible to find such unique expressions. Even in those cases the two functions  $f_1(z)$ ,  $f_2(z)$  with dissimilar appearances which are identical in the intersection  $D_1 \cap D_2$  of the two regions ( $f_1(z)$  analytic in  $D_1$  and  $f_2(z)$  analytic in  $D_2$ ) are considered as dissimilar manifestations of a really unique entity; i.e., in the two examples discussed

$$f_1(z) \equiv f_2(z) \quad .$$

Thus  $f_1(z) = 1 - z + z^2 - z^3 + \dots$

$= \frac{1}{1+z}$  is valid in the range  $z = -\frac{1}{2}$  to  $+\infty$

all along the positive real axis. Thus the restriction of  $\kappa^2 G(t) < 1$  no longer restricts the applicability of the formula, i.e.,  $\kappa^2$  need not be less than  $t^2$ . If  $\kappa^2$  is now allowed to be greater than  $t^2$ , then the formula holds over the whole range  $t = 0$  to  $\infty$ . Agreement of the correlation function calculated using theories that take the validity of the formulae of  $q(t)$  over the whole range of  $\infty$  and experiment at quite high values of  $\kappa$  confirm that this extension, using analytic continuation, is valid.

### 3.11 Problems in Calculation of the Transform of the Coulomb Potential

The  $g$  bond of the charge-charge interaction potential is given by

$$g(r) = \frac{1}{r}$$

Then its transform

$$\begin{aligned} G(t) &= \int_0^{\infty} g(r) 4\pi r^2 \frac{\sin tr}{tr} dr \\ &= \int_0^{\infty} \frac{1}{r} \cdot 4\pi r^2 \cdot \frac{\sin tr}{tr} dr \\ &= \frac{4\pi}{t} \int_0^{\infty} \sin tr dr. \end{aligned}$$

This integral does not

converge; since  $\sin(tr)$  is a function that oscillates upto infinity. To see this more explicitly, we consider (2),

$$\frac{4\pi}{t} \int_0^{\infty} \sin tr dr$$

$$\begin{aligned}
&= \lim_{\alpha \rightarrow 0} \frac{4\pi}{t} \int_0^{1/\alpha} \sin tr \, dr \\
&= \lim_{\alpha \rightarrow 0} \left[ \frac{4\pi}{t} \cdot \frac{1}{t} \cos tr \right]_0^{1/\alpha} \\
&= \lim_{\alpha \rightarrow 0} \frac{1}{t^2} \left( \cos \left( \frac{t}{\alpha} \right) - 1 \right)
\end{aligned}$$

Obviously in the limit  $\alpha \rightarrow 0$ ,  $\cos \frac{t}{\alpha}$  diverges.

To handle this integral, one uses a convergence factor  $e^{-\alpha r}$  i.e. writes  $g(r) = e^{-\alpha r}/4\pi r$  and calculates  $G(t)$  as follows

$$\begin{aligned}
G(t) &= \lim_{\alpha \rightarrow 0} G(\alpha, t) = \lim_{\alpha \rightarrow 0} \int_0^{\infty} \frac{e^{-\alpha r}}{4\pi r} 4\pi r^2 \frac{\sin tr}{tr} \, dr \\
&= \lim_{\alpha \rightarrow 0} \left\{ \frac{1}{t} \int_0^{\infty} e^{-\alpha r} \sin(tr) \, dr \right\} = \lim_{\alpha \rightarrow 0} \left( \frac{1}{\alpha^2 + t^2} \right) \\
&= 1/t^2
\end{aligned}$$

It is important to realize that  $G(t) = \lim_{\alpha \rightarrow 0} G(\alpha, t)$  is an assertion, verifiable only by agreement of results so derived with experiments. We actually used  $G(t)$ , which is integral of  $G(\alpha, t)$  with  $\alpha$  set equal to zero before integration is carried out, but then the integral diverges. What we are able to calculate is integral of  $G(\alpha, t)$  and then set  $\alpha = 0$  on the integrated function. We force convergence by using a convergence factor, which in this case is  $e^{-\alpha r}$ . Friedman (2) points out that  $e^{-\alpha r}$  is not the only convergence factor. He shows that if  $\tilde{g}(t, \alpha)$  is calculated from  $g(r, \alpha) = \frac{1}{4\pi r^{1+\alpha}}$ , one again obtains  $\lim_{\alpha \rightarrow 0} \tilde{g}(t, \alpha) = 1/t^2$ . He points out that transform

## CHAPTER IV

HNC CALCULATIONS ON MACROION SOLUTION : ANGLE DEPENDENT POTENTIAL



## Introduction

In this chapter, we present theoretical results on calculation of  $q$  bonds in a mixture of ions and dipoles in solution. This calculation is necessary for the calculation of correlation function in a solution of macroions carrying a charge and a dipole, containing macroions and small inorganic ions, the solvent being treated as a continuum. The calculation is based on the method of Friedman and Jepsen (1). We present a description of their method of calculation of  $q$  bond in section 1. We describe in section 2, the extension of their method, carried out by us, to ion-dipole mixtures at finite concentration of ions and dipoles. The application of the expressions derived in section 2 to the calculation of correlation function is shown in Sections 3 and 4. Reduction of the equations to Mayer's formula for ionic mixtures is shown in Section 5. The validity of the cluster expansion is discussed in Section 6 and that of the Allnatt equation in Section 7.

### 4.1 Jepsen and Friedman Theory

The potential of average force between the two solute particles with angle-dependent potential depend on orientation as well as the distance. Statistical mechanical calculation of the properties of such a system can be accomplished with the help of Mayer's technique of summation of cluster diagrams. According to the cluster expansion, the potential of average force is given by

$$W_{xy}(\{x\}, \{y\}) = U_{xy}(\{x\}, \{y\}) - kT \sum_{n>1} C'^n Q(\{x\}, \{y\}, :n)$$

$$Q(x, y, :n) = \frac{1}{n!} \int S(x, y : n) d\{n\}$$

$S(x,y:n)$  is the sum of all terms corresponding to graphs of  $n$  field points and 2 root points (i.e.  $X$  and  $Y$ )

- (i) In the graphs  $X$  and  $Y$  are not connected.
- (ii) There are at least two independent paths by which each of the field points is connected to both  $X$  and  $Y$ .
- (iii) The  $n$  field points are connected among themselves independent of  $X$  and  $Y$ .

The summation technique developed by Mayer and subsequently extended by Meeron sums the terms with the same topological classification rather than terms having the same  $n$ . This has been discussed in Chapter 3 in full detail for systems interacting through central forces only (i.e. forces having only radial dependence). Jepsen and Friedman (1) extended this to systems of molecules with orientation dependent forces (i.e. interaction between molecules depended not only on the distances between the centres, but also on their relative orientation). The summation method requires evaluation of convolution integrals of the type

$$\int f_{x1} f_{12} \dots f_{\nu y} d\{1\} \dots d\{\nu\}$$

and summing them over  $\nu = 1, \dots, \infty$ .

$f_{ij}$ : A function dependent on coordinates  $\{i\}$  and  $\{j\}$ .

When the forces are central, evaluation of this integral is done by convolution theorem of Fourier transform in three dimensions. Jepsen and Friedman (1) have developed a method to formulate convolution theorem for orientation dependent forces. We discuss the method following the presentation given in their paper.

In the following, an outline of the Montroll-Mayer derivation of the convolution theorem for systems of molecules with only central forces, is given. This is given in a form that is easy to

generalize to molecules with orientation-dependent for

If there are two molecules  $i$  and  $j$  with their centers at  $\vec{r}_i$  and  $\vec{r}_j$ , then an arbitrary square-integrable  $f$  which is a function of both  $\vec{r}_i$  and  $\vec{r}_j$  can be expanded in the following bilinear form

$$f_{ij}(\vec{r}_{ij}) = \sum_{\vec{t}_i, \vec{t}_j} \psi_{\vec{t}_i}^*(\vec{r}_i) a(\vec{t}_i, \vec{t}_j) \psi_{\vec{t}_j}(\vec{r}_j)$$

$\psi_{\vec{t}}(\vec{r})$ :  $\psi$  function, an element of a complete orthonormal set of functions of  $\vec{r}$ .

If the molecules are all contained in a cube of side  $\lambda$ , then

$$\psi_{\vec{t}}(\vec{r}) = \lambda^{-3/2} \exp(i\vec{r} \cdot \vec{t})$$

$\vec{t}$ : A lattice vector =  $t_1, t_2, t_3$

$$t_n = 0, \pm 2\pi/\lambda, \pm 2(2\pi/\lambda), \dots$$

The sum in eq.(1) is over all values of  $\vec{t}_i, \vec{t}_j$ . Since  $\psi$  is orthonormal, then

$$\left. \begin{aligned} \int \psi_{\vec{t}}(\vec{r}) \psi_{\vec{t}'}^*(\vec{r}) d\vec{r} &= \delta(\vec{t} : \vec{t}') \\ &= 1 \quad \text{if } \vec{t} = \vec{t}' \\ &= 0 \quad \text{if } \vec{t} \neq \vec{t}' \end{aligned} \right\} \quad (3)$$

$$\begin{aligned} & \int f_{12} f_{23} \dots f_{\nu, \nu+1} d\vec{r}_2 d\vec{r}_3 \dots d\vec{r}_\nu \\ &= \int \left\{ \sum_{\vec{t}_1, \vec{t}_2} \psi_{\vec{t}_1}^*(\vec{r}_1) a(\vec{t}_1, \vec{t}_2) \psi_{\vec{t}_2}(\vec{r}_2) \right\} \left\{ \sum_{\vec{t}_2, \vec{t}_3} \psi_{\vec{t}_2}^*(\vec{r}_2) a(\vec{t}_2, \vec{t}_3) \psi_{\vec{t}_3}(\vec{r}_3) \right\} \dots \\ & \quad \left\{ \sum_{\vec{t}_\nu, \vec{t}_{\nu+1}} \psi_{\vec{t}_\nu}^*(\vec{r}_\nu) a(\vec{t}_\nu, \vec{t}_{\nu+1}) \psi_{\vec{t}_{\nu+1}}(\vec{r}_{\nu+1}) \right\} d\vec{r}_2 d\vec{r}_3 \dots d\vec{r}_\nu \end{aligned}$$

$$\begin{aligned}
&= \sum_{\vec{t}_1, \vec{t}_2, \dots, \vec{t}_{\nu+1}} \int \psi_{\vec{t}_1}^*(\vec{r}_1) a(\vec{t}_1, \vec{t}_2) \psi_{\vec{t}_2}(\vec{r}_2) \psi_{\vec{t}_2}^*(\vec{r}_2) a(\vec{t}_2, \vec{t}_3) \\
&\quad \psi_{\vec{t}_3}(\vec{r}_3) \dots \psi_{\vec{t}_\nu}^*(\vec{r}_\nu) a(\vec{t}_\nu, \vec{t}_{\nu+1}) \psi_{\vec{t}_{\nu+1}}(\vec{r}_{\nu+1}) d\vec{r}_2 d\vec{r}_3 \dots d\vec{r}_\nu \\
&= \sum_{\vec{t}_1, \vec{t}_2, \dots, \vec{t}_{\nu+1}} \psi_{\vec{t}_1}^*(\vec{r}_1) a(\vec{t}_1, \vec{t}_2) a(\vec{t}_2, \vec{t}_3) \dots a(\vec{t}_\nu, \vec{t}_{\nu+1}) \psi_{\vec{t}_{\nu+1}}(\vec{r}_{\nu+1}) \\
&\quad \int \psi_{\vec{t}_2}(\vec{r}_2) \psi_{\vec{t}_2}^*(\vec{r}_2) d\vec{r}_2 \int \psi_{\vec{t}_3}(\vec{r}_3) \psi_{\vec{t}_3}^*(\vec{r}_3) d\vec{r}_3 \dots \\
&\quad \int \psi_{\vec{t}_\nu}(\vec{r}_\nu) \psi_{\vec{t}_\nu}^*(\vec{r}_\nu) d\vec{r}_\nu \\
&= \sum_{\vec{t}_1, \vec{t}_2, \dots, \vec{t}_{\nu+1}} \psi_{\vec{t}_1}(\vec{r}_1) a(\vec{t}_1, \vec{t}_2) \dots a(\vec{t}_\nu, \vec{t}_{\nu+1}) \psi_{\vec{t}_{\nu+1}}(\vec{r}_{\nu+1}) \\
&= \lambda^{-3} \sum_{\vec{t}} [(a(\vec{t}))^\nu e^{i \vec{r}_{1, \nu+1} \cdot \vec{t}}] \quad (4)
\end{aligned}$$

The last step is obtained with the help of equations (2) and (3).

The molecules with orientation dependent forces are described by different variables than above. The variables are distance vector as well as Euler angle.

$\vec{r}_j$  is the vector to the centre of molecule  $j$  from the origin of a standard Cartesian coordinate system. If there is another Cartesian coordinate system fixed in molecule  $j$  and rotating with it, then the orientational coordinates of the molecule are specified by the rotation which is necessary to make the standard coordinate system coincide with the  $j$ -coordinate system. Thus  $\{j\} = \vec{r}_j$ ,  $s \rightarrow j$ .

$\{j\} \rightarrow$  a set of six coordinates, is divided into two subsets of 3 coordinates each.

The components of  $\vec{r}_j$  are the 3 Cartesian coordinates. The components of  $s \rightarrow j$  ( $j$  from  $s$ ) are the 3 Euler angles  $\alpha, \beta, \gamma$ .

As a function of distance,  $\vec{r}_j$  can be expressed by a complete set of orthogonal expansion function which is of the form  $\exp(i\vec{\epsilon} \cdot \vec{r})$ , the function of rotation ( $s \rightarrow j$ ) can also be expressed by a set of orthogonal expansion functions. This set is given by the irreducible representation coefficient,  $D_{mn}^\ell(s \rightarrow j)$  of the three dimensional rotation group. Given below are some properties of the D-functions which are used in the subsequent calculation.

(1) The indices  $l, m, n$  of  $D_{mn}^l(s \rightarrow j)$  are conjugate respectively, to the Euler angles  $\beta, \gamma, \alpha$  of the rotation  $s \rightarrow j$ .

$l \rightarrow$  Integral values  $\rightarrow 0, 1, 2, \dots$

$m, n \rightarrow$  Also integral values  $\rightarrow -l \dots +l$

$$(2) D_{mn}^l(s \rightarrow j) = D_{nm}^{l*}(j \rightarrow s) \quad (\text{Inverse rotation}) \quad (5)$$

$$(3) \int D_{mn}^l(s \rightarrow j) D_{m'n'}^{l'*}(s \rightarrow j) d(s \rightarrow j) = \frac{8\pi^2}{2l+1} \delta(l, m, n : l', m', n') \quad (\text{Orthonormality}) \quad (6)$$

$$(4) \int D_{mn}^l(s \rightarrow j) D_{m'n'}^{l'*}(s \rightarrow j) d(s \rightarrow j) = \int_0^{2\pi} d\alpha \int_0^\pi \sin\beta d\beta \int_0^{2\pi} d\gamma D_{mn}^l(\alpha, \beta, \gamma) D_{m'n'}^{l'*}(\alpha, \beta, \gamma) \quad (7)$$

$$(4) \sum_{\nu=-l}^{+l} D_{m\nu}^l(b \rightarrow a) D_{\nu n}^l(c \rightarrow b) = D_{mn}^l(c \rightarrow a) \quad (8)$$

(5) The product of two D-functions of the same rotation can be

written as a finite linear combination of D functions by the formula

$$D_{mn}^1(s \rightarrow j) D_{m'n'}^{1'}(s \rightarrow j) = \sum_{LMN} (2L+1) (-)^{M+N} \left[ \begin{matrix} l & l' & L \\ m & m' & M \end{matrix} \right]_{3j} \left[ \begin{matrix} l & l' & L \\ n & n' & N \end{matrix} \right]_{3j} D_{-M-N}^L(s \rightarrow j) \quad (9)$$

where,

$$\left[ \begin{matrix} a & b & c \\ d & e & f \end{matrix} \right]_{3j} : \text{Wigner 3-j coefficient}$$

Terms of Eqn. (9) that do not vanish must have  $M = -m-m'$  and  $N = -n-n'$

$$(6) \quad D_{nm}^1(1 \rightarrow 1) = \delta(n:m) \quad (10)$$

$$(7) \quad D_{nm}^{1*}(2 \rightarrow 1) = (-)^{n-m} D_{-n-m}^1(2 \rightarrow 1) \quad (11)$$

$$(8) \quad D_{0m}^{1*}(\alpha, \beta, \gamma) = \left( \frac{4\pi}{2n+1} \right)^{1/2} Y_m^{1*}(\beta, \alpha) \\ = (\text{sgn } m)^m \left( \frac{(n-|m|)!}{(n+|m|)!} \right)^{1/2} P_1^m(\cos \beta) \exp(-im\alpha) \quad (12)$$

$$(9) \quad \int D_{n_1 m_1}^{l_1}(A \rightarrow B) D_{n_2 m_2}^{l_2}(A \rightarrow B) D_{n_3 m_3}^{l_3}(A \rightarrow B) d(A \rightarrow B) \\ = 8\pi^2 \left[ \begin{matrix} l_1 & l_2 & l_3 \\ n_1 & n_2 & n_3 \end{matrix} \right]_{3j} \left[ \begin{matrix} l_1 & l_2 & l_3 \\ m_1 & m_2 & m_3 \end{matrix} \right]_{3j} \quad (13)$$

$$\begin{aligned}
 (10) \quad & \sum_{n_1 n_2 n_3} D_{n_1 m_1}^{l_1 (1 \rightarrow 2)} D_{n_2 m_2}^{l_2 (1 \rightarrow 2)} D_{n_3 m_3}^{l_3 (1 \rightarrow 2)} \times \begin{bmatrix} l_1 & l_2 & l_3 \\ n_1 & n_2 & n_3 \end{bmatrix}_{3j} \\
 & = \begin{bmatrix} l_1 & l_2 & l_3 \\ m_1 & m_2 & m_3 \end{bmatrix}_{3j} \quad (14)
 \end{aligned}$$

$$\begin{aligned}
 (11) \quad & \sum_{\substack{m_1 m_2 | m_3 \text{ fixed} \\ n_1 n_2 | n_3 \text{ fixed}}} \begin{bmatrix} l_1 & l_2 & l_3 \\ m_1 & m_2 & m_3 \end{bmatrix} D_{m_1 n_1}^{l_1 (A \rightarrow B)} \times D_{m_2 n_2}^{l_2 (A \rightarrow B)} \\
 & \begin{bmatrix} l_1 & l_2 & l'_3 \\ n_1 & n_2 & n_3 \end{bmatrix}_{3j} = \frac{\delta(l_3 : l'_3)}{2l_3 + 1} D_{m_3 n_3}^{l_3^* (A \rightarrow B)} \quad (15)
 \end{aligned}$$

$$(12) \quad \begin{bmatrix} l_1 & l_2 & l_3 \\ m_1 & m_2 & m_3 \end{bmatrix}_{3j} = (-)^{l_1 + l_2 + l_3} \begin{bmatrix} l_1 & l_2 & l_3 \\ -m_1 & -m_2 & -m_3 \end{bmatrix}_{3j} \quad (16)$$

$$(13) \quad \sum_{m_1 m_2} \begin{bmatrix} l_1 & l_2 & l_3 \\ m_1 & m_2 & m \end{bmatrix}_{3j} \begin{bmatrix} l_1 & l_2 & l \\ m_1 & m_2 & m \end{bmatrix}_{3j} = \frac{\delta(l_3 : l)}{(2l + 1)} \quad (17)$$

$$\begin{aligned}
 (14) \quad & \begin{bmatrix} l_1 & l_2 & l_1 + l_2 \\ m_1 & m_2 & -m_1 - m_2 \end{bmatrix}_{3j} \left( \frac{(2l_1 + 2l_2 + 1)!}{(2l_1)! (2l_2)!} \right)^{1/2} \\
 & = \frac{(-)^{l_1 - l_2 + m_1 + m_2} [(l_1 + l_2 + m_1 + m_2)! (l_1 + l_2 - m_1 - m_2)!]^{1/2}}{[(l_1 + m_1)! (l_1 - m_1)! (l_2 + m_2)! (l_2 - m_2)!]^{1/2}} \quad (18)
 \end{aligned}$$

$$\begin{aligned}
 (15) \quad & \sum_{l_3} (2l_3 + 1) \begin{bmatrix} l_1 & l_2 & l_3 \\ m_1 & m_2 & m_3 \end{bmatrix}_{3j} \begin{bmatrix} l_1 & l_2 & l_3 \\ m'_1 & m'_2 & m_3 \end{bmatrix}_{3j} \\
 & = \delta(m_1, m_2 : m'_1, m'_2) \quad (19)
 \end{aligned}$$

$$\begin{aligned}
&= \sum_{\substack{l_1 l_2 l \\ m_1 m_2 m \\ n_1 n_2 n \\ s_1 s_2 s \\ 1 \quad 2}} \bar{F}_{12} D_{m_1 s_1}^{l_1} (T \rightarrow 1) D_{m_2 s_2}^{l_2} (T \rightarrow 2) D_{os}^1 (T \rightarrow r_{12}) \\
&\times D_{s_1 n_1}^{l_1} (S \rightarrow T) D_{s_2 n_2}^{l_2} (S \rightarrow T) D_{sn}^1 (S \rightarrow T) \quad (23)
\end{aligned}$$

With the help of Eqn.(9)

$$\begin{aligned}
&D_{s_1 n_1}^{l_1} (S \rightarrow T) D_{s_2 n_2}^{l_2} (S \rightarrow T) D_{sn}^1 (S \rightarrow T) \\
&= \sum_{LM} (2L+1) \begin{bmatrix} l_1 & l_2 & L \\ s_1 & s_2 & u \end{bmatrix}_{3j} \begin{bmatrix} l_1 & l_2 & L \\ n_1 & n_2 & v \end{bmatrix}_{3j} (2M+1) \\
&\begin{bmatrix} L & l & M \\ -u & s & \omega \end{bmatrix}_{3j} \begin{bmatrix} L & l & M \\ -v & n & x \end{bmatrix}_{3j} (-)^{u+v+\omega+x} D_{\omega x}^M (S \rightarrow T)
\end{aligned}$$

Because of invariance in rotation of the pairwise function

$$M = \omega = x = 0 \text{ and } D_{\omega x}^M (s \rightarrow T) = 1$$

$$M = 0 \Rightarrow L = 1$$

$$\left. \begin{aligned}
\omega = 0 &\Rightarrow -u = -s = s_1 + s_2 \\
x = 0 &\Rightarrow -v = -n = n_1 + n_2
\end{aligned} \right\} \text{ Properties of 3-j coefficient}$$

With the help of equation (19) the above summation reduces to

$$\begin{bmatrix} l_1 & l_2 & 1 \\ s_1 & s_2 & -s_1-s_2 \end{bmatrix}_{3j} \begin{bmatrix} l_1 & l_2 & 1 \\ n_1 & n_2 & -n_1-n_2 \end{bmatrix}_{3j} (-)^{-s_1-s_2-n_1-n_2}$$



$$\begin{aligned}
&= \begin{bmatrix} l_1 & l_2 & 1 \\ s_1 & s_2 & -s_1-s_2 \end{bmatrix}_{3j} \begin{bmatrix} l_1 & l_2 & 1 \\ n_1 & n_2 & -n_1-n_2 \end{bmatrix}_{3j} (-)^{-2(s_1-s_2)} \\
&= \begin{bmatrix} l_1 & l_2 & 1 \\ s_1 & s_2 & -s_1-s_2 \end{bmatrix}_{3j} \begin{bmatrix} l_1 & l_2 & 1 \\ n_1 & n_2 & -n_1-n_2 \end{bmatrix}_{3j} \quad (24)
\end{aligned}$$

Hence from equation (23) we have

$$\begin{aligned}
f_{12} &= \sum_{\substack{l_1, l_2, l \\ m_1, m_2, m \\ n_1, n_2, n \\ s_1, s_2, s}} \bar{F}_{12} \begin{pmatrix} l_1 & l_2 & 1 \\ m_1 & m_2 & r_{12} \\ n_1 & n_2 & n \end{pmatrix} \begin{bmatrix} l_1 & l_2 & 1 \\ s_1 & s_2 & -s_1-s_2 \end{bmatrix}_{3j} \\
&\quad \times \begin{bmatrix} l_1 & l_2 & 1 \\ n_1 & n_2 & -n_1-n_2 \end{bmatrix}_{3j} D_{m_1 s_1}^{l_1 (T \rightarrow 1)} D_{m_2 s_2}^{l_2 (T \rightarrow 2)} D_{os}^{l (T \rightarrow r_{12})} \\
&= \sum_{\substack{l_1, l_2, l \\ m_1, m_2, m}} \left\{ \sum_{n_1, n_2, n} \bar{F}_{12} \begin{pmatrix} l_1 & l_2 & 1 \\ m_1 & m_2 & r_{12} \\ n_1 & n_2 & n \end{pmatrix} \begin{bmatrix} l_1 & l_2 & 1 \\ n_1 & n_2 & -n_1-n_2 \end{bmatrix}_{3j} \right\} \\
&\quad \times \sum_{s_1, s_2, s} \begin{bmatrix} l_1 & l_2 & 1 \\ s_1 & s_2 & s \end{bmatrix}_{3j} D_{m_1 s_1}^{l_1 (T \rightarrow 1)} D_{m_2 s_2}^{l_2 (T \rightarrow 2)} D_{os}^{l (T \rightarrow r_{12})}
\end{aligned}$$

From the definition in equation (21), the summation  $\sum_{n_1, n_2, n}$  in the bracket { } reduces to  $(-)^{-m_1} \bar{f}_{12} \begin{pmatrix} l_1 & l_2 & 1 \\ m_1 & m_2 & r_{12} \end{pmatrix}$ .

From the definition in equation (11),

$$D_{m_1 s_1}^{l_1 (T \rightarrow 1)} = (-)^{-s_1+m_1} D_{-m_1 -s_1}^{l_1^* (T \rightarrow 1)}$$

$$\begin{aligned}
\text{Hence } f_{12} &= \sum_{\substack{l_1, l_2, l \\ m_1, m_2}} (-)^{-m_1} \bar{f}_{12} \begin{pmatrix} l_1 & l_2 & l \\ m_1 & m_2 & r_{12} \end{pmatrix} \\
&\times \sum_{s_1, s_2, s} \begin{bmatrix} l_1 & l_2 & l \\ s_1 & s_2 & s \end{bmatrix}_{3j} (-)^{-s_1+m_1} D_{-m_1-s_1}^{l_1*} (T \rightarrow 1) D_{m_2 s_2}^{l_2} (T \rightarrow 2) \\
&\times D_{0s}^l (T \rightarrow r_{12})
\end{aligned}$$

In the summation  $\sum_{s_1, s_2, s}$ , the indices of  $s_1$  over which the summation takes place, varies from  $-l_1$  through 0 to  $+l_1$ , Hence inside the summation  $s_1$  can be replaced by  $-s_1$ . Same is true with the index  $m_1$ . Hence,  $s$  which is equal to  $-s_1-s_2$  can be replaced by  $s_1-s_2$  inside the summation. Thus we have,

$$\begin{aligned}
f_{12} &= \sum_{\substack{l_1, l_2, l \\ m_1, m_2}} (-)^{m_1} \bar{f}_{12} \begin{pmatrix} l_1 & l_2 & l \\ m_1 & m_2 & r_{12} \end{pmatrix} \sum_{s_1, s_2, s} \begin{bmatrix} l_1 & l_2 & l \\ s_1 & s_2 & s \end{bmatrix}_{3j} \\
&\times (-)^{s_1-m_1} D_{m_1 s_1}^{l_1*} (T \rightarrow 1) D_{m_2 s_2}^{l_2} (T \rightarrow 2) D_{0s}^l (T \rightarrow r_{12}) \\
&= \sum_{\substack{l_1, l_2, l \\ m_1, m_2 \\ s_1, s_2}} (-)^{s_1} \bar{f}_{12} \begin{pmatrix} l_1 & l_2 & l \\ m_1 & m_2 & r_{12} \end{pmatrix} \begin{bmatrix} l_1 & l_2 & l \\ -s_1 & s_2 & s_1-s_2 \end{bmatrix}_{3j} D_{m_1 s_1}^{l_1*} (T \rightarrow 1) \\
&\times D_{m_2 s_2}^l (T \rightarrow 2) D_{0 s_1-s_2}^l (T \rightarrow r_{12}) \tag{25}
\end{aligned}$$

If S coordinate system is so chosen that  $T \rightarrow r_{12}$  rotation vanishes, then with the help of Eqn. (10), we have

$$D_{0 \ s_1-s_2}^1 (T \rightarrow r_{12}) = \delta(o: s_1-s_2).$$

and the equation survives for  $s_1-s_2=0$ . Hence  $s_1=s_2=s$

Now we have,

$$f_{12} = \sum_{\substack{l_1 l_2 l \\ m_1 m_2 s}} \bar{f}_{12} \begin{pmatrix} l_1 & l_2 & l \\ m_1 & m_2 & r_{12} \end{pmatrix} \begin{bmatrix} l_1 & l_2 & l \\ -s & s & 0 \end{bmatrix}_{3j} (-)^s D_{m_1 s}^{l_1*} (r_{12} \rightarrow 1) \\ D_{m_2 s}^{l_2} (r_{12} \rightarrow 2) \quad (26)$$

The above equation is inverted in the following way to get the expression for  $\bar{f}_{12}$  in terms of  $f_{12}$  :

$$\int f_{12} D_{m_1 s}^{l_1} (r_{12} \rightarrow 1) D_{m_2 s}^{l_2*} (r_{12} \rightarrow 2) d(r_{12} \rightarrow 1) d(r_{12} \rightarrow 2) \\ = \int \sum_{\substack{l'_1 l'_2 l' \\ m'_1 m'_2 s'}} \bar{f}_{12} \begin{pmatrix} l'_1 & l'_2 & l' \\ m'_1 & m'_2 & r_{12} \end{pmatrix} \begin{bmatrix} l'_1 & l'_2 & l' \\ -s' & s' & 0 \end{bmatrix}_{3j} (-)^{s'} D_{m'_1 s'}^{l'_1*} (r_{12} \rightarrow 1) \\ \times D_{m'_2 s'}^{l'_2} (r_{12} \rightarrow 2) D_{m_1 s}^{l_1} (r_{12} \rightarrow 1) D_{m_2 s}^{l_2*} (r_{12} \rightarrow 2) d(r_{12} \rightarrow 1) d(r_{12} \rightarrow 2) \quad (27)$$

By equation (6),

$$\sum_{l'_1, m'_1, s'} \int D_{m_1 s}^{l_1} (r_{12} \rightarrow 1) D_{m'_1 s'}^{l'_1*} (r_{12} \rightarrow 1) d(r_{12} \rightarrow 1) = \frac{8\pi^2}{2l_1+1}$$

$$\sum_{l'_2, m'_2, s'} \int D_{m_2 s}^{l_2} (r_{12} \rightarrow 2) D_{m'_2 s'}^{l'_2*} (r_{12} \rightarrow 2) d(r_{12} \rightarrow 2) = \frac{8\pi^2}{2l_2+1}$$

Hence equation (27) becomes

$$\int f_{12} D_{m_1}^{l_1} (r_{12} \longrightarrow 1) D_{m_2}^{l_2*} (r_{12} \longrightarrow 2) d(r_{12} \longrightarrow 1) d(r_{12} \longrightarrow 2)$$

$$= \sum_{l'} \bar{f}_{12} \begin{bmatrix} l_1 & l_2 & l \\ m_1 & m_2 & r_{12} \end{bmatrix} \begin{bmatrix} l_1 & l_2 & l \\ -s & s & 0 \end{bmatrix}_{3j} (-)^s \left( \frac{8\pi^2}{2l_1+1} \right) \left( \frac{8\pi^2}{2l_2+1} \right) \quad (28)$$

$$\sum_s \begin{bmatrix} l_1 & l_2 & l \\ -s & s & 0 \end{bmatrix}_{3j} (-)^s \int f_{12} D_{m_1}^{l_1} (r_{12} \longrightarrow 1) D_{m_2}^{l_2*} (r_{12} \longrightarrow 2) d(r_{12} \longrightarrow 1) \times d(r_{12} \longrightarrow 2)$$

$$= \sum_{s, l'} \begin{bmatrix} l_1 & l_2 & l \\ -s & s & 0 \end{bmatrix}_{3j} (-)^s \bar{f}_{12} \begin{bmatrix} l_1 & l_2 & l' \\ m_1 & m_2 & r_{12} \end{bmatrix} \begin{bmatrix} l_1 & l_2 & l' \\ -s & s & 0 \end{bmatrix}_{3j}$$

$$\times (-)^s \frac{(8\pi^2)^2}{(2l_1+1)(2l_2+1)}$$

$$= \sum_{s, l'} \bar{f}_{12} \begin{bmatrix} l_1 & l_2 & l' \\ m_1 & m_2 & r_{12} \end{bmatrix} (-)^{2s} \begin{bmatrix} l_1 & l_2 & l \\ -s & s & 0 \end{bmatrix}_{3j} \begin{bmatrix} l_1 & l_2 & l' \\ -s & s & 0 \end{bmatrix}_{3j}$$

$$\times \frac{(8\pi^2)^2}{(2l_1+1)(2l_2+1)}$$

$$= \bar{f}_{12} \begin{bmatrix} l_1 & l_2 & l \\ m_1 & m_2 & r_{12} \end{bmatrix} \frac{64\pi^4}{(2l+1)(2l_1+1)(2l_2+1)}$$

(both the 3j-coefficients are multiplied with the help of equation (17))

$$\therefore \bar{f}_{12} \begin{bmatrix} l_1 & l_2 & l \\ m_1 & m_2 & r_{12} \end{bmatrix} = \frac{(2l+1)(2l_1+1)(2l_2+1)}{64\pi^4} \sum_s \begin{bmatrix} l_1 & l_2 & l \\ s & s & 0 \end{bmatrix}$$

$$(-)^s \int f_{12} D_{m_1}^{l_1} (r_{12} \longrightarrow 1) D_{m_2}^{l_2} (r_{12} \longrightarrow 2) d(r_{12} \longrightarrow 1) d(r_{12} \longrightarrow 2) \quad (29)$$

## Convolution Theorem

### (i) General Pairwise Functions

$f_{12}(\{1\},\{2\})$  : a function of spatial and orientational coordinates of molecules 1 and 2. This can be expanded in terms of complete set of orthonormal functions. The expansion is given as

$$f_{12} = \sum_{\langle 1 \rangle, \langle 2 \rangle} \Psi_{\langle 1 \rangle}^* (\{1\}) \tilde{F}_{12} (\langle 1 \rangle, \langle 2 \rangle) \Psi_{\langle 2 \rangle} (\{2\}) \quad (30)$$

$\langle a \rangle \longrightarrow$  A set of coordinates conjugate of  $\{a\}$ .  $\Psi_{\langle a \rangle}$  constitutes a complete orthonormal set of functions of  $\langle a \rangle$ .

$$\Psi_{\langle a \rangle} (\{a\}) = \left( \frac{2l+1}{8\pi^2 \lambda^3} \right)^{1/2} \exp (i \vec{\ell}_1 \cdot \vec{r}_1) D_{mn}^l (L \longrightarrow a) \quad (31)$$

$\vec{\ell} \longrightarrow$  conjugate to  $\vec{r}$

$l, m, n \longrightarrow$  conjugate to Euler angle

$L \longrightarrow$  fixed laboratory coordinate system

$a \longrightarrow$  coordinate system of molecule  $a$

$\lambda \longrightarrow$  length of the cube to which the molecule is confined

$$\int \Psi_{\langle a \rangle}^* (\{a\}) \Psi_{\langle a \rangle} (\{a\}) d(\{a\}) = \delta (\langle a \rangle : \langle a \rangle') \quad (32)$$

From Eqn. (30):

$$f_{12} \Psi_{\langle 2 \rangle}^* (\{2\}) = \sum_{\langle 1 \rangle, \langle 2 \rangle} \Psi_{\langle 1 \rangle}^* (\{1\}) \tilde{F}_{12} (\langle 1 \rangle, \langle 2 \rangle) \Psi_{\langle 2 \rangle} (\{2\}) \Psi_{\langle 2 \rangle}^* (\{2\}) \quad (33)$$

$$\begin{aligned} & \int \Psi_{\langle 1 \rangle} (\{1\}) f_{12} \Psi_{\langle 2 \rangle}^* (\{2\}) d(\{1\}) d(\{2\}) \\ &= \int \sum_{\langle 1 \rangle', \langle 2 \rangle'} \Psi_{\langle 1 \rangle} (\{1\}) \Psi_{\langle 1 \rangle'}^* (\{1\}) \tilde{F}_{12} (\langle 1 \rangle', \langle 2 \rangle') \Psi_{\langle 2 \rangle'} (\{2\}) \Psi_{\langle 2 \rangle}^* (\{2\}) \\ & \quad d(\{1\}) d(\{2\}) \end{aligned}$$

$$\begin{aligned}
&= \sum_{\langle 1 \rangle', \langle 2 \rangle'} \tilde{F}(\langle 1 \rangle', \langle 2 \rangle') \int \Psi_{\langle 1 \rangle}(\{1\}) \Psi_{\langle 1 \rangle'}^*(\{1\}) d\{1\}) \\
&\quad \times \int \Psi_{\langle 2 \rangle}(\{2\}) \Psi_{\langle 2 \rangle'}^*(\{2\}) d\{2\}) \\
&= \tilde{F}(\langle 1 \rangle, \langle 2 \rangle)
\end{aligned} \tag{34}$$

The integrations above turned out to be unity with the help of equation (32).

$$\text{Hence, } \tilde{F}(\langle 1 \rangle, \langle 2 \rangle) = \int \Psi_{\langle 1 \rangle}(\{1\}) f_{12} \Psi_{\langle 2 \rangle}^*(\{2\}) d\{1\} d\{2\} \tag{35}$$

This orthogonal expansion is used in the evaluation of the convolution integral in the following way

$$p_{XY}(\nu f, \{X\}, \{Y\})$$

$$= \int f_{x1} f_{12} \dots f_{\nu-1, \nu} f_{\nu Y} d\{1\} d\{2\} \dots d\{\nu\} \tag{36}$$

(with the help of equation (30) and equation (32))

$$\begin{aligned}
&= \int \sum_{\langle X \rangle, \langle 1 \rangle} \Psi_{\langle X \rangle}^*(\{X\}) \tilde{F}_{x1}(\langle X \rangle, \langle 1 \rangle) \Psi_{\langle 1 \rangle}(\{1\}) \sum_{\langle 1 \rangle, \langle 2 \rangle} \Psi_{\langle 1 \rangle}^*(\{1\}) \tilde{F}(\{1\}, \{2\}) \\
&\times \Psi_{\langle 2 \rangle}(\{2\}) \dots \sum_{\langle \nu \rangle, \langle Y \rangle} \Psi_{\langle \nu \rangle}^*(\{\nu\}) \tilde{F}(\langle \nu \rangle, \langle Y \rangle) \Psi_{\langle Y \rangle}(\{Y\}) d\{1\} d\{2\} \dots d\{\nu\} \\
&= \sum_{\langle X \rangle, \langle 1 \rangle \dots \langle Y \rangle} \Psi_{\langle X \rangle}^*(\{X\}) \tilde{F}_{x1}(\langle X \rangle, \langle 1 \rangle) \tilde{F}(\langle 1 \rangle, \langle 2 \rangle) \dots \tilde{F}(\langle \nu \rangle, \langle Y \rangle) \\
&\times \Psi_{\langle Y \rangle}(\{Y\}) \int \Psi_{\langle 1 \rangle}(\{1\}) \Psi_{\langle 1 \rangle}^*(\{1\}) d\{1\} \dots \\
&\times \int \Psi_{\langle \nu \rangle}(\{\nu\}) \Psi_{\langle \nu \rangle}^*(\{\nu\}) d\{\nu\}
\end{aligned}$$

$$\begin{aligned}
&= \sum_{\langle X \rangle, \langle Y \rangle} \Psi_{\langle X \rangle}^* (\{X\}) \left[ \sum_{\langle 1 \rangle, \langle 2 \rangle, \dots, \langle \nu \rangle} \tilde{F}_{X1}(\langle X \rangle, \langle 1 \rangle) \tilde{F}_{12}(\langle 1 \rangle, \langle 2 \rangle) \dots \right. \\
&\quad \left. \dots \tilde{F}_{\nu Y}(\langle \nu \rangle, \langle Y \rangle) \right] \Psi_{\langle Y \rangle} (\{Y\}) \\
&= \sum_{\langle X \rangle, \langle Y \rangle} \Psi_{\langle X \rangle}^* (\{X\}) \tilde{P}_{XY}(\nu f)(\langle X \rangle, \langle Y \rangle) \Psi_{\langle Y \rangle} (\{Y\}) \quad (37)
\end{aligned}$$

$$\therefore \tilde{P}_{XY}(\nu f) = \sum_{\langle 1 \rangle, \langle 2 \rangle, \dots, \langle \nu \rangle} \tilde{F}_{X1}(\langle X \rangle, \langle 1 \rangle) \tilde{F}_{12}(\langle 1 \rangle, \langle 2 \rangle) \dots \tilde{F}_{\nu Y}(\langle \nu \rangle, \langle Y \rangle) \quad (38)$$

Let  $F_{ij}$  is a matrix with  $\tilde{F}_{ij}(\langle i \rangle, \langle j \rangle)$  being the element of the  $\langle i \rangle$ th row and  $\langle j \rangle$ th column, then  $\tilde{P}_{XY}$ 's are the elements of the matrix product  $F_{X1} F_{12} \dots F_{\nu Y}$ .

The sum of the convolution integral over all values of  $\nu$  gives

$$q_{XY} = f_{XY} + \sum_{\nu > 1} c' \nu p_{XY}(\nu f) \quad (39)$$

where  $P_{XY}(\nu f)$  is given by equation (36).

This when transformed by equation (35) one gets

$$\tilde{Q}_{XY} = \tilde{F}_{XY} + \sum_{\nu > 1} c'^{\nu} \tilde{P}_{XY}(\nu) \quad (40)$$

Each term of equations (39) and (40) is an element of a matrix. Hence one can write a corresponding matrix equation,

$$Q_{XY} = F_{XY} + F_{X1} \left( \sum_{\nu > 1} c'^{\nu} \left( \prod_{i=1}^{\nu-1} F_{i, i+1} \right) F_{\nu Y} \right) \quad (41)$$

If molecules 1, 2, ..... between X and Y are all of the same species, then

$$Q_{XY} = F_{XY} + c' F_{XA} (I - c' F_{AA})^{-1} F_{AY} \quad (42)$$

$$= \frac{[(2l_1+1)(2l_2+1)]^{1/2}}{16\pi^3} \sum_{l,n} \int_{\text{cube}} f_{12}(-i)^l (2l+1) j_1(rt) D_{\text{on}}^l(L \rightarrow t) D_{\text{on}}^{l*}(L \rightarrow r) \\ D_{m_1 n_1}^{l_1} D_{m_2 n_2}^{l_2*} r^2 dr d(L \rightarrow 1) d(L \rightarrow 2) d(L \rightarrow r)$$

$$= \frac{[(2l_1+1)(2l_2+1)]^{1/2}}{16\pi^3} \sum_{l,n} \sum_{\substack{l'_1 l'_2 l' \\ m'_1 m'_2 \\ n'_1 n'_2 n}} \int \bar{f}_{12} \begin{pmatrix} l'_1 & l'_2 & l' \\ m'_1 & m'_2 & r \end{pmatrix} \\ (-)^{n'_1} \begin{bmatrix} l'_1 & l'_2 & l' \\ -n'_1 & n'_2 & n \end{bmatrix}_{3j} D_{m'_1 n'_1}^{l'_1*}(L \rightarrow 1) D_{m'_2 n'_2}^{l'_2*}(L \rightarrow 2) D_{\text{on}}^{l'}(L \rightarrow r) (-i)^l (2l+1)$$

$$j_1(rt) D_{\text{on}}^l(L \rightarrow t) D_{\text{on}}^{l*}(L \rightarrow r) D_{m_1 n_1}^{l_1}(L \rightarrow 1) D_{m_2 n_2}^{l_2*}(L \rightarrow 2) r^2 dr d(L \rightarrow 1) d(L \rightarrow 2) d(L \rightarrow r)$$

(D functions are integrated over  $(L \rightarrow 1)$ ,  $(L \rightarrow 2)$ ,  $(L \rightarrow r)$  with the help of equation (6), and we get the following for  $l=l'$ ,  $m=m'$ ,  $n=n'$ )

$$= \frac{[(2l_1+1)(2l_2+1)]^{1/2}}{16\pi^3} \times \frac{(8\pi^2)^3 (2l+1)}{(2l_1+1)(2l_2+1)(2l+1)} \sum_{l,n} \int \bar{f}_{12} \begin{pmatrix} l_1 & l_2 & l \\ m_1 & m_2 & r \end{pmatrix} (-)^{n_1}$$

$$\times \begin{bmatrix} l_1 & l_2 & l \\ -n_1 & n_2 & n \end{bmatrix}_{3j} (-i)^l j_1(rt) D_{\text{on}}^l(L \rightarrow t) r^2 dr$$



$$= \frac{32 \pi^3 (-i)^1 (-)^{n_1}}{[(2l_1+1)(2l_2+1)]^{1/2}} \sum_{l,n} \int_{\text{cube}} \bar{f}_{12} \begin{pmatrix} l_1 & l_2 & l \\ m_1 & m_2 & r \end{pmatrix} D_{\text{on}}^1 (L \rightarrow t) \\ \times \begin{bmatrix} l_1 & l_2 & l \\ -n_1 & n_2 & n \end{bmatrix}_{3j} j_1 (rt) r^2 dr$$

By approaching the limit  $\lambda = \infty$ , we fix the limit of the integration from 0 to  $\infty$  and this limit is justified for statistical mechanical calculations, since the bulk properties are independent of  $\lambda$ . By using the definition in equation (49) and replacing  $\int_{\text{cube}}$  by  $\int_0^\infty$  we get equation (48).

$\bar{f}_{12}$  is not the desired transform, as it depends on the rotation  $L \rightarrow t$ , also it is a function of nine variables rather than six. So we carry out a further transformation to get the desired transform of  $f_{12}$ .

Let us define a quantity  $\tilde{f}_{12} \begin{pmatrix} l_1 & l_2 & t \\ m_1 & m_2 & n \end{pmatrix}$  by the following linear transform

$$\tilde{f}_{12} = \sum_{n_1 n_2} \bar{f}_{12} D_{n_1 n}^{l_1*} (L \rightarrow t) D_{n_2 n}^{l_2} (L \rightarrow t) \quad (50)$$

By applying equation (48) and equation (14) and equation (11) to the above equation, we find

$$\tilde{f}_{12} = \sum_{n_1 n_2} (-)^{n_1} \sum_{l,n} \begin{bmatrix} l_1 & l_2 & l \\ -n_1 & n_2 & n' \end{bmatrix}_{3j} D_{\text{on}'}^1 (L \rightarrow t) f_{12}^\dagger D_{n_1 n}^{l_1*} (L \rightarrow t) D_{n_2 n}^{l_2} (L \rightarrow t)$$

$$\begin{aligned}
&= \sum_1 \sum_{n_1, n_2, n'} (-)^{n_1} \begin{bmatrix} l_1 & l_2 & 1 \\ -n_1 & n_2 & n' \end{bmatrix}_{3j} D_{n_1 n}^{l_1*} (L \rightarrow t) D_{n_2 n}^{l_2} (L \rightarrow t) D_{on}^1 (L \rightarrow t) \\
&\times f_{12}^\dagger \begin{pmatrix} l_1 & l_2 & 1 \\ m_1 & m_2 & t \end{pmatrix} \\
&= \sum_1 \sum_{n_1 n_2 n'} (-)^{n_1} \begin{bmatrix} l_1 & l_2 & 1 \\ -n_1 & n_2 & n' \end{bmatrix}_{3j} (-)^{n_1 - n} D_{-n_1 - n}^{l_1} (L \rightarrow t) D_{n_2 n}^{l_2} (L \rightarrow t) \\
&\times D_{on}^1 (L \rightarrow t) f_{12}^\dagger \begin{pmatrix} l_1 & l_2 & 1 \\ m_1 & m_2 & t \end{pmatrix} \\
&= \sum_1 \sum_{n_1 n_2 n'} (-)^{2n_1 - n} \begin{bmatrix} l_1 & l_2 & 1 \\ -n_1 & n_2 & n' \end{bmatrix}_{3j} D_{-n_1 - n}^{l_1} (L \rightarrow t) D_{n_2 n}^{l_2} (L \rightarrow t) D_{on}^1 (L \rightarrow t) \\
&\times f_{12}^\dagger \begin{pmatrix} l_1 & l_2 & 1 \\ m_1 & m_2 & t \end{pmatrix} \\
&= \sum_1 \sum_{n_1 n_2 n'} (-)^{-n} \begin{bmatrix} l_1 & l_2 & 1 \\ -n_1 & n_2 & n' \end{bmatrix}_{3j} D_{-n_1 - n}^{l_1} (L \rightarrow t) D_{n_2 n}^{l_2} (L \rightarrow t) D_{on}^1 (L \rightarrow t) \\
&\times f_{12}^\dagger \begin{pmatrix} l_1 & l_2 & 1 \\ m_1 & m_2 & t \end{pmatrix} \\
&(\because (-)^{2n_1} = 1, (-)^{-n} = (-)^{-2n} (-)^n = (-)^n) \\
&= \sum_1 (-)^n f_{12}^\dagger \begin{pmatrix} l_1 & l_2 & 1 \\ m_1 & m_2 & t \end{pmatrix} \sum_{n_1 n_2 n'} \begin{bmatrix} l_1 & l_2 & 1 \\ -n_1 & n_2 & n' \end{bmatrix}_{3j} D_{-n_1 - n}^{l_1} (L \rightarrow t) \\
&\times D_{n_2 n}^{l_2} (L \rightarrow t) D_{on}^1 (L \rightarrow t)
\end{aligned}$$

Inner summation survives only if  $n'=0$  and becomes  $\begin{bmatrix} l_1 & l_2 & 1 \\ -n & n & 0 \end{bmatrix}_{3j}$

by equation (14).

Hence,

$$\tilde{f}_{12} \begin{pmatrix} l_1 & l_2 & t \\ m_1 & m_2 & n \end{pmatrix} = (-)^n \sum_1 \begin{pmatrix} l_1 & l_2 & 1 \\ -n & n & 0 \end{pmatrix}_{3j} f_{12}^\dagger \begin{pmatrix} l_1 & l_2 & 1 \\ m_1 & m_2 & t \end{pmatrix} \quad (51)$$

$$= \frac{(-)^n 32\pi^3}{[(2l_1+1)(2l_2+1)]^{1/2}} \sum_1 (-i)^1 \begin{pmatrix} l_1 & l_2 & 1 \\ -n & n & 0 \end{pmatrix}_{3j} \int_0^\infty \tilde{f}_{12} \begin{pmatrix} l_1 & l_2 & 1 \\ m_1 & m_2 & r \end{pmatrix} j_1(rt) r^2 dr \quad (52)$$

Equation (51) is multiplied on both sides by

$$\begin{pmatrix} l_1 & l_2 & 1' \\ -n & n & 0 \end{pmatrix}_{3j} \text{ and we get}$$

$$\begin{pmatrix} l_1 & l_2 & 1' \\ -n & n & 0 \end{pmatrix}_{3j} \tilde{f}_{12} = (-)^n \sum_1 \begin{pmatrix} l_1 & l_2 & 1' \\ -n & n & 0 \end{pmatrix}_{3j} \begin{pmatrix} l_1 & l_2 & 1 \\ -n & n & 0 \end{pmatrix}_{3j} f_{12}^\dagger$$

or

$$\begin{aligned} \sum_n (-)^n \begin{pmatrix} l_1 & l_2 & 1' \\ -n & n & 0 \end{pmatrix}_{3j} \tilde{f}_{12} &= \sum_n (-)^{2n} \sum_1 \begin{pmatrix} l_1 & l_2 & 1' \\ -n & n & 0 \end{pmatrix}_{3j} \begin{pmatrix} l_1 & l_2 & 1 \\ -n & n & 0 \end{pmatrix}_{3j} f_{12}^\dagger \\ &= \frac{1}{2l'+1} f_{12}^\dagger \text{ (By equation (17))} \end{aligned}$$

$$\implies f_{12}^\dagger \begin{pmatrix} l_1 & l_2 & 1 \\ m_1 & m_2 & t \end{pmatrix} = (2l+1) \sum_n (-)^n \begin{pmatrix} l_1 & l_2 & 1 \\ -n & n & 0 \end{pmatrix}_{3j} \tilde{f}_{12} \begin{pmatrix} l_1 & l_2 & t \\ m_1 & m_2 & n \end{pmatrix} \quad (53)$$

$f_{12}^\dagger$  is given by equation (49). Hence

$$\begin{aligned} &\frac{32\pi^3 (-i)^1}{[(2l_1+1)(2l_2+2)]^{1/2}} \int_0^\infty \tilde{f}_{12} \begin{pmatrix} l_1 & l_2 & 1 \\ m_1 & m_2 & r \end{pmatrix}_{3j} j_1(rt) r^2 dr \\ &= (2l+1) \sum_n (-)^n \begin{pmatrix} l_1 & l_2 & 1 \\ -n & n & 0 \end{pmatrix}_{3j} \tilde{f}_{12} \begin{pmatrix} l_1 & l_2 & t \\ m_1 & m_2 & n \end{pmatrix} \end{aligned}$$

or

$$\int_0^{\infty} \tilde{f}_{12} \begin{pmatrix} l_1 & l_2 & 1 \\ m_1 & m_2 & r \end{pmatrix} j_1(rt) r^2 dr$$

$$= \frac{(2l_1+1)[(2l_1+1)(2l_2+1)]^{1/2}}{32\pi^3 (-i)^1} \sum_n (-)^n \begin{bmatrix} l_1 & l_2 & 1 \\ -n & n & 0 \end{bmatrix} \tilde{f}_{12} \begin{pmatrix} l_1 & l_2 & t \\ m_1 & m_2 & n \end{pmatrix}$$

or,

$$\int_0^{\infty} dt j_1(r't) t^2 \int dr \tilde{f}_{12} j_1(rt) r^2 = \sum_n (-)^n \begin{bmatrix} l_1 & l_2 & 1 \\ -n & n & 0 \end{bmatrix} j_1$$

$$\times \int \tilde{f}_{12} \begin{pmatrix} l_1 & l_2 & 1 \\ m_1 & m_2 & r \end{pmatrix} j_1(rt) t^2 dt$$

$$\text{L.H.S.} = \int_0^{\infty} dr \tilde{f}_{12}(r) r^2 \int dt j_1(r't) j_1(rt) t^2$$

$$[\text{By Hankel's integral, inner integral} = \frac{\pi}{2} \frac{\delta(r-r')}{rr'}]$$

$$= \int_0^{\infty} dr \tilde{f}_{12}(r) r^2 \frac{\pi}{2} \frac{\delta(r-r')}{rr'}$$

$$= \frac{\pi}{2} \tilde{f}_{12}(r) \frac{r^2}{r^2} = \frac{\pi}{2} \tilde{f}_{12}(r)$$

$$\text{also } (-i)^1 = \frac{1}{(i)^1}$$

$$\therefore (-i)^1 (i)^1 = (-i^2)^1 = (1)^1 = 1$$

$$\therefore (-i)^1 = \frac{1}{(i)^1}$$

$$\therefore \tilde{f}_{12} \begin{pmatrix} l_1 & l_2 & 1 \\ m_1 & m_2 & r \end{pmatrix}$$

$$= \frac{(2l_1+1)[(2l_1+1)(2l_2+1)]^{1/2} (i)^1}{16\pi^4} \sum_n (-)^n \begin{bmatrix} l_1 & l_2 & 1 \\ -n & n & 0 \end{bmatrix} \int_0^{\infty} \tilde{f} \begin{pmatrix} l_1 & l_2 & t \\ m_1 & m_2 & n \end{pmatrix} \times j_1(rt) t^2 dt \quad (54)$$

With the help of equation (53), equation (48) can be written

as

$$\begin{aligned}
 \tilde{F}_{12} &= (-)^{n_1} \sum_{1n'} \begin{bmatrix} l_1 & l_2 & 1 \\ -n_1 & n_2 & n' \end{bmatrix}_{3j} D_{on'}^{l_1} (L \rightarrow t) \sum_n (2l+1) (-)^n \\
 &\quad \begin{bmatrix} l_1 & l_2 & 1 \\ -n & n & 0 \end{bmatrix}_{3j} \tilde{f}_{12} \begin{pmatrix} l_1 & l_2 & t \\ m_1 & m_2 & n \end{pmatrix} \\
 &= (-)^{n_1} \sum_{1, n', n} (-)^{n(2l+1)} \begin{bmatrix} l_1 & l_2 & 1 \\ n_1 & n_2 & n' \end{bmatrix}_{3j} \begin{bmatrix} l_1 & l_2 & 1 \\ -n & n & 0 \end{bmatrix}_{3j} D_{on'}^{l_1} (L \rightarrow t) \\
 &\quad \times \tilde{f}_{12} \begin{pmatrix} l_1 & l_2 & t \\ m_1 & m_2 & n \end{pmatrix} \tag{55}
 \end{aligned}$$

Now, we find;  $D_{nn_1}^{l_1} (L \rightarrow t) D_{-n-n_2}^{l_2} (L \rightarrow t)$

$$= \sum_{1, n'} (2l+1) (-)^{n'} \begin{bmatrix} l_1 & l_2 & 1 \\ n & -n & 0 \end{bmatrix}_{3j} \begin{bmatrix} l_1 & l_2 & 1 \\ n_1 & -n_2 & n' \end{bmatrix}_{3j} D_{on'}^{l_1} (L \rightarrow t)$$

$$= \sum_{1, n'} (2l+1) (-)^{n'} \begin{bmatrix} l_1 & l_2 & 1 \\ -n & n & 0 \end{bmatrix}_{3j} \begin{bmatrix} l_1 & l_2 & 1 \\ -n_1 & n_2 & -n' \end{bmatrix}_{3j} D_{on'}^{l_1} (L \rightarrow t)$$

(By equation 16)

$$= \sum_{1, n'} (2l+1) (-)^{n_1 - n_2} \begin{bmatrix} l_1 & l_2 & 1 \\ -n & n & 0 \end{bmatrix}_{3j} \begin{bmatrix} l_1 & l_2 & 1 \\ -n_1 & n_2 & n' \end{bmatrix}_{3j} D_{on'}^{l_1} (L \rightarrow t)$$

$$= (-)^{-n_2} \sum_{1, n'} (2l+1) (-)^{n_1} \begin{bmatrix} l_1 & l_2 & 1 \\ -n & n & 0 \end{bmatrix}_{3j} \begin{bmatrix} l_1 & l_2 & 1 \\ -n_1 & n_2 & n' \end{bmatrix}_{3j} D_{on'}^{l_1} (L \rightarrow t)$$

$$= (-)^{n_2} \sum_{1, n'} (2l+1) (-)^{n_1} \begin{bmatrix} l_1 & l_2 & 1 \\ -n & n & 0 \end{bmatrix}_{3j} \begin{bmatrix} l_1 & l_2 & 1 \\ -n_1 & n_2 & n' \end{bmatrix}_{3j} D_{on'}^{l_1} (L \rightarrow t)$$

Substituting this in equation (55), we get

$$\begin{aligned}\tilde{F}_{12} &= (-)^{-n_2} \sum_n (-)^n D_{nn_1}^{l_1} (L \rightarrow t) D_{-n-n_2}^{l_2} (L \rightarrow t) \tilde{f}_{12} \begin{pmatrix} l_1 & l_2 & t \\ m_1 & m_2 & r \end{pmatrix} \\ &= \sum_n D_{nn_1}^{l_1} (L \rightarrow t) D_{nn_2}^{l_2*} (L \rightarrow t) \tilde{f}_{12} \begin{pmatrix} l_1 & l_2 & t \\ m_1 & m_2 & n \end{pmatrix} \quad (56)\end{aligned}$$

With the help of equation (11)  $(-)^{n-n_2} D_{-n-n_2}^{l_2} (L \rightarrow t) = D_{nn_2}^{l_2*} (L \rightarrow t)$ .

The transform of convolution integral  $\tilde{P}_{XY}$  in equation (38) now can be simplified in the following way:

$$\begin{aligned}\tilde{P}_{XY}(\nu f, \langle X \rangle, \langle Y \rangle) &= \sum_{\langle 1 \rangle, \langle 2 \rangle, \dots, \langle \nu \rangle} \tilde{F}(\langle X \rangle, \langle 1 \rangle) \tilde{F}(\langle 1 \rangle, \langle 2 \rangle) \dots \tilde{F}(\langle \nu \rangle, \langle Y \rangle) \\ &= \sum_{\langle 1 \rangle, \langle 2 \rangle, \dots, \langle \nu \rangle} D_{n_{X1}n_X}^{l_1*} (L \rightarrow t) \tilde{f}_{X1}(n_{X1}) D_{n_{X1}n_1}^{l_1*} (L \rightarrow t) \dots D_{n_{\nu Y}n_\nu}^{l_\nu} \\ &\quad \tilde{f}_{\nu Y}(n_{\nu Y}) D_{n_{\nu Y}n_Y}^{l_Y*} (L \rightarrow t)\end{aligned}$$

From equation (5) and (8) and (10), we have

$$\begin{aligned}&\sum_n D_{n_a n}^{l_a*} (L \rightarrow t) D_{n_b n}^l (L \rightarrow t) \\ &= \sum_n D_{nn_a}^l (t \rightarrow L) D_{n_b n}^l (L \rightarrow t) \\ &= \sum_n D_{n_b n}^l (L \rightarrow t) D_{nn_a}^l (t \rightarrow L) \\ &= D_{n_b n_a}^l (t \rightarrow t) = \delta(n_b : n_a) \quad (57)\end{aligned}$$

$$\therefore \tilde{P}_{XY} (\nu f, \langle X \rangle, \langle Y \rangle)$$

$$= \sum_{\substack{l_1, l_2, \dots, l_\nu \\ m_1, m_2, \dots, m_\nu \\ n_1, n_2, \dots, n_\nu \\ n_{x1}, n_{12}, \dots, n_{\nu Y}}} D_{n_{x1} n_x}^{l_x} (L \rightarrow t) \tilde{f}_{x1}(n_{x1}) D_{n_{x1} n_1}^{l_1^*} (L \rightarrow t) D_{n_{12} n_1}^{l_1} (L \rightarrow t) \tilde{f}_{12}(n_{12}) \\ D_{n_{12} n_2}^{l_2^*} (L \rightarrow t) \dots D_{n_{\nu Y} n_\nu}^{l_\nu} \tilde{f}_{\nu Y}(n_{\nu Y}) D_{n_{\nu Y} n_Y}^{l_Y}$$

(If we sum over  $n_1, n_2, \dots, n_\nu$ , then we get a nonzero term for  $n_{x1} = n_{12} = \dots = n_{\nu Y} = n$ )

$$= \sum_{\substack{l_1, l_2, \dots, l_\nu \\ m_1, m_2, \dots, m_\nu, n}} D_{nn_x}^{l_x} \tilde{f}_{x1}(n) \tilde{f}_{12}(n) \dots \tilde{f}_{\nu Y}(n) D_{nn_Y}^{l_Y} \quad (58)$$

$$= \sum_n D_{nn_x}^{l_x} \left\{ \sum_{\substack{l_1, \dots, l_\nu \\ m_1, \dots, m_\nu}} \tilde{f}_{x1} \begin{pmatrix} l_x & l_1 & t \\ m_x & m_1 & n \end{pmatrix} \dots \tilde{f}_{\nu Y} \begin{pmatrix} l_\nu & l_Y & t \\ m_\nu & m_Y & n \end{pmatrix} \right\} D_{nn_Y}^{l_Y}$$

$$= \sum_n D_{nn_x}^{l_x} \tilde{P}_{XY} \left( \nu f, \begin{pmatrix} l_x & l_Y & t \\ m_x & m_Y & n \end{pmatrix} \right) D_{nn_Y}^{l_Y} \quad (59)$$

where,

$$\tilde{P}_{XY} = \sum_{\substack{l_1, l_2, \dots, l_\nu \\ m_1, m_2, \dots, m_\nu}} \tilde{f}_{x1} \begin{pmatrix} l_x & l_1 & t \\ m_x & m_1 & n \end{pmatrix} \tilde{f}_{12} \begin{pmatrix} l_1 & l_2 & t \\ m_1 & m_2 & n \end{pmatrix} \dots \tilde{f}_{\nu Y} \begin{pmatrix} l_\nu & l_Y & t \\ m_\nu & m_Y & n \end{pmatrix} \quad (60)$$

The relation between  $p_{XY} (\{X\}, \{Y\})$ ,  $\bar{p}_{XY}$  and  $\tilde{P}_{XY}$  is the same as the relation between  $f_{XY}$ ,  $\bar{f}_{XY}$ ,  $\tilde{f}_{XY}$ .

Also similar relation prevails for the sum over chains,

$$q_{XY} (f) = f_{XY} + \sum_{\nu \geq 1} c' \nu p_{XY} \quad (61)$$

its half transform

given by<sub>1</sub>

$$\bar{u}_{12} = (-)^{l_1} \delta(l_1+l_2:1) \left[ \frac{(2l_1+2l_2+1)!}{(2l_1)!(2l_2)!} \right]^{1/2} \frac{M_{m_1}^{l_1*} M_{m_2}^{l_2}}{r^{l_1+l_2+1}} \quad (69)$$

M functions are the multipole moments of the molecule.

Full transform can be found with the help of equation (52)

$$\tilde{u}_{12} \begin{pmatrix} l_1 & l_2 & t \\ m_1 & m_2 & n \end{pmatrix} = \frac{(-)^n 32\pi^3}{[(2l_1+1)(2l_2+1)]^{1/2}} \sum_i (-i)^l \begin{bmatrix} l_1 & l_2 & 1 \\ -n & n & 0 \end{bmatrix}_{3j}$$

$$\times \int_0^\infty \bar{u}_{12} \begin{pmatrix} l_1 & l_2 & 1 \\ m_1 & m_2 & r_{12} \end{pmatrix} j_1(rt) r^2 dr$$

(By replacing the expression for  $\bar{u}_{12}$  from equation (69), we get),

$$= \frac{(-)^n 32\pi^3}{[(2l_1+1)(2l_2+1)]^{1/2}} \sum_l (-i)^l \begin{bmatrix} l_1 & l_2 & 1 \\ -n & n & 0 \end{bmatrix}_{3j} \int_0^\infty (-)^{l_1} \delta(l_1+l_2:1)$$

$$\times \left[ \frac{(2l_1+2l_2+1)!}{(2l_1)!(2l_2)!} \right]^{1/2} \frac{M_{m_1}^{l_1*} M_{m_2}^{l_2}}{r_{12}^{l_1+l_2+1}} j_1(rt) r^2 dr$$

$$= \frac{(-)^n 32\pi^3}{[(2l_1+1)(2l_2+1)]^{1/2}} \sum_l (-i)^l \begin{bmatrix} l_1 & l_2 & 1 \\ -n & n & 0 \end{bmatrix}_{3j} (-)^{l_1} \delta(l_1+l_2:1)$$

$$\times \left[ \frac{(2l_1+2l_2+1)!}{(2l_1)!(2l_2)!} \right]^{1/2} M_{m_1}^{l_1} M_{m_2}^{l_2} \int_0^\infty \frac{j_1(rt)}{r_{12}^{l_1+l_2-1}} dr$$

[Evaluation of the integral:

$$\int_a^\infty \frac{j_{l_1+l_2}(rt)}{r_{12}^{l_1+l_2-1}} dr = \int_a^\infty \frac{j_{l_1+l_2}(rt)}{(rt)^{l_1+l_2-1}} d(rt) \quad t^{l_1+l_2-2}$$



$$= t^{l_1+l_2-2} \int_a^\infty \frac{j_{l_1+l_2}^{(rt)}}{(rt)^{l_1+l_2-1}} dr$$

From the relation  $\int j_n(x) x^{1-n} dx = \frac{j_{n-1}(x)}{x^{n-1}}$ , the above integral becomes

$$t^{l_1+l_2-2} \left. \frac{j_{l_1+l_2-1}^{(rt)}}{(rt)^{l_1+l_2-1}} \right|_a^\infty = \left. \frac{j_{l_1+l_2-1}^{(rt)}}{t r^{l_1+l_2-1}} \right|_a^\infty = - \left. \frac{j_{l_1+l_2-1}^{(at)}}{a^{l_1+l_2-1} t} \right] \quad (70)$$

$$= \frac{(-)^n 32\pi^3}{[(2l_1+1)(2l_2+1)]^{1/2}} (-i)^{l_1+l_2} \begin{bmatrix} l_1 & l_2 & l_1+l_2 \\ -n & n & 0 \end{bmatrix}_{3j} \\ \times (-)^{l_1} \left[ \frac{(2l_1+2l_2+1)!}{(2l_1)! (2l_2)!} \right]^{1/2} M_{m_1}^{l_1*} M_{m_2}^{l_2} \int_a^\infty \frac{j_{l_1+l_2-1}^{(rt)}}{r^{l_1+l_2-1}} dr \quad (71)$$

(With the help of equation (18)),

$$\left[ \frac{(2l_1+2l_2+1)!}{(2l_1)! (2l_2)!} \right]^{1/2} \begin{bmatrix} l_1 & l_2 & l_1+l_2 \\ -n & n & 0 \end{bmatrix}_{3j} \\ = \frac{(-)^{l_1-l_2} [(l_1+l_2)! (l_1+l_2)!]^{1/2}}{[(l_1+n)! (l_1-n)! (l_2+n)! (l_2-n)!]^{1/2}} \quad (72)$$

$$(-i)^{l_1+l_1} (-)^{l_1} (-)^{l_1-l_2} (i)^{-l_1-l_2} (-)^{2l_1-l_2} \\ \cdot (-i)^1 = \frac{1}{(i)^1} = (i)^{-1} \\ = (i)^{-l_1-l_2} (-)^{-l_2} = (i)^{-l_1-l_2} (-)^{l_2} \\ = (i)^{-l_1-l_2} (i^2)^{l_2} = (i)^{-l_1-l_2+2l_2} = (i)^{l_2-l_1} \quad (73)$$

Equations (71), (72) and (73) together give the following expression for  $\tilde{u}_{12}$ .

$$\tilde{u}_{12} = \frac{(-)^n 32\pi^3 (i)^{l_2 - l_1} (l_1 + l_2)! j_{l_1 + l_2 - 1}(at) M_{m_1}^{l_1*} M_{m_2}^{l_2}}{[(l_1 + n)! (l_1 - n)! (l_2 + n)! (l_2 - n)! (2l_1 + 1) (2l_2 + 1)]^{1/2} ta^{l_1 + l_2 - 1}} \quad (74)$$

$$\tilde{g}_{12} \begin{pmatrix} l_1 & l_2 & t \\ m_1 & m_2 & n \end{pmatrix} = -\beta \tilde{u}_{12} = M_{m_1}^{l_1*} \tilde{h} \begin{pmatrix} l_1 & l_2 \\ t & n \end{pmatrix} M_{m_2}^{l_2} \quad (75)$$

where

$$\tilde{h} \begin{pmatrix} l_1 & l_2 \\ t & n \end{pmatrix} = \frac{-\beta 32\pi^3 (-)^n (i)^{l_2 - l_1} (l_1 + l_2)! j_{l_1 + l_2 - 1}(at)}{[(l_1 + n)! (l_1 - n)! (l_2 + n)! (l_2 - n)! (2l_1 + 1) (2l_2 + 1)]^{1/2} ta^{l_1 + l_2 - 1}} \quad (76)$$

Now let us consider the expression for the  $n$  convolution integral given by equation (60) where we use  $\tilde{g}_{XY}$  as the function and there are two intermediate particles. Thus,

$$\begin{aligned} \tilde{p}_{XY}(2g) = \sum_{\substack{l_1 l_2 \\ m_1 m_2}} M_{m_X}^{l_X*} \tilde{h} \begin{pmatrix} l_X & l_1 \\ t & n \end{pmatrix} M_{m_1}^{l_1} M_{m_1}^{l_1*} \tilde{h} \begin{pmatrix} l_1 & l_2 \\ t & n \end{pmatrix} M_{m_2}^{l_2} \\ \times M_{m_2}^{l_2*} \tilde{h} \begin{pmatrix} l_2 & l_Y \\ t & n \end{pmatrix} M_{m_Y}^{l_Y} \end{aligned} \quad (77)$$

Let us define the following for a molecule of species  $s$

$$\sum_m M_m^{l*} M_m^l = M_s(l) \quad (78)$$

Hence, equation (77) becomes

$$\begin{aligned}
\tilde{p}_{XY}(2Y) &= \sum_{l_1 l_2} M_{m_X}^{l_X^*} \tilde{h} \begin{pmatrix} l_X & l_1 \\ t & n \end{pmatrix} M_1(l_1) \tilde{h} \begin{pmatrix} l_1 & l_2 \\ t & n \end{pmatrix} M_2(l_2) \\
&\times h \begin{pmatrix} l_2 & l_Y \\ 1 & n \end{pmatrix} M_{m_Y}^{l_Y} \\
&= M_{m_X}^{l_X^*} \langle l_X | H M_1 H M_2 H | l_Y \rangle M_{m_Y}^{l_Y} \quad (79)
\end{aligned}$$

where H matrix is the matrix of  $\tilde{h}$  and the elements are given by

$$\langle l_1 | H(t, n) | l_2 \rangle = \tilde{h} \begin{pmatrix} l_1 & l_2 \\ 1 & n \end{pmatrix} \quad (80)$$

$M_S$  matrix is the matrix of  $M_S(l)$  and the elements are given by

$$\langle l_1 | M_S | l_2 \rangle = M_S(l_1) \delta(l_1: l_2) \quad (81)$$

If we sum over chains of all lengths, we obtain the expression for  $\tilde{q}(t)$  from equation (63)

$$\begin{aligned}
\tilde{q}_{XY} &= \tilde{g}_{XY} + c' \tilde{p}_{XY}(1g) + c'^2 \tilde{p}_{XY}(2g) + \dots \\
&= \tilde{g}_{XY} + M_{m_X}^{l_X^*} \langle l_X | H c' M_1 H | l_Y \rangle M_{m_Y}^{l_Y} + M_{m_X}^{l_X^*} \langle l_X | H c' M_1 H c' M_2 H | l_Y \rangle M_{m_Y}^{l_Y} + \dots
\end{aligned}$$

From equation (76), we have

$$\begin{aligned}
\tilde{g}_{XY} &= M_{m_X}^{l_X^*} \langle l_X | H | l_Y \rangle M_{m_Y}^{l_Y} \\
\therefore \tilde{q}_{XY}(t) &= M_{m_X}^{l_X^*} \langle l_X | H(I + c' M_1 H + c' M_1 H c' M_1 H + \dots) | l_Y \rangle M_{m_Y}^{l_Y} \\
&= M_{m_X}^{l_X^*} \langle l_X | H (I - c' M_1 H)^{-1} | l_Y \rangle \quad (82)
\end{aligned}$$

## 4.2 Extension of Friedman-Jepsen Method to Mixture

If the system is a mixture (viz. an ionic solution) then, we have particles of more than one species in the system. So in order to find  $\tilde{q}_{XY}(t)$  we have to consider chains of all lengths and all possible sequences. If we sum over all of them, we obtain the following expression in place of equation (82) as the expression for  $\tilde{q}_{XY}(t)$ . Thus,

$$\tilde{q}_{XY}(t) = M_{m_X}^{l_X^*} < l_X | H \left[ I - (C_1 M_1 H + C_2 M_2 H + \dots + C_n M_n H) \right]^{-1} | l_Y > M_{m_Y}^{l_Y} \quad (83)$$

where  $1, 2, \dots, n$  represent the species present in the mixture.

This is apparent from the following consideration. Suppose, we have a mixture of two species. Then we consider the expression  $[I - (X+Y)]^{-1}$

$$[I - (X+Y)]^{-1} = I + (X+Y)^2 + (X+Y)^3 + (X+Y)^4 + \dots$$

$$(X+Y)^2 = X^2 + XY + YX + Y^2$$

Thus  $(X+Y)^2$  gives all possible sequences of length 2.

$$(X+Y)^3 = X^3 + XXY + XYX + YXX + XY Y + YXY + YYX + Y^3$$

and  $(X+Y)^3$  gives all possible sequences of length 3.

Similarly  $(X+Y)^n$  gives all possible sequences of length  $n$ .

Hence the expression for  $\tilde{q}_{XY}(t)$  is

$$M_{m_X}^{l_X^*} < l_X | H \left[ I - (C_1 M_1 H + C_2 M_2 H) \right]^{-1} | l_Y > M_{m_Y}^{l_Y}$$

If we have a mixture of three particles, then we consider the expression  $[I - (X+Y+Z)]^{-1}$

$$[ I - (X+Y+Z) ]^{-1} = I + (X+Y+Z) + (X+Y+Z)^2 + (X+Y+Z)^3 + \dots$$

$(X+Y+Z)$  gives all possible sequences of length one. Then, we consider,

$$(X+Y+Z)^2 = X^2 + XY + YX + Y^2 + YZ + ZY + Z^2 + ZX + XZ$$

and this gives all possible sequences of length two. Then consider  $(X+Y+Z)^3$

$$\begin{aligned} = & XXX + XXY + XYX + YXX + XXZ + XZX + ZXX + XYY + YXY + YYX \\ & + XYZ + XZY + YXZ + YZX + ZXY + ZYX + XZZ + ZXZ + ZZX + YYZ \\ & + YZY + ZYY + YZZ + ZYZ + YZZ + YYY + ZZZ \end{aligned}$$

and this gives all possible sequences of length three and thus  $(X+Y+Z)^n$  will give all possible sequences of length  $n$ .

Hence the expression for  $\tilde{q}_{XY}(t)$  is

$$M_{m_X}^{l_X*} < l_X | H \left[ I - (C_1 M_1 H + C_2 M_2 H + C_3 M_3 H) \right]^{-1} | l_Y > M_{m_Y}^{l_Y}$$

And the expression for  $\tilde{q}_{XY}(t)$  for a system of mixture of  $n$  particles is

$$M_{m_X}^{l_X*} < l_X | H \left[ I - (C_1 M_1 H + C_2 M_2 H + \dots + C_n M_n H) \right]^{-1} | l_Y > M_{m_Y}^{l_Y}$$

In the above expressions  $C_1, C_2, \dots, C_n$  are concentration in number of particles per unit volume of species  $1, 2, \dots, n$  respectively, each divided by  $8\pi^2$ .

$M_1, M_2, M_n$  are the  $M$  matrices as defined in equation (81) for species  $1, 2, \dots, n$ .

$H$  is the matrix of  $\tilde{h}$  as defined in equation (80).

The system that we will discuss in detail is an ionic solution containing a positive ion, a negative ion and a

macroion. They are embedded in water which is considered to be a continuum characterized by a dielectric constant. The macroion has negative charge as well as dipole moment on it.

Since the particles in the system have only charge and dipole, the M and H matrices are two dimensional.

In order to find the correlation function by HNC calculation we have to calculate q function between all pairs of particles of the three particles. This q is calculated from  $\bar{q}_{12} \begin{pmatrix} l_1 l_2 l \\ m_1 m_2 r \end{pmatrix}$  by eqn. (26) and  $\bar{q}_{12}$  is calculated from  $\tilde{q}_{12} \begin{pmatrix} l_1 l_2 t \\ m_1 m_2 r \end{pmatrix}$  by eqn. (54). So we need to evaluate  $\tilde{q}_{12}$  from the M and H matrices.

The M and H matrices are constructed as follows :

Let  $q_+$  be the charge of the positive ion,  
 $q_-$  be the charge of the negative ion,  
and  $q_m$  be the charge of the macroion,  
and  $\mu_m$  be the dipole of the macroion.

The elements of the M matrix are defined as

$$\begin{aligned} (l_1 | M | l_2) &= M(l_1) \delta(l_1 : l_2) \\ &= \sum_m M_m^{l*} M_m^l \end{aligned} \quad (84)$$

$M_m^l$  = The multipole moments of the charge distribution

If  $l = 0$ , (viz. a charge)  $\sum_m M_m^{l*} M_m^l = M_0^0 * M_0^0 = q \times q = q^2$

If  $l = 1$ , (viz a dipole), then

$$\sum_m M_m^{l*} M_m^l = M_0^1 * M_0^1 + M_1^1 * M_1^1 + M_{-1}^1 * M_{-1}^1 \quad (85)$$

If the coordinate system, fixed in the molecule, is so chosen that the dipole lies in the z-direction, then  $M_0^1 = \mu$ , the dipole moment,  $M_{\pm 1}^1 = 0$ .

$$\text{Hence } \sum_m M_m^{I*} M_m^{I*} = \mu^2 \quad (86)$$

This relation holds irrespective of the choice of z-axis.

Hence  $M_+$  = M matrix for the positive ion

$$= \begin{bmatrix} q_+^2 & 0 \\ 0 & 0 \end{bmatrix} \quad (87)$$

$M_-$  = M matrix for the negative ion

$$= \begin{bmatrix} q_-^2 & 0 \\ 0 & 0 \end{bmatrix} \quad (88)$$

$M_m$  = M matrix for the macroion

$$= \begin{bmatrix} q_m^2 & 0 \\ 0 & \mu_m^2 \end{bmatrix} \quad (89)$$

The elements of the H matrix are defined as

$$(l_1 | H(t, n) | l_2) = \tilde{h}_{l_1 l_2}(t, n) \quad (90)$$

Thus the H matrices for our system, where  $l_1 = 0$ ,  $l_2 = 1$  and  $n = 1, 0, -1$  are

$$H(t, 0) = \begin{bmatrix} \tilde{h}_{00}(t, 0) & \tilde{h}_{01}(t, 0) \\ \tilde{h}_{10}(t, 0) & \tilde{h}_{11}(t, 0) \end{bmatrix} \quad (91)$$

$$H(t, 1) = \begin{bmatrix} \tilde{h}_{00}(t, 1) & \tilde{h}_{01}(t, 1) \\ \tilde{h}_{10}(t, 1) & \tilde{h}_{11}(t, 1) \end{bmatrix} \quad (92)$$

$$H(t, -1) = \begin{bmatrix} \tilde{h}_{00}(t, -1) & \tilde{h}_{01}(t, -1) \\ \tilde{h}_{10}(t, -1) & \tilde{h}_{11}(t, -1) \end{bmatrix} \quad (93)$$

$$= \begin{pmatrix} \frac{1 + c_m \mu_m^2 \frac{2xj_1(a_{11}t)}{3a_{11}t}}{\det 1} & \frac{-(\sum_i c_i q_i^2) \frac{ixj_0(a_{10}t)}{\sqrt{3}t}}{\det 1} \\ \frac{c_m \mu_m^2 \frac{ixj_0(a_{01}t)}{\sqrt{3}t}}{\det 1} & \frac{1 + (\sum_i c_i q_i^2) \frac{xa_{00}j_{-1}(a_{00}t)}{t}}{\det 1} \end{pmatrix} \quad (99)$$

$$H(I - C_+ M_+ H - C_- M_- H - C_m M_m H)^{-1}$$

$$= \begin{pmatrix} \tilde{h}_{00} & \tilde{h}_{01} \\ \tilde{h}_{10} & \tilde{h}_{11} \end{pmatrix} \begin{pmatrix} \frac{1 + c_m \mu_m^2 \frac{2xj_1(a_{11}t)}{3a_{11}t}}{\det 1} & \frac{-(\sum_i c_i q_i^2) \frac{ixj_0(a_{10}t)}{\sqrt{3}t}}{\det 1} \\ \frac{c_m \mu_m^2 \frac{ixj_0(a_{01}t)}{\sqrt{3}t}}{\det 1} & \frac{+ (\sum_i c_i q_i^2) \frac{x a_{00}j_{-1}(a_{00}t)}{t}}{\det 1} \end{pmatrix}$$

$$= \begin{pmatrix} P_{11} & P_{12} \\ P_{21} & P_{22} \end{pmatrix} \quad (100)$$

where

$$P_{11}(n=0) = \tilde{h}_{00} \frac{1 + \frac{c_m \mu_m^2 2xj_1(a_{11}t)}{3a_{11}t}}{\det 1} + \tilde{h}_{01} \frac{\frac{c_m \mu_m^2 ixj_0(a_{01}t)}{\sqrt{3}t}}{\det 1}$$

$$= \frac{1}{\det 1} x \left\{ \frac{(-x a_{00} j_{-1}(a_{00}t))}{t} \right\} \left[ 1 + c_m \mu_m^2 \frac{2xj_1(a_{11}t)}{3a_{11}t} \right]$$

$$+ \frac{1}{\det 1} x c_m \mu_m^2 x^2 \frac{j_0(a_{01}t) j_0(a_{01}t)}{3t^2} \quad (101)$$



$$\begin{aligned}
P_{12}(n=0) &= \tilde{h}_{00} \left( \frac{-(\sum_i c_i q_i^2) \frac{ix j_0(a_{01}t)}{\sqrt{3} t}}{\det 1} \right) \\
&+ \tilde{h}_{01} \left( \frac{1 + (\sum_i c_i q_i^2) \frac{x a_{00} j_{-1}(a_{00}t)}{t}}{\det 1} \right) \\
&= \left[ i \frac{x^2 a_{00} j_0(a_{01}t) j_{-1}(a_{00}t)}{\sqrt{3} t^2} \left( \sum_i c_i q_i^2 \right) \right. \\
&\quad - \frac{ix j_0(a_{01}t)}{\sqrt{3} t} - \left. \left( \frac{ix^2 a_{00} j_0(a_{01}t) j_{-1}(a_{00}t)}{\sqrt{3} t^2} \right) \right. \\
&\quad \left. \times \left( \sum_i c_i q_i^2 \right) \right] \times \frac{1}{\det 1} \\
&= \frac{ix j_0(a_{01}t)}{\sqrt{3} t} \times \frac{1}{\det 1} \\
&= -i P, \text{ where } P = \frac{x j_0(a_{01}t)}{\sqrt{3} t} \times \frac{1}{\det 1} \tag{102}
\end{aligned}$$

$$\begin{aligned}
P_{21}(n=0) &= \tilde{h}_{10} \left( \frac{1 + c_m \mu_m^2 \frac{2x j_1(a_{11}t)}{3a_{11}t}}{\det 1} \right) \\
&+ \tilde{h}_{11} \left( \frac{c_m \mu_m^2 \frac{ix j_0(a_{01}t)}{\sqrt{3} t}}{\det 1} \right) \\
&= \frac{ix j_0(a_{10}t)}{\sqrt{3} t} \left( \frac{1 + c_m \mu_m^2 \frac{2x j_1(a_{11}t)}{3a_{11}t}}{\det 1} \right)
\end{aligned}$$

$$\begin{aligned}
& + \frac{-2x j_1(a_{11}t)}{3a_{11}t} \left( \frac{C_m \mu_m^2 \frac{ix j_0(a_{01}t)}{\sqrt{3} t}}{\det 1} \right) \\
& = \frac{1}{\det 1} \times \left( \frac{ix j_0(a_{10}t)}{\sqrt{3} t} + \frac{i2x^2 C_m \mu_m^2 j_0(a_{01}t) j_1(a_{11}t)}{3 \sqrt{3} a_{11} t^2} \right. \\
& \quad \left. - \frac{-i2x^2 C_m \mu_m^2 j_0(a_{01}t) j_1(a_{11}t)}{3\sqrt{3} a_{11} t^2} \right) \quad (103) \\
& = i P
\end{aligned}$$

$$\begin{aligned}
P_{22}(n=0) &= \tilde{h}_{10} \left( \frac{-(\sum_i C_i q_i^2) \frac{ix j_0(a_{10}t)}{\sqrt{3} t}}{\det 1} \right) + \tilde{h}_{11} \left( \frac{1 + (\sum_i C_i q_i^2) \frac{xa_{00} j_{-1}(a_{00}t)}{t}}{\det 1} \right) \\
&= \frac{x^2 j_0(a_{01}t) j_0(a_{10}t)}{3t^2} \times (\sum_i C_i q_i^2) \times \frac{1}{\det 1} \\
&\quad - \frac{2x j_1(a_{11}t)}{3a_{11}t} \left[ \frac{1 + (\sum_i C_i q_i^2) \frac{xa_{00} j_{-1}(a_{00}t)}{t}}{\det 1} \right] \quad (104)
\end{aligned}$$

For  $n = 1$  and  $n = -1$ , the H matrix is given as

$$\begin{bmatrix} 0 & 0 \\ 0 & \frac{x j_1(a_{11}t)}{3a_{11}t} \end{bmatrix} \quad (105)$$

$$\begin{aligned}
C_+ M_+ H &= C_+ \begin{bmatrix} q_+^2 & 0 \\ 0 & 0 \end{bmatrix} \begin{bmatrix} 0 & 0 \\ 0 & \frac{x j_1(a_{11}t)}{3a_{11}t} \end{bmatrix} \\
&= \begin{bmatrix} 0 & 0 \\ 0 & 0 \end{bmatrix} \quad (106)
\end{aligned}$$

$$\begin{aligned}
C_{-M-H} &= C_- \begin{bmatrix} q_-^2 & 0 \\ 0 & 0 \end{bmatrix} \begin{bmatrix} 0 & \frac{xj_1^0(a_{11}t)}{3a_{11}t} \\ 0 & 0 \end{bmatrix} \\
&= \begin{bmatrix} 0 & 0 \\ 0 & 0 \end{bmatrix}
\end{aligned} \tag{107}$$

$$\begin{aligned}
C_{mM_mH} &= C_m \begin{bmatrix} q_m^2 & 0 \\ 0 & \mu_m^2 \end{bmatrix} \begin{bmatrix} 0 & \frac{xj_1^0(a_{11}t)}{3a_{11}t} \\ 0 & 0 \end{bmatrix} \\
&= \begin{bmatrix} 0 & \frac{xj_1^0(a_{11}t)}{3a_{11}t} \\ 0 & C_m \mu_m^2 \frac{xj_1^0(a_{11}t)}{3a_{11}t} \end{bmatrix}
\end{aligned} \tag{108}$$

$$\begin{aligned}
(I - C_{+M_+H} - C_{-M-H} - C_{mM_mH}) \\
= \begin{bmatrix} 1 & \frac{xj_1^0(a_{11}t)}{3a_{11}t} \\ 0 & 1 - C_m \mu_m^2 \frac{xj_1^0(a_{11}t)}{3a_{11}t} \end{bmatrix}
\end{aligned} \tag{109}$$

Determinant of the above matrix = det2

$$= 1 - C_m \mu_m^2 \frac{xj_1^0(a_{11}t)}{3a_{11}t} \tag{110}$$

$$\begin{aligned}
(I - C_{+M_+H} - C_{-M-H} - C_{mM_mH})^{-1} \\
= \begin{bmatrix} 1 - \frac{C_m \mu_m^2 xj_1^0(a_{11}t)}{3a_{11}t} & 0 \\ \frac{C_m \mu_m^2 xj_1^0(a_{11}t)}{3a_{11}t} & 1 \end{bmatrix}
\end{aligned} \tag{111}$$

$$H (I - C_{+M_+H} - C_{-M-H} - C_{mM_mH})^{-1}$$

$$\begin{aligned}
&= \begin{bmatrix} 0 & 0 \\ 0 & \frac{xj_1(a_{11}t)}{3a_{11}t} \end{bmatrix} \begin{bmatrix} 1 - \frac{c_m \mu_m^2 xj_1(a_{11}t)}{3a_{11}t \det 2} & 0 \\ 0 & 1 \end{bmatrix} \\
&= \begin{bmatrix} 0 & 0 \\ 0 & \frac{xj_1(a_{11}t)}{3a_{11}t(\det 2)} \end{bmatrix} \quad (112)
\end{aligned}$$

$$\begin{aligned}
P_{11} \quad (n = 1, -1) &= 0 \\
P_{12} \quad (n = 1, -1) &= 0 \\
P_{21} \quad (n = 1, -1) &= 0 \\
P_{22} \quad (n = 1, -1) &= \frac{xj_1(a_{11}t)}{3a_{11}t(\det 2)} \quad (113)
\end{aligned}$$

#### CALCULATION OF q FUNCTIONS:

In the following the subscript '++' represents that the quantity being calculated is that between two positive ions. Similarly '-' represents a negative ion and 'm' represents a macroion. To avoid any possible confusion, let us state that  $\tilde{q}$  is the full transform of q bond and  $q_{+, -, m}$  are charges.

$$\begin{aligned}
\tilde{q}_{++} \begin{pmatrix} 0 & 0 & t \\ 0 & 0 & 0 \end{pmatrix} &= q_+ P_{11} (n = 0) q_+ \\
&= q_+^2 P_{11} (n = 0)
\end{aligned}$$

$$\tilde{q}_{+-} \begin{pmatrix} 0 & 0 & t \\ 0 & 0 & 0 \end{pmatrix} = q_+ q_- P_{11} (n = 0)$$

$$\tilde{q}_{-+} \begin{pmatrix} 0 & 0 & t \\ 0 & 0 & 0 \end{pmatrix} = \tilde{q}_{+-} \begin{pmatrix} 0 & 0 & t \\ 0 & 0 & 0 \end{pmatrix}$$

$$\tilde{q}_{--} \begin{pmatrix} 0 & 0 & t \\ 0 & 0 & 0 \end{pmatrix} = q_-^2 P_{11} (n = 0)$$

$$\tilde{q}_{+m} \begin{pmatrix} 0 & 0 & t \\ 0 & 0 & 0 \end{pmatrix} = q_+ q_m P_{11} \quad (n = 0)$$

$$\tilde{q}_{-m} \begin{pmatrix} 0 & 0 & t \\ 0 & 0 & 0 \end{pmatrix} = q_- q_m P_{11} \quad (n = 0).$$

$$\tilde{q}_{+m} \begin{pmatrix} 0 & 0 & t \\ 0 & 0 & 0 \end{pmatrix} = \tilde{q}_{m+} \begin{pmatrix} 0 & 0 & t \\ 0 & 0 & 0 \end{pmatrix}$$

$$\tilde{q}_{-m} \begin{pmatrix} 0 & 0 & t \\ 0 & 0 & 0 \end{pmatrix} = \tilde{q}_{m-} \begin{pmatrix} 0 & 0 & t \\ 0 & 0 & 0 \end{pmatrix}$$

$$\begin{aligned} \tilde{q}_{+m} \begin{pmatrix} 0 & 1 & t \\ 0 & 0 & 0 \end{pmatrix} &= q_+ P_{12} \quad (n = 0) \quad \mu_m \\ &= q_+ \mu_m P_{12} \quad (n = 0) \end{aligned}$$

$$\begin{aligned} \tilde{q}_{m+} \begin{pmatrix} 1 & 0 & t \\ 0 & 0 & 0 \end{pmatrix} &= \mu_m P_{21} \quad (n = 0) \quad q_+ \\ &= q_+ \mu_m P_{21} \quad (n = 0) \end{aligned}$$

$$\tilde{q}_{-m} \begin{pmatrix} 0 & 1 & t \\ 0 & 0 & 0 \end{pmatrix} = q_- \mu_m P_{12} \quad (n = 0)$$

$$\tilde{q}_{m-} \begin{pmatrix} 1 & 0 & t \\ 0 & 0 & 0 \end{pmatrix} = q_- \mu_m P_{21} \quad (n = 0)$$

$$\tilde{q}_{mm} \begin{pmatrix} 0 & 0 & t \\ 0 & 0 & 0 \end{pmatrix} = q_m^2 P_{11} \quad (n = 0)$$

$$\tilde{q}_{mm} \begin{pmatrix} 0 & 1 & t \\ 0 & 0 & 0 \end{pmatrix} = q_m \mu_m P_{12} \quad (n = 0)$$

$$\tilde{q}_{mm} \begin{pmatrix} 1 & 0 & t \\ 0 & 0 & 0 \end{pmatrix} = q_m \mu_m P_{21} \quad (n = 0)$$

$$\tilde{q}_{mm} \begin{pmatrix} 1 & 1 & t \\ 0 & 0 & 0 \end{pmatrix} = \mu_m P_{22} \mu_m = \mu_m^2 P_{22} \quad (n = 0)$$

$$\tilde{q}_{mm} \begin{pmatrix} 1 & 1 & t \\ 0 & 0 & 1 \end{pmatrix} = \mu_m^2 P_{22} \quad (n = 1)$$

$$\tilde{q}_{mm} \begin{pmatrix} 1 & 1 & t \\ 0 & 0 & -1 \end{pmatrix} = \mu_m^2 P_{22} \quad (n = -1)$$

Since  $\mu_1^1 = 0$  and  $\mu_{-1}^1 = 0$  (other  $\tilde{q}_{mm}$  values are zero)

Using Eq<sup>n</sup> (54), we calculate the half transform  $\bar{q}$ . They are given as follows. (Values of the Bessel function and Wigner 3-j coefficients, are given in the Appendix).

$$\begin{aligned} \bar{q}_{++} \begin{pmatrix} 0 & 0 & 0 \\ 0 & 0 & r_{++} \end{pmatrix} \\ = \frac{1}{16\pi^4} \times (-)^0 \times \begin{bmatrix} 0 & 0 & 0 \\ 0 & 0 & 0 \end{bmatrix}_{3j} \int \tilde{q}_{++} j_0(rt) t^2 dt \\ = \frac{q_+^2}{16\pi^4 r_{++}} \int_0^\infty P_{11}(n=0) t \sin(rt) dt \end{aligned}$$

$$\bar{q}_{+-} \begin{pmatrix} 0 & 0 & 0 \\ 0 & 0 & r_{+-} \end{pmatrix} = \frac{q_+ q_-}{16\pi^4 r_{+-}} \int_0^\infty P_{11}(n=0) t \sin(rt) dt$$

$$\bar{q}_{-+} \begin{pmatrix} 0 & 0 & 0 \\ 0 & 0 & r_{-+} \end{pmatrix} = \bar{q}_{+-} \begin{pmatrix} 0 & 0 & 0 \\ 0 & 0 & r_{+-} \end{pmatrix}$$

$$\bar{q}_{--} \begin{pmatrix} 0 & 0 & 0 \\ 0 & 0 & r_{--} \end{pmatrix} = \frac{q_-^2}{16\pi^4 r_{--}} \int_0^\infty P_{11}(n=0) t \sin(rt) dt$$

$$\bar{q}_{+m} \begin{pmatrix} 0 & 0 & 0 \\ 0 & 0 & r_{+m} \end{pmatrix} = \frac{q_+ q_m}{16\pi^4 r_{+m}} \int_0^\infty P_{11}(n=0) t \sin(rt) dt$$

$$\bar{q}_{-m} \begin{pmatrix} 0 & 0 & 0 \\ 0 & 0 & r_{-m} \end{pmatrix} = \frac{q_- q_m}{16\pi^4 r_{-m}} \int_0^\infty P_{11}(n=0) t \sin(rt) dt$$

$$\bar{q}_{m+} \begin{pmatrix} 0 & 0 & 0 \\ 0 & 0 & r_{m+} \end{pmatrix} = \bar{q}_{+m} \begin{pmatrix} 0 & 0 & 0 \\ 0 & 0 & r_{+m} \end{pmatrix}$$

$$\bar{q}_{m-} \begin{pmatrix} 0 & 0 & 0 \\ 0 & 0 & r_{m-} \end{pmatrix} = \bar{q}_{-m} \begin{pmatrix} 0 & 0 & 0 \\ 0 & 0 & r_{-m} \end{pmatrix}$$

$$\bar{q}_{+m} \begin{pmatrix} 0 & 1 & 1 \\ 0 & 0 & r_{+m} \end{pmatrix} = \frac{1}{16\pi^4} \times (i)^1 \times (3)^{1/2} \times 3$$

$$\times (-)^0 \begin{bmatrix} 0 & 1 & 1 \\ 0 & 0 & 0 \end{bmatrix}_{3j} \int_0^\infty \tilde{q}_{+m} \begin{pmatrix} 0 & 1 & t \\ 0 & 0 & 0 \end{pmatrix} j_1(r_{+m}t) t^2 dt$$

$$= \frac{i \times 3\sqrt{3}}{16\pi^4} \times \left(-\frac{1}{\sqrt{3}}\right) \times q_+ \mu_m \int_0^\infty P_{12} (n=0) j_1(r_{+m}t) t^2 dt$$

$$= -\frac{i \times 3}{16\pi^4} \times q_+ \mu_m \int_0^\infty -i P \left( \frac{\sin(r_{+m}t)}{r_{+m}^2 t^2} - \frac{\cos(r_{+m}t)}{r_{+m}t} \right) t^2 dt$$

(we recall  $P_{12} = -iP$ , Eq. 102)

$$= \frac{+3i^2}{16\pi^4} \times q_+ \mu_m \int_0^\infty \left\{ P \left( \frac{\sin(r_{+m}t)}{r_{+m}^2} \right) - P \left( \frac{\cos(r_{+m}t)}{r_{+m}} \right) t \right\} dt$$

$$= -\frac{3}{16\pi^4} \times q_+ \mu_m \left[ \frac{1}{r_{+m}^2} \int_0^\infty P \sin(r_{+m}t) dt - \frac{1}{r_{+m}} \int_0^\infty P \cos(r_{+m}t) t dt \right]$$

$$\bar{q}_{-m} \begin{pmatrix} 0 & 1 & 1 \\ 0 & 0 & r_{-m} \end{pmatrix} = -\frac{3}{16\pi^4} \times q_- \mu_m \left[ \frac{1}{r_{-m}^2} \int_0^\infty P \sin(r_{-m}t) dt - \frac{1}{r_{-m}} \int_0^\infty P t \cos(r_{-m}t) dt \right]$$

$$\bar{q}_{m+} \begin{pmatrix} 1 & 0 & 1 \\ 0 & 0 & r_{m+} \end{pmatrix}$$

$$= \frac{3}{16\pi^4} \times (i)^1 \times 3\sqrt{3} \times (-)^0 \begin{bmatrix} 1 & 0 & 1 \\ 0 & 0 & 0 \end{bmatrix}_{3j} \int_0^\infty \tilde{q}_{m+} \begin{pmatrix} 0 & 1 & t \\ 0 & 0 & 0 \end{pmatrix} j_1(r_{m+}t) t^2 dt$$

$$\begin{aligned}
= & - \frac{(30)^{1/2}}{16\pi^4} \left[ \frac{3}{r_{mm}^3} \mu_m^2 \int_0^\infty P_{22}(n=0) \times \frac{1}{t} \sin(r_{mm}t) dt \right. \\
& - \frac{\mu_m^2}{r_{mm}} \int_0^\infty P_{22}(n=0) t \sin(r_{mm}t) dt \\
& \left. - \frac{3\mu_m^2}{r_{mm}^2} \int_0^\infty P_{22}(n=0) \cos(r_{mm}t) dt \right] \quad (114)
\end{aligned}$$

$$\begin{aligned}
+ & \left(\frac{15}{2}\right)^{1/2} \times \frac{1}{16\pi^4} \left[ \frac{3}{r_{mm}^3} \mu_m^2 \int_0^\infty P_{22}(n=1) \times \frac{1}{t} \sin(r_{mm}t) dt \right. \\
& - \frac{\mu_m^2}{r_{mm}} \int_0^\infty P_{22}(n=1) t \sin(r_{mm}t) dt \\
& \left. - \frac{3}{r_{mm}^2} \mu_m^2 \int_0^\infty P_{22}(n=1) \cos(r_{mm}t) dt \right] \quad (114a)
\end{aligned}$$

$$\begin{aligned}
+ & \left(\frac{15}{2}\right)^{1/2} \times \frac{1}{16\pi^4} \left[ \frac{3}{r_{mm}^3} \mu_m^2 \int_0^\infty P_{22}(n=-1) \times \frac{1}{t} \sin(r_{mm}t) dt \right. \\
& - \frac{\mu_m^2}{r_{mm}} \int_0^\infty P_{22}(n=-1) t \sin(r_{mm}t) dt \\
& \left. - \frac{3}{r_{mm}^2} \mu_m^2 \int_0^\infty P_{22}(n=-1) \cos(r_{mm}t) dt \right] \quad (114b)
\end{aligned}$$

$$\bar{q}_{mm} \begin{pmatrix} 1 & 1 & 1 \\ 0 & 0 & r_{mm} \end{pmatrix}$$



$$= \frac{(i) (3)^{1/2} (3)^{1/2} 3}{16\pi^4} \left[ (-)^0 \begin{bmatrix} 1 & 1 & 1 \\ 0 & 0 & 0 \end{bmatrix}_{3j} \int_0^\infty \tilde{q}_{mm} \begin{pmatrix} 1 & 1 & t \\ 0 & 0 & 0 \end{pmatrix} t^2 j_1(rt) dt \right.$$

$$+ (-)^0 \begin{bmatrix} 1 & 1 & 1 \\ -1 & 1 & 0 \end{bmatrix}_{3j} \int_0^\infty \tilde{q}_{mm} \begin{pmatrix} 1 & 1 & t \\ 0 & 0 & 1 \end{pmatrix} t^2 j_1(rt) dt$$

$$\left. + (-)^0 \begin{bmatrix} 1 & 1 & 1 \\ 1 & -1 & 0 \end{bmatrix}_{3j} \int_0^\infty \tilde{q}_{mm} \begin{pmatrix} 1 & 1 & t \\ 0 & 0 & -1 \end{pmatrix} t^2 j_1(rt) dt \right]$$

$$= \frac{9i}{16\pi^4} \left[ 0 - \frac{1}{\sqrt{6}} \int_0^\infty P_{22}(n=1) t^2 j_1(rt) dt \right. \\ \left. + \frac{1}{\sqrt{6}} \int_0^\infty P_{22}(n=-1) t^2 j_1(rt) dt \right]$$

$$= \frac{9i}{16\pi^4} \left[ - \frac{1}{\sqrt{6}} \int_0^\infty P_{22}(n=1) t^2 j_1(rt) dt \right. \\ \left. + \frac{1}{\sqrt{6}} \int_0^\infty P_{22}(n=-1) t^2 j_1(rt) dt \right]$$

$$= 0 \quad (\text{since } P_{22}(n=1) = P_{22}(n=-1))$$

$$\bar{q}_{mm} \begin{pmatrix} 1 & 1 & 0 \\ 0 & 0 & r_{mm} \end{pmatrix} = \frac{(i)^0 x(3)^{1/2} (3)^{1/2} 1}{16\pi^4} x$$

$$\left[ (-)^{-1} \begin{bmatrix} 1 & 1 & 0 \\ 1 & -1 & 0 \end{bmatrix}_{3j} \int_0^\infty \tilde{q}_{mm} \begin{pmatrix} 1 & 1 & t \\ 0 & 0 & -1 \end{pmatrix} t^2 j_0(r_{mm} t) dt \right.$$

$$\begin{aligned}
& + (-)^0 \begin{bmatrix} 1 & 1 & 0 \\ 0 & 0 & 0 \end{bmatrix}_{3j} \int_0^\infty \tilde{q}_{mm} \begin{pmatrix} 1 & 1 & t \\ 0 & 0 & 0 \end{pmatrix} t^2 j_0(r_{mm}t) dt \\
& + (-)^1 \begin{bmatrix} 1 & 1 & 0 \\ -1 & 1 & 0 \end{bmatrix}_{3j} \int_0^\infty \tilde{q}_{mm} \begin{pmatrix} 1 & 1 & t \\ 0 & 0 & 1 \end{pmatrix} t^2 j_0(r_{mm}t) dt \Big] \\
& = \frac{3}{16\pi^4} \left[ \left( -\frac{1}{\sqrt{3}} \right) \mu_m^2 \int_0^\infty P_{22}(n=-1) t^2 \frac{\sin(r_{mm}t)}{r_{mm}t} dt \right. \\
& + \left( -\frac{1}{\sqrt{3}} \right) \mu_m^2 \int_0^\infty P_{22}(n=0) t^2 \frac{\sin(r_{mm}t)}{r_{mm}t} dt \\
& + \left. \left( -\frac{1}{\sqrt{3}} \right) \mu_m^2 \int_0^\infty P_{22}(n=1) t^2 \frac{\sin(r_{mm}t)}{r_{mm}t} dt \right] \\
& = -\frac{\sqrt{3} \mu_m^2}{16\pi^4} \left[ \frac{1}{r} \int_0^\infty P_{22}(n=1) t \sin(r_{mm}t) dt \right. \\
& + \frac{1}{r} \int_0^\infty P_{22}(n=0) t \sin(r_{mm}t) dt \\
& + \left. \frac{1}{r} \int_0^\infty P_{22}(n=-1) t \sin(r_{mm}t) dt \right]
\end{aligned}$$

In the above, when calculating  $\bar{q}$  from  $\tilde{q}$ , we have to do sine integration of the various matrix elements  $P_{ij}$  multiplied by  $\sin(rt)$  over the variable  $t$  between  $0, \infty$ . This can be done both numerically and wherever possible analytically. The  $\lim_{a \rightarrow 0}$  has to be obtained for each integral.

The following consideration is useful in evaluation of the limit  $a \rightarrow 0$  of the integral. In each of the expressions  $P_{11}$ ,  $P_{12}$  etc. (Eq. 101-104 and 112a) and in the expression of the determinant (Eq. 98(a)), there appears terms with  $j_1(at)$  in the numerator with  $t$  or  $t^2$  in the denominator, as well as terms with  $j_1(at)$  in the numerator and  $at$  in the denominator. The former fall off to negligible values at a large  $t$  called  $t_{\max}$ , whose value is independent of the value of the parameter  $a$ . In the limit  $x \gg 1$ ,  $j_1(x) \rightarrow \frac{1}{x} \sin(x - \frac{1\pi}{2})$ . So,  $j_1(at)$  fall off when  $at \gg 1$ , where 1 is a small number. As the parameter 'a' becomes smaller, the value of  $t$  for which  $at \gg 1$  becomes larger. But irrespective of the value of  $t$  at which  $j_1(at)$  falls off to a small value, the denominator ( $t$  or  $t^2$ ) will become large independent of the value of  $a$ , and make the magnitude of the term negligible. The latter which have  $at$  in the denominator, do not have this feature. As  $a \rightarrow 0$ , the value of  $t$  at which it falls off keeps on increasing indefinitely. These infinitely spread out (on the  $t$ -axis) functions can be dropped on the basis of following considerations. The integral of these functions with  $\sin(rt)$  is calculated by symmetrizing these functions and then calculating their Fourier transform. The symmetrized functions are also infinitely spread out. It is known that if F.T. of  $f(t)$  is  $g(\omega)$ , then F.T. of  $f(at)$  is  $\frac{1}{|a|} g(\frac{\omega}{a})$ . If  $a$  is small then  $g(\frac{\omega}{a})$  shrinks to zero frequency and  $\frac{1}{|a|} \rightarrow \infty$ . Therefore the contribution of these functions is a  $\delta$ -function at  $\omega=0$ . The  $\delta$ -function in  $q(r)$  contributes a  $\delta$ -function to  $\phi(r)$ . The convolution  $a*b$ , where  $a$  has a  $\delta$ -function at  $r=0$  gives  $b(0)$ , which is a  $\delta$ -function if both  $a$  and  $b$  are  $q(r)$ , or if both are  $\phi(r)$ . Thus  $\tau(r)$  also has a  $\delta$ -function at  $r=0$ .  $h(r)$  calculated as  $e^{\tau+q}$  is however set equal

to -1 within hard sphere radius. The  $\delta$ -function thus disappears. The function  $x(\vec{r}) = h(\vec{r}) - \tau(\vec{r}) - q(\vec{r})$  again procures a  $\delta$ -function, the recalculated  $\tau$ , as sums of convolutions of functions having  $\delta$ -functions, has a  $\delta$ -function at  $r=0$ . The recalculated  $h(\vec{r})$  once again is free of the  $\delta$ -function, because within the hardsphere, one deliberately sets it equal to -1. Since the  $\delta$ -function is inconsequential, we drop the terms  $j_1(at)/at$  terms from  $P_{ij}$  ( $i,j=1,2$ ) altogether. The terms that remain fall off at a certain  $t = t_{\max}$ . Then, one obtains  $\lim_{a \rightarrow 0} \int_0^\infty = \lim_{a \rightarrow 0} \int_0^{t_{\max}}$ . Now one can always choose  $a$  to be so small that over the whole range 0 to  $t_{\max}$ ,  $at$  is very small. Then one can evaluate the integrand in the limit at  $\rightarrow 0$ , make it free of  $at$ , obtain a function of  $t$  only and integrate it within the limit 0 to  $\infty$ . Since the integrand is negligible above  $t_{\max}$ , its behaviour above this value of  $t$  makes no difference to the calculated values. Thus, we use in the integrations that follow:

$$\lim_{a \rightarrow 0} \int_0^\infty I(t, at) dt = \int_0^\infty \left\{ \lim_{at \rightarrow 0} I(t, at) \right\} dt$$

Then we can analytically integrate several integrals that appear in expressions of different  $\bar{q}$ 's.

$$\begin{aligned} (1) \quad & \lim_{a \rightarrow 0} \int_0^\infty P_{11}(n=0) t^2 j_0(rt) dt \\ &= \frac{1}{r} \int_0^\infty \left\{ \lim_{at \rightarrow 0} P_{11}(n=0) t \right\} \sin(rt) dt \end{aligned}$$

$$\lim_{at \rightarrow 0} P_{11}(n=0)$$

$$= -\frac{x}{t^2} \left[ \frac{1 + C_m \mu_m^2 \frac{2x}{3} - C_m \mu_m^2 \frac{x}{3}}{1 + \frac{(\sum C_i q_i^2) x}{t^2} + \frac{2C_m \mu_m^2 x}{3} + \frac{(\sum C_i q_i^2) (C_m \mu_m^2) x^2}{3t^2}} \right]$$

$$= \frac{-3x \left( 1 + C_m \mu_m^2 \frac{x}{3} \right)}{3 + 2C_m \mu_m^2 x} \left[ \frac{1}{t^2 + \frac{3(\sum C_i q_i^2) x + (\sum C_i q_i^2) C_m \mu_m^2 x^2}{3 + 2C_m \mu_m^2 x}} \right]$$

$$\text{Let } C = \frac{-3x(1 + C_m \mu_m^2 \frac{x}{3})}{3 + 2C_m \mu_m^2 x}$$

$$k^2 = \frac{3(\sum_i C_i q_i^2) x + (\sum_i C_i q_i^2) C_m \mu_m^2 x^2}{3 + 2C_m \mu_m^2 x}$$

$$\text{Then } \lim_{a \rightarrow 0} P_{11}(n=0) = C \cdot \frac{1}{t^2 + k^2}$$

$$\therefore \int_0^{\infty} \left( \lim_{a \rightarrow 0} P_{11}(t) \right) t \sin rt \, dt$$

$$= C \int_0^{\infty} \frac{t}{t^2 + k^2} \sin rt \, dt$$

$$= C \frac{\pi}{2} \exp(-kr) \quad (115)$$

this analytical value of the integral is taken from Meeron (6).

|   |   |
|---|---|
| $(2) (a) \quad \lim_{a \rightarrow 0} \int_0^{\infty} P \sin(rt) dt,$       | $(b) \quad \lim_{a \rightarrow 0} \int_0^{\infty} P t \cos(rt) dt$            |
| $= \int_0^{\infty} \left\{ \lim_{a \rightarrow 0} P \right\} \sin rt \, dt$ | $= \int_0^{\infty} \left\{ \lim_{a \rightarrow 0} P \right\} t \cos rt \, dt$ |

The integral 2(a) reduces to

$$= \frac{\sqrt{3}x}{3+2C_m\mu_m^2x} \int_0^\infty \frac{t}{t^2 + \frac{3(\sum C_i q_i^2)x + (\sum C_i q_i^2)C_m\mu_m^2x^2}{3+2C_m\mu_m^2x}} \sin(rt) dt$$

$$= c \int_0^\infty \frac{t}{t^2+k^2} \sin(rt) dt$$

$$= c \times \frac{\pi}{2} \exp(-kr) \quad (116)$$

where

$$c = \frac{\sqrt{3}x}{3 + 2C_m\mu_m^2x}$$

$$k^2 = \frac{3(\sum_i C_i q_i^2)x + (\sum_i C_i q_i^2)C_m\mu_m^2x^2}{3 + 2C_m\mu_m^2x}$$

This integral is evaluated analytically the same way as in eqn.

(115).

Integral 2(b) equals a  $\delta$ -function at  $r=0$  because  $Pt$  is  $[j_0(at)/\det 1]$ ,  $\det 1$  falls off at a certain value of  $t$  (called  $t_{\max}$ ), but  $j_0(at)$  infinitely spreads on  $t$  axis in the limit  $a \rightarrow 0$ .  $\therefore \int_0^\infty Pt \cos rt dt$  is a  $\delta$ -function at  $r=0$ . We have discussed above why such an integral can be dropped altogether.

Eq. (114) has three parts. They reduce to

$$(i) \frac{-3(\sum C_i q_i^2)x^2}{(3+2C_m\mu_m^2x)} \int_0^\infty \frac{\sin(rt)}{t \left( t^2 + \frac{3(\sum C_i q_i^2)x + C_m\mu_m^2(\sum C_i q_i^2)x^2}{3+2C_m\mu_m^2x} \right)} dt$$

$$(ii) \frac{-(\sum C_i q_i^2) x^2}{(3+2C_m \mu_m^2 x)} \int_0^\infty \frac{t \sin(rt)}{t^2 + \frac{3(\sum C_i q_i^2) x + C_m \mu_m^2 (\sum C_i q_i^2) x^2}{3+2C_m \mu_m^2 x}} dt$$

$$(iii) \frac{-3(\sum C_i q_i^2) x^2}{(3+2C_m \mu_m^2 x)} \int_0^\infty \frac{\cos(rt)}{t^2 + \frac{3(\sum C_i q_i^2) x + C_m \mu_m^2 (\sum C_i q_i^2) x^2}{3+2C_m \mu_m^2 x}} dt$$

The analytical value of the integral in (ii) is taken from Meeron (6).

$$\frac{-(\sum C_i q_i^2) x^2}{(3+2C_m \mu_m^2 x)} \times \frac{\pi}{2} \exp(-k|r|)$$

where  $k^2 = \frac{3(\sum C_i q_i^2) x + C_m \mu_m^2 (\sum C_i q_i^2) x^2}{3+2C_m \mu_m^2 x}$

The integral in (iii) is evaluated analytically as follows:

$$\frac{-3(\sum C_i q_i^2) x^2}{(3+2C_m \mu_m^2 x)} \int_0^\infty \frac{\cos(rt)}{t^2 + \frac{3(\sum C_i q_i^2) x + C_m \mu_m^2 (\sum C_i q_i^2) x^2}{3+2C_m \mu_m^2 x}} dt$$

$$= C \int_0^\infty \frac{1}{t^2 + k^2} \cos(rt) dt$$

The analytical integration is shown in Appendix 3 and is equal to

$$C \times \frac{\pi}{2} \times \frac{1}{k} \times \exp(-k|r|).$$

The integral in (i) is evaluated numerically and is always too small. It may be possible to show analytically that it

$$\begin{aligned}
& + \bar{q}_{mm} \begin{pmatrix} 1 & 0 & 1 \\ 0 & 0 & r_{mm} \end{pmatrix} \begin{bmatrix} 1 & 0 & 1 \\ 0 & 0 & 0 \end{bmatrix}_{3j} (-)^0 D_{00}^{1*}(r_{mm} \rightarrow m) D_{00}^0(r_{mm}) \\
& + \bar{q}_{mm} \begin{pmatrix} 1 & 1 & 2 \\ 0 & 0 & r_{mm} \end{pmatrix} \begin{bmatrix} 1 & 1 & 2 \\ 0 & 0 & 0 \end{bmatrix}_{3j} (-)^0 D_{00}^{1*}(r_{mm} \rightarrow m) D_{00}^1(r_{mm} \rightarrow m) \\
& + \bar{q}_{mm} \begin{pmatrix} 1 & 1 & 2 \\ 0 & 0 & r_{mm} \end{pmatrix} \begin{bmatrix} 1 & 1 & 2 \\ -1 & 1 & 0 \end{bmatrix}_{3j} (-)^1 D_{01}^{1*}(r_{mm} \rightarrow m) D_{01}^1(r_{mm} \rightarrow m) \\
& + \bar{q}_{mm} \begin{pmatrix} 1 & 1 & 2 \\ 0 & 0 & r_{mm} \end{pmatrix} \begin{bmatrix} 1 & 1 & 2 \\ 1 & -1 & 0 \end{bmatrix}_{3j} (-)^{-1} D_{0-1}^{1*}(r_{mm} \rightarrow m) D_{0-1}^1(r_{mm} \rightarrow m) \\
& + \bar{q}_{mm} \begin{pmatrix} 1 & 1 & 1 \\ 0 & 0 & r_{mm} \end{pmatrix} \begin{bmatrix} 1 & 1 & 1 \\ 0 & 0 & 0 \end{bmatrix}_{3j} (-)^0 D_{00}^{1*}(r_{mm} \rightarrow m) D_{00}^1(r_{mm} \rightarrow m) \\
& + \bar{q}_{mm} \begin{pmatrix} 1 & 1 & 1 \\ 0 & 0 & r_{mm} \end{pmatrix} \begin{bmatrix} 1 & 1 & 1 \\ -1 & 1 & 0 \end{bmatrix}_{3j} (-)^1 D_{01}^{1*}(r_{mm} \rightarrow m) D_{00}^1(r_{mm} \rightarrow m) \\
& + \bar{q}_{mm} \begin{pmatrix} 1 & 1 & 1 \\ 0 & 0 & r_{mm} \end{pmatrix} \begin{bmatrix} 1 & 1 & 1 \\ 1 & -1 & 0 \end{bmatrix}_{3j} (-)^{-1} D_{0-1}^{1*}(r_{mm} \rightarrow m) D_{0-1}^1(r_{mm} \rightarrow m) \\
& + \bar{q}_{mm} \begin{pmatrix} 1 & 1 & 0 \\ 0 & 0 & r_{mm} \end{pmatrix} \begin{bmatrix} 1 & 1 & 0 \\ 0 & 0 & 0 \end{bmatrix}_{3j} (-)^0 D_{00}^{1*}(r_{mm} \rightarrow m) D_{00}^1(r_{mm} \rightarrow m) \\
& + \bar{q}_{mm} \begin{pmatrix} 1 & 1 & 0 \\ 0 & 0 & r_{mm} \end{pmatrix} \begin{bmatrix} 1 & 1 & 0 \\ -1 & 1 & 0 \end{bmatrix}_{3j} (-)^1 D_{01}^{1*}(r_{mm} \rightarrow m) D_{01}^1(r_{mm} \rightarrow m) \\
& + \bar{q}_{mm} \begin{pmatrix} 1 & 1 & 0 \\ 0 & 0 & r_{mm} \end{pmatrix} \begin{bmatrix} 1 & 1 & 0 \\ 1 & -1 & 0 \end{bmatrix}_{3j} (-)^{-1} D_{0-1}^{1*}(r_{mm} \rightarrow m) D_{0-1}^1(r_{mm} \rightarrow m) \\
& = \bar{q}_{mm} \begin{pmatrix} 0 & 0 & 0 \\ 0 & 0 & r_{mm} \end{pmatrix} - \frac{1}{\sqrt{3}} \bar{q}_{mm} \begin{pmatrix} 0 & 1 & 1 \\ 0 & 0 & r_{mm} \end{pmatrix} \cos \beta_2 \\
& - \frac{1}{\sqrt{3}} \bar{q}_{mm} \begin{pmatrix} 1 & 0 & 1 \\ 0 & 0 & r_{mm} \end{pmatrix} \cos \beta_1 \\
& + \left( \frac{2}{15} \right)^{1/2} \bar{q}_{mm} \begin{pmatrix} 1 & 1 & 2 \\ 0 & 0 & r_{mm} \end{pmatrix} \cos \beta_1 \cos \beta_2
\end{aligned}$$



$$\begin{aligned}
& - \frac{1}{2(30)^{1/2}} \bar{q}_{mm} \begin{pmatrix} 1 & 1 & 2 \\ 0 & 0 & r_{mm} \end{pmatrix} \sin \beta_1 \sin \beta_2 e^{-i(\alpha_1 - \alpha_2)} \\
& - \frac{1}{2(30)^{1/2}} \bar{q}_{mm} \begin{pmatrix} 1 & 1 & 2 \\ 0 & 0 & r_{mm} \end{pmatrix} \sin \beta_1 \sin \beta_2 e^{+i(\alpha_1 - \alpha_2)} + 0 + 0 + 0 \\
& - \frac{1}{\sqrt{3}} \bar{q}_{mm} \begin{pmatrix} 1 & 1 & 0 \\ 0 & 0 & r_{mm} \end{pmatrix} \cos \beta_1 \cos \beta_2 \\
& - \frac{1}{2\sqrt{3}} \bar{q}_{mm} \begin{pmatrix} 1 & 1 & 0 \\ 0 & 0 & r_{mm} \end{pmatrix} \sin \beta_1 \sin \beta_2 e^{-i(\alpha_1 - \alpha_2)} \\
& - \frac{1}{2\sqrt{3}} \bar{q}_{mm} \begin{pmatrix} 1 & 1 & 0 \\ 0 & 0 & r_{mm} \end{pmatrix} \sin \beta_1 \sin \beta_2 e^{+i(\alpha_1 - \alpha_2)} \\
& = \bar{q}_{mm} \begin{pmatrix} 0 & 0 & 0 \\ 0 & 0 & r_{mm} \end{pmatrix} - \frac{1}{\sqrt{3}} \bar{q} \begin{pmatrix} 0 & 1 & 1 \\ 0 & 0 & r_{mm} \end{pmatrix} \cos \beta_2 \\
& - \frac{1}{\sqrt{3}} \bar{q} \begin{pmatrix} 1 & 0 & 1 \\ 0 & 0 & r_{mm} \end{pmatrix} \cos \beta_1 \\
& + \bar{q}_{mm} \begin{pmatrix} 1 & 1 & 2 \\ 0 & 0 & r_{mm} \end{pmatrix} \left\{ \left( \frac{2}{15} \right)^{1/2} \cos \beta_1 \cos \beta_2 \right. \\
& \left. - \frac{1}{2(30)^{1/2}} \sin \beta_1 \sin \beta_2 \left( e^{-i(\alpha_1 - \alpha_2)} + e^{i(\alpha_1 - \alpha_2)} \right) \right\} \\
& + \bar{q}_{mm} \begin{pmatrix} 1 & 1 & 0 \\ 0 & 0 & r_{mm} \end{pmatrix} \left\{ - \frac{1}{\sqrt{3}} \cos \beta_1 \cos \beta_2 \right. \\
& \left. - \frac{1}{2\sqrt{3}} \sin \beta_1 \sin \beta_2 \left( e^{-i(\alpha_1 - \alpha_2)} + e^{i(\alpha_1 - \alpha_2)} \right) \right\} \\
& = \bar{q}_{mm} \begin{pmatrix} 0 & 0 & 0 \\ 0 & 0 & r_{mm} \end{pmatrix} - \frac{1}{\sqrt{3}} \bar{q} \begin{pmatrix} 0 & 1 & 1 \\ 0 & 0 & r_{mm} \end{pmatrix} \cos \beta_2 \\
& - \frac{1}{\sqrt{3}} \bar{q} \begin{pmatrix} 1 & 0 & 1 \\ 0 & 0 & r_{mm} \end{pmatrix} \cos \beta_1
\end{aligned}$$

$$\begin{aligned}
& + \bar{q}_{mm} \begin{pmatrix} 1 & 1 & 2 \\ 0 & 0 & r_{mm} \end{pmatrix} \left\{ \left( \frac{2}{15} \right)^{1/2} \cos \beta_1 \cos \beta_2 \right. \\
& - \frac{1}{(30)^{1/2}} \sin \beta_1 \sin \beta_2 \cos (\alpha_1 - \alpha_2) \left. \right\} \\
& - \frac{1}{\sqrt{3}} \bar{q}_{mm} \begin{pmatrix} 1 & 1 & 0 \\ 0 & 0 & r_{mm} \end{pmatrix} \left\{ \cos \beta_1 \cos \beta_2 + \sin \beta_1 \sin \beta_2 \cos (\alpha_1 - \alpha_2) \right\}
\end{aligned}$$

In the above calculations, i.e., calculation of  $\hat{q}$ ,  $\bar{q}$  and  $q$  we have used values of Bessel function, Wigner 3j-coefficient and Rotation matrices. These values are given in the Appendix.

In Chapter 3, we have used the method Rasaiah and Friedman (2) to solve Alnatt's HNC equation (3). Alnatt's method uses the subdivision of  $\tau$  diagrams into two subsets, called A and B (the details are in Chapter 3). This classification was made first by Meeron (4). Meeron's theory is developed for very general  $f$  bonds. The development of Alnatt (3) applies generally excepting that one has to use  $q$  functions appropriate to the particular system. Alnatt (3) uses  $q$  for ion-ion interactions. All we need to do is to use  $q$  for ion-dipole and dipole-dipole interaction and follow the same procedure given by Rasaiah and Friedman (2). The integrals that requires evaluation are multidimensional, since integration over three relative coordinates and the angular variables that specify orientation of the two particles is to be carried out. As shown below, the convolution integral that is evaluated over and over again is in one variable only. Numerical integration over angular variables also become necessary, but these are not convolution integrals.

### 4.3 Calculation of Initial value of $\tau$

The function  $q$  calculated in the previous section are used for calculation of  $\tau$ .

As defined previously,  $\phi_{ij} = \exp(q_{ij}) - 1$

$$\tau = (\phi * \phi) - (q * q)$$

Hence (we recall  $\tau_{ij} = \sum_k \phi_{ik} * \phi_{kj} - \sum_k q_{ik} * q_{kj}$ )

$$\begin{aligned}\tau_{11} &= \left( \phi_{11} * \phi_{11} + \phi_{12} * \phi_{21} + \phi_{13} * \phi_{31} \right) \\ &\quad - \left( q_{11} * q_{11} + q_{12} * q_{21} + q_{13} * q_{31} \right)\end{aligned}$$

$$\begin{aligned}\tau_{12} &= \left( \phi_{11} * \phi_{12} + \phi_{12} * \phi_{22} + \phi_{13} * \phi_{32} \right) \\ &\quad - \left( q_{11} * q_{12} + q_{12} * q_{22} + q_{13} * q_{32} \right)\end{aligned}$$

$$\begin{aligned}\tau_{13} &= \left( \phi_{11} * \phi_{13} + \phi_{12} * \phi_{23} + \phi_{13} * \phi_{33} \right) \\ &\quad - \left( q_{11} * q_{13} + q_{12} * q_{23} + q_{13} * q_{33} \right)\end{aligned}$$

$$\begin{aligned}\tau_{21} &= \left( \phi_{21} * \phi_{11} + \phi_{22} * \phi_{21} + \phi_{23} * \phi_{31} \right) \\ &\quad - \left( q_{21} * q_{11} + q_{22} * q_{21} + q_{23} * q_{31} \right)\end{aligned}$$

$$\begin{aligned}\tau_{22} &= \left( \phi_{21} * \phi_{12} + \phi_{22} * \phi_{22} + \phi_{23} * \phi_{32} \right) \\ &\quad - \left( q_{21} * q_{12} + q_{22} * q_{22} + q_{23} * q_{32} \right)\end{aligned}$$

$$\begin{aligned}\tau_{23} &= \left( \phi_{21} * \phi_{13} + \phi_{22} * \phi_{23} + \phi_{23} * \phi_{33} \right) \\ &\quad - \left( q_{21} * q_{13} + q_{22} * q_{23} + q_{23} * q_{33} \right)\end{aligned}$$

$$\tau_{31} = \left( \phi_{31} * \phi_{11} + \phi_{32} * \phi_{21} + \phi_{33} * \phi_{31} \right) \\ - \left( q_{31} * q_{11} + q_{32} * q_{21} + q_{33} * q_{31} \right)$$

$$\tau_{32} = \left( \phi_{31} * \phi_{12} + \phi_{32} * \phi_{22} + \phi_{33} * \phi_{32} \right) \\ - \left( q_{31} * q_{12} + q_{32} * q_{22} + q_{33} * q_{32} \right)$$

$$\tau_{33} = \left( \phi_{31} * \phi_{13} + \phi_{32} * \phi_{23} + \phi_{33} * \phi_{33} \right) \\ - \left( q_{31} * q_{13} + q_{32} * q_{23} + q_{33} * q_{33} \right)$$

The functions  $q$  and therefore  $\phi$  are functions of the relative co-ordinates of the two centers of mass and the angular variables specifying the orientation of the two particles.

Of all the  $\tau$ 's given above  $\tau_{11}, \tau_{12}, \tau_{21}, \tau_{22}$  (where 1 and 2 are small ions) are functions of only  $r$ , the distance between their centres, since 1 and 2 carry only charge and interact through angle-independent potential.

$\tau_{13}, \tau_{23}, \tau_{31}$  and  $\tau_{32}$  (where 3 is macroion and 1, 2 are small ions) are functions of their distance as well as orientation of the macroion, since the macroion carries a dipole moment as well as charge and the interaction potential is angle dependent. We will show below that they are functions of  $r$ , the distance and  $\beta$ , only one of the Euler angles, specifying the orientation of the macroion.

$\tau_{33}$  is a function involving a pair of macroions and is a function of four variables,  $r$  the distance and  $\beta_1, \beta_2, \alpha_1 - \alpha_2$ , where  $\alpha_1, \beta_1$  are two of the Euler angles of one macroion and  $\alpha_2,$

$\beta_2$ , are those of the other. The other Euler angles  $\gamma_1, \gamma_2$  do not appear in the expressions. None of the  $\tau$ 's depend on the orientation of the interparticle vector, since external angle dependent field is absent.

In the above expressions, \* implies integration. For example,

$$\phi_{11'} * \phi_{1'1''} = c_1 \int \phi_{11'}(\vec{r}_{11'}) \phi_{1'1''}(\vec{r}_{1'1''}) d\{1'\} d\Gamma$$

1, 1', 1'' are three different positive ions. The 1' in the middle signifies the positive ion of variable coordinates over the coordinates of which the integration is carried out to obtain a function that depends on the distance between the particles 1 and 1'', which are held fixed.  $d\{1'\}$  shows that the integration should take place over the three spatial coordinates of the center of the mass of particle 1'. Integration over  $d\Gamma$  gives  $8\pi^2$  since  $\phi$ 's are angle independent. The integration is carried out only over  $\{1'\}$ . The only numerical procedure is to calculate convolution integrals in  $r$  variable only. This is described in Chapter 5, section 1.

$$\phi_{13} * \phi_{31'} = c_3 \int \phi_{13}(\vec{r}_{13}) \phi_{31'}(\vec{r}_{31'}) d\{3\}$$

The 3 in the middle signifies the mobile macroion over the coordinates of which the integration takes place to give the function that depends on the distance between a pair of static positive ions. Since 3 is a macroion,  $d\{3\}d\Gamma$  stands for  $d\{3\} d\alpha_3 \sin \beta_3 d\beta_3 d\gamma_3$  where  $\alpha, \beta$  and  $\gamma$  are the Euler angles associated with the macroion and  $\{3\}$  denotes the coordinates of center of mass of particle 3.

Hence, there are two types of integration

- (1) The integration takes place over the coordinates of a positive (or negative) ion with only radial dependence of the functions, whose product is being integrated.
- (2) The integration takes place over the coordinates of a macroion with radial as well as angle dependence.

In the calculation of  $\tau$ 's described above, the integrals are clasified as follows :

(i) ion-ion-ion interaction :

$$\begin{aligned} & \phi_{11}*\phi_{11} , \phi_{12}*\phi_{21} , \phi_{11}*\phi_{12} , \phi_{12}*\phi_{22} , \phi_{21}*\phi_{11} , \phi_{22}*\phi_{21} , \\ & \phi_{21}*\phi_{12} , \phi_{22}*\phi_{22} \\ & q_{11}*q_{11} , q_{12}*q_{21} , q_{11}*q_{12} , q_{12}*q_{22} , q_{21}*q_{11} , q_{22}*q_{21} , \\ & q_{21}*q_{12} , q_{22}*q_{22} \end{aligned}$$

(ii) ion-macroion-ion interaction :

$$\begin{aligned} & \phi_{13}*\phi_{31} , \phi_{13}*\phi_{32} , \phi_{23}*\phi_{31} , \phi_{23}*\phi_{32} \\ & q_{13}*q_{31} , q_{13}*q_{32} , q_{23}*q_{31} , q_{23}*q_{32} \end{aligned}$$

(iii) ion-ion-macroion interaction :

$$\begin{aligned} & \phi_{11}*\phi_{13} , \phi_{12}*\phi_{23} , \phi_{21}*\phi_{13} , \phi_{22}*\phi_{23} , \phi_{31}*\phi_{11} , \phi_{32}*\phi_{21} , \\ & \phi_{31}*\phi_{12} , \phi_{32}*\phi_{22} \\ & q_{11}*q_{13} , q_{12}*q_{23} , q_{21}*q_{13} , q_{22}*q_{23} , q_{31}*q_{11} , q_{32}*q_{21} , \\ & q_{31}*q_{12} , q_{32}*q_{22} \end{aligned}$$

(iv) ion-macroion-macroion interaction :

$$\begin{aligned} & \phi_{13}*\phi_{33} , \phi_{23}*\phi_{33} , \phi_{33}*\phi_{31} , \phi_{33}*\phi_{32} \\ & q_{13}*q_{33} , q_{23}*q_{33} , q_{33}*q_{31} , q_{33}*q_{32} \end{aligned}$$

(v) macroion-ion-macroion interaction :

$$\begin{aligned} & \phi_{31}*\phi_{13} , \phi_{32}*\phi_{23} \\ & q_{31}*q_{13} , q_{32}*q_{23} \end{aligned}$$

(vi) macroion-macroion-macroion interaction :

$$\phi_{33} * \phi_{33}$$

$$q_{33} * q_{33}$$

(i) The evaluation of the integrals given in (i) require calculation of convolution integrals in  $r$  variable only. The details are in Chapter 5, section 1. The situation is exactly the same as those encountered in systems interacting through central potential. The only difference is multiplication by  $8\pi^2$  which is obtained from the integration over angular variables. The concentration values used are also actual chemical concentrations divided by  $8\pi^2$ .

(ii) The integrals given in (ii) are evaluated as follows :

$$\begin{aligned} \phi_{13} * \phi_{31} &= \int \phi_{13}(\vec{r}_{13}, \beta_3) \phi_{31}(\vec{r}_{31}, \beta_3) d\{3\} d\alpha_3 \sin \beta_3 d\beta_3 d\gamma_3 \\ &= \int_0^{2\pi} d\alpha_3 \int_0^{2\pi} d\beta_3 \int_0^{\pi} d\beta_3 \sin \beta_3 \int_0^{\infty} \phi_{13}(\vec{r}_{13}, \beta_3) \phi_{31}(\vec{r}_{31}, \beta_3) d\{3\} \\ &= 4\pi^2 \int_0^{\pi} d\beta_3 \sin \beta_3 \int_0^{\infty} \phi_{13}(\vec{r}_{13}, \beta_3) \phi_{31}(\vec{r}_{31}, \beta_3) d\{3\} \end{aligned}$$

At constant  $\beta_3$ , the innermost integral becomes independent of  $\beta_3$  and is only dependent on  $\vec{r}$ . Hence, it can be evaluated as the integrals in (i). When the procedure is carried out for all the values of  $\beta_3$ , the result becomes a function of  $r_{11}$  and  $\beta_3$ . For each value of  $\vec{r}_{11}$ , the value of the results for all  $\beta_3$  are multiplied by  $\sin \beta_3$  and numerically integrated over  $\beta_3$  between the limits of 0 and  $\pi$ . This is repeated for all the values of  $r_{11}$  and

Thus  $\phi_{33}, (\vec{r}_{33}, \beta_3, \beta_3, \alpha_3 - \alpha_3)$  is numerically integrated over  $\alpha_3 - \alpha_3$ , between the limit of  $-2\pi$  and  $0$  and we get  $f_{33}, (\vec{r}_{33}, \beta_3, \beta_3)$ . Other integrals in (iv) are evaluated the same way.

(v) The integrals given in (v) are evaluated as follows :

$$\phi_{31} * \phi_{13} = \int \phi_{31}(\vec{r}_{31}, \beta_3) \phi_{13}(\vec{r}_{13}, \beta_3) d\{1\} d\Gamma$$

For each value of  $\beta_3$  and  $\beta_3$ , the integral becomes dependent on  $\vec{r}$  and evaluated as in the integral in (i) and the result becomes a function of  $r_{33}, \beta_3, \beta_3$ , and hence is three-dimensional. This is multiplied by  $8\pi^2$  as a result of integration over  $d\Gamma$ .

The other integrals are evaluated in the same way.

(vi) The integral given in (vi) is evaluated as follows :

$$\begin{aligned} \phi_{33} * \phi_{3'3''} &= \int \phi_{33}(\vec{r}_{33}, \beta_3, \beta_3, \alpha_3 - \alpha_3) \\ &\quad \phi_{3'3''}(\vec{r}_{3'3''}, \beta_3, \beta_3, \alpha_3 - \alpha_3) d\{3'\} d\alpha_3, \sin\beta_3, d\beta_3, d\gamma_3, \\ &= \int_0^{2\pi} d\gamma_3, \int_0^\pi \sin\beta_3, d\beta_3, \int \phi_{33}, \phi_{3'3''} d\{3'\} d\alpha_3, \\ &= 2\pi \int_0^\pi \sin\beta_3, d\beta_3, \int_0^{2\pi} d\alpha_3, \int \phi_{33}, (\vec{r}_{33}, \beta_3, \beta_3, \alpha_3 - \alpha_3) \\ &\quad \phi_{3'3''}(\vec{r}_{3'3''}, \beta_3, \beta_3, \alpha_3 - \alpha_3) d\{3'\} \end{aligned}$$

At constant  $\beta_3, \beta_3, \beta_3$ , the functions in the inner integral are function of  $r_{33}$ , and  $\alpha_3 - \alpha_3$ ; and  $r_{3'3''}$  and  $\alpha_3 - \alpha_3$  respectively.  $\alpha_3$  and  $\alpha_3$  are constant values and  $\alpha_3$ , varies from  $0$  to  $2\pi$ . We have to evaluate the following integral



$$g(r_{33''}, \alpha_3 - \alpha_{3''}) = \int \phi_{33'}(\vec{r}_{33'}, \alpha_3 - \alpha_{3'}) \phi_{3'3''}(\vec{r}_{3'3''}, \alpha_3, -\alpha_{3''}) d\{3'\} d\alpha_3,$$

$$g(k_{r_{33''}}, \alpha_3 - \alpha_{3''}) = \int \phi_{33'}(\vec{r}_{33'}, \alpha_3 - \alpha_{3'}) \phi_{3'3''}(\vec{r}_{3'3''}, \alpha_3, -\alpha_{3''}) \\ e^{-2\pi i k_{r_{33''}} \cdot \vec{r}_{33''}} d\vec{r}_{33''}, d\vec{r}_{33'}, d\alpha_3, \\ \vec{r}_{33''} = \vec{r}_{33'} + \vec{r}_{3'3''} \\ \alpha_3 - \alpha_{3''} = (\alpha_3 - \alpha_{3'}) + (\alpha_3, -\alpha_{3''})$$

$d\vec{r}_{33''} d\vec{r}_{33'} = d\vec{r}_{33'}, d\vec{r}_{3'3''}$  - The Jacobian of the transformation is unity.

$d(\alpha_3 - \alpha_{3''}) d(\alpha_3 - \alpha_{3'}) = d(\alpha_3 - \alpha_{3'}) d(\alpha_3, -\alpha_{3''})$  - The Jacobian of the transformation is unity.

Hence the above expression is separated into two parts as follows :

$$\int_0^{2\pi} d\alpha_3, \int \phi_{33'}(\vec{r}_{33'}, \alpha_3 - \alpha_{3'}) e^{-2\pi i k_{r_{33''}} \cdot \vec{r}_{33''}} d\vec{r}_{33'}, \\ \times \int \phi_{3'3''}(\vec{r}_{3'3''}, \alpha_3, -\alpha_{3''}) e^{-2\pi i k_{r_{33''}} \cdot \vec{r}_{3'3''}} d\vec{r}_{3'3''}$$

Each of the above integrations involving the  $\phi$  functions are evaluated as described in Chapter 5 and the expression reduces to

$$\int_0^{2\pi} d\alpha_3, f(k_r, \alpha_3 - \alpha_{3'}) g(k_r, \alpha_3, -\alpha_{3''})$$

For a constant  $k_r$ , the above expression becomes

$$F(\alpha_3 - \alpha_{3'}) = \int_0^{2\pi} f'(\alpha_3 - \alpha_{3'}) g'(\alpha_3 - \alpha_{3'})$$

$$= - \int_{\alpha_3}^{\alpha_3 - 2\pi} f'(\alpha_3 - \alpha_{3'}) g'(\alpha_3 - \alpha_{3'}) d(\alpha_3 - \alpha_{3'})$$

When Fourier Transformed, it becomes

$$\hat{F} = - \int_{-2\pi}^{2\pi} \int_{\alpha_3 - 2\pi}^{\alpha_3} f'(\alpha_3 - \alpha_{3'}) g'(\alpha_3, -\alpha_{3''}) e^{-2\pi i k \cdot (\alpha_3 - \alpha_{3''})} d(\alpha_3 - \alpha_{3''}) d(\alpha_3 - \alpha_{3'})$$

$$= - \int_0^{2\pi} \int_{2\pi}^0 f' g' e^{-2\pi i k \cdot \{(\alpha_3 - \alpha_{3'}) + (\alpha_3, -\alpha_{3''})\}} d(\alpha_3 - \alpha_{3'}) d(\alpha_3 - \alpha_{3''})$$

$$= - \int_0^{2\pi} \int_{2\pi}^0 f' g' e^{-2\pi i k \cdot \{(\alpha_3 - \alpha_{3'}) + (\alpha_3, -\alpha_{3''})\}} d(\alpha_3 - \alpha_{3'}) d(\alpha_3, -\alpha_{3''})$$

$$= \int_{-2\pi}^0 f'(\alpha_3 - \alpha_{3'}) e^{-2\pi i k \cdot (\alpha_3 - \alpha_{3'})} d(\alpha_3 - \alpha_{3'})$$

$$\times \int_0^{2\pi} g'(\alpha_3, -\alpha_{3''}) e^{-2\pi i k \cdot (\alpha_3, -\alpha_{3''})} d(\alpha_3, -\alpha_{3''})$$

Then we take  $f'(\alpha_3 - \alpha_{3'})$  from  $f(k_r, \alpha_3 - \alpha_{3'})$  and perform one-dimensional Fourier Transform, the limits of  $\alpha_3 - \alpha_{3'}$ , is from  $-2\pi$  to  $0$ . Similar operation is done with  $g'(\alpha_3, -\alpha_{3''})$ , the limits of  $\alpha_3, -\alpha_{3''}$  being from  $0$  to  $2\pi$ . We multiply them. The result is a function of  $k_{\alpha_3 - \alpha_{3''}}$ . This is back fourier transformed. The result is the value of the integration over  $d\alpha_3$ , and it is a

function of  $\alpha_3 - \alpha_{3''}$ . If we vary  $k_r$ , the result is a function of  $k_r$  and  $\alpha_3 - \alpha_{3''}$ . Keeping  $\alpha_3 - \alpha_{3''}$  fixed, we take the values as a function of  $k_r$  and carry out the sine transformation as in the previous chapter. By varying  $\alpha_3 - \alpha_{3''}$ , we get the values as a function of  $r_{33''}$  and  $\alpha_3 - \alpha_{3''}$ . Then we vary  $\beta_3, \beta_{3'}, \beta_{3''}$  and obtain  $\phi_{33}, * \phi_{3',3''} (r_{33''}, \beta_3, \beta_{3'}, \beta_{3''}, \alpha_3 - \alpha_{3''})$ . Now we integrate over the values of  $\beta_3$ , to obtain  $\phi_{33}, * \phi_{3',3''} (r_{33''}, \beta_3, \beta_{3''}, \alpha_3 - \alpha_{3''})$ .  $q_{33}, * q_{3',3''}$  is also evaluated the same way.

#### 4.4 Calculation of $g(r, \Gamma)$

In the method of Rasaiah and Friedman (2) given in Chapter 3 (Section 8) one uses  $\tau_{\text{initial}}$  and  $q$  to calculate  $h_{\text{initial}}$ ;  $q$ ,  $\tau$  and  $h$  depend on same number of variables, which can be 1, 2, 4, as seen above. One then calculates  $x = h - \tau - q$  and recalculate  $\tau$  using the formula.

$$\tau = x * h + q * x + q * x * h$$

(1) Calculation of  $\tau_{11}$

$$\tau_{11} = \sum_{i=1}^3 x_{1i} * h_{i1} + \sum_{i=1}^3 q_{1i} * x_{i1} + \sum_{i,j=1}^3 q_{1i} * x_{ij} * h_{j1}$$

We first consider

$$\begin{aligned} \sum_{i=1}^3 x_{1i} * h_{i1} &= C_1 \int x_{11} h_{11} d\{1\} d\Gamma_1 + C_2 \int x_{12} h_{21} d\{2\} d\Gamma_2 \\ &+ C_3 \int x_{13} h_{31} d\{3\} d\Gamma_3 \end{aligned}$$

The first two integrals are evaluated as  $\phi_{11} * \phi_{11}$  in the previous section. The third integral involves integration over radial as well as angular variables and is evaluated as  $\phi_{13} * \phi_{31}$

in 4.3 above. We then consider

$$\sum_{i=1}^3 q_{1i} * x_{i1} \text{ which is also evaluated as } \sum_{i=1}^3 x_{1i} * h_{i1}$$

Finally, we consider

$$\begin{aligned} & \sum_{i,j=1}^3 q_{1i} * x_{ij} * h_{j1} \\ &= c_1^2 \int q_{11} x_{11} h_{11} d\{1\} d\Gamma_1 d\Gamma_1 + c_1 c_2 \int q_{11} x_{12} h_{21} d\{1\} d\{2\} d\Gamma_1 d\Gamma_2 \\ &+ c_1 c_3 \int q_{11} x_{13} h_{31} d\{1\} d\{3\} d\Gamma_1 d\Gamma_3 + c_2 c_1 \int q_{12} x_{21} h_{11} d\{2\} d\{1\} d\Gamma_2 d\Gamma_1 \\ &+ c_2^2 \int q_{12} x_{22} h_{21} d\{2\} d\{2\} d\Gamma_2 d\Gamma_2 + c_2 c_3 \int q_{12} x_{23} h_{31} d\{2\} d\{3\} d\Gamma_2 d\Gamma_3 \\ &+ c_3 c_1 \int q_{13} x_{31} h_{11} d\{3\} d\Gamma_3 d\Gamma_1 + c_3 c_2 \int q_{13} x_{32} h_{21} d\{3\} d\Gamma_3 d\Gamma_2 \\ &+ c_3^2 \int q_{13} x_{33} h_{31} d\{3\} d\{3'\} d\Gamma_3 d\Gamma_3, \end{aligned}$$

Here and in similar cases that will follow, the integrals arising from  $q*x*h$  are evaluated as follows. First the integral involving  $x$  and  $h$  is evaluated. Then the integral involving  $q$  and the resultant from the integral involving  $x$  and  $h$  are evaluated

$$\begin{aligned} & \int q_{11} x_{11} h_{11} d\{1\} d\Gamma_1 d\Gamma_1 = \int d\{1\} d\Gamma_1 q_{11} \int x_{11} h_{11} d\{1\} d\Gamma_1 \\ &= \int d\{1\} d\Gamma_1 q_{11} (xh)_{111} = (qxh)_{1111} \\ & \int q_{11} x_{12} h_{21} d\{1\} d\{2\} d\Gamma_1 d\Gamma_2 = \int d\{1\} d\Gamma_1 q_{11} \int x_{12} h_{21} d\{2\} d\Gamma_2 \\ &= \int d\{1\} d\Gamma_1 q_{11} (xh)_{121} = (qxh)_{1121} \\ & \int q_{12} x_{21} h_{11} d\{2\} d\{1\} d\Gamma_2 d\Gamma_1 = \int d\{2\} d\Gamma_2 q_{12} \int x_{21} h_{11} d\{1\} d\Gamma_1 \end{aligned}$$

$$= \int d\{2\} d\Gamma_2 q_{12}(xh)_{211} = (qxh)_{1211}$$

$$\begin{aligned} \int q_{12} x_{22} h_{21} d\{2\} d\{2\} d\Gamma_2 d\Gamma_2 &= \int d\{2\} d\Gamma_2 q_{12} \int x_{22} h_{21} d\{2\} d\Gamma_2 \\ &= \int d\{2\} d\Gamma_2 q_{12}(xh)_{221} = (qxh)_{1221} \end{aligned}$$

$(xh)_{111}$ ,  $(xh)_{121}$ ,  $(xh)_{211}$ ,  $(xh)_{221}$  are evaluated as  $\phi_{11} * \phi_{11}$  in 4.3 above.  $(qxh)_{1111}$ ,  $(qxh)_{1121}$ ,  $(qxh)_{1211}$ ,  $(qxh)_{1221}$ , are also evaluated as  $\phi_{11} * \phi_{11}$ .

$$\begin{aligned} \int q_{11} x_{13} h_{31} d\{1\} d\Gamma_1 d\{3\} d\Gamma_3 &= \int d\{1\} d\Gamma_1 q_{11} \int x_{13} h_{31} d\{3\} d\Gamma_3 \\ &= \int d\{1\} d\Gamma_1 q_{11}(xh)_{131} = (qxh)_{1131} \end{aligned}$$

$$\begin{aligned} \int q_{12} x_{23} h_{31} d\{2\} d\Gamma_2 d\{3\} d\Gamma_3 &= \int d\{2\} d\Gamma_2 q_{12} \int x_{23} h_{31} d\{3\} d\Gamma_3 \\ &= \int d\{2\} d\Gamma_2 q_{12}(xh)_{231} = (qxh)_{1231} \end{aligned}$$

$(xh)_{131}$ ,  $(xh)_{231}$  are evaluated as  $\phi_{13} * \phi_{31}$  in 4.3 above.

$(qxh)_{1131}$ ,  $(qxh)_{1231}$  are also evaluated as  $\phi_{11} * \phi_{11}$ .

$$\begin{aligned} \int q_{13} x_{31} h_{11} d\{3\} d\Gamma_3 d\{1\} d\Gamma_1 &= \int d\{3\} d\Gamma_3 q_{13} \int x_{31} h_{11} d\{1\} d\Gamma_1 \\ &= \int d\{3\} d\Gamma_3 q_{13}(xh)_{311} = (qxh)_{1311} \end{aligned}$$

$$\begin{aligned} \int q_{13} x_{32} h_{21} d\{3\} d\Gamma_3 d\{2\} d\Gamma_2 &= \int d\{3\} d\Gamma_3 q_{13} \int x_{32} h_{21} d\{2\} d\Gamma_2 \\ &= \int d\{3\} d\Gamma_3 q_{13}(xh)_{321} = (qxh)_{1321} \end{aligned}$$

$(xh)_{311}$ ,  $(xh)_{321}$  are evaluated as  $\phi_{31} * \phi_{11}$  and  $(qxh)_{1311}$ ,

$(qxh)_{1321}$  are evaluated as  $\phi_{13} * \phi_{31}$  in 4.3 above.

$$\begin{aligned} \int q_{13} x_{33} h_{3,1} d\{3\} d\Gamma_3 d\{3'\} d\Gamma_{3'} &= \int d\{3\} d\Gamma_3 q_{13} \int x_{33} h_{3,1} d\{3'\} d\Gamma_{3'} \\ &= \int d\{3\} d\Gamma_3 q_{13}(xh)_{33,1} = (qxh)_{133,1} \end{aligned}$$

$(xh)_{33,1}$  is evaluated as  $\phi_{33} * \phi_{31}$  and  $(qxh)_{1331}$  is evaluated as  $\phi_{13} * \phi_{31}$  in 4.3 above.

ii) Calculation of  $\tau_{12}$

$$\tau_{12} = \sum_{i=1}^3 x_{1i} * h_{i2} + \sum_{i=1}^3 q_{1i} * x_{i2} + \sum_{i,j=1}^3 q_{1i} * x_{ij} * h_{j2}$$

Consider the first term:

$$\begin{aligned} \sum_i x_{1i} * h_{i2} &= c_1 \int x_{11} h_{12} d\{1\} d\Gamma_1 + c_2 \int x_{12} h_{22} d\{2\} d\Gamma_2 \\ &\quad + c_3 \int x_{13} h_{32} d\{3\} d\Gamma_3 \end{aligned}$$

The first two integrals are evaluated as  $\phi_{11} * \phi_{11}$  and the third integral is evaluated as  $\phi_{13} * \phi_{31}$  in 4.3 above.

$$\begin{aligned} \sum_i q_{1i} * x_{i2} &= c_1 \int q_{11} x_{12} d\{1\} d\Gamma_1 + c_2 \int q_{12} x_{22} d\{2\} d\Gamma_2 \\ &\quad + c_3 \int q_{13} x_{32} d\{3\} d\Gamma_3 \end{aligned}$$

The first two integrals are evaluated as  $\phi_{11} * \phi_{11}$  and the third integral is evaluated as  $\phi_{13} * \phi_{31}$  in 4.3 above.

Finally, consider the third term,

$$\begin{aligned} \sum_{i,j=1}^3 q_{1i} * x_{ij} * h_{j2} &= c_1^2 \int q_{11} x_{11} h_{12} d\{1\} d\{1\} d\Gamma_1 d\Gamma_1 \\ &\quad + c_1 c_2 \int q_{11} x_{12} h_{22} d\{1\} d\{2\} d\Gamma_1 d\Gamma_2 \\ &\quad + c_1 c_3 \int q_{11} x_{13} h_{32} d\{1\} d\{3\} d\Gamma_1 d\Gamma_3 + c_2 c_1 \int q_{12} x_{21} h_{12} d\{2\} d\{1\} d\Gamma_2 d\Gamma_1 \\ &\quad + c_2^2 \int q_{12} x_{22} h_{22} d\{2\} d\{2\} d\Gamma_2 d\Gamma_2 + c_2 c_3 \int q_{12} x_{23} h_{32} d\{2\} d\{3\} d\Gamma_2 d\Gamma_3 \\ &\quad + c_3 c_1 \int q_{13} x_{31} h_{12} d\{3\} d\{1\} d\Gamma_3 d\Gamma_1 + c_3 c_2 \int q_{13} x_{32} h_{22} d\{3\} d\{2\} d\Gamma_3 d\Gamma_2 \end{aligned}$$

$$+ c_3^2 \int q_{13} x_{33} h_{3,2} d\{3\} d\Gamma_3 d\{3'\} d\Gamma_3,$$

$$\begin{aligned} \int q_{11} x_{11} h_{12} d\{1\} d\Gamma_1 d\{1\} d\Gamma_1 &= \int d\{1\} d\Gamma_1 q_{11} \int x_{11} h_{12} d\{1\} d\Gamma_1 \\ &= \int d\{1\} d\Gamma_1 q_{11} (xh)_{112} = (qxh)_{1112} \end{aligned}$$

$$\begin{aligned} \int q_{11} x_{12} h_{22} d\{1\} d\Gamma_1 d\{2\} d\Gamma_2 &= \int d\{1\} d\Gamma_1 q_{11} \int x_{12} h_{22} d\{2\} d\Gamma_2 \\ &= \int d\{1\} d\Gamma_1 q_{11} (xh)_{122} = (qxh)_{1122} \end{aligned}$$

$$\begin{aligned} \int q_{12} x_{21} h_{12} d\{2\} d\Gamma_2 d\{1\} d\Gamma_1 &= \int d\{2\} d\Gamma_2 q_{12} \int x_{21} h_{12} d\{1\} d\Gamma_1 \\ &= \int d\{2\} d\Gamma_2 q_{12} (xh)_{212} = (qxh)_{1212} \end{aligned}$$

$$\begin{aligned} \int q_{12} x_{22} h_{22} d\{2\} d\Gamma_2 d\{2\} d\Gamma_2 &= \int d\{2\} d\Gamma_2 q_{12} \int x_{22} h_{22} d\{2\} d\Gamma_2 \\ &= \int d\{2\} d\Gamma_2 q_{12} (xh)_{222} = (qxh)_{1222} \end{aligned}$$

$(xh)_{112}$  ,  $(xh)_{122}$  ,  $(xh)_{212}$  ,  $(xh)_{222}$  are evaluated as  $\phi_{11} * \phi_{11}$  and  $(qxh)_{1112}$  ,  $(qxh)_{1122}$  ,  $(qxh)_{1212}$  ,  $(qxh)_{1222}$  , are also evaluated as  $\phi_{11} * \phi_{11}$  in 4.3 above.

$$\begin{aligned} \int q_{11} x_{13} h_{32} d\{1\} d\Gamma_1 d\{3\} d\Gamma_3 &= \int d\{1\} d\Gamma_1 q_{11} \int x_{13} h_{32} d\{3\} d\Gamma_3 \\ &= \int d\{1\} d\Gamma_1 q_{11} (xh)_{132} = (qxh)_{1132} \end{aligned}$$

$$\begin{aligned} \int q_{12} x_{23} h_{32} d\{2\} d\Gamma_2 d\{3\} d\Gamma_3 &= \int d\{2\} d\Gamma_2 q_{12} \int x_{23} h_{32} d\{3\} d\Gamma_3 \\ &= \int d\{2\} d\Gamma_2 q_{12} (xh)_{232} = (qxh)_{1232} \end{aligned}$$

$(xh)_{132}$  ,  $(xh)_{232}$  are evaluated as  $\phi_{13} * \phi_{31}$  and  $(qxh)_{1132}$  ,  $(qxh)_{1232}$  are evaluated as  $\phi_{11} * \phi_{11}$  in 4.3 above

$$\int q_{13} x_{31} h_{12} d\{3\} d\Gamma_3 d\{1\} d\Gamma_1 = \int d\{3\} d\Gamma_3 q_{13} \int x_{31} h_{12} d\{1\} d\Gamma_1$$

$$= \int d\{1\} d\Gamma_1 q_{11}(xh)_{13,3} = (qxh)_{113,3}$$

$$\begin{aligned} \int q_{12} x_{23, h_{3,3}} d\{2\} d\Gamma_2 d\{3'\} d\Gamma_3, &= \int d\{2\} d\Gamma_2 q_{12} \int x_{23, h_{3,3}} d\{3'\} d\Gamma_3, \\ &= \int d\{2\} d\Gamma_2 q_{12}(xh)_{23,3} = (qxh)_{123,3} \end{aligned}$$

$(xh)_{13,3}$ ,  $(xh)_{23,3}$  are evaluated the same way as  $\phi_{13} * \phi_{33}$  and  $(qxh)_{113,3}$ ,  $(qxh)_{123,3}$  are evaluated the same way as  $\phi_{11} * \phi_{13}$  in 4.3 above.

$$\begin{aligned} \int q_{13, x_{3,1} h_{13}} d\{3'\} d\Gamma_3, d\{1\} d\Gamma_1 &= \int d\{3'\} d\Gamma_3, q_{13,} \int x_{3,1} h_{13} d\{1\} d\Gamma_1 \\ &= \int d\{3'\} d\Gamma_3, q_{13,} (xh)_{3,13} = (qxh)_{13,13} \end{aligned}$$

$$\begin{aligned} \int q_{13, x_{3,2} h_{23}} d\{3'\} d\Gamma_3, d\{2\} d\Gamma_2 &= \int d\{3'\} d\Gamma_3, q_{13,} \int x_{3,2} h_{23} d\{2\} d\Gamma_2 \\ &= \int d\{3'\} d\Gamma_3, q_{13,} (xh)_{3,23} = (qxh)_{13,23} \end{aligned}$$

$(xh)_{3,13}$ ,  $(xh)_{3,23}$  are evaluated the same way as  $\phi_{3,1} * \phi_{13}$  and  $(qxh)_{13,13}$ ,  $(qxh)_{13,23}$  are evaluated the same way  $\phi_{13} * \phi_{33}$  in 4.3 above.

$$\begin{aligned} \int q_{13,} x_{3,3''} h_{3''3} d\{3'\} d\Gamma_3, d\{3''\} d\Gamma_{3''} \\ &= \int d\{3'\} d\Gamma_3, q_{13,} \int x_{3,3''} h_{3''3} d\{3''\} d\Gamma_{3''} \\ &= \int d\{3'\} d\Gamma_3, q_{13,} (xh)_{3,3''3} = (qxh)_{13,3''3} \end{aligned}$$

$(xh)_{3,3''3}$  is evaluated the same way as  $\phi_{33} * \phi_{33}$  and  $(qxh)_{13,3''3}$  is evaluated the same way as  $\phi_{13} * \phi_{33}$  in 4.3 above.

(iv) calculation of  $\tau_{21}$  :

$$\tau_{21} = \sum_{i=1}^3 x_{2i} * h_{i1} + \sum_{i=1}^3 q_{2i} * x_{i1} + \sum_{i,j=1}^3 q_{21} * x_{ij} * h_{j1}$$



$\sum_i x_{2i} * h_{i1}$  is evaluated the same way as  $\sum_i x_{1i} * h_{i1}$  in (i) of this section.

$\sum_i q_{2i} * h_{i1}$  is also evaluated the same way as  $\sum_i x_{2i} * h_{i1}$

$$\sum_{i,j} q_{2i} * x_{ij} * h_{j1}$$

$$= c_1^2 \int q_{21} x_{11} h_{11} d\{1\} d\Gamma_1 d\{1\} d\Gamma_1$$

$$+ c_1 c_2 \int q_{21} x_{12} h_{21} d\{1\} d\Gamma_1 d\{2\} d\Gamma_2 + c_1 c_3 \int q_{21} x_{13} h_{31} d\{1\} d\Gamma_1 d\{3\} d\Gamma_3$$

$$+ c_2 c_1 \int q_{22} x_{21} h_{11} d\{2\} d\Gamma_2 d\{1\} d\Gamma_1 + c_2^2 \int q_{22} x_{22} h_{21} d\{2\} d\Gamma_2 d\{1\} d\Gamma_1$$

$$+ c_2 c_3 \int q_{22} x_{23} h_{31} d\{2\} d\Gamma_2 d\{3\} d\Gamma_3$$

$$+ c_3 c_1 \int q_{23} x_{31} h_{11} d\{3\} d\Gamma_3 d\{1\} d\Gamma_1 + c_3 c_2 \int q_{23} x_{32} h_{21} d\{3\} d\Gamma_3 d\{2\} d\Gamma_2$$

$$+ c_3^2 \int q_{23} x_{33} h_{31} d\{3\} d\Gamma_3 d\{3'\} d\Gamma_3,$$

$$\int q_{21} x_{11} h_{11} d\{1\} d\Gamma_1 d\{1\} d\Gamma_1, \int q_{21} x_{12} h_{21} d\{1\} d\Gamma_1 d\{2\} d\Gamma_2,$$

$$\int q_{22} x_{21} h_{11} d\{2\} d\Gamma_2 d\{1\} d\Gamma_1,$$

$\int q_{22} x_{22} h_{21} d\{2\} d\Gamma_2 d\{2\} d\Gamma_2$ , are evaluated the same way as  $(q_x h)_{1111}$  in (i) of this section.

$$\int q_{21} x_{13} h_{31} d\{1\} d\Gamma_1 d\{3\} d\Gamma_3, \int q_{22} x_{23} h_{31} d\{2\} d\Gamma_2 d\{3\} d\Gamma_3 \text{ are}$$

evaluated the same way as  $(q_{xh})_{1131}$  in (i) of this section.

$$\int q_{23} x_{31} h_{11} d\{3\} d\Gamma_3 d\{1\} d\Gamma_1, \quad \int q_{23} x_{32} h_{21} d\{3\} d\Gamma_3 d\{2\} d\Gamma_2,$$

are evaluated the same way as  $(q_{xh})_{1311}$  in (i) of this section.

$$\int q_{23} x_{33} h_{3,1} d\{3\} d\Gamma_3 d\{3'\} d\Gamma_3, \text{ is evaluated the same way as } (q_{xh})_{133,1} \text{ in (i) of this section.}$$

(v) Calculation of  $\tau_{22}$  :

$$\tau_{22} = \sum_{i=1}^3 x_{2i} * h_{i2} + \sum_{i=1}^3 q_{2i} * x_{i2} + \sum_{i,j=1}^3 q_{2i} * x_{ij} * h_{j2}$$

$\sum_i x_{2i} * h_{i2}$  is evaluated the same way as  $\sum_i x_{1i} * h_{i1}$  in (i) of this section.

$\sum_i q_{2i} * x_{i2}$  is evaluated the same way as  $\sum_i x_{2i} * h_{i2}$  above.

$\sum_i q_{2i} * x_{ij} * h_{j2}$  is evaluated the same way as  $\sum_i q_{1i} * x_{ij} * h_{j1}$  in (i) of this section.

(vi) Calculation of  $\tau_{23}$  :

$$\tau_{23} = \sum_{i=1}^3 x_{2i} * h_{i3} + \sum_{i=1}^3 q_{2i} * x_{i3} + \sum_{i,j=1}^3 q_{2i} * x_{ij} * h_{j3}$$

$\sum_i x_{2i} * h_{i3}$  is evaluated the same way as  $\sum_i x_{1i} * h_{i3}$  in (iii) of this section.

$\sum_i q_{2i} * x_{i3}$  is evaluated the same way as  $\sum_i x_{1i} * h_{i3}$  in (iii) of this section.

$\sum_{i,j} q_{2i} * x_{ij} * h_{j3}$  is evaluated the same way as  $\sum_{i,j} q_{1i} * x_{ij} * h_{j3}$  in (iii) of this section.

(vii) Calculation of  $\tau_{31}$  :

$$\tau_{31} = \sum_{i=1}^3 x_{3i} * h_{i1} + \sum_{i=1}^3 q_{3i} * x_{i1} + \sum_{i,j=1}^3 q_{3i} * x_{ij} * h_{j1}$$

$$\sum_i x_{3i} * h_{i1}$$

$$= c_1 \int x_{31} h_{11} d\{1\} d\Gamma_1 + c_2 \int x_{32} h_{21} d\{2\} d\Gamma_2 + c_3 \int x_{33} h_{31} d\{3\} d\Gamma_3,$$

$$\sum q_{3i} * x_{i1}$$

$$= c_1 \int q_{31} x_{11} d\{1\} d\Gamma_1 + c_2 \int q_{32} x_{21} d\{2\} d\Gamma_2 + c_3 \int q_{33} x_{31} d\{3\} d\Gamma_3,$$

$\int x_{31} h_{11} d\{1\} d\Gamma_1$ ,  $\int x_{32} h_{21} d\{2\} d\Gamma_2$  are evaluated the same way as  $\phi_{31} * \phi_{11}$  in 4.3 above.

$\int x_{33} h_{31} d\{3\} d\Gamma_3$ , is evaluated the same way as  $\phi_{33} * \phi_{31}$  in 4.3 above.

$\sum_i q_{3i} * x_{i1}$  is evaluated the same way as  $\sum_i x_{3i} * h_{i1}$ .

$$\sum_{i,j=1}^3 q_{3i} * x_{ij} * h_{j1}$$

$$= c_1^2 \int q_{31} x_{11} h_{11} d\{1\} d\Gamma_1$$

$$+ c_1 c_2 \int q_{31} x_{12} h_{21} d\{1\} d\Gamma_1 d\{2\} d\Gamma_2 + c_1 c_3 \int q_{31} x_{13} h_{31} d\{1\} d\Gamma_1 d\{3\} d\Gamma_3$$

$$+ c_2 c_1 \int q_{32} x_{21} h_{11} d\{2\} d\Gamma_2 d\{1\} d\Gamma_1 + c_2^2 \int q_{32} x_{22} h_{21} d\{2\} d\Gamma_2 d\{2\} d\Gamma_2$$

$$+ c_2 c_3 \int q_{32} x_{23} h_{31} d\{2\} d\{3\} d\Gamma_3 + c_3 c_1 \int q_{33} x_{31} h_{11} d\{3\} d\Gamma_3 d\{1\} d\Gamma_1$$

$$+ c_3 c_2 \int q_{33} x_{32} h_{21} d\{3\} d\Gamma_3 d\{2\} d\Gamma_2$$

$$+ c_3^2 \int q_{33}, x_{3'3''} h_{3''1} d\{3'\} d\Gamma_{3'}, d\{3''\} d\Gamma_{3''}$$

$$\int q_{31} x_{11} h_{11} d\{1\} d\Gamma_1 d\{1\} d\Gamma_2 = \int d\{1\} d\Gamma_1 q_{31} \int x_{11} h_{11} d\{1\} d\Gamma_2$$

$$= \int d\{1\} d\Gamma_1 q_{31} (xh)_{111} = (qxh)_{3111}$$

$$\int q_{31} x_{12} h_{21} d\{1\} d\Gamma_1 d\{2\} d\Gamma_2 = \int d\{1\} d\Gamma_1 q_{31} \int x_{12} h_{21} d\{2\} d\Gamma_2$$

$$= \int d\{1\} d\Gamma_1 q_{31} (xh)_{121} = (qxh)_{3121}$$

$$\int q_{32} x_{21} h_{11} d\{2\} d\Gamma_2 d\{1\} d\Gamma_1 = \int d\{2\} d\Gamma_2 q_{32} \int x_{21} h_{11} d\{1\} d\Gamma_1$$

$$= \int d\{2\} d\Gamma_2 q_{32} (xh)_{211} = (qxh)_{3211}$$

$$\int q_{32} x_{22} h_{21} d\{2\} d\Gamma_2 d\{2\} d\Gamma_2 = \int d\{2\} d\Gamma_2 q_{32} \int x_{22} h_{21} d\{2\} d\Gamma_2$$

$$= \int d\{2\} d\Gamma_2 q_{32} (xh)_{221} = (qxh)_{3221}$$

$(xh)_{111}$ ,  $(xh)_{121}$ ,  $(xh)_{211}$ ,  $(xh)_{221}$  are evaluated the same way as  $\phi_{11} * \phi_{11}$  in 4.3 above.

$(qxh)_{3111}$ ,  $(qxh)_{3121}$ ,  $(qxh)_{3211}$ ,  $(qxh)_{3221}$  are evaluated the same way as  $\phi_{31} * \phi_{11}$  in 4.3 above.

$$\int q_{31} x_{13}, h_{3,1} d\{1\}d\Gamma_1 d\{3'\}d\Gamma_3, = \int d\{1\}d\Gamma_1 q_{31} \int x_{13}, h_{3,1} d\{3'\} d\Gamma_3,$$

$$= \int d\{1\}d\Gamma_1 q_{31} (xh)_{13,1} = (qxh)_{313,1}$$

$$\int q_{32} x_{23}, h_{3,1} d\{2\}d\Gamma_2 d\{3'\} d\Gamma_3, = \int d\{2\}d\Gamma_2 q_{32} \int x_{23}, h_{3,1} d\{3'\} d\Gamma_3,$$

$$= \int d\{2\}d\Gamma_2 q_{32} (xh)_{23,1} = (qxh)_{323,1}$$

$(xh)_{13,1}$  ,  $(xh)_{23,1}$  are evaluated the same way as  $\phi_{13} * \phi_{31}$  in 4.3 above.

$(qxh)_{313,1}$  ,  $(qxh)_{323,1}$ , are evaluated the same way as  $\phi_{31} * \phi_{11}$  in 4.3 above.

$$\int q_{33}, x_{3,1} h_{11} d\{3'\}d\Gamma_3, d\{1\}d\Gamma_1 = \int d\{3'\} d\Gamma_3, q_{33}, \int x_{3,1} h_{11} d\{1\}d\Gamma_1$$

$$= \int d\{3'\} d\Gamma_3, q_{33}, (xh)_{3,11} = (qxh)_{33,11}$$

$$\int q_{33}, x_{3,2} h_{21} d\{3'\}d\Gamma_3, d\{2\}d\Gamma_2 = \int d\{3'\} d\Gamma_3, q_{33}, \int x_{3,2} h_{21} d\{2\}d\Gamma_2$$

$$= \int d\{3'\} d\Gamma_3, q_{33}, (xh)_{3,21} = (qxh)_{33,21}$$

$(xh)_{3,11}$  ,  $(xh)_{3,21}$  are evaluated the same way as  $\phi_{31} * \phi_{11}$  in 4.3 above.

$(qxh)_{33,11}$  ,  $(qxh)_{33,21}$ , are evaluated the same way as  $\phi_{33} * \phi_{31}$  in 4.3 above.

$$\begin{aligned}
\int q_{33}, x_{3,3} h_{3,1} d\{3'\} d\Gamma_3, d\{3''\} d\Gamma_{3''} &= \int d\{3'\} d\Gamma_3, q_{33}, \int x_{3,3} h_{3,1} d\{3''\} d\Gamma_{3''} \\
&= \int d\{3'\} d\Gamma_3, q_{33}, (xh)_{3,3,1} \\
&= (qxh)_{33,3,1}
\end{aligned}$$

$(xh)_{3,3,1}$  is evaluated the same way as  $\phi_{33} * \phi_{31}$  in 4.3 above.

$(qxh)_{33,3,1}$  is evaluated the same way as  $\phi_{33} * \phi_{31}$  in 4.3 above.

(viii) Calculation of  $\tau_{32}$  :

$$\tau_{32} = \sum_{i=1}^3 x_{3i} * h_{i2} + \sum_{i=1}^3 q_{3i} * x_{i2} + \sum_{i,j=1}^3 q_{3i} * x_{ij} * h_{j2}$$

$\sum_i x_{3i} * h_{i2}$  is evaluated the same way as  $\sum_i x_{3i} * h_{i1}$  in (vii) of this section.

$\sum_i q_{3i} * x_{i2}$  is evaluated the same way as  $\sum_i x_{3i} * h_{i1}$  in (vii) of this section.

$\sum_i q_{3i} * x_{ij} * h_{j2}$  is evaluated the same way as  $\sum_i q_{3i} * x_{ij} * h_{j1}$  in (vii) of this section.

(ix) Calculation of  $\tau_{33}$  :

$$\tau_{33} = \sum_{i=1}^3 x_{3i} * h_{i3}, + \sum_{i=1}^3 q_{3i} * x_{i3}, + \sum_{i,j=1}^3 q_{3i} * x_{ij} * h_{j3},$$

$$\sum_i x_{3i} * h_{i3},$$

$$= c_1 \int x_{31} h_{13}, d\{1\} d\Gamma_1 + c_2 \int x_{32} h_{23}, d\{2\} d\Gamma_2$$

$$+ c_3 \int x_{33''} h_{3''3}, d\{3''\} d\Gamma_{3''}$$

$\int x_{31} h_{13}, d\{1\} d\Gamma_1$  and  $\int x_{32} h_{23}, d\{2\} d\Gamma_2$  are evaluated the same way as  $\phi_{31} * \phi_{13}$  in 4.3 above.

$\int x_{33''} h_{3''3}, d\{3''\} d\Gamma_{3''}$  is evaluated the same way as  $\phi_{33''} * \phi_{3''3}$ , in 4.3 above.

$\sum_i q_{3i} * x_{i3}$ , is evaluated the same way as  $\sum q_{3i} * h_{i3}$  above.

$$\sum_{i,j} q_{3i} * x_{ij} * h_{j3},$$

$$= c_1^2 \int q_{31} x_{11} h_{13}, d\{1\} d\Gamma_1 d\{1\} d\Gamma_1$$

$$+ c_1 c_2 \int q_{31} x_{12} h_{23}, d\{1\} d\Gamma_1 d\{2\} d\Gamma_2$$

$$+ c_1 c_3 \int q_{31} x_{13''} h_{3''3}, d\{1\} d\Gamma_1 d\{3''\} d\Gamma_{3''}$$

$$+ c_2 c_1 \int q_{32} x_{21} h_{13}, d\{2\} d\Gamma_2 d\{1\} d\Gamma_1 + c_2^2 \int q_{32} x_{22} h_{23}, d\{2\} d\Gamma_2 d\{2\} d\Gamma_2$$

$$+ c_2 c_3 \int q_{32} x_{23''} h_{3''3}, d\{2\} d\Gamma_2 d\{3''\} d\Gamma_{3''}$$

$$+ c_3 c_1 \int q_{33''} x_{3''1} h_{13}, d\{3''\} d\Gamma_{3''} d\{1\} d\Gamma_1$$

$$+ c_3 c_2 \int q_{33''} x_{3''2} h_{23}, d\{3''\} d\Gamma_{3''} d\{2\} d\Gamma_2$$

$$+ c_3^2 \int q_{33''} x_{3''3'''} h_{3'''3}, d\{3''\} d\Gamma_{3''} d\{3'''\} d\Gamma_{3'''}$$

$$\int q_{31} x_{11} h_{13}, d\{1\} d\Gamma_1 d\{1\} d\Gamma_1 = \int d\{1\} d\Gamma_1 q_{31} \int x_{11} h_{13}, d\{1\} d\Gamma_1$$

$\phi_{31} * \phi_{13}$  in 4.3 above.

$(xh)_{3''',3''3'}$ ,  $(qxh)_{33'',13}$ ,  $(qxh)_{33'',23}$ ,  $(qxh)_{33''',3''3'}$  are evaluated the same way as  $\phi_{33} * \phi_{33}$  in 4.3 above.

The calculation repeats itself till convergence is achieved. The final result is  $g$  as a function of  $r$  and angular variables. To obtain  $g(r)$  irrespective of angle one integrates over the angular variables ( $d\Gamma = \sin\beta \, d\beta \, d\gamma \, d\alpha$ ).

#### 4.5 Calculation of $q$ for a mixture of ions only from the equations derived above: Reduction to the Mayer formula

A function with a positive ion at both the fixed terminal points is given by

$$\begin{aligned} q_{++}(r) &= \bar{q}_{++} \begin{pmatrix} 0 & 0 & 0 \\ 0 & 0 & r \end{pmatrix} = \frac{q_+^2}{16\pi^4 r_{++}} \int_0^\infty P_{11}(n=0) t \sin r t dt \\ &= \frac{q_+^2}{16\pi^4 r_{++}} c \frac{\pi}{2} \exp(-kr) \end{aligned}$$

(the value of the integral is given in equation (115) in section 4.2. Also the values of  $c$  and  $k$  are given there. Calculation of  $q(r)$  from  $\bar{q}(r)$  and  $\bar{q}(r)$  from  $\bar{q}(t)$  is also given in section 4.2).

Thus,

$$c = - \frac{3(32\pi^3/kT) (1 + c_m \mu_m^2 \frac{32\pi^3}{3\epsilon kT})}{3 + 2 c_m \mu_m^2 (32\pi^3/\epsilon kT)}$$

$$k^2 = \frac{3(\sum_i c_i q_i^2) (\frac{32\pi^3}{\epsilon kT}) + (\sum_i c_i q_i^2) c_m \mu_m^2 (32\pi^3/\epsilon kT)^2}{3 + 2 c_m \mu_m^2 (32\pi^3/\epsilon kT)}$$

The values of  $q$ 's and  $\mu$  used in section 4.2 are the actual value of the charge and dipole moment divided by  $\epsilon$ , the dielectric permittivity of the medium. Hence, we have  $\sigma$  in the denominator



here and the  $q$ 's and  $\mu$  are the actual charge and dipole moment. Let us set  $\mu_m = 0$ , to obtain a formula valid for a mixture of ions. Then,

$$C = -\frac{32\pi^3}{kT}, \quad k^2 = \left( \sum_i C_i q_i^2 \right) \left( \frac{32\pi^3}{\epsilon kT} \right)$$

The concentration used in this method are  $\frac{1}{8\pi^2}$  of the actual chemical concentrations, in order to take into account integration over angular coordinates. Thus  $k^2 \left( \sum_i C_i q_i^2 \right) \frac{4\pi}{\epsilon kT}$ , if we are using actual chemical concentrations, as has been done in Mayer's work (5).

$$\begin{aligned} q_{++}(r) &= \frac{q_+^2}{16\pi^4 \epsilon r_{++}} \left( -\frac{32\pi^3}{kT} \right) \cdot \frac{\pi}{2} \exp(-kr) \\ &= -\frac{q_+^2}{\epsilon kT} \left\{ \frac{\exp(-kr)}{r} \right\} \end{aligned}$$

This is identical with Mayer's formula (5) for  $q$  function in a mixture of ions derived by a different method, in particular by using  $e^{-\alpha r}$  as the convergence factor and then taking the limit  $\alpha \rightarrow 0$ .

#### 4.6 Problem of Convergence of the Cluster Expansion of Angle Dependent $q(t)$

The condition of validity of Eq. 83 is the condition of convergence of the power series of matrices

$$I + A + A^2 + \dots + A^n = (I - A)^{-1}$$

We have considered specific elements of the matrix sum on the L.H.S. and found, by explicit expansion, that they can be expressed as the product of appropriate elements of the transpose of the cofactor matrix of  $A$  multiplied by a power

series, which if it converges becomes the inverse of  $\det (I-A)$ , i.e.,  $I+A+A^2+\dots+A^n$  can be equated to  $(I-A)_{C.F.}^T / \det (I-A)$ , i.e.  $(I-A)^{-1}$  only if this power series converges.

Now  $\det (I-A) = 1 - (a_{\alpha\alpha} + a_{\beta\beta} - a_{\alpha\alpha} a_{\beta\beta} + a_{\alpha\beta} a_{\beta\alpha})$ , for a  $2 \times 2$  matrix.

For the matrix under consideration

$$a_{\alpha\alpha} = -\frac{x}{t^2} \sum_i c_i q_i^2 \quad a_{\alpha\beta} = -\frac{ix}{\sqrt{3}t} \sum_i c_i q_i^2 \quad a_{\beta\alpha} = +\frac{ix}{\sqrt{3}t} c_m \mu_m^2$$

$$a_{\beta\beta} = -\frac{2x}{3} c_m \mu_m^2$$

(Having taken the limit, all the convergence factors  $a_{oo}$  etc. going to 0.)

We now call  $\sum_i c_i q_i^2 = \alpha$ ,  $c_m \mu_m^2 = \beta$ . Then, the condition necessary to be able to write the equality

$$I + A + \dots + A^n = (I - A)^{-1} \text{ is}$$

$$|a_{\alpha\alpha} + a_{\beta\beta} - a_{\alpha\alpha} a_{\beta\beta} + a_{\alpha\beta} a_{\beta\alpha}| < 1$$

$$\text{or } \left| -\frac{x}{t^2} \alpha - \frac{2x}{3} \beta - \frac{2x^2}{3t^2} \alpha\beta + \frac{x^2}{3t^2} \alpha\beta \right| < 1$$

$$\text{or } \frac{x}{t^2} \alpha + \frac{2x}{3} \beta + \frac{x^2}{3t^2} \alpha\beta < 1$$

The well known condition for the convergence of a power series of matrices, i.e. to be able to write  $I + A + \dots + A^n = (I-A)^{-1}$  is that the absolute value of the largest eigenvalue of  $A$  has to be less than unity. The eigenvalues of  $A$  are

$$\frac{1}{2} \left[ -\left\{ \frac{x}{t^2} \alpha + \frac{2x}{3} \beta \right\} \pm \left\{ \frac{x^2}{t^4} \alpha^2 + \frac{4x^2}{9} \beta^2 \right\}^{1/2} \right].$$

$x, t, \alpha, \beta$  are all positive. The second term in curly bracket within the square bracket is positive. Simple algorithm

manipulation shows that the condition that the mod of largest eigenvalue is  $<1$  reduces to

$$\frac{x}{t^2} \alpha + \frac{2x}{3} \beta + \frac{x^2}{3t^2} \alpha\beta < 1,$$

the same condition stated earlier. The more well known condition being the same as the condition we worked out ourselves, by considering the convergence of a power series, makes us reach the following conclusion.

The power series that must converge for our formulae to be valid is the expansion of

$$\left( 1 - \left\{ a_{\alpha\alpha} + a_{\beta\beta} - a_{\alpha\alpha} a_{\beta\beta} + a_{\alpha\beta} a_{\beta\alpha} \right\} \right)^{-1}$$

or,  $\left( 1 - \left\{ T - D \right\} \right)^{-1}$ , where  $T$  is the trace and  $D$  the

determinant.  $(T - D)$  in our case is  $-\frac{x}{t^2} \alpha - \frac{2x}{3} \beta - \frac{x^2}{3t^2} \alpha\beta$ ;

$x, \alpha, \beta$  being positive,  $T - D$  is negative, i.e., the power series

is the expansion of  $(1 + \frac{x}{t^2} \alpha + \frac{2x}{3} \beta + \frac{x^2}{3t^2} \alpha\beta)^{-1} = (1+z)^{-1}$ ,

where  $z = \frac{x}{t^2} \alpha + \frac{2x}{3} \beta + \frac{x^2}{3t^2} \alpha\beta$ . By method of analytic

continuation, the validity of the expansion can be extended to  $z > 1$

on the positive axis, i.e., for  $\frac{1}{t^2} (x\alpha + \frac{1}{3} x^2 \alpha\beta) + \frac{2x}{3} \beta > 1$ ,

i.e., for all  $t$ . In case of a system of pure dipoles ( $c_i = 0$  for

all  $i$ ), the same statement holds. Jepsen and Friedman (1) state

that their theory holds only at lower dipole density e.g. that of

supercritical steam rather than liquid densities. Friedman in his

book on Ionic Solution Theory (11) is also hesitant about the

validity of the argument based on analytic continuation. It is

because of this, that we have taken the conservative stand and

stated in various parts of this thesis that for dipoles the theory

is valid only at low densities of solutes in a dilute solution.

We however do not see any reason why it should not be valid over the whole range of concentration as is true of mixtures of ions in Mayer's theory of ionic solution. We are studying this aspect more thoroughly.

#### 4.7 The Validity of Allnatt Equation for Angle-dependent Potential

In Chapter III, we solved Allnatt's HNC equation to obtain correlation function in ionic solution. Briefly, recapitulating, Allnatt (3) uses Meeron's results (6) on the calculation of potential of average force  $w_{ij}(r)$  or equivalently  $g_{ij}(r)$  from their diagrammatic expansion. The formula is

$$g_{ij}(r) = \exp (q_{ij} - \beta u_{ij}^* + \alpha_{ij})$$

where  $q_{ij}$  is the sum of  $g$ -bond chains between  $i$  and  $j$ ,  $u_{ij}^*$  is the hard sphere potential and  $\alpha_{ij}$  are defined as

$$\alpha_{ij} = \sum_{m \geq 1}^{\infty} \frac{\rho^m}{m!} \int \theta(ij;m) dm$$

$\theta$  diagrams are made up of  $\phi$  bonds ( $\phi = e^q - 1$ ) and  $q$  bonds, with only isolated  $q$  bonds. Details are given in Chapter III, section 7. Jepsen and Friedman in their paper (1) use an identical equation, except that  $q$  bond is different and is angle dependent (Eq. 5.5-5.7 and Eq. 5.12 of Jepsen and Friedman (1)). Since their  $q$  bond is different, their  $\phi$  bond is also different

Allnatt classified the  $\alpha_{ij}$  diagram into  $\tau_{ij}$  and  $\eta_{ij}$  on the basis of their topology and  $\eta_{ij}$  is set equal to zero in the HNC approximation.  $\tau$  is further classified into A and B (details in Chapter III, section 7). These steps also remain unchanged in systems with angle-dependent potential, because the diagrams are the same, only the bonds are different. One then obtains Allnatt HNC equation for angle dependent potential.

## APPENDIX

### 1. Bessel function :

$$j_n(x) = \left( \frac{\pi}{2x} \right)^{1/2} J_{n+\frac{1}{2}}(x) \quad (\text{Ref. 1})$$

$$\text{where } J_{n+\frac{1}{2}}(x) = \sqrt{\frac{2}{\pi}} x^{n+\frac{1}{2}} \left( -\frac{1}{x} \frac{d}{dx} \right)^n \frac{\sin x}{x} \quad (\text{Ref. 7})$$

$$J_{1/2}(x) = \sqrt{\frac{2}{\pi x}} \sin x \quad (\text{Ref. 7})$$

$$J_{-1/2}(x) = \sqrt{\frac{2}{\pi x}} \cos x \quad (\text{Ref. 7})$$

$$\begin{aligned} \therefore j_0(x) &= \left( \frac{\pi}{2x} \right)^{1/2} J_{1/2}(x) \\ &= \left( \frac{\pi}{2x} \right)^{1/2} \left( \frac{2}{\pi x} \right)^{1/2} \sin x \\ &= \frac{\sin x}{x} \end{aligned}$$

$$\begin{aligned} j_{-1}(x) &= \left( \frac{\pi}{2x} \right)^{1/2} J_{-1/2}(x) \\ &= \frac{\cos x}{x} \end{aligned}$$

$$\begin{aligned} j_1(x) &= \left( \frac{\pi}{2x} \right)^{1/2} J_{1+1/2}(x) \\ &= \left( \frac{\pi}{2x} \right)^{1/2} \left( \frac{2}{\pi} \right)^{1/2} x^{3/2} \left( -\frac{1}{x} \frac{d}{dx} \right) \frac{\sin x}{x} \\ &= \frac{\sin x}{x^2} - \frac{\cos x}{x} \end{aligned}$$

$$j_2(x) = \left( \frac{\pi}{2x} \right)^{1/2} J_{2+\frac{1}{2}}(x)$$

$$= \left(\frac{\pi}{2x}\right)^{1/2} \left(\frac{2}{\pi}\right)^{1/2} x^{5/2} \left(-\frac{1}{x} \frac{d}{dx}\right)^2 \frac{\sin x}{x}$$

$$= \frac{3\sin x}{x^3} - \frac{3\cos x}{x^2} - \frac{\sin x}{x}$$

## 2. Wigner 3j-coefficient:

$$\begin{bmatrix} \ell_1 & \ell_2 & \ell \\ m_1 & m_2 & m \end{bmatrix}_{3j} = (-)^{\ell_1+\ell_2+m} (2\ell+1)^{-1/2} C(\ell_1, \ell_2, \ell; m_1, m_2, m) \quad (\text{Ref.8})$$

C is the Clebsch-Gordon coefficient. The values of C are obtained from Tinkham (Ref. 9)

$$\begin{bmatrix} 0 & 0 & 0 \\ 0 & 0 & 0 \end{bmatrix}_{3j} = 1$$

$$\begin{bmatrix} 1 & 0 & 1 \\ 0 & 0 & 0 \end{bmatrix}_{3j} = -\frac{1}{\sqrt{3}}$$

$$\begin{bmatrix} 1 & 1 & 1 \\ 0 & 0 & 0 \end{bmatrix}_{3j} = 0$$

$$\begin{bmatrix} 0 & 1 & 1 \\ 0 & 0 & 0 \end{bmatrix}_{3j} = -\frac{1}{\sqrt{3}}$$

$$\begin{bmatrix} 1 & 1 & 2 \\ 0 & 0 & 0 \end{bmatrix}_{3j} = \left(\frac{2}{15}\right)^{1/2}$$

$$\begin{bmatrix} 1 & 1 & 2 \\ -1 & 1 & 0 \end{bmatrix}_{3j} = \left(\frac{1}{30}\right)^{1/2}$$

$$\begin{bmatrix} 1 & 1 & 2 \\ 1 & -1 & 0 \end{bmatrix}_{3j} = \left(\frac{1}{30}\right)^{1/2}$$

$$\begin{bmatrix} 1 & 1 & 1 \\ -1 & 1 & 0 \end{bmatrix}_{3j} = -\frac{1}{\sqrt{6}}$$

$$\begin{bmatrix} 1 & 1 & 1 \\ 1 & -1 & 0 \end{bmatrix}_{3j} = -\frac{1}{\sqrt{6}}$$

$$\begin{bmatrix} 1 & 1 & 0 \\ 0 & 0 & 0 \end{bmatrix}_{3j} = -\frac{1}{\sqrt{3}}$$

$$\begin{bmatrix} 1 & 1 & 0 \\ -1 & 1 & 0 \end{bmatrix}_{3j} = \frac{1}{\sqrt{3}}$$

$$\begin{bmatrix} 1 & 1 & 0 \\ 1 & -1 & 0 \end{bmatrix}_{3j} = \frac{1}{\sqrt{3}}$$

### 3. Rotation Matrices (Ref. 1 and 8):

$$D_{00}^{\ell}(\alpha, \beta, \gamma) = P_{\ell}(\cos \beta)$$

$$D_{00}^0(\alpha, \beta, \gamma) = 1$$

$$D_{00}^1(\alpha, \beta, \gamma) = \cos \beta$$

$$D_{00}^{1*}(\alpha, \beta, \gamma) = \cos \beta$$

$$D_{0m}^{\ell*}(\alpha, \beta, \gamma) = (-)^m \left[ \frac{4\pi}{2\ell+1} \right]^{1/2} Y_{\ell m}^*(\beta, \alpha)$$

$$D_{0m}^{\ell}(\alpha, \beta, \gamma) = (-)^m \left[ \frac{4\pi}{2\ell+1} \right]^{1/2} Y_{\ell m}(\beta, \alpha)$$

$$D_{0m}^{\ell*}(\alpha, \beta, \gamma) = (-)^{0-m} D_{0, -m}^{\ell}(\alpha, \beta, \gamma) = (-)^m D_{0, -m}^{\ell}(\alpha, \beta)$$

$$\therefore D_{0-m}^{\ell}(\alpha, \beta, \gamma) = (-)^m D_{0m}^{\ell*}(\alpha, \beta, \gamma)$$

$$= (-)^m (-)^m \left[ \frac{4\pi}{2\ell+1} \right]^{1/2} Y_{\ell m}^*(\beta, \alpha)$$

$$f(t) = \frac{1}{k^2 + t^2} \Rightarrow \text{an even function}$$

$$\begin{aligned}
 & \int_{-\infty}^{\infty} f(t) e^{-irt} dt \\
 &= \int_{-\infty}^0 f(t) e^{-irt} dt + \int_0^{\infty} f(t) e^{-irt} dt \\
 &= -\int_0^{-\infty} f(t) e^{-irt} dt + \int_0^{\infty} f(t) e^{-ir} dt \\
 &= -\int_0^{\infty} f(-t) e^{-ir(-t)} d(-t) + \int_0^{\infty} f(t) e^{-irt} dt \\
 &= \int_0^{\infty} f(t) e^{irt} dt + \int_0^{\infty} f(t) e^{-irt} dt \\
 &= \int_0^{\infty} f(t) (e^{irt} + e^{-irt}) dt \\
 &= 2 \int_0^{\infty} f(t) \cos(rt) dt
 \end{aligned}$$

##### 5. Elements of the H-matrix

Let us define a quantity  $x = \frac{32\pi^3}{kT}$



$$\tilde{h}_{00}(t, 0) = \frac{-x a_{00} j_{-1}(a_{00}t)}{3^{1/2} t}$$

$$\tilde{h}_{01}(t, 0) = \frac{-x j_0(a_{01}t)}{3^{1/2} t}$$

$$\tilde{h}_{10}(t, 0) = \frac{-ix j_0(a_{10}t)}{3^{1/2} t}$$

$$\tilde{h}_{11}(t, 0) = \frac{-2x j_1(a_{11}t)}{3a_{11}t}$$

$$\tilde{h}_{00}(t, 1) = 0$$

$$\tilde{h}_{01}(t, 1) = 0$$

$$\tilde{h}_{10}(t, 1) = 0$$

$$\tilde{h}_{11}(t, 1) = \frac{-x j_1(a_{11}t)}{3a_{11}t}$$

$$\tilde{h}_{00}(t, -1) = 0$$

$$\tilde{h}_{01}(t, -1) = 0$$

$$\tilde{h}_{10}(t, -1) = 0$$

$$\tilde{h}_{11}(t, -1) = \frac{x j_1(a_{11}t)}{3a_{11}t}$$

## REFERENCES

1. D.W. Jepsen and H.L. Friedman, J. Chem. Phys., 38, 846, 1963.
2. J.C. Rasaiah and H.L. Friedman, J. Chem. Phys., 48, 2742, 1968.
3. A.R. Allnatt, Mol. Phy., 8, 533, 1964.
4. E. Meeron, J. Math. Phys., 1, 192, 1960.
5. J.E. Mayer, J. Chem. Phys., 18, 1426, 1950.
6. E. Meeron, J. Chem. Phys., 28, 630, 1958.
7. E. Kraut, Fundamentals of Mathematical Physics, McGraw Hill, 1967, pp. 267-8.
8. C.G. Gray and K.E. Gubbins, Theory of Molecular Fluids, Oxford University Press, 1984, Appendix A.
9. M. Tinkham: Group Theory and Quantum Mechanics, McGraw Hill, 1964, Tata McGraw Hill ed., 1974, Chapter 5, p. 124.
10. A. Messiah : Quantum Mechanics, Vol. I, North Holland Publishers, Amsterdam and John Wiley, N.Y., 1966, p. 478.
11. Friedman, H.L., Ionic Solution Theory Based on Cluster Expansion Methods (New York, Interscience Publishers), 1962.

$$\Rightarrow \frac{1}{\sqrt{2\pi}} \int_{-\infty}^{\infty} e^{irt} \left(\frac{2k^3}{\pi}\right)^{1/2} \frac{1}{k^2+t^2} dt = (k)^{1/2} e^{-k|r|} \quad (\text{Ref. 10})$$

$$\text{or } \frac{(2k^3)^{1/2}}{\sqrt{2} \pi} \int_{-\infty}^{\infty} \frac{1}{k^2+t^2} e^{irt} dt = (k)^{1/2} e^{-k|r|}$$

$$\text{or } \int_{-\infty}^{\infty} \frac{1}{k^2+t^2} e^{irt} dt = \frac{\pi}{k} e^{-k|r|} \quad (1)$$

Since  $\frac{1}{t^2+k^2}$  is an even function

$$\int_{-\infty}^{\infty} \frac{1}{k^2+t^2} e^{irt} dt = \int_{-\infty}^{\infty} \frac{1}{k^2+t^2} e^{-irt} dt$$

and

$$\frac{1}{2} \int_{-\infty}^{\infty} \frac{1}{k^2+t^2} e^{-irt} dt = \int_0^{\infty} \frac{1}{k^2+t^2} \cos(rt) dt \quad (2)$$

(The proof of (2) is given later)

$$\therefore \int_0^{\infty} \frac{1}{k^2+t^2} \cos(rt) dt = \frac{1}{2} \int_{-\infty}^{\infty} \frac{1}{k^2+t^2} e^{-irt} dt$$

(From equation 1)

$$= \frac{1}{2} \times \frac{\pi}{k} e^{-k|r|}$$

$$= \frac{\pi}{2} \times \frac{1}{k} \times e^{-k|r|}$$

Proof of (2)

In this chapter, we describe the computational aspects of the solution of the integral equation and discuss the implications of the numerical results obtained. The single most important result is that Allnatt's HNC equation converges at particle charges and packing fractions much larger than reported in recent literature.

### 5.1 Calculation of Convolution integrals $a*b$ :

In Chapter III (Section 8) we have described the method used by Rasaiah and Friedman (1) to solve HNC equation of Allnatt (2).

An examination of this method shows that we need to calculate several convolution integrals  $a*b$  ( $a$  and  $b$  can be  $q, h, x$ ). The same is needed in the solution of angle-dependent HNC equation described in Chapter IV. This is done by fourier transformation technique, as described below. The integrals present as  $a*b$  are of the kind

$$\begin{aligned} I(\vec{r}_{ij}) &= \int a(\vec{r}_{ik}) b(\vec{r}_{kj}) d(k) \\ &= \int a(\vec{r}_{ik}) b(\vec{r}_{kj}) d(\vec{r}_{ik}) \end{aligned} \quad (1)$$

Fourier Transform of  $I(\vec{r}_{ij})$  is  $I(\vec{k})$ . Then,

$$\begin{aligned} I(\vec{k}) &= \iint a(\vec{r}_{ik}) b(\vec{r}_{kj}) \exp[-2\pi i \vec{k} \cdot \vec{r}_{ij}] d(\vec{r}_{ik}) d(\vec{r}_{ij}) \\ &= \int \int a(\vec{r}_{ik}) b(\vec{r}_{kj}) \exp[-2\pi i \vec{k} \cdot (\vec{r}_{ik} + \vec{r}_{kj})] d(\vec{r}_{ik}) d(\vec{r}_{ij}) \end{aligned} \quad (2)$$

We now transform variables of integration;  $\vec{r}_{ik} \vec{r}_{ij} \longrightarrow \vec{r}_{ik} \vec{r}_{kj}$ .

$$d(\vec{r}_{ik}) d(\vec{r}_{ij}) = |J| d(\vec{r}_{ik}) d(\vec{r}_{kj})$$

$|J|$  = The Jacobian of co-ordinate transformation = 1

Then,

$$\begin{aligned}
 I(\vec{k}) &= \int a(\vec{r}_{ik}) \exp \left[ -2\pi i \vec{k} \cdot \vec{r}_{ik} \right] d(\vec{r}_{ik}) \\
 &\quad \int b(\vec{r}_{kj}) \exp \left[ -2\pi i \vec{k} \cdot \vec{r}_{kj} \right] d(\vec{r}_{kj}) \\
 &= \hat{a}(\vec{k}) \cdot \hat{b}(\vec{k})
 \end{aligned} \tag{3}$$

where,

$$\begin{aligned}
 \hat{a}(\vec{k}) &= \int a(\vec{r}_{ik}) \exp \left[ -2\pi i \vec{k} \cdot \vec{r}_{ik} \right] d\vec{r}_{ik} \\
 &= \int a(\vec{r}_{ik}) \exp \left[ -2\pi i r_{ik} K \cos\theta \right] r_{ik}^2 \sin\theta d\theta d\phi dr_{ik}
 \end{aligned}$$

(where  $\theta, \phi$  specify the orientation of  $\vec{r}_{ik}$  with respect to  $\vec{k}$ )

$$\begin{aligned}
 &= \int_0^{2\pi} d\phi \left\{ \int_0^{\infty} dr_{ik} a(\vec{r}_{ik}) r_{ik}^2 \right\} \left\{ \int_0^{\pi} d\theta \sin\theta \exp \left[ -2\pi i r_{ik} K \cos\theta \right] \right\} \\
 &= 2\pi \left\{ \int dr_{ik} a(\vec{r}_{ik}) r_{ik}^2 \right\} [I_0]
 \end{aligned} \tag{4}$$

where

$$\begin{aligned}
 I_0 &= \int_0^{\pi} \exp \left[ -2\pi i r_{ik} K \cos\theta \right] \sin\theta d\theta \\
 &= \int_{-1}^{+1} \exp \left[ -2\pi i r_{ik} K \cos\theta \right] d(-\cos\theta) \\
 &= \left[ \frac{\exp[-2\pi i r_{ik} K \cos\theta]}{-2\pi i r_{ik} K} \right]_{-1}^{+1} \\
 &= \frac{\exp(2\pi i r_{ik} K) - \exp(-2\pi i r_{ik} K)}{2\pi i r_{ik} K} = \frac{2i \sin(2\pi r_{ik} K)}{2\pi i r_{ik} K}
 \end{aligned}$$

$$= \frac{\sin(2\pi r_{ik}K)}{\pi r_{ik}K} \quad (5)$$

We rewrite Eq. (4), using Eq. (5)

$$\begin{aligned} \therefore \hat{a}(\vec{K}) &= 2\pi \int_0^\infty a(\vec{r}_{ik}) r_{ik}^2 \frac{\sin(2\pi r_{ik}K)}{\pi r_{ik}K} dr_{ik} \\ &= 2 \int_0^\infty a(\vec{r}_{ik}) r_{ik} \sin(2\pi r_{ik}K) dr_{ik} \\ &= \frac{2}{K} \int_0^\infty a(\vec{r}_{ik}) r_{ik} \sin(2\pi r_{ik}K) dr_{ik} \end{aligned} \quad (6)$$

$$\text{Similarly } \hat{b}(\vec{K}) = \frac{2}{K} \int_0^\infty b(\vec{r}_{kj}) r_{kj} \sin(2\pi r_{kj}K) dr_{kj}$$

Hence  $\hat{I}(\vec{K})$  can be calculated by calculating  $\hat{a}(\vec{K})$  and  $\hat{b}(\vec{K})$ . In the calculation of  $\hat{a}(\vec{K})$  and  $\hat{b}(\vec{K})$  we see that we have to do the sine transformation of the corresponding quantities. We have done this with the help of a subroutine for calculation of the FFT by NAG Library (C06FJF). The method of calculation of the sine transform using the FFT algorithm is shown below.

$$(b) \text{ Calculation of the integral } \int_0^\infty f(r) \sin kr \, dr \text{ or } \int_0^\infty f(r) \cos kr \, dr$$

for all  $k$  using an FFT algorithm:

An FFT algorithm accomplishes the following transformation of a set of  $N$  numbers,  $f_j$  ( $j=0\dots N-1$ ) to a set of  $N$  number  $f_k$ :

$$f_k = \frac{1}{\sqrt{N}} \sum_{j=0}^{N-1} f_j \exp\left(-\frac{2\pi i j k}{N}\right) \quad (7)$$

Let us consider a set  $f_j$  ( $j = 0;\dots N$ ) obtained by symmetrizing (or antisymmetrizing) a set  $f_j'$ . Then the  $N$  numbers  $f_j$  can be

subdivided into two groups  $f_j$ , and  $f_{j''}$  such that  $j' = N - j''$  and  $f_{j'} = \pm f_{j''}$ . Then, we obtain, with  $j'' = \frac{N}{2}$ ,

$$\sum_{j=0}^{N-1} = \sum_{j=0}^{N/2} + \sum_{j=(N/2)+1}^{N-1} \quad \text{if } N \text{ is even and} \quad (8a)$$

$$\text{with } J'' = \frac{(N-1)}{2}$$

$$\sum_{j=0}^{N-1} = \sum_{j=0}^{(N-1)/2} + \sum_{j=(N+1)/2}^{N-1} \quad \text{if } N \text{ is odd.} \quad (8b)$$

In both cases ( $N$  even or odd)  $f_0 = \pm f_N$  (+ for symmetrized set, - for antisymmetrized set) but  $f_N$  is not a member of the set  $f_j$  ( $j=0 \dots N-1$ ). Thus in this set, there is a small asymmetry present in the midst of symmetry and antisymmetry; otherwise the last number  $f_{N-1} = \pm f_1$ , which is the second member of the set ( $f_0$  being the first) and  $f_N$  does not appear, making  $f_0$  without its counterpart. If  $N$  is even, the symmetry or antisymmetry is around  $f_{N/2}$ , which acts as the center of symmetry. Thus, we have a mid point of the set. If  $N$  is odd, no point can be identified as the midpoint; the change over to the symmetrized or the antisymmetrized set takes place in going from  $f_{(N-1)/2}$  to  $f_{(N+1)/2}$ , i.e.,  $f_{(N-1)/2} = \pm f_{(N+1)/2}$ .

Let us take  $N$  to be even. Let us write the expression of

$f_k$  as

$$f_k = \frac{1}{\sqrt{N}} \sum_{j=0}^{N/2} + \frac{1}{\sqrt{N}} \sum_{j=(N/2)+1}^{N-1} = S_1 + S_2$$

(Combining terms with  $j' = j''$ )

$$= f_0 + 2 \sum_{j'=1}^{(N-1)/2} f_j \cos \frac{2\pi j' k}{N} \text{ (if the set is symmetrized)}$$

or

$$f_0 - 2i \sum_{j=2}^{(N-1)/2} f_j \sin \frac{2\pi j k}{N} \text{ (if the set is antisymmetrized)}$$

In this case it is not necessary to set  $f_{N/2} = 0$ .

Hence to obtain sine transform we antisymmetrize our data set and call the Fourier transformation subroutine from the NAG library, (C06FJF). When we obtain the transformed values we discard the real part which is equivalent to  $f_0$  described above and we take the imaginary part into consideration and divide it by -2. Also we multiply this by  $\sqrt{N}$  and  $T/N$ , where  $T$  is the total range of the value which is Fourier transformed. Then each value is multiplied by corresponding value of  $2/K$  (Eq. 6). We thus obtain  $\hat{a}(\vec{k})$  and  $\hat{b}(\vec{k})$ . The two sets are multiplied (for the same  $\vec{k}$ ) to obtain  $I(\vec{k})$  (Eq. 3). Once we get  $\hat{I}(\vec{k})$ , we carry out inverse Fourier transformation to get the value of the integral as a function of  $\vec{r}_{ij}$ .



$$\begin{aligned}
 I(\vec{r}_{ij}) &= \int \hat{I}(\vec{k}) e^{2\pi i \vec{k} \cdot \vec{r}_{ij}} d\{\vec{k}\} \\
 &= \int \hat{I}(\vec{k}) e^{2\pi i k r_{ij} \cos\theta} k^2 \sin\theta d\theta d\phi dk
 \end{aligned}$$

( $\theta, \phi$  specify orientation of  $\vec{k}$  vector with respect to  $\vec{r}_{ij}$ ,  $k$  is the magnitude of  $\vec{k}$ )

$$= \int_0^{2\pi} d\phi \int_0^\infty dk k^2 \hat{I}(k) \int_0^\pi e^{2\pi i k r_{ij} \cos\theta} (\sin\theta d\theta)$$

Using  $\int_0^\pi e^{2\pi i k r_{ij} \cos\theta} \sin\theta d\theta = \frac{2i \sin(2\pi k r_{ij})}{2\pi k r_{ij}}$ , we obtain

$$\begin{aligned}
 I(\vec{r}_{ij}) &= \frac{4\pi}{2\pi r_{ij}} \int_0^\infty \hat{I}(k) k \sin(2\pi k r_{ij}) dk \\
 &= \frac{2}{r_{ij}} \int_0^\infty \hat{I}(k) k \sin(2\pi k r_{ij}) dk
 \end{aligned}$$

Hence the inverse Fourier Transformation is also a sine transformation. After getting the transformed values, we multiply them by  $\sqrt{N}$ ,  $\frac{T}{N}$ ,  $-\frac{1}{2}$  and  $\frac{2}{r_{ij}}$ . Thus we get the value of the integral  $a*b$ .

In a nutshell, the procedure of calculating  $a*b$  is: Take  $a(r_{ij})$  (i) multiply by  $r_{ij}$ , (ii) antisymmetrize, (iii) FT, (iv) multiply imaginary part by  $\sqrt{N}$ ,  $\frac{T}{N}$ ,  $-\frac{1}{2}$  and  $\frac{2}{k}$ ; now we have  $\hat{a}(k)$ , (v) do the same to obtain  $\hat{b}(k)$ , (vi) multiply  $\hat{a}(k)$  by  $\hat{b}(k)$  for same  $k$ ; obtain  $\hat{I}(\vec{k})$  multiply by  $k$ , (vii) antisymmetrize (viii) FT, (ix) multiply imaginary part by  $\sqrt{N}$ ,  $\frac{T}{N}$ ,  $-\frac{1}{2}$  and  $\frac{2}{r}$ .

In the discussion that follows we use the following abbreviations.

$c_m$  = Concentration of macroion (M),

$r_m$  = Macroion radius, ( $\text{\AA}^0$ ),

$c^-$  = Concentration of univalent negative ion (M),

$cdnst$  = Charge density on macroion surface as one electronic charge per so many  $\text{\AA}^{02}$

IS = Ionic strength of the solution,

Reduced distance  $d_r$  = actual distance/macroion radius.

The same abbreviations have been used in the graphs.

## 5.2 Number of Points in F.T. Operations

To begin with we used 1400 points in Fourier Transformation. This seems to give correct values of transformation both in the forward ( $r \rightarrow t$ ) and backward ( $t \rightarrow r$ ) direction. Correctness has been verified by calculating the integral  $g(t) = \int_0^{\infty} f(r) \sin tr \, dr$  (and its inverse  $f(r) = \int_0^{\infty} g(t) \sin tr \, dt$ ) by direct numerical integration using a NAG subroutine and by Fourier Transformation method described above and then comparing the values. The error increases as the function becomes more steep. The solution of the problem is to increase the number of points in the steep part of the function. The ideal way to handle it is to have a larger density of points in the steep part and a smaller density of points in the not so steep part of the function. This has been done by Rossky and Friedman (1) using an algorithm by Talman (2). We have not used this algorithm even though we perhaps should have. We now plan to use Talman's algorithm and verify that the results remain unchanged. However being conscious of

this problem we have carried out the Fourier transformation at two different values of the number of points (1400, 5200) used to cover the same range in r-space ( $1000 \text{ \AA}^0$ ). The results have not changed at  $\text{cdnst} = 19200, 4800$  and  $1200$  at  $r_m = 200$  and  $300$ . The results change marginally near the hard sphere radius for  $\text{cdnst} = 300$  and  $600$  at  $r_m = 200$ . At  $\text{cdnst} = 100$ , the change is larger, once again near the hard sphere radii. This is why we have not reported these values. In several systems studied, the correlation function did not level off to 1 even at  $r = 1000 \text{ \AA}^0$ . Quite obviously these systems require a larger range and a larger number of points to acquire correct results. The reason why larger number of points ( $> 5200$ ) could not be used in this work is very easily rectifiable. We used NAG software which has been implemented only in our HP-9000 supermini systems. The programme was originally developed using NAG in HP. It was not anticipated that a larger number of points will become crucial. We can without much difficulty upgrade our programme to the Convex-220 mini super system. The software library changes to VECLIB, a small alteration.

Two purposes are served by increasing the number of points in F.T. operations. The first is to scan the r-space more properly. The second is that as the number of points to represent the function in r-space is increased, the range covered in t-space ( $t_{\text{max}} = \frac{N - 1}{\text{range of } r}$ , where  $N$  is the total number of points used in representing the function in r-space) increases. For a system with a large value of kappa i.e. systems with high packing fraction and high charge density (viz.  $r_m = 200 \text{ \AA}^0$  or  $300 \text{ \AA}^0$ ,  $c_m = 1 \times 10^{-6}$ ,  $\text{cdnst} = 100$ ), the function in r-space has a

short range (functional form being  $e^{-\kappa r}/r$ ). This means that the function spreads out in t-space. If increasing the number of points did not alter the results, it must mean that we have adequately covered the function in t-space. It is therefore understandable that we obtain changes (when we change number of points) in numerical results only for systems with high charge and high packing fraction. We note that there are several recent literature reports (3,4) on highly charged asymmetric polyionic system where no change in numerical results were obtained by carrying out F.T. operations using the Talman algorithm of using unevenly spaced data samples. The particle charges studied in our work is however higher than those in Refs. 3 and 4. This aspect needs more careful investigation.

### .3 The Problem of Nonconvergent Iterations in Solution of HNC Equation

We now discuss the problem, already known in the literature (5-8), of not obtaining convergence of the iterative procedure used in solving the HNC equation. Our experience is as follows:

We have not been able to run systems with macroion radius ( $r_m$ ) = 400  $\text{\AA}$  and above, at  $\text{cdnst} = 4800$  and several ionic strengths. Since systems with this charge density have been run successfully with lower  $r_m$ 's (200  $\text{\AA}$ , 300  $\text{\AA}$ ), we decided not to investigate other parameters at  $r_m = 400$ . Macroion radii larger than 400  $\text{\AA}$  were also tried, but without success.

At macroion concentrations  $5 \times 10^{-6} \text{M}$  and above, we did not obtain convergent solutions over a wide range of parameters.

3. The most thoroughly investigated systems are with macroion concentration  $1 \times 10^{-6} \text{M}$ . At this concentration with  $200 \text{ \AA}^0$  macroion radii and at all charge densities studied we could not obtain convergent solutions above a  $c^-$  value greater than  $0.001 \text{ M}$ . The same is true with  $300 \text{ \AA}^0$  macroion radius except for the  $\text{cdnst} = 4800$ , where the system with  $c^- = 0.001$  did not converge.
4. At macroion radius  $20 \text{ \AA}^0$ , there is virtually no problem in obtaining convergent solutions. However, quite surprisingly at  $50 \text{ \AA}^0$  radius we had problem with systems having  $\text{cdnst} = 100, 300$  at all ionic strength. The macroion concentration is  $1 \times 10^{-6} \text{M}$ . But at a  $\text{cdnst} = 600$ , we are able to get convergence. We did not investigate lower charge density. We note that, contrary to our expectation there is no problem in obtaining the convergence at higher charge densities for a macroion radius of  $200 \text{ \AA}^0$ , whereas at  $r_m = 50 \text{ \AA}^0$ , we had difficulties.
5. At macroion concentration of  $1 \times 10^{-7} \text{M}$ , systems with  $c^- = 0.01 \text{M}$  and higher values did not converge. In general we did not have problem at other values of parameters here, as well as at lower macroion concentration. However, the variation of parameters at these macroion concentration is less extensive.
6. The calculation of the total volume occupied by the small ions of the background electrolyte shows that they contribute to the packing fraction (fraction of the total volume occupied by the hard sphere) by about  $0.003$ . Since HNC theory is known to handle solutions of electrolytes of

symmetrical small ions upto molar concentrations, the failure to obtain convergence at 0.01 M concentration of the background electrolyte of the macroionic solution studied is not related to high packing fraction.

7. The major contributor to packing fraction is the macroion. A  $1 \times 10^{-6}$  M solution of 200 Å<sup>0</sup> macroion radius has a packing fraction contribution from macroions of about 0.0192. The maximum charge studied at  $c^- = 0.0$  M (two component system) and  $cdnst = 100$  is 5024 electronic charge. Because of the difficulties discussed in section 5.2, our results at  $cdnst = 100$  may not be fully reliable, yet we think the convergence problems will not be there even when these difficulties were removed. However the convergence obtained with systems having  $cdnst = 300$  is reliable. The total particle charge is about 1700 electronic charge.
8. Numerical experiments on systems with  $r_m = 300$ , show that convergence is not obtained at  $cdnst = 300, 600$ , but is obtained at  $cdnst = 1200$  at  $c_m = 1 \times 10^{-6}$  and  $c^- = 0, 10^{-5}, 10^{-4}, 10^{-3}$ . The packing fraction of this system is 0.064. The total particle charge studied at this packing fraction is 900e.
9. Recent application of HNC theory to macroion solution with high asymmetry of charge and size has found it difficult to obtain solution for particle charges greater than 100e at a lower packing fraction of 0.04 (6), in spite of considerably modified numerical technique. The only paper that reports a study of colloids of higher particle charge is due to Khan et al (7). They treat macroion-macroion correlation by HNC

and macroion-small ion correlation by MSA. They have studied larger macroion radii than we could study viz. radius of  $436 \text{ \AA}^0$ , but at considerably lower packing fraction (.0002), with particle charges upto 450. Particle radius of  $1170 \text{ \AA}^0$ , particle charge of 432 e, and radius  $436 \text{ \AA}^0$ , charge 500 e and 11000 e, have been studied but at a particle density two orders of magnitude less than that in our study. The maximum packing fraction they study is in the system with  $Z = 432e$  and  $r_m = 1170 \text{ \AA}^0$ . The value is  $\sim 0.01$ , significantly less than that in the  $r_m = 300 \text{ \AA}^0$  system studied by us, where  $Z = 900 e$  is studied at a packing fraction of 0.064. The 11000 e particle charge studied by Khan et al (7) is at a packing fraction of 0.001. The other recent reports (8-16) study particle charge below 100 e.

10. It is therefore a fair claim that the use of Allnatt's HNC equation considerably improves the situation regarding the difficulty of obtaining convergent solution of the HNC equation. This must be due to the use of a different closure than used by other workers. They use the usual HNC closure (Eq. 5.19 of Ref. 17) which can be written as

$$c(r) = -\beta u(r) + h(r) - \log (h(r) + 1)$$

Now  $\tau(r) = h(r) - c(r)$ . <sup>(Eq 63, p146)</sup> Hence  $h(r) = e^{g(r)+\tau(r)}$  where  $g(r) = -\beta u(r) = -\frac{z_1 z_2}{rkT}$ . The closure used in Allnatt equation is

$$h(r) = e^{g(r) + \tau(r)}$$

where  $q(r) = (e^{-\kappa r}/r) z_1 z_2$ ,  $q(r)$  is a sum of g-bond chains and its range is considerably less than a g(r) bond.

a certain particle number density ( $c^- < 10^{-5}$ ) however, this number density does not affect the graphs. (Figs. 5.1 and 5.2). This is expected because then even Belloni's  $\kappa$  is affected to a smaller extent. As one goes to  $c^- = 1 \times 10^{-3}$  (Fig. 5.4) at  $r_m = 300$  and  $cdnst = 4800$ , we obtain a  $g(r)$  vs.  $r$  graph that shows substantial attraction ( $g(r) > 1$ ) almost all over, if  $c_m = 1 \times 10^{-7}$ , in sharp contrast to  $c_m = 1 \times 10^{-8}$  which remains repulsive althrough and shows no feature of attractive correlation at all. The system at  $c_m = 1 \times 10^{-6}$  fails to converge. The large attraction ( $cdnst = 4800$ ,  $r_m = 300$ ) at  $d_r \sim 2.66$  is a significant change in going from  $c^- = 1 \times 10^{-4}$  to  $c^- = 1 \times 10^{-3}$ . Of course, the increase in small ion concentration ( $c^-$ ) in going from  $1 \times 10^{-4}$  to  $1 \times 10^{-3}$  is also more significant in absolute terms than an increase from  $1 \times 10^{-5}$  to  $1 \times 10^{-4}$  even though it is ten fold in both cases. Even though in both  $c_m = 1 \times 10^{-7}$  and  $1 \times 10^{-8}$ , features of attractive correlation increase with rise in  $c^-$ , at  $c_m = 1 \times 10^{-6}$ , attractive features diminish in going from  $c^- = 1 \times 10^{-5}$  to  $1 \times 10^{-4}$ . The iteration gives nonadmissible numbers and fails to converge at  $c^- = 1 \times 10^{-3}$  ( $c_m = 1 \times 10^{-6}$ ). Thus the increase in features of attractive interaction with increase in  $c^-$  is not always seen. Thus, it is a complicated effect and cannot be always understood in terms of a simple model of interaction between dressed macroions whose effective charge decreases as  $c^-$  increases with increased counterion condensation. Effective charge of a dressed macroion is a complicated quantity involving both the counterion and the coion distribution. One more point about the graph at  $c^- = 1 \times 10^{-3}$  : The scale used to accommodate a large value of  $g(r)$  at its maximum hides the fact that the curve starts being



repulsive, becomes attractive to level off to  $g = 1$  at large  $d_r$ . We note that a value of  $g = 88$ , in terms of energy is not as large,  $w = -kT \ln g$  gives  $w$  per mole to be  $-2.76 \text{ k cal mole}^{-1}$ , whereas  $g = 10$  would give half as much. The graphs in Figs. 5.1, 5.4 are given at a fixed  $c^-$  as a function of  $c_m$ . Turned around they are shown at a fixed  $c_m$  as a function of  $c^-$  in Figs. 5.5 and 5.6.

(ii)  $r_m = 300$ ,  $cdnst = 19200$  (Figs. 5.7-5.11)

The trends discussed above are now studied at  $cdnst = 19200$ . The graphs at  $c^- = 0$  (Fig. 5.7) and  $1 \times 10^{-5}$  (Fig. 5.8) are nearly superimposable, but those at  $c^- = 1 \times 10^{-4}$  (Fig. 5.9) once again differ from those at  $c^- = 1 \times 10^{-5}$  (Fig. 5.8). Whereas at  $c^- = 0$  and  $1 \times 10^{-5}$ , the  $c_m = 1 \times 10^{-8}$  graphs are highly repulsive such that even at  $r = 1000 \text{ \AA}^0$ , they do not level off to  $g(r) = 1$  and remain fixed to the x-axis; they observably rise towards  $g(r) = 1$  at  $c^- = 1 \times 10^{-4}$ . The graph at  $c_m = 1 \times 10^{-6}$  although repulsive ( $g(r) < 1$ ) at all  $r$  at both  $c^- = 1 \times 10^{-5}$  and  $1 \times 10^{-4}$  shows visible difference in shape. In contrast to  $c_m = 1 \times 10^{-6}$  graphs at  $cdnst = 4800$  (at all  $c^-$  values), which show predominantly attractive  $g(r)$ , the corresponding graphs at  $cdnst = 19200$  are repulsive althrough. The extent of repulsive effects is smaller at higher  $c^-$ . The graphs in Figs. 5.7 to 5.9 are at fixed  $c^-$  as a function of  $c_m$ . The same graphs at a fixed  $c_m$  as a function of  $c^-$  are shown in Figs. 5.10 and 5.11. Figure 5.11 shows a progressively decreasing repulsive feature of the graphs as  $c^-$  goes from 0,  $10^{-5}$ ,  $10^{-4}$  to  $10^{-3}$  ( $c_m = 1 \times 10^{-7}$ ,  $cdnst = 19200$ ), the last graph shows an attractive peak. This last graph is not shown in Figs.

5.7 to 5.9 because at  $c^- = 1 \times 10^{-3}$ , systems with  $c_m = 1 \times 10^{-6}$  did not converge.

(iii)  $r_m = 200$ ,  $cdnst = 4800$  (Figs. 5.12-5.18)

Once again  $c^- = 1 \times 10^{-5}$  graphs (Fig. 5.13) are superimposable on  $c^- = 0$  graphs (Fig. 5.12) but differ from those at  $1 \times 10^{-4}$  (Fig. 5.14) and  $1 \times 10^{-3}$  (Fig. 5.15) significantly at all values of  $c_m$ . Once again  $c_m = 1 \times 10^{-6}$  graphs show peaks. They are repulsive at lower  $d_r$ , become attractive at larger  $d_r$ , show a peak, only to level off to  $g(r) = 1$  at  $d_r \sim 5.0$ , i.e.  $r = 1000 \text{ \AA}$ . The peak becomes more intense and shifts to larger  $d_r$  as  $c^-$  decreases from  $1 \times 10^{-3}$  to  $1 \times 10^{-4}$  to  $1 \times 10^{-5}$ . This is reminiscent of shorter bond distance in diatomic molecules with larger electron density in between them. In this case larger  $c^-$  means larger counterion condensation and therefore the equivalence to larger electron density. However, as the peak shifts to shorter  $\tilde{r}$ , the  $g$  value at the peak becomes smaller. At shorter distances increase in the magnitude of repulsion is responsible for making the  $g$ -value smaller. In agreement with the trend discussed above, the decreased repulsion at higher ionic strength the graphs at  $c_m = 10^{-7}$  and  $10^{-8}$  are less repulsive at  $c^- = 10^{-3}$  compared to those at  $c^- = 10^{-4}$  and  $10^{-5}$ . The more attractive  $g(r)$  vs.  $r$  graphs at higher  $c_m$  values also corroborate the trend seen at  $r_m = 300$ , which we may call, effective shielding of macroion-macroion correlation due to macroions. The graphs in Figs. 5.12-5.15 are at fixed  $c^-$  as a function of  $c_m$ . The same graphs at a fixed  $c_m$  as a function of  $c^-$  are shown in Figs. 5.16-5.18.

(iv)  $r_m = 200$ ,  $cdnst = 19200$  (Fig. 5.19-5.25)

At  $c^- = 0$  (Fig. 5.19) and  $c^- = 10^{-5}$  (Fig. 5.20), graphs of this system for  $c_m = 1 \times 10^{-7}$  and  $1 \times 10^{-8}$  differ from each other to some extent in sharp contrast to similar pairs of systems (at  $r_m = 300$ ,  $cdnst = 4800$ ,  $19200$  and  $r_m = 200$ ,  $cdnst = 19200$ ) considered earlier, where virtually no difference existed and graphs were nearly superimposable. This has its origin perhaps in the fact that the change in ionic strength is not insignificant (for  $c_m = 1 \times 10^{-7}$  and  $1 \times 10^{-8}$ ) in going from  $c^- = 0$  to  $c^- = 10^{-5}$  whereas the corresponding change is comparatively much less (~3% compared to 30% and 400%) in  $c_m = 1 \times 10^{-6}$  graph, which does not change significantly.  $c^- = 0$  to  $10^{-5}$  changes not only,  $\kappa$  but also particle density in HNC equation. However, the change in particle density is small since  $10^{-5}$  is on an absolute scale small. We recall that in the system  $r_m = 300$ ,  $cdnst = 4800$  particle density change had an observable effect in going from  $c^- = 10^{-5}$  to  $10^{-4}$ , the ionic strength did not change significantly. Similar ionic strength effect actually exists in  $r_m = 300$ ,  $cdnst = 19200$  system also, but shows up insignificantly on the graphs. At  $c_m = 1 \times 10^{-8}$ , the graph shows some change, hard to see on the scale used in the graph, as one goes from  $c^- = 0$  to  $c^- = 1 \times 10^{-5}$ , but absolutely no change is seen at  $c_m = 1 \times 10^{-7}$  and  $1 \times 10^{-6}$ . This is connected with the fact that  $c^- = 0$  to  $c^- = 1 \times 10^{-5}$  introduces more significant ionic strength change only at  $c_m = 1 \times 10^{-8}$  (~50%) than at  $c_m = 1 \times 10^{-6}$  (~5%) and  $1 \times 10^{-7}$  (~2%). On going to  $c^- = 1 \times 10^{-4}$  (Fig. 5.21) and  $1 \times 10^{-3}$  (Fig. 5.22) all the graphs show progressive decrease in features of repulsive correlation. The graphs seen in Fig. 5.19-5.22 are at a fixed

$c^-$  as a function of  $c_m$ . The same graphs at a fixed  $c_m$  as a function of  $c^-$  are shown in Figs. 5.23-5.25.

(v) Higher  $cdnst$ , 600 and 1200 (Fig. 5.26-5.29)

We now examine graphs in Figs. 5.26, 5.27 and 5.28. At  $cdnst = 600$  and  $c_m = 1 \times 10^{-7}$ ,  $r_m = 200$  (Fig. 5.26),  $c^- = 0$  and  $10^{-5}$  graphs are indistinguishable, both showing a peak in the graph. At  $c^- = 10^{-4}$ , the peak increases in magnitude and shifts towards lower  $d_r$ , both shifts are small. At  $c^- = 10^{-3}$ , significantly more change is seen, the peak shifts much closer to  $d_r = 2$ , and increases in amplitude significantly. At  $cdnst = 1200$ ,  $c_m = 1 \times 10^{-6}$  (Fig. 5.27),  $r_m = 200$ ,  $c^- = 0$ ,  $10^{-5}$ ,  $10^{-4}$  are superimposable but the graph corresponding to  $c^- = 10^{-3}$  changes significantly. However the feature of attractive correlation decreases at  $c^- = 10^{-3}$ . All the graphs show attraction at hard sphere contact. Fig. 5.28 ( $cdnst = 600$ ,  $c_m = 1 \times 10^{-7}$ ,  $r_m = 300$ ) shows identical features as Fig. 5.27, only the numbers change a little bit.

We have seen earlier in Figs. 5.12-5.18 that at  $r_m = 200$ ,  $cdnst = 4800$ ,  $c_m = 1 \times 10^{-6}$ , the  $g(r)$  vs.  $r$  plot shows a peak that shifts towards smaller  $d_r$  and the magnitude of  $g$  at the peak decreases monotonically as  $c^-$  increases. Fig. 5.27 shows systems with  $c_m = 1 \times 10^{-6}$  and show the same trend; since all the graphs show attraction at hard sphere contact, we do not see any shift, but the magnitude of  $g$  at  $d_r = 2$  falls at  $c^- = 10^{-3}$  from those at  $c^- = 0$ ,  $10^{-5}$ ,  $10^{-4}$ . The trend in Fig. 5.26 is the same as that discussed above as far as shift is concerned, but the change in magnitude shows opposite trend. We note that these figures are obtained at  $c_m = 1 \times 10^{-7}$ . When  $r_m$  is increased to 300 at the same

cdnst as shown in Fig. 5.28, the trends shift over to that seen in Fig. 5.27 where cdnst is larger (1200 instead of 600) but size is smaller ( $r_m = 200$ ). We note that the net charge on  $r_m = 300$  particle is 943 e, and that on  $r_m = 200$  particle is 838 e. The features of  $g(r)$  vs.  $r$  graphs seem to depend only on the total charge, in these cases.

Figure 5.29 is the graph of a system with  $r_m = 300$ ,  $c_m = 1 \times 10^{-8}$ ,  $cdnst = 600$ ,  $c^- = 1 \times 10^{-3}$ . It shows a sharp peak at very close to hard sphere contact, which falls off rapidly to unity at  $d_r \sim 2.05$ . In Fig. 5.28, we studied  $r_m = 300$ ,  $cdnst = 600$ ,  $c_m = 1 \times 10^{-7}$  systems. The  $c^- = 10^{-3}$  plot shows an attraction at hard sphere contact, but a  $g$ -value which is smaller, yet attractive. The change is due to change in  $c_m$ . Increase in  $c_m$  causes shielding of macroion-macroion repulsive interaction, because at  $c_m = 1 \times 10^{-8}$ ,  $g \sim 1$  at hard sphere contact, but at  $c_m = 1 \times 10^{-7}$ ,  $g \sim 5$ . The peak in  $g(r)$  vs.  $r$  graph that we see at  $c_m = 1 \times 10^{-8}$  (Fig. 5.29) is however larger than that at  $c_m = 1 \times 10^{-7}$  (Fig. 5.28) seen at hard sphere contact.

(vi)  $r_m = 20$  (Fig. 5.30-5.35)

Figures 5.30 and 5.31 show graphs at  $r_m = 20$ ,  $c_m = 1 \times 10^{-8}$  and  $cdnst = 300$  and  $600$  respectively as a function of  $c^-$ . In both figures, we observe a progressive shielding of repulsive interaction as  $c^-$  increases. The repulsive correlation is less for  $cdnst = 600$  compared to that at  $cdnst = 300$  at low  $c^-$ . The difference disappears at high  $c^-$ . All this is anticipated according to classical models of colloidal interaction. The same comments hold for Figs. 5.32 and 5.33 which are for systems at  $c_m = 1 \times 10^{-7}$  but are otherwise identical to those in Figs. 5.30

and 5.31. Comparison between these two pairs show that repulsive correlation is less severe (both at  $cdnst = 600$  and  $300$ ) at higher macroion concentration, at low  $c^-$  ( $0, 10^{-5}$ ). This effect has been seen earlier. The shielding by macroions disappears at higher  $c^-$ . A look at graphs with  $r_m = 20$ , and  $c_m = 1 \times 10^{-6}$  (Figs. 5.34-5.35), show that shielding of macroion-macroion correlation by macroions increases at higher  $c_m$  and the difference is visible even at higher  $c^-$  values, e.g.,  $cdnst = 600$  graphs show considerably less repulsive correlation (difference exists even for  $c^- = 10^{-3}$  and  $10^{-2}$ , but very little for  $10^{-1}$ ). We note that ionic strength differs significantly ( $\sim 10\%$ ) at  $c^- = 10^{-3}$ , less so at  $c^- = 10^{-2}$  and  $10^{-1}$  ( $\sim 1\%$ ).

**Effect of Charge:** The effect of  $cdnst$  alone is brought out in Figs. 5.37 to 5.39. These graphs are all at  $c_m = 1 \times 10^{-6}$  and  $r_m = 200$  at different  $c^-$  values. The  $cdnst = 1200$  is the least repulsive graph.  $cdnst = 4800$  is more repulsive than the lower  $cdnst = 19200$  in Fig. 5.38 nearly over all  $r$  values. In Fig. 5.37 and 5.39 these two plots cross each other. There is clearly a balance between their larger intrinsic charge, which increases repulsion and their increased ability to condense counterions which decreases repulsion. In Figs. 5.40 to 5.42, are shown systems with  $r_m = 200$ ,  $c_m = 1 \times 10^{-7}$  at different  $c^-$  values. The  $cdnst = 1200$  is once again the least repulsive graph.  $cdnst = 4800$  is clearly the least repulsive and  $cdnst = 19200$  lies in between. The factors responsible for this relative ordering are the same as those in Figs. 5.37-5.39. The relative ordering of 4800 and 19200 change as one goes to  $r_m = 300$ ,  $c_m = 1 \times 10^{-6}$  at

different  $c^-$  values (Figs. 5.43-5.44). This is a result of increased particle charge (even though  $cdnst$  values are the same), which affect both intrinsic repulsion and increased counterion condensation and resulting shielding. In Fig. 5.45 and Fig. 5.46 ( $r_m = 300$ ,  $c_m = 1 \times 10^{-7}$ ,  $c^- = 0$ ), we find  $cdnst = 600$  to be least repulsive of all three graphs,  $cdnst = 4800$  being most repulsive, whereas  $cdnst = 19200$  lies in between.

In Fig. 5.47 ( $r_m = 300$ ,  $c_m = 1 \times 10^{-7}$ ,  $c^- = 1 \times 10^{-4}$ )  $cdnst = 600$  is least repulsive,  $cdnst = 4800$  is most repulsive,  $cdnst = 19200$  lies in between. In Fig. 5.48 ( $r_m = 300$ ,  $c_m = 1 \times 10^{-7}$ ,  $c^- = 1 \times 10^{-3}$ ) there is a cross-over between  $cdnst = 600$  and  $cdnst = 19200$  graphs, but it is fair to say that  $cdnst = 600$  is less repulsive over a wide range of  $r$  values.  $cdnst = 4800$  (Fig. 5.6(b)) shows a significant attractive peak in contrast to that seen in  $c^- = 1 \times 10^{-4}$  graph (Fig. 5.47).

Figs. 5.49-5.57 show  $g(r)$  vs.  $r$  graphs at  $r_m = 20$  at  $c_m = 1 \times 10^{-6}$  and  $1 \times 10^{-7}$ . Each graph is shown as a function of  $cdnst$  and  $c^-$  is varied from one graph to another. In all of them, shielding is more at lower  $cdnst$  (600) than at higher (300). As  $c^-$  increases, keeping  $c_m$  constant (Figs. 5.49-5.52), shielding increases. The same is true with  $c_m = 1 \times 10^{-7}$  system (Figs. 5.53-5.57).

**Effect of Size:** An examination of Figs. 5.58 to 5.60 show three graphs at  $cdnst = 4800$ ,  $c_m = 1 \times 10^{-6}$  at varying values of  $c^- = 0$ ,  $1 \times 10^{-5}$ ,  $1 \times 10^{-4}$ . The graph of  $r_m = 300$  shows attractive correlation at hard sphere contact, but shows features of

The shielding due to macroions increases at a given charge density with size. This is visibly clear on comparing say Figs. 5.9 and 5.21. However, this may be purely an effect of increasing total particle charge. A comparison of shielding by macroions of  $r_m = 200$ ,  $cdnst = 4800$  (Fig. 5.14) with that of  $r_m = 300$ ,  $cdnst = 19200$  (Fig. 5.8) shows that the former is more efficient in screening. In this case the total particle charge is larger for  $r_m = 200$  system. It would be of some interest to compare two systems with identical total charge, but different size, to fish out size effect alone.

The attractive peak in  $g(r)$  versus  $r$  graphs: This aspect is discussed in Chapter I. We discuss it here in connection with our results. Patey (18) observed strongly attractive forces between a pair of similarly charged macroions in his HNC calculation on an infinitely dilute macroion solution. This observation is contrary to classical ideas on colloids, which are believed to have repulsive interactions at all distances. Teubner (19) pointed out that this attraction may be an artifact of the HNC theory and suggested that the inclusion of the highly connected bridge diagrams neglected in the HNC approximation will lead to the disappearance of the peak in  $g(r)$  versus  $r$  graphs discovered by Patey (18). The calculation of  $g(r)$  of macroionic particles by the three point extension (TPE) of HNC theory by Sanchez and Lozada-Cassou (20) show no peak. The proponents of TPE of HNC theory believe that the bridge diagrams of interaction of two particles held by a dumbbell in this calculation get included in the two particle correlation function eventually



calculated. Sanchez and Lozada-Cassou (20) claim that the TPE-HNC results which show no peak in the  $g(r)$  versus  $r$  graphs prove Teubner's contention (19) that the peak in  $g(r)$  vs.  $r$  graph is an artifact of the neglect of bridge diagrams in HNC theory, since TPE-HNC introduce the effect of bridge diagrams. However, in the investigations carried out on application of the HNC theory to macroionic solution in the 1980's and early 1990's, show these attractive features over and over again. Bratko et al (4) observe an attractive maximum in the  $g_{MM}$  (macroion-macroion) vs.  $r$  graphs at a distance of  $5.1 \text{ \AA}$  (reduced distance  $d_r = 3.0$ ),  $Z_m$  (macroion charge) = -40 with HNC (for all ion pairs) and HNC-PY (HNC for macroion-macroion and PY for macroion-ion, ion-ion) closures. A similar attractive maximum is seen in systems with  $Z_m = -60$  at a distance  $\sim 5 \text{ \AA}$  ( $d_r = 5.0$ ), where solutions are obtained from integral equations (HNC and HNC-PY, as above) and Monte-Carlo calculations. The magnitude of  $g$  at its maximum is  $\sim 1.2$ . Macroion-ion  $g(r)$  values are also highly attractive indicating that the attractive maxima in  $g_{MM}$  -  $r$  graphs results from piling up of counterions near macroion surface. Linse (15) observed an attractive maximum in  $g_{MM}$  vs.  $r$  graph at a value  $r = 65 \text{ nm}$  ( $d_r \approx 4.0$ ) by HNC and RHNC theory and Molecular Dynamics simulation. The value of  $g$  at the maximum is  $\sim 1.2$ . Attractive maxima are seen in  $g_{MI}$  (macroion-ion) and  $g_{II}$  (ion-ion) vs.  $r$  graphs. Linse (16) also observes a very similar maximum. Khan et al (7) observe an attractive maximum in  $g(r)$  vs.  $r$  graph for a system of colloidal particles of  $872 \text{ \AA}$  diameter, particle density  $2.56 \times 10^{12} \text{ cm}^{-3}$ , a total particle charge of  $11,000e$ . The height of the peak for macroion-macroion

correlation is 22.3 at a point close to the distance of closest hard sphere contact (not explicitly shown in the published graph) and that for macroion-counterion is 104.3. Linse and Jonsson (14) observe an attractive maximum in the  $g_{MM}(r)$  (macroion-macroion) vs.  $r$  plot obtained from Monte-Carlo calculation at a distance of  $50 \text{ \AA}^0$  ( $r_m = 10$ ,  $d_r \approx 5$ ). A similar maximum is obtained in  $g_{II}$  (ion-ion) vs.  $r$  plot. Patey (18) obtains attractive minima in his  $\beta w(r)$  vs.  $r$  plot, where  $\beta w(r) = -\ln g(r)$ . The minima would correspond to maxima in  $g(r)$  vs.  $r$  graph. Patey calculates at infinite dilution, i.e., he has only two macroions with electrolytes in a continuous dielectric in between. The values of  $\ln g(r)$  are 200 (particle charge = 5000e), 100 (4400e), 70 ( $\sim 4000e$ ), 25 ( $\sim 3600 e$ ). Similar large values are obtained in calculations done on system with different parameters but similar values of charge. These values are exceptionally large and are not seen in the calculations done at finite macroion concentrations, in the papers discussed above. The values of  $g$  at the attractive maxima are usually 1.2 to 1.4 but then the particle charges at which these calculations are done are very low ( $< 100e$ ), whereas Patey's calculations are done at values of particle charge that are more than an order of magnitude larger. Linse (16) reports a small maximum ( $g$  value  $\sim 1.4$ ) in the  $g_{MM}(r)$  vs.  $r$  plot. Beresford-Smith et al (21) obtain macroion-macroion correlation function using  $v^{\text{eff}}(r)$  calculated in the OCM using an approximate model and obtain an attractive maximum. The value of  $g$  at the maximum is  $\sim 2$  (at  $r = 500 \text{ \AA}^0$ ,  $r_m = 160 \text{ \AA}^0$ ,  $d_r \approx 3.1$ ;  $Z_m$ , particle charge = 300e). Once again, we have, a small  $g$  at maximum for a small charge.

In the systems studied by us, we have not found values of  $w$  as large as those found by Patey (18). The maximum  $g$  we have found is of the order of  $10^2$ , i.e.,  $w = -4.606 \text{ kT}$ , in contrast to  $w \approx -200 \text{ kT}$  (in one case, even larger negative values). A value of  $-4.606 \text{ kT}$  for  $w$  means a ratio of  $(e^5 : 1$  or  $\sim 100 : 1$  probability of finding the two particles together at that  $r$  where  $g$  vs.  $r$  graph has an attractive maximum compared to that at a larger  $r$  where  $g \approx 1$ . More commonly, the value of  $g$  at the (sometimes at the hard sphere contact) are  $\sim 10$ , i.e.,  $w$  equals  $-2.303 \text{ kT}$ . This means a ratio of  $\sim 10:1$  instead of  $\sim 100:1$ . A ratio of  $100:1$  can perhaps be described as formation of a dimer. A ratio of  $10:1$  indicates a weak dimer. Patey's values (18) of  $-200 \text{ kT}$ , were almost as strong as that of formation of a diatomic molecule. We may point out that Patey also observed stronger "bond", i.e., more negative  $w$  as the macroionic charge increased. We have also observed this trend. Detailed comparison of our results with Patey's cannot be made because the values of macroionic particle charges studied by him are much larger than those used by us. Also he studies a system at infinite dilution. Patey studied three different sized systems,  $d_c = 100 d$  ( $d_c$  = diameter of the colloid,  $d$  = diameter of the counterion),  $d_c = 50 d$ ,  $d_c = 200 d$ . The lowest particle charge studied at which attraction is seen in the first family is  $\sim 1200 e$  (in his notation  $\sigma^* = 0.044$ , particle charge (in units of  $e$ ) =  $\pi (\frac{d_c}{d})^2 \sigma^*$ ), a little less than the maximum charge studied by us at  $r_m = 200$  ( $\sim 1700e$ ) and a little more than that at  $r_m = 300$  ( $\sim 900e$ ). Patey finds in this system,  $w(r)$  at the minimum =  $-50 \text{ kT}$ . We find much less attractive force at higher packing fraction.

The lowest charge studied in the second family ( $d_c/d = 50$ ) is  $\sim 150e$  ( $\sigma^* = 0.021$ ), but at this value of particle charge, repulsive interaction is obtained. Attractive minima in the plot of  $w(r)$  versus  $r$  is obtained at a particle charge of  $\sim 375e$  ( $\sigma^* = 0.050$ ) and the value at the minimum is  $w(r) = -30$  kT. We obtain considerably less attractive correlation in a system of similar charge but at higher packing fraction. The lowest charge studied in the third family ( $d_c/d = 200$ ) at which attractive interaction is seen is quite high ( $15600e$ ). We have not studied any system at this charge. We also note that in Patey's results as salt concentration changes, the value at the minimum of  $w(r)$  vs.  $r$  graph changes, e.g. at 0.1 M. Salt concentration  $w(r)$  (at minimum) =  $-200$  kT at a particle charge of  $\sim 5000e$ , whereas at 0.01M salt concentration,  $w(r)$  at minimum =  $-400$  kT at a particle charge of  $\sim 1900e$ . This is qualitatively the effect of decreased particle charge, which even at low ionic strength (i.e., in a less shielded condition) show stronger attractive forces than a particle with larger charge at higher ionic strength (i.e., more shielded). At much larger packing fraction, we find that  $w(r)$  becomes less negative, i.e., more repulsive. This is not unreasonable. But in the range studied by us, we have also observed decrease of repulsive correlation with increase in macroion concentration, i.e., if we combine Patey's results with ours, the repulsive correlation, first increases and then decreases as macroion concentration increases. The matter needs closer scrutiny.

## 5.5 Calculation of transform of Coulomb Potential for systems with distance-dependent screening constant

In Chapter II, we conclude that the effects of polarization of macroionic dielectric by ions in solution become significant for non-spherical particles. In such a case, screening constant of Coulombic interaction becomes a function of distance. In Chapter III, section 9, we derive an expression of  $q$  bond in  $t$ -space ( $q(t)$ ) for such a system. In order to calculate  $q(t)$ , we require an expression of  $g(t)$ , the transform of the Coulomb potential  $\frac{1}{\epsilon(r)r}$ . We multiply it by  $e^{-\lambda r}$  to handle the problem of divergence

$$g(t) = \frac{4\pi}{t} \int_0^{\infty} g(r) r \sin tr dr = \int_0^{r_0} + \int_{r_0}^{r_{\max}} + \int_{r_{\max}}^{\infty}$$

where  $r_0$  is the macroion radius and  $r_{\max}$  is the distance at which the  $\epsilon(r)$  effectively becomes equal to the bulk dielectric constant  $\epsilon_s$  of the solvent. Between 0 to  $r_0$ , we assume that  $\epsilon(r) = \epsilon_s$  and between  $r_{\max}$  and  $\infty$   $\epsilon(r)$  once again equals  $\epsilon_s$ . First of all, let us comment on why  $\epsilon(r) = \epsilon_s$  between 0 and  $r_0$ . In the treatment of small ions (Mayer-Meeron theory) the potential energy is broken into a hard sphere part and a Coulombic part, the latter extends from zero to infinity. Obviously, the Coulomb potential between  $r=0$  to hard sphere radius adds to hard sphere potential to give hard sphere potential again. So, strictly, for the part other than the hard sphere part (which we call  $g$ -bond), it makes no difference what we set it to be within the hard sphere. It is set equal to Coulomb potential from 0 to  $\infty$ , to make it possible to carry out  $g$ -bond summation by analytical means. We also do the same, but

not with the objective of using analytical methods, because the problem with distance dependent screening constant has to be handled numerically. However setting  $\epsilon(r) = \epsilon_s$  within the hard sphere allows us to check the limiting case where macroion permittivity equals that of the solvent. The  $\int_0^{r_0}$  integral can be done analytically

$$\int_0^{r_0} \frac{e^{-\lambda r}}{\epsilon_s r} 4\pi r^2 \frac{\sin tr}{tr} dr = \frac{4\pi}{\epsilon_s t} \int_0^{r_0} e^{-\lambda r} \sin tr dr$$

Let us evaluate the indefinite integral  $I = \int e^{-\lambda r} \sin tr dr$  in the limit  $\lambda \rightarrow 0$

$$\begin{aligned} I &= \text{Im} \int e^{-\lambda r} e^{itr} dr \\ &= \text{Im} \int e^{-(\lambda - it)r} dr \\ &= \text{Im} \left[ -\frac{1}{-(\lambda - it)} e^{-(\lambda - it)r} \right] \\ &= \frac{t e^{-\lambda r} \cos tr + \lambda e^{-\lambda r} \sin tr}{-t^2 - \lambda^2} \end{aligned}$$

Setting limits 0,  $r_0$

$$I = \frac{t e^{-\lambda r_0} \cos r_0 t + \lambda e^{-\lambda r_0} \sin r_0 t}{-t^2 - \lambda^2} - \frac{t}{-t^2 - \lambda^2}$$

$$\lim_{\lambda \rightarrow 0} I = -\frac{\cos r_0 t}{t} + \frac{1}{t}$$

The same integral is to be evaluated between  $r_{\max}$  and  $\infty$ . This calculation yields,

$$\lim_{\lambda \rightarrow 0} I = \frac{\cos r_{\max} t}{t}$$

$$\therefore g(t) = \frac{\cos r_{\max} t - \cos r_0 t}{t^2} \cdot \frac{4\pi}{\epsilon_s} + \frac{4\pi}{\epsilon_s t^2}$$

$$+ \left[ \lim_{\lambda \rightarrow 0} \int_{r_0}^{r_{\max}} \frac{e^{-\lambda r}}{\epsilon(r)} \sin tr \, dr \right] \times \frac{4\pi}{t}$$

The integral within bracket equals  $\int_0^{r_{\max}} \frac{\sin tr \, dr}{\epsilon(r)}$

The integral between  $r_{\max}$  and  $\infty$  has to be handled analytically, because the range of the potential is too large to allow handling by numerical method.

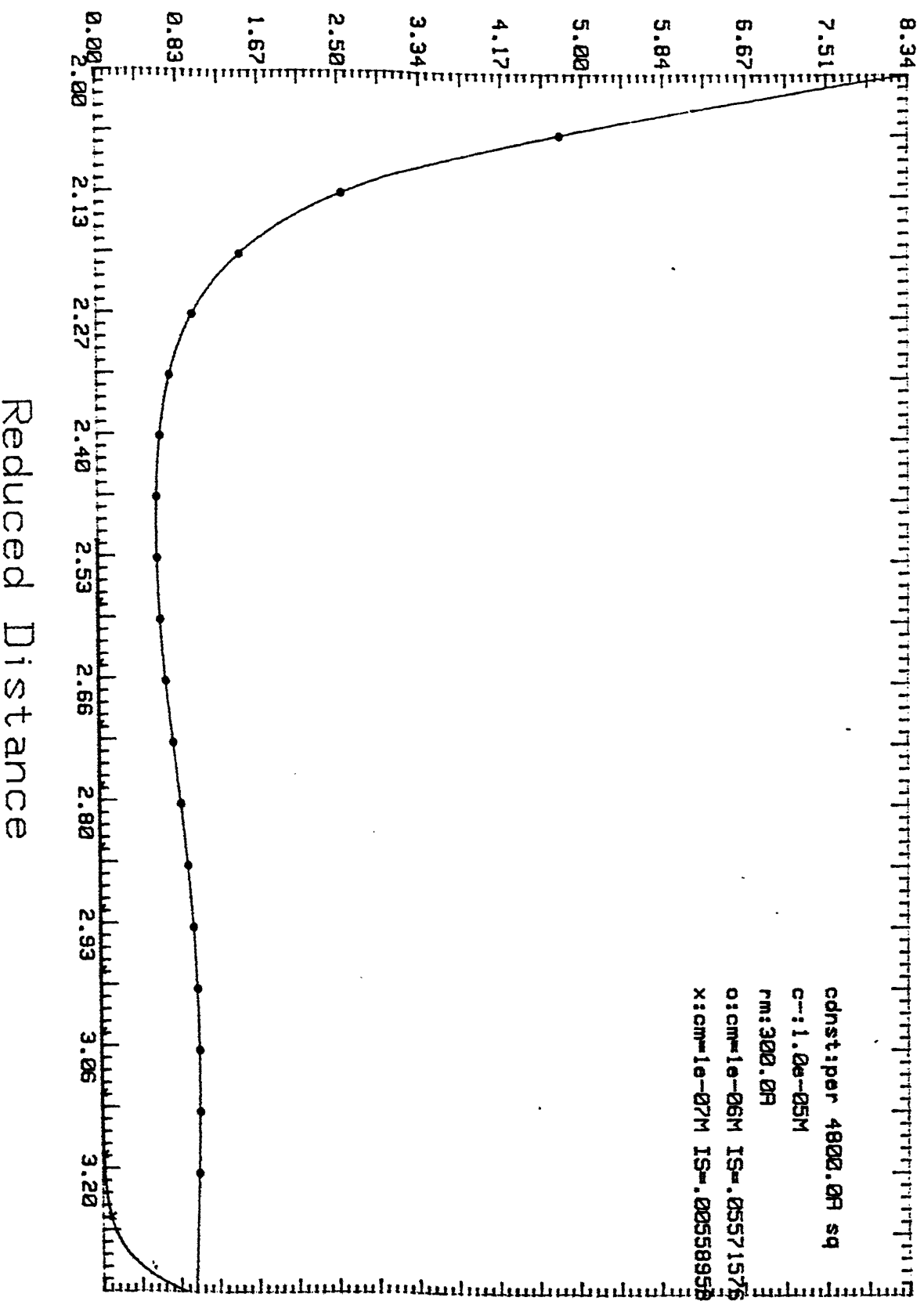
The transform of the Coulomb potential with distance dependent screening constant is used in the calculation of  $q(r)$  (Chapter III, Section 9). A programme was written to calculate correlation function of such systems. Having arrived at the conclusion in Chapter II, that the effects of polarization will be significant in nonspherical macroions only, we have postponed numerical calculation till an expression of  $\epsilon(r)$  for such a system is worked out. However to verify the programme, we have calculated  $g(r)$  for a system with  $\epsilon(\text{macroion}) = \epsilon(\text{solvent})$ . This system should be identical to the usual systems considered in Chapter 3, where macroions and ions all interact through the usual Coulomb potential, with a screening constant equal to the dielectric permittivity of the solvent. The  $g(r)$  so calculated is exactly the same as that calculated by the method described in Chapter III. The agreement is shown in Fig. 5.74.

## 5.6 Systems with angle-dependent interaction:

Figure 5.75 shows that the program for calculation of  $g(r)$  for angle dependent potential gives nearly the same result as that calculated by the method of Chapter III when  $\mu_m$  is set equal to zero (both for one iteration). A system with  $\mu_m = 20,000D$  (again with one iteration only) shows a significant

# Correlation Function Vs. Distance F-5.2

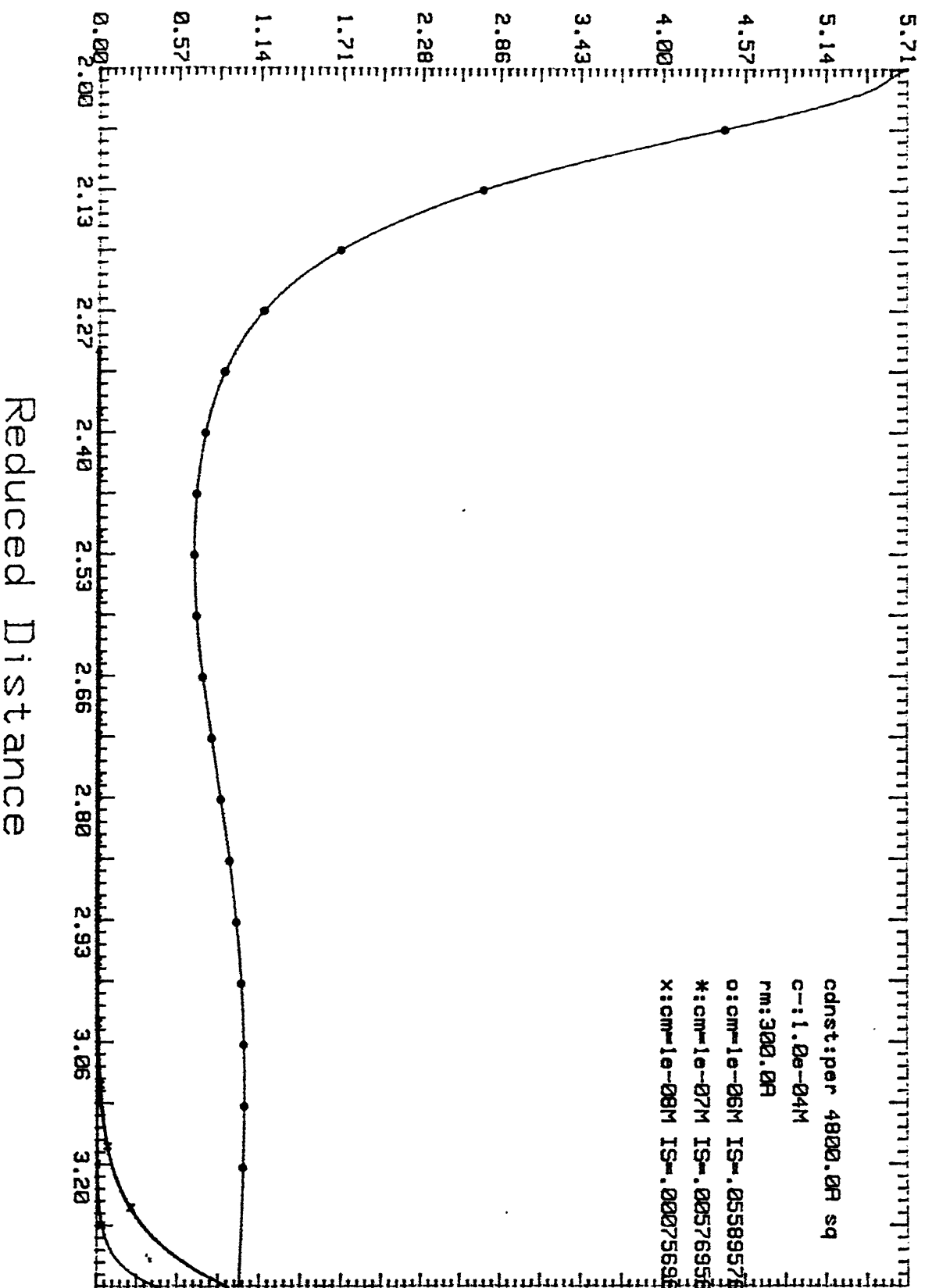
Macro Ion-Macro Ion Correlation;  $g(r)$





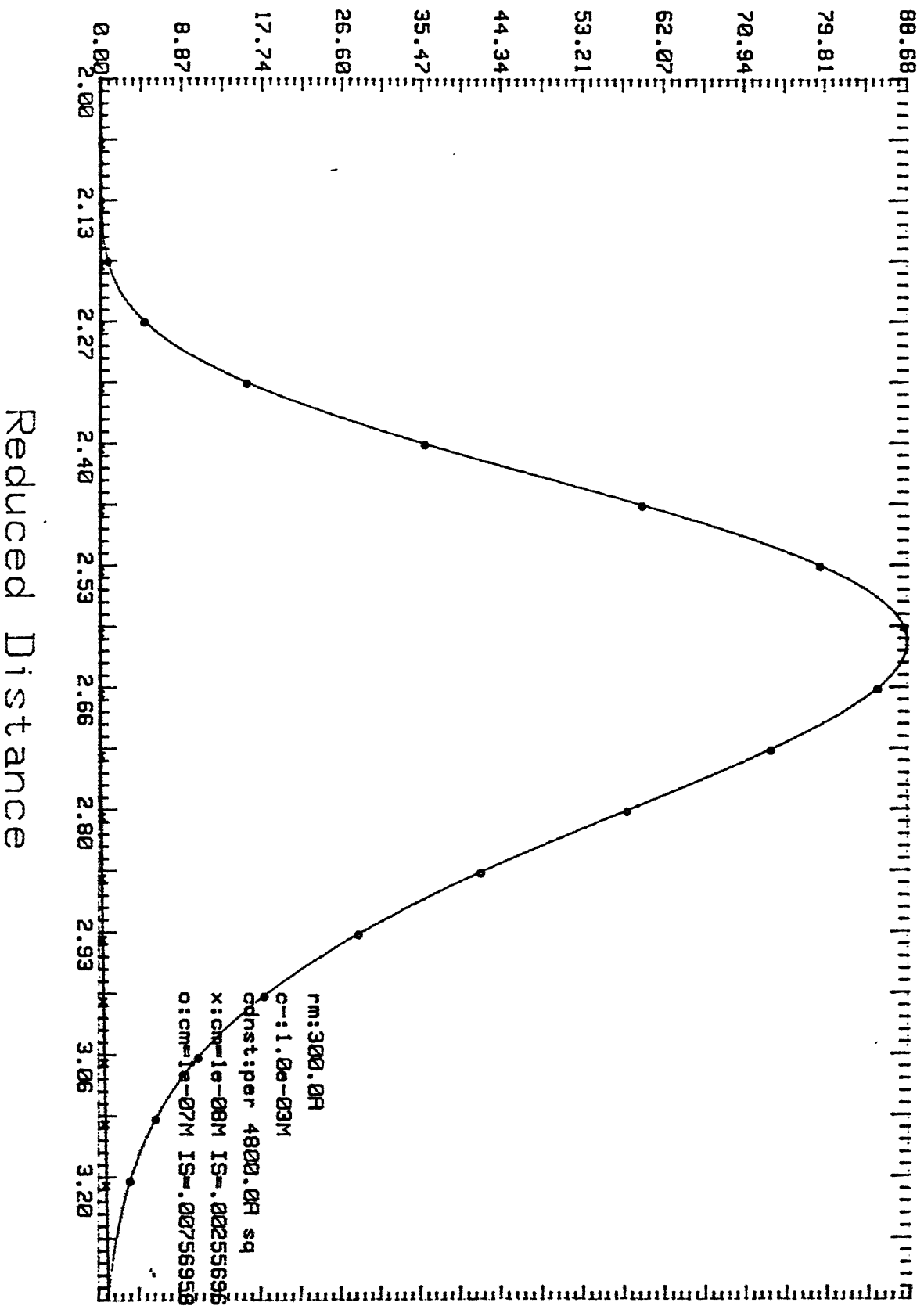
# Correlation Function Vs. Distance F-5.3

Macro Ion-Macro Ion Correlation;  $g(r)$

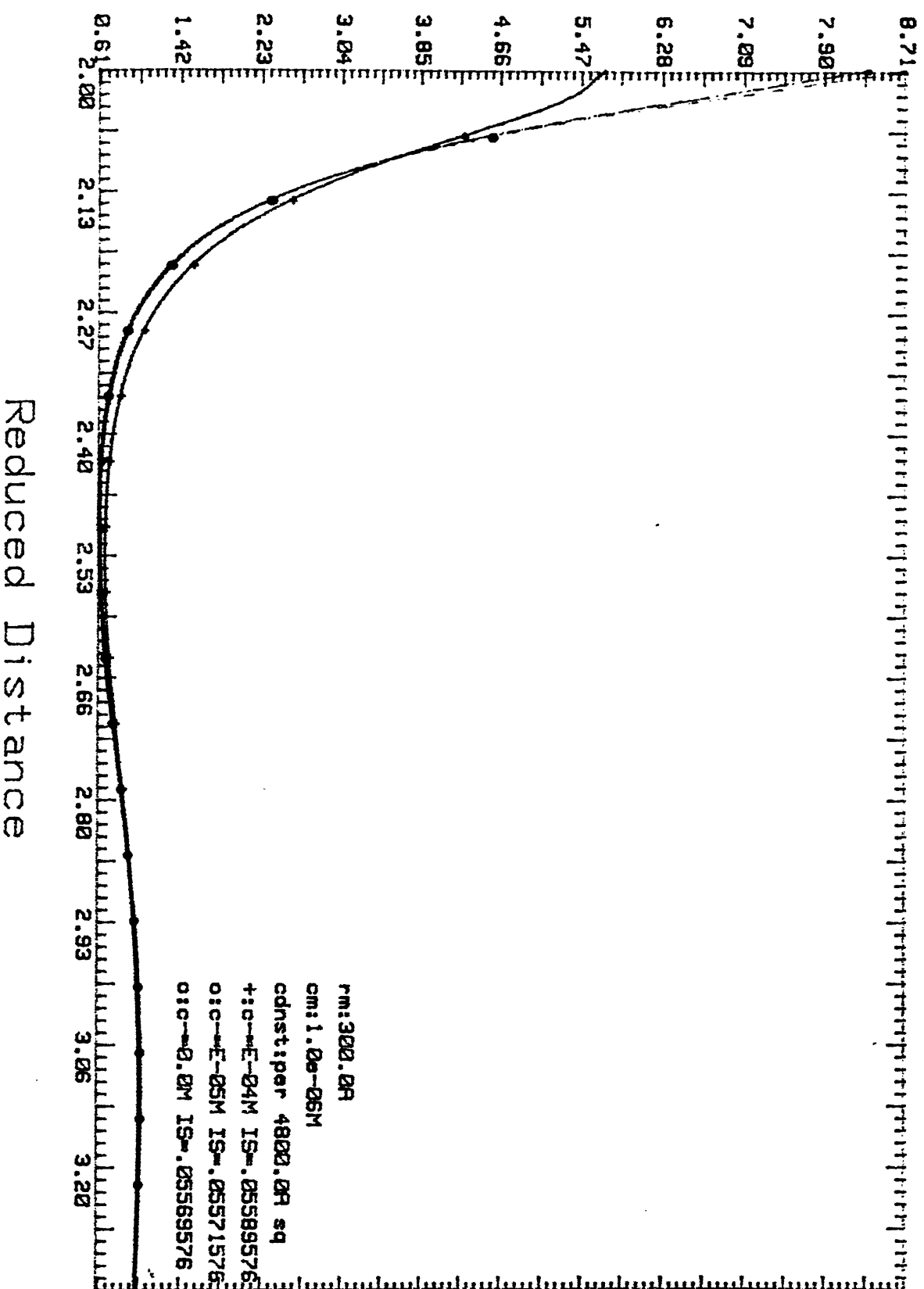


# Correlation Function Vs. Distance F-5.4

Macro Ion-Macro Ion Correlation;  $g(r)$

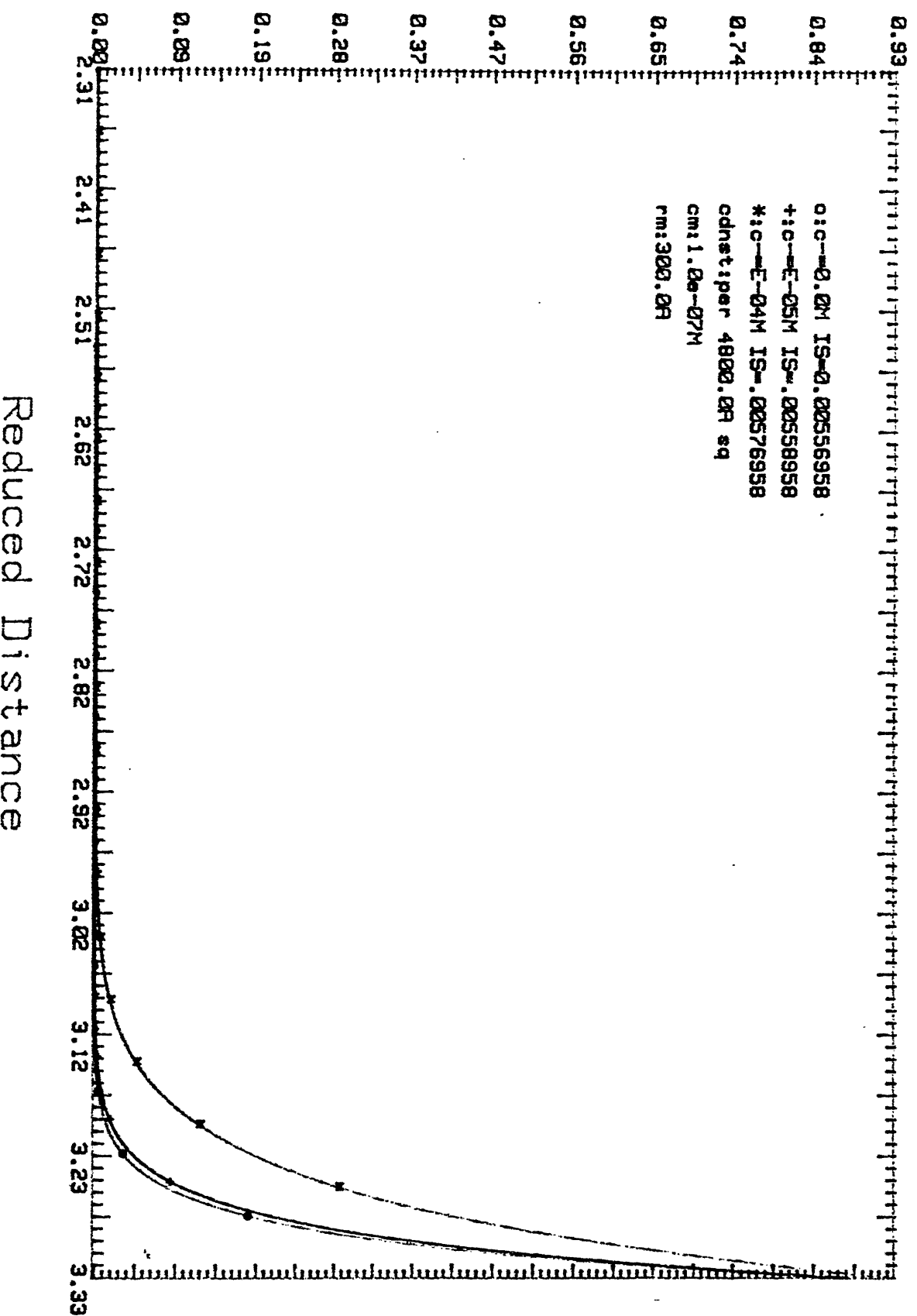


# Correlation Function Vs. Distance F-5.5



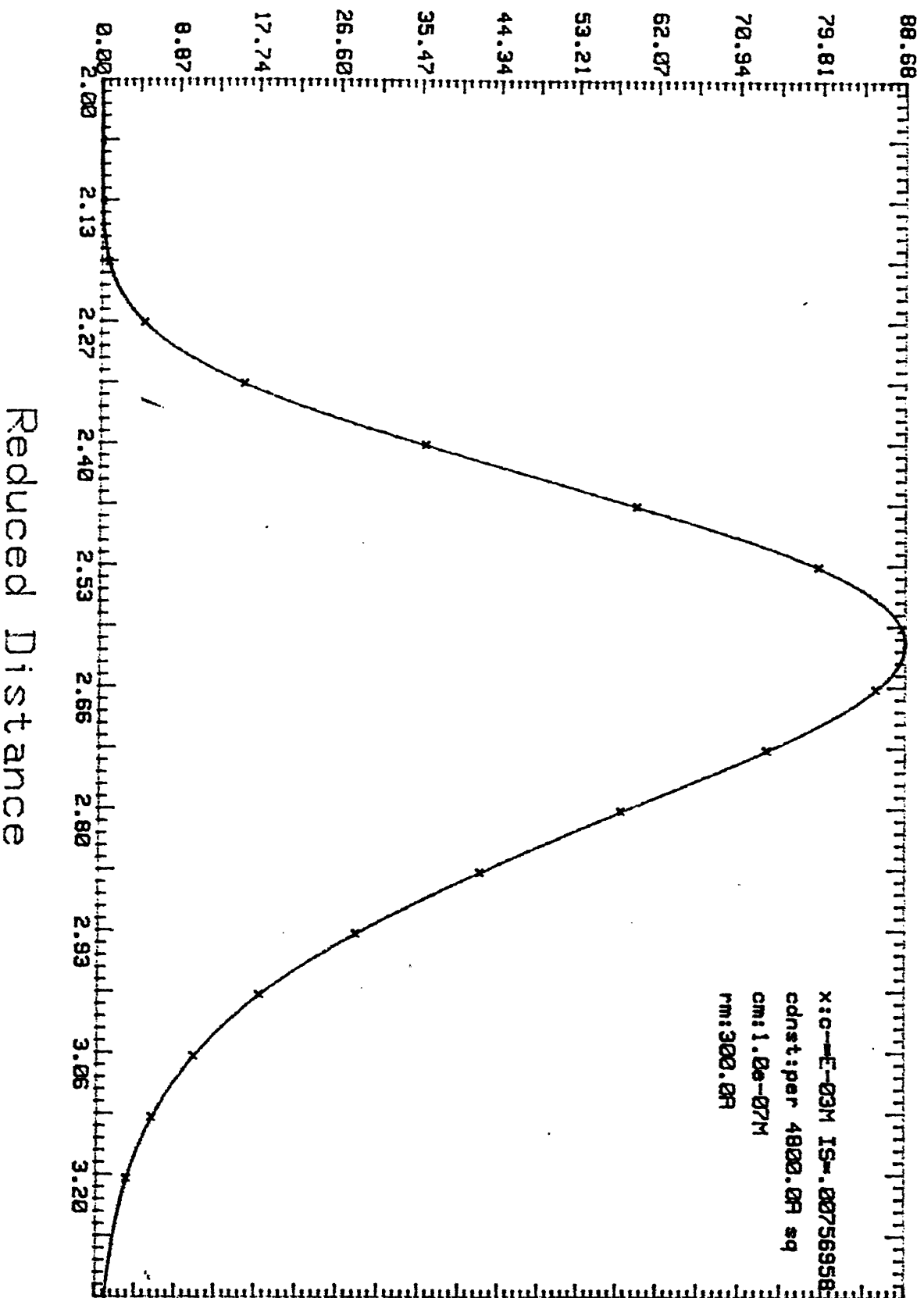
# Correlation Function Vs. Distance F-5.6(a)

Macro Ion-Macro Ion Correlation;  $g(r)$



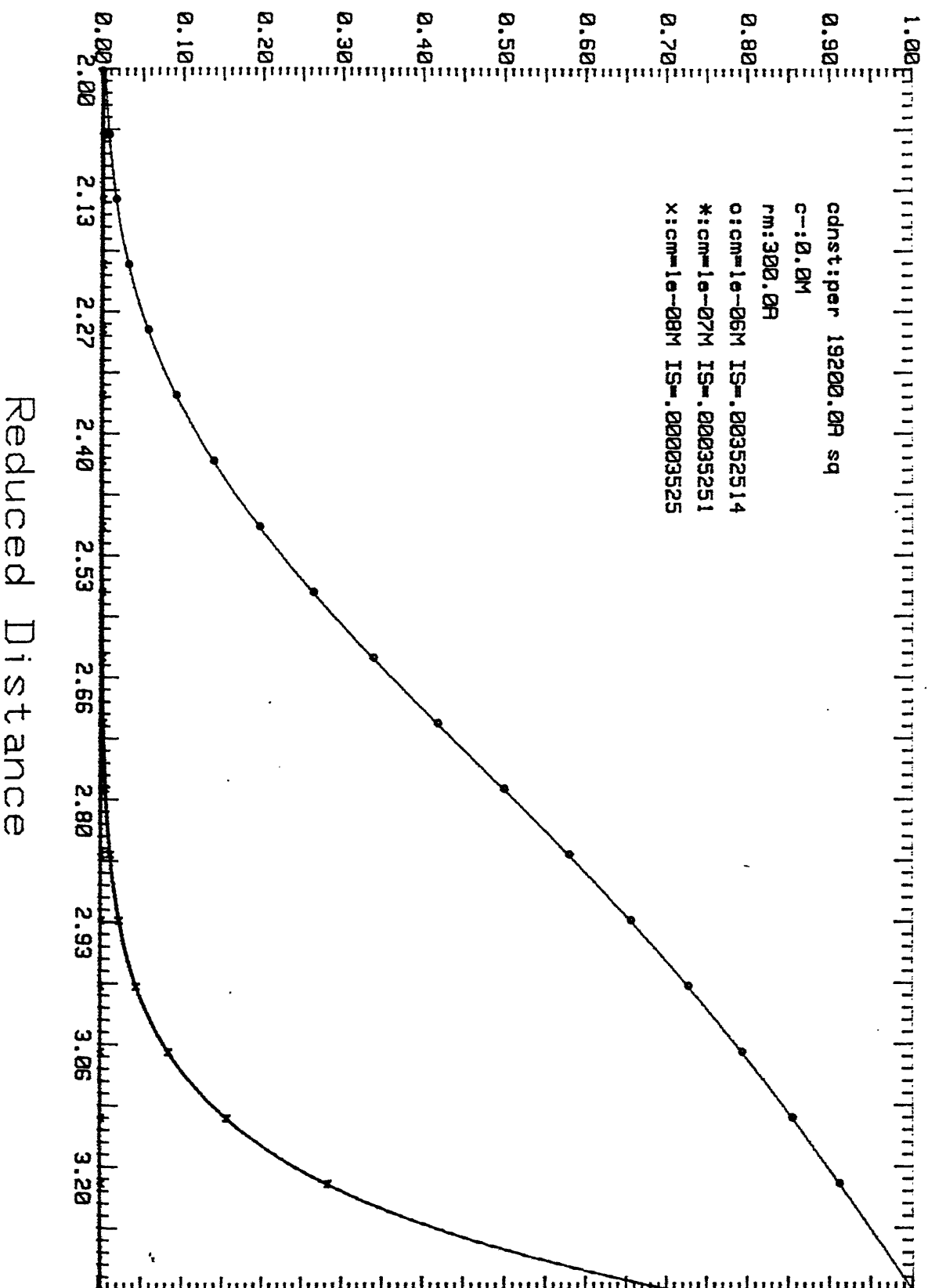
# Correlation Function Vs. Distance F-5.6(b)

Macro Ion-Macro Ion Correlation;  $g(r)$



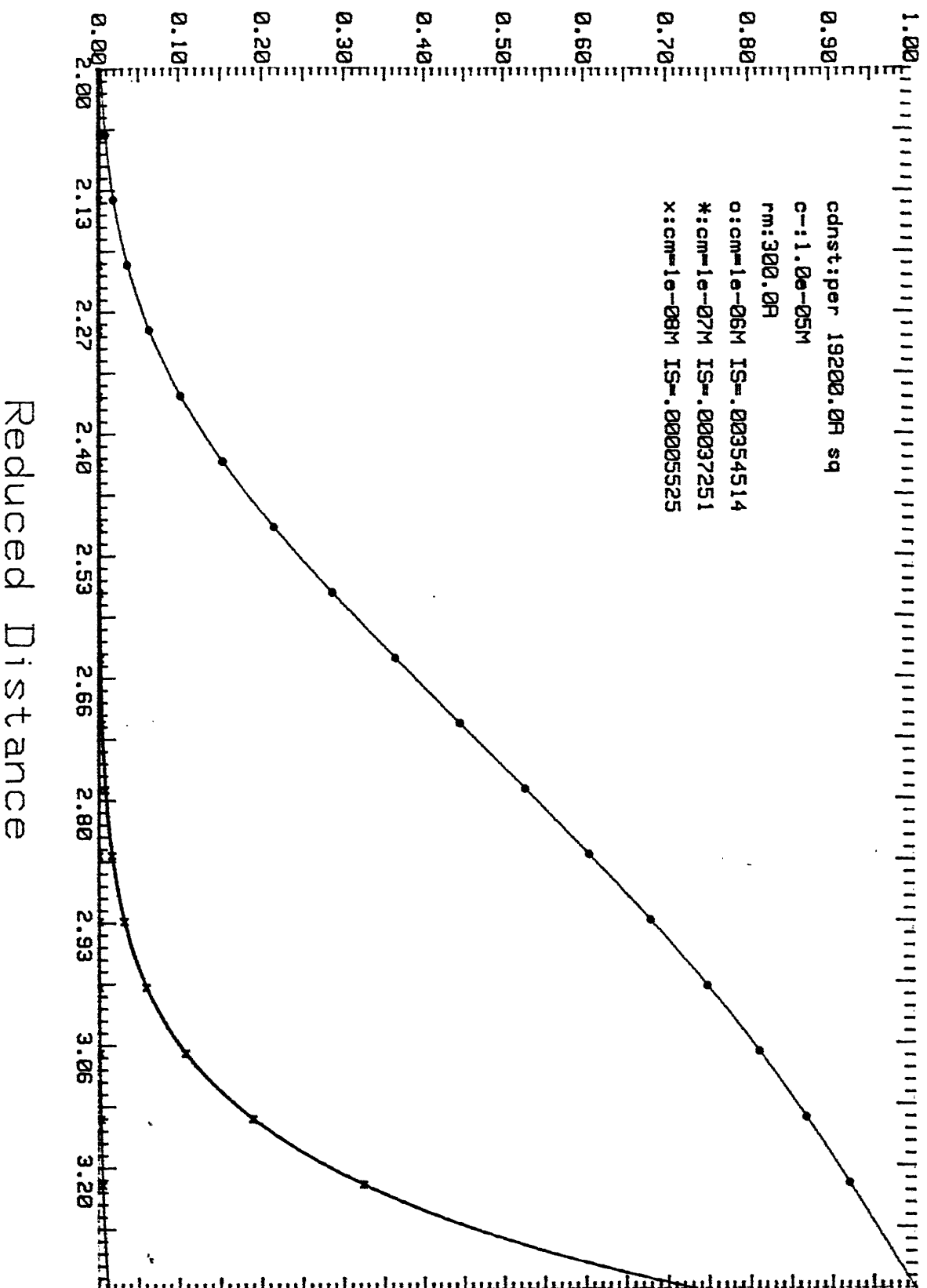
# Correlation Function Vs. Distance F-5.7

Macro Ion-Macro Ion Correlation;g(r)



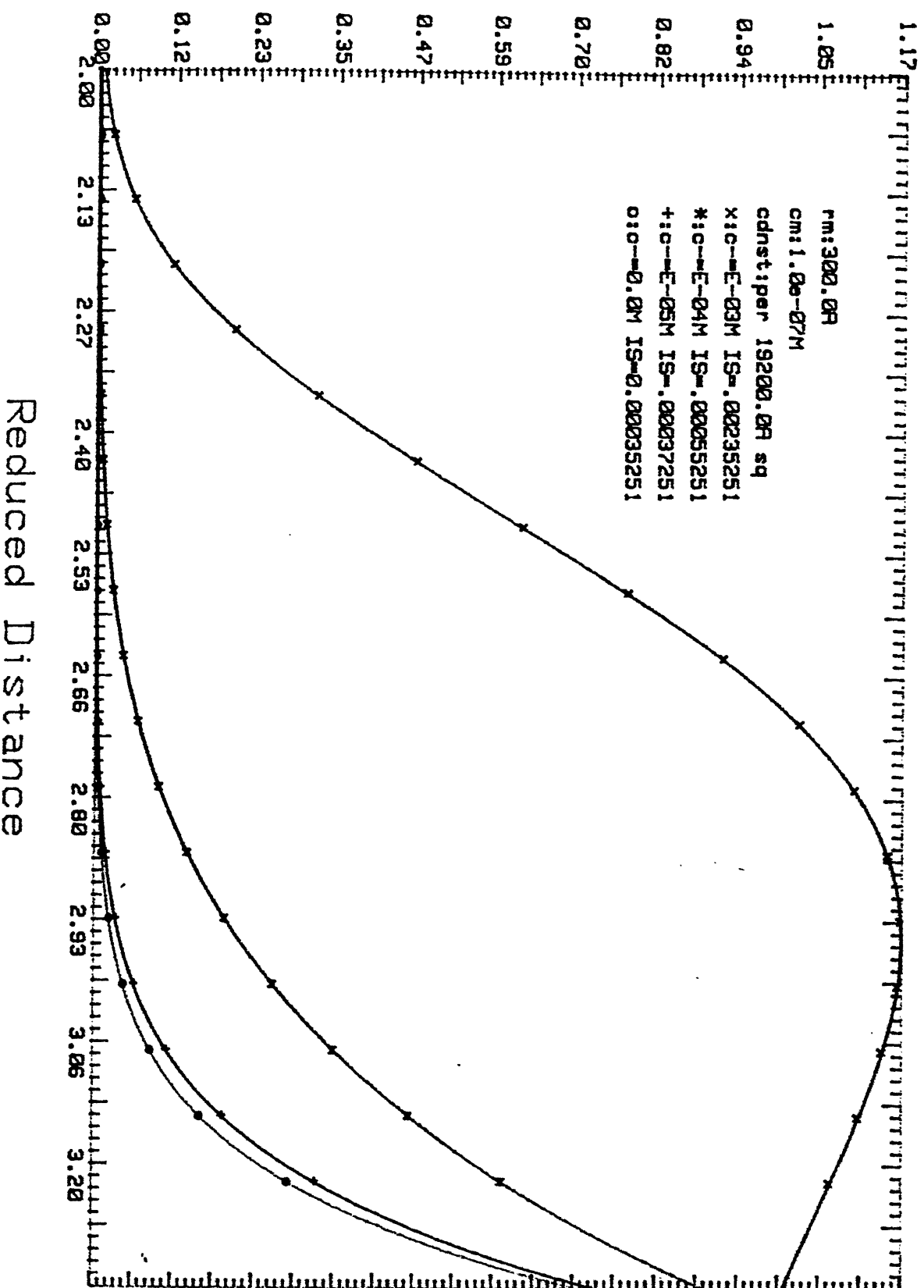
# Correlation Function Vs. Distance F-5.8

Macro Ion-Macro Ion Correlation;  $g(r)$



# Correlation Function Vs. Distance F-5.11

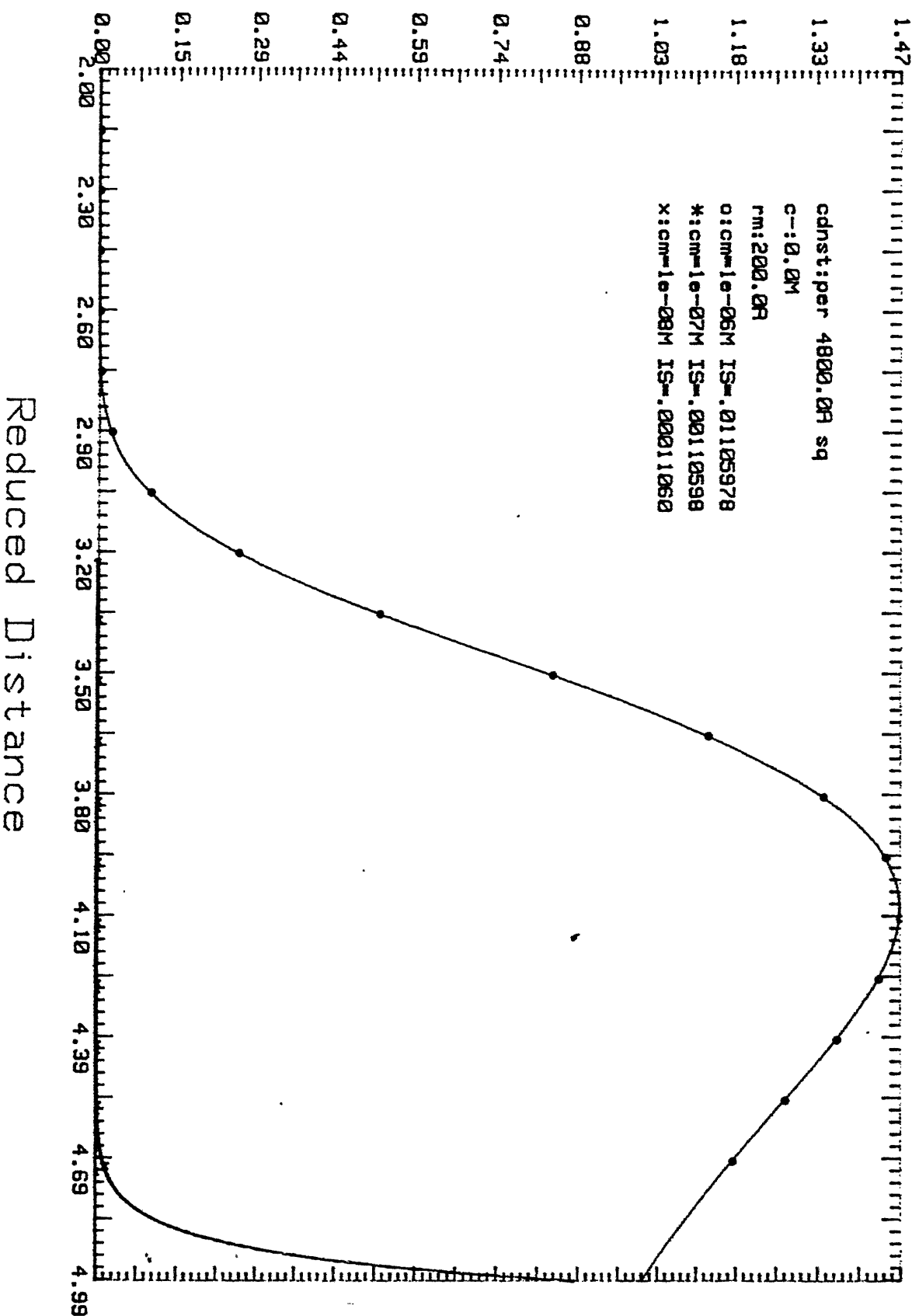
Macro Ion-Macro Ion Correlation;  $g(r)$





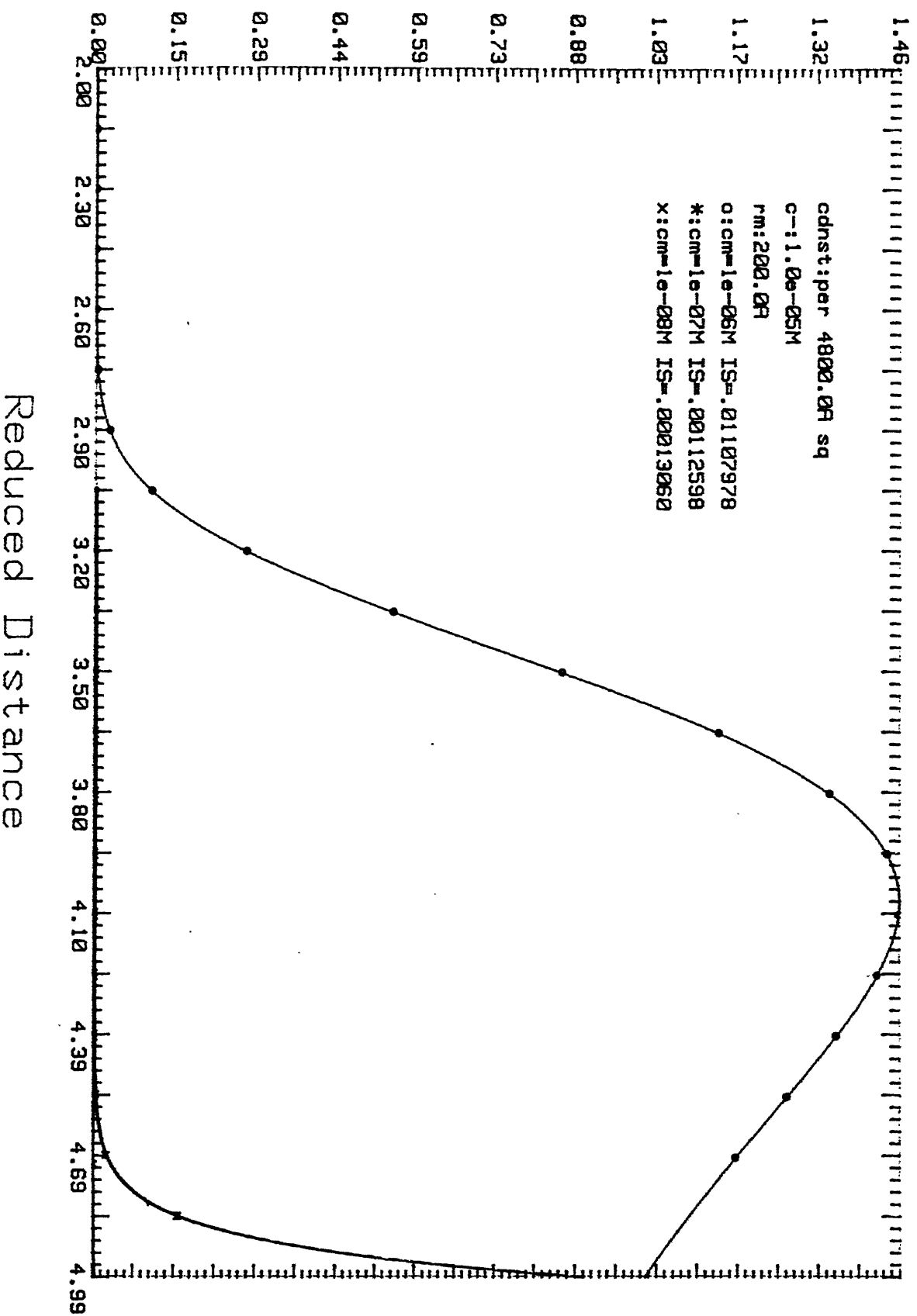
# Correlation Function Vs. Distance F-5.12

Macro Ion-Macro Ion Correlation;g(r)

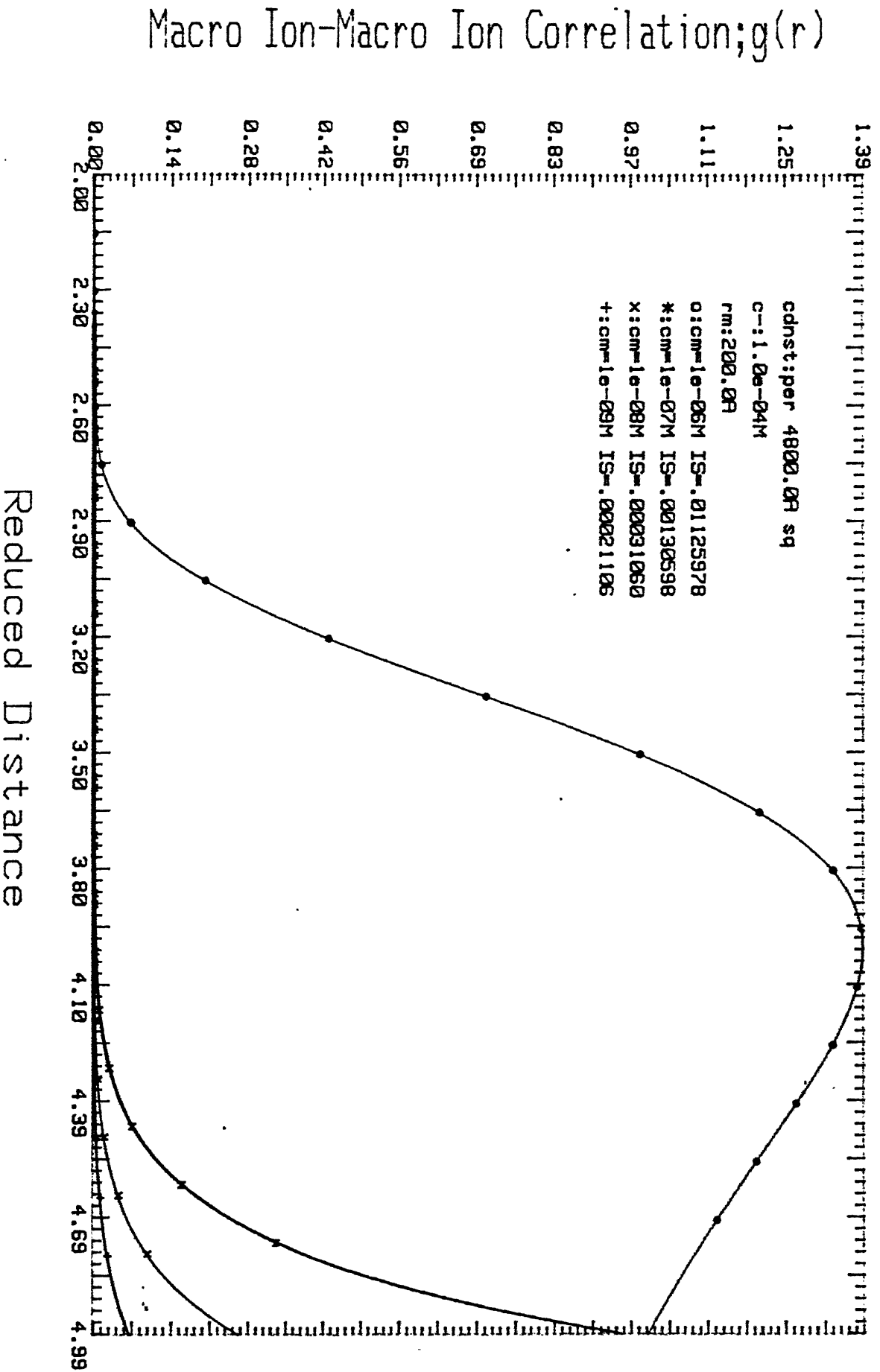


# Correlation Function Vs. Distance F-5.1

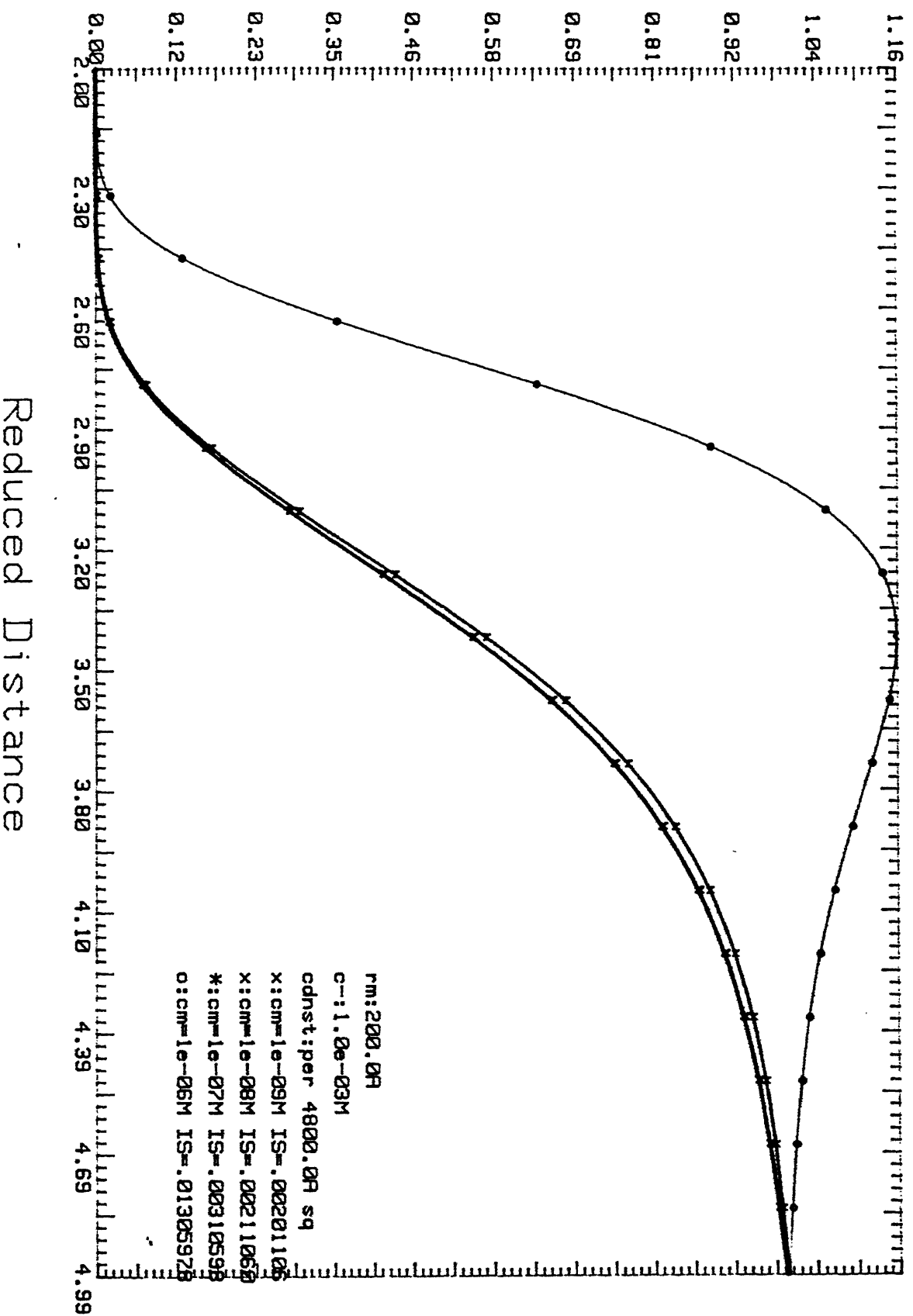
Macro Ion-Macro Ion Correlation; $g(r)$



# Correlation Function Vs. Distance F-5.14

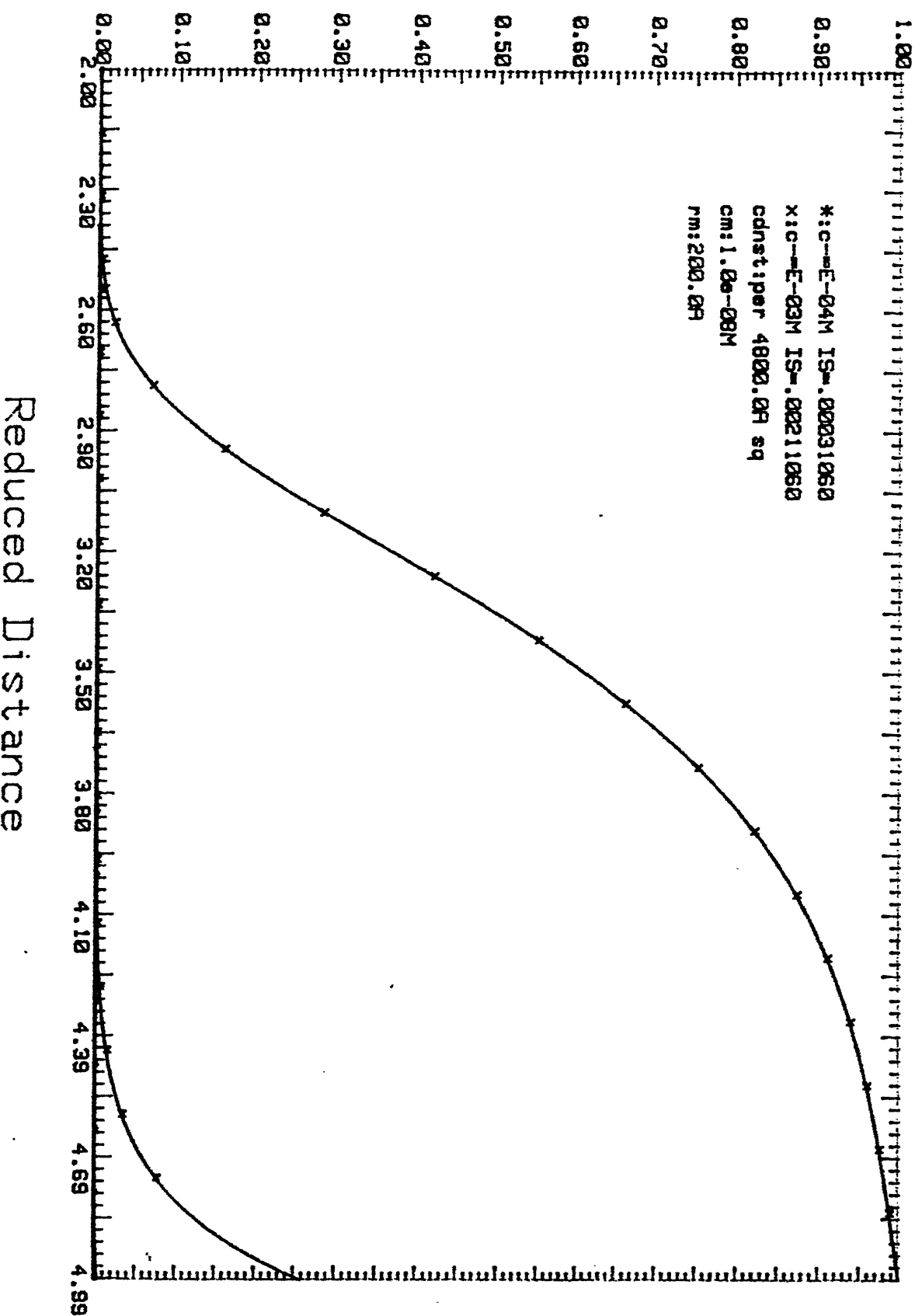


# Correlation Function Vs. Distance F-5.15



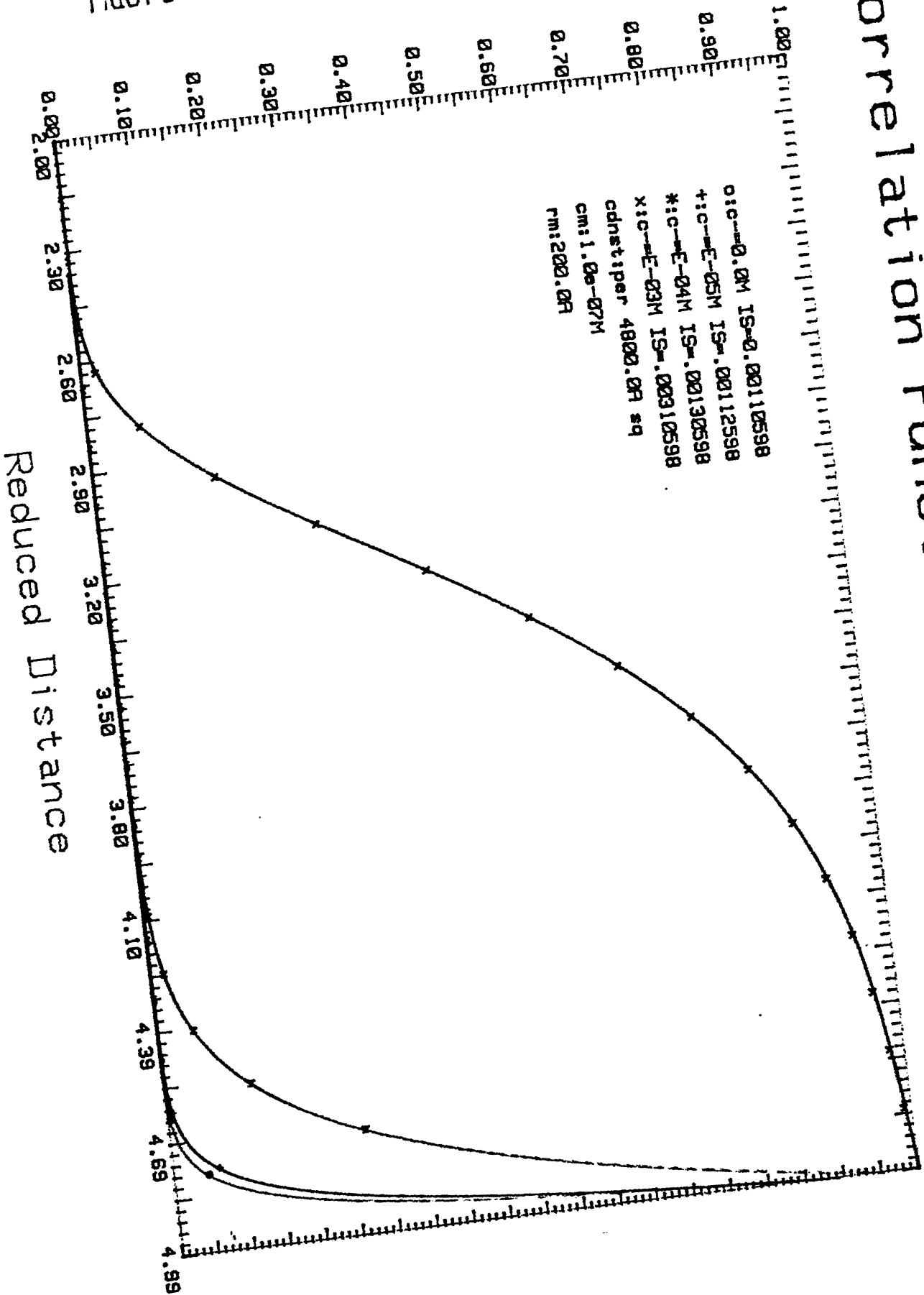
# Correlation Function Vs. Distance F-5.16

Macro Ion-Macro Ion Correlation;g(r)

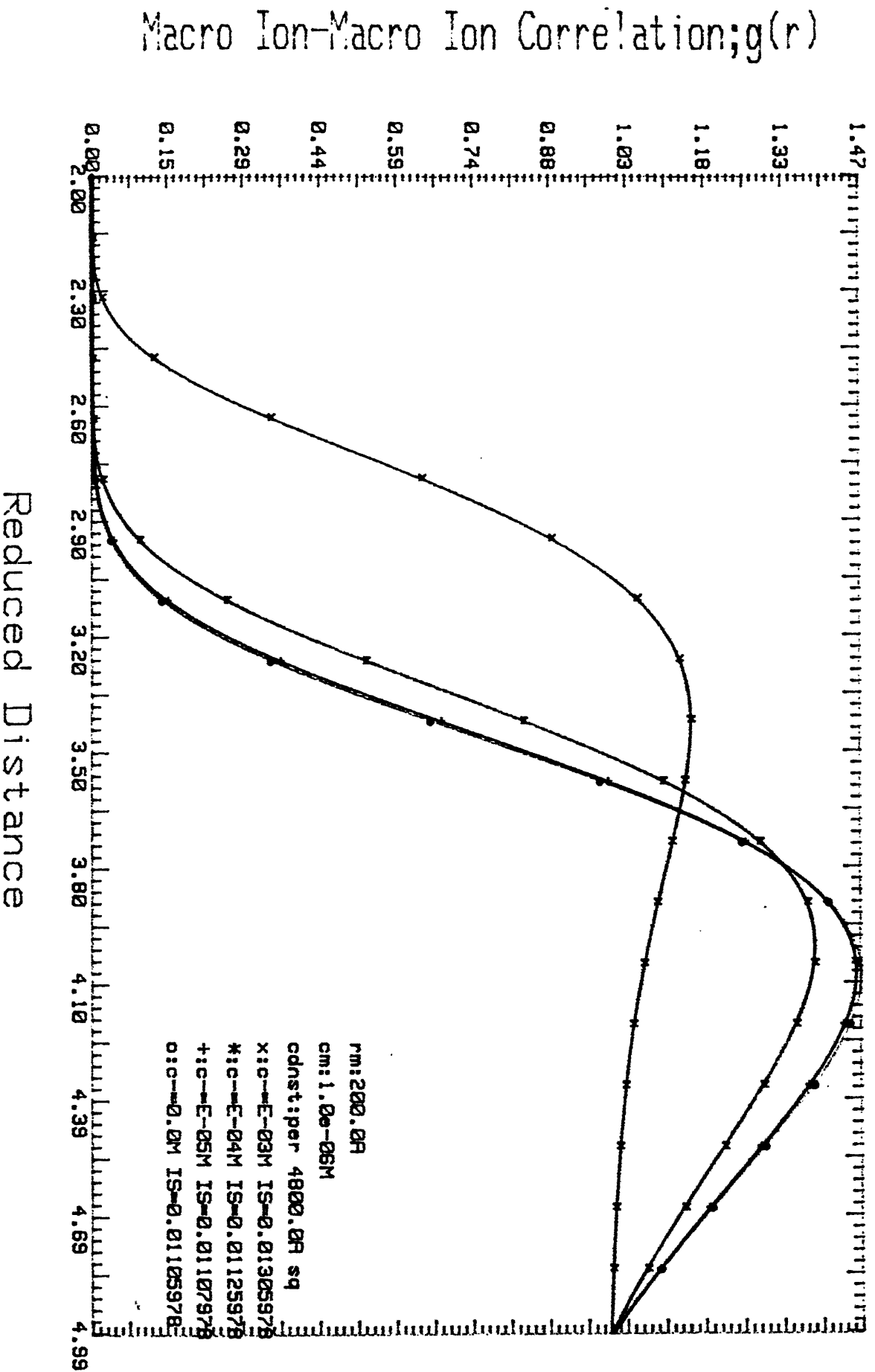


# Correlation Function Vs. Distance F-5.17

Macro Ion-Macro Ion Correlation;  $g(r)$

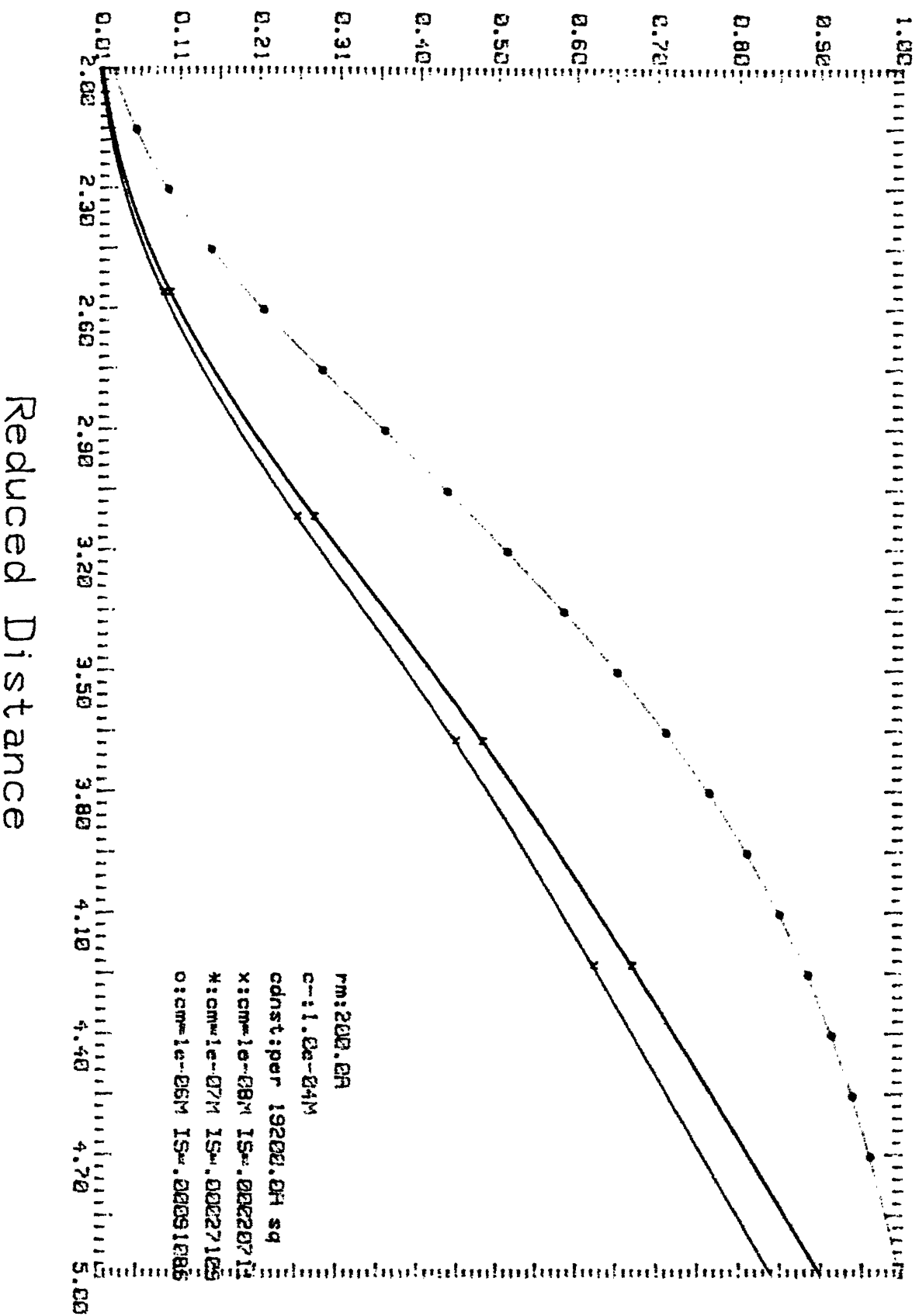


# Correlation Function Vs. Distance F-5.18



# Correlation Function Vs. Distance

F - 5.21



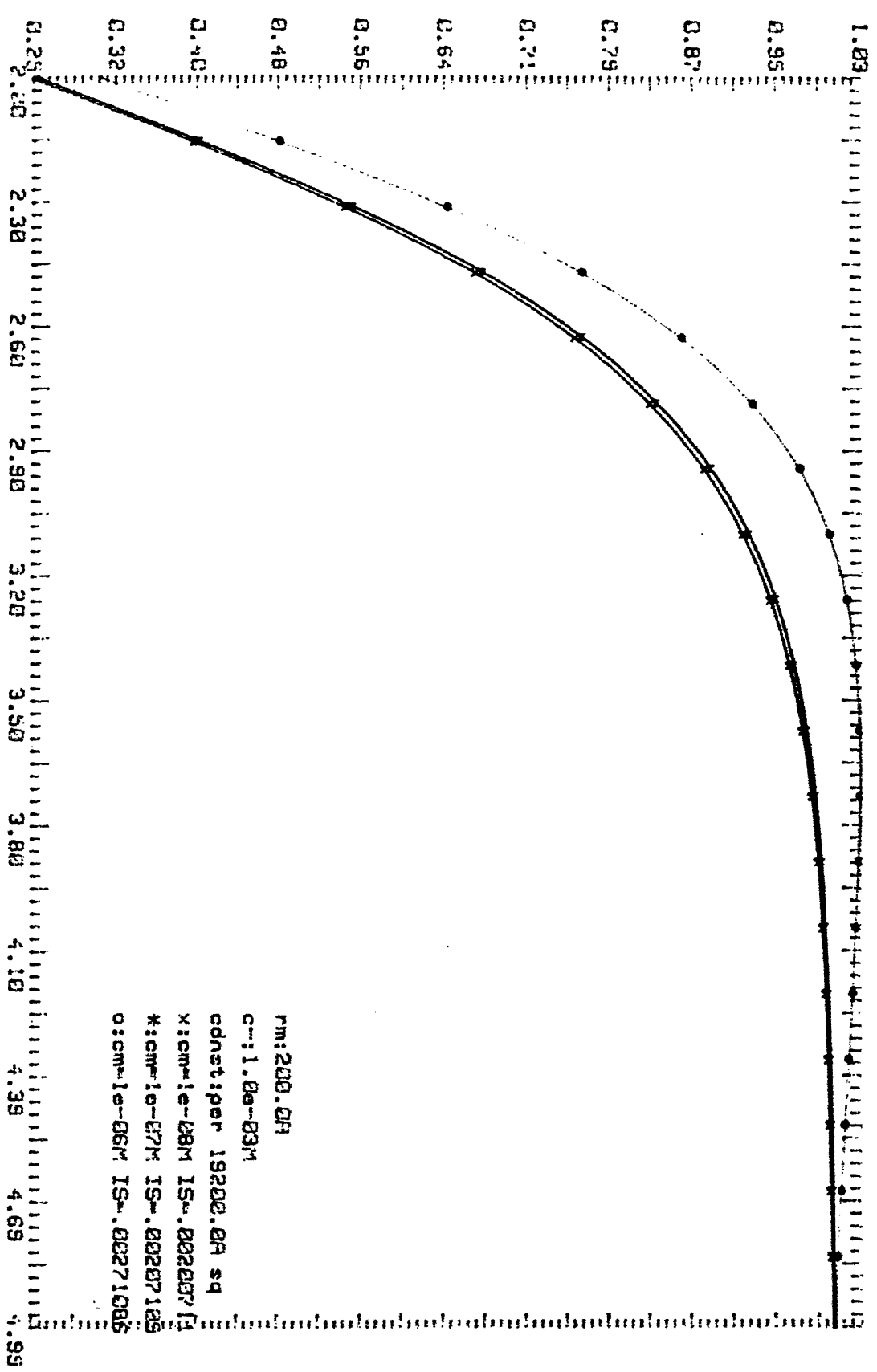


# Correlation Function Vs. Distance

F-5.22

F - 5.22

Macro Ion-Macro Ion Correlation;  $g(r)$



rm:200.0A  
 cm:1.0e-03M  
 cdnst:per 19200.0A sq  
 x:cm:1e-08M IS-.00200714  
 o:cm:1e-07M IS-.00207105  
 o:cm:1e-06M IS-.00271005

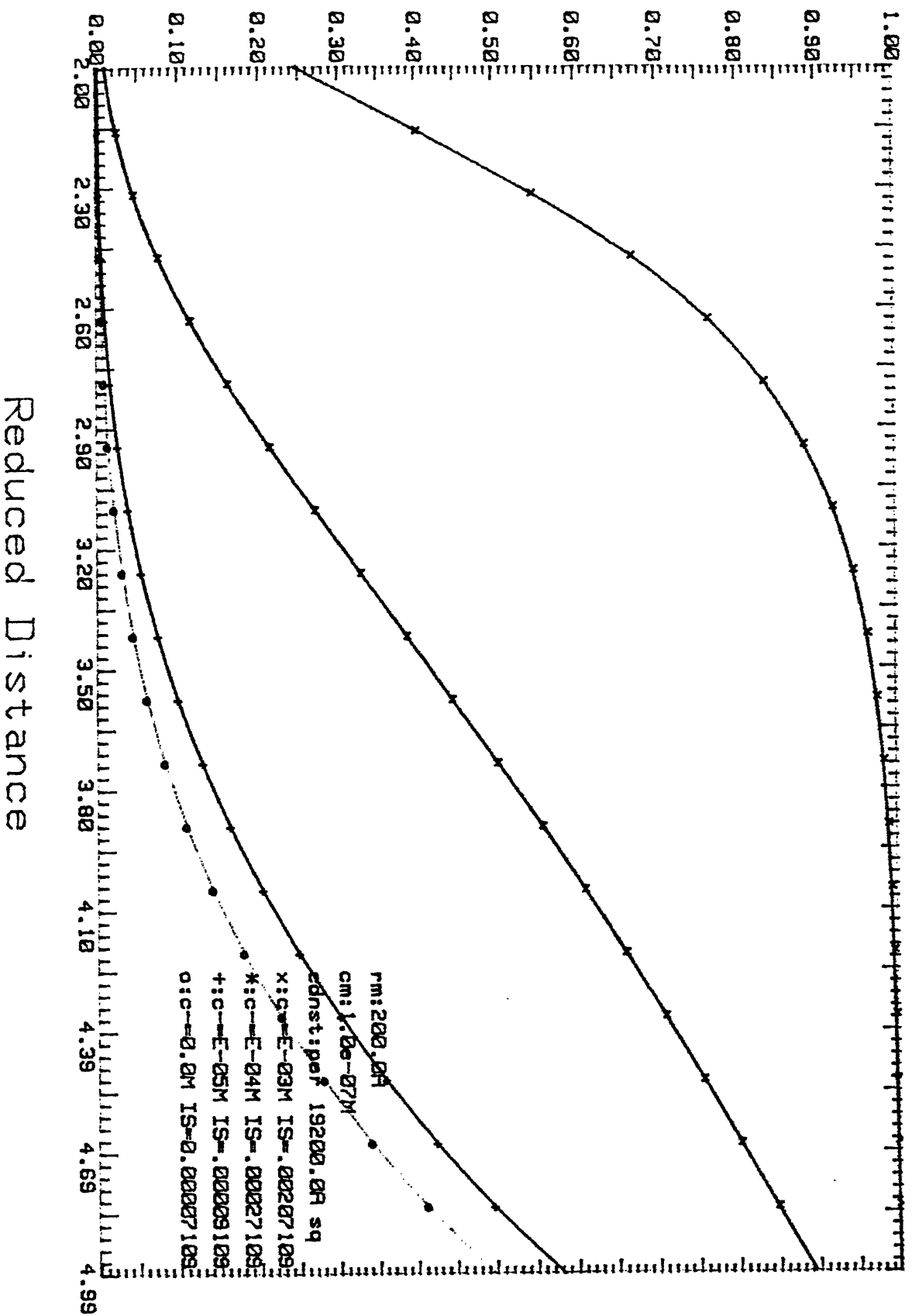
Reduced Distance

F - 5.22

# Correlation Function Vs. Distance

F-5.22

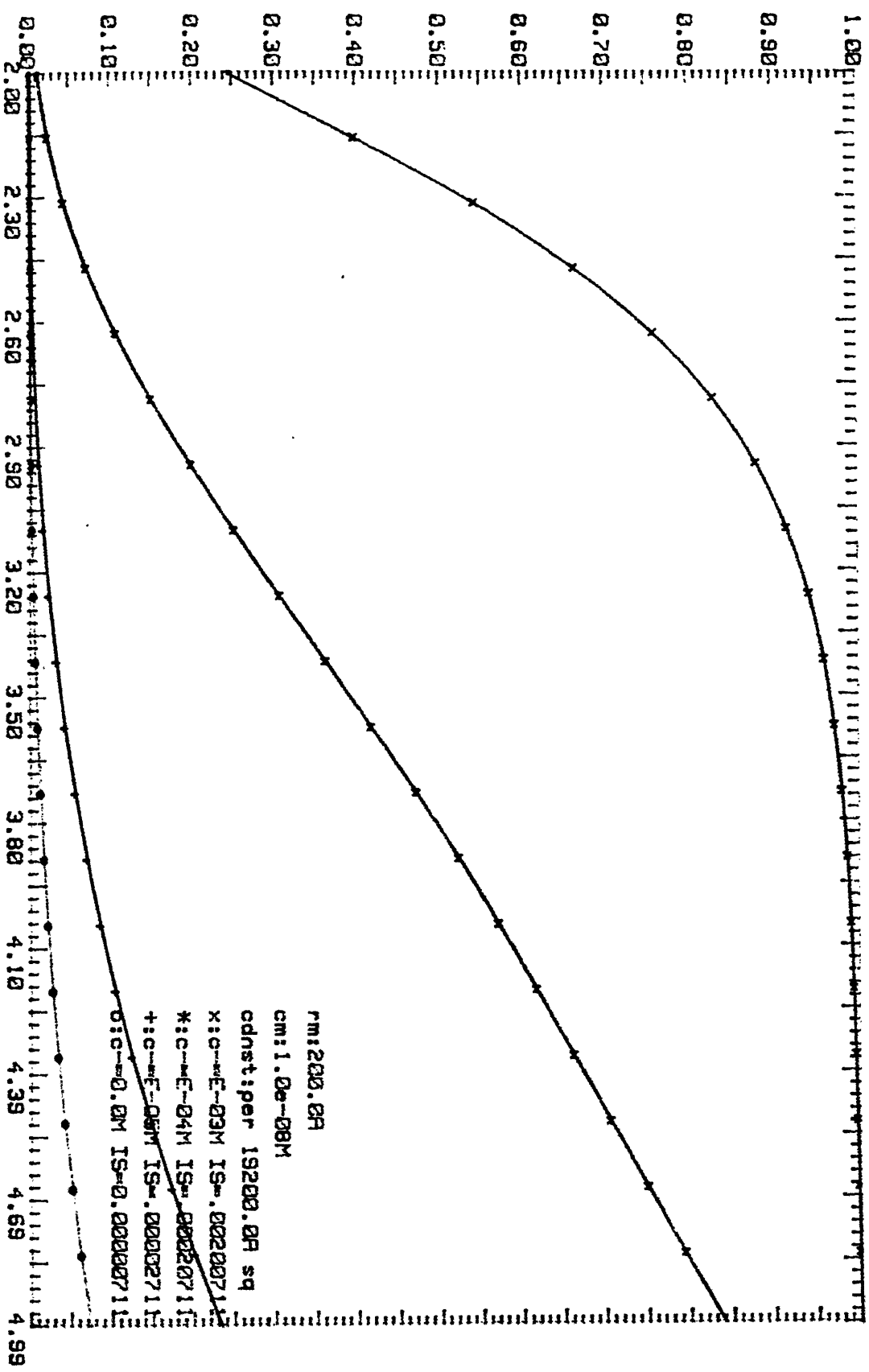
Macro Ion-Macro Ion Correlation; $g(r)$



# Macro Ion-Macro Ion Correlation;g(r)

Correlation Function Vs. Distance

F-5.24

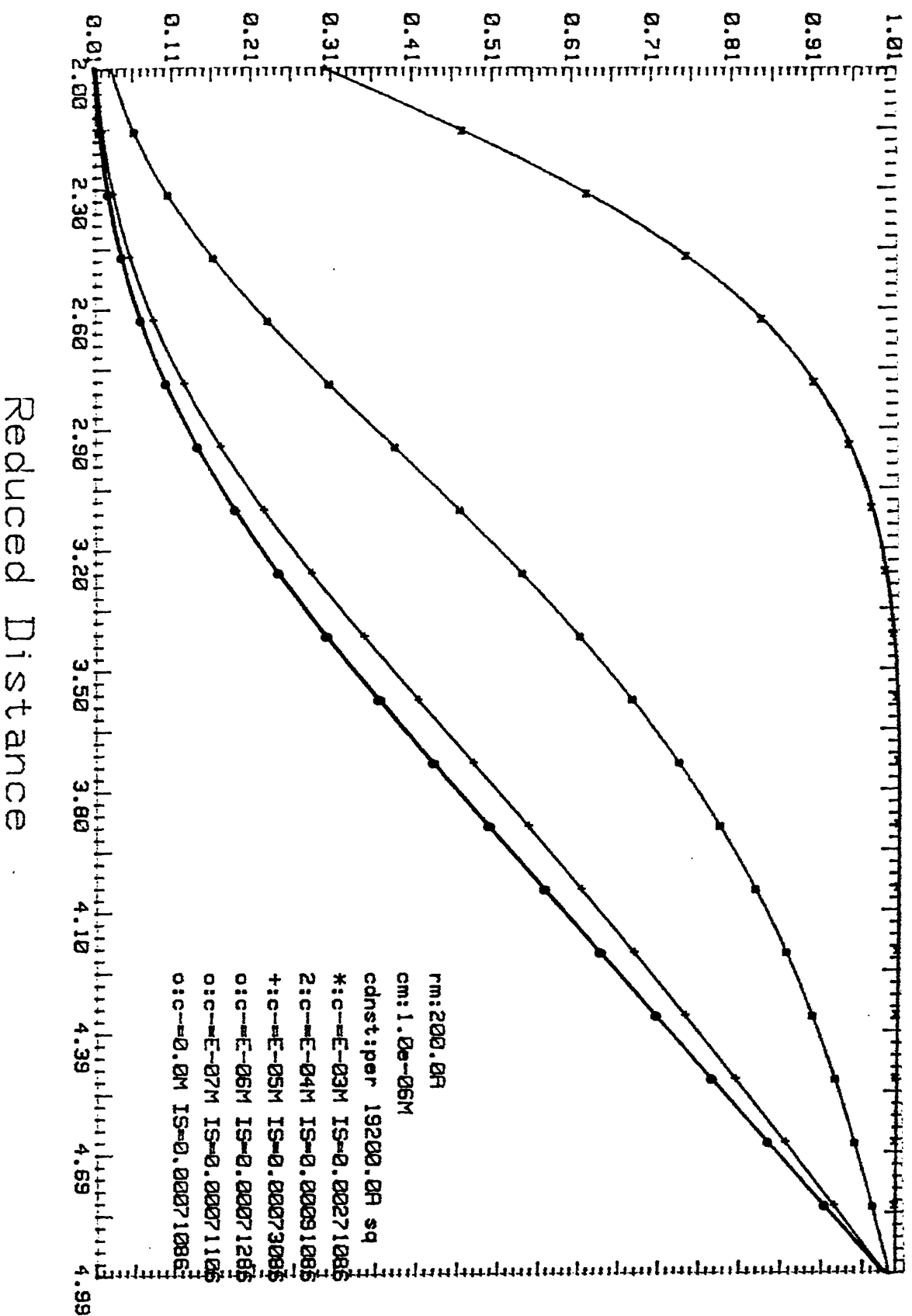


Reduced Nitrogen

# Correlation Function Vs. Distance

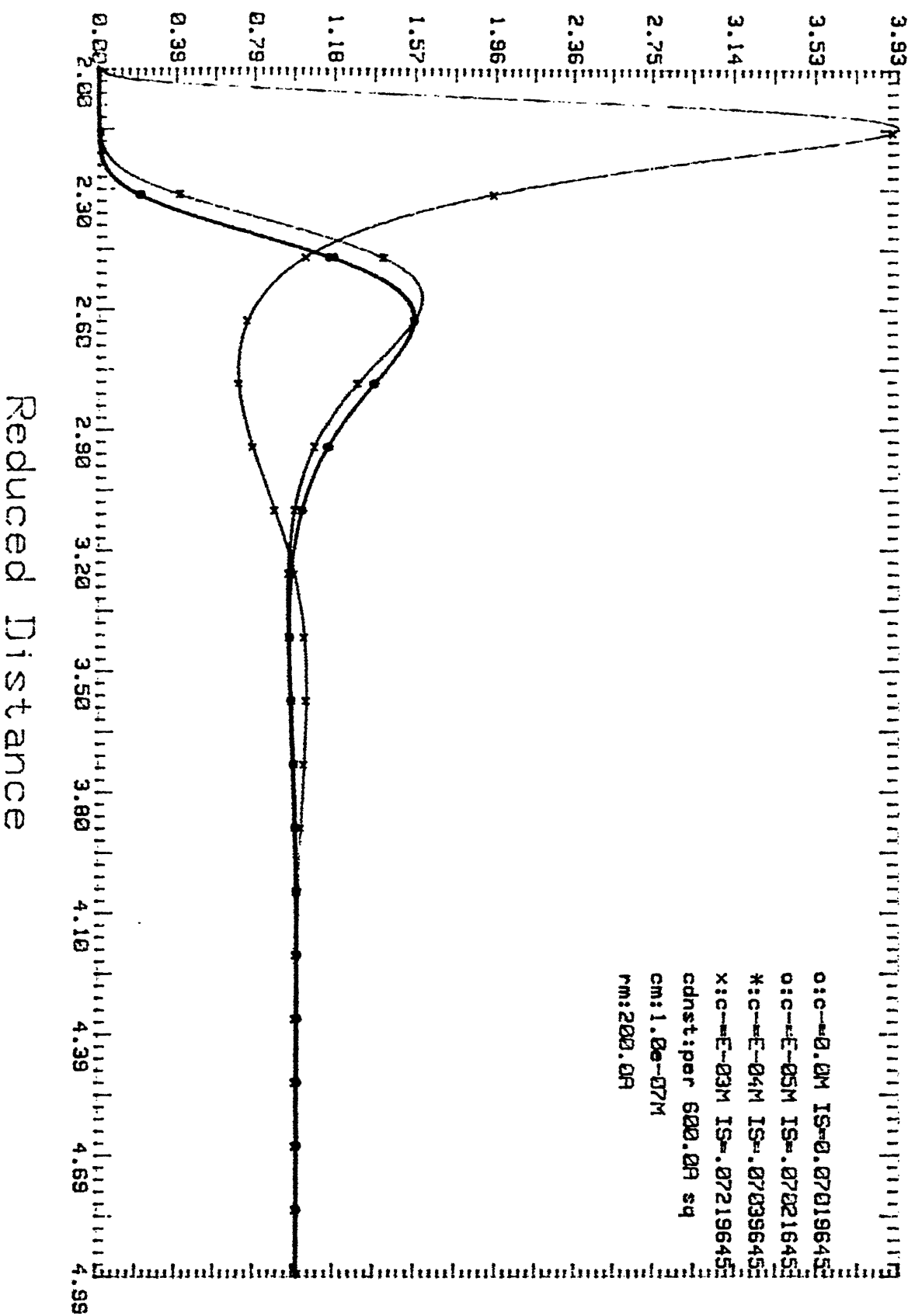
F-5.25

Macro Ion-Macro Ion Correlation;  $g(r)$

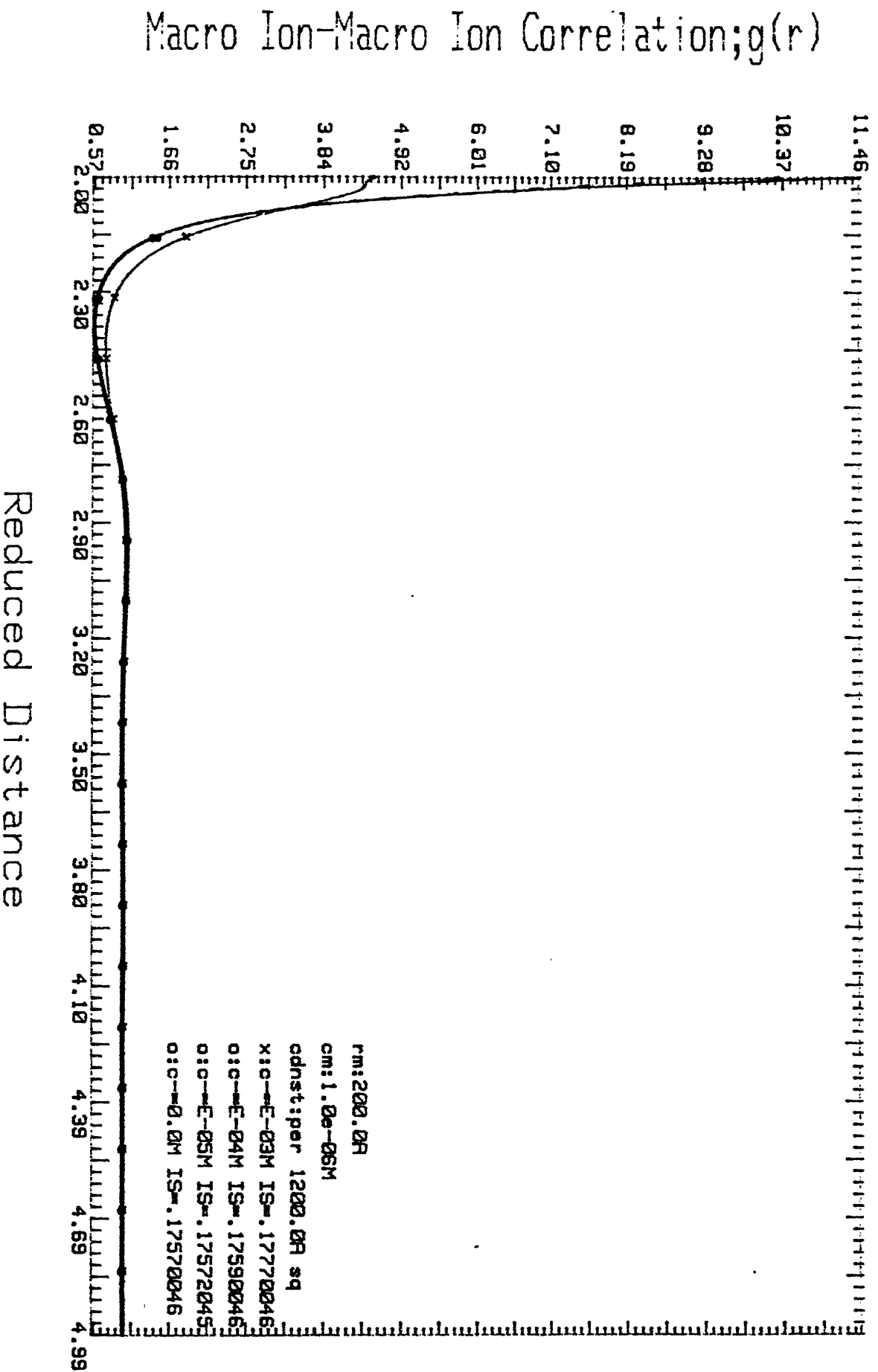


# Correlation Function Vs. Distance F-5.26

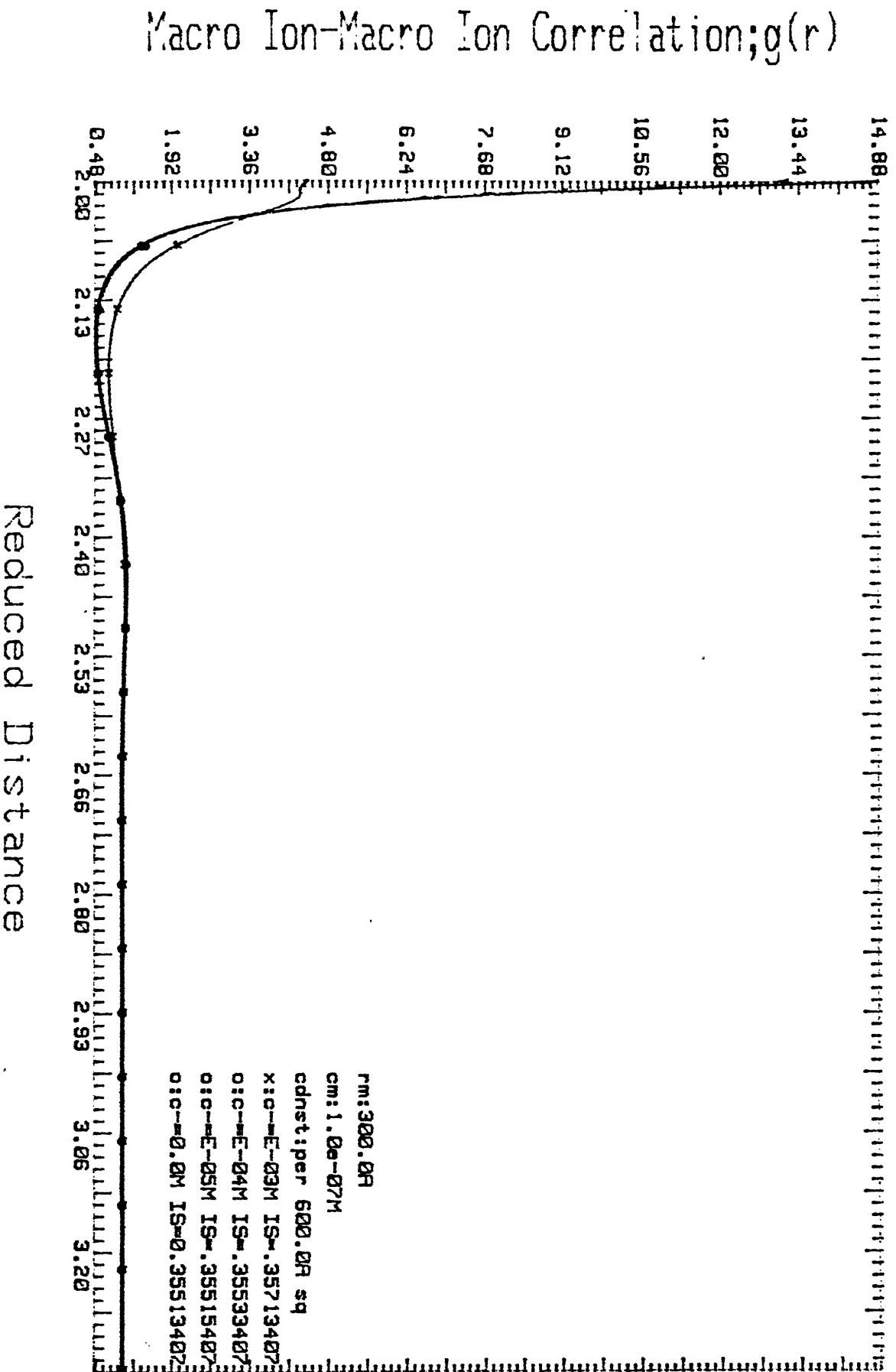
Macro Ion-Macro Ion Correlation;  $g(r)$



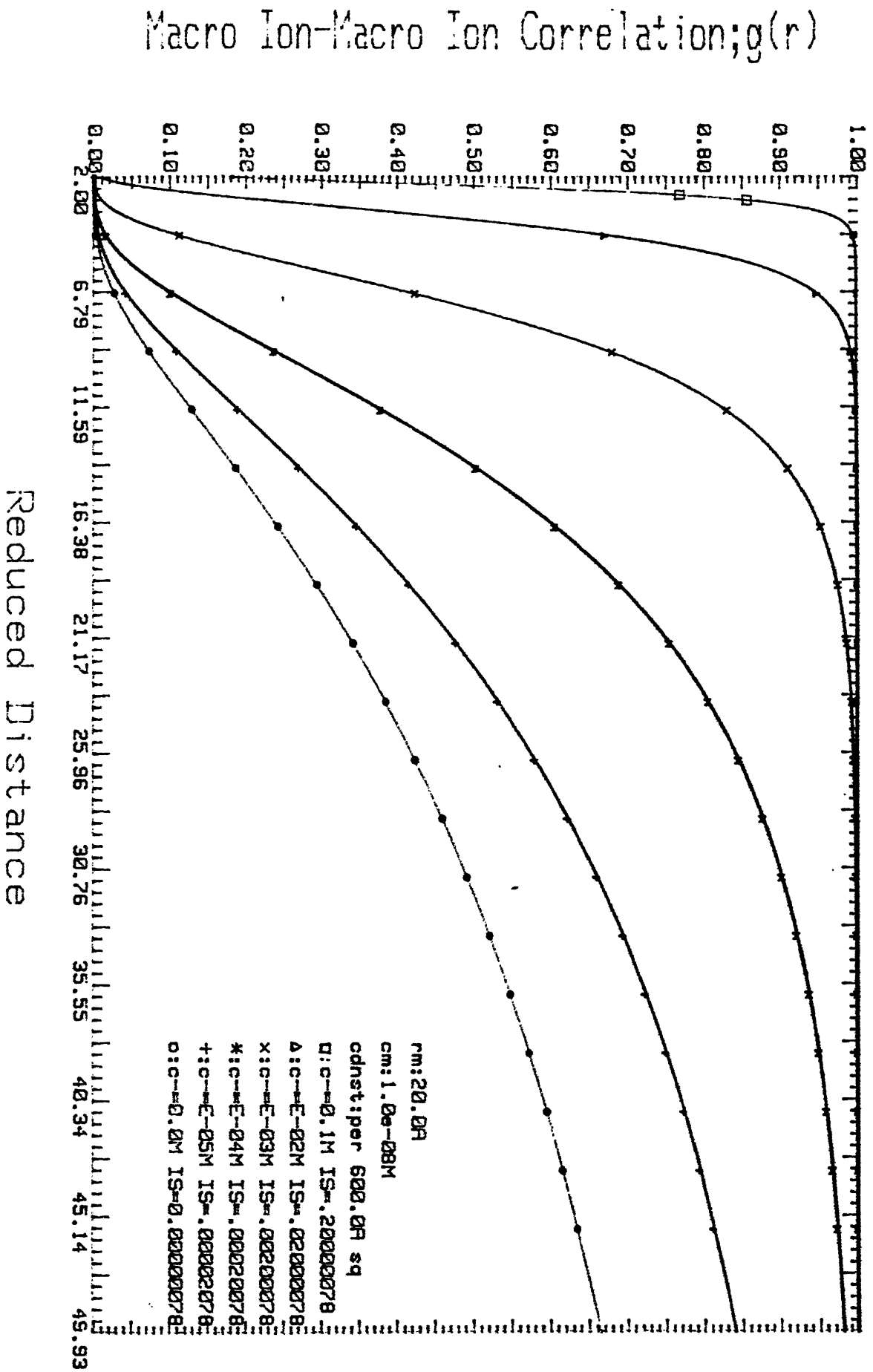
# Correlation Function Vs. Distance F-5.27



# Correlation Function Vs. Distance F-5.28



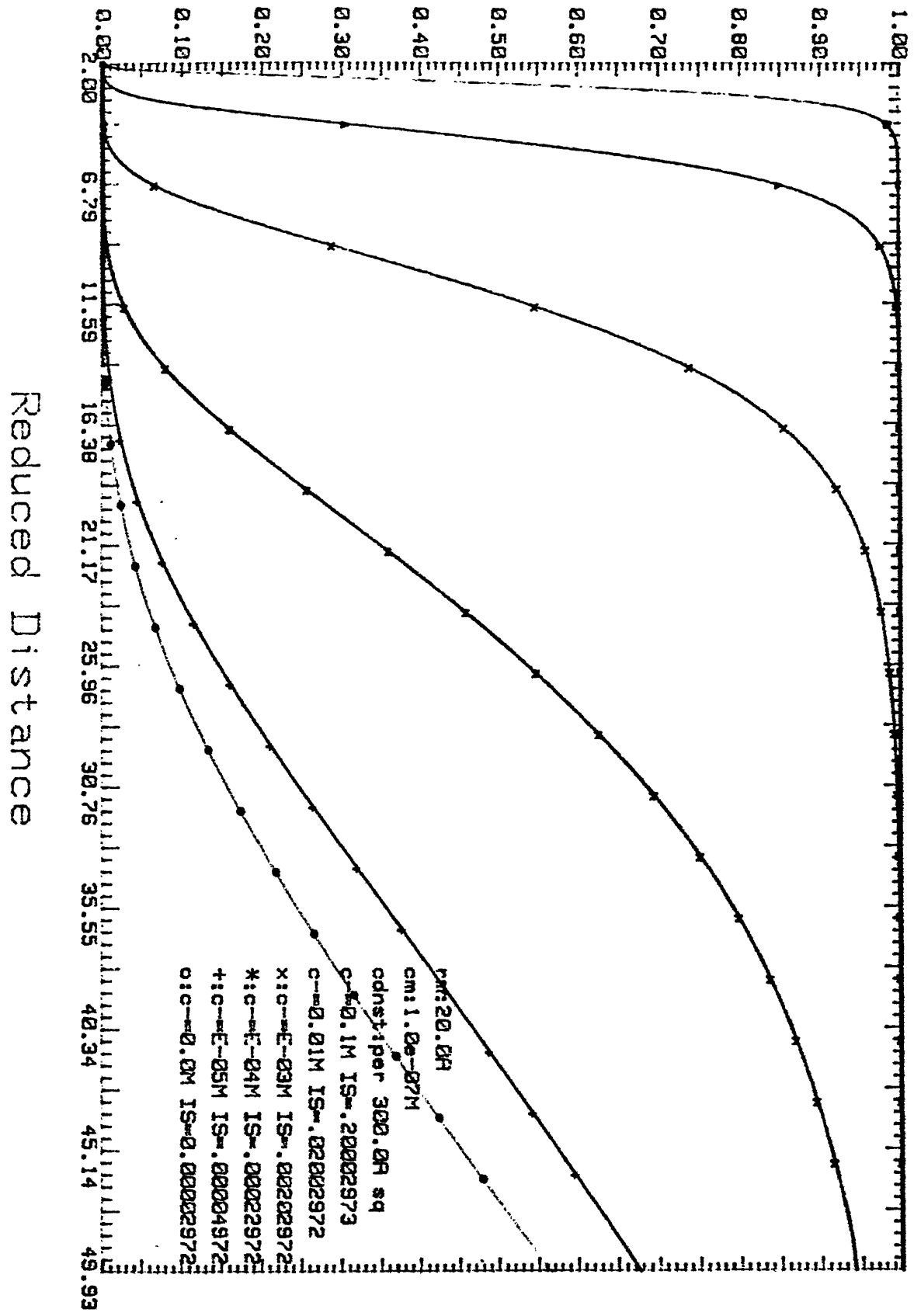
# Correlation Function Vs. Distance F-5.31



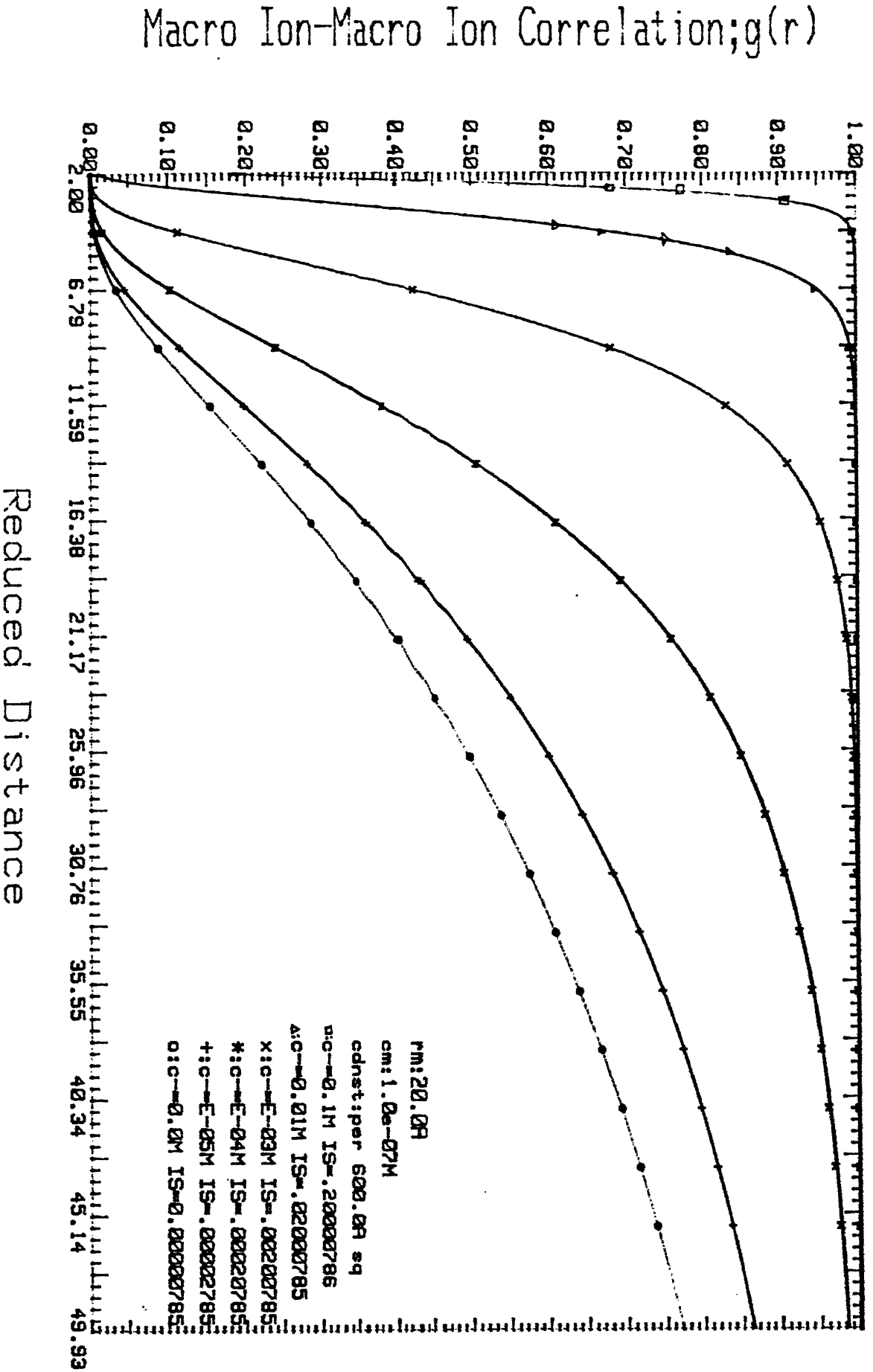


# Correlation Function Vs. Distance F.5.32

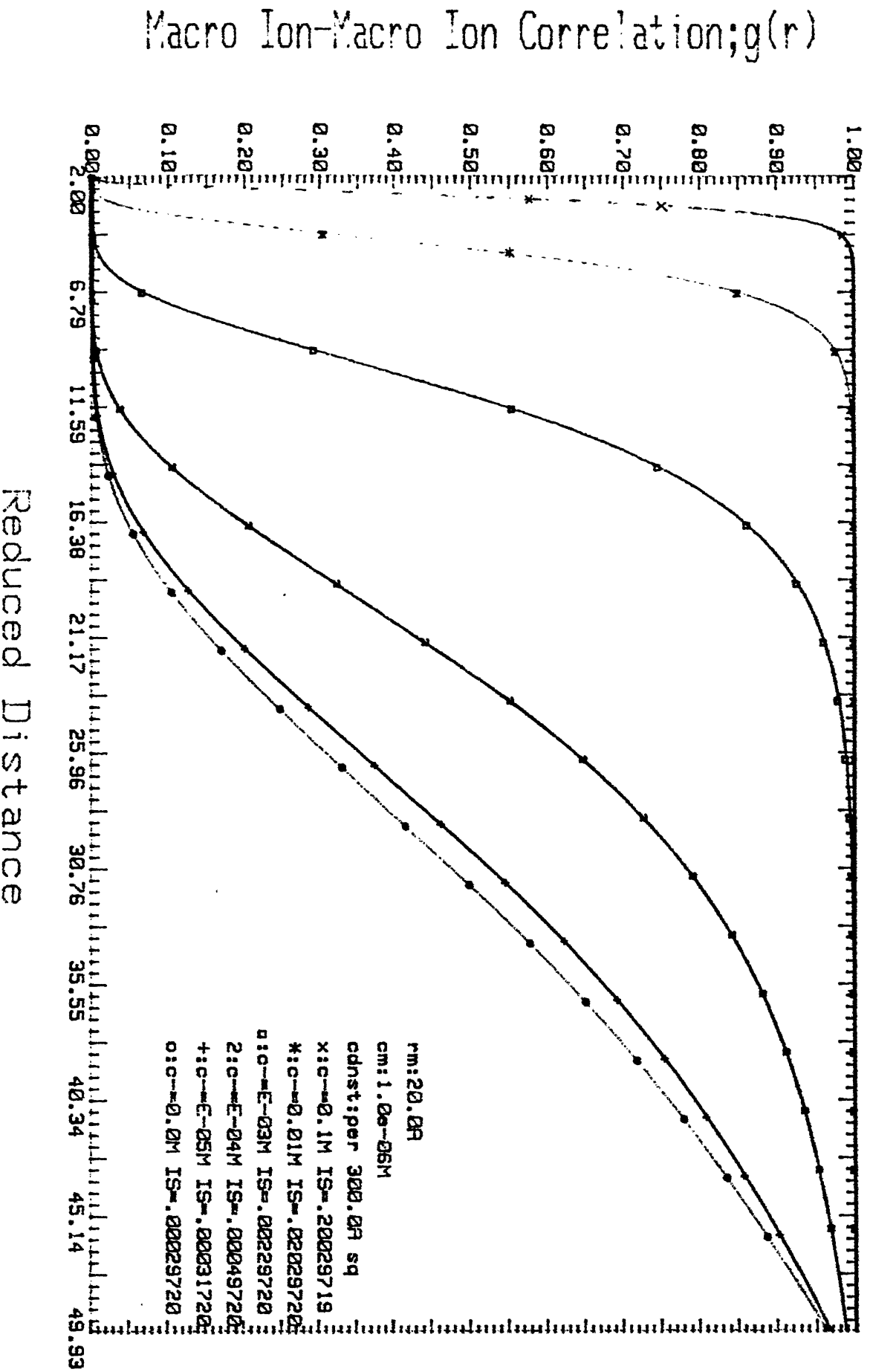
Macro Ion-Macro Ion Correlation;g(r)



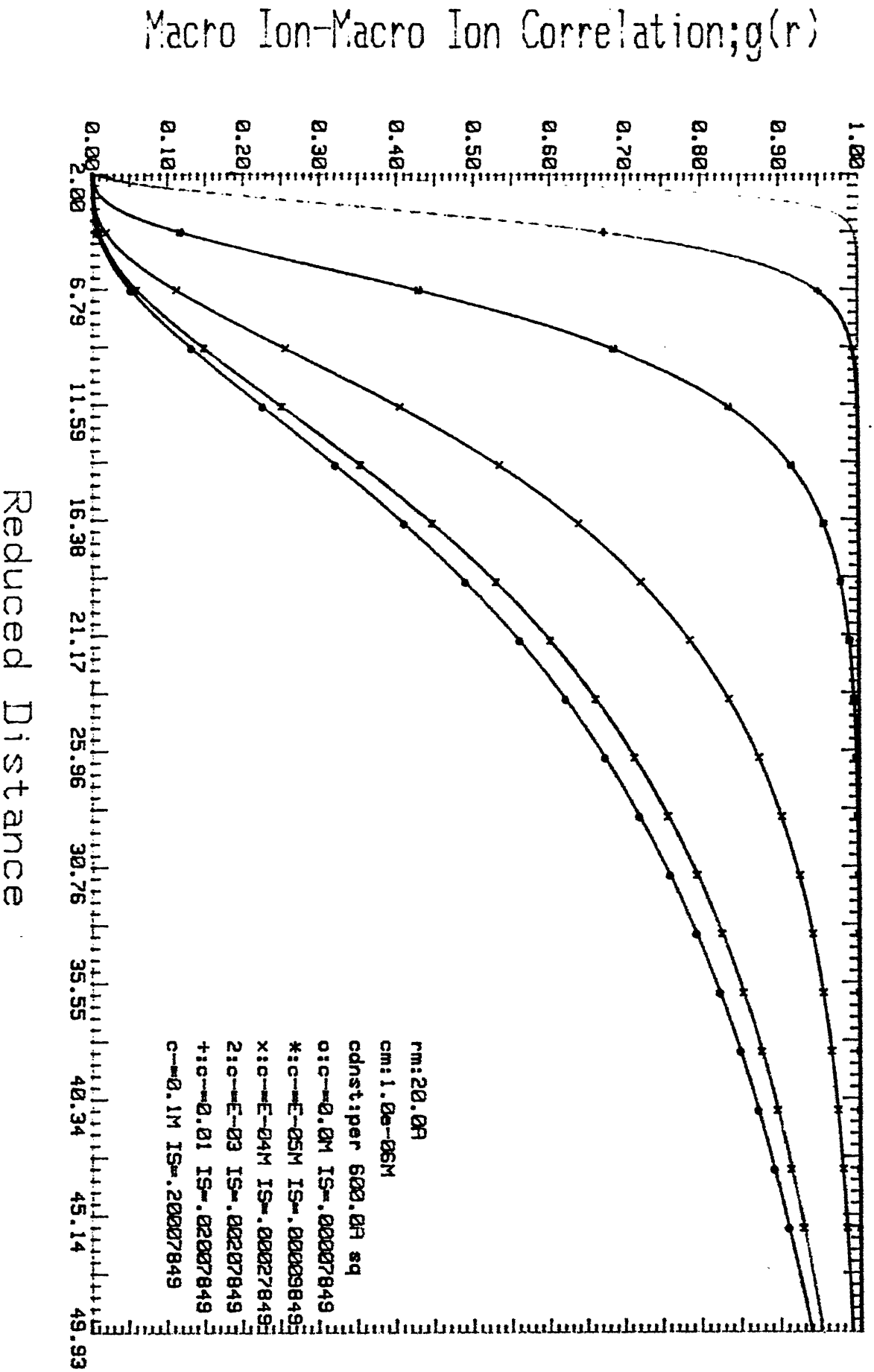
# Correlation Function Vs. Distance F-5.3i



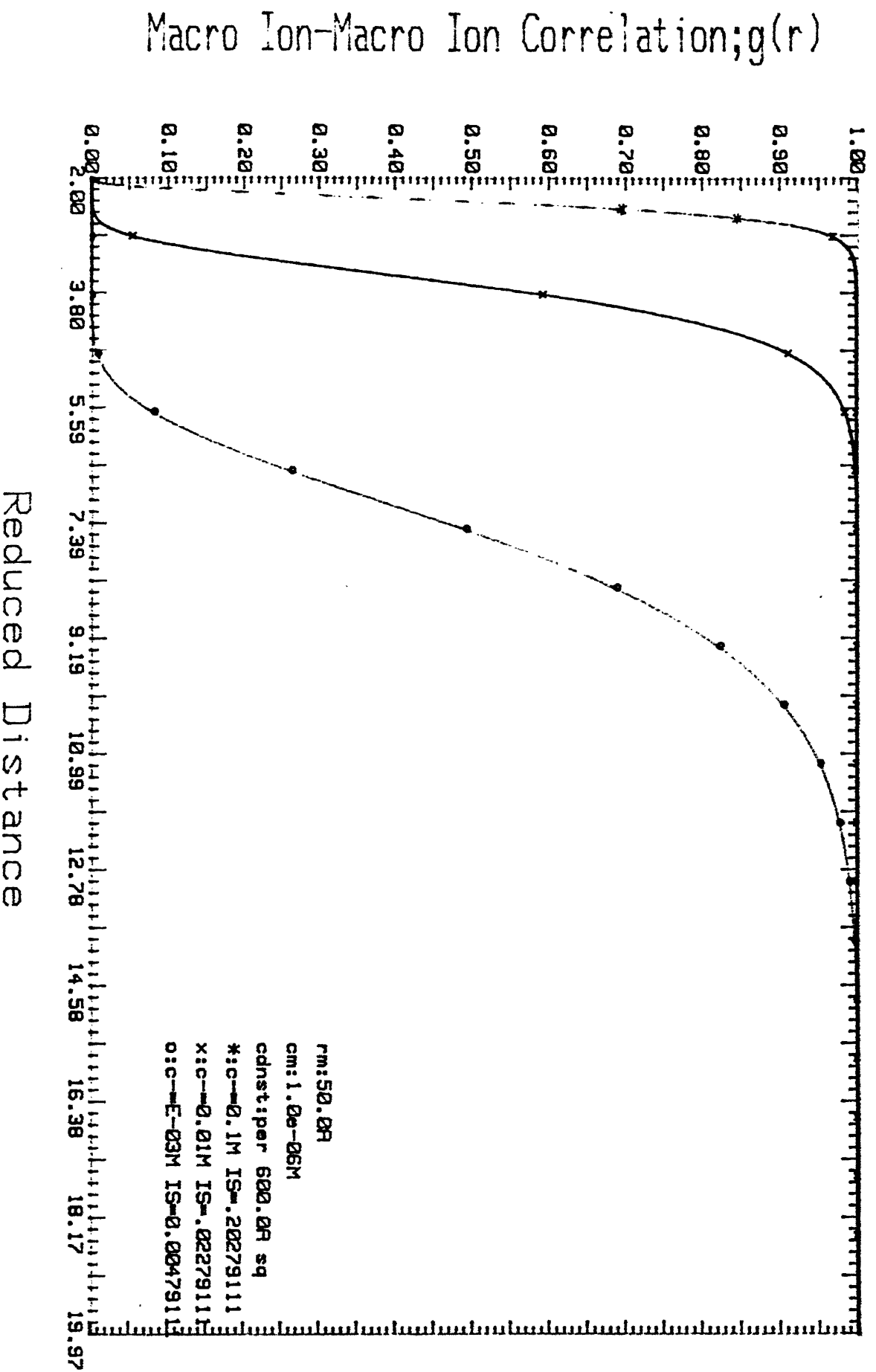
# Correlation Function Vs. Distance F-5.34



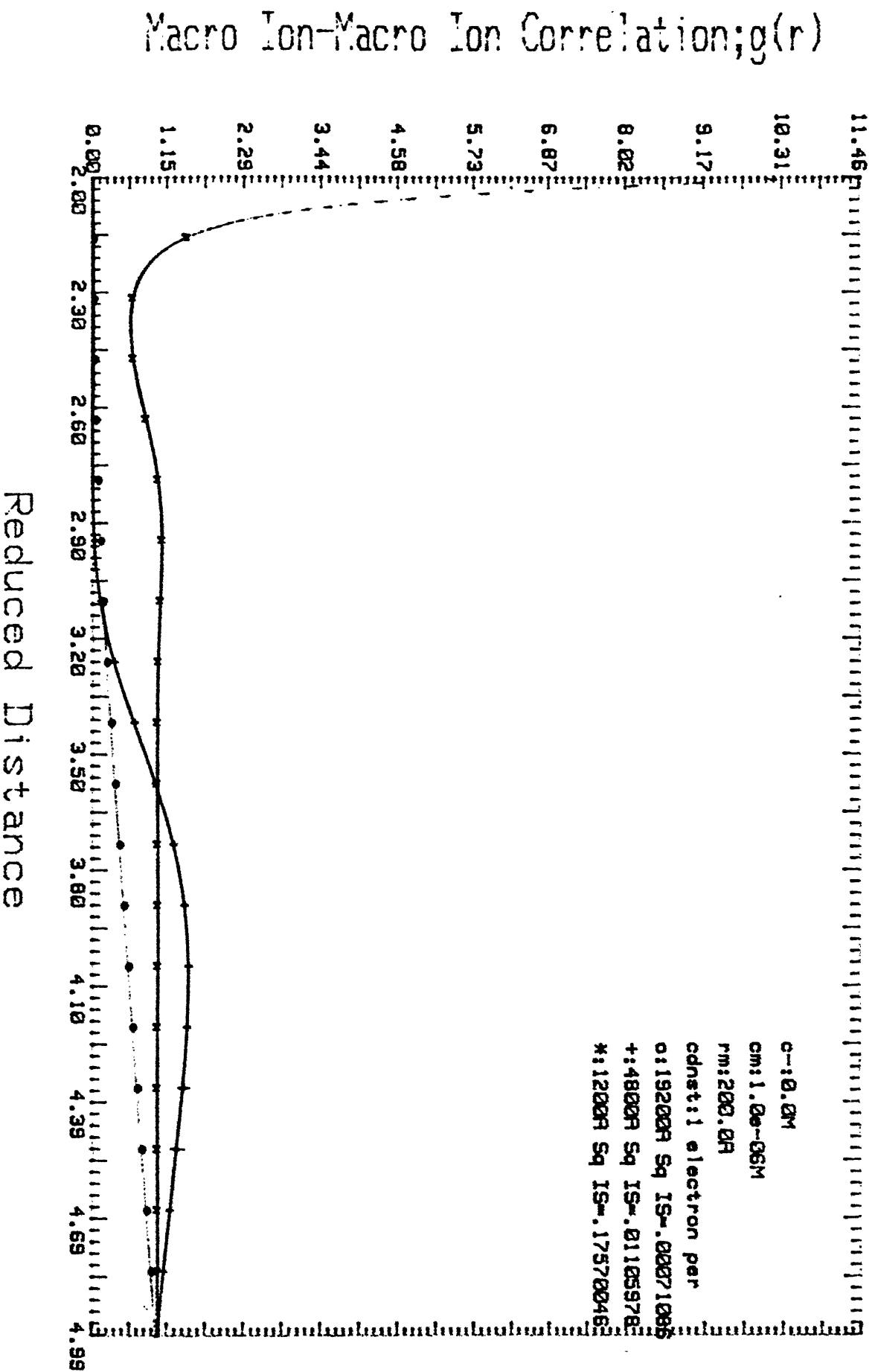
# Correlation Function Vs. Distance F-5.35



# Correlation Function Vs. Distance F-5.36

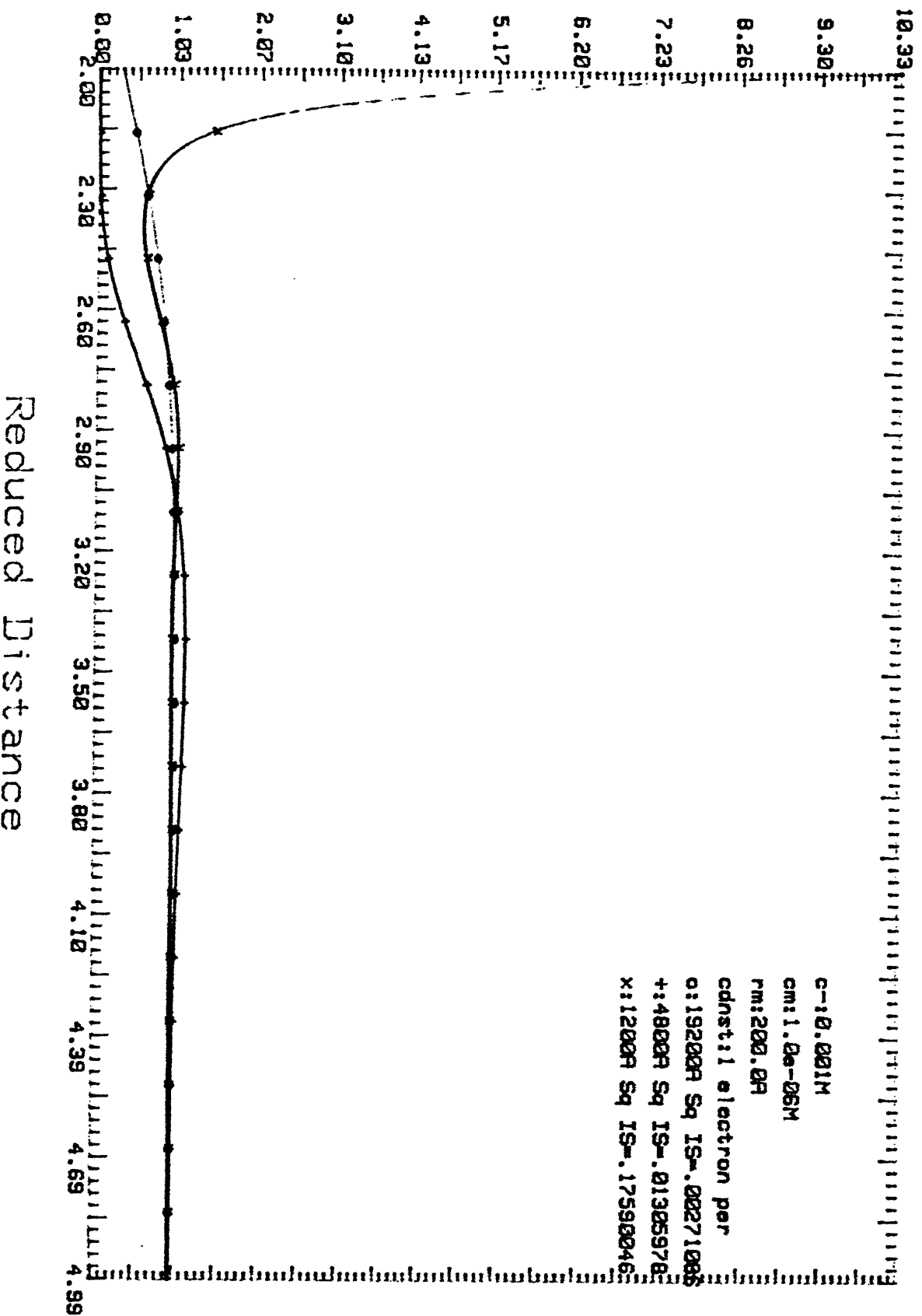


# Correlation Function Vs. Distance F-5.37

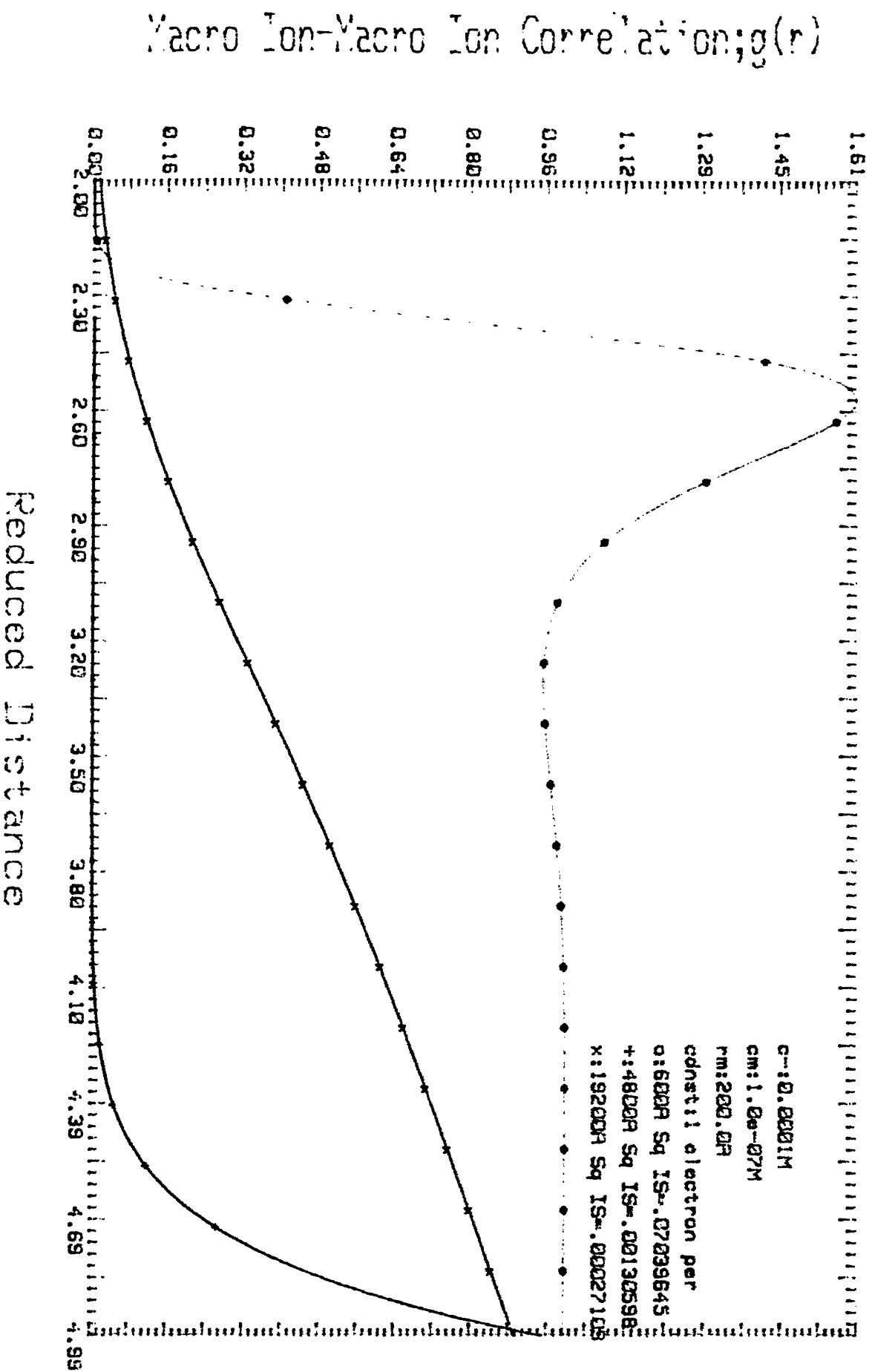


# Correlation Function Vs. Distance F-5.38

Macro Ion-Macro Ion Correlation;  $g(r)$

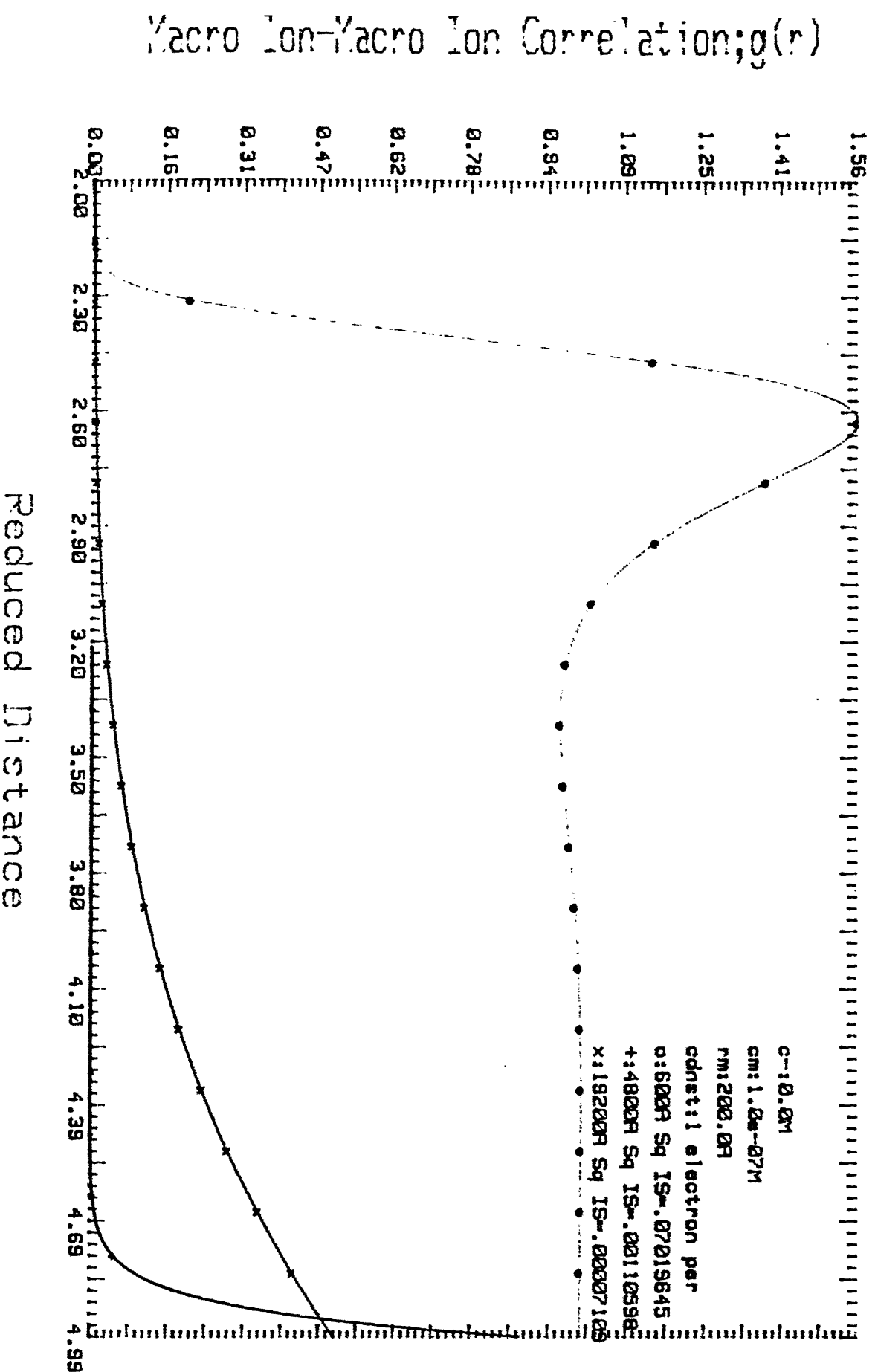


# Correlation Function Vs. Distance F-5.41

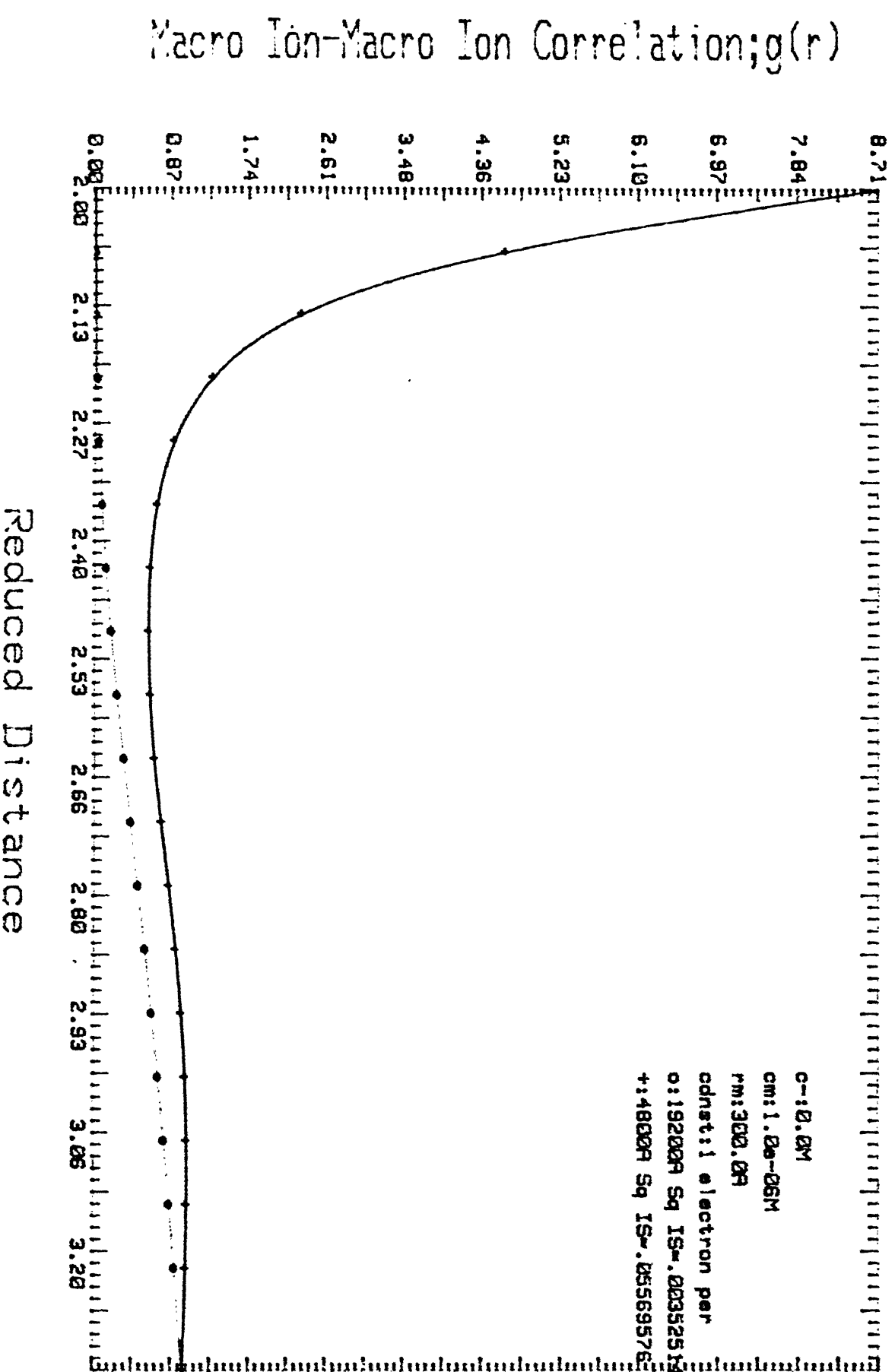




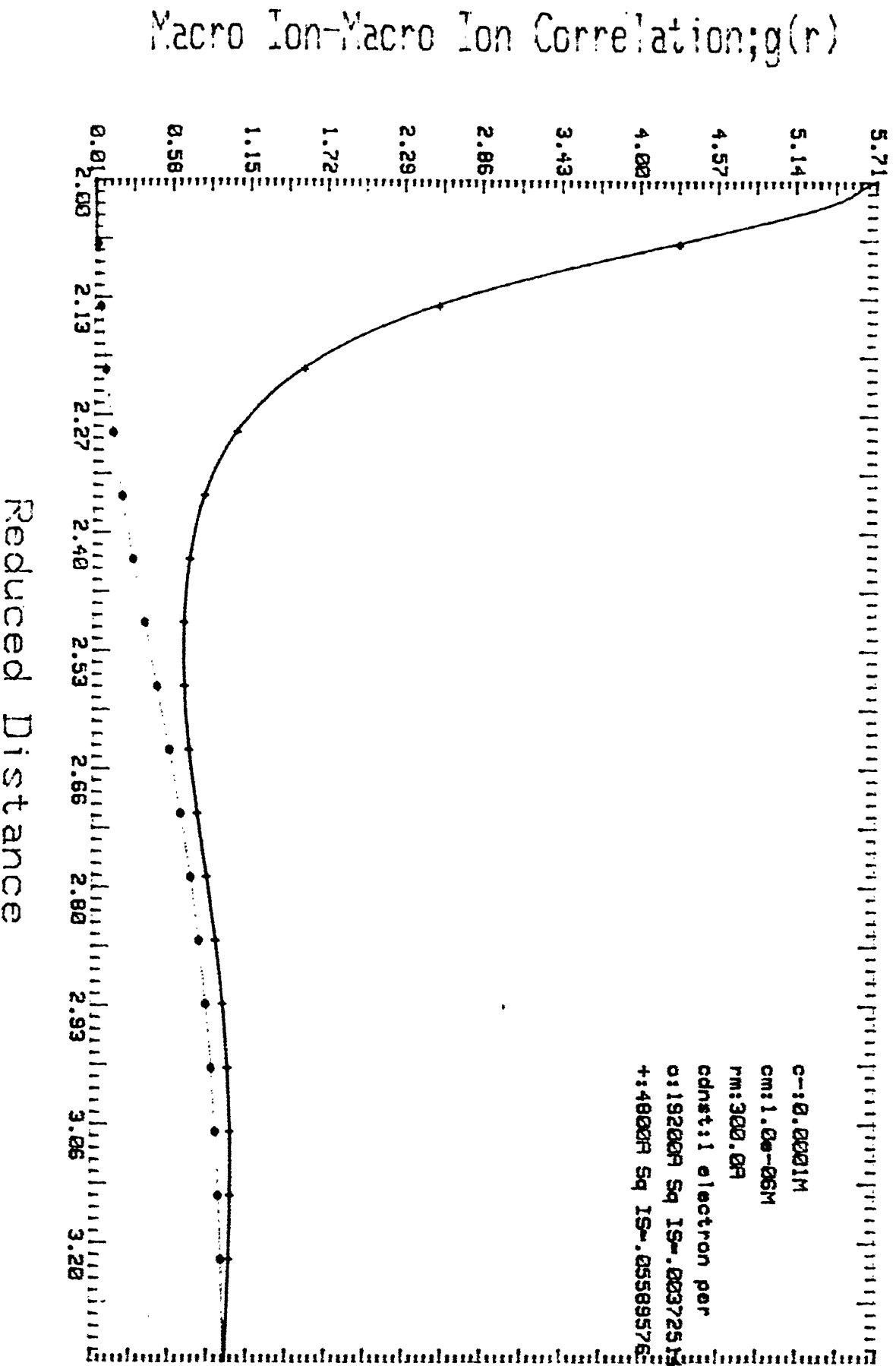
# Correlation Function Vs. Distance F-5.42



# Correlation Function Vs. Distance F-5.43

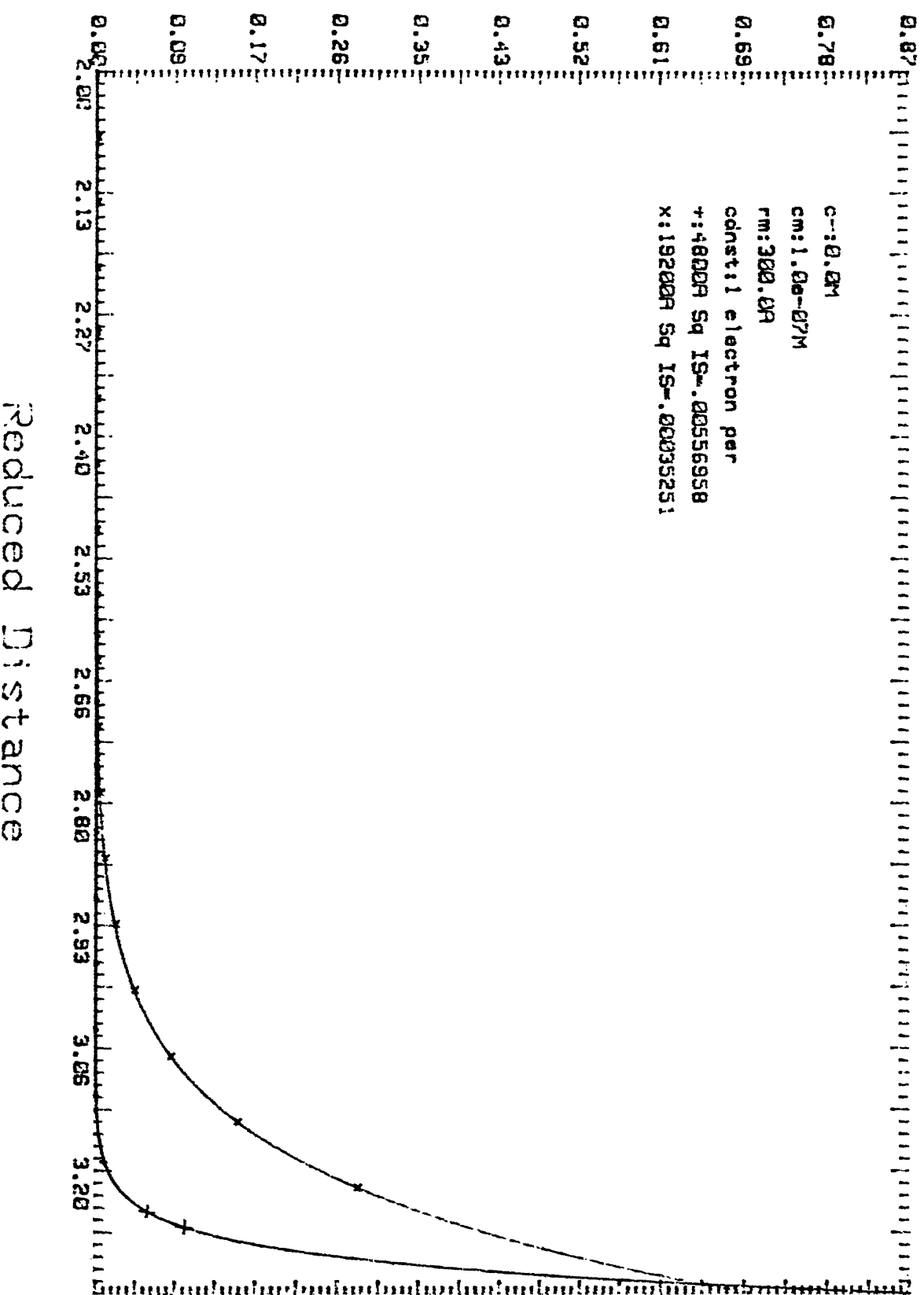


# Correlation Function Vs. Distance F-5.44

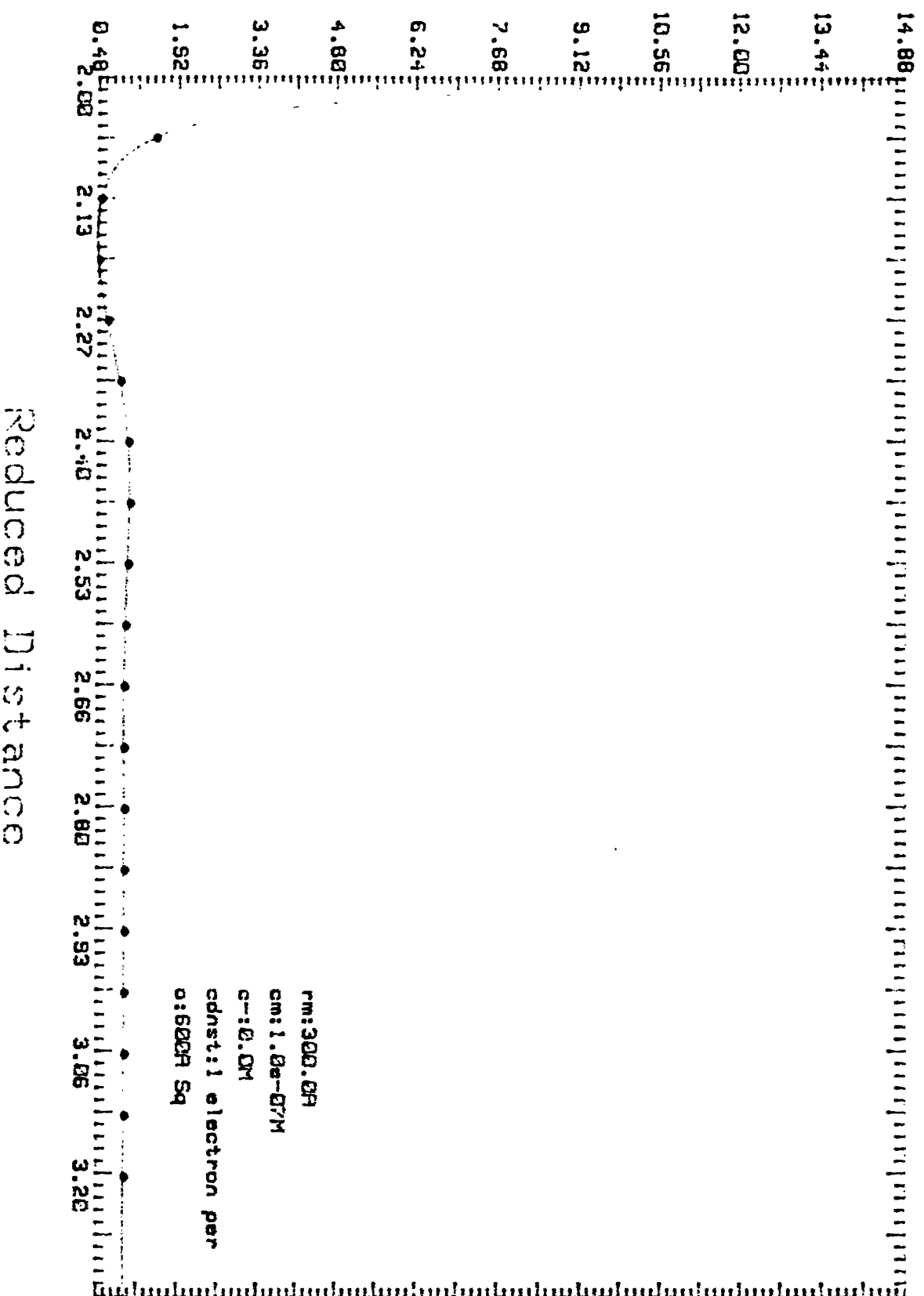


# Correlation Function Vs. Distance F-5.45

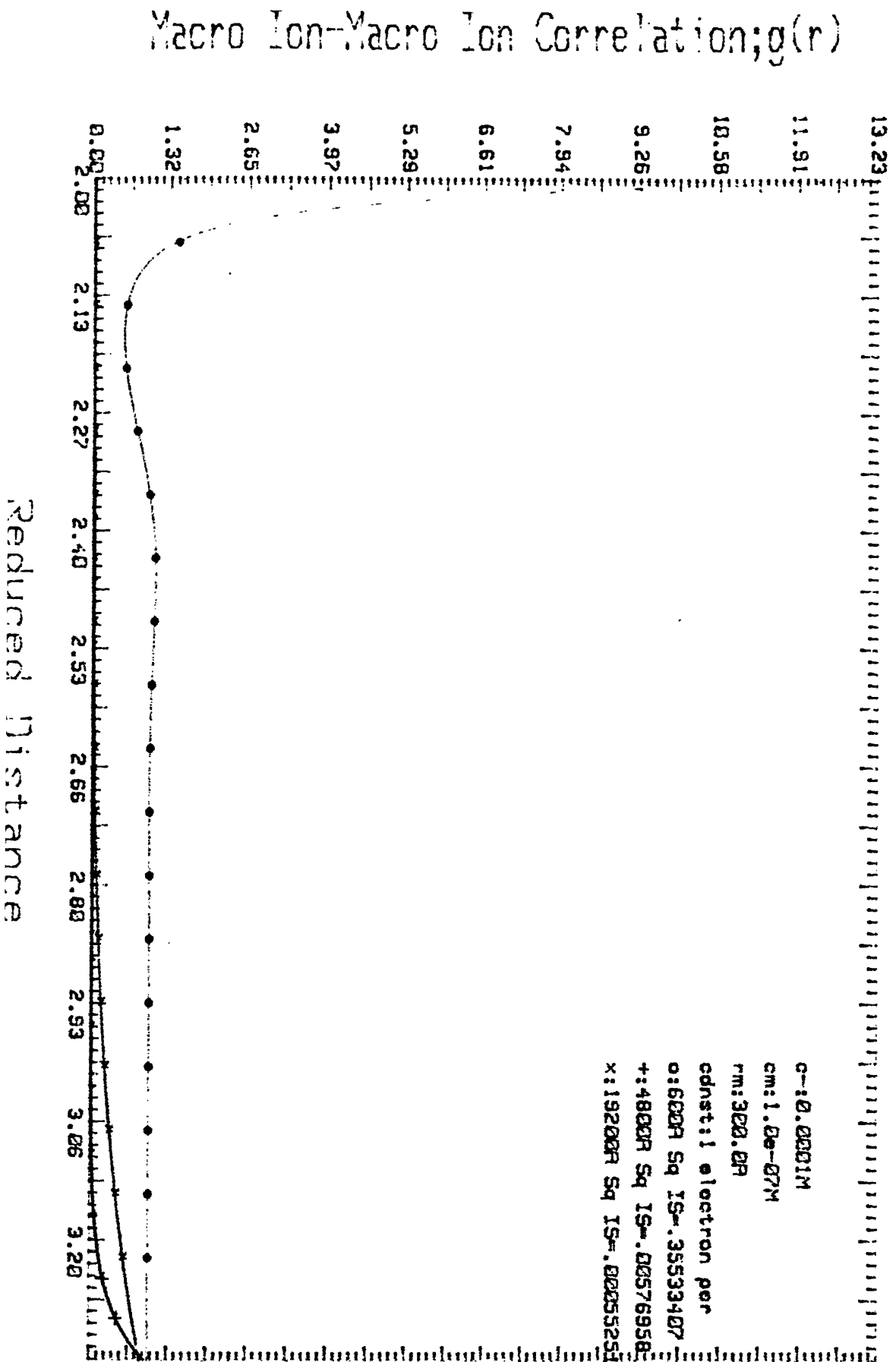
Macro Ion-Macro Ion Correlation;  $g(r)$



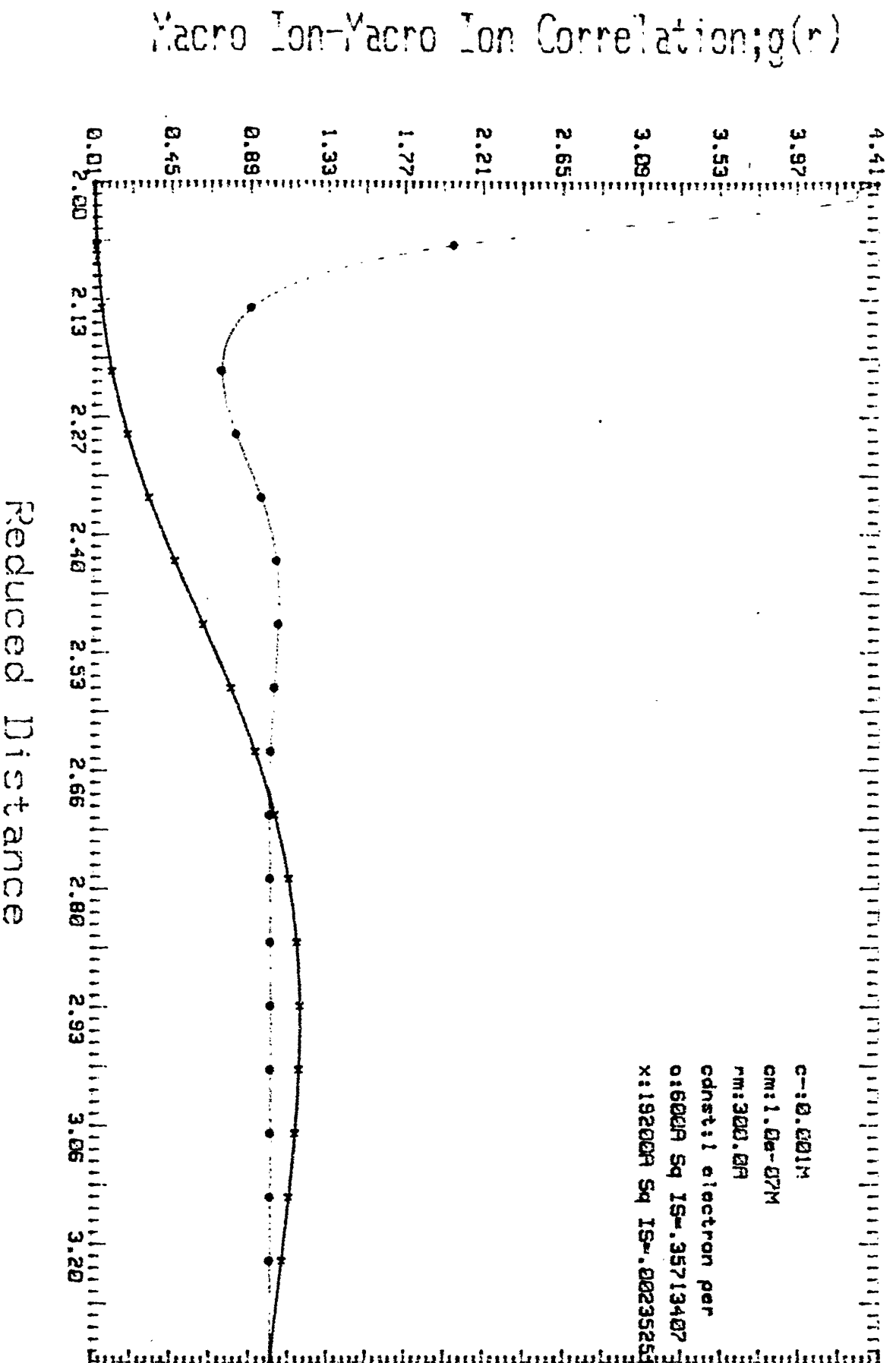
# Correlation Function Vs. Distance F-5.46



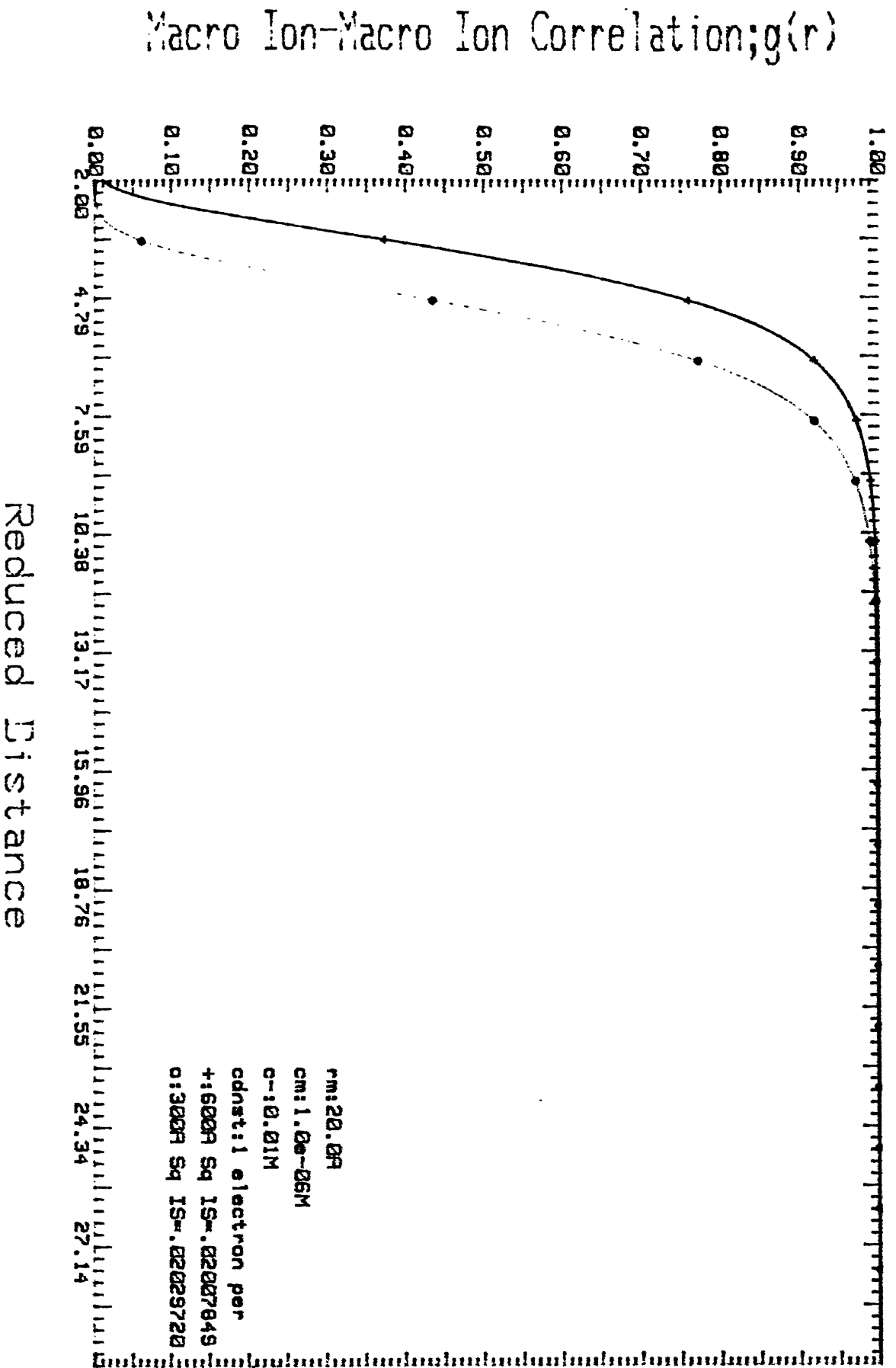
# Correlation Function Vs. Distance F-5.47



# Correlation Function Vs. Distance F-5.48

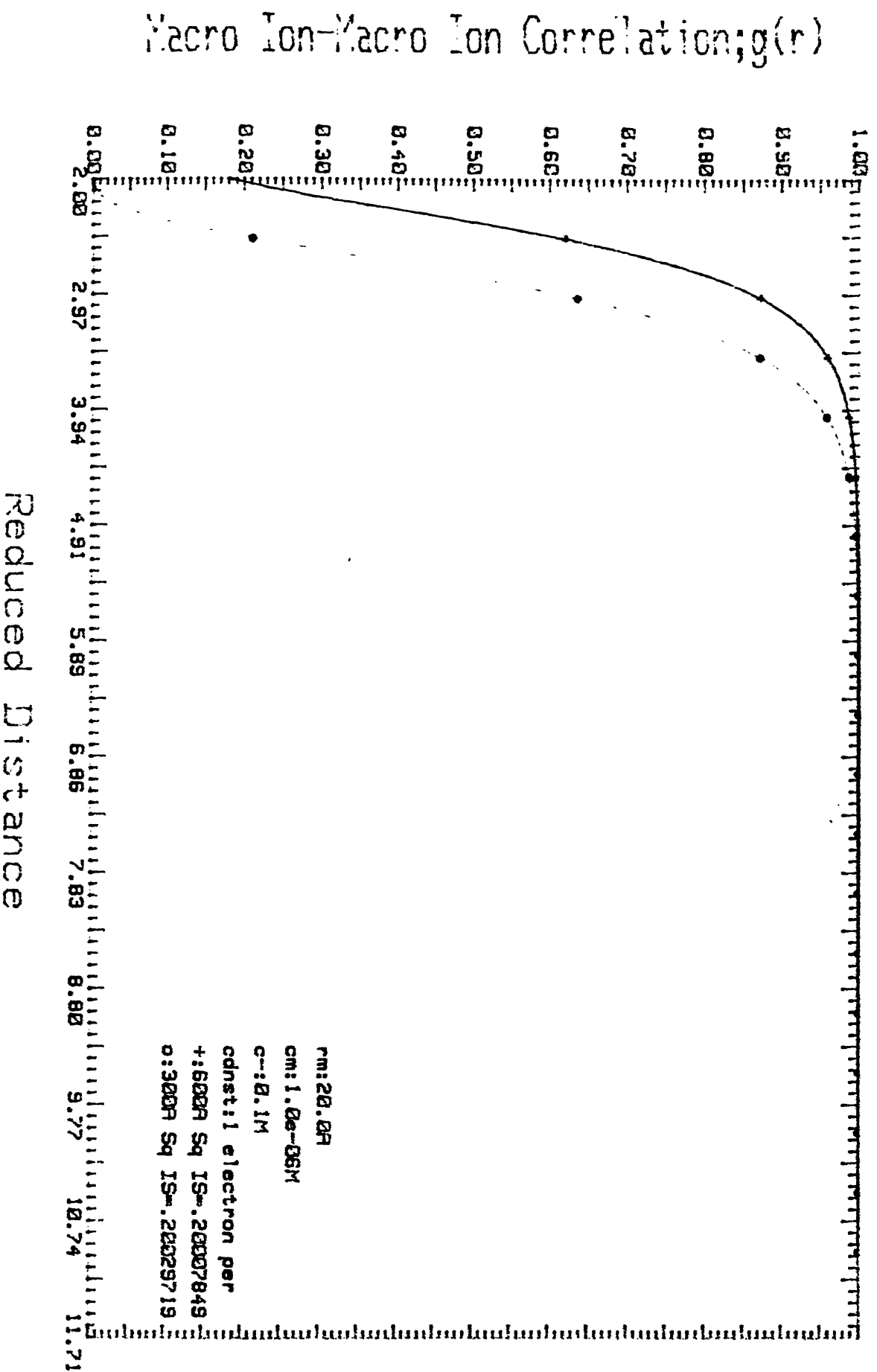


# Correlation Function Vs. Distance F-5.51

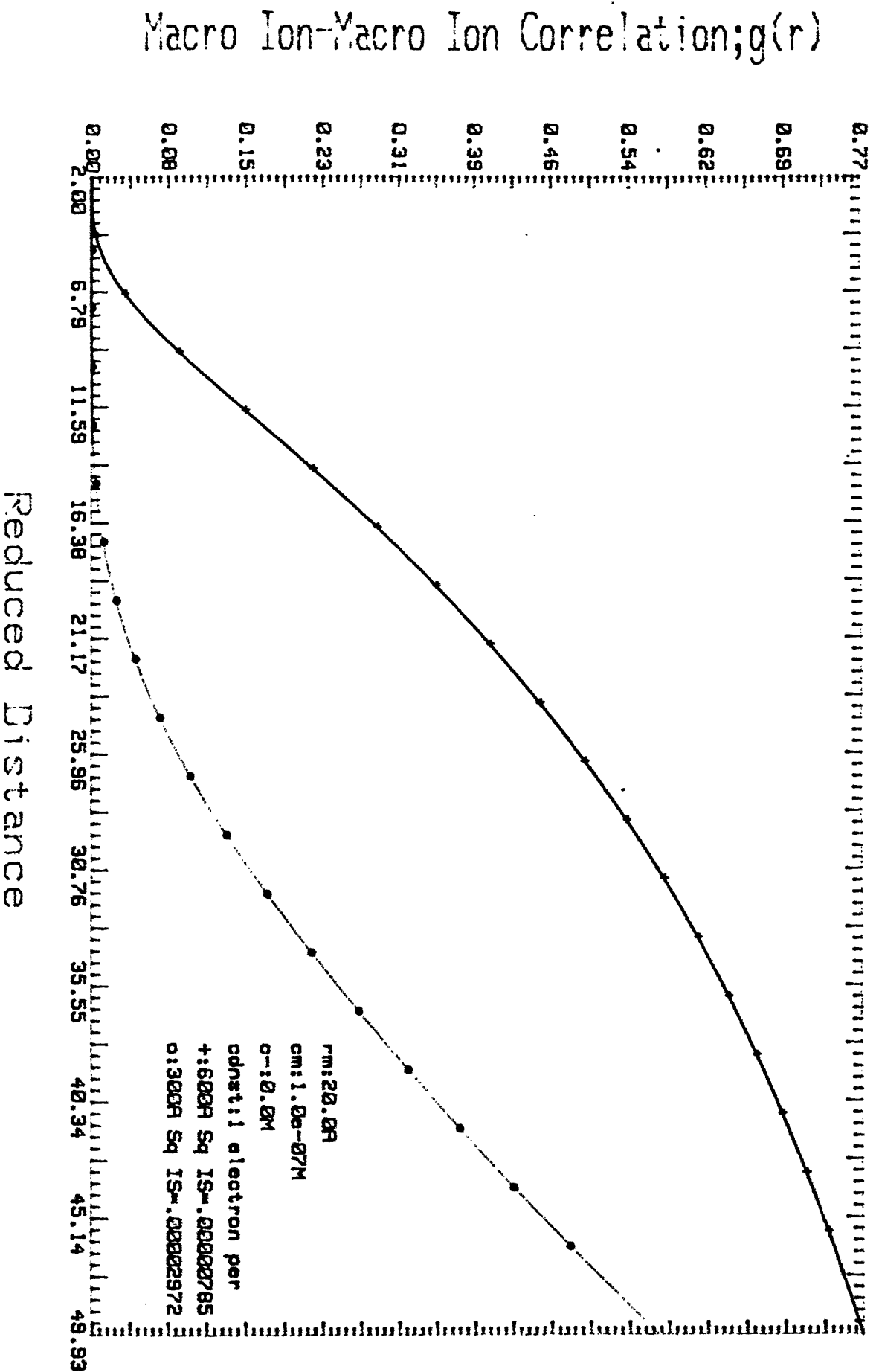




# Correlation Function Vs. Distance F-5.52

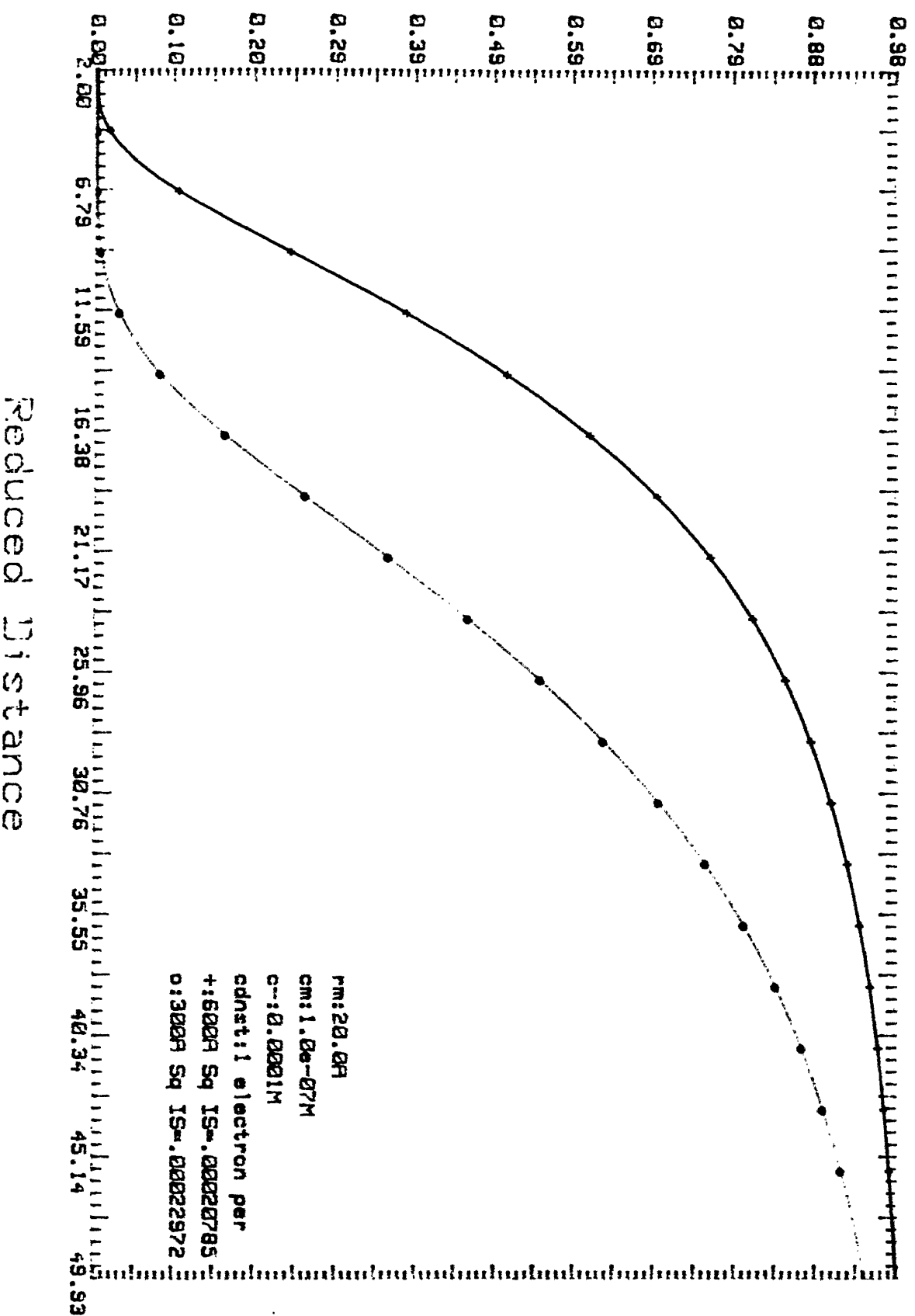


# Correlation Function Vs. Distance F-5.53



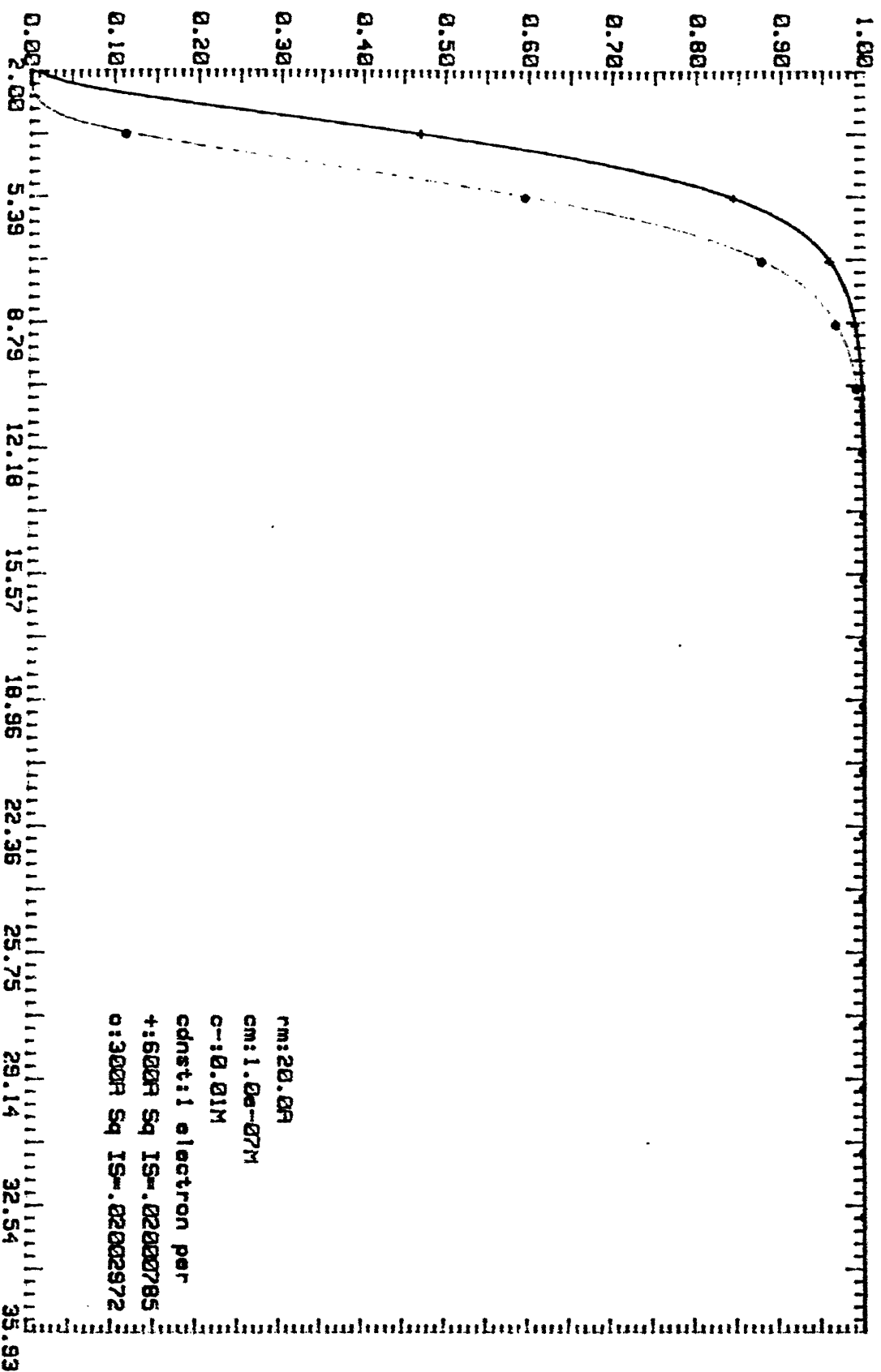
# Correlation Function Vs. Distance F-5.54

Macro Ion-Macro Ion Correlation;  $g(r)$



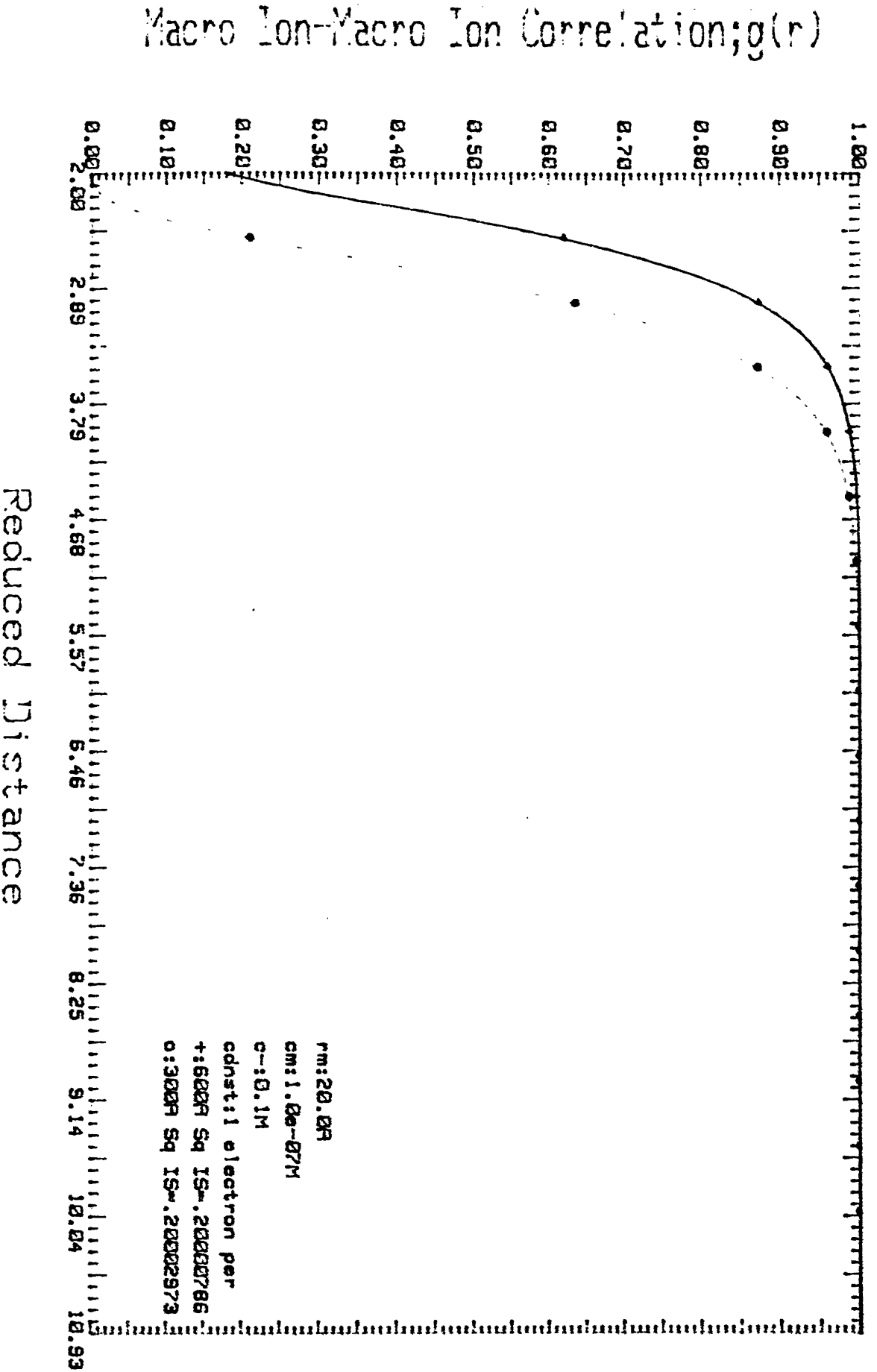
# Correlation Function Vs. Distance F-5.55

Macro Ion-Macro Ion Correlation;g(r)



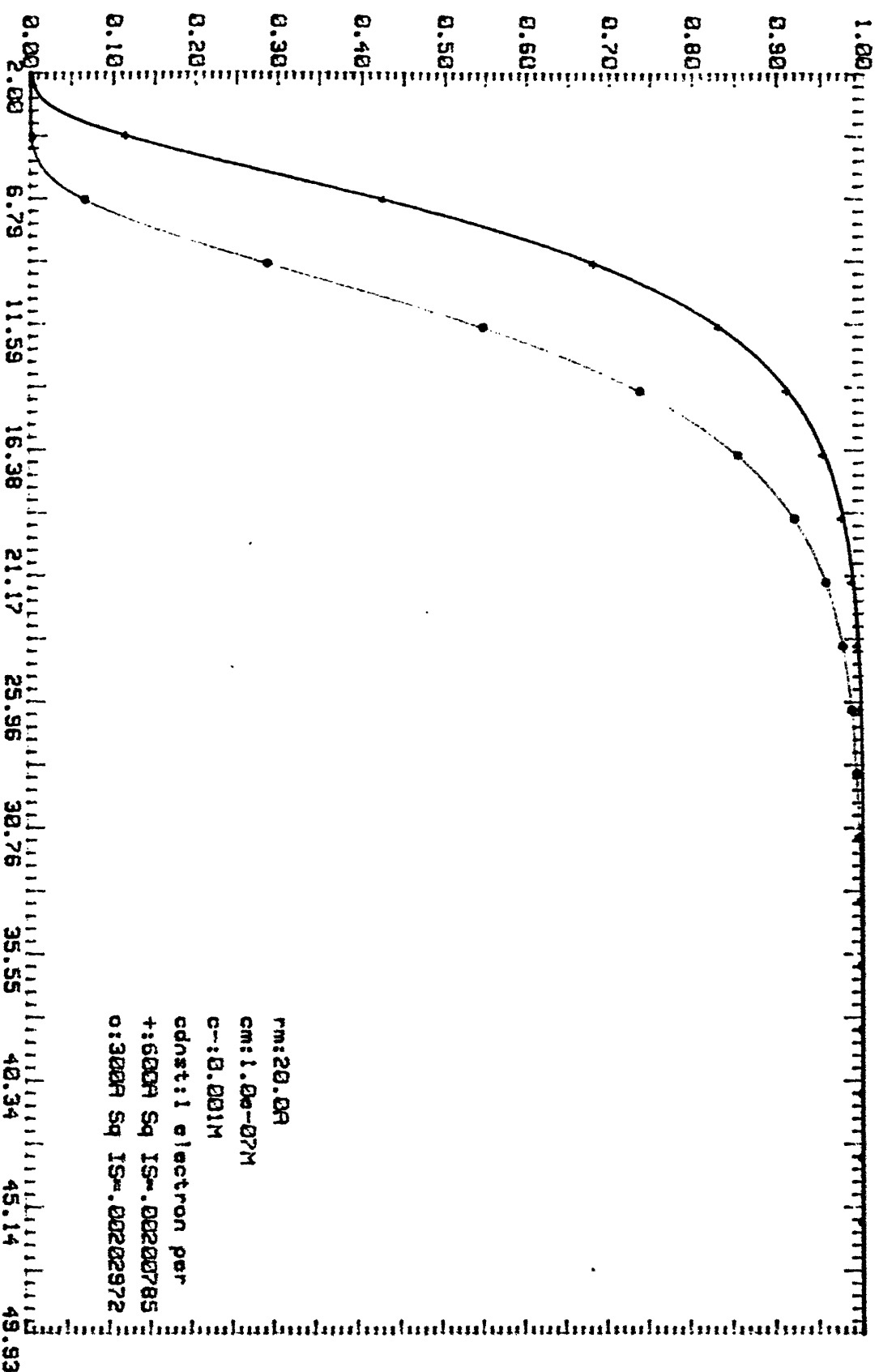
Reduced Distance

# Correlation Function Vs. Distance F-5.56



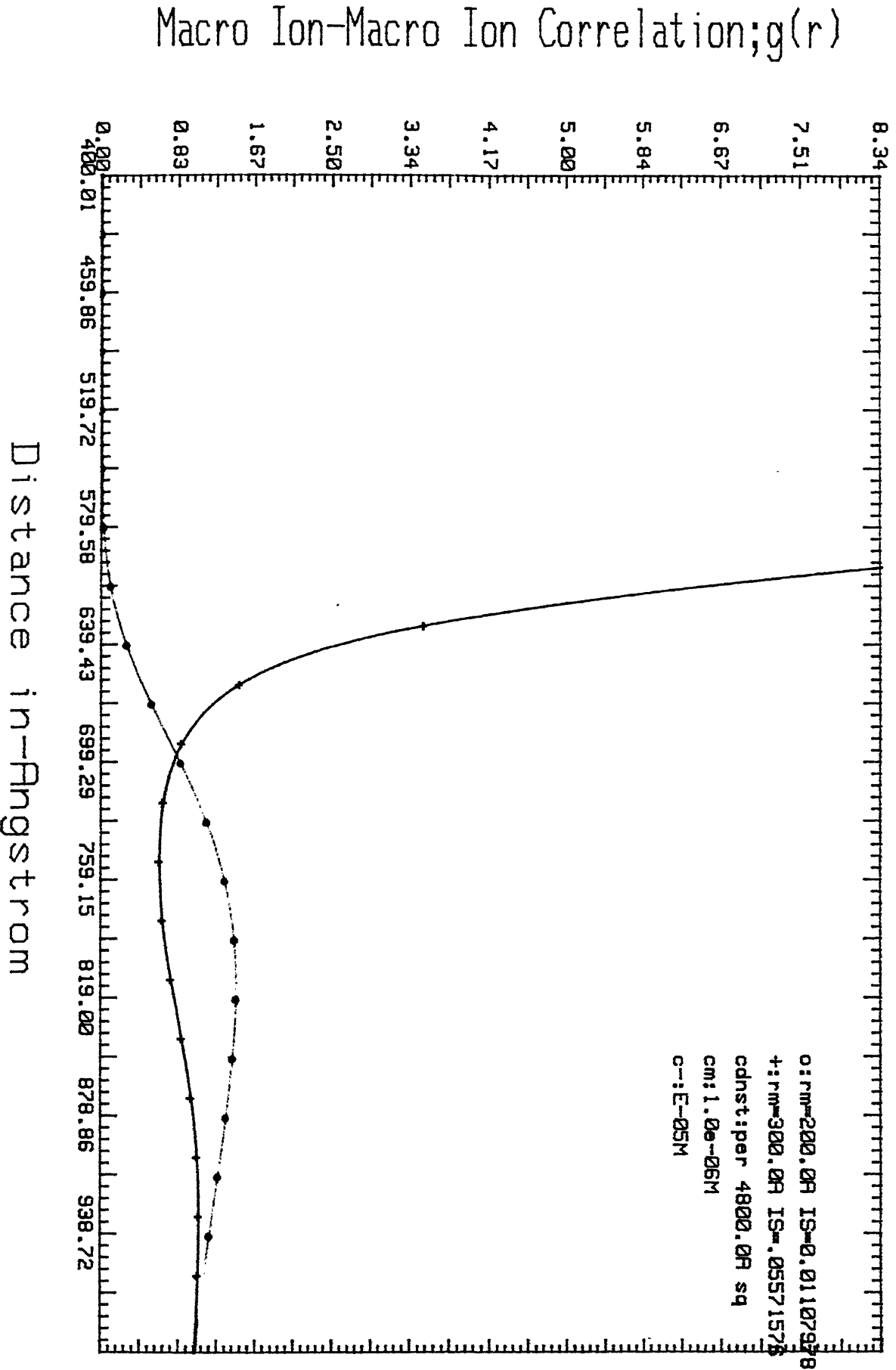
# Correlation Function Vs. Distance F-5.57

Macro Ion-Macro Ion Correlation;  $g(r)$

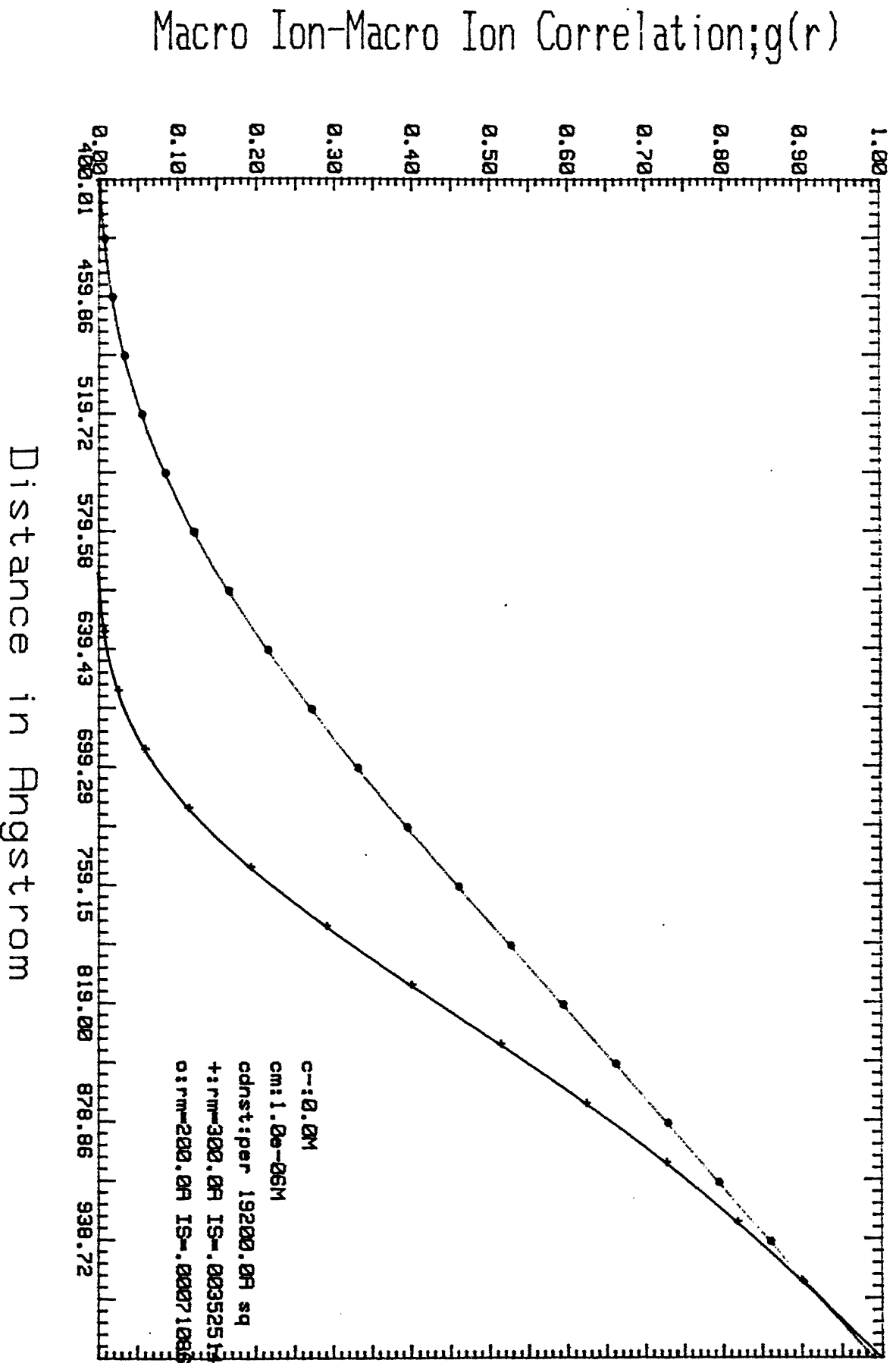


Reduced Distance

# Correlation Function Vs. Distance F-5.58

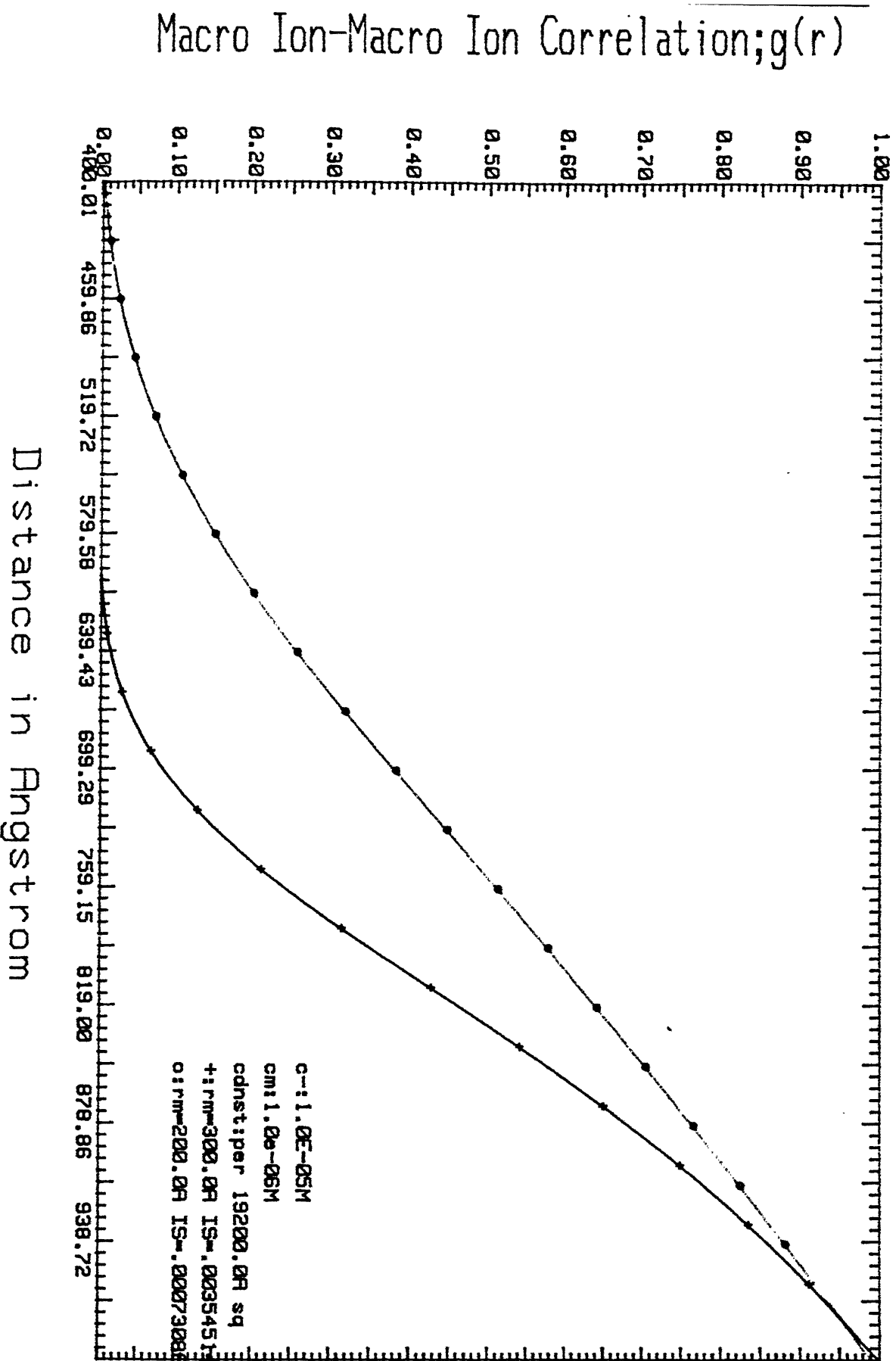


# Correlation Function Vs. Distance F-5.61

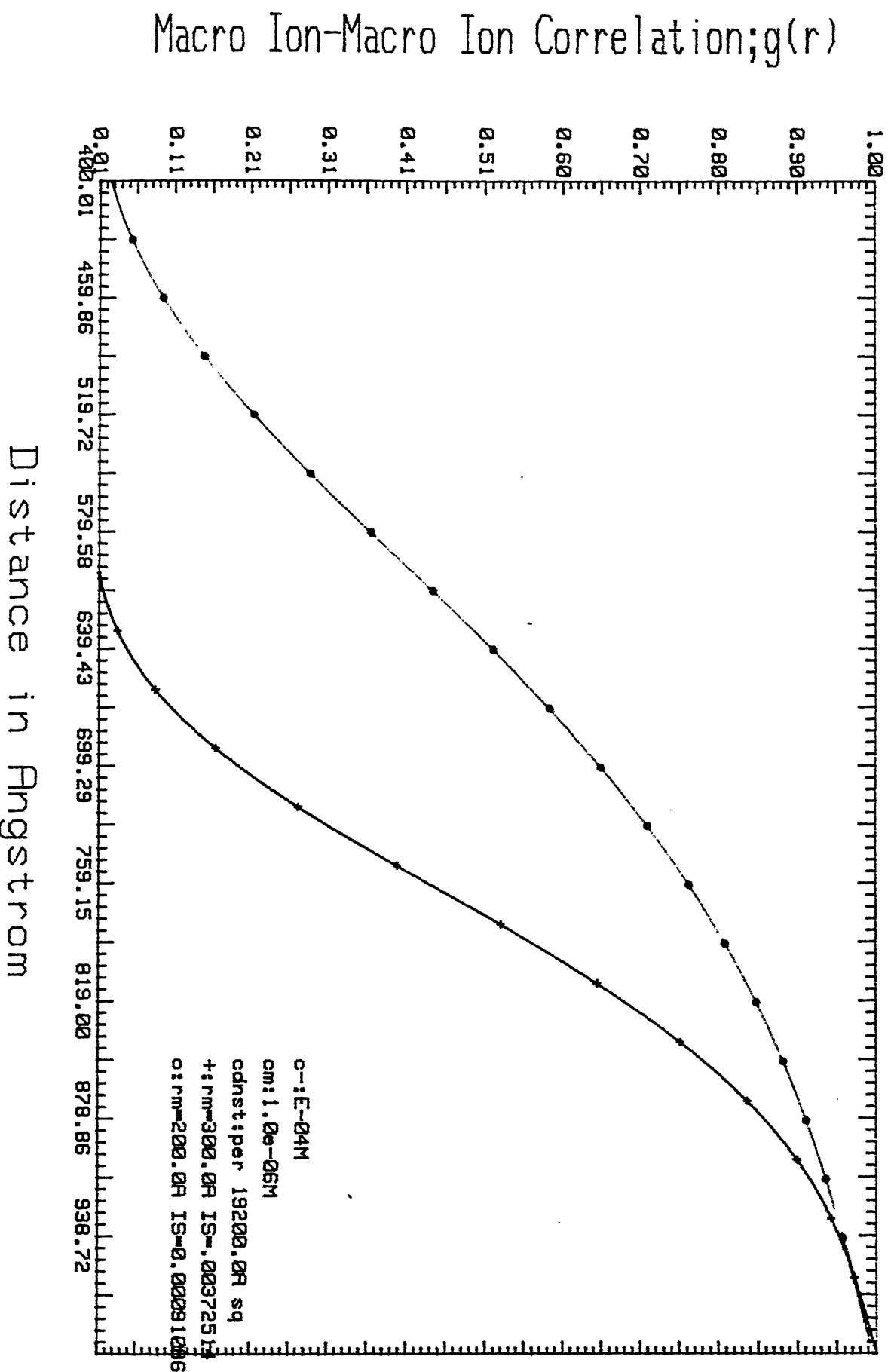




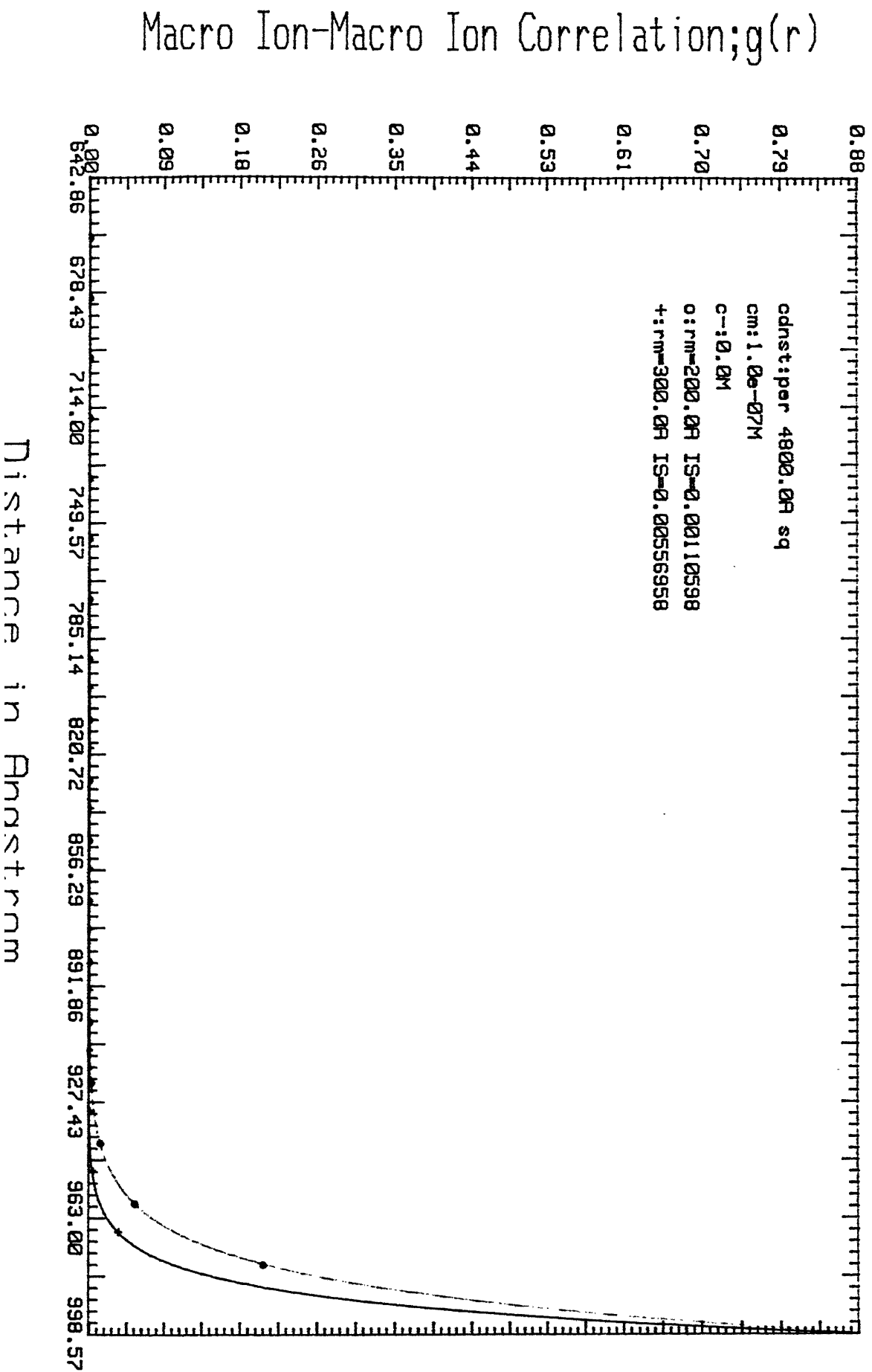
# Correlation Function Vs. Distance F-5.62



# Correlation Function Vs. Distance F-5.62

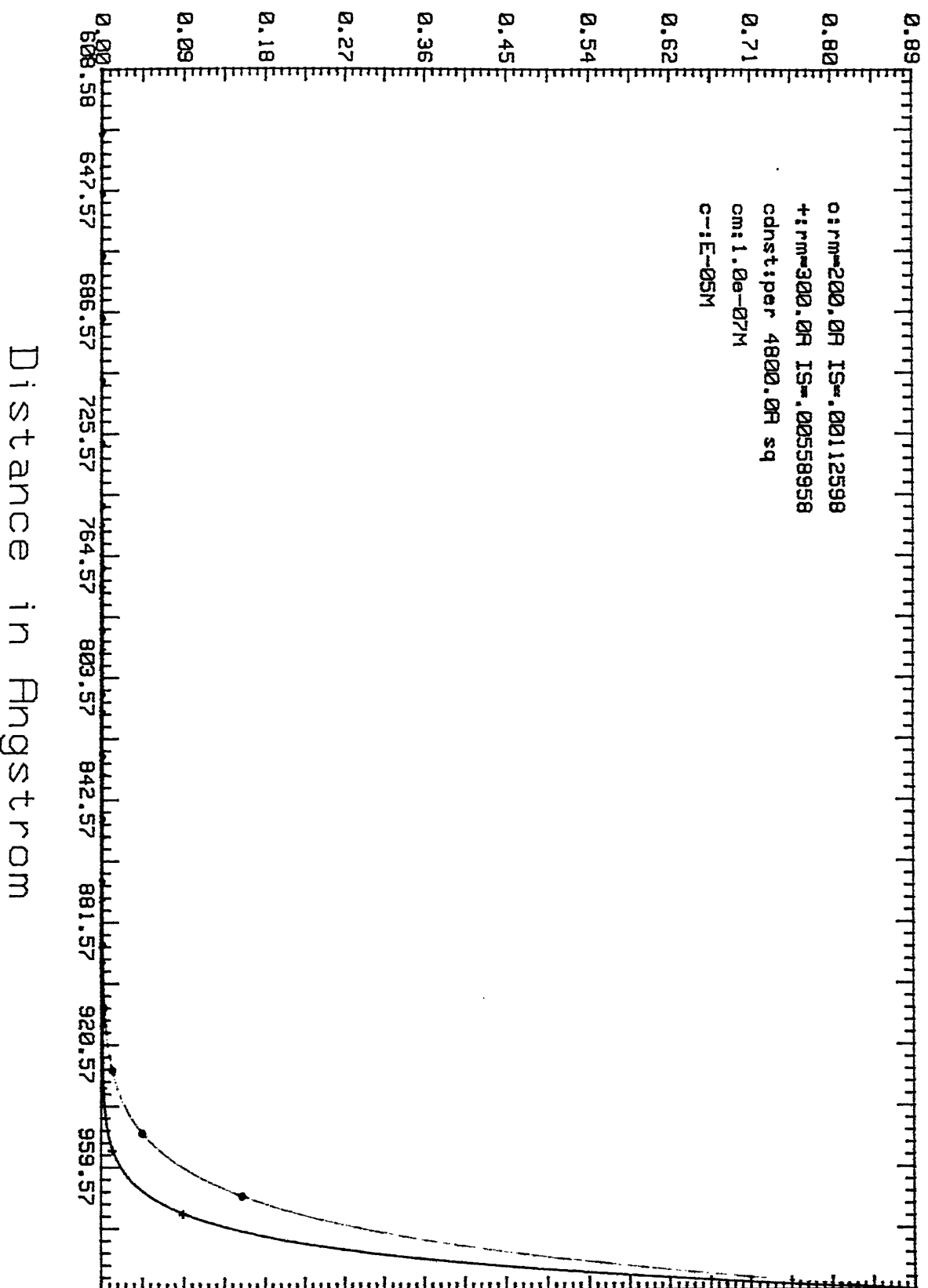


# Correlation Function Vs. Distance F-5.64



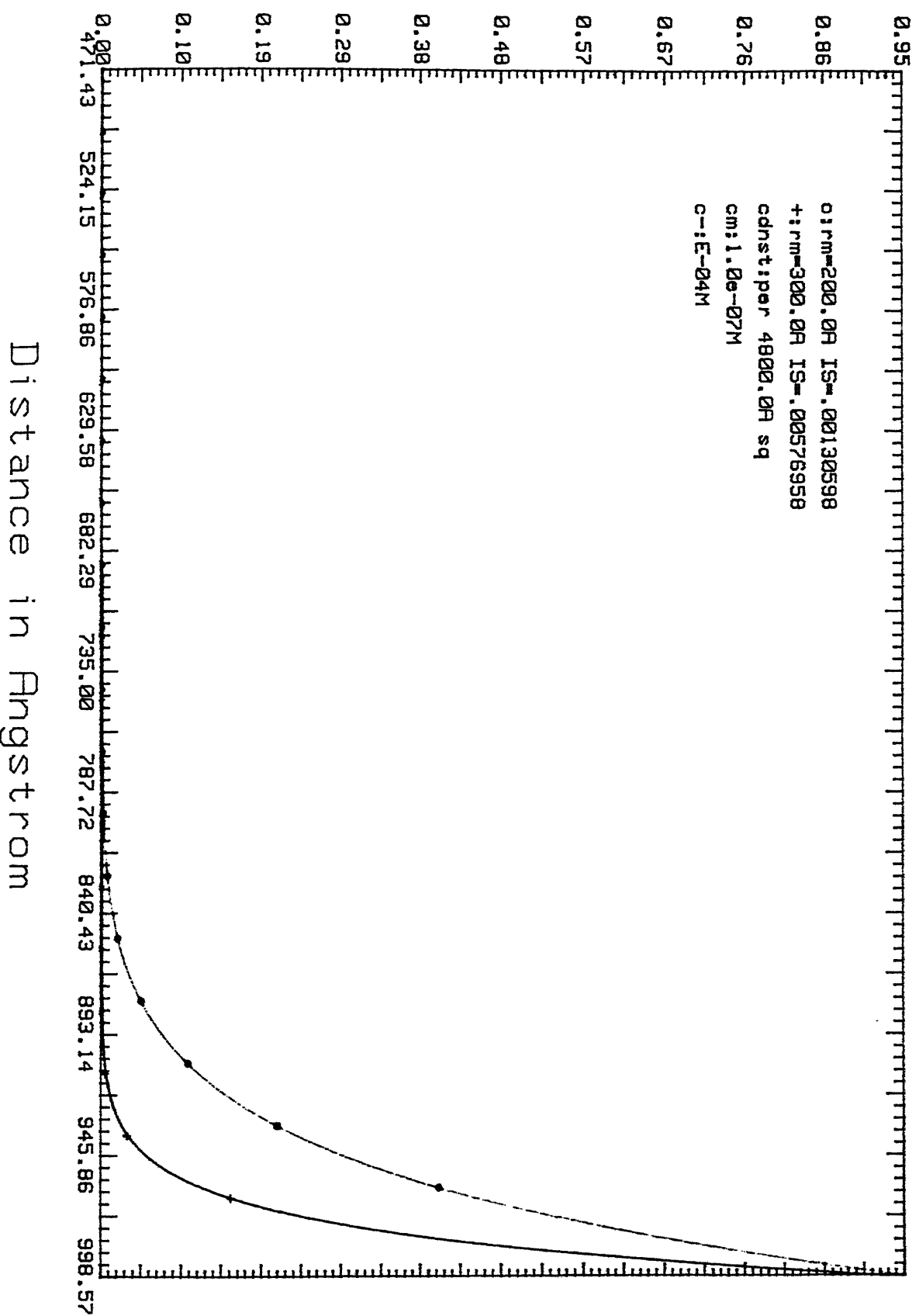
# Correlation Function Vs. Distance F-5.65

Macro Ion-Macro Ion Correlation;g(r)



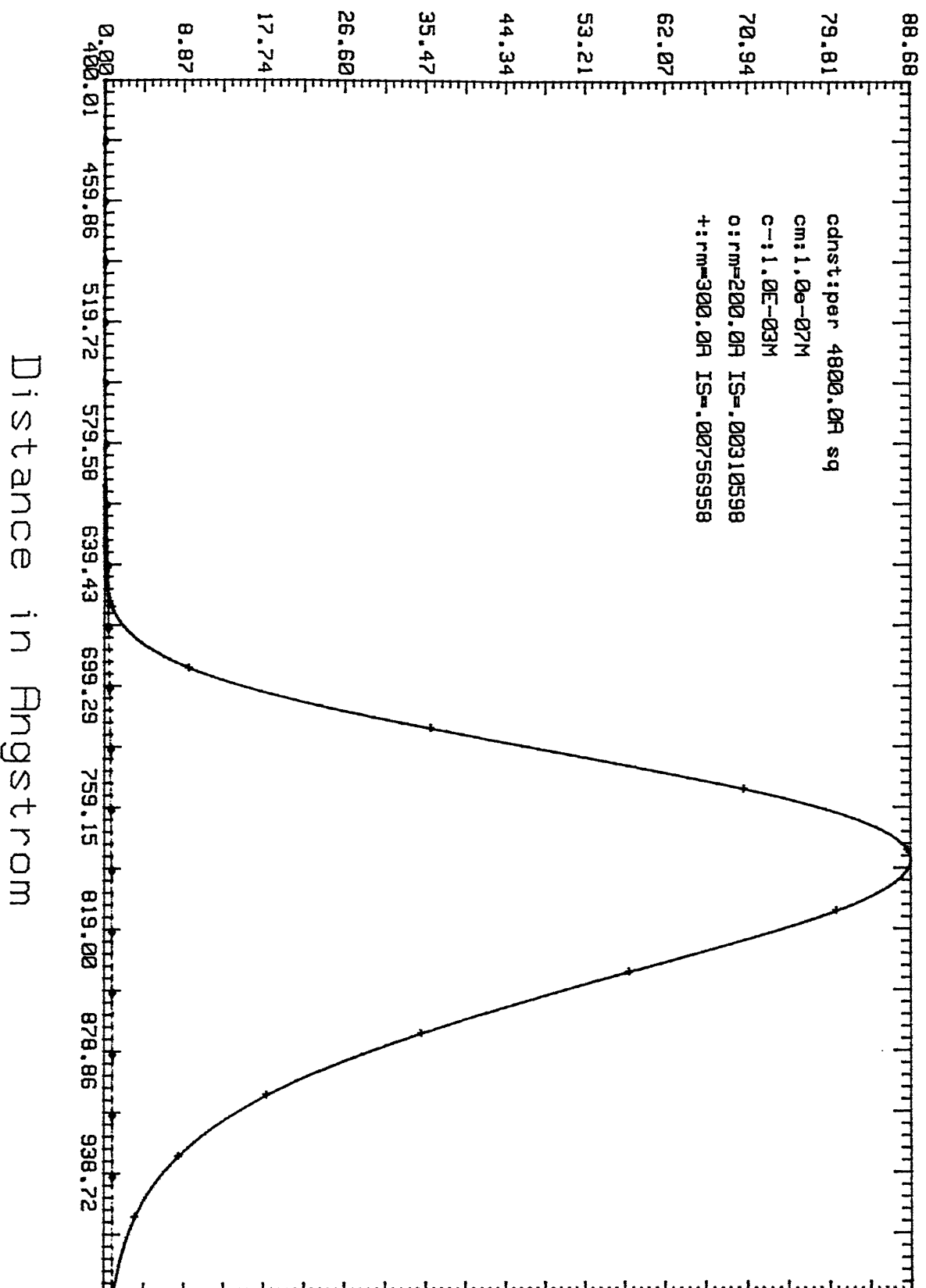
# Correlation Function Vs. Distance F-5.66

Macro Ion-Macro Ion Correlation;g(r)



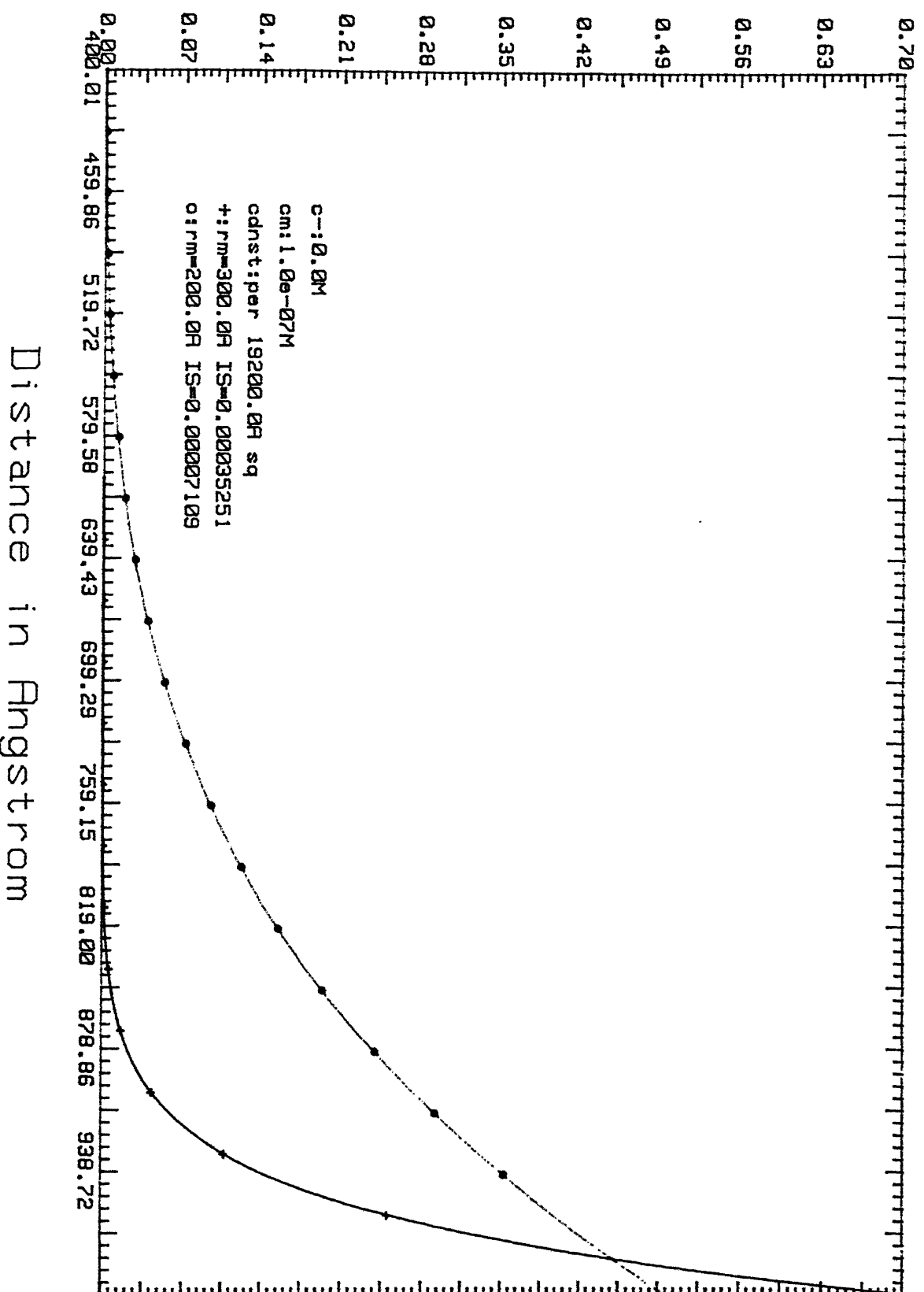
# Correlation Function Vs. Distance F-5.67

Macro Ion-Macro Ion Correlation;g(r)



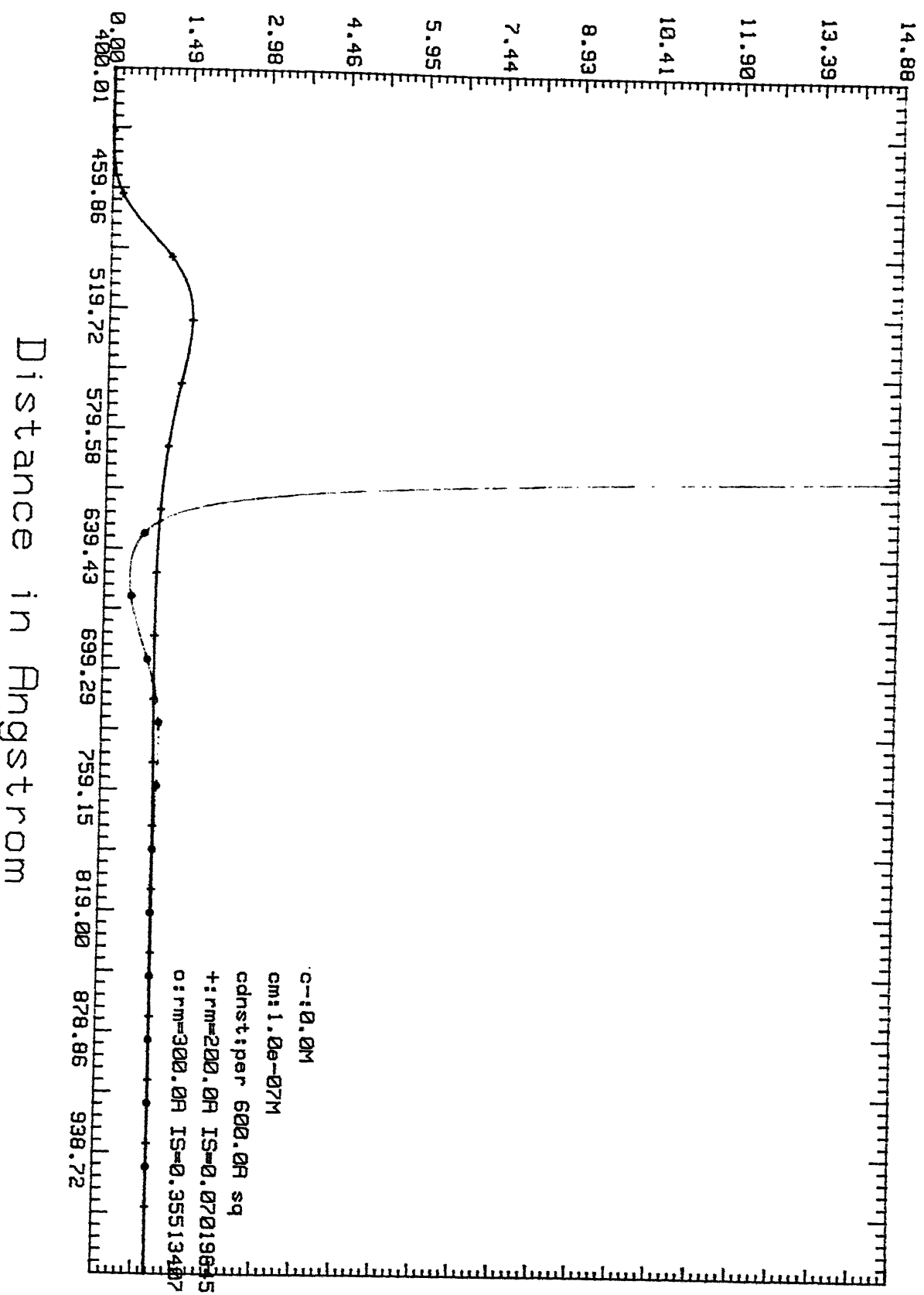
# Correlation Function Vs. Distance F-5.68

Macro Ion-Macro Ion Correlation;  $g(r)$



# Correlation Function Vs. Distance F-5.71

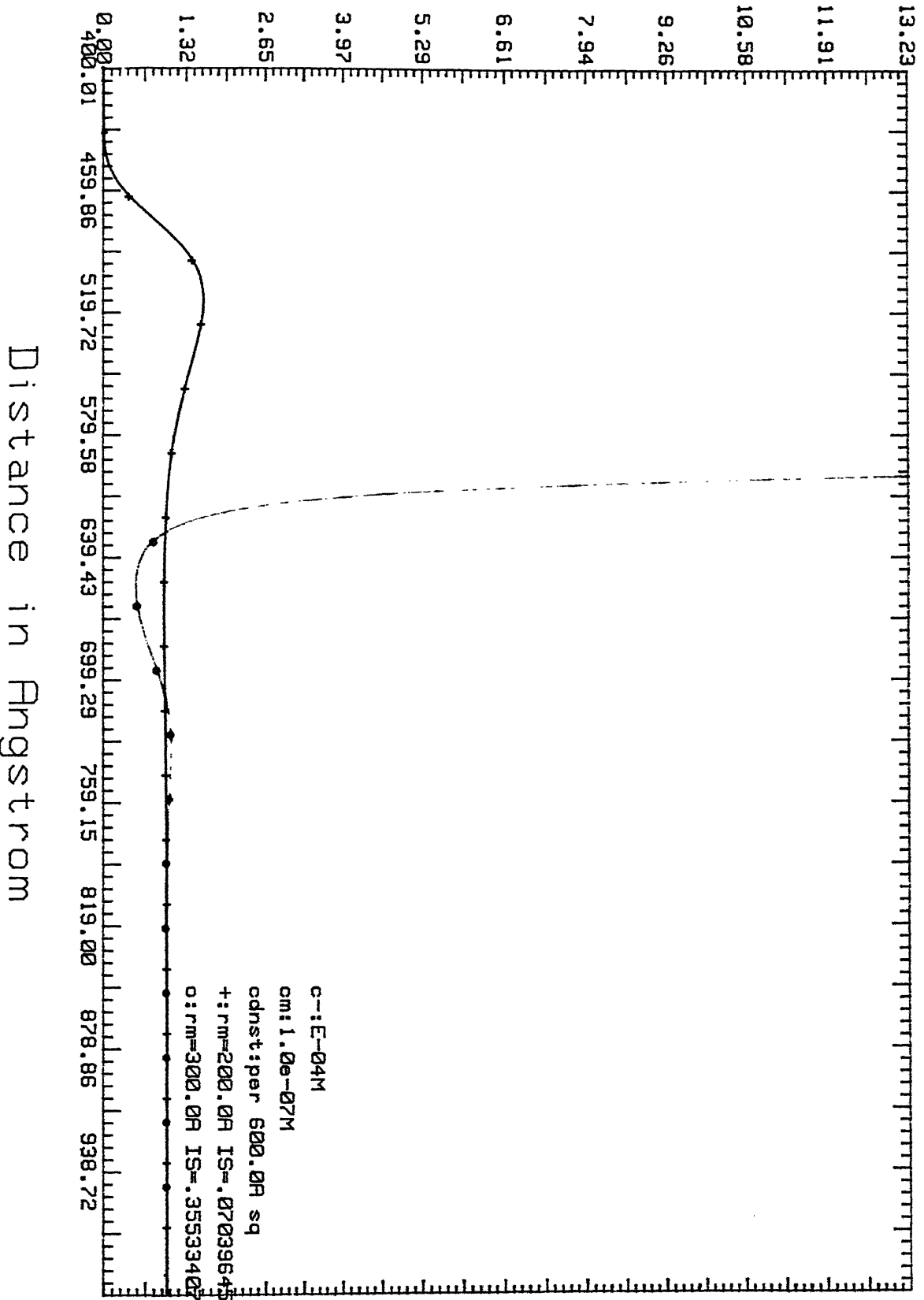
Macro Ion-Macro Ion Correlation;  $g(r)$



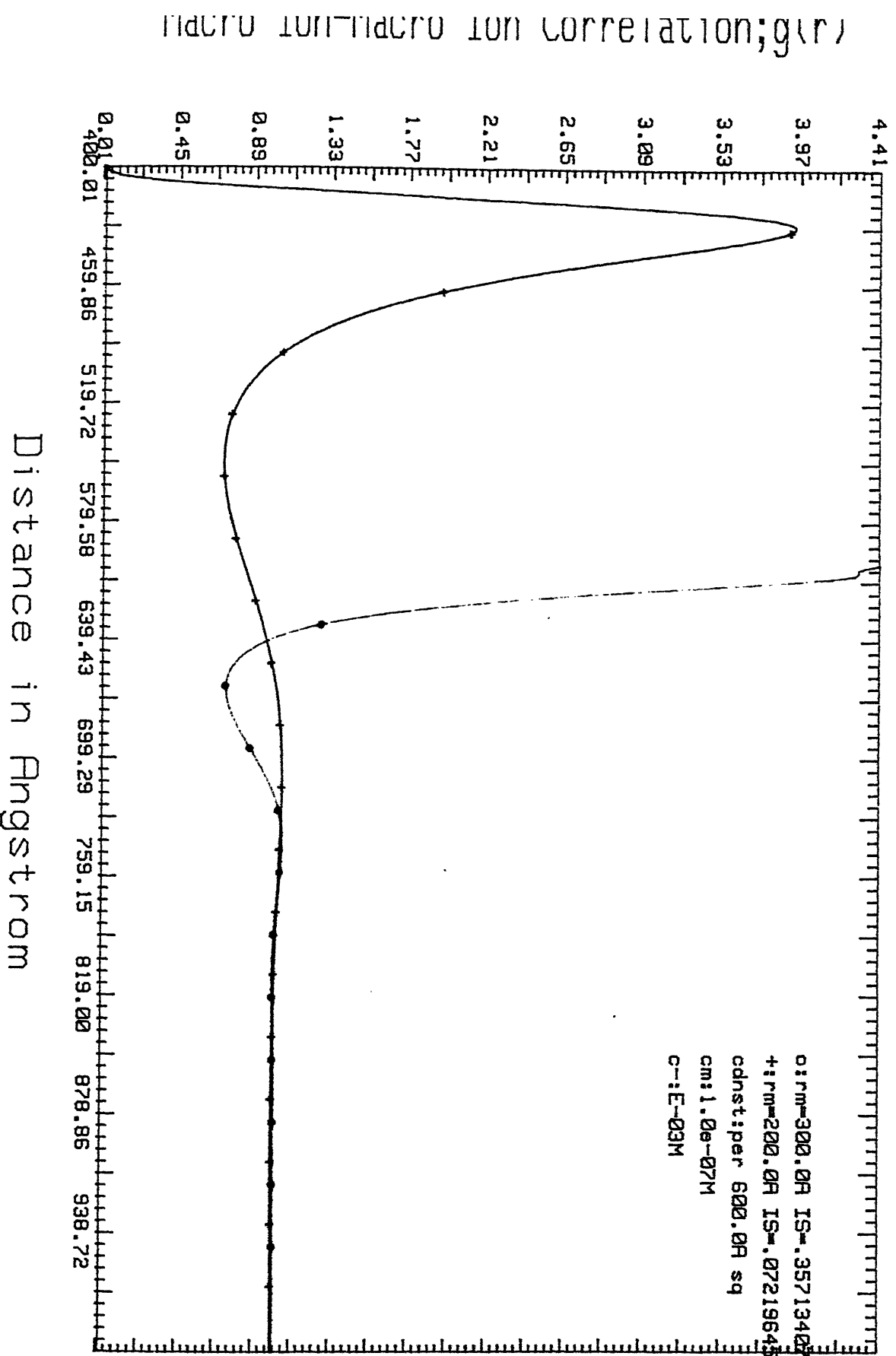


# Correlation Function Vs. Distance $r = 5.72$

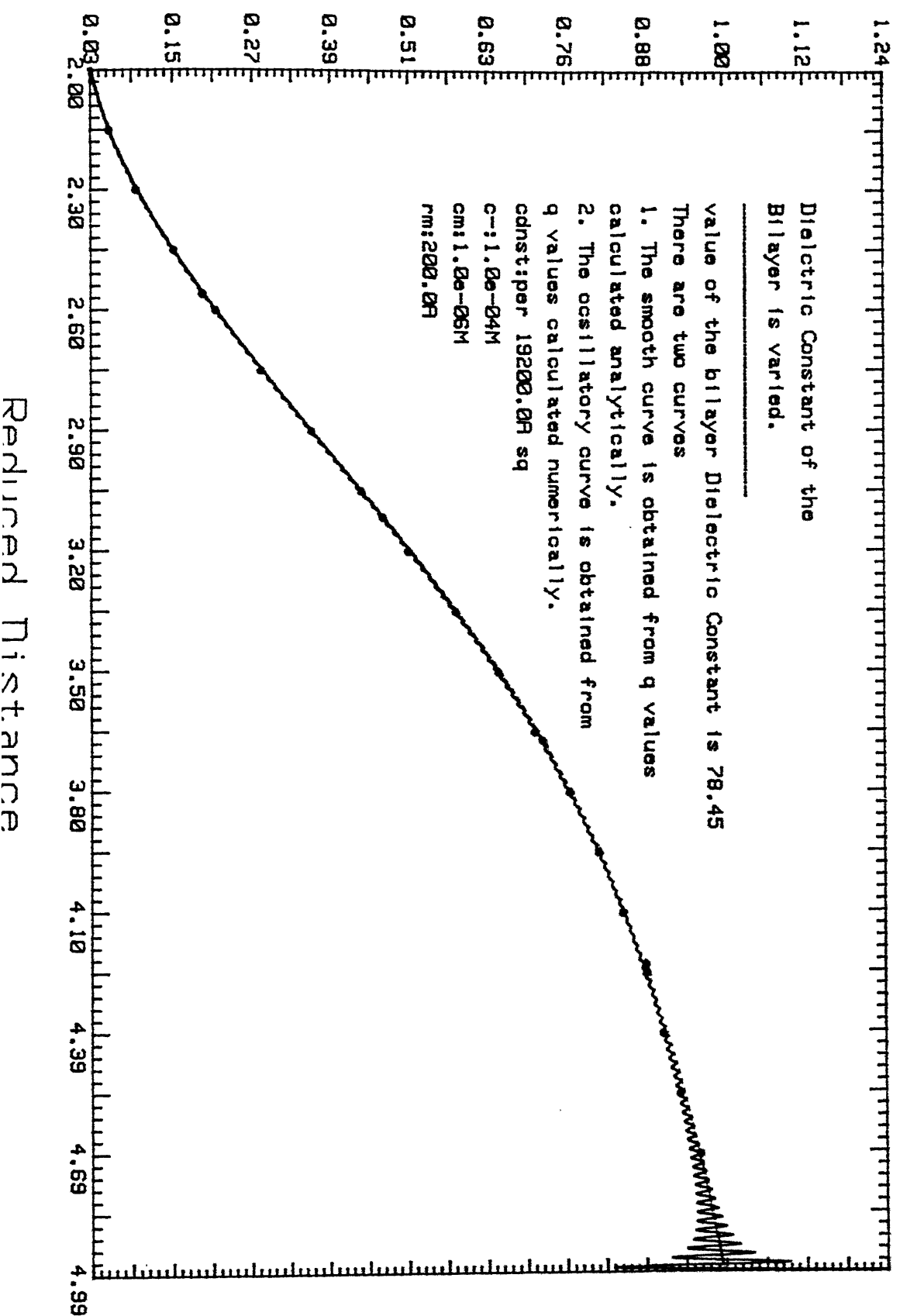
Macro Ion-Macro Ion Correlation;  $g(r)$



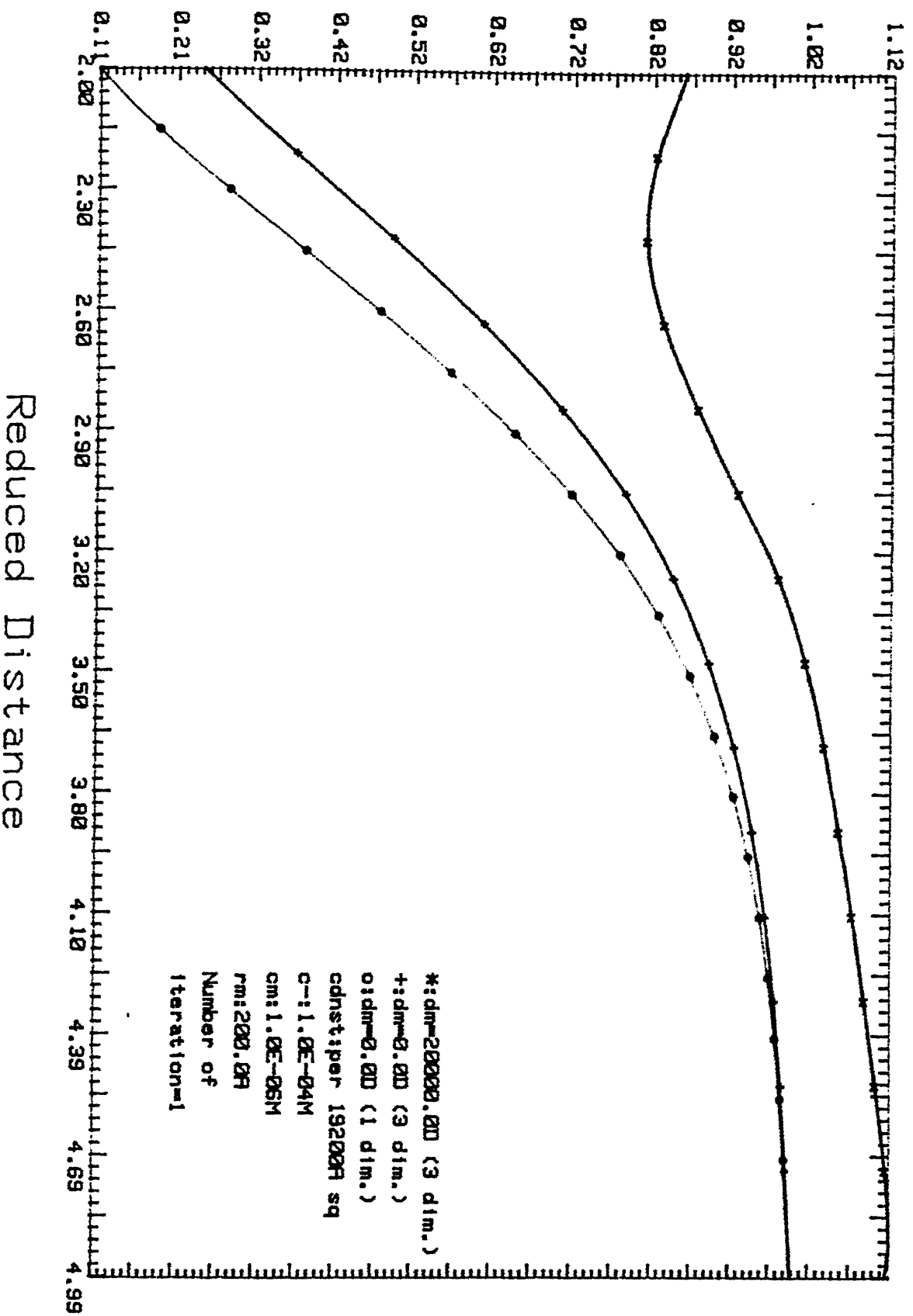
# Correlation Function Vs. Distance F-5.73



Correlation Function Vs. Distance Fig. 5. 74



# Correlation Function Vs. Distance Fig- 5.7c



## References

1. Rossky, P.J., and Friedman, H.L., J. Chem. Phys., 72, 5694, 1980.
2. Talman, J.D., J. Comput. Phys., 29, 35, 1978.
3. Beresford-Smith, B. and Chan, D.Y.C., Chem. Phys. Lett., 92, 474, 1982.
4. Bratko, D., Friedman, H.L. and Zhong, E.C., J. Chem. Phys., 85, 377, 1986.
5. Abernethy, G.M. and Gillan, M.J., Mol. Phys., 39, 839, 1980.
6. Fushiki, M., J. Chem. Phys., 89, 7445, 1988.
7. Khan, S., Morton, T.L. and Ronis, D., Phys. Rev. A, 35, 4295, 1987.
8. Belloni, L., J. Chem. Phys., 88, 5143, 1988.
9. Elkoubi, D., Turq, D. and Hansen, J.P., Chem. Phys. Lett., 52, 493, 1977.
10. Rogers, F.J., J. Chem. Phys., 73, 6272, 1980.
11. Beresford-Smith, B. and Chan, D.Y.C., Chem. Phys. Lett., 92, 474, 1982.
12. Belloni, L., Chem. Phys. Lett., 99, 43, 1985.
13. Bratko, D., Friedman, H.L., Chen, S.H. and Blum, L., Phys. Rev. A 34, 2215, 1986.
14. Linse, P. and Jonsson, B., J. Chem. Phys., 78, 3167, 1983.
15. Linse, P., *ibid*, 93, 1376, 1990.
16. Linse, P., *ibid*, 94, 3817, 1991.
17. Hansen, J. and McDonald, I.R., Theory of Simple Fluids, Academic Press, 1986.
18. Patey, G.N., J. Chem. Phys., 72, 5763, 1980.

19. Teubner, M., J. Chem. Phys., 75, 1907, 1981.
20. Sanchez, J. and Lozada-Cassou, M., Chem.Phys. Lett., 190, 22, 1992.
21. Beresford-Smith, B., Chan, D.Y.C. and Mitchell, D.J., J. Colloid Interface Sci., 105, 216, 1985.
22. Belloni, L., J. Chem. Phys., 85, 519, 1986.

# APPENDIX-1

```

c -----
c The system is a 3-component system.The particles are
c 1=Na+,2=Cl-,3=A macroion with negative charge density.
c -----

integer ndim,lwork,l,m,n,j,ni
parameter(ndim=1,l=3,m=3,n=1400,nn=n/2,lwork=4*n)
integer nphi,nq,nh,nx,ifail,ntao1,ntao2,ntao
double precision work(lwork),xq(1,m,n),yq(1,m,n),xh(1,m,n),yh(1,
1 m,n),xx(1,m,n),yx(1,m,n),xtao1(1,m,n),ytao1(1,m,n),xtao2(1,m,n),
1 ytao2(1,m,n),xtao(1,m,n),ytao(1,m,n)
integer ndq(ndim),ndh(ndim),ndx(ndim),ndtao1(ndim),ndtao2(ndim)
1 ,ndtao(ndim)
double precision v(nn),r(1,m,n),q(1,m,n),h(1,m,n),x(1,m,n)
double precision ansd(1,m),ansq(1,m),ansh(1,m),ansx(1,m),g(1,m,n)
double precision xphi(1,m,n),yphi(1,m,n),error,rng,tbn,tbn1,kp
integer ndphi(ndim)
double precision phi(1,m,n),yp(nn),z(1),xa(1,m,n)
double precision xb(n),yb(n),ad,hh(nn),xxd(nn),rd(nn)
double precision res1(1,m),res2(1,m),res3(1,m),res4(1,m),res5(1,m)
1 ,res6(1,m),res7(1,m),res8(1,m),res9(1,m),res10(1,m),mat3(1,m),is
double precision a(1,m,n),e(1),c(m,l),mat(1,m),mat1(1,m),mat2(1,m)
external c06fjff,d01gaf,fun,f01ckf
common e,dc,bc,temp,c,kp
open(unit=35,file='value.in')
open(unit=42,file='tao2.out')
open(unit=43,file='graph')
read(35,*)dc,bc,temp
read(35,*)(e(i),i=1,l)
read(35,*)((c(i,j),i=1,m),j=1,l)
read(35,*)rm,r1,r2,dnst,tmax,tmin
read(35,*)e1,e2,ni
e(1)=e1*e(1)
e(2)=e2*e(2)
e3=(4.0*3.14*(rm**2))/dnst
e(3)=e3*e(3)

```

```

if((i.eq.3).and.(j.eq.1)) then
if(r(i,j,k).le.(r1+rm))then
phi(i,j,k)=-1.0
else
phi(i,j,k)=dexp(q(i,j,k))-1.0d0
endif
endif
if(r(i,j,k).le.(r2+rm))then
phi(i,j,k)=-1.0
else
phi(i,j,k)=dexp(q(i,j,k))-1.0d0
endif
endif
xphi(i,j,k)=phi(i,j,k)*r(i,j,k)
yphi(i,j,k)=0.0d0
r(i,j,k+1)=r(i,j,k)+tbn
end do
end do
end do
do k=nnn,n
do i=1,l
do j=1,m
xphi(i,j,k)=-xphi(i,j,((n+2)-k))
yphi(i,j,k)=0.0d0
c r(i+1)=r(i)+tbn
end do
end do
end do
c*****
c    CALCULATION OF INITIAL VALUE OF tao
c*****
c*****
c CALCULATION OF THE CONVOLUTION INTEGRAL phi*phi
c*****
ifail=1
do i=1,l

```



```

do j=1,m
do k=1,nn
yp(k)=phi(i,j,k)*(r(i,j,k)**2)
rd(k)=r(i,j,k)
end do
call d01gaf(rd,yp,nn,ad,error,ifail)
ansd(i,j)=ad
end do
end do
do i=1,l
do j=1,m
ndphi(1)=n
nphi=ndphi(1)
do k=1,n
xb(k)=xphi(i,j,k)
yb(k)=yphi(i,j,k)
end do
ifail=0
call c06fjf(ndim,ndphi,nphi,xb,yb,work,lwork,ifail)
yphi(i,j,1)=ansd(i,j)*4.0d0*3.14d0
do k=2,n
xk=dfloat(k)
yphi(i,j,k)=-yb(k)*(rng/(xk-1.0d0))*tbn*sqrt(xn)
end do
end do
end do

do i=1,l
do j=1,m
mat(i,j)=yphi(i,j,k)
end do
end do
call f01ckf(res1,mat,c,l,l,m,z,l,l,ifail)
call f01ckf(res2,res1,mat,l,m,l,z,l,l,ifail)
do ii=1,l

```

```

do jj=1,m
ytaol(ii,jj,k)=res2(ii,jj)
end do
end do
end do
do i=1,l
do j=1,m
do k=1,nn
xk=float(k)
xtaol(i,j,k)=ytaol(i,j,k)*((xk-1.0d0)/rng)
ytaol(i,j,k)=0.0
end do
end do
end do
do i=1,l
do j=1,m
do k=nnn,n
xtaol(i,j,k)=-xtaol(i,j,((n+2)-k))
ytaol(i,j,k)=0.0
end do
end do
end do
tbn1=(xn-1.0d0)/(rng*xn)
do i=1,l
do j=1,m
ndtaol(1)=n
ntaol=ndtaol(1)
do k=1,n
xb(k)=xtaol(i,j,k)
yb(k)=ytaol(i,j,k)
end do
ifail=0
call c06fjf(ndim,ndtaol,ntaol,xb,yb,work,lwork,ifail)
do k=1,nn
xk=dfloat(k)
ytaol(i,j,k)=-((1.0d0/r(i,j,k))*yb(k)*tbn1*sqrt(xn)

```

```

end do
end do
end do
C*****
C CALCULATION OF THE CONVOLUTION INTEGRAL q*q
C*****
do i=1,l
do j=1,m
do k=1,nn
xq(i,j,k)=q(i,j,k)*r(i,j,k)
yq(i,j,k)=0.0
v(k)=q(i,j,k)*(r(i,j,k)**2)
rd(k)=r(i,j,k)
ifail=1
call d01gaf(rd,v,nn,ad,error,ifail)
ansq(i,j)=ad
end do
end do
do k=nnn,n
do i=1,l
do j=1,m
xq(i,j,k)=-xq(i,j,(n+2-k))
yq(i,j,k)=0.0
end do
end do
end do
do i=1,l
do j=1,m
ndq(1)=n
nq=ndq(1)
do k=1,n
xb(k)=xq(i,j,k)
yb(k)=yq(i,j,k)
end do
ifail=0
call c06fjf(ndim,ndq,nq,xb,yb,work,lwork,ifail)

```

```

yq(i,j,1)=ansq(i,j)*4.0d0*3.14d0
do k=2,nn
  xk=dfloat(k)
  yq(i,j,k)=-yb(k)*(rng/(xk-1.0d0))*tbn*sqrt(xn)
end do
end do
end do
do k=1,nn
  do i=1,l
    do j=1,m
      mat(i,j)=yq(i,j,k)
    end do
  end do
  call f01ckf(res1,mat,c,l,l,m,z,1,1,ifail)
  call f01ckf(res2,res1,mat,l,m,l,z,1,1,ifail)
  do ii=1,l
    do jj=1,m
      ytao2(ii,jj,k)=res2(ii,jj)
    end do
  end do
end do
do i=1,l
  do j=1,m
    do k=1,nn
      xk=float(k)
      xtao2(i,j,k)=ytao2(i,j,k)*((xk-1.0d0)/rng)
      ytao2(i,j,k)=0.0
    end do
  end do
end do

do i=1,l
  do j=1,m

```

```

xtao2(i,j,k)=-xtao2(i,j,((n+2)-k))
ytao2(i,j,k)=0.0
end do
end do
end do
do i=1,l
do j=1,m
ndtao2(1)=n
ntao2=ndtao2(1)
do k=1,n
xb(k)=xtao2(i,j,k)
yb(k)=ytao2(i,j,k)
end do
ifail=0
call c06fjf(ndim,ndtao2,ntao2,xb,yb,work,lwork,ifail)
do k=1,nn
xk=dfloat(k)
ytao2(i,j,k)=-((1.0d0/r(i,j,k))*yb(k)*tbn1*sqrt(xn)
ytao(i,j,k)=ytao1(i,j,k)-ytao2(i,j,k)
end do
end do
end do
C*****
C INITIAL VALUE OF tao IS CALCULATED
C*****
C-----
rm1=rm*1.0e08
cn=c(2,2)/6.023e20
cp=c(1,1)/6.023e20
cmn=c(3,3)/6.023e20
ed3=dnst*1.0e16
is=(cp*(e1**2))+(cn*(e2**2))+(cmn*(e3**2))
write(43,11)ed3,rm1,cn,cmn,is,cp
11 format('The charge density on the Macroion:one electron per',
1 f10.2,'angstrom square',/'The radius of the Macroion=',f8.2,'A'
1 /'The concentration of the univalent negative ion=',e10.4,'M'

```

```

1 /'The concentration of the Macroion=',e10.4,'M'/'Ionic Strength
1 ='f12.8,
1 /'The concentration of the univalent positive ion=',f6.5,'M')

```

```

c-----

```

```

jd=0

```

```

c*****

```

```

c CALCULATION OF FINAL VALUE OF tao

```

```

c*****

```

```

c*****

```

```

c CALCULATION OF h AND x FUNCTION

```

```

c*****

```

```

300 do i=1,l

```

```

do j=1,m

```

```

do k=1,nn

```

```

if((i.ne.3).and.(j.ne.3))then

```

```

if(i.ne.j)then

```

```

if(r(i,j,k).le.(r1+r2))then

```

```

h(i,j,k)=-1.0

```

```

else

```

```

end if

```

```

else

```

```

if((i.ne.2).and.(j.ne.2))then

```

```

if(r(i,j,k).le.(2.0*r1))then

```

```

h(i,j,k)=-1.0

```

```

else

```

```

h(i,j,k)=exp(q(i,j,k)+ytao(i,j,k))-1.0d0

```

```

end if

```

```

else

```

```

if(r(i,j,k).le.(2.0*r2))then

```

```

h(i,j,k)=-1.0

```

```

else

```

```

h(i,j,k)=exp(q(i,j,k)+ytao(i,j,k))-1.0d0

```

```

end if

```

```

end if

```

```

end if

```

```

else

```

```

if(r(i,j,k).le.(2.0*rm))then
h(i,j,k)=-1.0
else
h(i,j,k)=exp(q(i,j,k)+ytao(i,j,k))-1.0d0
endif
endif
if((i.eq.1).and.(j.eq.3)) then
if(r(i,j,k).le.(r1+rm))then
h(i,j,k)=-1.0
else
h(i,j,k)=exp(q(i,j,k)+ytao(i,j,k))-1.0d0
endif
endif
if((i.eq.2).and.(j.eq.3)) then
if(r(i,j,k).le.(r2+rm))then
h(i,j,k)=-1.0
else
h(i,j,k)=exp(q(i,j,k)+ytao(i,j,k))-1.0d0
endif
endif
if((i.eq.3).and.(j.eq.1)) then
if(r(i,j,k).le.(r1+rm))then
h(i,j,k)=-1.0
else
h(i,j,k)=exp(q(i,j,k)+ytao(i,j,k))-1.0d0
endif
endif
if((i.eq.3).and.(j.eq.2)) then
if(r(i,j,k).le.(r2+rm))then
h(i,j,k)=-1.0
else
h(i,j,k)=exp(q(i,j,k)+ytao(i,j,k))-1.0d0
endif
endif
x(i,j,k)=h(i,j,k)-q(i,j,k)-ytao(i,j,k)
end do

```

```

call f01ckf(res4,res3,mat2,1,m,1,z,1,1,ifail)
call f01ckf(res5,mat1,c,1,1,m,z,1,1,ifail)
call f01ckf(res6,res5,mat3,1,m,1,z,1,1,ifail)
call f01ckf(res7,mat1,c,1,1,m,z,1,1,ifail)
call f01ckf(res8,res7,mat3,1,m,1,z,1,1,ifail)
call f01ckf(res9,res8,c,1,1,m,z,1,1,ifail)
call f01ckf(res10,res9,mat2,1,m,1,z,1,1,ifail)
do ii=1,1
do jj=1,m
ytaa(ii,jj,k)=res4(ii,jj)+res6(ii,jj)+res10(ii,jj)
end do
end do
end do
do k=1,nn
xk=dfloat(k)
do i=1,1
do j=1,m
xtao(i,j,k)=ytaa(i,j,k)*((xk-1.0d0)/rng)
ytaa(i,j,k)=0.0d0
end do
end do
end do
do k=nnn,n
do i=1,1
do j=1,m
xtao(i,j,k)=-xtao(i,j,((n+2)-k))
ytaa(i,j,k)=0.0d0
end do
end do
end do
do i=1,1
do j=1,m
ndtao(1)=n
ntao=ndtao(1)
do k=1,n
xb(k)=xtao(i,j,k)

```



```

yb(k)=ytao(i,j,k)
end do
ifail=0
call c06fjf(ndim,ndtao,ntao,xb,yb,work,lwork,ifail)
do k=1,nn
xk=dfloat(k)
ytao(i,j,k)=-(1.0d0/r(i,j,k))*yb(k)*tbn1*sqrt(xn)
end do
end do
end do
c FINAL VALUE OF tao IS CALCULATED. THIS tao VALUE IS USED
c IN THE CALCULATION OF h AND x VALUES FOR THE CALCULATION OF
c IMPROVED VALUE OF tao BY MEANS OF A go to LOOP GIVVEN BELOW.
c*****
if(jd.eq.ni)then
go to 5
else
go to 300
endif
c*****
c CALCULATION OF g FUNCTION-THE CORRELATION FUNCTION
c*****
5 do i=1,l
do j=1,m
do k=1,nn
xk=dfloat(k)
if((i.ne.3).and.(j.ne.3))then
if(i.ne.j)then
if(r(i,j,k).le.(r1+r2))then
h(i,j,k)=-1.0d0
else
h(i,j,k)=exp(q(i,j,k)+ytao(i,j,k))-1.0d0
end if
else
if((i.ne.2).and.(j.ne.2))then
if(r(i,j,k).le.(2.0*r1))then

```

```

h(i,j,k)=-1.0d0
else
h(i,j,k)=exp(q(i,j,k)+ytao(i,j,k))-1.0d0
end if
else
if(r(i,j,k).le.(2.0*r2))then
h(i,j,k)=-1.0d0
else
h(i,j,k)=exp(q(i,j,k)+ytao(i,j,k))-1.0d0
end if
end if
end if
else
if(r(i,j,k).le.(2.0*rm))then
h(i,j,k)=-1.0d0
else
h(i,j,k)=exp(q(i,j,k)+ytao(i,j,k))-1.0d0
endif
endif
if((i.eq.1).and.(j.eq.3)) then
if(r(i,j,k).le.(r1+rm))then
h(i,j,k)=-1.0d0
else
h(i,j,k)=exp(q(i,j,k)+ytao(i,j,k))-1.0d0
endif
endif
if((i.eq.2).and.(j.eq.3)) then
if(r(i,j,k).le.(r2+rm))then
h(i,j,k)=-1.0d0
else
h(i,j,k)=exp(q(i,j,k)+ytao(i,j,k))-1.0d0
endif
endif
if((i.eq.3).and.(j.eq.1)) then
if(r(i,j,k).le.(r1+rm))then
h(i,j,k)=-1.0d0
else

```

```

h(i,j,k)=exp(q(i,j,k)+ytao(i,j,k))-1.0d0
endif
endif
if((i.eq.3).and.(j.eq.2)) then
if(r(i,j,k).le.(r2+rm))then
h(i,j,k)=-1.0d0
else
h(i,j,k)=exp(q(i,j,k)+ytao(i,j,k))-1.0d0
endif
endif
g(i,j,k)=h(i,j,k)+1.0
end do
end do
end do
do i=1,l
do k=1,nn
if(g(i,3,k).ne.0.0)then
r(i,3,k)=r(i,3,k)/rm
write(43,10)r(i,3,k),g(i,3,k)
else
continue
end if
end do
write(43,1)
end do
write(42,*)jd
1 format('-----')
10 format(f12.8,3x,f12.8)
stop
end

```

## APPENDIX-2

c CALCULATION OF THE CORRELATION FUNCTION

c -----

c The system is a 3-component system. The particles are

c 1=Na<sup>+</sup>, 2=Cl<sup>-</sup>, 3=A macroion with negative charge density.

c -----

```
integer ndim,lwork,l,m,n,j,ni,np
```

```
parameter(ndim=1,l=3,m=3,n=5200,nn=n/2,lwork=4*n)
```

```
integer nphi,nq,nh,nx,ifail,ntao1,ntao2,ntao
```

```
double precision gb(nn),ygb(nn),ad,delta,q1t(nn),q2t(nn),
```

```
1 q3t(nn),q11t(nn),q21t(nn),q31t(nn),xq1t(nn),xq2t(nn)
```

```
1 ,xq3t(nn),yq1t(nn),yq2t(nn),yq3t(nn),xq11t(nn),xq21t
```

```
1 (nn),xq31t(nn),yq11t(nn),yq21t(nn),yq31t(nn),tm,
```

```
1 det(nn),dbts(nn),ktinv,td(nn+1)
```

```
double precision work(lwork),xq(l,m,n),yq(l,m,n),xh(l,m,n),yh(l,
```

```
1 m,n),xx(l,m,n),yx(l,m,n),xtao1(l,m,n),ytao1(l,m,n),xtao2(l,m,n),
```

```
1 ytao2(l,m,n),xtao(l,m,n),ytao(l,m,n),d0(nn),epsln(nn),kp
```

```
integer ndq(ndim),ndh(ndim),ndx(ndim),ndtao1(ndim),ndtao2(ndim)
```

```
1 ,ndtao(ndim)
```

```
double precision v(nn),r(l,m,n),q(l,m,n),h(l,m,n),x(l,m,n)
```

```
double precision ansd(l,m),ansq(l,m),ansh(l,m),ansx(l,m),g(l,m,n)
```

```
double precision xphi(l,m,n),yphi(l,m,n),error,rng,tbn,tbn1
```

```
integer ndphi(ndim)
```

```
double precision phi(l,m,n),yp(nn),z(1),xa(l,m,n)
```

```
double precision xb(n),yb(n),hh(nn),xxd(nn),rd(nn)
```

```
double precision res1(l,m),res2(l,m),res3(l,m),res4(l,m),res5(l,m)
```

```
1 ,res6(l,m),res7(l,m),res8(l,m),res9(l,m),res10(l,m),mat3(l,m),is
```

```
double precision a(l,m,n),e(1),c(m,1),mat(l,m),mat1(l,m),mat2(l,m)
```

```
external c06fjf,d01gaf,fun,f01ckf
```

```
open(unit=35,file='value.in')
```

```
open(unit=42,file='tao2.out')
```

```
open(unit=43,file='graph')
```

```
read(35,*)dc,bc,temp,em
```

```
read(35,*)(e(i),i=1,l)
```

```
read(35,*)((c(i,j),i=1,m),j=1,l)
```

```

read(35,*)rm,r1,r2,dnst,tmax,tmin
read(35,*)e1,e2,ni,alpha,tm
pi=22.0/7.0
fp=4.0*pi
epc=1.0/(8.0*(pi**3))
ktinv=1.0/(bc*temp)
delta=fp*ktinv
e(1)=e1*e(1)
e(2)=e2*e(2)
e3=(4.0*pi*(rm**2))/dnst
e(3)=e3*e(3)
c(1,1)=(e2/e1)*c(2,2)+(e3/e1)*c(3,3)
nnn=nn+1
xn=dfloat(n)
sum=0.0
do i=1,m
do j=1,l
    sum=sum+(c(i,j)*(e(j)**2))
end do
end do
kp=sqrt((4.0d0*pi*sum)/(dc*bc*temp))
write(6,*)kp
rng=2.0d0*(tmax-tmin)
tbn=rng/xn
tbn1=(xn-1.0d0)/(rng*xn)
xnp=((2.0*rm)-tmin)/tbn
np=ifix(xnp)+1
do i=1,l
do j=1,m
    r(i,j,1)=tmin
end do
end do
do i=1,l
do j=1,m
do k=1,nn
    r(i,j,k+1)=r(i,j,k)+tbn

```

```

end do
end do
end do
tbn2=tm/dfloat(nn)
td(1)=0.0
do i=1,nn
td(i+1)=td(i)+tbn2
end do
C*****
C CALCULATION OF SCREENING CONSTANT AS A FUNCTION
C OF DISTANCE.
C*****
call eps(rm,dc,em,nn,l,m,r,epsln,d0,np)
do i=1,nn
write(*,*)epsln(i)
end do
C*****
C SCREENING CONSTANT AS A FUNCTION OF DISTANCE
C IS CALCULATED.
C*****
C-----
C*****
C CALCULATION OF q(t) BY NUMERICAL INTEGRATION
C*****
do j=2,nn
do i=1,nn-np
gb(i)=(dexp(-alpha*d0(i)))/epsln(i)
v(i)=gb(i)*sin(d0(i)*td(j))
end do
ifail=1
call d0lgaf(d0,v,(nn-np),ad,error,ifail)
ygb(j)=ad+((cos(tmax*td(j))-cos(2.0*rm*td(j))+1.0)/(dc*td(j)))
end do
do i=2,nn
ygb(i)=fp*ktinv*ygb(i)*(1.0/td(i))
end do

```

```

q1t(1)=0.0
q2t(1)=0.0
q3t(1)=0.0
q11t(1)=0.0
q21t(1)=0.0
q31t(1)=0.0
do i=2,nn
dbts(i)=delta/(dc*(td(i)**2))
a1=c(1,1)*(e(1)**2)*dbts(i)
a2=c(2,2)*(e(2)**2)*dbts(i)
a3=c(3,3)*(e(3)**2)*dbts(i)
a4=c(2,2)*c(3,3)*(e(2)**2)*(e(3)**2)*dbts(i)*ygb(i)
a5=c(2,2)*c(3,3)*(e(2)**2)*(e(3)**2)*(dbts(i)**2)
a6=c(1,1)*c(3,3)*(e(1)**2)*(e(3)**2)*dbts(i)*ygb(i)
a7=c(1,1)*c(3,3)*(e(1)**2)*(e(3)**2)*(dbts(i)**2)
a8=c(3,3)*(e(3)**2)*ygb(i)
det(i)=1.0+a1+a2+a3+a4-a5+a6-a7
c11=1.0+a2+a8+a4-a5
c12=-a1-a6+a7
c13=-a1
c21=-a2-a4+a5
c22=1.0+a1+a8+a6-a7
c23=-a2
c31=-a3
c32=-a3
c33=1+a1+a2
q1t(i)=-(dbts(i)*(c11+c21+c31))/det(i)
q2t(i)=-(dbts(i)*(c12+c22+c32))/det(i)
q3t(i)=-(dbts(i)*(c13+c23+c33))/det(i)
q11t(i)=-(dbts(i)*(c11+c21)+(ygb(i)*c31))/det(i)
q21t(i)=-(dbts(i)*(c12+c22)+(ygb(i)*c32))/det(i)
q31t(i)=-(dbts(i)*(c13+c23)+(ygb(i)*c33))/det(i)
end do
do j=1,nn
do i=1,nn
xq1t(i)=q1t(i)*td(i)*sin(r(1,1,j)*td(i))

```

```

phi(i,j,k)=dexp(q(i,j,k))-1.0d0
endif
endif
if((i.eq.1).and.(j.eq.3)) then
if(r(i,j,k).le.(r1+rm))then
phi(i,j,k)=-1.0
else
phi(i,j,k)=dexp(q(i,j,k))-1.0d0
endif
endif
if((i.eq.2).and.(j.eq.3)) then
if(r(i,j,k).le.(r2+rm))then
phi(i,j,k)=-1.0
else
phi(i,j,k)=dexp(q(i,j,k))-1.0d0
endif
endif
if((i.eq.3).and.(j.eq.1)) then
if(r(i,j,k).le.(r1+rm))then
phi(i,j,k)=-1.0
else
phi(i,j,k)=dexp(q(i,j,k))-1.0d0
endif
endif
if((i.eq.3).and.(j.eq.2)) then
if(r(i,j,k).le.(r2+rm))then
phi(i,j,k)=-1.0
else
phi(i,j,k)=dexp(q(i,j,k))-1.0d0
endif
endif
xphi(i,j,k)=phi(i,j,k)*r(i,j,k)
yphi(i,j,k)=0.0d0
end do
end do
end do

```



```

C*****
C CALCULATION OF INITIAL VALUE OF tao
C*****
C*****
C CALCULATION OF THE CONVOLUTION INTEGRAL phi*phi
C*****
  do k=nnn,n
  do i=1,l
  do j=1,m
    xphi(i,j,k)=-xphi(i,j,((n+2)-k))
    yphi(i,j,k)=0.0d0
  c r(i+1)=r(i)+tbn
  end do
  end do
  end do
  ifail=1
  do i=1,l
  do j=1,m
  do k=1,nn
    yp(k)=phi(i,j,k)*(r(i,j,k)**2)
    rd(k)=r(i,j,k)
  end do
  call d01gaf(rd,yp,nn,ad,error,ifail)
  ansd(i,j)=ad
  end do
  end do
  do i=1,l
  do j=1,m
    ndphi(1)=n
    nphi=ndphi(1)
  do k=1,n
    xb(k)=xphi(i,j,k)
    yb(k)=yphi(i,j,k)
  end do
  ifail=0
  call c06fjf(ndim,ndphi,nphi,xb,yb,work,lwork,ifail)

```

```

yphi(i,j,1)=ansd(i,j)*4.0d0*pi
do k=2,n
xk=dfloat(k)
yphi(i,j,k)=-yb(k)*(rng/(xk-1.0d0))*tbn*sqrt(xn)
end do
end do
end do
do k=1,nn
do i=1,l
do j=1,m
mat(i,j)=yphi(i,j,k)
end do
end do
call f01ckf(res1,mat,c,l,l,m,z,1,1,ifail)
call f01ckf(res2,res1,mat,l,m,l,z,1,1,ifail)
do ii=1,l
do jj=1,m
ytaol(ii,jj,k)=res2(ii,jj)
end do
end do
end do
do i=1,l
do j=1,m
do k=1,nn
xk=float(k)
xtaol(i,j,k)=ytaol(i,j,k)*((xk-1.0d0)/rng)
ytaol(i,j,k)=0.0
end do
end do
end do
do i=1,l
do j=1,m
do k=nnn,n
xtaol(i,j,k)=-xtaol(i,j,((n+2)-k))
ytaol(i,j,k)=0.0
end do

```

```

end do
end do
do i=1,l
do j=1,m
ndtaol(1)=n
ntaol=ndtaol(1)
do k=1,n
xb(k)=xtaol(i,j,k)
yb(k)=ytaol(i,j,k)
end do
ifail=0
call c06fjf(ndim,ndtaol,ntaol,xb,yb,work,lwork,ifail)
do k=1,nn
xk=dfloat(k)
ytaol(i,j,k)=-(1.0d0/r(i,j,k))*yb(k)*tbn1*sqrt(xn)
end do
end do
end do
C*****
C  CALCULATION OF THE CONVOLUTION INTEGRAL q*q
C*****
do i=1,l
do j=1,m
do k=1,nn
xq(i,j,k)=q(i,j,k)*r(i,j,k)
yq(i,j,k)=0.0
v(k)=q(i,j,k)*(r(i,j,k)**2)
rd(k)=r(i,j,k)
end do
ifail=1
call d01gaf(rd,v,nn,ad,error,ifail)
ansq(i,j)=ad
end do
end do
do k=nnn,n
do i=1,l

```

```

do j=1,m
  xq(i,j,k)=-xq(i,j,(n+2-k))
  yq(i,j,k)=0.0
end do
end do
end do
do i=1,l
  do j=1,m
    ndq(1)=n
    nq=ndq(1)
    do k=1,n
      xb(k)=xq(i,j,k)
      yb(k)=yq(i,j,k)
    end do
    ifail=0
    call c06fjf(ndim,ndq,nq,xb,yb,work,lwork,ifail)
    yq(i,j,1)=ansq(i,j)*4.0d0*pi
    do k=2,nn
      xk=dfloat(k)
      yq(i,j,k)=-yb(k)*(rng/(xk-1.0d0))*tbn*sqrt(xn)
    end do
  end do
end do
do k=1,nn
  do i=1,l
    do j=1,m
      mat(i,j)=yq(i,j,k)
    end do
  end do
  call f01ckf(res1,mat,c,l,l,m,z,1,1,ifail)
  call f01ckf(res2,res1,mat,l,m,l,z,1,1,ifail)
  do ii=1,l
    do jj=1,m
      ytao2(ii,jj,k)=res2(ii,jj)
    end do
  end do
end do

```

```

end do
do i=1,l
do j=1,m
do k=1,nn
xk=float(k)
xtao2(i,j,k)=y tao2(i,j,k)*((xk-1.0d0)/rng)
y tao2(i,j,k)=0.0
end do
end do
end do
do k=nnn,n
do i=1,l
do j=1,m
xtao2(i,j,k)=-xtao2(i,j,((n+2)-k))
y tao2(i,j,k)=0.0
end do
end do
end do
do i=1,l
do j=1,m
ndtao2(1)=n
ntao2=ndtao2(1)
do k=1,n
xb(k)=xtao2(i,j,k)
yb(k)=y tao2(i,j,k)
end do
ifail=0
call c06fjf(ndim,ndtao2,ntao2,xb,yb,work,lwork,ifail)
do k=1,nn
xk=dfloat(k)
y tao2(i,j,k)=-((1.0d0/r(i,j,k))*yb(k)*tbn1*sqrt(xn)
y tao(i,j,k)=y tao1(i,j,k)-y tao2(i,j,k)
end do
end do
end do
C*****

```

c INITIAL VALUE OF tao IS CALCULATED.

c\*\*\*\*\*

c-----

rm1=rm\*1.0e08

cn=c(2,2)/6.023e20

cp=c(1,1)/6.023e20

cmn=c(3,3)/6.023e20

ed3=dnst\*1.0e16

is=(cp\*(e1\*\*2))+(cn\*(e2\*\*2))+(cmn\*(e3\*\*2))

write(43,11)ed3,rm1,cn,cmn,is,cp,em

11 format('The charge density on the Macroion:one electron per',

1 f10.2,'angstrom square',/'The radius of the Macroion=',f8.2,'A'

1 /'The concentration of the univalent negative ion=',e10.4,'M'

1 /'The concentration of the Macroion=',e10.4,'M'/'Ionic Strength

1 ='f12.8,

1 /'The concentration of the univalent positive ion=',f6.5,'M',

1 /'The dielectric constant of the Bilayer='f10.5)

c-----

jd=0

c\*\*\*\*\*

c CALCULATION OF FINAL VALUE OF tao

c\*\*\*\*\*

c\*\*\*\*\*

c CALCULATION OF h AND x FUNCTION

c\*\*\*\*\*

300 do i=1,1

do j=1,m

do k=1,nn

if((i.ne.3).and.(j.ne.3))then

if(i.ne.j)then

if(r(i,j,k).le.(r1+r2))then

h(i,j,k)=-1.0

else

h(i,j,k)=exp(q(i,j,k)+ytao(i,j,k))-1.0d0

end if

else

```

if((i.ne.2).and.(j.ne.2))then
if(r(i,j,k).le.(2.0*r1))then
h(i,j,k)=-1.0
else
h(i,j,k)=exp(q(i,j,k)+ytao(i,j,k))-1.0d0
end if
else
if(r(i,j,k).le.(2.0*r2))then
h(i,j,k)=-1.0
else
h(i,j,k)=exp(q(i,j,k)+ytao(i,j,k))-1.0d0
end if
end if
end if
else
if(r(i,j,k).le.(2.0*rm))then
h(i,j,k)=-1.0
else
h(i,j,k)=exp(q(i,j,k)+ytao(i,j,k))-1.0d0
endif
endif
if((i.eq.1).and.(j.eq.3)) then
if(r(i,j,k).le.(r1+rm))then
h(i,j,k)=-1.0
else
h(i,j,k)=exp(q(i,j,k)+ytao(i,j,k))-1.0d0
endif
endif
if((i.eq.2).and.(j.eq.3)) then
if(r(i,j,k).le.(r2+rm))then
h(i,j,k)=-1.0
else
h(i,j,k)=exp(q(i,j,k)+ytao(i,j,k))-1.0d0
endif
endif
if((i.eq.3).and.(j.eq.1)) then

```

```

call c06fjff(ndim,ndx,nx,xb,yb,work,lwork,ifail)
yx(i,j,1)=ansx(i,j)*4.0d0*pi
do k=2,nn
  xk=dfloat(k)
  yx(i,j,k)=-yb(k)*(rng/(xk-1.0d0))*tbn*sqrt(xn)
end do
end do
end do
do k=1,nn
  do i=1,l
    do j=1,m
      mat1(i,j)=yq(i,j,k)
      mat2(i,j)=yh(i,j,k)
      mat3(i,j)=yx(i,j,k)
    end do
  end do
  call f01ckf(res3,mat3,c,l,l,m,z,1,1,ifail)
  call f01ckf(res4,res3,mat2,l,m,l,z,1,1,ifail)
  call f01ckf(res5,mat1,c,l,l,m,z,1,1,ifail)
  call f01ckf(res6,res5,mat3,l,m,l,z,1,1,ifail)
  call f01ckf(res7,mat1,c,l,l,m,z,1,1,ifail)
  call f01ckf(res8,res7,mat3,l,m,l,z,1,1,ifail)
  call f01ckf(res9,res8,c,l,l,m,z,1,1,ifail)
  call f01ckf(res10,res9,mat2,l,m,l,z,1,1,ifail)
  do ii=1,l
    do jj=1,m
      ytao(ii,jj,k)=res4(ii,jj)+res6(ii,jj)+res10(ii,jj)
    end do
  end do
end do
do k=1,nn
  xk=dfloat(k)
  do i=1,l
    do j=1,m
      xtao(i,j,k)=ytao(i,j,k)*((xk-1.0d0)/rng)
      ytao(i,j,k)=0.0d0
    end do
  end do
end do

```



```

end do
end do
end do
do k=nnn,n
do i=1,l
do j=1,m
xtao(i,j,k)=-xtao(i,j,((n+2)-k))
ytao(i,j,k)=0.0d0
end do
end do
end do
do i=1,l
do j=1,m
ndtao(1)=n
ntao=ndtao(1)
do k=1,n
xb(k)=xtao(i,j,k)
yb(k)=ytao(i,j,k)
end do
ifail=0
call c06fjf(ndim,ndtao,ntao,xb,yb,work,lwork,ifail)
do k=1,nn
xk=dfloat(k)
ytao(i,j,k)=-(1.0d0/r(i,j,k))*yb(k)*tbn1*sqrt(xn)
end do
end do
end do
C*****:
c FINAL VALUE OF tao IS CALCULATED. THIS tao VALUE IS USED
c IN THE CALCULATION OF h AND x VALUES FOR THE CALCULATION OF
c IMPROVED VALUE OF tao BY MEANS OF A go to LOOP GIVVEN BELOW.
C*****:
if(jd.eq.ni)then
go to 5
else
go to 300

```

```

endif
C*****
c CALCULATION OF g FUNCTION-THE CORRELATION FUNCTION
C*****
5 do i=1,l
  do j=1,m
    do k=1,nn
      xk=dfloat(k)
      if((i.ne.3).and.(j.ne.3))then
        if(i.ne.j)then
          if(r(i,j,k).le.(r1+r2))then
            h(i,j,k)=-1.0d0
          else
            h(i,j,k)=exp(q(i,j,k)+ytao(i,j,k))-1.0d0
          end if
        else
          if((i.ne.2).and.(j.ne.2))then
            if(r(i,j,k).le.(2.0*r1))then
              h(i,j,k)=-1.0d0
            else
              h(i,j,k)=exp(q(i,j,k)+ytao(i,j,k))-1.0d0
            end if
          else
            if(r(i,j,k).le.(2.0*r2))then
              h(i,j,k)=-1.0d0
            else
              h(i,j,k)=exp(q(i,j,k)+ytao(i,j,k))-1.0d0
            end if
          end if
        end if
      else
        if(r(i,j,k).le.(2.0*rm))then
          h(i,j,k)=-1.0d0
        else
          h(i,j,k)=exp(q(i,j,k)+ytao(i,j,k))-1.0d0
        end if
      endif
    end if
  end if
end do

```

```

endif
if((i.eq.1).and.(j.eq.3)) then
if(r(i,j,k).le.(r1+rm))then
h(i,j,k)=-1.0d0
else
h(i,j,k)=exp(q(i,j,k)+ytao(i,j,k))-1.0d0
endif
endif
if((i.eq.2).and.(j.eq.3)) then
if(r(i,j,k).le.(r2+rm))then
h(i,j,k)=-1.0d0
else
h(i,j,k)=exp(q(i,j,k)+ytao(i,j,k))-1.0d0
endif
endif
if((i.eq.3).and.(j.eq.1)) then
if(r(i,j,k).le.(r1+rm))then
h(i,j,k)=-1.0d0
else
h(i,j,k)=exp(q(i,j,k)+ytao(i,j,k))-1.0d0
endif
endif
if((i.eq.3).and.(j.eq.2)) then
if(r(i,j,k).le.(r2+rm))then
h(i,j,k)=-1.0d0
else
h(i,j,k)=exp(q(i,j,k)+ytao(i,j,k))-1.0d0
endif
endif
g(i,j,k)=h(i,j,k)+1.0
end do
end do
end do
do i=1,l
do k=1,nñ
if(g(i,3,k).ne.0.0)then

```

```

r(i,3,k)=r(i,3,k)/rm
write(43,10)r(i,3,k),g(i,3,k)
else
continue
end if
end do
write(43,1)
end do
  write(42,*)jd
1 format('-----')
10 format(f12.8,3x,f12.8)
stop
end
C*****
C SUBROUTINE FOR THE CALCULATION OF THE SCREENING CONSTANT
C*****
subroutine eps(r0,es,e1,nn,l,m,r,epsln,d0,np)
integer nt
parameter(nt=36)
double precision d0(nn),epsln(nn),r(1,m,nn)
do i=1,nn
d0(i)=r(1,1,i)
end do
do j=1,nn
if(d0(j).le.(2.0*r0))then
epsln(j)=0.0
else
a1=1.0/es
a2=1.0/(1.0+(2.0*(es/e1)))
a3=((r0/d0(j))**3)
a4=(es-e1)-1.0
epsln(j)=a1*(1.0+(a2*a3*a4))
end if
end do
do i=np+1,nn
d0(i-np)=d0(i)

```

```
epsln(i-np)=epsln(i)  
end do  
return  
end
```

### APPENDIX-3

#### C CALCULATION OF THE CORRELATION FUNCTION

C -----

C The system is a 3-component system. The particles are  
 C 1=Na<sup>+</sup>, 2=Cl<sup>-</sup>, 3=A macroion with negative charge density  
 C as well as dipole moment. The convolution integral is  
 C calculated along with the angular integration.

C -----

```

external sine, cosine, c06fff
integer m, mm, lwork, i, ndim, n, nd, jd, md, mmd, lw, j, kk, l, lw1, id
      1 , ifail, nitr, nu
parameter (ndim=1, m=1000, n=9, nd=18, mm=m/2, lwork=4*m, mmd=mm
      1 , md=2*mmd, lw=4*md, lw1=4*nd, np=1000)
double precision t(np), f1, f2, f3, det1, det2, k(mm+1), w1(lw1)
      1 , p11n0, q11b(mm), q12b(mm), q130b(mmd), q131b(mmd), q22b(mm)
      1 , q230b(mmd), q231b(mmd), q311b(mmd), q312b(mmd), q3030b(mmd),
      1 q3031b(mmd), q3130b(mmd), q31312b(mmd), q31310b(mmd), r(mm+1)
double precision p22n01(mm), p22n02(mm), p22n03(mm), rr(mm+1)
      1 , work(lwork), w(lw)
double precision p110(mm), p12n0(mm), p22n0t(np)
double precision f33(mmd, n, n), q33(mmd, n, n, nd), phi33(mmd, n, n, nd)
      double precision q11(md), q12(md), q22(md)
double precision yq111(md), yq121(md)
double precision yq112(md), yq122(md)
double precision phi11(mmd), phi12(mmd), phi22(mmd)
double precision yph111(md), yph112(md), yph121(md), yph122(md)
double precision yq211(md), yq221(md), yq222(md)
double precision yph211(md), yph221(md), yph222(md)
double precision ytemp1(md), ytemp2(md), yxij(md), yxjk(md)
      1 , xijkdd(md), yxijkd(mmd, n), xijkd(mmd, n, n)
double precision tmp(n), ans, error, yph131(mmd), yph132(mmd),
      1 yph231(mmd), yph232(mmd), xx(nd/2)
double precision yq131(mmd), yq132(mmd), yq231(mmd), yq232(mmd)
      double precision q13(mmd, n), q23(mmd, n), q31(mmd, n), q32(mmd, n)
double precision yq113(mmd, n), yq123(mmd, n), yq213(mmd, n),

```

```

1 yq223(mmd,n),yq311(mmd,n),yq321(mmd,n),yq312(mmd,n),yq322(mmd,n)
double precision yph113(mmd,n),yph123(mmd,n),
1 yph213(mmd,n),yph223(mmd,n)
double precision yph311(mmd,n),yph312(mmd,n),x1(mmd,nd),
1 yph321(mmd,n),yph322(mmd,n),x2(mmd,nd)
double precision phi13(mmd,n),phi23(mmd,n),phi31(mmd,n),
1 phi32(mmd,n)
double precision xtmpr1(nd),ytmpr1(nd),xtmpr2(nd),ytmpr2(nd)
1 ,xtmpr3(nd),ytmpr3(nd),al(nd)
double precision yph133(mmd,n),yph233(mmd,n),yph331(mmd,n)
1 ,yph332(mmd,n)
double precision yq133(mmd,n),yq233(mmd,n),yq331(mmd,n)
1 ,yq332(mmd,n)
double precision yq313(mmd,n,n),
1 yq323(mmd,n,n),yph313(mmd,n,n),yph323(mmd,n,n)
double precision xtemp1(md)
double precision yq333(mmd,n,n,nd),
1 y1(mmd,n,n,nd),yph333(mmd,n,n,nd)
double precision betamin,betamax,alphamin,alphamax,tbn1
1 ,tbn2,rngbeta,rngalpha,beta(n),alpha(nd+1)
double precision mu3,bc,temp,q1,q2,q3,c1,c2,c3,r3,dnst,nne,npe
1 ,eln,tmin,tmax,rng,tbn,ktinv,pi,x,kppsq,jm1,j1,j0,dpn
double precision a,b,c,d,e,f,g,cd,r1,r2,fps,epc,fp,tp,ps,is
double precision rrng,krng,tbn3,tbn4,temp1,temp2,temp3,temp4
C*****
double precision qx11(mmd),qx12(mmd),qx13(mmd,n),qx21(mmd),
1 qx22(mmd),qx23(mmd,n),qx31(mmd,n),qx32(mmd,n),qx33(mmd,n)
double precision h11(mmd),h12(mmd),h21(mmd),h22(mmd)
double precision x11(mmd),x12(mmd),x21(mmd),x22(mmd)
double precision h13(mmd,n),h31(mmd,n),h23(mmd,n),h32(mmd,n)
double precision x13(mmd,n),x31(mmd,n),x23(mmd,n),x32(mmd,n)
double precision h33(mmd,n,n,nd),x33(mmd,n,n,nd)
equivalence (phi11,h11),(phi12,h12),(phi22,h22),(phi13,h13),
1 (phi23,h23),(phi31,h31),(phi32,h32),(yph131,h21),
1 (yq131,x11),(yq132,x12),(yq231,x21),(yq232,x22)
equivalence (x13,yq133),(x31,yq331),(x23,yq233),(x32,yq332)

```

```

C*****
double precision tao11,tao12,tao21,tao22,tao13,tao31,tao23,
1 tao32,tao33,t33(mmd,n,n,nd)
double precision h13d(mmd),h23d(mmd),h31d(mmd),h32d(mmd),
1 h33d(mmd)
equivalence (qx11,h13d),(qx12,h23d),(qx21,h31d),(qx22,h32d),
1 (x11,h33d)
double precision g11(mmd),g12(mmd),g13(mmd),g21(mmd),g22(mmd),
1 g23(mmd),g31(mmd),g32(mmd),g33(mmd)
real*4 CPUTIME,btzero,btime
open(unit=33,file='input')
open(unit=34,file='output')
read(33,*) bc,temp,mu3,dpn
read(33,*) q1,q2,q3,nne,npe
read(33,*) c1,c2,c3
read(33,*) r3,dnst,r1,r2
read(33,*) rmin,rmax
read(33,*) tmin,tmax
read(33,*) nu
pi=22.0/7.0
fps=4.0*(pi**2)
epc=8.0*(pi**3)
eps=8.0*(pi**2)
ps=pi**2
fp=4.0*pi
tp=2.0*pi
eln=(4.0*pi*(r3**2))/dnst
q1=(q1*npe)/(sqrt(78.45))
q2=(q2*nne)/(sqrt(78.45))
mu3=(mu3*dpn)/(sqrt(78.45))
q3=(eln*q3)/(sqrt(78.45))
c1=(nne/npe)*c2+(eln/npe)*c3
C-----
rml=r3*1.0e08
cn=c2/6.023e20
cp=c1/6.023e20

```



```

cmn=c3/6.023e20
ed3=dnst*1.0e16
is=(cp*(npe**2))+(cn*(nne**2))+(cmn*(eln**2))
write(34,11)ed3,rm1,cn,cmn,is,cp,dpn
11 format('The charge density on the Macroion:one electron per',
1 f10.2,'angstrom square',/'The radius of the Macroion=',f8.2,'A'
1 /'The concentration of the univalent negative ion=',e10.4,'M'
1 /'The concentration of the Macroion=',e10.4,'M'/'Ionic Strength
1 ='f12.8,
1 /'The concentration of the univalent positive ion=',f6.5,'M',
1 /'The dipole moment of the macroion='f10.3,'Debye')
C-----
C*****
C CALCULATION OF q-tilde(t)
C*****
c1=c1/(8.0*(pi**2))
c2=c2/(8.0*(pi**2))
c3=c3/(8.0*(pi**2))
rng=2.0*(tmax-tmin)
tbn=rng/dfloat(np)
t(1)=tmin
do i=2,np
t(i)=t(i-1)+tbn
end do
rrng=2.0*(rmax-rmin)
tbn3=rrng/dfloat(m)
r(1)=rmin
do i=2,mm
r(i)=r(i-1)+tbn3
end do
do i=1,mm
k(i)=(dfloat(i)-1.0)/rrng
end do
krng=2.0*(k(mm)-k(1))
tbn4=krng/dfloat(m)
ktinv=1.0/(bc*temp)

```

```

x=ktinv*32.0*(pi**3)
kpps=(c1*(q1**2))+(c2*(q2**2))+(c3*(q3**2))
a=c3*(mu3**2)
b=(2.0/3.0)*x
d=(3.0+(2.0*a*x))
c=-(3.0*x*(1.0+((a*b)/2.0)))/d
e=((3.0*kpps*x)+(kpps*a*(x**2)))/d
f=(sqrt(3.0)*x)/d
g=-(kpps*(x**2))/(3.0*d)
do i=1,mm
do j=1,np
p22n0t(j)=(1.0/(t(j)*((t(j)**2)+e)))*(sin(r(i)*t(j)))
end do
call d01gaf(t,p22n0t,n,ans,error,ifail)
p22n01(i)=3.0*g*ans
end do
do i=1,mm
p110(i)=c*(pi/2.0)*dexp(-sqrt(e)*r(i))
p12n0(i)=f*(pi/2.0)*dexp(-sqrt(e)*r(i))
p22n02(i)=g*(pi/2.0)*dexp(-sqrt(e)*r(i))
p22n03(i)=3.0*g*(pi/2.0)*(1.0/sqrt(e))*dexp(-sqrt(e)*r(i))
end do
C*****
C CALCULATION OF q-bar(r)
C*****
do i=1,mm
q11b(i)=(1.0/(16.0*(pi**4)))*(q1**2)*p110(i)*(1.0/r(i))
q12b(i)=(1.0/(16.0*(pi**4)))*(q1*q2)*p110(i)*(1.0/r(i))
q130b(i)=(1.0/(16.0*(pi**4)))*(q1*q3)*p110(i)*(1.0/r(i))
q22b(i)=(1.0/(16.0*(pi**4)))*(q2*q2)*p110(i)*(1.0/r(i))
q230b(i)=(1.0/(16.0*(pi**4)))*(q2*q3)*p110(i)*(1.0/r(i))
q3030b(i)=(1.0/(16.0*(pi**4)))*(q3*q3)*p110(i)*(1.0/r(i))
c q21b(i)=q12b(i)
c q301b(i)=q130b(i)
c q302b(i)=q230b(i)
q131b(i)=-(3.0/(16.0*(pi**4)))*q1*mu3*(p12n0(i)*(1.0/(r(i)**2)

```

```

1 )))
q231b(i)=- (3.0/(16.0*(pi**4)))*q2*mu3*(p12n0(i)*(1.0/(r(i)**2
1 )))
q3031b(i)=- (3.0/(16.0*(pi**4)))*q3*mu3*(p12n0(i)*(1.0/(r(i)**2
1 )))
q311b(i)= (3.0/(16.0*(pi**4)))*q1*mu3*(p12n0(i)*(1.0/(r(i)**2
1 )))
q312b(i)= (3.0/(16.0*(pi**4)))*q2*mu3*(p12n0(i)*(1.0/(r(i)**2
1 )))
q3130b(i)= (3.0/(16.0*(pi**4)))*q3*mu3*(p12n0(i)*(1.0/(r(i)**2
1 )))
q31312b(i)= (- (sqrt(30.0)/(16.0*(pi**4)))*(mu3**2)*(((3.0/(r(i)
1 **3))*p22n01(i))-((1.0/r(i))*p22n02(i))-((3.0/(r(i)**2)
1 *p22n03(i))))))
c q31311b(i)=0.0
q31310b(i)= (- (sqrt(3.0)/(16.0*(pi**4)))*(mu3**2)*((1.0/r(i))*
1 p22n02(i)))
end do
betamin=0.0
betamax=3.14
alphamin=-6.28
alphamax=6.28
rngbeta=betamax-betamin
tbn1=rngbeta/dfloat(n)
rngalpha=alphamax-alphamin
tbn2=rngalpha/dfloat(nd)
beta(1)=betamin+tbn1
do i=1,n-1
beta(i+1)=beta(i)+tbn1
end do
alpha(1)=alphamin
do i=1,nd
alpha(i+1)=alpha(i)+tbn2
end do
c*****
c CALCULATION OF q AND phi FUNCTION.

```

```

C*****
do i=1,mmd
  id=i*(mm/mmd)
  r(i)=r(id)
  q11(i)=q11b(id)
  q12(i)=q12b(id)
c  q21(i)=q21b(id)
  q22(i)=q22b(id)
  if(r(i).le.(r1*2.0)) then
    phi11(i)=-1.0
  else
    phi11(i)=dexp(q11(i))-1.0d0
  end if
  if(r(i).le.(r1+r2)) then
    phi12(i)=-1.0
c  phi21(i)=-1.0
  else
    phi12(i)=dexp(q12(i))-1.0d0
c  phi21(i)=dexp(q21(i))-1.0d0
  end if
  if(r(i).le.(2.0*r2)) then
    phi22(i)=-1.0
  else
    phi22(i)=dexp(q22(i))-1.0d0
  end if
end do
do i=1,mmd
  id=i*(mm/mmd)
  do j=1,n
    q13(i,j)=q130b(id)-(sqrt(1.0/3.0)*q131b(id)*cos(beta(j)))
    q31(i,j)=q130b(id)-(sqrt(1.0/3.0)*q311b(id)*cos(beta(j)))
    q23(i,j)=q230b(id)-(sqrt(1.0/3.0)*q231b(id)*cos(beta(j)))
    q32(i,j)=q230b(id)-(sqrt(1.0/3.0)*q312b(id)*cos(beta(j)))
    if(r(i).le.(r1+r3)) then
      phi13(i,j)=-1.0
      phi31(i,j)=-1.0

```

```

else
phi13(i,j)=dexp(q13(i,j))-1.0d0
phi31(i,j)=dexp(q31(i,j))-1.0d0
end if
if(r(i).le.(r2+r3)) then
phi23(i,j)=-1.0
phi32(i,j)=-1.0
else
phi23(i,j)=dexp(q23(i,j))-1.0d0
phi32(i,j)=dexp(q32(i,j))-1.0d0
end if
end do
end do
do i=1,mmd
do j=1,n
do kk=1,n
do l=1,nd
      q33(i,j,kk,l)=q3030b(i)-((1.0/sqrt(3.0))*q3031b(i)*
1  cos(beta(kk)))-((1.0/sqrt(3.0))*q3130b(i)*cos(beta(j)))+
1  (q31312b(i)*(((sqrt(2.0/15.0))*cos(beta(j))*cos(beta(kk)))-
1  ((sqrt(1.0/30.0))*sin(beta(j))*sin(beta(kk))*cos(alpha(l)))))-
1  ((1.0/sqrt(3.0))*q31310b(i)*((cos(beta(j))*cos(beta(kk)))+
1  (sin(beta(j))*sin(beta(kk))*cos(alpha(l))))))
if(r(i).le.(2.0*r3)) then
phi33(i,j,kk,l)=-1.0
else
phi33(i,j,kk,l)=dexp(q33(i,j,kk,l))-1.0d0
end if
end do
end do
end do
end do

```

```

C-----
C*****
C CALCULATION OF INITIAL VALUE OF tao
C*****

```

C IN THE FOLLOWING, SUBROUTINES ARE CALLED FOR THE CALCULATION  
C OF THE CONVOLUTION INTEGRAL.

C\*\*\*\*\*

call iii(q11,q11,yq111,yxij,yxjk,r,k,tbn3,tbn4,md,mmd,w,lw  
1 ,xtempl,eps)

call iii(q12,q12,yq121,yxij,yxjk,r,k,tbn3,tbn4,md,mmd,w,lw  
1 ,xtempl,eps)

call iii(q11,q12,yq112,yxij,yxjk,r,k,tbn3,tbn4,md,mmd,w,lw  
1 ,xtempl,eps)

call iii(q12,q22,yq122,yxij,yxjk,r,k,tbn3,tbn4,md,mmd,w,lw  
1 ,xtempl,eps)

call iii(q12,q11,yq211,yxij,yxjk,r,k,tbn3,tbn4,md,mmd,w,lw  
1 ,xtempl,eps)

call iii(q22,q12,yq221,yxij,yxjk,r,k,tbn3,tbn4,md,mmd,w,lw  
1 ,xtempl,eps)

C yq212=yq121

call iii(q22,q22,yq222,yxij,yxjk,r,k,tbn3,tbn4,md,mmd,w,lw  
1 ,xtempl,eps)

C-----

call iii(phi11,phi11,yph111,yxij,yxjk,r,k,tbn3,tbn4,md,mmd,w,  
1 lw,xtempl,eps)

call iii(phi12,phi12,yph121,yxij,yxjk,r,k,tbn3,tbn4,md,mmd,w,  
1 lw,xtempl,eps)

call iii(phi11,phi12,yph112,yxij,yxjk,r,k,tbn3,tbn4,md,mmd,w,  
1 lw,xtempl,eps)

call iii(phi12,phi22,yph122,yxij,yxjk,r,k,tbn3,tbn4,md,mmd,w,  
1 lw,xtempl,eps)

call iii(phi12,phi11,yph211,yxij,yxjk,r,k,tbn3,tbn4,md,mmd,w,  
1 lw,xtempl,eps)

call iii(phi22,phi12,yph221,yxij,yxjk,r,k,tbn3,tbn4,md,mmd,w,  
1 lw,xtempl,eps)

C yph212=yph121

call iii(phi22,phi22,yph222,yxij,yxjk,r,k,tbn3,tbn4,md,mmd,w,  
1 lw,xtempl,eps)

C-----

call imi(q13,q31,yq131,beta,r,k,tbn3,tbn4,w,lw,mmd,n,md,

```

1  xtempl,ytempl,ytemp2,xijkdd,yxijkd,tmp,ans,error)
call imi(q23,q31,yq231,beta,r,k,tbn3,tbn4,w,lw,mmd,n,md,
1  xtempl,ytempl,ytemp2,xijkdd,yxijkd,tmp,ans,error)
call imi(q13,q32,yq132,beta,r,k,tbn3,tbn4,w,lw,mmd,n,md,
1  xtempl,ytempl,ytemp2,xijkdd,yxijkd,tmp,ans,error)
call imi(q23,q32,yq232,beta,r,k,tbn3,tbn4,w,lw,mmd,n,md,
1  xtempl,ytempl,ytemp2,xijkdd,yxijkd,tmp,ans,error)
call imi(phi13,phi31,yph131,beta,r,k,tbn3,tbn4,w,lw,mmd,n,md,
1  xtempl,ytempl,ytemp2,xijkdd,yxijkd,tmp,ans,error)
call imi(phi23,phi31,yph231,beta,r,k,tbn3,tbn4,w,lw,mmd,n,md,
1  xtempl,ytempl,ytemp2,xijkdd,yxijkd,tmp,ans,error)
call imi(phi13,phi32,yph132,beta,r,k,tbn3,tbn4,w,lw,mmd,n,md,
1  xtempl,ytempl,ytemp2,xijkdd,yxijkd,tmp,ans,error)
call imi(phi23,phi32,yph232,beta,r,k,tbn3,tbn4,w,lw,mmd,n,md,
1  xtempl,ytempl,ytemp2,xijkdd,yxijkd,tmp,ans,error)
c-----
call iim(q13,q11,yq113,r,k,tbn3,tbn4,w,lw,mmd,n,md,
1  xtempl,ytempl,ytemp2,xijkdd,eps)
call iim(q23,q12,yq123,r,k,tbn3,tbn4,w,lw,mmd,n,md,
1  xtempl,ytempl,ytemp2,xijkdd,eps)
call iim(q13,q12,yq213,r,k,tbn3,tbn4,w,lw,mmd,n,md,
1  xtempl,ytempl,ytemp2,xijkdd,eps)
call iim(q23,q22,yq223,r,k,tbn3,tbn4,w,lw,mmd,n,md,
1  xtempl,ytempl,ytemp2,xijkdd,eps)
call iim(q31,q11,yq311,r,k,tbn3,tbn4,w,lw,mmd,n,md,
1  xtempl,ytempl,ytemp2,xijkdd,eps)
call iim(q32,q12,yq321,r,k,tbn3,tbn4,w,lw,mmd,n,md,
1  xtempl,ytempl,ytemp2,xijkdd,eps)
call iim(q31,q12,yq312,r,k,tbn3,tbn4,w,lw,mmd,n,md,
1  xtempl,ytempl,ytemp2,xijkdd,eps)
call iim(q32,q22,yq322,r,k,tbn3,tbn4,w,lw,mmd,n,md,
1  xtempl,ytempl,ytemp2,xijkdd,eps)
call iim(phi13,phi11,yph113,r,k,tbn3,tbn4,w,lw,mmd,n,md,
1  xtempl,ytempl,ytemp2,xijkdd,eps)
call iim(phi23,phi12,yph123,r,k,tbn3,tbn4,w,lw,mmd,n,md,
1  xtempl,ytempl,ytemp2,xijkdd,eps)

```

```

if(r(i).le.(r1+r2)) then
h12(i)=-1.0
else
h12(i)=dexp(q12(i)+tao12)-1.0d0
end if
x12(i)=h12(i)-q12(i)-tao12
temp1=fps*yq231(i)
temp2=fps*yph231(i)
temp3=((c1*yph211(i))+(c2*yph221(i))+(c3*temp2))
temp4=((c1*yq211(i))+(c2*yq221(i))+(c3*temp1))
tao21=temp3-temp4
if(r(i).le.(r1+r2)) then
h21(i)=-1.0
else
h21(i)=dexp(q12(i)+tao21)-1.0d0
end if
x21(i)=h21(i)-q12(i)-tao21
temp1=fps*yq232(i)
temp2=fps*yph232(i)
temp3=((c1*yph121(i))+(c2*yph222(i))+(c3*temp2))
temp4=((c1*yq121(i))+(c2*yq222(i))+(c3*temp1))
tao22=temp3-temp4
if(r(i).le.(2.0*r2)) then
h22(i)=-1.0
else
h22(i)=dexp(q22(i)+tao22)-1.0d0
end if
x22(i)=h22(i)-q22(i)-tao22
end do
c-----
do i=1,mmd
do j=1,n
temp1=tp*yph133(i,j)
temp2=tp*yq133(i,j)
temp3=(c1*yph113(i,j))+(c2*yph123(i,j))+(c3*temp1)
temp4=(c1*yq113(i,j))+(c2*yq123(i,j))+(c3*temp2)

```



```

tao13=temp3-temp4
if(r(i).le.(r1+r3)) then
h13(i,j)=-1.0
else
h13(i,j)=dexp(q13(i,j)+tao13)-1.0d0
end if
x13(i,j)=h13(i,j)-q13(i,j)-tao13
temp1=tp*yph233(i,j)
temp2=tp*yq233(i,j)
temp3=(c1*yph213(i,j))+(c2*yph223(i,j))+(c3*temp1)
temp4=(c1*yq213(i,j))+(c2*yq223(i,j))+(c3*temp2)
tao23=temp3-temp4
if(r(i).le.(r2+r3)) then
h23(i,j)=-1.0
else
h23(i,j)=dexp(q23(i,j)+tao23)-1.0d0
end if
x23(i,j)=h23(i,j)-q23(i,j)-tao23
temp1=tp*yph331(i,j)
temp2=tp*yq331(i,j)
temp3=(c1*yph311(i,j))+(c2*yph321(i,j))+(c3*temp1)
temp4=(c1*yq311(i,j))+(c2*yq321(i,j))+(c3*temp2)
tao31=temp3-temp4
if(r(i).le.(r1+r3)) then
h31(i,j)=-1.0
else
h31(i,j)=dexp(q31(i,j)+tao31)-1.0d0
end if
x31(i,j)=h31(i,j)-q31(i,j)-tao31
temp1=tp*yph332(i,j)
temp2=tp*yq332(i,j)
temp3=(c1*yph312(i,j))+(c2*yph322(i,j))+(c3*temp1)
temp4=(c1*yq312(i,j))+(c2*yq322(i,j))+(c3*temp2)
tao32=temp3-temp4
if(r(i).le.(r2+r3)) then
h32(i,j)=-1.0

```

```

    else
      h32(i,j)=dexp(q32(i,j)+tao32)-1.0d0
    end if
    x32(i,j)=h32(i,j)-q32(i,j)-tao32
  end do
end do

C-----
do i=1,mmd
  do j=1,n
    do jd=1,n
      do l=1,nd
        temp2=(c1*yq313(i,j,jd))+(c2*yq323(i,j,jd))+(c3*tp*
          1 yq333(i,j,jd,l))
        temp3=(c1*yph313(i,j,jd))+(c2*yph323(i,j,jd))+(c3*tp*
          1 yph333(i,j,jd,l))
        tao33=temp3-temp2
        if(r(i).le.(2.0*r3)) then
          h33(i,j,jd,l)=-1.0
        else
          h33(i,j,jd,l)=dexp(q33(i,j,jd,l)+tao33)-1.0d0
        end if
        x33(i,j,jd,l)=h33(i,j,jd,l)-q33(i,j,jd,l)-tao33
      end do
    end do
  end do
end do

C*****
C INITIAL VALUE OF tao ,h AND x FUNCTIONS ARE CALCULATED
C*****
nitr=0
btzero = CPUTIME(0.0d0)

C-----
C*****
C CALCULATION OF FINAL VALUE OF tao
C*****
300 nitr=nitr+1

```

```

call iii(q11,x11,yqx111,yxij,yxjk,r,k,tbn3,tbn4,md,mmd,w,
1 lw,xtemp1,eps)
call iii(q12,x21,yqx121,yxij,yxjk,r,k,tbn3,tbn4,md,mmd,w,
1 lw,xtemp1,eps)
call imi(q13,x31,yqx131,beta,r,k,tbn3,tbn4,w,lw,mmd,n,md,
1 xtemp1,ytemp1,ytemp2,xijkdd,yxijkd,tmp,ans,error)
do i=1,mmd
qx11(i)=(c1*yqx111(i))+(c2*yqx121(i))+(c3*fps*yqx131(i))
end do
C-----
call iii(q11,x12,yqx112,yxij,yxjk,r,k,tbn3,tbn4,md,mmd,w,
1 lw,xtemp1,eps)
call iii(q12,x22,yqx122,yxij,yxjk,r,k,tbn3,tbn4,md,mmd,w,
1 lw,xtemp1,eps)
call imi(q13,x32,yqx132,beta,r,k,tbn3,tbn4,w,lw,mmd,n,md,
1 xtemp1,ytemp1,ytemp2,xijkdd,yxijkd,tmp,ans,error)
do i=1,mmd
qx12(i)=(c1*yqx112(i))+(c2*yqx122(i))+(c3*fps*yqx132(i))
end do
C-----
call iim(x13,q11,yqx113,r,k,tbn3,tbn4,w,lw,mmd,n,md,
1 xtemp1,ytemp1,ytemp2,xijkdd,eps)
call iim(x23,q12,yqx123,r,k,tbn3,tbn4,w,lw,mmd,n,md,
1 xtemp1,ytemp1,ytemp2,xijkdd,eps)
call xint2(x33,alpha,mmd,n,nd,f33,xx,ans,error,al)
call imm(q13,f33,yqx133,beta,r,k,tbn3,tbn4,w,lw,mmd,n,md,
1 xtemp1,ytemp1,ytemp2,xijkdd,xijkd,tmp,ans,error)
do i=1,mmd
do j=1,n
qx13(i,j)=(c1*yqx113(i,j))+(c2*yqx123(i,j))+(c3*tp*
1 yqx133(i,j))
end do
end do
C-----
call iii(q12,x11,yqx211,yxij,yxjk,r,k,tbn3,tbn4,md,mmd,w,
1 lw,xtemp1,eps)

```

```

call iii(q22,x21,yqx221,yxij,yxjk,r,k,tbn3,tbn4,md,mmd,w,
1 lw,xtemp1,eps)
call imi(q23,x31,yqx231,beta,r,k,tbn3,tbn4,w,lw,mmd,n,md,
1 xtemp1,ytemp1,ytemp2,xijkdd,yxijkd,tmp,ans,error)
do i=1,mmd
qx21(i)=(c1*yqx211(i))+(c2*yqx221(i))+(c3*fps*yqx231(i))
end do
C-----
call iii(q12,x12,yqx212,yxij,yxjk,r,k,tbn3,tbn4,md,mmd,w,
1 lw,xtemp1,eps)
call iii(q22,x22,yqx222,yxij,yxjk,r,k,tbn3,tbn4,md,mmd,w,
1 lw,xtemp1,eps)
call imi(q23,x32,yqx232,beta,r,k,tbn3,tbn4,w,lw,mmd,n,md,
1 xtemp1,ytemp1,ytemp2,xijkdd,yxijkd,tmp,ans,error)
do i=1,mmd
qx22(i)=(c1*yqx212(i))+(c2*yqx222(i))+(c3*fps*yqx232(i))
end do
C-----
call iim(x13,q12,yqx213,r,k,tbn3,tbn4,w,lw,mmd,n,md,
1 xtemp1,ytemp1,ytemp2,xijkdd,eps)
call iim(x23,q22,yqx223,r,k,tbn3,tbn4,w,lw,mmd,n,md,
1 xtemp1,ytemp1,ytemp2,xijkdd,eps)
call xint2(x33,alpha,mmd,n,nd,f33,xx,ans,error,al)
call imm(q23,f33,yqx233,beta,r,k,tbn3,tbn4,w,lw,mmd,n,md,
1 xtemp1,ytemp1,ytemp2,xijkdd,xijkd,tmp,ans,error)
do i=1,mmd
do j=1,n
qx23(i,j)=(c1*yqx213(i,j))+(c2*yqx223(i,j))+(c3*tp*
1 yqx233(i,j))
end do
end do
C-----
call iim(q31,x11,yqx311,r,k,tbn3,tbn4,w,lw,mmd,n,md,
1 xtemp1,ytemp1,ytemp2,xijkdd,eps)
call iim(q32,x21,yqx321,r,k,tbn3,tbn4,w,lw,mmd,n,md,
1 xtemp1,ytemp1,ytemp2,xijkddi,eps)

```

```

call xint1(q33,alpha,mmd,n,nd,f33,xx,ans,error,a1)
call imm(x31,f33,yqx331,beta,r,k,tbn3,tbn4,w,lw,mmd,n,md,
      1 xtemp1,ytemp1,ytemp2,xijkdd,xijkd,tmp,ans,error)
do i=1,mmd
do j=1,n
qx31(i,j)=(c1*yqx311(i,j))+(c2*yqx321(i,j))+(c3*tp*
      1 yqx331(i,j))
end do
end do

C-----
call iim(q31,x12,yqx312,r,k,tbn3,tbn4,w,lw,mmd,n,md,
      1 xtemp1,ytemp1,ytemp2,xijkdd,eps)
call iim(q32,x22,yqx322,r,k,tbn3,tbn4,w,lw,mmd,n,md,
      1 xtemp1,ytemp1,ytemp2,xijkdd,eps)
call xint1(q33,alpha,mmd,n,nd,f33,xx,ans,error,a1)
call imm(x32,f33,yqx332,beta,r,k,tbn3,tbn4,w,lw,mmd,n,md,
      1 xtemp1,ytemp1,ytemp2,xijkdd,xijkd,tmp,ans,error)
do i=1,mmd
do j=1,n
qx32(i,j)=(c1*yqx312(i,j))+(c2*yqx322(i,j))+(c3*tp*
      1 yqx332(i,j))
end do
end do

C-----
call mim(q31,x13,yqx313,r,k,tbn3,tbn4,w,lw,mmd,n,md,xtemp1,
      1 ytemp1,ytemp2,xijkdd,eps)
call mim(q32,x23,yqx323,r,k,tbn3,tbn4,w,lw,mmd,n,md,xtemp1,
      1 ytemp1,ytemp2,xijkdd,eps)
call mmm(q33,x33,yqx333,beta,r,k,tbn3,tbn4,w,lw,w1,lw1,mmd,
      1 n,md,nd,xtemp1,ytemp1,ytemp2,xtmpr1,ytmpr1,xtmpr2,ytmpr2,
      1 xtmpr3,ytmpr3,x1,x2,y1,tmp,ans,error,alpha)

C-----
do i=1,mmd
do j=1,n
do jd=1,n
do l=1,nd

```

```

t33(i,j,jd,1)=(c1*yqx313(i,j,jd))+(c2*yqx323(i,j,jd))+
1 (c3*tp*yqx333(i,j,jd,1))
end do
end do
end do
end do
C-----
call iii(x11,h11,yxh111,yxij,yxjk,r,k,tbn3,tbn4,md,mmd,w,
1 lw,xtemp1,eps)
call iii(x12,h21,yxh121,yxij,yxjk,r,k,tbn3,tbn4,md,mmd,w,
1 lw,xtemp1,eps)
call imi(x13,h31,yxh131,beta,r,k,tbn3,tbn4,w,lw,mmd,n,md,
1 xtemp1,ytemp1,ytemp2,xijkdd,yxijkd,tmp,ans,error)
call iii(x11,h12,yxh112,yxij,yxjk,r,k,tbn3,tbn4,md,mmd,w,
1 lw,xtemp1,eps)
call iii(x12,h22,yxh122,yxij,yxjk,r,k,tbn3,tbn4,md,mmd,w,
1 lw,xtemp1,eps)
call imi(x13,h32,yxh132,beta,r,k,tbn3,tbn4,w,lw,mmd,n,md,
1 xtemp1,ytemp1,ytemp2,xijkdd,yxijkd,tmp,ans,error)
call iim(h13,x11,yxh113,r,k,tbn3,tbn4,w,lw,mmd,n,md,
1 xtemp1,ytemp1,ytemp2,xijkdd,eps)
call iim(h23,x12,yxh123,r,k,tbn3,tbn4,w,lw,mmd,n,md,
1 xtemp1,ytemp1,ytemp2,xijkdd,eps)
call xint2(h33,alpha,mmd,n,nd,f33,xx,ans,error,al)
call imm(x13,f33,yxh133,beta,r,k,tbn3,tbn4,w,lw,mmd,n,md,
1 xtemp1,ytemp1,ytemp2,xijkdd,xijkd,tmp,ans,error)
call iii(x21,h11,yxh211,yxij,yxjk,r,k,tbn3,tbn4,md,mmd,w,
1 lw,xtemp1,eps)
call iii(x22,h21,yxh221,yxij,yxjk,r,k,tbn3,tbn4,md,mmd,w,
1 lw,xtemp1,eps)
call imi(x23,h31,yxh231,beta,r,k,tbn3,tbn4,w,lw,mmd,n,md,
1 xtemp1,ytemp1,ytemp2,xijkdd,yxijkd,tmp,ans,error)
call iii(x21,h12,yxh212,yxij,yxjk,r,k,tbn3,tbn4,md,mmd,w,
1 lw,xtemp1,eps)
call iii(x22,h22,yxh222,yxij,yxjk,r,k,tbn3,tbn4,md,mmd,w,
1 lw,xtemp1,eps)

```

```

call imi(x23,h32,yxh232,beta,r,k,tbn3,tbn4,w,lw,mmd,n,md,
  1 xtemp1,ytemp1,ytemp2,xijkdd,yxijkd,tmp,ans,error)
call iim(h13,x21,yxh213,r,k,tbn3,tbn4,w,lw,mmd,n,md,
  1 xtemp1,ytemp1,ytemp2,xijkdd,eps)
call iim(h23,x22,yxh223,r,k,tbn3,tbn4,w,lw,mmd,n,md,
  1 xtemp1,ytemp1,ytemp2,xijkddi,eps)
call xint2(h33,alpha,mmd,n,nd,f33,xx,ans,error,al)
call imm(x23,f33,yxh233,beta,r,k,tbn3,tbn4,w,lw,mmd,n,md,
  1 xtemp1,ytemp1,ytemp2,xijkdd,xijkd,tmp,ans,error)
call iim(x31,h11,yxh311,r,k,tbn3,tbn4,w,lw,mmd,n,md,
  1 xtemp1,ytemp1,ytemp2,xijkdd,eps)
call iim(x32,h21,yxh321,r,k,tbn3,tbn4,w,lw,mmd,n,md,
  1 xtemp1,ytemp1,ytemp2,xijkdd,eps)
call xint1(x33,alpha,mmd,n,nd,f33,xx,ans,error,al)
call imm(h31,f33,yxh331,beta,r,k,tbn3,tbn4,w,lw,mmd,n,md,
  1 xtemp1,ytemp1,ytemp2,xijkdd,xijkd,tmp,ans,error)
call iim(x31,h12,yxh312,r,k,tbn3,tbn4,w,lw,mmd,n,md,
  1 xtemp1,ytemp1,ytemp2,xijkdd,eps)
call iim(x32,h22,yxh322,r,k,tbn3,tbn4,w,lw,mmd,n,md,
  1 xtemp1,ytemp1,ytemp2,xijkdd,eps)
call xint1(x33,alpha,mmd,n,nd,f33,xx,ans,error,al)
call imm(h32,f33,yxh332,beta,r,k,tbn3,tbn4,w,lw,mmd,n,md,
  1 xtemp1,ytemp1,ytemp2,xijkdd,xijkd,tmp,ans,error)
C-----
call iii(q11,yxh111,y1111,yxij,yxjk,r,k,tbn3,tbn4,md,mmd,w,
  1 lw,xtemp1,eps)
call iii(q11,yxh121,y1121,yxij,yxjk,r,k,tbn3,tbn4,md,mmd,w,
  1 lw,xtemp1,eps)
call iii(q11,yxh131,y1131,yxij,yxjk,r,k,tbn3,tbn4,md,mmd,w,
  1 lw,xtemp1,eps)
call iii(q12,yxh211,y1211,yxij,yxjk,r,k,tbn3,tbn4,md,mmd,w,
  1 lw,xtemp1,eps)
call iii(q12,yxh221,y1221,yxij,yxjk,r,k,tbn3,tbn4,md,mmd,w,
  1 lw,xtemp1,eps)
call iii(q12,yxh231,y1231,yxij,yxjk,r,k,tbn3,tbn4,md,mmd,w,
  1 lw,xtemp1,eps)

```

```

      1 (i,j))
temp3=(c1*c1*y1113(i,j))+(c1*c2*y1123(i,j))+(c1*
      1 c3*tp*y1133(i,j))+(c2*c1*y1213(i,j))+(c2*c2*
      1 y1223(i,j))+(c2*c3*tp*y1233(i,j))
qx13(i,j)=qx13(i,j)+temp1+temp3
end do
end do
c-----
call iii(q12,yxh111,y2111,yxij,yxjk,r,k,tbn3,tbn4,md,mmd,w,
      1 lw,xtemp1,eps)
call iii(q12,yxh121,y2121,yxij,yxjk,r,k,tbn3,tbn4,md,mmd,w,
      1 lw,xtemp1,eps)
call iii(q12,yxh131,y2131,yxij,yxjk,r,k,tbn3,tbn4,md,mmd,w,
      1 lw,xtemp1,eps)
call iii(q22,yxh211,y2211,yxij,yxjk,r,k,tbn3,tbn4,md,mmd,w,
      1 lw,xtemp1,eps)
call iii(q22,yxh221,y2221,yxij,yxjk,r,k,tbn3,tbn4,md,mmd,w,
      1 lw,xtemp1,eps)
call iii(q22,yxh231,y2231,yxij,yxjk,r,k,tbn3,tbn4,md,mmd,w,
      1 lw,xtemp1,eps)
call imi(q23,yxh311,y2311,beta,r,k,tbn3,tbn4,w,lw,mmd,n,md,
      1 xtemp1,ytemp1,ytemp2,xijkdd,yxijkd,tmp,ans,error)
call imi(q23,yxh321,y2321,beta,r,k,tbn3,tbn4,w,lw,mmd,n,md,
      1 xtemp1,ytemp1,ytemp2,xijkdd,yxijkd,tmp,ans,error)
call imi(q23,yxh331,y2331,beta,r,k,tbn3,tbn4,w,lw,mmd,n,md,
      1 xtemp1,ytemp1,ytemp2,xijkdd,yxijkd,tmp,ans,error)
c-----
do i=1,mmd
temp1=(c1*yxh211(i))+(c2*yxh221(i))+(c3*fps*yxh231(i))
temp3=(c1*c1*y2111(i))+(c1*c2*y2121(i))+(c1*c3*
      1 fps*y2131(i))+(c2*c1*y2211(i))+(c2*c2*y2221
      1 (i))+(c2*c3*fps*y2231(i))+(c3*c1*fps*y2311(i))+(c3*c2*
      1 fps*y2321(i))+(c3*c3*epc*y2331(i))
tao21=temp1+qx21(i)+temp3
if(r(i).le.(r1+r2)) then
h21(i)=-1.0

```



```

else
h21(i)=dexp(q12(i)+tao21)-1.0d0
end if
x21(i)=h21(i)-q12(i)-tao21
end do

c-----
call iii(q12,yxh112,y2112,yxij,yxjk,r,k,tbn3,tbn4,md,mmd,w,
1 lw,xtemp1,eps)
call iii(q12,yxh122,y2122,yxij,yxjk,r,k,tbn3,tbn4,md,mmd,w,
1 lw,xtemp1,eps)
call iii(q12,yxh132,y2132,yxij,yxjk,r,k,tbn3,tbn4,md,mmd,w,
1 lw,xtemp1,eps)
call iii(q22,yxh212,y2212,yxij,yxjk,r,k,tbn3,tbn4,md,mmd,w,
1 lw,xtemp1,eps)
call iii(q22,yxh222,y2222,yxij,yxjk,r,k,tbn3,tbn4,md,mmd,w,
1 lw,xtemp1,eps)
call iii(q22,yxh232,y2232,yxij,yxjk,r,k,tbn3,tbn4,md,mmd,w,
1 lw,xtemp1,eps)
call imi(q23,yxh312,y2312,beta,r,k,tbn3,tbn4,w,lw,mmd,n,md,
1 xtemp1,ytemp1,ytemp2,xijkdd,yxijkd,tmp,ans,error)
call imi(q23,yxh322,y2322,beta,r,k,tbn3,tbn4,w,lw,mmd,n,md,
1 xtemp1,ytemp1,ytemp2,xijkdd,yxijkd,tmp,ans,error)
call imi(q23,yxh332,y2332,beta,r,k,tbn3,tbn4,w,lw,mmd,n,md,
1 xtemp1,ytemp1,ytemp2,xijkdd,yxijkd,tmp,ans,error)
c-----
do i=1,mmd
temp1=(c1*yxh212(i))+(c2*yxh222(i))+(c3*fps*yxh232(i))
temp3=(c1*c1*y2112(i))+(c1*c2*y2122(i))+(c1*c3*
1 fps*y2132(i))+(c2*c1*y2212(i))+(c2*c2*y222
1 (i))+(c2*c3*fps*y2232(i))+(c3*c1*fps*y2312(i))+(c3*c2*
1 fps*y2322(i))+(c3*c3*epc*y2332(i))
tao22=temp1+qx22(i)+temp3
if(r(i).le.(r2+r2)) then
h22(i)=-1.0
else
h22(i)=dexp(q22(i)+tao22)-1.0d0

```

```

end if
x22(i)=h22(i)-q22(i) -tao22
end do

```

```

c-----
call iim(yxh113,q12,y2113,r,k,tbn3,tbn4,w,lw,mmd,n,md,
1  xtemp1,ytemp1,ytemp2,xijkdd,eps)
call iim(yxh123,q12,y2123,r,k,tbn3,tbn4,w,lw,mmd,n,md,
1  xtemp1,ytemp1,ytemp2,xijkdd,eps)
call iim(yxh133,q12,y2133,r,k,tbn3,tbn4,w,lw,mmd,n,md,
1  xtemp1,ytemp1,ytemp2,xijkdd,eps)
call iim(yxh213,q22,y2213,r,k,tbn3,tbn4,w,lw,mmd,n,md,
1  xtemp1,ytemp1,ytemp2,xijkdd,eps)
call iim(yxh223,q22,y2223,r,k,tbn3,tbn4,w,lw,mmd,n,md,
1  xtemp1,ytemp1,ytemp2,xijkdd,eps)
call iim(yxh233,q22,y2233,r,k,tbn3,tbn4,w,lw,mmd,n,md,
1  xtemp1,ytemp1,ytemp2,xijkdd,eps)

```

```

c-----
do i=1,mmd
do j=1,n
temp1=(c1*yxh213(i,j))+(c2*yxh223(i,j))+(c3*tp*yxh233
1  (i,j))
temp3=(c1*c1*y2113(i,j))+(c1*c2*y2123(i,j))+(c1*
1  c3*tp*y2133(i,j))+(c2*c1*y2213(i,j))+(c2*c2*
1  y2223(i,j))+(c2*c3*tp*y2233(i,j))
qx23(i,j)=qx23(i,j)+temp1+temp2
end do
end do

```

```

c-----
call iim(q31,yxh111,y3111,r,k,tbn3,tbn4,w,lw,mmd,n,md,
1  xtemp1,ytemp1,ytemp2,xijkdd,eps)
call iim(q31,yxh121,y3121,r,k,tbn3,tbn4,w,lw,mmd,n,md,
1  xtemp1,ytemp1,ytemp2,xijkdd,eps)
call iim(q31,yxh131,y3131,r,k,tbn3,tbn4,w,lw,mmd,n,md,
1  xtemp1,ytemp1,ytemp2,xijkdd,eps)
call iim(q32,yxh211,y3211,r,k,tbn3,tbn4,w,lw,mmd,n,md,
1  xtemp1,ytemp1,ytemp2,xijkdd,eps)

```

```

call iim(q32,yxh221,y3221,r,k,tbn3,tbn4,w,lw,mmd,n,md,
1  xtemp1,ytemp1,ytemp2,xijkdd,eps)
call iim(q32,yxh231,y3231,r,k,tbn3,tbn4,w,lw,mmd,n,md,
1  xtemp1,ytemp1,ytemp2,xijkdd,eps)
call xint1(q33,alpha,mmd,n,nd,f33,xx,ans,error,al)
call imm(yxh311,f33,y3311,beta,r,k,tbn3,tbn4,w,lw,mmd,n,md,
1  xtemp1,ytemp1,ytemp2,xijkdd,xijkd,tmp,ans,error)
call imm(yxh321,f33,y3321,beta,r,k,tbn3,tbn4,w,lw,mmd,n,md,
1  xtemp1,ytemp1,ytemp2,xijkdd,xijkd,tmp,ans,error)
call imm(yxh331,f33,y3331,beta,r,k,tbn3,tbn4,w,lw,mmd,n,md,
1  xtemp1,ytemp1,ytemp2,xijkdd,xijkd,tmp,ans,error)
C-----
call iim(q31,yxh112,y3112,r,k,tbn3,tbn4,w,lw,mmd,n,md,
1  xtemp1,ytemp1,ytemp2,xijkdd,eps)
call iim(q31,yxh122,y3122,r,k,tbn3,tbn4,w,lw,mmd,n,md,
1  xtemp1,ytemp1,ytemp2,xijkdd,eps)
call iim(q31,yxh132,y3132,r,k,tbn3,tbn4,w,lw,mmd,n,md,
1  xtemp1,ytemp1,ytemp2,xijkdd,eps)
call iim(q32,yxh212,y3212,r,k,tbn3,tbn4,w,lw,mmd,n,md,
1  xtemp1,ytemp1,ytemp2,xijkdd,eps)
call iim(q32,yxh222,y3222,r,k,tbn3,tbn4,w,lw,mmd,n,md,
1  xtemp1,ytemp1,ytemp2,xijkdd,eps)
call iim(q32,yxh232,y3232,r,k,tbn3,tbn4,w,lw,mmd,n,md,
1  xtemp1,ytemp1,ytemp2,xijkdd,eps)
call imm(yxh312,f33,y3312,beta,r,k,tbn3,tbn4,w,lw,mmd,n,md,
1  xtemp1,ytemp1,ytemp2,xijkdd,xijkd,tmp,ans,error)
call imm(yxh322,f33,y3322,beta,r,k,tbn3,tbn4,w,lw,mmd,n,md,
1  xtemp1,ytemp1,ytemp2,xijkdd,xijkd,tmp,ans,error)
call imm(yxh332,f33,y3332,beta,r,k,tbn3,tbn4,w,lw,mmd,n,md,
1  xtemp1,ytemp1,ytemp2,xijkdd,xijkd,tmp,ans,error)
C-----
call mmm(x33,h33,yxh333,beta,r,k,tbn3,tbn4,w,lw,w1,lw1,mmd,
1  n,md,nd,xtemp1,ytemp1,ytemp2,xtmp1,ytmp1,xtmp2,ytmp2,
1  xtmp3,ytmp3,x1,x2,y1,tmp,ans,error,alpha)
C-----
call mim(x31,h13,f33,r,k,tbn3,tbn4,w,lw,mmd,n,md,xtemp1,

```

```

      1 ytemp1,ytemp2,xijkdd,eps)
call imm(q13,f33,y1313,beta,r,k,tbn3,tbn4,w,lw,mmd,n,md,
      1 xtemp1,ytemp1,ytemp2,xijkdd,xijkd,tmp,ans,error)
call imm(q23,f33,y2313,beta,r,k,tbn3,tbn4,w,lw,mmd,n,md,
      1 xtemp1,ytemp1,ytemp2,xijkdd,xijkd,tmp,ans,error)
do i=1,mmd
do j=1,n
do jd=1,n
do l=1,nd
yxh313(i,j,jd,l)=f33(i,j,jd)
end do
end do
end do
end do
call mim(x32,h23,f33,r,k,tbn3,tbn4,w,lw,mmd,n,md,xtemp1,
      1 ytemp1,ytemp2,xijkdd,eps)
call imm(q13,f33,y1323,beta,r,k,tbn3,tbn4,w,lw,mmd,n,md,
      1 xtemp1,ytemp1,ytemp2,xijkdd,xijkd,tmp,ans,error)
call imm(q23,f33,y2323,beta,r,k,tbn3,tbn4,w,lw,mmd,n,md,
      1 xtemp1,ytemp1,ytemp2,xijkdd,xijkd,tmp,ans,error)
do i=1,mmd
do j=1,n
do jd=1,n
do l=1,nd
yxh323(i,j,jd,l)=f33(i,j,jd)
end do
end do
end do
end do
c-----
do i=1,mmd
do j=1,n
do jd=1,n
do l=1,nd
t33(i,j,jd,l)=t33(i,j,jd,l)+(c1*yxh313(i,j,jd,l))+
      1 (c2*yxh323(i,j,jd,l))+(c3*tp*yxh333(i,j,jd,l))

```

```

end do
end do
end do
end do
c-----
call xint2(yxh333,alpha,mmd,n,nd,f33,xx,ans,error,a1)
call imm(q13,f33,y1333,beta,r,k,tbn3,tbn4,w,lw,mmd,n,md,
1 xtemp1,ytemp1,ytemp2,xijkdd,xijkd,tmp,ans,error)
call imm(q23,f33,y2333,beta,r,k,tbn3,tbn4,w,lw,mmd,n,md,
1 xtemp1,ytemp1,ytemp2,xijkdd,xijkd,tmp,ans,error)
c-----
do i=1,mmd
do j=1,n
temp1=(c3*c1*fps*y1313(i,j))+(c3*c2*fps*
1 y1323(i,j))+(c3*c3*fps*y1333(i,j))
tao13=qx13(i,j)+temp1
if(r(i).le.(r1+r3)) then
h13(i,j)=-1.0
else
h13(i,j)=dexp(q13(i,j)+tao13)-1.0d0
end if
x13(i,j)=h13(i,j)-q13(i,j)-tao13
temp1=(c3*c1*fps*y2313(i,j))+(c3*c2*fps*
1 y2323(i,j))+(c3*c3*fps*y2333(i,j))
tao23=qx23(i,j)+temp1
if(r(i).le.(r2+r3)) then
h23(i,j)=-1.0
else
h23(i,j)=dexp(q23(i,j)+tao23)-1.0d0
end if
x23(i,j)=h23(i,j)-q23(i,j)-tao23
end do
end do
do i=1,mmd
do j=1,n
temp1=(c1*yxh311(i,j))+(c2*yxh321(i,j))+(c3*tp*yxh331(i,j))

```

```

temp3=(c1*c1*y3111(i,j))+(c1*c2*y3121(i,j))+(c1*c3*tp*
1  y3131(i,j))+(c2*c1*y3211(i,j))+(c2*c2*y3221(i,j))+
1  (c2*c3*tp*y3231(i,j))+(c3*c1*fps*y3311(i,j))+(c3*c2*fps*
1  y3321(i,j))+(c3*c3*fps*y3331(i,j))
tao31=temp1+qx31(i,j)+temp3
if(r(i).le.(r1+r3)) then
h31(i,j)=-1.0
else
h31(i,j)=dexp(q31(i,j)+tao31)-1.0d0
end if
x31(i,j)=h31(i,j)-q31(i,j)-tao31
end do
end do
do i=1,mmd
do j=1,n
temp1=(c1*yxh312(i,j))+(c2*yxh322(i,j))+(c3*tp*yxh332(i,j))
temp3=(c1*c1*y3112(i,j))+(c1*c2*y3122(i,j))+(c1*c3*tp*
1  y3132(i,j))+(c2*c1*y3212(i,j))+(c2*c2*y3222(i,j))+
1  (c2*c3*tp*y3232(i,j))+(c3*c1*fps*y3312(i,j))+(c3*c2*fps*
1  y3322(i,j))+(c3*c3*fps*y3332(i,j))
tao32=temp1+qx32(i,j)+temp3
if(r(i).le.(r2+r3)) then
h32(i,j)=-1.0
else
h32(i,j)=dexp(q32(i,j)+tao32)-1.0d0
end if
x32(i,j)=h32(i,j)-q32(i,j)-tao32
end do
end do
c-----
call mim(q31,yxh113,y3113,r,k,tbn3,tbn4,w,lw,mmd,n,md,xtemp1,
1  ytemp1,ytemp2,xijkdd,eps)
call mim(q31,yxh123,y3123,r,k,tbn3,tbn4,w,lw,mmd,n,md,xtemp1,
1  ytemp1,ytemp2,xijkdd,eps)
call mim(q31,yxh133,y3133,r,k,tbn3,tbn4,w,lw,mmd,n,md,xtemp1,
1  ytemp1,ytemp2,xijkdd,eps)

```

```

call mim(q32,yxh213,y3213,r,k,tbn3,tbn4,w,lw,mmd,n,md,xtemp1,
1 ytemp1,ytemp2,xijkdd,eps)
call mim(q32,yxh223,y3223,r,k,tbn3,tbn4,w,lw,mmd,n,md,xtemp1,
1 ytemp1,ytemp2,xijkdd,eps)
call mim(q32,yxh233,y3233,r,k,tbn3,tbn4,w,lw,mmd,n,md,xtemp1,
1 ytemp1,ytemp2,xijkdd,eps)
call mmm(q33,yxh313,y3313,beta,r,k,tbn3,tbn4,w,lw,w1,lw1,mmd,
1 n,md,nd,xtemp1,ytemp1,ytemp2,xtmp1,ytmp1,xtmp2,ytmp2,
1 xtmp3,ytmp3,x1,x2,y1,tmp,ans,error,alpha)
call mmm(q33,yxh323,y3323,beta,r,k,tbn3,tbn4,w,lw,w1,lw1,mmd,
1 n,md,nd,xtemp1,ytemp1,ytemp2,xtmp1,ytmp1,xtmp2,ytmp2,
1 xtmp3,ytmp3,x1,x2,y1,tmp,ans,error,alpha)
call mmm(q33,yxh333,y3333,beta,r,k,tbn3,tbn4,w,lw,w1,lw1,mmd,
1 n,md,nd,xtemp1,ytemp1,ytemp2,xtmp1,ytmp1,xtmp2,ytmp2,
1 xtmp3,ytmp3,x1,x2,y1,tmp,ans,error,alpha)
c-----
c call flush(34)
do i=1,mmd
do j=1,n
do jd=1,n
do l=1,nd
temp3=(c1*c1*y3113(i,j,jd))+(c1*c2*y3123(i,j,jd))+
1 (c1*c3*tp*y3133(i,j,jd))+(c2*c1*y3213(i,j,jd))+
1 (c2*c2*y3223(i,j,jd))+(c2*c3*tp*y3233(i,j,jd))+
1 (c3*c1*tp*y3313(i,j,jd,l))+(c3*c2*tp*y3323(i,j,jd,l))+
1 (c3*c3*fps*y3333(i,j,jd,l))
t33(i,j,jd,l)=t33(i,j,jd,l)+temp3
if(r(i).le.(2.0*r3)) then
h33(i,j,jd,l)=-1.0
else
h33(i,j,jd,l)=dexp(q33(i,j,jd,l)+t33(i,j,jd,l))-1.0d0
end if
x33(i,j,jd,l)=h33(i,j,jd,l)-q33(i,j,jd,l)-t33(i,j,jd,l)
end do
end do
end do

```

```

xtmpr1(1)=h33(i,j,jd,1)
end do
ifail=1
call d01gaf(alpha,xtmpr1,nd,f33(i,j,jd),error,ifail)
f33(i,j,jd)=f33(i,j,jd)/(4.0*pi)
tmp(jd)=f33(i,j,jd)*sin(beta(jd))
end do
ifail=1
call d01gaf(beta,tmp,n,yxijkd(i,j),error,ifail)
yxijkd(i,j)=yxijkd(i,j)*0.5
tmp(j)=yxijkd(i,j)*sin(beta(j))
end do
ifail=1
call d01gaf(beta,tmp,n,h33d(i),error,ifail)
h33d(i)=h33d(i)*0.5
end if
end do
C*****
C CALCULATION OF g-THE CORRELATION FUNCTION
C*****
do i=1,mmd
g11(i)=h11(i)+1.0
g12(i)=h12(i)+1.0
g13(i)=h13d(i)+1.0
g21(i)=h21(i)+1.0
g22(i)=h22(i)+1.0
g23(i)=h23d(i)+1.0
g31(i)=h31d(i)+1.0
g32(i)=h32d(i)+1.0
g33(i)=h33d(i)+1.0
end do
do i=1,mmd
if(g13(i).ne.0.0)then
rr(i)=r(i)/r3
write(34,1)rr(i),g13(i)
else

```



```

continue
end if
end do
write(34,*)'-----'
do i=1,mmd
if(g23(i).ne.0.0)then
rr(i)=r(i)/r3
write(34,1)rr(i),g23(i)
else
continue
end if
end do
write(34,*)'-----'
do i=1,mmd
if(g33(i).ne.0.0)then
rr(i)=r(i)/r3
write(34,1)rr(i),g33(i)
else
continue
end if
end do
write(34,*)'-----'
btime = CPU TIME(btzero)
write(34,*)btime,btzero
c-----
1 format(f12.8,3x,f12.8)
stop
end
c -----
c*****
c SUBROUTINE TO INTEGRATE x33 OVER THE ANGLE (alpha1-alpha2)
c BETWEEN -2pi TO 0.
c*****
subroutine xint1(x33,alpha,mmd,n,nd,f33,xx,ans,error,al)
double precision x33(mmd,n,n,nd),alpha(nd),f33(mmd,n,n),
1 xx(nd/2),ans,error,al(nd)

```

```

integer i,j,jd,l,mmd,n,nd,ifail
do i=1,mmd
do j=1,n
do jd=1,n
do l=1,nd/2
xx(l)=x33(i,j,jd,l)
al(l)=alpha(l)
end do
ifail=1
call d01gaf(al,xx,nd/2,f33(i,j,jd),error,ifail)
end do
end do
end do
return
end

c -----
c*****
c SUBROUTINE TO INTEGRATE x33 OVER THE ANGLE (alpha1-alpha2)
c BETWEEN 0 TO 2pi.
c*****
subroutine xint2(x33,alpha,mmd,n,nd,f33,xx,ans,error,al)
double precision x33(mmd,n,n,nd),alpha(nd),f33(mmd,n,n),
1 xx(nd/2),ans,error,al(nd)
integer i,j,jd,l,mmd,n,nd,ifail
do i=1,mmd
do j=1,n
do jd=1,n
do l=1,nd/2
xx(l)=x33(i,j,jd,(nd/2+1))
al(l)=alpha(nd/2+1)
end do
ifail=1
call d01gaf(al,xx,nd/2,ans,error,ifail)
f33(i,j,jd)=ans
end do
end do

```

```

end do
return
end

c -----
c*****
c SUBROUTINE TO CALCULATE THE CONVOLUTION INTEGRAL WITH
c ion-ion-ion INTERACTION.
c*****
subroutine iii(xij,xjk,xijk,yxij,yxjk,r,k,tbn3,tbn4,md,mmd
1 ,w,lw,xtempl,eps)
integer i,md,mmd,lw
double precision xij(mmd),xjk(mmd),xijk(md),yxij(md),yxjk(md)
1 ,tbn3,tbn4,w(lw),xtempl(md),r(mmd+1),k(mmd+1)
do i=1,mmd
yxij(i)=xij(i)
end do
do i=1,mmd
yxjk(i)=xjk(i)
end do
call fft(r,k,tbn3,xtempl,yxij,md,mmd,w,lw)
call fft(r,k,tbn3,xtempl,yxjk,md,mmd,w,lw)
call bft(yxij,yxjk,r,k,tbn4,xtempl,xijk,md,mmd,w,lw)
do i=1,md
xijk(i)=xijk(i)*eps
end do
return
end

c -----
c*****
c SUBROUTINE TO CALCULATE THE CONVOLUTION INTEGRAL WITH
c ion-macroion-ion INTERACTION.
c*****
subroutine imi(xij,xjk,yxijk,beta,r,k,tbn3,tbn4,w,lw,mmd,n,md,
1 xtempl,ytempl,ytemp2,xijkdd,yxijkd,tmp,ans,error)
integer i,j,mmd,n,md,lw,ifail
double precision xij(mmd,n),xjk(mmd,n),r(mmd),k(mmd),w(lw)

```

```

      1 ,beta(n),yxijk(mmd),tbn3,tbn4
double precision xtempl(md),ytempl(md),ytemp2(md),xijkdd(md),
      1 yxijkd(mmd,n),tmp(n),ans,error
do j=1,n
do i=1,mmd
ytempl(i)=xij(i,j)
end do
call fft(r,k,tbn3,xtempl,ytempl,md,mmd,w,lw)
do i=1,mmd
ytemp2(i)=xjk(i,j)
end do
call fft(r,k,tbn3,xtempl,ytemp2,md,mmd,w,lw)
call bft(ytempl,ytemp2,r,k,tbn4,xtempl,xijkdd,md,mmd,w,lw)
do i=1,mmd
yxijkd(i,j)=xijkdd(i)
end do
end do
do i=1,mmd
do j=1,n
tmp(j)=yxijkd(i,j)*sin(beta(j))
end do
ifail=1
call d01gaf(beta,tmp,n,ans,error,ifail)
yxijk(i)=ans
end do
return
end

```

```

C -----
C*****
C SUBROUTINE TO CALCULATE THE CONVOLUTION INTEGRAL WITH
C ion-ion-macroion INTERACTION.
C*****
subroutine iim(x1,x2,yxijk,r,k,tbn3,tbn4,w,lw,mmd,n,md,
      1 xtempl,ytempl,ytemp2,xijkdd,eps)
integer i,j,mmd,n,lw,md
double precision x1(mmd,n),x2(mmd),yxijk(mmd,n),r(mmd),k(mmd)

```

```

      1 ,w(lw),tbn3,tbn4,xijkdd(md)
double precision xtemp1(md),ytemp1(md),ytemp2(md)
do i=1,mmd
ytemp2(i)=x2(i)
end do
call fft(r,k,tbn3,xtemp1,ytemp2,md,mmd,w,lw)
do j=1,n
do i=1,mmd
ytemp1(i)=x1(i,j)
end do
call fft(r,k,tbn3,xtemp1,ytemp1,md,mmd,w,lw)
call bft(ytemp2,ytemp1,r,k,tbn4,xtemp1,xijkdd,md,mmd,w,lw)
do i=1,mmd
yxijk(i,j)=xijkdd(i)*eps
end do
end do
return
end

c -----
c *****
c SUBROUTINE TO CALCULATE THE CONVOLUTION INTEGRAL WITH
c ion-macroion-macroion INTERACTION.
c *****
subroutine imm(xij,xjk,xijk,beta,r,k,tbn3,tbn4,w,lw,mmd,n,md,
      1 xtemp1,ytemp1,ytemp2,xijkdd,xijkd,tmp,ans,error)
integer i,j,kk,mmd,n,md,lw,ifail
double precision xij(mmd,n),xjk(mmd,n,n),beta(n),r(mmd),k(mmd)
      1 ,tbn3,tbn4,w(lw),xijk(mmd,n),xtemp1(md),ytemp1(md),
      1 ytemp2(md),xijkd(mmd,n,n),tmp(n),ans,error,xijkdd(md)
do kk=1,n
do j=1,n
do i=1,mmd
ytemp1(i)=xij(i,j)
end do
call fft(r,k,tbn3,xtemp1,ytemp1,md,mmd,w,lw)
do i=1,mmd

```

```

ytemp2(i)=xjk(i,j,kk)
end do
call fft(r,k,tbn3,xtemp1,ytemp2,md,mmd,w,lw)
call bft(ytemp2,ytemp1,r,k,tbn4,xtemp1,xijkdd,md,mmd,w,lw)
do i=1,mmd
xijkd(i,j,kk)=xijkdd(i)
end do
end do
end do
do i=1,mmd
do kk=1,n
do j=1,n
tmp(j)=xijkd(i,j,kk)*sin(beta(j))
end do
ifail=1
call d0lgaf(beta,tmp,n,ans,error,ifail)
xijk(i,kk)=ans
end do
end do
return
end

```

```

c -----
c*****
c SUBROUTINE TO CALCULATE THE CONVOLUTION INTEGRAL WITH
c macroion-ion-macroion INTERACTION.
c*****
subroutine mim(xij,xjk,xijk,r,k,tbn3,tbn4,w,lw,mmd,n,md,xtemp1,
1 ytemp1,ytemp2,xijkdd,eps)
integer i,j,jd,mmd,n,lw,md
double precision xij(mmd,n),xjk(mmd,n),xijk(mmd,n,n),r(mmd),
1 k(mmd),w(lw),tbn3,tbn4,xtemp1(md),ytemp1(md),ytemp2(md),
1 xijkdd(md)
do j=1,n
do i=1,mmd
ytemp1(i)=xij(i,j)
end do

```

```

call fft(r,k,tbn3,xtemp1,ytemp1,md,mmd,w,lw)
do jd=1,n
do i=1,mmd
ytemp2(i)=xjk(i,jd)
end do
call fft(r,k,tbn3,xtemp1,ytemp2,md,mmd,w,lw)
call bft(ytemp2,ytemp1,r,k,tbn4,xtemp1,xijkdd,md,mmd,w,lw)
do i=1,mmd
xijk(i,j,jd)=xijkdd(i)*eps
end do
end do
end do
return
end

c -----
c*****
c SUBROUTINE TO CALCULATE THE CONVOLUTION INTEGRAL WITH
c macroion-macroion-macroion INTERACTION.
c*****
subroutine mmm(xij,xjk,xijk,beta,r,k,tbn3,tbn4,w,lw,w1,lw1,mmd,
1 n,md,nd,xtemp1,ytemp1,ytemp2,xtmpr1,ytmpr1,xtmpr2,ytmpr2,
1 xtmpr3,ytmpr3,x1,x2,y1,tmp,ans,error,alpha)
integer ndim
parameter(ndim=1)
integer ndfn(ndim),nfn,i,j,jd,jdd,l,lw,lw1,mmd,md,n,nd,ifail
double precision xij(mmd,n,n,nd),xjk(mmd,n,n,nd),xijk(mmd,n,n,
1 nd),beta(n),r(mmd),k(mmd),tbn3,tbn4,w(lw),w1(lw1),xtemp1(md),
1 y1(mmd,n,n,nd),ytemp1(md),ytemp2(md),x1(mmd,nd),x2(mmd,nd),
1 xtmpr1(nd),ytmpr1(nd),xtmpr2(nd),ytmpr2(nd)
1 ,xtmpr3(nd),ytmpr3(nd),tmp(n),ans,error
do j=1,n
do jd=1,n
do l=1,nd
do i=1,mmd
ytemp1(i)=xij(i,j,jd,l)
end do

```

```

        end do
    end do
end do
return
end
c -----
c*****
c SUBROUTINE TO CALCULATE FORWARD FOURIER TRANSFORM
c*****
subroutine fft(r,k,tbn3,xfn,yfn,md,mmd,w,lw)
integer md,mmd,lw,i
double precision r(mmd),xfn(md),yfn(md),k(mmd),w(lw),tbn3
    1 ,ans,error
do i=1,mmd
yfn(i)=yfn(i)*r(i)
end do
call sine(md,mmd,w,lw,xfn,yfn,tbn3)
yfn(1)=0.0
do i=2,mmd
yfn(i)=yfn(i)*(2.0/k(i))
end do
return
end
c -----
c*****
c SUBROUTINE TO CALCULATE BACKWARD FOURIER TRANSFORM OF THE
c PRODUCT OF x AND y.
c*****
subroutine bft(x,y,r,k,tbn4,xfn,yfn,md,mmd,w,lw)
integer md,mmd,lw,i
double precision x(mmd),r(mmd),xfn(md),yfn(md),k(mmd)
double precision w(lw),tbn4,y(mmd)
do i=1,mmd
yfn(i)=x(i)*y(i)*k(i)
end do
call sine(md,mmd,w,lw,xfn,yfn,tbn4)

```



```

do i=1,mmd
yfn(i)=yfn(i)*(2.0/r(i))
end do
return
end

c -----
c*****
c SUBROUTINE TO CALCULATE THE SINE TRANSFORM
c*****
subroutine sine(m,mm,work,lwork,xfn,yfn,tbn)
integer ndim,m,mm,i,lwork
parameter(ndim=1)
integer ndfn(ndim),nfn,ifail,mmm
double precision xfn(m),yfn(m),work(lwork),tbn
mmm=mm+1
do i=1,mm
xfn(i)=yfn(i)
yfn(i)=0.0
end do
xfn(mmm)=0.0
do i=mmm,m
xfn(i)=-xfn(m+2-i)
yfn(i)=0.0
end do
ndfn(1)=m
nfn=ndfn(1)
ifail=0
call c06fjf(ndim,ndfn,nfn,xfn,yfn,work,lwork,ifail)
do i=1,m
yfn(i)=-0.5*yfn(i)*tbn*sqrt(dfloat(m))
end do
return
end
c-----

```

```

      do l=1,nd
        xtmpr3(l)=(xtmpr1(l)*xtmpr2(l))-(ytmpr1(l)*ytmpr2(l))
        ytmpr3(l)=(xtmpr1(l)*ytmpr2(l))+(ytmpr1(l)*xtmpr2(l))
      end do
      ndfn(1)=nd
      nfn=ndfn(1)
      ifail=0
      call c06gcf(ytmpr3,nfn,ifail)
      call c06fjf(ndim,ndfn,nfn,xtmpr3,ytmpr3,w1,lw1,ifail)
      call c06gcf(ytmpr3,nfn,ifail)
      do l=1,nd
        y1(i,jd,jdd,l)=xtmpr3(l)
      end do
    end do
  end do
  do l=1,nd
    do jdd=1,n
      do i=1,mmd
        ytemp1(i)=y1(i,jd,jdd,l)
      end do
      call fft(k,r,tbn4,xtemp1,ytemp1,md,mmd,w,lw)
      do i=1,mmd
        y1(i,jd,jdd,l)=ytemp1(i)
      end do
    end do
  end do
  end do
  end do
  do l=1,nd
    do jdd=1,n
      do i=1,mmd
        do jd=1,n
          tmp(jd)=y1(i,jd,jdd,l)*sin(beta(jd))
        end do
        ifail=1
        call d01gaf(beta,tmp,n,xijk(i,j,jdd,l),error,ifail)
      end do
    end do
  end do

```

$$- \rho_+ \rho_- \rho_m z_+^2 z_-^2 z_m^2 \frac{\delta}{t^2} \lambda \tilde{g}'_{+m} \lambda \tilde{g}'_{m+} - \rho_+ \rho_m z_+^2 z_m^2 \lambda \tilde{g}'_{+m} \lambda \tilde{g}'_{m+}$$

$\rho_{ij} \longrightarrow ij$  element of the transposed cofactor matrix

$$\begin{aligned} \rho_{11} = 1 + \rho_- z_-^2 \frac{\delta}{t^2} + \rho_m z_m^2 \lambda \tilde{g}'_{mm} + \rho_- \rho_m z_-^2 z_m^2 \frac{\delta}{t^2} \lambda \tilde{g}'_{mm} \\ - \rho_- \rho_m z_-^2 z_m^2 \lambda \tilde{g}'_{m-} \lambda \tilde{g}'_{-m} . \end{aligned}$$

$$\rho_{12} = -\rho_+ z_+^2 \frac{\delta}{t^2} - \rho_+ \rho_m z_+^2 z_m^2 \frac{\delta}{t^2} \lambda \tilde{g}'_{mm} + \rho_+ \rho_m z_+^2 z_m^2 \lambda \tilde{g}'_{m-} \lambda \tilde{g}'_{m+}$$

$$\rho_{13} = -\rho_+ z_+^2 \lambda \tilde{g}'_{+m} + \rho_+ \rho_- z_+^2 z_-^2 \frac{\delta}{t^2} \lambda \tilde{g}'_{-m} - \rho_+ \rho_- z_+^2 z_-^2 \frac{\delta}{t^2} \lambda \tilde{g}'_{+m}$$

$$\rho_{21} = -\rho_- z_-^2 \frac{\delta}{t^2} - \rho_- \rho_m z_-^2 z_m^2 \frac{\delta}{t^2} \lambda \tilde{g}'_{mm} + \rho_- \rho_m z_-^2 z_m^2 \lambda \tilde{g}'_{m-} \lambda \tilde{g}'_{m+}$$

$$\begin{aligned} \rho_{22} = 1 + \rho_+ z_+^2 \frac{\delta}{t^2} + \rho_m z_m^2 \lambda \tilde{g}'_{mm} + \rho_+ \rho_m z_+^2 z_m^2 \frac{\delta}{t^2} \lambda \tilde{g}'_{mm} \\ - \rho_+ \rho_m z_+^2 z_m^2 \lambda \tilde{g}'_{m+} \lambda \tilde{g}'_{+m} \end{aligned}$$

$$\rho_{23} = -\rho_- z_-^2 \frac{\delta}{t^2} - \rho_+ \rho_- z_+^2 z_-^2 \frac{\delta}{t^2} \lambda \tilde{g}'_{-m} + \rho_+ \rho_- z_+^2 z_-^2 \frac{\delta}{t^2} \lambda \tilde{g}'_{+m}$$

$$\rho_{31} = -\rho_m z_m^2 \lambda \tilde{g}'_{m+} + \rho_- \rho_m z_-^2 z_m^2 \frac{\delta}{t^2} \lambda \tilde{g}'_{m-} - \rho_- \rho_m z_-^2 z_m^2 \frac{\delta}{t^2} \lambda \tilde{g}'_{m+}$$

$$\rho_{32} = -\rho_m z_m^2 \lambda \tilde{g}'_{m-} + \rho_+ \rho_m z_+^2 z_m^2 \frac{\delta}{t^2} \lambda \tilde{g}'_{m-} + \rho_+ \rho_m z_+^2 z_m^2 \frac{\delta}{t^2} \lambda \tilde{g}'_{m+}$$

$$\rho_{33} = 1 + \rho_+ z_+^2 \frac{\delta}{t^2} + \rho_- z_-^2 \frac{\delta}{t^2}$$

$$\therefore (-\lambda H') \left[ I - Z' (-\lambda H') \right]^{-1}$$

## REFERENCES

1. Hill, T.L., Statistical Mechanics, McGraw Hill Book Company, 1956.
2. Friedman, H.L., Ionic Solution Theory, Wiley Interscience, 1962.
3. Mayer, J.E. and Montroll, E., J. Chem. Phys., 9, 2-16, 1941.
4. Meeron, E., J. Chem. Phys., 27, 1238-46, 1957.
5. McMillan, W.G. and Mayer, J.E., J. Chem. Phys., 13, 276-305, 1945.
6. Mayer, J.E., J. Chem. Phys., 18, 1426-36, 1950.
7. Meeron, E., J. Chem. Phys., 28, 630-643, 1958.
8. Meeron, E., Physics of Fluids, 1, 139-149, 1958.
9. Meeron, E. and Rodemich, E.R., Physics of Fluids 1, 246-250, 1958.
10. Meeron, E., J. Math. Phys. 1, 192-201, 1960.
11. Van Leeuwen, J.M.J., Groeneveld and de Boer, J., Physica, 25, 792-808, 1959.
12. Alnatt, A.R., Mol. Phys. 8, 533-539, 1964.
13. Meeron, E., Physica 26, 445, 1960
14. Rasaiah, J.C. and Friedman, H.L., J. Chem. Phys. 48, 2742-2752, 1968.
15. Jepsen, D.W. and Friedman, H.L., J. Chem. Phys., 38, 846-864, 1963.
16. Dennery, P. and Krzywicki, A. Mathematics for Physicists, Harper and Row, 1967 (Chapter 1, Section 26).

Let  $f_{12}$  be a pairwise invariant function and a function of the variables  $r_{12}$ ,  $S \rightarrow 1$ ,  $S \rightarrow 2$ ,  $S \rightarrow r_{12}$ . Its orthogonal expansion in terms of the complete orthogonal set of D functions is given by

$$f_{12}(r_{12}, S \rightarrow 1, S \rightarrow 2, S \rightarrow r_{12})$$

$$= \sum_{\substack{l_1, l_2, l \\ m_1, m_2 \\ n_1, n_2, n}} \bar{F}_{12} \begin{pmatrix} l_1 & l_2 & l \\ m_1 & m_2 & r_{12} \\ n_1 & n_2 & n \end{pmatrix} D_{m_1 n_1}^{l_1}(S \rightarrow 1) D_{m_2 n_2}^{l_2}(S \rightarrow 2) D_{on}^l(S \rightarrow r_{12}) \quad (22)$$

$\bar{F}_{12}$  : A partial transform of  $f_{12}$

$l_1, l_2, l, m_1, m_2, n_1, n_2$ , and  $n$  are the conjugate variables of the Euler angle of rotation  $S \rightarrow r_{12}$

$m = 0$ : the  $\gamma$  angle of  $S \rightarrow r_{12}$  rotation has no effect on  $f_{12}$ .

The  $\alpha$  and  $\beta$  angles correspond to the azimuthal and polar angles of  $r_{12}$  in coordinate system  $S$ .

With the help of eqn.(8), eqn.(22) is written as

$$f_{12} = \sum_{\substack{l_1, l_2, l \\ m_1, m_2 \\ n_1, n_2}} \bar{F}_{12} \begin{pmatrix} l_1 & l_2 & l \\ m_1 & m_2 & r_{12} \\ n_1 & n_2 & n \end{pmatrix} \left\{ \sum_S D_{m_1 s_1}^{l_1}(T \rightarrow 1) D_{s_1 n_1}^{l_1}(S \rightarrow T) \right\} \\ \left\{ \sum_{S_2} D_{m_2 s_2}^{l_2}(T \rightarrow 2) D_{s_2 n_2}^{l_2}(S \rightarrow T) \right\}, \left\{ \sum_S D_{os}^l(T \rightarrow r_{12}) D_{sn}^l(S \rightarrow T) \right\},$$

$$r = |\vec{r}|, t = |\vec{t}|, j_1(rt) \text{ is the spherical Bessel function}$$

$$d\vec{r} = \frac{1}{2\pi} r^2 dr d(L \longrightarrow r) \quad (46)$$

From equations (8) and (5), we get the identity

$$D_{00}^1(r \longrightarrow t) = \sum_n D_{0n}^1(L \longrightarrow t) D_{0n}^{1*}(L \longrightarrow r) \quad (47)$$

With the help of equations (44,45,46,47) and equation (9), equation (43) is integrated to give

$$\tilde{F}_{12} \left( \begin{array}{cccc} l_1 & l_2 & t & L \longrightarrow t \\ m_1 & m_2 & n_1 & n_2 \end{array} \right)$$

$$= (-)^{n_1} \sum_{l,n} \left[ \begin{array}{ccc} l_1 & l_2 & l \\ -n_1 & n_2 & n \end{array} \right] D_{0n}^1(L \longrightarrow t) f_{12}^\dagger \left( \begin{array}{ccc} l_1 & l_2 & l \\ m_1 & m_2 & t \end{array} \right) \quad (48)$$

where

$$f_{12}^\dagger \left( \begin{array}{ccc} l_1 & l_2 & l \\ m_1 & m_2 & t \end{array} \right) = \frac{32 \pi^3 (-i)^l}{[(2l_1+1)(2l_2+1)]^{1/2}} \int_0^\infty \tilde{f}_{12} \left( \begin{array}{ccc} l_1 & l_2 & l \\ m_1 & m_2 & r \end{array} \right) j_1(rt) r^2 dr \quad (49)$$

Derivation of equation (48) is shown below. With the help of equation (43), (44), (45), we carry out the following steps to get equation (48),

$$\tilde{F}_{12} = \frac{[(2l_1+1)(2l_2+1)]^{1/2}}{8\pi^2} \int_{\text{cube}} f_{12} e^{-i\vec{t} \cdot \vec{r}} D_{m_1 n_1}^{l_1}(L \longrightarrow 1) D_{m_2 n_2}^{l_2*}(L \longrightarrow 2) \\ \times d(L \longrightarrow 1) d(L \longrightarrow 2) dr$$

$$= \frac{[(2l_1+1)(2l_2+1)]^{1/2}}{8\pi^2} \sum_l \int f_{12} (-i)^l (2l+1) j_1(rt) D_{00}^l(r \longrightarrow t) D_{m_1 n_1}^{l_1}(L \longrightarrow 1) \\ \times D_{m_2 n_2}^{l_2*}(L \longrightarrow 2) d(L \longrightarrow 1) d(L \longrightarrow 2) d(L \longrightarrow r) r^2 dr / 2\pi$$

distributions overlap. Because of this we can eliminate the convergence difficulties occurring in the cluster integral.

- (ii) The other is the remainder  $u_{12}^* = u_{12} - u_{12}^C$  of the total potential. This is predominant at small separation and is of the nature of short range.

$$\text{Hence } \gamma_{12} = \exp(-\beta (u_{12}^* + u_{12}^C)) - 1 \quad (65)$$

$$\begin{aligned} &= \exp(-\beta u_{12}^*) \exp(-\beta u_{12}^C) - 1 \\ &= (1+k_{12}) (1 + (-\beta u_{12}^C) + \frac{1}{2!}(-\beta u_{12}^C)^2 + \dots) - 1 \\ &= (1+k_{12}) (1 + g_{12} + \frac{1}{2!} g_{12}^2 + \dots) - 1 \\ &= (1+k_{12}) + (1 + k_{12}) \sum_{n \geq 1} g_{12}^n / n! - 1 \end{aligned}$$

$$= k_{12} + (1 + k_{12}) \sum_{n \geq 1} \frac{g_{12}^n}{n!} \quad (66)$$

where,

$$k_{12} = \exp(-\beta u_{12}^*) - 1 \quad (67)$$

$$g_{12} = -\beta u_{12}^C \quad (68)$$

In Mayer's procedure of summation, g-bond chains of all length between two particles are summed which gives the  $q(g)$  bonds. The parallel combination of  $q(g)$  bonds with or without  $k_{12}$  bonds are further summed to sum over the infinite set of graphs and this summation is necessary for calculation of potential of average force and other properties. These properties can also be calculated from the results of graph summation with the help of hypernetted chain approximation. This requires analytical evaluation of various  $q$ -bonds that occur in the given problem. This is illustrated below:

For two fixed charge distribution on molecules 1 and 2, expansion of the half transform of potential of interaction is

$$= \left( \begin{array}{c|c} \left[ 1 - \tilde{h}_{00} (c_+ q_+^2 + c_- q_-^2 + c_m q_m^2) \right] & (-\tilde{h}_{01} (c_+ q_+^2 + c_- q_-^2 + c_m q_m^2)) \\ \hline -c_m \mu_m^2 \tilde{h}_{10} & 1 - c_m \mu_m^2 \tilde{h}_{11} \end{array} \right)$$

$$= \left( \begin{array}{cc} 1 - \tilde{h}_{00} (\sum_i c_i q_i^2) & -\tilde{h}_{01} (\sum_i c_i q_i^2) \\ -\tilde{h}_{10} c_m \mu_m^2 & 1 - c_m \mu_m^2 \tilde{h}_{11} \end{array} \right) \quad (97)$$

For  $n = 0$ , the values for  $\tilde{h}$ 's are taken from the Appendix and

$$(I - C_+ M_+ H - C_- M_- H - C_m M_m H)$$

$$= \left( \begin{array}{c|c} 1 + \frac{x a_{00} j_{-1}(a_{00} t)}{t} (\sum_i c_i q_i^2) & \frac{ix j_0(a_{01} t)}{\sqrt{3} t} (\sum_i c_i q_i^2) \\ \hline \frac{-ix j_0(a_{10} t)}{\sqrt{3} t} c_m \mu_m^2 & 1 + \frac{2x j_1(a_{11} t)}{3a_{11} t} c_m \mu_m^2 \end{array} \right) \quad (98)$$

where  $x = 32\pi^3/kT$

Determinant of the above matrix

$$(\det 1) = \left\{ 1 + (\sum_i c_i q_i^2) \frac{x a_{00} j_{-1}(a_{00} t)}{t} \right\} \left\{ 1 + c_m \mu_m^2 \frac{2x j_1(a_{11} t)}{3a_{11} t} \right\}$$

$$- \frac{x^2 j_0(a_{10} t) j_0(a_{01} t) (\sum_i c_i q_i^2) (c_m \mu_m^2)}{3t^2} \quad (98a)$$

$$\therefore (I - C_+ M_+ H - C_- M_- H - C_m M_m H)^{-1}$$

$$= (\det 1)^{-1} \left( \begin{array}{cc} 1 + c_m \mu_m^2 \frac{2x j_1(a_{11} t)}{3a_{11} t} & - (\sum_i c_i q_i^2) \frac{ix j_0(a_{10} t)}{\sqrt{3} t} \\ c_m \mu_m^2 \frac{ix j_0(a_{01} t)}{\sqrt{3} t} & 1 + \frac{(\sum_i c_i q_i^2) x a_{00} j_{-1}(a_{00} t)}{t} \end{array} \right)$$



$$= \frac{-3}{16\pi^4} \times q_m \mu_m \left[ \frac{1}{r_{mm}^2} \int_0^\infty P \sin(r_{mm}t) dt - \frac{1}{r_{mm}} \int_0^\infty P t \cos(r_{mm}t) dt \right]$$

$$\bar{q}_{mm} \begin{pmatrix} 1 & 0 & 1 \\ 0 & 0 & r_{mm} \end{pmatrix}$$

$$= \frac{3}{16\pi^4} \times q_m \mu_m \times \left[ \frac{1}{r_{mm}^2} \int_0^\infty P \sin(r_{mm}t) dt - \frac{1}{r_{mm}} \int_0^\infty P t \cos(r_{mm}t) dt \right]$$

$$\bar{q}_{mm} \begin{pmatrix} 1 & 1 & 2 \\ 0 & 0 & r_{mm} \end{pmatrix}$$

$$= \frac{(i)^2 (3)^{1/2} (3)^{1/2} 5}{16\pi^4} \left[ (-)^0 \begin{bmatrix} 1 & 1 & 2 \\ 0 & 0 & 0 \end{bmatrix}_{3j} \int_0^\infty \tilde{q}_{mm} \begin{pmatrix} 1 & 1 & t \\ 0 & 0 & 0 \end{pmatrix} j_2(r_{mm}t) t^2 dt \right.$$

$$+ (-)^1 \begin{bmatrix} 1 & 1 & 2 \\ -1 & 1 & 0 \end{bmatrix}_{3j} \int_0^\infty \tilde{q}_{mm} \begin{pmatrix} 1 & 1 & t \\ 0 & 0 & 1 \end{pmatrix} j_2(r_{mm}t) t^2 dt$$

$$+ (-)^1 \begin{bmatrix} 1 & 1 & 2 \\ 1 & -1 & 0 \end{bmatrix}_{3j} \int_0^\infty \tilde{q}_{mm} \begin{pmatrix} 1 & 1 & t \\ 0 & 0 & -1 \end{pmatrix} j_2(r_{mm}t) t^2 dt \left. \right]$$

$$= - \frac{15}{16\pi^4} \left[ \left( \frac{2}{15} \right)^{1/2} \mu_m^2 \int_0^\infty P_{22}(n=0) \left( \frac{3 \sin(r_{mm}t)}{r_{mm}^3 t^3} - \frac{\sin(r_{mm}t)}{r_{mm}t} \right. \right.$$

$$- \left. \frac{3 \cos(r_{mm}t)}{r_{mm}^2 t^2} \right) t^2 dt - \left( \frac{1}{30} \right)^{1/2} \mu_m^2 \int_0^\infty P_{22}(n=1) \left( \frac{3 \sin(r_{mm}t)}{r_{mm}^3 t^3} - \frac{\sin(r_{mm}t)}{r_{mm}t} \right.$$

$$- \left. \frac{3 \cos(r_{mm}t)}{r_{mm}^2 t^2} \right) t^2 dt - \left( \frac{1}{30} \right)^{1/2} \mu_m^2 \int_0^\infty P_{22}(n=-1) \left( \frac{3 \sin(r_{mm}t)}{r_{mm}^3 t^3} - \frac{\sin(r_{mm}t)}{r_{mm}t} \right.$$

$$- \left. \frac{3 \cos(r_{mm}t)}{r_{mm}^2 t^2} \right) t^2 dt \left. \right]$$

$$= \bar{q}_{--} \begin{pmatrix} 0 & 0 & 0 \\ 0 & 0 & r_{--} \end{pmatrix}$$

$$\begin{aligned} q_{-m} &= \bar{q}_{-m} \begin{pmatrix} 0 & 0 & 0 \\ 0 & 0 & r_{-m} \end{pmatrix} \begin{bmatrix} 0 & 0 & 0 \\ 0 & 0 & 0 \end{bmatrix}_{3j} (-)^0 D_{00}^{0*} (r_{-m} \rightarrow -) D_{00}^0 (r_{-m} \rightarrow m) \\ &+ \bar{q}_{-m} \begin{pmatrix} 0 & 0 & 0 \\ 0 & 0 & r_{-m} \end{pmatrix} \begin{bmatrix} 0 & 1 & 1 \\ 0 & 0 & 0 \end{bmatrix}_{3j} (-)^0 D_{00}^{0*} (r_{-m} \rightarrow -) D_{00}^1 (r_{-m} \rightarrow m) \\ &= \bar{q}_{-m} \begin{pmatrix} 0 & 0 & 0 \\ 0 & 0 & r_{-m} \end{pmatrix} - \frac{1}{\sqrt{3}} \bar{q}_{-m} \begin{pmatrix} 0 & 1 & 1 \\ 0 & 0 & r_{-m} \end{pmatrix} \cos \beta_1 \end{aligned}$$

$$\begin{aligned} q_{m+} &= \bar{q}_{m+} \begin{pmatrix} 0 & 0 & 0 \\ 0 & 0 & r_{m+} \end{pmatrix} \begin{bmatrix} 0 & 0 & 0 \\ 0 & 0 & 0 \end{bmatrix}_{3j} (-)^0 D_{00}^{0*} (r_{m+} \rightarrow m) D_{00}^0 (r_{m+} \rightarrow +) \\ &+ \bar{q}_{m+} \begin{pmatrix} 1 & 0 & 1 \\ 0 & 0 & r_{m+} \end{pmatrix} \begin{bmatrix} 1 & 0 & 1 \\ 0 & 0 & 0 \end{bmatrix}_{3j} (-)^0 D_{00}^{1*} (r_{m+} \rightarrow m) D_{00}^0 (r_{m+} \rightarrow +) \\ &= \bar{q}_{m+} \begin{pmatrix} 0 & 0 & 0 \\ 0 & 0 & r_{m+} \end{pmatrix} - \frac{1}{\sqrt{3}} \bar{q}_{m+} \begin{pmatrix} 1 & 0 & 1 \\ 0 & 0 & r_{m+} \end{pmatrix} \cos \beta_2 \end{aligned}$$

$$\begin{aligned} q_{m-} &= \bar{q}_{m-} \begin{pmatrix} 0 & 0 & 0 \\ 0 & 0 & r_{m-} \end{pmatrix} \begin{bmatrix} 0 & 0 & 0 \\ 0 & 0 & 0 \end{bmatrix}_{3j} (-)^0 D_{00}^{0*} (r_{m-} \rightarrow m) D_{00}^0 (r_{m-} \rightarrow -) \\ &+ \bar{q}_{m-} \begin{pmatrix} 1 & 0 & 1 \\ 0 & 0 & r_{m-} \end{pmatrix} \begin{bmatrix} 1 & 0 & 1 \\ 0 & 0 & 0 \end{bmatrix}_{3j} (-)^0 D_{00}^{1*} (r_{m-} \rightarrow m) D_{00}^0 (r_{m-} \rightarrow -) \\ &= \bar{q}_{m-} \begin{pmatrix} 0 & 0 & 0 \\ 0 & 0 & r_{m-} \end{pmatrix} - \frac{1}{\sqrt{3}} \bar{q}_{m-} \begin{pmatrix} 1 & 0 & 1 \\ 0 & 0 & r_{m-} \end{pmatrix} \cos \beta_2 \end{aligned}$$

$$\begin{aligned} q_{mm} &= \bar{q}_{mm} \begin{pmatrix} 0 & 0 & 0 \\ 0 & 0 & r_{mm} \end{pmatrix} \begin{bmatrix} 0 & 0 & 0 \\ 0 & 0 & 0 \end{bmatrix}_{3j} (-)^0 D_{00}^{0*} (r_{mm} \rightarrow m) D_{00}^0 (r_{mm} \rightarrow m) \\ &+ \bar{q}_{mm} \begin{pmatrix} 0 & 1 & 1 \\ 0 & 0 & r_{mm} \end{pmatrix} \begin{bmatrix} 0 & 1 & 1 \\ 0 & 0 & 0 \end{bmatrix}_{3j} (-)^0 D_{00}^{0*} (r_{mm} \rightarrow m) D_{00}^1 (r_{mm} \rightarrow m) \end{aligned}$$

$$= \int_0^{2\pi} \phi_{3,3''}(\vec{r}_{3,3''}, \beta_3, \beta_{3''}, \alpha_3, -\alpha_{3''}) d(\alpha_3, -\alpha_{3''})$$

Thus  $\phi_{3,3''}$  is numerically integrated over  $\alpha_3, -\alpha_{3''}$  between the limits of 0 and  $2\pi$  and the result is  $f_{3,3''}(\vec{r}_{3,3''}, \beta_3, \beta_{3''})$ .

$$\text{Hence } \phi_{13} * \phi_{3,3''} = 2\pi \int_0^\pi \sin\beta_3 d\beta_3 \int_0^\infty \phi_{13}(\vec{r}_{13}, \beta_3) f_{3,3''}(\vec{r}_{3,3''}, \beta_3, \beta_{3''}) d\{3'\}$$

At constant  $\beta_3$ , and  $\beta_{3''}$  the inner integral is only dependent on  $\vec{r}$  and is evaluated by the same method as (i). The result is a function of  $r_{13''}$ ,  $\beta_3, \beta_{3''}$  and keeping  $r_{13''}$  and  $\beta_{3''}$  constant, the values of the integral are multiplied by  $\sin\beta_3$ , and integrated over  $\beta_3$ . Thus  $\phi_{13} * \phi_{3,3''}$  becomes a function of  $r_{13''}$  and  $\beta_{3''}$ .

$$\phi_{33} * \phi_{3,1} = \int \phi_{33}(\vec{r}_{3,3'}, \beta_3, \beta_{3'}, \alpha_3 - \alpha_{3'}) \phi_{3,1}(r_{3,1}, \beta_3) d\{3'\} d\alpha_3, \sin\beta_3, d\beta_3, dr_3,$$

is evaluated as above except for the fact that

$$\int_0^{2\pi} \phi_{33} d\alpha_3 \text{ is evaluated in a slightly different way,}$$

$$\int_0^{-2\pi} \phi_{33}(\alpha_3 - \alpha_{3'}) d(-(\alpha_3 - \alpha_{3'})) = - \int_0^{-2\pi} \phi_{33}(\alpha_3 - \alpha_{3'}) d(\alpha_3 - \alpha_{3'})$$

$$= \int_{-2\pi}^0 \phi_{33}(\alpha_3 - \alpha_{3'}) d(\alpha_3 - \alpha_{3'})$$

$$\begin{aligned}
& \sum_{i,j=1}^3 q_{1i} * x_{ij} * h_{j3} = c_1^2 \int q_{11} x_{11} h_{13} d\{1\} d\Gamma_1 d\{1\} d\Gamma_1 \\
& \quad + c_1 c_2 \int q_{11} x_{12} h_{23} d\{1\} d\Gamma_1 d\{2\} d\Gamma_2 \\
& + c_1 c_3 \int q_{11} x_{13} h_{3,3} d\{1\} d\Gamma_1 d\{3'\} d\Gamma_3 + c_2 c_1 \int q_{12} x_{21} h_{13} d\{2\} d\Gamma_2 d\{1\} d\Gamma_1 \\
& + c_2^2 \int q_{12} x_{22} h_{23} d\{2\} d\Gamma_2 d\{2\} d\Gamma_2 + c_2 c_3 \int q_{12} x_{23} h_{3,3} d\{2\} d\Gamma_2 d\{3'\} d\Gamma_3, \\
& + c_3 c_1 \int q_{13} x_{3,1} h_{13} d\{3'\} d\Gamma_3 d\{1\} d\Gamma_1 + c_3 c_2 \int q_{13} x_{3,2} h_{23} d\{3'\} d\Gamma_3 d\{2\} d\Gamma_2 \\
& + c_3^2 \int q_{13} x_{3,3} h_{3,3} d\{3'\} d\Gamma_3 d\{3''\} d\Gamma_3
\end{aligned}$$

$$\begin{aligned}
\int q_{11} x_{11} h_{13} d\{1\} d\Gamma_1 d\{1\} &= \int d\{1\} d\Gamma_1 q_{11} \int x_{11} h_{13} d\{1\} d\Gamma_1 \\
&= \int d\{1\} d\Gamma_1 q_{11} (xh)_{113} = (qxh)_{1113}
\end{aligned}$$

$$\begin{aligned}
\int q_{11} x_{12} h_{23} d\{1\} d\Gamma_1 d\{2\} d\Gamma_2 &= \int d\{1\} d\Gamma_1 q_{11} \int x_{12} h_{23} d\{2\} d\Gamma_2 \\
&= \int d\{1\} d\Gamma_1 q_{11} (xh)_{123} = (qxh)_{1123}
\end{aligned}$$

$$\begin{aligned}
\int q_{12} x_{21} h_{13} d\{2\} d\Gamma_2 d\{1\} d\Gamma_1 &= \int d\{2\} d\Gamma_2 q_{12} \int x_{21} h_{13} d\{1\} d\Gamma_1 \\
&= \int d\{2\} d\Gamma_2 q_{12} (xh)_{213} = (qxh)_{1213}
\end{aligned}$$

$$\begin{aligned}
\int q_{12} x_{22} h_{23} d\{2\} d\Gamma_2 d\{2\} d\Gamma_2 &= \int d\{2\} d\Gamma_2 q_{12} \int x_{22} h_{23} d\{2\} d\Gamma_2 \\
&= \int d\{2\} d\Gamma_2 q_{12} (xh)_{223} = (qxh)_{1223}
\end{aligned}$$

$(xh)_{113}$ ,  $(xh)_{123}$ ,  $(xh)_{213}$ ,  $(xh)_{223}$  are evaluated as  $\phi_{11} * \phi_{13}$   
 and  $(qxh)_{1113}$ ,  $(qxh)_{1123}$ ,  $(qxh)_{1213}$ ,  $(qxh)_{1223}$  are evaluated as  
 $\phi_{11} * \phi_{13}$  in 4.3 above.

$$\int q_{11} x_{13} h_{3,3} d\{1\} d\Gamma_1 d\{3'\} d\Gamma_3 = \int d\{1\} d\Gamma_1 q_{11} \int x_{13} h_{3,3} d\{3'\} d\Gamma_3,$$

$$= \int d\{2\} d\Gamma_2 q_{32} (xh)_{23}{}_{3'}, = (qxh)_{323}{}_{3'},$$

$(xh)_{13}{}_{3'}$  ,  $(xh)_{23}{}_{3'}$  , are evaluated the same way as  $\phi_{13} * \phi_{33}$  in 4.3 above.

$(qxh)_{313}{}_{3'}$  ,  $(qxh)_{323}{}_{3'}$  , are evaluated the same way as  $\phi_{31} * \phi_{13}$  in 4.3 above.

$$\begin{aligned} & \int q_{33}{}_{''} x_{3''1} h_{13}, d\{3''\} d\Gamma_{3''} d\{1\} d\Gamma_1 \\ &= \int d\{3''\} d\Gamma_{3''} q_{33}{}_{''} \int x_{3''1} h_{13} d\{1\} d\Gamma_1 \\ &= \int d\{3''\} d\Gamma_{3''} q_{33}{}_{''} (xh)_{3''13}, = (qxh)_{33''13}, \end{aligned}$$

$$\begin{aligned} & \int q_{33}{}_{''} x_{3''2} h_{23}, d\{3''\} d\Gamma_{3''} d\{2\} d\Gamma_2 \\ &= \int d\{3''\} d\Gamma_{3''} q_{33}{}_{''} \int x_{3''2} h_{23}, d\{2\} d\Gamma_2 \\ &= \int d\{3''\} d\Gamma_{3''} q_{33}{}_{''} (xh)_{3''23}, = (qxh)_{33''23}, \end{aligned}$$

$$\begin{aligned} & \int q_{33}{}_{'''} x_{3'''3'''} h_{3'''} d\{3'''\} d\Gamma_{3'''} d\{3''''\} d\Gamma_{3''''} \\ &= \int d\{3'''\} d\Gamma_{3'''} q_{33}{}_{'''} \int x_{3'''3'''} h_{3'''} d\{3''''\} d\Gamma_{3''''} \\ &= \int d\{3'''\} d\Gamma_{3'''} q_{33}{}_{'''} (xh)_{3'''3'''} d\Gamma_{3''''} \\ &= (qxh)_{33'''3'''} \end{aligned}$$

$(xh)_{3'''13'}$  ,  $(xh)_{3'''23}$  , are evaluated the same way as

and

$$\frac{1}{\sqrt{N}} f_0 + \frac{1}{\sqrt{N}} f_{N/2} \exp(-\pi i k) + \frac{1}{\sqrt{N}} \sum_{j'=1}^{(N/2)-1} f_{j'} \left\{ -2i \sin((2\pi j'k)/N) \right\} \text{ if the set is anti-symmetrized}$$

Let  $f_{N/2}$  be set = 0

. . For symmetric input data

$$S = \frac{1}{\sqrt{N}} f_0 + \frac{1}{\sqrt{N}} \sum_{j=1}^{(N/2)-1} f_j \cos \frac{2\pi jk}{N}$$

For antisymmetric input data

$$S = \frac{1}{\sqrt{N}} f_0 - \frac{1}{\sqrt{N}} \sum_{j=1}^{N/2-1} 2i \sin \frac{2\pi jk}{N}$$

For N odd:

$$S_2 = \sum_{j'=\frac{N+1}{2}}^{N-1} f_{j'} \exp(-(2\pi i j'k)/N) = \sum_{j''=\frac{N-1}{2}}^{j''=1} f_{N-j''} \exp - \left( \frac{2\pi i (N-j'')k}{N} \right) \\ = \pm \sum_{j''=1}^{(N-1)/2} f_{j''} \exp \frac{2\pi i j''k}{N}$$

(using  $\exp(-2\pi i k) = 1$ , k integer)

$$S = S_1 + S_2 = \sum_{j'=0}^{(N-1)/2} f_{j'} \exp(-\frac{2\pi i j'k}{N}) \pm \sum_{j''=1}^{(N-1)/2} f_{j''} \exp(\frac{2\pi i j''k}{N})$$

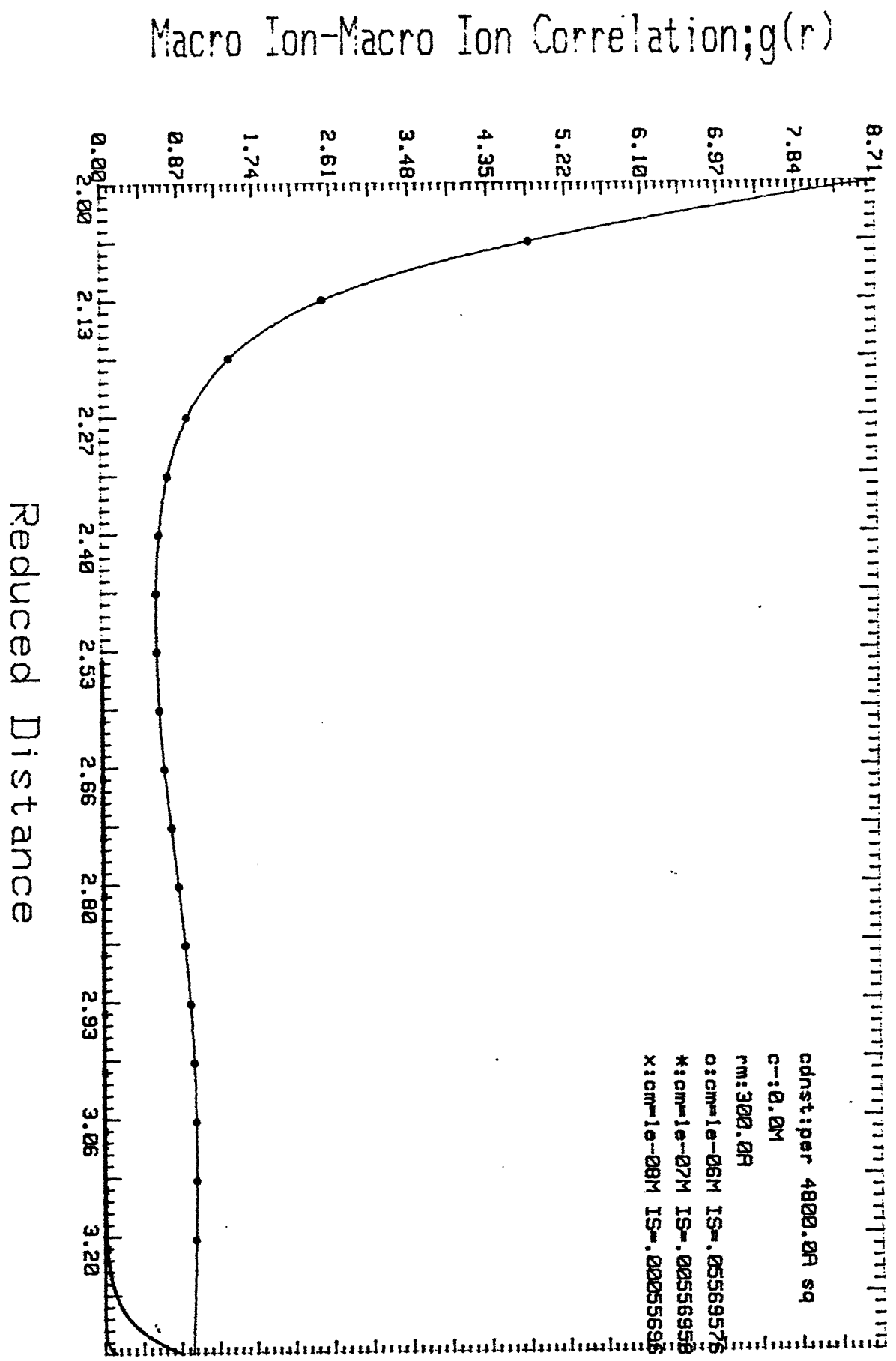
$g(r)$  versus  $r$  plots as a function of  $c_m$  remains unchanged. However quantitatively, the graph at  $c_m = 1 \times 10^{-6}$  shows less attractive correlation. In contrast to the same system at  $c^- = 1 \times 10^{-5}$ , in which  $g(r)$  falls from 8.34 at  $d_r = 2.0$  to a little below 0.83 before rising again to 1.00, we have at  $c^- = 1 \times 10^{-4}$  a similar shaped  $g(r)$  versus  $r$  graph where  $g(r)$  falls from 5.71 at  $d_r = 2.0$  to a little below 0.57 before rising again to 1.00. However, even though the graphs at  $c_m = 1 \times 10^{-7}$  and  $1 \times 10^{-8}$  remain repulsive althrough, they start rising to  $g(r) = 1.00$ , a little earlier on the  $d_r$  axis. The rise to  $g(r) = 1$  was not visible (Fig. 5.2) at  $c^- = 1 \times 10^{-5}$  and  $c_m = 1 \times 10^{-8}$  graph in the range shown in graphs whereas it is clearlay seen at  $c^- = 1 \times 10^{-4}$  and  $c_m = 1 \times 10^{-8}$  (Fig.5.3). Thus, one can say qualitatively that at large  $d_r$ , repulsion is lowered for  $c_m = 10^{-8}$  and  $10^{-7}$ . The nature of graphs at  $c^- = 0$  (Fig. 5.1) is superimposable on top of those at  $c^- = 1 \times 10^{-5}$ , showing that the  $g(r)$  versus  $r$  graphs, are insensitive to the value of  $c^-$  in the range 0 to  $1 \times 10^{-5}$ . The ionic strength changes very little ( $< 0.1\%$  for  $c_m = 1 \times 10^{-6}$  system) in going from  $c^- = 10^{-5}$  to  $10^{-4}$  and remains unchanged between  $c^- = 0$  to  $c^- = 10^{-5}$ . Quite clearly, ionic strength, as a single quantity does not determine macroion-macroion screening. The particle number densities that appear in the expressions of the HNC theory do affect, even if their total effect on ionic strength is marginal, the ionic strength being dominated by macroionic charge. In an expression of  $V_{\text{eff}}(r)$  due to Belloni (22),  $\kappa$  is calculated by taking only small ions into account. Thus the change in particle density of small ions would modify  $V_{\text{eff}}(r)$  even if macroion charge dominates ionic strength. Below

$= 10^{-3}$ . This larger attractive peak is nearly equal to the maximum (at hard sphere contact) of  $r_m = 300$ , whose maximum value of  $g$  (at hard sphere contact) falls in magnitude as we go from  $c^- = 0$  to  $10^{-4}$  to  $10^{-3}$ .

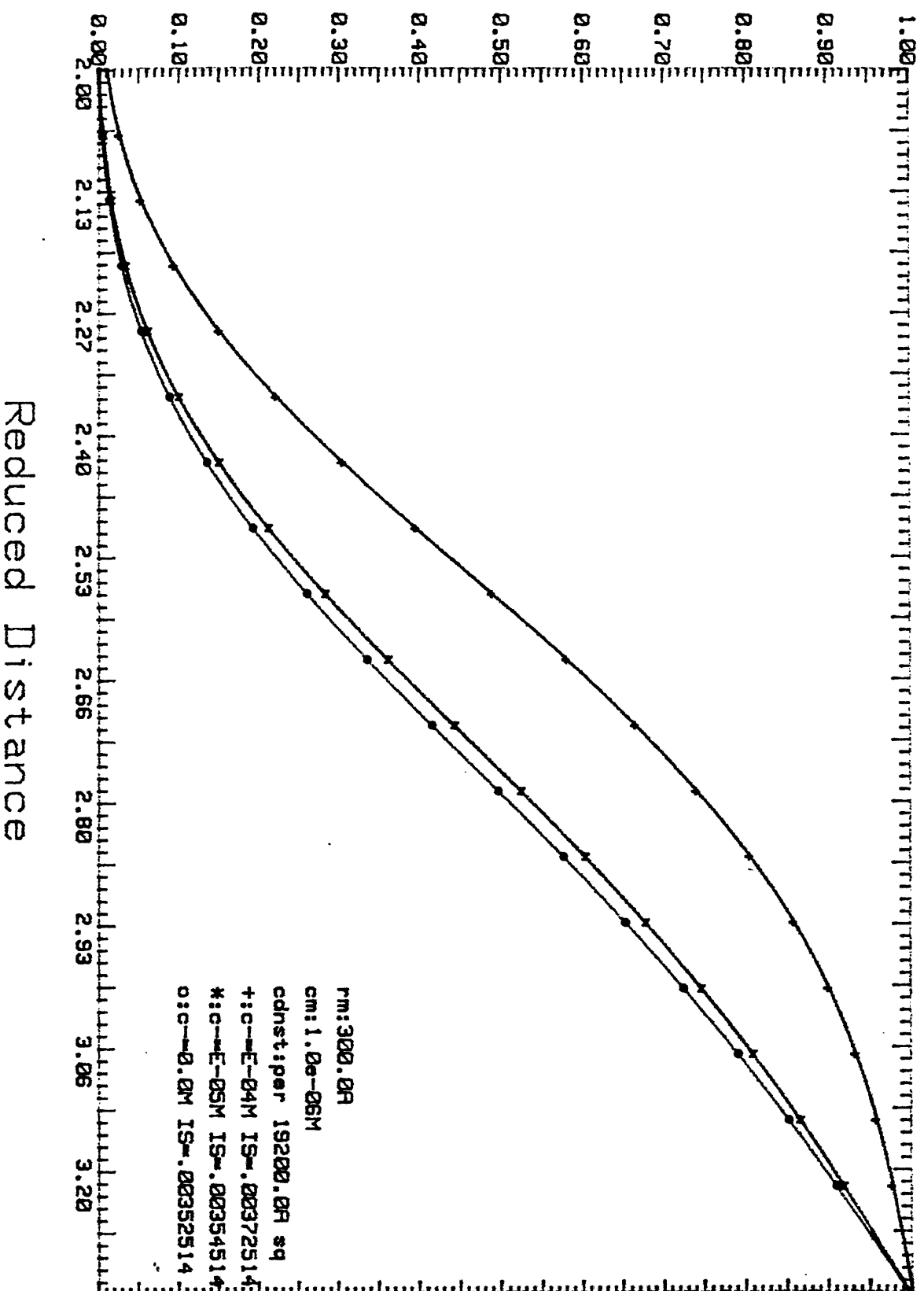
**Range of Interaction:** In systems studied at  $r_m = 200$ , the range of interaction be it repulsive althrough or attractive over a range with a peak in the  $g(r)$  versus  $r$  graph is about  $1000 \text{ \AA}^0$ , if  $c_m = 1 \times 10^{-6}$  at all values of  $c^-$  (Figs. 5.18-5.25). At this  $c_m$  the mean interparticle distance is  $\sim 1,000 \text{ \AA}^0$ . At  $c_m = 1 \times 10^{-7}$ , the interparticle distance is about  $10,000 \text{ \AA}^0$ ; the range of interaction increases, but the range at high  $c^-$  ( $1 \times 10^{-3}$ ,  $1 \times 10^{-4}$ ) remains about the same. The values of the range at  $c^- = 1 \times 10^{-5}$  go beyond  $1000 \text{ \AA}^0$ , but the graphs are slightly inaccurate because maximum range is set at  $1000 \text{ \AA}^0$ . At  $c_m = 1 \times 10^{-8}$  the graphs at lower  $c^-$  values are progressively more inaccurate but clearly the range increases well beyond  $1000 \text{ \AA}^0$ . The trends in  $r_m = 300$  systems are qualitatively the same (Figs. 5.10-5.11). The  $r_m = 20$  systems show a progressive decrease in the range as ionic strength increases at all values of  $c_m$  (Figs. 5.30-5.35). At  $c^- = 10^{-1}$ , the range is  $d_r \sim 4$ . At low  $c^- = 0, 10^{-5}, 10^{-4}$ , the range exceeds  $1000 \text{ \AA}^0$ . The lone graph at  $r_m = 50$  (Fig. 5.36) shows progressive decrease in range values with increasing  $c^-$ ,  $d_r \sim 2$  at  $c^- = 1 \times 10^{-1}$  to  $d_r \sim 11$  at  $c^- = 1 \times 10^{-3}$ . The central feature is that increasing ionic strength leads to increasing condensation of counterions and therefore decreases long range interaction, i.e. shields the macroions. Increasing macroion concentration also gives rise to shielding of macroion-macroion correlation.



# Correlation Function Vs. Distance F-5.1



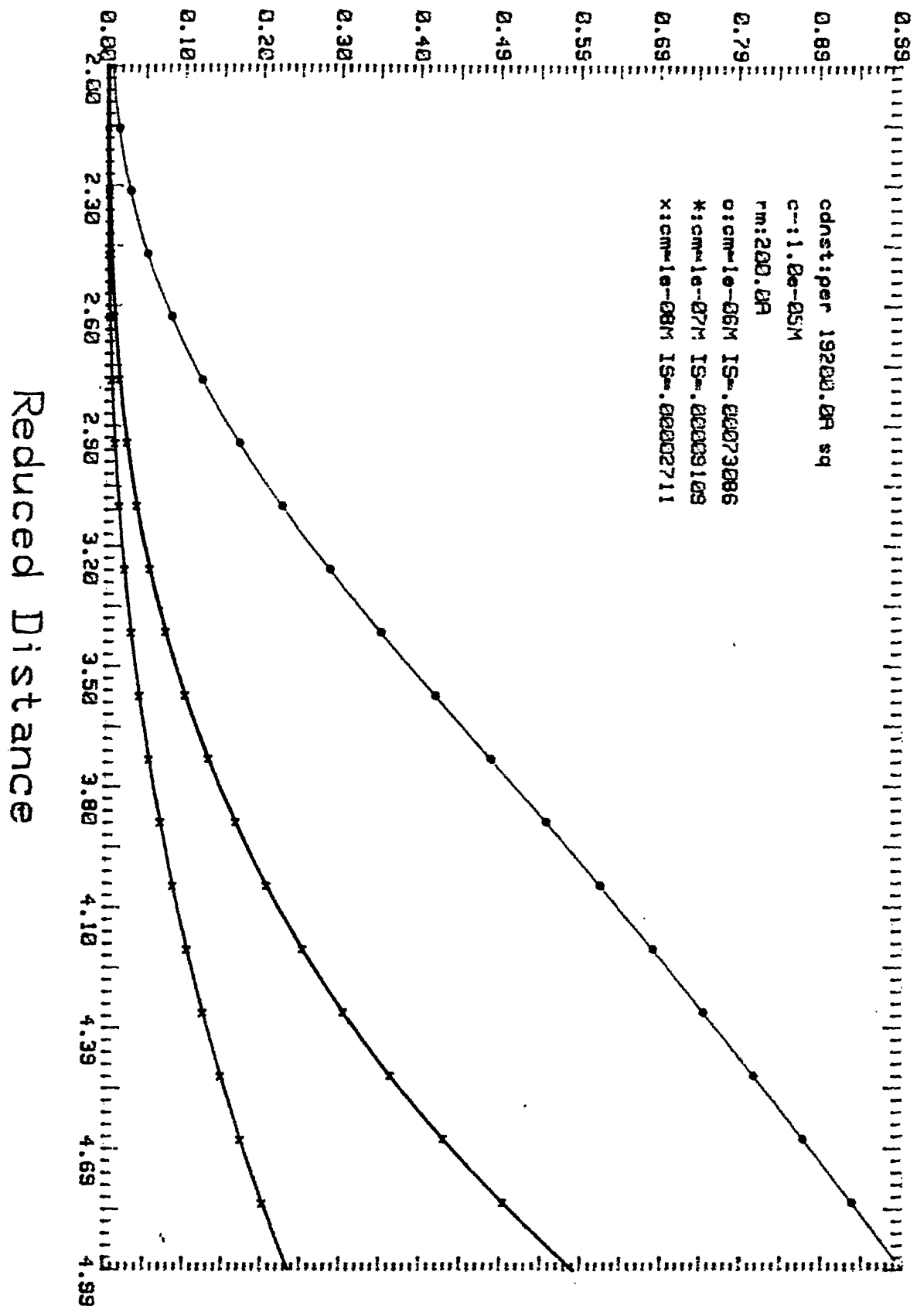
# Correlation Function Vs. Distance F-5.1C



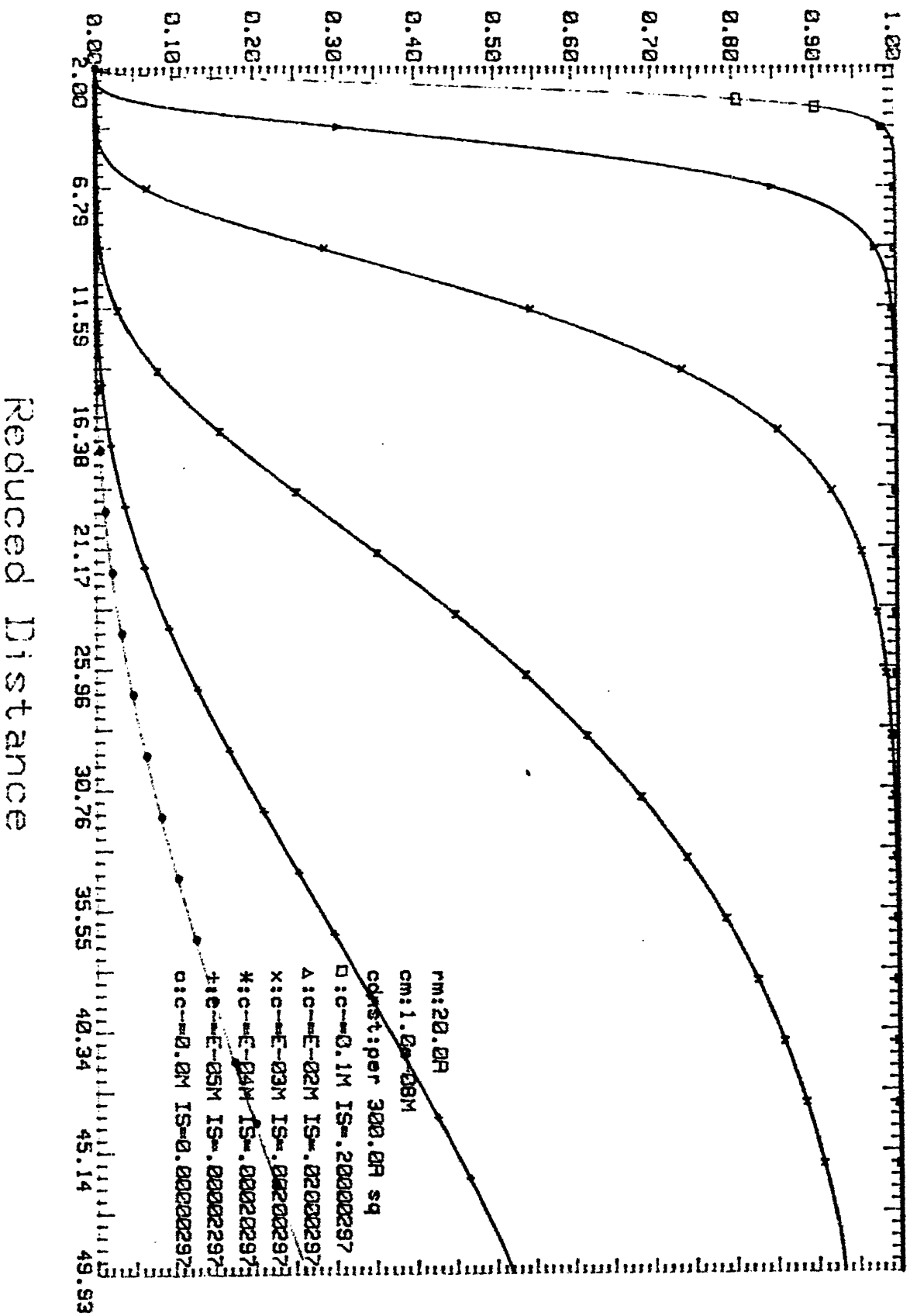
# Correlation Function Vs. Distance

F-5.2d

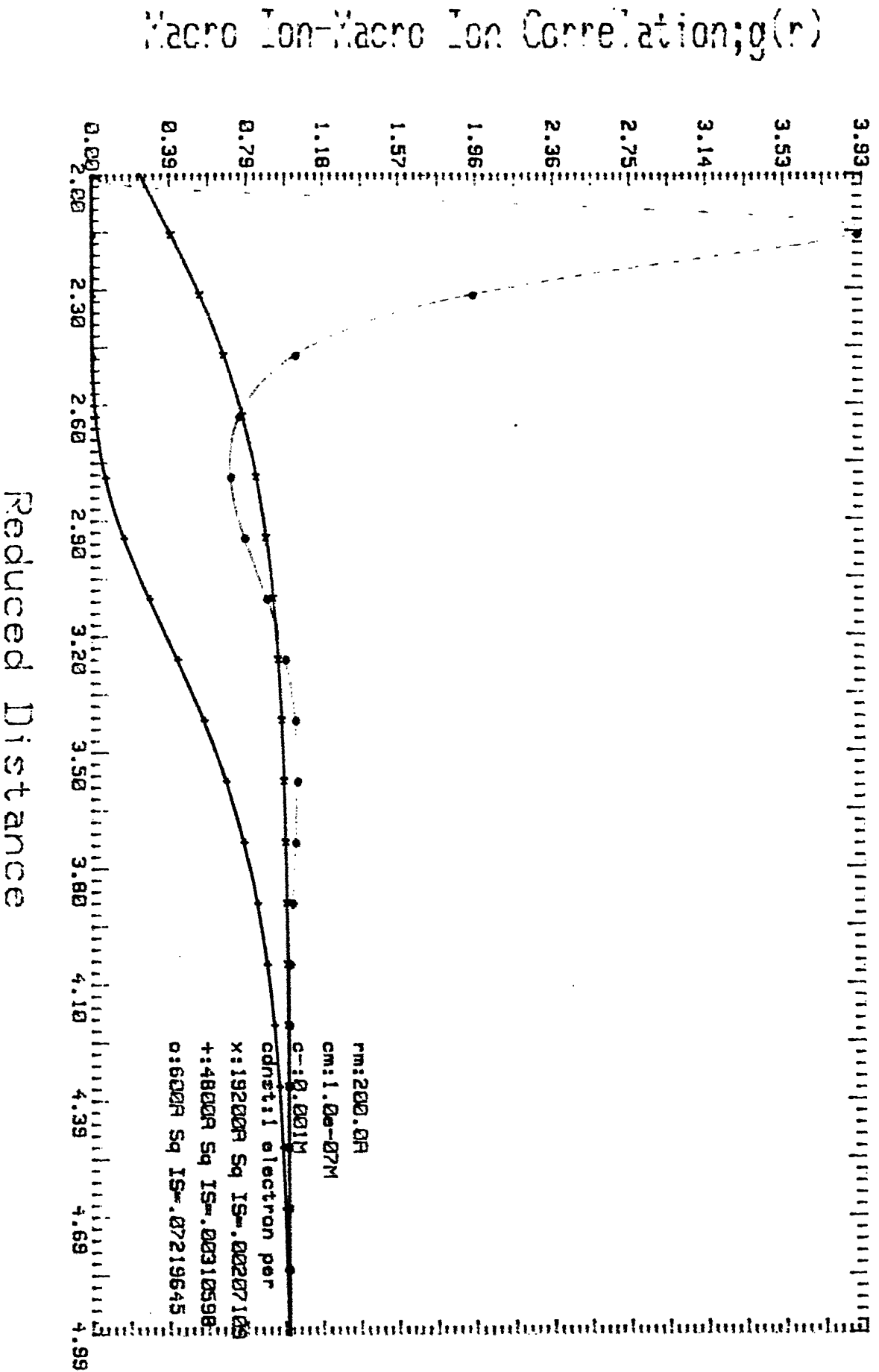
Macro Ion-Macro Ion Correlation;  $g(r)$



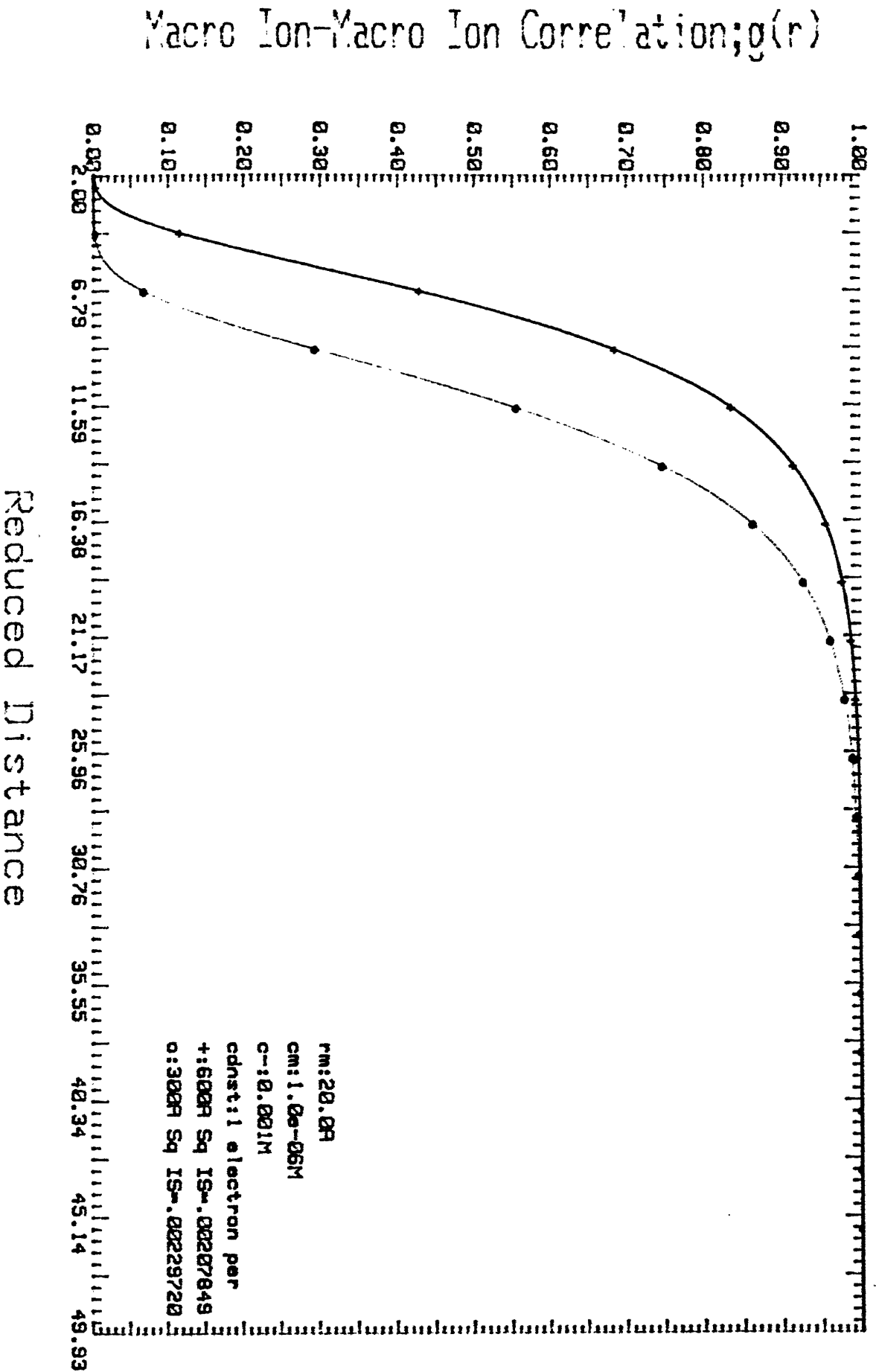
# Correlation Function Vs. Distance F-5.30



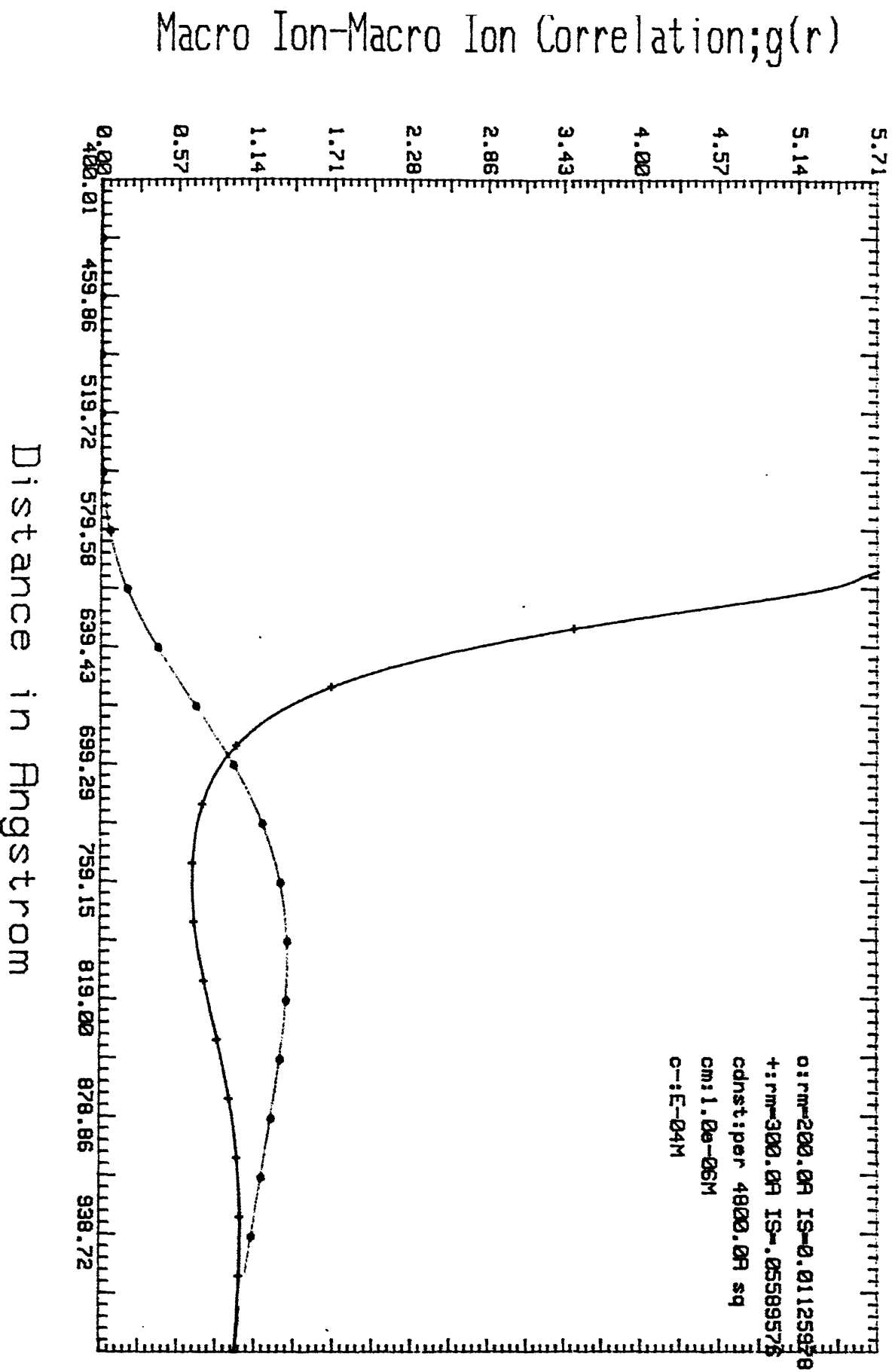
# Correlation Function Vs. Distance F-5.40



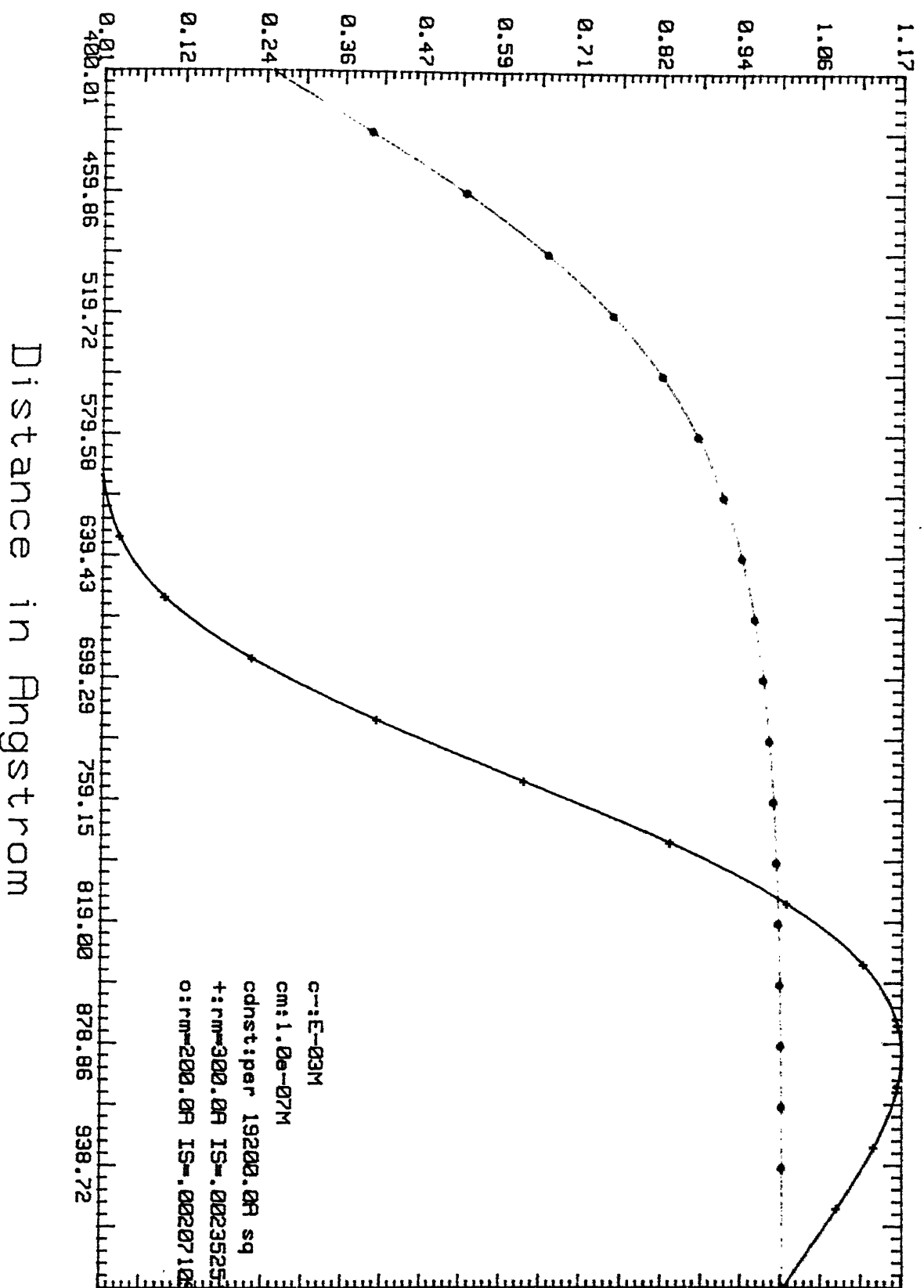
# Correlation Function Vs. Distance F-5.50



# Correlation Function Vs. Distance F-5.60



## Correlation Function Vs. Distance F-5.70





```

else
  if((i.ne.2).and.(j.ne.2))then
    if(r(i,j,k).le.(2.0*r1))then
      phi(i,j,k)=-1.0
    else
      phi(i,j,k)=dexp(q(i,j,k))-1.0d0
    end if
  else
    if(r(i,j,k).le.(2.0*r2))then
      phi(i,j,k)=-1.0
    else
      phi(i,j,k)=dexp(q(i,j,k))-1.0d0
    end if
  end if
end if
else
  if(r(i,j,k).le.(2.0*rm))then
    phi(i,j,k)=-1.0
  else
    phi(i,j,k)=dexp(q(i,j,k))-1.0d0
  endif
endif
if((i.eq.1).and.(j.eq.3)) then
  if(r(i,j,k).le.(r1+rm))then
    phi(i,j,k)=-1.0
  else
    phi(i,j,k)=dexp(q(i,j,k))-1.0d0
  endif
endif
if((i.eq.2).and.(j.eq.3)) then
  if(r(i,j,k).le.(r2+rm))then
    phi(i,j,k)=-1.0
  else
    phi(i,j,k)=dexp(q(i,j,k))-1.0d0
  endif
endif
endif

```

```

ndh(1)=n
nh=ndh(1)
ndx(1)=n
nx=ndx(1)
do k=1,n
xb(k)=xh(i,j,k)
yb(k)=yh(i,j,k)
end do
ifail=0
call c06fjf(ndim,ndh,nh,xb,yb,work,lwork,ifail)
yh(i,j,1)=ansh(i,j)*4.0d0*3.14d0
do k=2,nn
xk=dfloat(k)
yh(i,j,k)=-yb(k)*(rng/(xk-1.0d0))*tbn*sqrt(xn)
end do
do k=1,n
xb(k)=xx(i,j,k)
yb(k)=yx(i,j,k)
end do
ifail=0
call c06fjf(ndim,ndx,nx,xb,yb,work,lwork,ifail)
yx(i,j,1)=ansx(i,j)*4.0d0*3.14d0
do k=2,nn
xk=dfloat(k)
yx(i,j,k)=-yb(k)*(rng/(xk-1.0d0))*tbn*sqrt(xn)
end do
end do
do k=1,nn
do i=1,l
do j=1,m
mat1(i,j)=yq(i,j,k)
mat2(i,j)=yh(i,j,k)
mat3(i,j)=yx(i,j,k)
end do
end do
call f01ckf(res3,mat3,c,l,l,m,z,1,1,ifail)

```

```

q(3,2,i)=e(3)*e(2)*yq21t(i)
q(3,3,i)=e(3)*e(3)*yq31t(i)
end do
c-----
c*****
c CALCULATION OF phi FUNCTION
c*****
do i=1,l
do j=1,m
do k=1,nn
if((i.ne.3).and.(j.ne.3))then
if(i.ne.j)then
if(r(i,j,k).le.(r1+r2))then
phi(i,j,k)=-1.0
else
phi(i,j,k)=dexp(q(i,j,k))-1.0d0
end if
else
if((i.ne.2).and.(j.ne.2))then
if(r(i,j,k).le.(2.0*r1))then
phi(i,j,k)=-1.0
else
phi(i,j,k)=dexp(q(i,j,k))-1.0d0
end if
else
if(r(i,j,k).le.(2.0*r2))then
phi(i,j,k)=-1.0
else
phi(i,j,k)=dexp(q(i,j,k))-1.0d0
end if
end if
end if
else
if(r(i,j,k).le.(2.0*rm))then
phi(i,j,k)=-1.0
else

```

```

call d01gaf(rd,xxd,nn,ad,error,ifail)
ansx(i,j)=ad
end do
end do
do k=nnn,n
do i=1,l
do j=1,m
xh(i,j,k)=-xh(i,j,(n+2-k))
yh(i,j,k)=0.0d0
xx(i,j,k)=-xx(i,j,(n+2-k))
yx(i,j,k)=0.0d0
end do
end do
end do
do i=1,l
do j=1,m
ndh(1)=n
nh=ndh(1)
ndx(1)=n
nx=ndx(1)
do k=1,n
xb(k)=xh(i,j,k)
yb(k)=yh(i,j,k)
end do
ifail=0
call c06fjff(ndim,ndh,nh,xb,yb,work,lwork,ifail)
yh(i,j,1)=ansh(i,j)*4.0d0*pi
do k=2,nn
xk=dfloat(k)
yh(i,j,k)=-yb(k)*(rng/(xk-1.0d0))*tbn*sqrt(xn)
end do
do k=1,n
xb(k)=xx(i,j,k)
yb(k)=yx(i,j,k)
end do
ifail=0

```

```

double precision yxh112(md),yxh122(md),yxh132(md),yqx112(md),
1 yqx122(md),yqx132(md),y1112(md),y1122(md),y1132(md),
1 y2112(md),y2122(md),y2132(md),y3112(mmd,n),
1 y3122(mmd,n),y3132(mmd,n)
double precision yxh111(md),yxh121(md),yxh131(mmd),yqx111(md),
1 yqx121(md),yqx131(mmd),y1111(md),y1121(md),y1131(md),
1 y2111(md),y2121(md),y2131(md),y3111(mmd,n),
1 y3121(mmd,n),y3131(mmd,n)
equivalence (yph111,y1111),(yph112,y1121),(yph121,y1131),
1 (yph122,y1211),(yph211,y1221),(yph221,y1231),(yph232,y1311),
1 (yph132,y1321),(yph231,y1331)
equivalence (qx13,yph133),(qx23,yph233),(qx31,yph331),
1 (qx32,yph332)
equivalence (yqx111,yxh111),(yqx121,yxh121),(yqx131,yxh131),
1 (yqx112,yxh112),(yqx122,yxh122),(yqx132,yxh132),(yqx113,yxh113),
1 (yqx123,yxh123),(yqx133,yxh133),(yqx211,yxh211),(yqx221,yxh221),
1 (yqx231,yxh231),(yqx212,yxh212),(yqx222,yxh222),(yqx232,yxh232),
1 (yqx311,yxh311),(yqx321,yxh321),(yqx331,yxh331),(yqx312,yxh312),
1 (yqx322,yxh322),(yqx332,yxh332)
equivalence (y1111,y1112),(y1121,y1122),(y1131,
1 y1132),(y1211,y1212),(y1221,y1222),(y1231,
1 y1232),(y1311,y1312),(y1321,y1322),(y1331,y1332)
equivalence (y1111,y2111),(y1121,y2121),(y1131,y2131),
1 (y1211,y2211),(y1221,y2221),(y1231,y2231),(y1311,y2311)
1 ,(y1321,y2321),(y1331,y2331)
equivalence (y1111,y2112),(y1121,y2122),(y1131,
1 y2132),(y1211,y2212),(y1221,y2222),(y1231,
1 y2232),(y1311,y2312),(y1321,y2322),(y1331,y2332)
equivalence (yq313,y3213),(yq323,y3223),(yph313,
1 y3233),(yph323,y3113),(yqx313,y3123),(yqx323,y3133)
equivalence (phi33,h33,yxh313,y3323),(yq333,x33,yxh323,
1 y3333),(yph333,yqx333,yxh333)
equivalence (y1113,y2113),(y1123,y2123),(y1133,
1 y2133),(y1213,y2213),(y1223,y2223),(y1233,y2233)
equivalence (qx11(1),yq111(1)),(qx12(1),yq121(1)),(qx21(1),
1 yq112(1)),(qx22(1),yq122(1))

```

```

      1 ytemp1,ytemp2,xijkdd,eps)
call mim(q32,q23,yq323,r,k,tbn3,tbn4,w,lw,mmd,n,md,xtemp1,
      1 ytemp1,ytemp2,xijkdd,eps)
call mim(phi31,phi13,yph313,r,k,tbn3,tbn4,w,lw,mmd,n,md,xtemp1,
      1 ytemp1,ytemp2,xijkdd,eps)
call mim(phi32,phi23,yph323,r,k,tbn3,tbn4,w,lw,mmd,n,md,xtemp1,
      1 ytemp1,ytemp2,xijkdd,eps)
c-----
call mmm(q33,q33,yq333,beta,r,k,tbn3,tbn4,w,lw,w1,lw1,mmd,
      1 n,md,nd,xtemp1,ytemp1,ytemp2,xtmpr1,ytmpr1,xtmpr2,ytmpr2,
      1 xtmpr3,ytmpr3,x1,x2,y1,tmp,ans,error,alpha)
c-----
call mmm(phi33,phi33,yph333,beta,r,k,tbn3,tbn4,w,lw,w1,lw1,mmd,
      1 n,md,nd,xtemp1,ytemp1,ytemp2,xtmpr1,ytmpr1,xtmpr2,ytmpr2,
      1 xtmpr3,ytmpr3,x1,x2,y1,tmp,ans,error,alpha)
c-----
c*****
c  CALCULATION OF h AND x FINCTIONS FROM THE CALCULATED VALUE OF tao
c*****
do i=1,mmd
temp1=fps*yq131(i)
temp2=fps*yph131(i)
temp3=((c1*yph111(i))+(c2*yph121(i))+(c3*temp2))
temp4=((c1*yq111(i))+(c2*yq121(i))+(c3*temp1))
tao11=temp3-temp4
if (r(i).le.(2.0*r1)) then
h11(i)=-1.0
else
h11(i)=dexp(q11(i)+tao11)-1.0d0
end if
x11(i)=h11(i)-q11(i)-tao11
temp1=fps*yq132(i)
temp2=fps*yph132(i)
temp3=((c1*yph112(i))+(c2*yph122(i))+(c3*temp2))
temp4=((c1*yq112(i))+(c2*yq122(i))+(c3*temp1))
tao12=temp3-temp4

```

```

call imi(q13,yxh322,y1322,beta,r,k,tbn3,tbn4,w,lw,mmd,n,md,
1  xtemp1,ytemp1,ytemp2,xijkdd,yxijkd,tmp,ans,error)
call imi(q13,yxh332,y1332,beta,r,k,tbn3,tbn4,w,lw,mmd,n,md,
1  xtemp1,ytemp1,ytemp2,xijkdd,yxijkd,tmp,ans,error)
C-----
do i=1,mmd
temp1=(c1*yxh112(i))+(c2*yxh122(i))+(c3*fps*yxh132(i))
temp3=(c1*c1*y1112(i))+(c1*c2*y1122(i))+(c1*c3*
1  fps*y1132(i))+(c2*c1*y1212(i))+(c2*c2*y1222
1  (i))+(c2*c3*fps*y1232(i))+(c3*c1*fps*y1312(i))+(c3*c2*
1  fps*y1322(i))+(c3*c3*epc*y1332(i))
tao12=temp1+qx12(i)+temp3
if(r(i).le.(r1+r2)) then
h12(i)=-1.0
else
h12(i)=dexp(q12(i)+tao12)-1.0d0
end if
x12(i)=h12(i)-q12(i)-tao12
end do
C-----
call iim(yxh113,q11,y1113,r,k,tbn3,tbn4,w,lw,mmd,n,md,
1  xtemp1,ytemp1,ytemp2,xijkdd,eps)
call iim(yxh123,q11,y1123,r,k,tbn3,tbn4,w,lw,mmd,n,md,
1  xtemp1,ytemp1,ytemp2,xijkdd,eps)
call iim(yxh133,q11,y1133,r,k,tbn3,tbn4,w,lw,mmd,n,md,
1  xtemp1,ytemp1,ytemp2,xijkdd,eps)
call iim(yxh213,q12,y1213,r,k,tbn3,tbn4,w,lw,mmd,n,md,
1  xtemp1,ytemp1,ytemp2,xijkdd,eps)
call iim(yxh223,q12,y1223,r,k,tbn3,tbn4,w,lw,mmd,n,md,
1  xtemp1,ytemp1,ytemp2,xijkdd,eps)
call iim(yxh233,q12,y1233,r,k,tbn3,tbn4,w,lw,mmd,n,md,
1  xtemp1,ytemp1,ytemp2,xijkdd,eps)
C-----
do i=1,mmd
do j=1,n
temp1=(c1*yxh113(i,j))+(c2*yxh123(i,j))+(c3*tp*yxh133

```

```

ifail=1
call d01gaf(beta,tmp,n,h23d(i),error,ifail)
h23d(i)=0.5*h23d(i)
end if
end do
do i=1,mmd
if(r(i).le.(r1+r3))then
h31d(i)=-1.0
else
do j=1,n
tmp(j)=h31(i,j)*sin(beta(j))
end do
ifail=1
call d01gaf(beta,tmp,n,h31d(i),error,ifail)
h31d(i)=0.5*h31d(i)
end if
end do
do i=1,mmd
if(r(i).le.(r2+r3))then
h32d(i)=-1.0
else
do j=1,n
tmp(j)=h32(i,j)*sin(beta(j))
end do
ifail=1
call d01gaf(beta,tmp,n,h32d(i),error,ifail)
h32d(i)=0.5*h32d(i)
end if
end do
do i=1,mmd
if(r(i).le.(r3+r3))then
h33d(i)=-1.0
else
do j=1,n
do jd=1,n
do l=1,nd

```